

Application of lichen-biomonitoring to assess spatial variability of urban air quality in Manchester, UK

Daniel Niepsch

A thesis submitted in partial fulfilment of the
requirements of Manchester Metropolitan University for
the degree of Doctor of Philosophy

Department of Natural Sciences

2019

Acknowledgments

First and foremost, I would like to thank my supervisory team: Dr Leon J. Clarke, Dr Konstantinos Tzoulas and Dr Gina Cavan for all their valuable help and support throughout this project. Thank you for your persistent and invaluable supervision throughout the project, your time, effort and patience during this PhD project.

Sincere thanks also go to Dr David Megson and Dr Robert Sparkes for their suggestions and valuable inputs during analytical work, especially PAH extraction. Special gratitude to David McKendry for his help during laboratory work, analysis and technical support. Furthermore, I would like to thank the technical staff at MMU for their support, including David Groom, Alistair Battersby, Graham Tinsley, Claire Dean, John Stainton and Sue Hutchinson.

I would also like to thank everyone that I had the pleasure to meet and work with during my time at MMU. A special thanks goes to everyone in rooms JD E402 and E401, who is still present or has already left, for all the valuable time I could spend with you in (or outside) MMU.

There are a number of additional people and organisations that deserve my gratefulness:

- Dr Jason Newton at the Scottish Universities Research Centre (SUERC) and his help with stable-isotope analysis
- Rhys Jones at Waters Corporation (Stockport, UK) for his help and advice during PAH analysis and the possibility to use his equipment to analyse my samples

I sincerely express my gratitude to my former supervisors Dr Michael Zierdt, Dr Gerd Schmidt and Professor Dr Dr Manfred Frühauf, who supervised me during my Bachelor and Master Degree at the Martin-Luther-University Halle-Wittenberg. Especially Dr Zierdt, whom I have to thank for introducing me to lichens and awakening my passion for these amazing organisms.

Finally yet importantly, I would like to thank my friends and family and their ongoing support throughout the years. Especially, I would like to thank my mother Ellen Niepsch for her positivity that helped me to get that far.

Abstract

Airborne pollutants are increasingly impacting on urban populations, contributing to acute and chronic human health issues, e.g. cardiovascular and lung diseases, leading to approximately 40,000 premature deaths within the UK. Within the City of Manchester, two automated monitoring stations record atmospheric pollutants (i.e. CO, SO₂, NO_x and PM), but do not record airborne metal and PAH concentrations and are restricted in number, thus only recording localised air quality. This necessitates the application of additional monitoring methods to assess spatial variability of air quality, i.e. using biomonitors and passive monitoring devices.

Lichens are proven biomonitors for atmospheric pollution, due to their morphology, lacking roots, cuticle and stomata, and thus absorbing, adsorbing and accumulating nutrients and atmospheric pollutants within their biological tissue. The aim of the study was to document and assess spatial variability of air quality in the City of Manchester, by applying a high spatial resolution lichen biomonitoring approach. *Xanthoria parietina* and *Physcia* spp. lichens (N=94) were analysed for carbon, nitrogen and sulphur contents and their stable-isotope-ratio signatures ($\delta^{13}\text{C}$, $\delta^{15}\text{N}$ and $\delta^{34}\text{S}$). Furthermore, a new method was developed to extract nitrate and ammonium from lichen material, to investigate relative importance of both compounds on bulk nitrogen and $\delta^{15}\text{N}$ values. Airborne metal and polycyclic aromatic hydrocarbon concentrations were further analysed to investigate potential sources (i.e. vehicular emissions) and potential human health risks. Lichen chemical data, was in part, ground-truthed by NO_x diffusion tube analysis for NO₂ concentrations.

Findings indicated the beneficial use of lichens to biomonitor air quality at a high spatial resolution. Elevated pollutant loadings in lichens illustrated deteriorated air quality in Manchester. However, a complex mixture of pollutants affecting air quality in Manchester were indicated, with regard to its urban layout (i.e. road network, traffic counts and building heights) and subsequent dispersion and distribution of pollutants. This work contributed to a better insight into the variability of urban air quality, which could then be applied to (comparable) urban environments. Moreover, a high spatial lichen biomonitoring approach can be used to investigate and identify areas of concern regarding human health risks.

Table of Contents

Acknowledgments.....	I
Abstract.....	II
Table of Contents.....	III
Table of Figures.....	IX
Table tables.....	XX
Abbreviations.....	XXVII
Chapter 1- Introduction	
1.1 Scientific rationale.....	1
1.2 Aims & Objectives.....	4
1.2.1 Aims.....	4
1.2.2 Objectives.....	4
1.3 Thesis outline, chapter content, project justification and predictions.....	5
Chapter 2 - Literature review	
2.1 Air Quality, air pollution and health impacts in urban environments.....	13
2.2 Atmospheric pollutants.....	17
2.2.1 Atmospheric carbon, nitrogen and sulphur compounds.....	18
2.2.2 Atmospheric nitrate, ammonia and ammonium.....	22
2.2.3 Atmospheric stable-isotope ratios ($\delta^{13}\text{C}$, $\delta^{15}\text{N}$ and $\delta^{34}\text{S}$).....	23
2.2.4 Airborne metals.....	26
2.2.5 Atmospheric polycyclic aromatic hydrocarbons (PAHs).....	29
2.3 Biomonitoring with Lichens.....	32
2.3.1 <i>Xanthoria parietina</i>	36
2.3.2 <i>Physcia</i> spp.....	36
2.4 Lichens and air quality.....	37
2.4.1 Lichens and CNS.....	39
2.4.2 Lichens and stable-isotope ratios of carbon, nitrogen and sulphur.....	40
2.4.3 Lichens and nitrate and ammonium.....	40
2.4.4 Lichens and airborne metals.....	42
2.4.5 Lichens and PAHs.....	44
2.5 Passive sampling devices.....	46
2.6 Conclusion.....	48
2.7 The case study area – the City of Manchester (UK).....	49
2.7.1 Air quality in the City of Manchester.....	50
2.7.2 Meteorology and weather in (Greater) Manchester.....	57
2.7.3 Population and health characteristics of the City of Manchester.....	61
2.7.4 Building and road structures within the City of Manchester.....	62

2.8 Methodological Framework – sampling site identification, lichen sampling and geo-statistical modelling approach	68
2.8.1 Identification of sampling sites within the city centre of Manchester	69
2.8.2 Lichen sampling across Manchester	71
2.8.3 Geospatial modelling to assess spatial variability of air quality across Manchester	74
Chapter 3 - Epiphytic lichen diversity and air quality in Manchester	
3.1 Introduction – Lichen diversity and NO _x diffusion tubes	81
3.2 Research Methodology – Lichen frequency and diversity	83
3.2.1 Epiphytic lichen diversity to assess ‘environmental conditions’ in Manchester	83
3.2.2 Lichen species identification growing on street tree trunks across Manchester	86
3.2.3 Methodology to assess lichen frequency and diversity on tree trunks of street trees	89
3.3 Research Methodology – NO _x diffusion tubes	94
3.3.1 NO _x diffusion tube deployment procedure	94
3.3.2 Preparation and extraction of NO _x diffusion tubes before analysis	98
3.3.3 NO _x diffusion tube analysis by ion chromatography (IC)	99
3.3.4 NO _x diffusion tube calculations for NO ₂ in ambient air	100
3.4 Statistical data analysis	101
3.5 Geospatial data analysis	102
3.6 Results – Lichen diversity across Manchester	103
3.7 Results – NO _x diffusion tubes	109
3.7.1 Assessment of accuracy and precision of NO _x diffusion tube analysis by IC ..	109
3.7.2 Nitrogen dioxide (NO ₂) concentrations in the City of Manchester	111
3.8 Interpretation and discussion	116
3.8.1 Lichen diversity across Manchester in relation to air quality	116
3.8.2 Lichen species diversity and NO _x tube-derived NO ₂ concentrations	120
3.8.3 Discussion of influencing factors resulting in over- or underestimation of NO _x diffusion tube measurements	122
3.8.4 Comparison of NO _x diffusion tube measurements with automated air quality monitoring stations in Manchester to evaluate reliable performance of tubes	125
3.8.5 Comparison of NO ₂ concentrations across Manchester with other urban studies	130
3.8.6 ‘Seasonal’ variability of NO ₂ concentrations for a yearlong deployment period across Manchester	133
3.8.7 Assessment of potential influences of Manchester’s urban structure on recorded NO ₂ concentrations	140
3.9 Conclusion	144
Chapter 4 - Assessing urban air quality in Manchester (UK) at high spatial resolution using lichen carbon, nitrogen and sulphur contents and stable-isotope ratio signatures	
4.1 Introduction	147

4.2 Research Methodology	150
4.2.1 Lichen sampling and preparation	150
4.2.2 Lichen analysis for total carbon and total nitrogen contents – by CN analyser	153
4.2.3 Lichen analysis for stable-isotope ratios – by IRMS	153
4.2.4 NO _x diffusion tube analysis.....	154
4.2.5 Statistical data analysis.....	156
4.2.6 Geospatial data analysis	158
4.3 Results – Lichen CNS in urban and rural environments	159
4.3.1 Assessment of accuracy and precision of CNS and stable-isotope analysis ..	159
4.3.2 Assessment of temporal variability of CNS contents (wt%) in urban <i>X. parietina</i> samples	166
4.3.3 Carbon, nitrogen and sulphur contents (wt%) and stable-isotope-ratios in rural <i>X. parietina</i> samples	167
4.3.4 Spatial variability of carbon, nitrogen and sulphur contents (wt%) in lichens (<i>X. parietina</i> and <i>Physcia</i> spp.) sampled across the City of Manchester.....	170
4.3.5 Spatial variability of stable-isotope ratio signatures ($\delta^{13}\text{C}$, $\delta^{15}\text{N}$ and $\delta^{34}\text{S}$) in lichens (<i>X. parietina</i> and <i>Physcia</i> spp.) sampled across the City of Manchester	176
4.3.6 Comparison of rural and urban <i>X. parietina</i> samples.....	183
4.3.7 Urban NO _x diffusion tube measurements in relation to analysed lichen CNS contents (wt%) and stable-isotope-ratio-signatures ($\delta^{13}\text{C}$, $\delta^{15}\text{N}$ and $\delta^{34}\text{S}$)	186
4.3.8 Urban influences on spatial variability of CNS contents and stable-isotope-ratio signatures recorded in <i>X. parietina</i> and <i>Physcia</i> spp. in Manchester (UK)	189
4.4 Interpretation and Discussion	193
4.4.1 Temporal variability of carbon, nitrogen and sulphur contents (wt%) in urban <i>X. parietina</i> samples.....	193
4.4.2 Comparison of rural and urban lichen samples and the applicability of rural <i>X. parietina</i> as ‘control samples’.....	194
4.4.3 Comparison of carbon, nitrogen and sulphur contents (wt%) in lichens (<i>X. parietina</i> and <i>Physcia</i> spp.) with other urban studies and the relation to air quality in the City of Manchester	197
4.4.4 Comparison of stable-isotope ratio signatures in lichens (<i>X. parietina</i> and <i>Physcia</i> spp.) with other urban studies and the relation to air quality in the City of Manchester.....	203
4.4.5 Urban NO _x diffusion tube measurements	210
4.4.6 Investigating potential urban influences on spatial variability of CNS contents and stable-isotope ratio signatures recorded in <i>X. parietina</i> and <i>Physcia</i> spp. in Manchester (UK)	211
4.5 Conclusion	213
Chapter 5 - Development of a new method to quantify nitrate and ammonium in lichens	
5.1 Introduction	217

5.2 Research Methodology – Development of an extraction method to enable quantification of lichen nitrate and ammonium concentrations by ion chromatography (IC).....	219
5.2.1 Lichen sampling and preparation	219
5.2.2 Experimental design to determine lichen nitrate and ammonium concentrations	222
5.2.3 Detailed testing of different chemical extraction approaches using a single urban lichen sample.....	223
5.2.4 Determination of nitrate and ammonium by ion chromatography (IC).....	224
5.3 Statistical data analysis	225
5.4 Geospatial data analysis	226
5.5 Determination of nitrate and ammonium concentrations extracted from a single lichen sample and analysis by ion chromatography.....	228
5.5.1 Experiment 1: Extraction using DI, 1%, 7.5% and 15% KCl	228
5.5.2 Experiment 2: Extraction using DI, 1%, 3% and 6% KCl	232
5.5.3 Experiment 3: Extraction using 3% KCl.....	235
5.5.4 Application of optimised chemical extraction method to urban and rural lichen samples.	238
5.6 Results – nitrate and ammonium in rural and urban lichen samples	238
5.6.1 Assessment of accuracy and precision of nitrate and ammonium concentrations by ion chromatography (IC)	238
5.6.2 Temporal variability of lichen nitrate and ammonium concentrations.....	240
5.6.3 Nitrate and ammonium concentrations in urban lichen samples (<i>X. parietina</i> and <i>Physcia</i> spp.).....	242
5.6.4 Nitrate and ammonium concentrations in rural lichen samples.....	249
5.6.5 Comparison of nitrate and ammonium in urban and rural lichen samples	254
5.6.6 Spatial variability of nitrate and ammonium concentrations recorded in <i>X. parietina</i> and <i>Physcia</i> spp.....	256
5.7 Interpretation and Discussion	261
5.7.1 Nitrogen speciation (NO_3^- and NH_4^+) using DI and KCl and subsequent analysis by ion chromatography (IC)	261
5.7.2 What does temporal variability imply for spatial variability of NO_3^- and NH_4^+ across Manchester?	263
5.7.3 Assessment of nitrate and ammonium concentrations in rural <i>X. parietina</i> and influences on bulk nitrogen (N wt%) contents and $\delta^{15}\text{N}$ values.....	267
5.7.4 Comparison of urban lichen samples (<i>X. parietina</i> and <i>Physcia</i> spp.) nitrate and ammonium concentrations in relation to bulk nitrogen and $\delta^{15}\text{N}$ values.....	270
5.8 Conclusion	273

Chapter 6 - Lichen biomonitoring of spatial variability of airborne metal pollution in the City of Manchester

6.1 Introduction	277
6.2 Research Methodology – metal concentrations by ICP-OES and ICP-MS	279
6.2.1 Lichen sampling for analysis of metal concentrations.....	279

6.2.2	Microwave-assisted acid digestion of lichen material	281
6.2.3	Analysis of acid-digested lichen samples by ICP-OES and ICP-MS.....	282
6.2.4	Statistical analysis.....	285
6.2.5	Geospatial data analysis.....	287
6.3	Results – lichen metal concentrations.....	287
6.3.1	Assessment of accuracy and precision of metals dataset	287
6.3.2	Temporal variability of metal concentrations in urban lichen samples	292
6.3.3	Metal concentrations in rural <i>X. parietina</i> samples	297
6.3.4	Comparison of metal concentrations in <i>X. parietina</i> and <i>Physcia</i> spp. sampled across Manchester	301
6.3.5	Spatial variability of metal concentrations recorded in <i>X. parietina</i> and <i>Physcia</i> spp. samples across Manchester.....	309
6.3.6	Comparison of metal concentrations in rural and urban <i>X. parietina</i> lichens ..	318
6.4	Interpretation and Discussion	321
6.4.1	Temporal variability of metal concentrations	321
6.4.2	Can rural <i>X. parietina</i> lichens be used as ‘control’ samples for comparison with urban <i>X. parietina</i> for airborne metal concentrations?.....	323
6.4.3	Assessment of whether urban metal concentrations exhibit similar patterns and the potential for source apportionment.....	324
6.4.4	Do <i>X. parietina</i> and <i>Physcia</i> spp. lichens record different airborne metal concentrations in the City of Manchester?	328
6.4.5	Are lichen metal concentrations recorded for the City of Manchester comparable with other urban biomonitoring studies?.....	330
6.4.6	Exploring potential controls on urban metal concentrations in the City of Manchester Spatial variability of metal concentrations recorded in the City of Manchester.....	337
6.4.7	Modelling approach of metal concentrations in urban <i>X. parietina</i> samples applying urban control factors.....	346
6.5	Conclusion	351

Chapter 7 - Lichen biomonitoring for atmospheric PAH source apportionment and toxicity assessment

7.1	Introduction	354
7.2	Research area – Manchester city centre	357
7.2.1	Lichen sampling for PAH extractions	359
7.2.2	Solvent extraction of PAHs from lichen material.....	363
7.2.3	Testing SPE clean-up to determine best analytical practice	364
7.2.4	PAH extraction applied to Manchester urban lichen samples.....	366
7.2.5	PAH analysis using GC-MS, GC-APCI-TOF-MS/MS and GC-APCI-TQ-MS/MS	370
7.2.6	Calculating of recovery rates and limits of detection and limits of quantification for PAHs recorded by GC-APCI-TQ-MS/MS	372
7.2.7	Statistical analysis and data visualisation.....	373

7.3 Results – lichen PAH concentrations.....	375
7.3.1 Type and concentrations of PAHs recorded in <i>X. parietina</i> and <i>Physcia</i> spp..	375
7.3.2 Spatial variability of PAH concentrations.....	382
7.4 Interpretation and Discussion	392
7.4.1 Comparison of PAH concentrations recorded in <i>X. parietina</i> and <i>Physcia</i> spp.	392
7.4.2 Comparison of PAH concentrations recorded in Manchester with urban lichen- biomonitoring studies.....	393
7.4.3 Spatial variability of PAH concentrations in the urban environment of Manchester.....	398
7.4.4 Using PAH ratios to 'fingerprint' major sources of PAHs in the urban environment of Manchester	403
7.4.5 The carcinogenic potential of PAHs recorded across Manchester.....	418
7.5 Conclusion	422

Chapter 8 - Conclusions and recommendations

References

Appendices

Table of Figures

Chapter 1

Figure 1-1: Schematic thesis outline and chapter contents to assess high-spatial resolution of air quality in Manchester, dashed arrows indicate linkages between chapters and analytical data (e.g. NO_x diffusion tube measurements in relation to lichen nitrogen contents (N wt%) and stable-nitrogen isotope-ratios ($\delta^{15}\text{N}$))6

Chapter 2

Figure 2-1: Effects of air pollutants (specified for some) on the human system, with pollution related diseases (pollutant impacts summarized from Kampa and Castanas, 2008; Regan, 2018).....17

Figure 2-2: UK (a) carbon monoxide (CO) emission in kilo tonnes [kt] for all sources, industrial, commercial and residential combustion and road transport and (b) sulphur dioxide (SO₂) emissions in kilo tonnes [kt] for all sources and industrial, commercial and residential combustion (NAEI, 2018a).....19

Figure 2-3: Road traffic SO₂ emissions in kilo tonnes [kt] for the years 2000 to 2016 (NAEI, 2018a)20

Figure 2-4: UK nitrogen dioxides - NO_x (as NO₂) emissions in kilo tonnes [kt] for all sources, industrial, commercial combustion and road transport from 2000 to 2016 (NAEI, 2018b)....21

Figure 2-5: UK emissions NH₃ [in kilotonnes] (total NH₃ including industrial and commercial combustion and road transport; NH₃ including agriculture and road transport) from 2000 to 2016 (NAEI, 2016)23

Figure 2-6: Representative δ -values of CNS isotopes in natural systems (taken from Fry (2006); *Annual Review of Ecology and Systematics*, Volume 18, copyright 1987 by Annual Reviews: www.annualreview.org).....25

Figure 2-7: UK emissions of Cd, Pb, Ni and Zn between 2000 and 2016 (NAEI, 2018c) by major anthropogenic sources (i.e. industrial/ commercial combustion, production processes and road traffic)28

Figure 2-8: Semi-schematic profile of a foliose lichen (left) and SEM-profile (160x) of the foliose lichen *Lobaria scrobiculata* (layered structure) (right) (modified illustration after Wirth, 1995; Kirschbaum and Wirth, 2010)34

Figure 2-9: *Xanthoria parietina* [left] and *Physcia tenella* and *Physcia adscendens* (socialized) [right] (author [left]; Kirschbaum and Wirth, 2010:154 [right])36

Figure 2-10: 'Palmer-type' diffusion sampler (schematic overview, with dimensions) [left] and sampling tube components [right].....47

Figure 2-11: The case study area, together with automated air quality monitoring stations (Oxford Road [left] and Piccadilly Gardens [right]) and major road network in the city centre of Manchester; the study area location within Greater Manchester (inset map) is also shown.51

Figure 2-12: Monthly mean NO₂ at monitoring stations on Oxford Road and at Piccadilly Gardens (2010 to 2018; King et al., 2016 ;Air Quality England, 2018b, 2018a); the WHO limit value (40 $\mu\text{g}/\text{m}^3$) is also shown52

Figure 2-13: Total NO_x [$\mu\text{g}/\text{m}^3$] pollution map (sum of all sectors for 2017) for the City of Manchester (and bordering districts) – displayed as 1x1km raster data (QGIS 3.4.2; DEFRA, 2017b).....53

Figure 2-14: ΣPAH concentrations in air for the urban centre of Manchester (measured at Manchester Law Courts') for the years 1991 to 1995 (Coleman et al., 1997; Howsam and Jones, 1998)54

Figure 2-15: Recent quarterly measurements (Q) of PAH concentrations (particulate- and gaseous-phase) at Manchester Law Courts for the years 2010 to 2011 and 2013 to 2014; PAHs have

been classified by number of rings; naphthalene and dibenzo[a,h]anthracene were not measured, benzo[b]fluoranthene is included with benzo[j]fluoranthene (DEFRA, 2014b)55

Figure 2-16: Monthly mean temperature [°C], total precipitation [Σ mm] and sunshine hours [Σ hours] for the NO_x deployment period of NO_x diffusion tubes in Manchester, obtained from the Whitworth Meteorological Observatory59

Figure 2-17: Mean wind direction (frequencies) for Manchester during the NO_x deployment period (01/07/2017 to 01/07/2018).....59

Figure 2-18: Temperature [°C] (minimum, maximum and mean; with lowest and highest temperatures) and total precipitation [Σ mm] displayed as day-by-day data for the NO_x deployment period.....60

Figure 2-19: 2.5D model of building heights (OS Building Heights; Digimap - Ordnance Survey, 2017) across Manchester, displayed with automated monitoring stations and major road network62

Figure 2-20: Average traffic speed – AM and PM peak (Sept. 2013 to Aug. 2014) on the primary road network in Manchester, indicating potentially high traffic emissions (Highway Forecasting and Analytical Services, 2015).....65

Figure 2-21: Identified research area for the city centre of Manchester, including point sources (and main pollutant; NAEI, 2013) and major roads (including A- and B-roads and motorways; UK Department of Transport, 2012).....67

Figure 2-22: Methodological framework to assess high spatial resolution of air quality of Manchester, including the sampling procedure (schematic) and the use of secondary data to explore spatial variability of lichen-derived pollutant loadings.....68

Figure 2-23: Tree coverage (%) per ward (a; ‘Tree Audit Phase 2’ Red Rose Forest, 2008) and per Urban Morphology Type (UMT) across the city centre (b), displayed with major roads and monitoring stations.....70

Figure 2-24: Lichen sampling procedure (a), including tree height estimation and processing procedure (b), including freeze drying step (on Buchi L-200) for PAH analysis.....73

Figure 2-25: Secondary datasets used for description of the close surrounding of the sampling sites, which were included into spatial regression methods within each analytical chapter.....78

Figure 2- 26: Categorisation of datasets for spatial analysis of chemically analysed lichen pollutant loadings; urban factor datasets were implemented into GIS and sampling sites were categorised/grouped based on literature informed pollutant declines (i.e. NO_x); distances were measured from the specific sampling location79

Chapter 3

Figure 3-1: Lichen sampling sites (grey circles; N=94) sampled for *X. parietina* and *Physcia* spp. off street tree twigs and small branches to chemically analyse elemental composition and trees that were suitable to assess lichen frequency and diversity on bark (dark grey triangle; N=58)85

Figure 3-2: Comparison of lichens of the genus *Xanthoria*, including *X. parietina*, *X. polycarpa* and *X. ucrainica*; their main identification characteristics and habitats (Dobson, 2011)88

Figure 3-3: Sampling grid (‘lichen ladder’) attached to the tree trunk between 1.00 to 1.50 m height at each cardinal direction (Asta, Erhardt, et al., 2002)90

Figure 3-4: Evaluation matrix used to colour-code air quality across Manchester, based on lichen diversity (i.e. red illustrating deteriorated air quality) on 58 analysed trees (the evaluation matrix was adopted from Kirschbaum and Wirth, 2010)93

Figure 3-5: Lichen sampling sites for analysis of CNS contents, stable-isotope ratios and metal concentrations, together with NO_x diffusion tubes locations (N=45; and site ID) across Manchester; displayed with automated monitoring stations within the city centre.96

Figure 3-6: (a) NO _x diffusion tube - schematic view of NO _x diffusion tubes with dimensions and deployed tube at sampling site (with spacer block and information tag) (b) NO _x tube components and re-charged and fully assembled tube.....	97
Figure 3-7: Pie chart of lichen families recorded on examined trees to assess lichen diversity across Manchester; reference species are displayed as white patterns, eutrophication species as black patterns.....	104
Figure 3-8: Lichen diversity map – (a) 1x1 km grid, included analysed trees (N=58), LDI for reference and eutrophication species and (b) 1x1 km grid colour codes according to Figure 3-3 and AQI for each area (N/A – one tree analysed, no evaluation matrix used); displayed with major road classes and attribute table	106
Figure 3-9: Lichen diversity – (a) by tree approach, classified as ratio between reference and eutrophication species, major road classes and Σ of reference and eutrophication species at the site (displayed as pie charts) with frequencies of recorded lichen species (b)	107
Figure 3-10: Box-Whisker plots (25 th to 75 th percentile) of (a) reference species and traffic counts (grouped, N=46), (b) reference species and distance to major road (grouped, N=46), (c) eutrophication species and traffic counts (grouped, N=58) and (d) eutrophication species and distance to major road (grouped, N=58); Pearson's' r and ANOVA p-values are displayed for eutrophication species (normally distributed); Spearman ρ and Kruskal-Wallis p-values are displayed for reference species.	108
Figure 3-11: (a) Analysed nitrite concentrations (N=230) in certified reference material (CRM Simple Nutrients – Whole Volume QC3198; with upper and lower 95% confidence interval) and (b) mean nitrite concentrations (in CRM) by batch (red dashed line illustrates the certified value 2.95; error bars presented as 1x standard deviation of repeated CRM measurements for each analytical batch)	110
Figure 3-12: NO _x tube deployment sites that exceeded the WHO limit value of 40 $\mu\text{g}/\text{m}^3$ (colour coded by percentage of exceedance), displayed with number of exceedance out of 24 bi-weekly deployments; one site was recorded (grey circle) with no exceedance for the deployment period.....	114
Figure 3-13: Analysed mean concentrations [in $\mu\text{g}/\text{m}^3$] of NO ₂ concentrations for all deployment sites (N=45) between the 03/07/2017 and the 28/06/2018; no influencing factors (i.e. building heights, distance to road etc.) were used for spatial interpolation of data (mean NO ₂ values were interpolated by ordinary kriging; kriging error map is displayed in the Appendix A-4)	115
Figure 3-14: Reference and eutrophication species (summarised by tree) with mean NO ₂ concentrations for sites where NO _x diffusion tubes were located and that were analysed for lichen diversity (N=26)	121
Figure 3-15: Biweekly (mean) concentrations of NO ₂ in $\mu\text{g}/\text{m}^3$ measured at Manchester Piccadilly Gardens (red circle) and Oxford Road (grey square) between June 2017 and June 2018 (displayed with WHO limit value – red dotted line); numbers (1) represent a bi-weekly deployment period.....	126
Figure 3-16: Biweekly NO ₂ concentrations at 'co-located' sites recorded for 24-weeks (361 days); dummy value (white diamond) with CRM-derived nitrite value, as 1x standard deviation (± 0.108) and WHO limit value (red dotted line); numbers (1) represent a bi-weekly deployment period; missing values for ID: 17 indicate missing tubes.....	127
Figure 3-17: Automatically measured NO ₂ concentrations at (a) Manchester Oxford Road and (b) Manchester Piccadilly Gardens with closest NO _x diffusion tube (ID: 17 and ID: 34 for Oxford Road; ID: 18 for Piccadilly Gardens); error bars are presented as 1x Std. Dev. On 'dummy value'(CRM by IC analysis: ± 0.108)	129
Figure 3-18: Bar graphs of urban mean NO ₂ concentrations [in $\mu\text{g}/\text{m}^3$] (following Table 3-13) reported for UK and European studies to compare recorded NO ₂ in Manchester (with error	

bars, as 1 x Std. Dev. where applicable); WHO limit value of 40 $\mu\text{g}/\text{m}^3$ displayed as dashed-dotted line.....	131
Figure 3-19: ‘Seasonal’ NO_2 concentrations and meteorological data, to assess influences of (a) temperature [$^{\circ}\text{C}$], (b) sunshine hours [Σ hours] and (c) precipitation [Σ mm] on NO_2 concentrations	135
Figure 3-20: Seasonal variation of NO_2 concentration in Manchester (1) ‘Summer’ and (2) ‘Autumn; interpolated by Ordinary Kriging (OK), colour-coded by NO_2 concentration	137
Figure 3-21: Seasonal variation of NO_2 concentration in Manchester (3) ‘Winter’ and (4) ‘Spring; interpolated by Ordinary Kriging (OK), colour-coded by NO_2 concentration’	138
Figure 3-22: Nitrogen dioxide (NO_2) concentrations with distance to major road distance (displayed with correlation coefficient Pearson’s r , for normal distributed NO_2).....	141
Figure 3-23: Modelled NO_2 concentrations (mean concentrations) to investigate potential urban influences of Manchester’s urban structure on NO_2 concentrations, using Geographically Weighted Regression (GWR).....	143

Chapter 4

Figure 4-1: Lichen sampling sites (<i>X. parietina</i> : grey circle; <i>Physcia</i> spp.: black triangle and re-visited sampling sites in 2018: blue outline) across Manchester city centre; two automated instrumented air quality monitoring stations are also shown.....	151
Figure 4-2: Rural lichen sampling sites (<i>X. parietina</i> ; N=12) distributed around a poultry farm in Shrewsbury, UK (sampled in May 2018); displayed with location of poultry farm in relation to Greater Manchester (upper left corner, red square).....	152
Figure 4-3: NO_x tube deployment sites (N=45; with site IDs), displayed with two automated instrumented air quality monitoring stations (pictures displayed in the upper left corner) and lichen sampling sites (N=94)	155
Figure 4-4: Mean concentrations (presented as bar plots with 1x standard deviation) of recorded (a) nitrogen and (b) carbon contents (in wt%) in lichen CRM (No. 482) for each analytical batch using a CN analyser (with number of individual samples run; dashed lines represent certified values, N wt%: 1.743 and C wt%: 44.7).....	161
Figure 4-5: CNS contents (wt%; above) and stable-isotope-ratio signatures (‰; below) recorded for analytical batches recorded in lichen CRM (No. 482) using IRMS; dashed red lines presents certified values, blue dashed line represents indicative values for sulphur contents (wt%; Quevauviller et al., 1996)	165
Figure 4-6: Box-Whisker plots (25th to 75th percentile) of carbon contents (C wt%) recorded in <i>X. parietina</i> for sampling periods (undertaken during 2016/17 displayed as (1) and in 2018, as (2)), displayed with mean value: white square and extreme values (black diamond)	166
Figure 4-7: Comparison of nitrogen (wt%) [above] and $\delta^{34}\text{S}$ (‰) [below] in rural <i>X. parietina</i> samples, with distance to poultry farm (<500 m and >500 m).....	168
Figure 4-8: (a) Nitrogen contents (wt%) and (b) $\delta^{15}\text{N}$ (‰) values recorded in <i>X. parietina</i> , sampled around a poultry farm (in Shrewsbury, UK); displayed with sampling area and poultry farm location.....	169
Figure 4-9: Comparison of urban <i>X. parietina</i> and <i>Physcia</i> spp. samples for (a) carbon, (b) sulphur and (c) nitrogen contents, presented as Box-Whisker plots (with mean value: white square, median line and extreme values: black diamond) and scatter-plots for (d) carbon, (e) nitrogen and (f) sulphur contents to illustrate species-specific differences (with correlation statistics; error bars are presented on dummy value C wt%: ± 0.55 ; N wt%: ± 0.04 and S wt%: ± 0.02 ; two significant outliers (identified by Grubbs test, $p < 0.05$) in (d) <i>Physcia</i> spp. at 11.73 wt% and 18.37 wt% not shown)	171

Figure 4-10: Carbon contents (C wt%) in (a) <i>X. parietina</i> and (b) <i>Physcia</i> spp. (colour-coded, low to high) across the City of Manchester; displayed with automated air quality monitoring stations	173
Figure 4-11: Nitrogen contents (N wt%) in (a) <i>X. parietina</i> and (b) <i>Physcia</i> spp. (colour-coded, low to high) across the City of Manchester; displayed with automated air quality monitoring stations.....	174
Figure 4-12: Sulphur contents (S wt%) in (a) <i>X. parietina</i> and (b) <i>Physcia</i> spp. (colour-coded, low to high) across the City of Manchester; displayed with automated air quality monitoring stations	175
Figure 4-13: Comparison of urban <i>X. parietina</i> and <i>Physcia</i> spp. samples for (a) $\delta^{13}\text{C}$, (b) $\delta^{15}\text{N}$ and (c) $\delta^{34}\text{S}$, presented as Box-Whisker plots (with mean value: white square, median line and extreme values: black diamond) and scatter-plots for (d) $\delta^{13}\text{C}$, (e) $\delta^{15}\text{N}$ and (f) $\delta^{34}\text{S}$ to illustrate species-specific differences (with correlation statistics; error bars are presented on dummy value $\delta^{13}\text{C}$: $\pm 0.61\text{‰}$; $\delta^{15}\text{N}$: $\pm 0.23\text{‰}$ and $\delta^{34}\text{S}$: $\pm 0.62\text{‰}$).....	177
Figure 4-14: $\delta^{13}\text{C}$ values of (a) <i>X. parietina</i> and (b) <i>Physcia</i> spp. (colour-coded, low to high) across the City of Manchester; displayed with automated air quality monitoring stations.....	179
Figure 4-15: $\delta^{34}\text{S}$ values of (a) <i>X. parietina</i> and (b) <i>Physcia</i> spp. (colour-coded, low to high) across the City of Manchester; displayed with automated air quality monitoring stations.....	180
Figure 4-16: $\delta^{15}\text{N}$ values of (a) <i>X. parietina</i> and (b) <i>Physcia</i> spp. (colour-coded, low to high) across the City of Manchester; displayed with automated air quality monitoring stations.....	181
Figure 4-17: Scatter-plots of lichen CNS contents and stable isotope signatures ($\delta^{13}\text{C}$, $\delta^{15}\text{N}$ and $\delta^{34}\text{S}$) with correlation coefficients (Pearson's r and Spearman ρ); lichen CRM (No. 482) derived error bars are presented as \pm one standard deviation (on dummy value); lines (dark grey: <i>X. parietina</i> , light grey <i>Physcia</i> spp.) represent correlation slopes	182
Figure 4-18: Box-Whisker plots (25 th to 75 th percentile; displayed with mean: white square for normally distributed data, median line for non-normally distributed data; extreme values: black diamond) for (a) carbon, (b) nitrogen, (c) sulphur contents (in wt%) and (d) $\delta^{13}\text{C}$, (e) $\delta^{15}\text{N}$ and (f) $\delta^{34}\text{S}$ values (in ‰) in urban (left) and rural (right) <i>X. parietina</i> samples	185
Figure 4-19: Scatter plots of NO ₂ concentrations (NO ₂ mean concentration in $\mu\text{g}/\text{m}^3$) and lichen (a) N wt%, and (b) $\delta^{15}\text{N}$ with correlation coefficients correlation (Pearson's r , R^2 and significance level; **significant at the level $p < 0.05$, ***significant at the level $p < 0.01$); error bars on dummy value derived from lichen CRM (No. 482; N contents and δ -values, displayed in figure) and IC-CRM (QC3198; nitrite concentrations); lines (dark grey: <i>X. parietina</i> , light grey: <i>Physcia</i> spp.)	188
Figure 4-20: Box-Whisker plots (25 th to 75 th percentile, displayed with mean: white square, median line and extreme values: black diamond) of urban influencing factors and (a) nitrogen contents (wt%) with surrounding building heights, (b) sulphur contents (wt%) with surrounding building heights, (c) $\delta^{15}\text{N}$ values (‰) with road class (M = motorway, A = A-road, B = B-road and U = unclassified) and (d) $\delta^{15}\text{N}$ values (‰) with distance to major road (including motorway, A- and B-roads) recorded in <i>X. parietina</i> (see Table 4-12)	190
Figure 4-21: Geographically Weighed Regression (GWR) used to model urban influencing factors (as described in Table 4-10) of (a) N wt% and (b) $\delta^{15}\text{N}$ (‰) recorded in <i>X. parietina</i>	192
Figure 4-22: $\delta^{13}\text{C}$ values of atmospheric pollutants and pollution sources, reported in carbon isotope studies (Widory, 2006; López-Veneroni, 2009) to identify potential sources, displayed with analysed $\delta^{13}\text{C}$ values for lichen samples (<i>X. parietina</i> and <i>Physcia</i> spp.) in Manchester.....	205
Figure 4-23: $\delta^{15}\text{N}$ values of atmospheric pollutants and pollution sources, reported in nitrogen isotope studies (Heaton, 1986; Elliott et al., 2007; Widory, 2007; Felix et al., 2012, 2013; Felix and Elliott, 2014; Liu et al., 2016) to identify potential sources; displayed with analysed $\delta^{15}\text{N}$ values for lichen samples (<i>X. parietina</i> and <i>Physcia</i> spp.) in Manchester	207

Figure 4-24: $\delta^{34}\text{S}$ values of atmospheric pollutants and pollution sources reported in sulphur isotope studies (Cortecci and Longinelli, 1970; Case and Krouse, 1980; Wadleigh and Blake, 1999; Wadleigh, 2003; Norman, 2004) to identify potential sources, displayed with $\delta^{34}\text{S}$ values of lichens (*X. parietina* and *Physcia* spp.) in Manchester.....209

Chapter 5

Figure 5-1: Urban lichen sampling sites (*X. parietina*: grey circles, N=87; *Physcia* spp.: black triangles, N=48 and re-visited sites: blue circle, N=17) across the city centre of Manchester, displayed with method development site (red hexagon and picture of sampled tree)220

Figure 5-2: Rural lichen sampling sites (*X. parietina*; N=12) around a poultry farm in Shrewsbury, UK (sampled in May 2018); displayed with location of poultry farm in relation to Greater Manchester (upper left corner, red square)221

Figure 5-3: Summary of lichen chemical extraction procedure (schematic) for nitrate and ammonium223

Figure 5-4: Extracted (a) nitrate and (b) ammonium from lichen material (triplicates; in mg/kg) using DI, 1%, 7.5 and 15% KCl, grouped by solvent and solvent volume used [in ml], presented as box-whisker plots (25th to 75th percentile, with mean value: white square and median line)229

Figure 5-5: Comparison plot of (a) nitrate concentrations by extraction solvent, (b) ammonium by extraction solvent and (c) ammonium by solvent volumes (presented as bar graphs, with 1x standard error of the mean concentration); displayed with statistical significance of differences (as presented in Table 5-5).....231

Figure 5-6: Extracted (a) nitrate and (b) ammonium from lichen material (triplicates, in mg/kg) using different solvents KCl, grouped by solvent and solvent volume), error-bars are presented as 1x standard deviation (CRM-derived: NO_3^- 6.42% and NH_4^+ 6.30%).....233

Figure 5-7: Comparison of nitrate with extraction volumes (presented as bar charts with 1x standard error of the mean concentration); displayed with statistical significance of differences (as presented in Table 5-6)234

Figure 5-8: Concentrations of nitrate and ammonium (in mg/kg) (\log_{10} scale; bar charts, presented with CRM derived 1x standard deviation of NO_3^- : $\pm 0.91\%$ and NH_4^+ : $\pm 1.07\%$); shown for 3% KCl, with 2 ml and 3 ml, 24 and 6 hours extraction time and vortexing (v) and non-vortexing (nv)236

Figure 5-9: Comparison of nitrate with extraction volumes (in mg/kg) (presented as bar charts with 1x standard error of the mean); displayed with statistical significance of differences (as presented in Table 5-7); *indicates that no nitrate was extracted (or blank subtraction resulted in negative value)237

Figure 5-10: (a) Nitrate and (b) ammonium concentrations analysed for each KCl extraction batch (N=62), displayed with number analysed per batch (error bars are presented as 1x standard deviation); dashed line represent certified values (nitrate: 10.5 mg/l and ammonium: 3.125 mg/l)239

Figure 5-11: Box-Whisker plots (25th to 75th percentile) of nitrate [left] and ammonium concentrations [lower panel] concentrations recorded for sampling periods undertaken in 2016/17 (1) and 2018 at the same site (2); displayed with median line (non-normal distributed data) and mean: whit square (normally distributed data).....241

Figure 5-12: Box-whisker plots (25th and 75th percentile, displayed with mean (red square) and median line and extreme values: black diamonds) for comparison of nitrate [above] and ammonium concentrations [below] (in mg/kg) recorded in *X. parietina* (left, N=84) and *Physcia* spp. (right, N=48).....243

Figure 5-13: Nitrate concentrations (in mg/kg) (interpolated by ordinary kriging) in (a) <i>X. parietina</i> and (b) <i>Physcia</i> spp. to analyse spatial patterns across Manchester (kriging error maps in Appendix C-4).....	245
Figure 5-14: Ammonium concentrations (in mg/kg) (interpolated by ordinary kriging) in (a) <i>X. parietina</i> and (b) <i>Physcia</i> spp. to analyse spatial patterns across Manchester (kriging error maps in Appendix C-5)	246
Figure 5-15: Scatterplot of nitrate concentrations (in mg/kg) for comparison with (a) nitrogen contents [wt%] and (b) $\delta^{15}\text{N}$ [‰] in <i>X. parietina</i> and <i>Physcia</i> spp. (CRM-derived error bars on dummy value: N wt% ± 0.04 ; $\delta^{15}\text{N}$ ± 0.23 ; NO_3^- ± 0.45 and NH_4^+ ± 0.25); displayed with correlation statistics (Spearman ρ ; *significant at the level $p < 0.05$; **significant at the level $p < 0.01$) ..	247
Figure 5-16: Scatterplot of ammonium concentrations (in mg/kg) for comparison with nitrogen contents [wt%] and $\delta^{15}\text{N}$ [‰] in <i>X. parietina</i> and <i>Physcia</i> spp. (CRM-derived error bars on dummy value: N wt% ± 0.04 ; $\delta^{15}\text{N}$ ± 0.23 ; NO_3^- ± 0.45 and NH_4^+ ± 0.25); displayed with correlation statistics (Spearman ρ ; *significant at the level $p < 0.05$; **significant at the level $p < 0.01$) ..	248
Figure 5-17: (a) Nitrate, (b) ammonium (both in mg/kg) and (c) NO_3^- and NH_4^+ presented as percentage (of total recorded nitrate and ammonium) for each rural sampling site; error bars in (a) and (b) are presented as 1x standard deviation (CRM-derived: NO_3^- : ± 0.42 and NH_4^+ : ± 0.25)	250
Figure 5-18: (a) Nitrate and (b) ammonium concentrations (mg/kg) in <i>X. parietina</i> around a poultry farm (colour-coded by concentration ranges), displayed with poultry farm, site-ID and sampling area around the farm.....	251
Figure 5-19: Concentrations of nitrate (above) and ammonium (below) in <i>X. parietina</i> , displayed with distance to poultry farm (<500 m and >500m), in ascending order; distances below 150 m are also shown (error bars are presented as 1x standard deviation of IC-CRMs, NO_3^- : ± 0.42 and NH_4^+ : ± 0.25).....	252
Figure 5-20: Scatter-plots of nitrate and ammonium concentrations recorded in rural <i>X. parietina</i> (N=12) samples, with nitrogen contents [wt%] (a) and (b) and $\delta^{15}\text{N}$ [‰] (c) and (d); error bars presented as 1x standard deviation, CRM-derived: N wt% ± 0.04 ; $\delta^{15}\text{N}$ ± 0.23 ; NO_3^- ± 0.42 and NH_4^+ ± 0.25 ; displayed with correlation statistics (Pearson's r , R^2 value and significance level; *significant at the level $p < 0.05$, **significant at the level $p < 0.01$).....	253
Figure 5-21: Box-whisker plots (25th to 75th percentile, displayed with mean: white square, median line and extreme values: black diamonds) for nitrate [above] and ammonium [below] in urban (N=87) and rural (N=12) <i>X. parietina</i> samples.....	255
Figure 5-22: Box-Whisker plots (25th to 75th percentile; displayed with mean: white square, median line and extreme values: black diamond) for significant relationships of NO_3^- [upper panel] and NH_4^+ [lower panel] with building heights in <i>Physcia</i> spp.	257
Figure 5-23: Box-Whisker plots (25th to 75th percentile; displayed with mean: white square, median line and extreme values: black diamond) for significant relationships of (a) NO_3^- with distance to major road, (b) NO_3^- with surrounding building heights, (c) NO_3^- with distance to large point sources and (d) NH_4^+ with traffic counts in <i>X. parietina</i>	258
Figure 5-24: Modelled (Ordinary Least Square - OLS) NO_3^- and NH_4^+ concentrations in <i>X. parietina</i> based on urban influencing factors (i.e. traffic counts, surrounding building heights, distance to major road, green space and large point source) to evaluate spatial dispersion and distribution.....	260

Chapter 6

Figure 6-1: Sampling sites (and re-visited sites) for <i>X. parietina</i> (N=84) and <i>Physcia</i> spp. (N=17) lichens analysed for metal concentrations, with automated air quality monitoring stations also shown (overview map with site ID labels is included in Appendix D-1)	280
--	-----

Figure 6-2: ICP-MS signal drift correction procedure, showing calculation steps and application to each analysed unknown solution (lichen sample or lichen CRM).....	285
Figure 6-3: Lichen CRM (482) metal concentrations measured per sample batch (N=4, left to right) for Cd (by ICP-MS; upper left), Cr (by ICP-MS), Mn (by ICP-OES) and lower left for Ni (by ICP-OES), Pb (by ICP-OES) and Zn (by ICP-OES). Results presented as mean values with error bars as 1xSD of CRM values measured within a batch; displayed with certified CRM values (red dashed line; Quevauviller et al., 1996), and concentrations reported by Baffi et al. (2002) (blue dashed line). Palladium (Pd) and Platinum (Pt) not shown, due to unavailability of certified values	289
Figure 6-4: Box-Whisker plots (25 th to 75 th percentile, displayed with mean: red square, for normally distributed metal concentrations; median line for non-normally distributed metal concentrations; extreme values: black diamond) of target metal concentrations in <i>X. parietina</i> for both sampling periods 2016/17 and 2018, for (a) Cd, (b) Cr, (c) Mn, (d) Ni, (e) Pb and (f) Pd	295
Figure 6-5: Box-Whisker plots (25 th to 75 th percentile, displayed with mean: red square for normally distributed metal concentrations; median line for non-normally distributed metal concentrations; extreme values: black diamond) of target metal concentrations in <i>X. parietina</i> for both sampling periods 2016/17 and 2018, for Pt (upper panel) and Zn (lower panel) ...	296
Figure 6-6: Box-Whisker plots (25 th to 75 th percentile, displayed with mean: red square for normally distributed metal concentrations; median line for non-normally distributed metal concentrations; extreme values: black diamond) of metal concentrations (y-axes presented as log ₁₀ -scale) in rural samples of <i>X. parietina</i> (N=12), for all analysed metals (a) and for the key target metals that are the focus of this study (b)	298
Figure 6-7: Box-whisker plots (25 th and 75 th percentile) of rural <i>X. parietina</i> metal concentrations against distance to poultry farm (<500m and >500 m), displayed with mean values (red square; for normally distributed group data) and median line (dashed line; for non-normally distributed group data)	300
Figure 6-8: Box-Whisker plots (25 th to 75 th percentile, displayed with mean: red square, median line and extreme values: black diamond) of metal concentrations (y-axes presented as log ₁₀ -scale) recorded in urban samples of <i>X. parietina</i> (N=84), (a) for all analysed metals and (b) for target metals in this study	303
Figure 6-9: Box-Whisker plots (25 th to 75 th percentile, displayed with mean: red square, median line and extreme values: black diamond) of metal concentrations (y-axes presented as log ₁₀ -scale) recorded in urban samples of <i>Physcia</i> spp. (N=17), (a) for all analysed metals and (b) for target metals in this study	304
Figure 6-10: Comparison of (a) Cd, (b) Cr, (c) Mn, (d) Ni, (e) Pb, (f) Pd, (g) Pt and (h) Zn concentrations in <i>X. parietina</i> and <i>Physcia</i> spp. (X and Y error bars displayed on 'dummy value [white diamond]': lichen CRM derived, displayed as 1x SD; together with Spearman ρ for concentrations in lichen species)	308
Figure 6-11: Cadmium (Cd) concentrations in (a) <i>X. parietina</i> (N = 84) and (b) <i>Physcia</i> spp. (N=17), displayed as colour-coded symbols and automated air quality monitoring stations are also shown.	310
Figure 6-12: Chromium (Cr) concentrations in (a) <i>X. parietina</i> (N = 84) and (b) <i>Physcia</i> spp. (N=17), displayed as colour-coded symbols and automated air quality monitoring stations are also shown. A potential temporal influence, overlaid onto spatial variability needs to be considered for Cr concentrations in lichens	311
Figure 6-13: Manganese (Mn) concentrations in (a) <i>X. parietina</i> (N = 84) and (b) <i>Physcia</i> spp. (N=17), displayed as colour-coded symbols and automated air quality monitoring stations are also shown.	312

Figure 6-14: Nickel (Ni) concentrations in (a) <i>X. parietina</i> (N = 84) and (b) <i>Physcia</i> spp. (N=17), displayed as colour-coded symbols and automated air quality monitoring stations are also shown.....	313
Figure 6-15: Lead (Pb) concentrations in (a) <i>X. parietina</i> (N = 84) and (b) <i>Physcia</i> spp. (N=17), displayed as colour-coded symbols and automated air quality monitoring stations are also shown. A temporal influence, overlaid onto spatial variability for needs to be considered for Pb concentrations in lichens	315
Figure 6-16: Platinum (Pt) concentrations in (a) <i>X. parietina</i> (N = 84) and (b) <i>Physcia</i> spp. (N=17), displayed as colour-coded symbols and automated air quality monitoring stations are also shown	316
Figure 6-17: Zinc (Zn) concentrations in (a) <i>X. parietina</i> (N = 84) and (b) <i>Physcia</i> spp. (N=17), displayed as colour-coded symbols and automated air quality monitoring stations are also shown	317
Figure 6-18: Box-whisker plots (25 th to 75 th percentile; with mean: red square for normally distributed metal concentrations; median line for non-normally distributed metal concentrations; extreme values: black diamonds) for (a) Cd, (b) Cr, (c) Mn, (d) Ni, (e) Pb, (f) Pt and (g) Zn in urban and rural samples of <i>X. parietina</i>	320
Figure 6-19: Dendrogram of elements in urban samples of <i>X. parietina</i> (using complete linkage and squared Euclidian Distance); shorter distances between elements show higher similarity, further distances illustrate dissimilarities.	326
Figure 6-20: Maximum recorded concentrations of (a) Cd, (b) Cr, (c) Mn and (d) Ni recorded in this study, in comparison to urban lichen biomonitoring studies as presented in Table 6-16.....	332
Figure 6-21: Maximum recorded concentrations of Lead (Pb) [above] and Zinc (Zn) [below] recorded in this study, in comparison to urban lichen biomonitoring studies as presented in Table 6-16	333
Figure 6-22: Box-whisker plots (25 th to 75 th percentile) of Cr, Mn and Zn concentration in <i>X. parietina</i> with distance to major road (major roads include A- and B- roads and motorways); displayed with mean values (white rectangle), median lines (red dashed line) and outliers (black diamonds).....	340
Figure 6-23: Box-whisker Plot (25 th to 75 th percentile, with mean value: white square, median line and extreme values: black diamond) of (significant) target metal concentrations in <i>X. parietina</i> (a) Zn and (b) Pb and <i>Physcia</i> spp. (c) Ni and (d) Pb and with traffic counts (AADF - annual average daily traffic flow, 2017).....	342
Figure 6-24: Box-whisker plots (25 th to 75 th percentile; displayed with mean value: white square, median and extreme values: black diamonds) of building density/surrounding building heights and (significant) target metal concentrations for (1) Mn, (2) Pb, (3) Cr, (4) Ni and (5) Zn	345
Figure 6-25: Predicted concentrations of (a) Cd and (b) Cr [$\mu\text{g/g}$] across the research area, with R ² -value to display goodness of fit by GWR; air quality monitoring stations and sampling sites are also shown.....	348
Figure 6-26: Predicted concentrations of (a) Mn and (b) Ni [$\mu\text{g/g}$] across the research area, with R ² -value to display goodness of fit by GWR; air quality monitoring stations and sampling sites are also shown.....	349
Figure 6-27: Predicted concentrations of (a) Pb and (b) Pt [$\mu\text{g/g}$] across the research area, with R ² -value to display goodness of fit by GWR; air quality monitoring stations and sampling sites are also shown.....	350
Figure 6-28: Predicted concentrations of (a) Zn [$\mu\text{g/g}$] across the research area, with R ² -value to display goodness of fit by GWR; air quality monitoring stations and sampling sites are also shown	351

Chapter 7

- Figure 7-1:** Total (Σ) PAHs measured at ‘Manchester Law Courts’ between 1991 and 1995 by high-volume air samplers (Coleman et al., 1997; Howsam and Jones, 1998).....358
- Figure 7-2:** Quarterly PAH concentrations (particulate-phase and vapour-phase) measured at Manchester Law Court between 2010 and 2014; PAHs classified by number of rings; naphthalene and dibenzo[a,h]anthracene were not measured, benzo[b]fluoranthene is included with benzo[j]fluoranthene (DEFRA, 2014b).....358
- Figure 7-3:** Lichen sampling sites (*X. parietina*, N=20; *Physcia* spp., N=3) for PAH extraction across the City of Manchester. Sampling sites are colour-coded by site rationale, as displayed in Table 7-2 (MR= major road, GS= greenspace and RES= residential). The two automated air quality monitoring stations and the PAH Andersen Sampler at ‘Manchester Law Court’ (PAH measurements undertaken until 2014) also are shown.362
- Figure 7-4:** Schematic overview of solvent extraction process used for identification and quantification of lichen PAHs using ultrasonic-assisted extraction, sample concentration, SPE clean-up procedure and analysis by GC-MS and GC-APCI-TQ/TOF-MS/MS369
- Figure 7-5:** Total PAH concentrations (Σ by rings) recorded in: (a) *X. parietina* (N=20) and (b) *Physcia* spp. (N=3), with error bars and values within the bars (presented as 1x standard deviation of summarised ring-PAH concentrations, separately for *X. parietina* (a) and *Physcia* spp. (b)) 376
- Figure 7-6:** PAH concentrations (summarised by carcinogenic group 1: red, 2A: orange and 2B: yellow; traffic-related: green Σ PAHs: white) recorded at sampling sites for *X. parietina* (top panel) and PAHs (%) by ring-structure at sampling sites (bottom panel).....378
- Figure 7-7:** PAH concentrations (summarised by carcinogenic group 1: red, 2A: orange and 2B: yellow; traffic-related: green and other Σ PAHs: white) recorded at sampling sites for *Physcia* spp. (top panel) and PAHs (%) by ring-structure at sampling sites (bottom panel).379
- Figure 7-8:** Box-Whisker plots (25th to 75th percentile) for PAH concentrations [in ng/g] recorded in *X. parietina* and *Physcia* spp. for (1) and (2) carcinogenicity group 1 and 2A: benzo[a]pyrene (BaP) and benz[a]anthracene (BaA); (2) carcinogenicity group 2B: dibenzo[a,h]anthracene (DaA), (3) benzo[b]fluoranthene (BbF), benzo[k]fluoranthene (BkF) and indeno[1,2,3-cd]pyrene (IcdP); (4) chrysene (CHRY) and (5) pyrene (PYR), fluoranthene (FLT) and phenanthrene (PHE).....381
- Figure 7-9:** Summarized PAHs (Σ by rings) in *X. parietina* at analysed sites in Manchester, with major roads (A-, B-roads and motorway) and automated monitoring stations (blue) and PAH Andersen sampler (used for PAH measurements until 2014, red), illustrating lichen PAH profiles across Manchester.383
- Figure 7-10:** Concentrations of ‘group 1 and group 2A’ toxicity PAHs (a) benz[a]pyrene, (b) dibenzo[a,h]anthracene and (c) benz[a]anthracene [in ng/g] recorded in *X. parietina* across the city centre of Manchester; displayed with automated monitoring stations (blue diamonds) and PAH monitoring station (in use until 2014; red diamond)384
- Figure 7-11:** Concentrations of ‘group 2B’ toxicity PAHs (a) chrysene, (b) benzo[b]fluoranthene, (c) benzo[k]fluoranthene and (d) indeno[1,2,3-cd]pyrene [in ng/g] recorded in *X. parietina* across the city centre of Manchester; displayed with automated monitoring stations (blue diamonds) and PAH monitoring station (in use until 2014; red diamond)386
- Figure 7-12:** Concentrations of ‘traffic-related PAHs’ (a) phenanthrene, (b) fluoranthene and (c) pyrene [in ng/g] recorded in *X. parietina* across the city centre of Manchester; displayed with automated monitoring stations (blue diamonds) and PAH monitoring station (in use until 2014; red diamond).....387
- Figure 7-13:** Box-Whisker plots (25th to 75th percentile) of (a) phenanthrene (PHE) and (b) pyrene (PYR) with distance to major road and traffic counts, (c) benzo[k]fluoranthene (BkF) and (d) indeno[1,2,3-cd]pyrene [IcdP] with distance to road and traffic counts; displayed median line (red dashed line) and Spearman ρ value and Mann-Whitney test, with significance level...389

Figure 7-14: Box-Whisker plots (25th to 75th percentile) of Σ 5-ring PAHs with traffic counts [upper panel] and phenanthrene concentrations with distance to green space [lower panel]; displayed with median line (red dashed line) and correlation statistics (Spearman ρ) and significance level	390
Figure 7-15: Box-Whisker plots (25th to 75th percentile) of Σ 2-ring PAHs with (a) distance to road and (b) distance to greenspace and Σ 3-ring PAHs with distance to road (c) and distance to greenspace (d); displayed with median line (red dashed line) and correlation and group statistics (with significance level; *significant at level $p < 0.05$; **significant at the level $p < 0.01$)	391
Figure 7-16: Maximum PAH concentrations recorded in <i>X. parietina</i> and <i>Physcia</i> spp. for 'target PAHs' (upper panel); displayed with 1x specific PAH-derived standard deviation in the lichen species (<i>X. p.</i> : 0.31 ng/g to 1.85 ng/g; <i>Ph. spp.</i> : 0.02 ng/g to 0.36 ng/g) and maximum PAH concentrations (same PAHs) from European (urban/traffic) biomonitoring studies (lower panel); PHE= phenanthrene, FLT= fluoranthene, PYR= pyrene, BbF= benzo[b]fluoranthene, BkF= benzo[k]fluoranthene, IcdP= indeno[1,2,3-cd]pyrene, BaA= benz[a]anthracene, DahA= dibenzo[a,h]anthracene, BaP= benzo[a]pyrene	397
Figure 7-17: Ratios of ANT/(ANT+PHE) at analysed sites (recorded in <i>X. parietina</i>); displayed with monitoring stations and PAH measurement station (in use until 2014), N/A – ANT has not been found in samples	408
Figure 7-18: Ratios of PHE/ANT at analysed sites (recorded in <i>X. parietina</i>); displayed with monitoring stations (blue diamond) and PAH measurement station (in use until 2014).....	409
Figure 7-19: Ratios of BaA/(BaA+CHRY) at analysed sites (recorded in <i>X. parietina</i>); displayed with monitoring stations and PAH measurement station (in use until 2014)	409
Figure 7-20: Ratios of FLT/PYR at analysed sites (recorded in <i>X. parietina</i>); displayed with monitoring stations (blue diamond) and PAH measurement station (in use until 2014).....	410
Figure 7-21: Ratios of FLT/(FLT+PYR) at analysed sites (recorded in <i>X. parietina</i>); displayed with monitoring stations (blue diamond) and PAH measurement station (in use until 2014).....	410
Figure 7-22: Scatter-plot of ANT/ANT+PHE and BaA/BaA+CHRY ratios recorded at sampling sites (<i>X. parietina</i>); displayed with cluster of primary sources, i.e. petrogenic, petrogenic/combustion (mixture) and fuel combustion; dotted lines represent ratio thresholds	412
Figure 7-23: Scatter-plot of PHE+ANT and FLT+PYR ratios recorded at sampling sites (<i>X. parietina</i>); displayed with cluster of primary sources, i.e. vehicular emissions; lines represent ratio thresholds.....	413
Figure 7-24: Scatter-plot of PHE+ANT and FLT/FLT+PYR ratios recorded at sampling sites (<i>X. parietina</i>); displayed with cluster of primary sources, i.e. vehicular emissions; lines represent ratio thresholds	414
Figure 7-25: Total PAHs (PAH_{total}) and combustion PAHs (PAH_{comb}) at each sampling site (error bars presented as 10 μ g/ μ l standard CV% of total PAHs and combustion PAHs [4,5 and 6-ring] with 5.86% PAH_{total} and 6.12% PAH_{comb}).....	415
Figure 7-26: PAH ratios and distances to major road of (a) ANT/ANT+PHE, (b) PHE/ANT (c) BaA/BaA+CHRY, (d) FLT/PYR and (e) FLT/PFLT+PYR and (f) PAH_{comb}/PAH_{total} ; displayed with thresholds and potential PAH origins.....	416
Figure 7-27: TEF of PAHs contribution to toxicity/carcinogenicity of the PAH mixture recorded in <i>X. parietina</i> , presented as pie-chart and exploded bar-chart; colour-coded by carcinogenicity of target PAHs, group 1: red, group 2A: orange, group 2B: yellow and traffic-related PAHs: green	420

List of tables

Chapter 2

Table 2-1: UK ambient air quality standard pollutants, pollutant definitions and potential sources with EU limit values and average periods (Sutton et al., 2000; Bourguignon, 2018; Defra, 2018a; European Commission, 2018; NAEI, 2018c)	14
Table 2-2: CNS isotopes (low – ‘light’ and high – ‘heavy’ mass) and natural abundance (Fry, 2006; Sharp, 2017)	24
Table 2-3: Metals present in the environment, their sources and potential human health impacts	27
Table 2-4: Additional considered PAHs and methylated PAHs in the UK PAH network (non-automated) that are not continuously measured within Manchester (UK)	30
Table 2-5: List of identified European Union (EU) and U.S. Environmental Protection Agency (EPA) PAHs (Lerda, 2011; National Center for Biotechnology Information, 2018; Royal Society of Chemistry, 2018)	31
Table 2-6: Definitions of lichen-related terms (Wirth, 1995; Shukla et al., 2014; Cole, 2015).....	33
Table 2-7: Advantages and disadvantages of monitoring approaches, applicable for air quality monitoring studies, with major differences outlined in detail (WHO, 1999; Tuduri et al., 2012; Pienaar et al., 2015)	46
Table 2-8: Idling traffic emissions by pollutant and vehicle type (extract) (EPA, 2008).....	64
Table 2-9: Datasets used to investigate the urban context of Manchester, including source for each dataset; data was used for geo-spatial modelling (further presented in section 2.8.3)	69

Chapter 3

Table 3-1: Reference and eutrophication species that have been used to analyse lichen diversity across Manchester (adapted from Bartholomeß (n.d.) and modified by species mentioned by Wolseley et al. (2009), shaded in yellow, to include common British lichen species (Smith et al., 2009; Sutcliffe, 2009).....	87
Table 3-2: Trees applicable for the lichen diversity index, based on bark properties and girth at 150 cm height (adopted by Kirschbaum and Wirth, 2010; tree translations from: Sterry, 2007)..	89
Table 3-3: (a) Five recorded trees as an example to illustrate the calculation of the AQI; lichens found divided into reference and eutrophication species; numbers display frequencies of the species found at a cardinal site (max. 5); summed up frequencies for reference and eutrophication species per tree and cardinal site; (b) summed up frequencies for each tree and cardinal direction (for reference and eutrophication species), mean for the sampling area and ‘Lichen Diversity Value (LDV)’ of the sampling unit, with colour coding following Figure 3-3.....	92
Table 3-4: Suggested ‘per tree’ lichen species ratios that potentially indicate influences of eutrophication compounds on lichen diversity; colour-coded by influence of eutrophication compounds (i.e. NO _x and NH _x)	94
Table 3-5: Calibration concentrations NO _x tube analysis made from ‘Dionex™ Seven Anion Standard II’	99
Table 3-6: Specifications for calculations of NO ₂ concentrations from NO _x diffusion tubes; diffusion coefficients for NO ₂ in air, together with tube dimensions and correction factor for EU comparability	100
Table 3-7: Urban environmental variables [grouped] with potential influences on lichen diversity and NO ₂ concentrations in the City of Manchester	102

Table 3-8: Certified Reference Material – certified values and for IC analysis of NO _x diffusion tubes for nitrite and nitrate (N=230; in mg/l) (Sigma-Aldrich, 2017)	111
Table 3-9: NO ₂ concentrations recorded at deployment sites (N=45), displayed as minimum - maximum range (mean ± 1x standard deviation, due to normal distribution of data) to illustrate spatial variability across Manchester (data for 24 biweekly deployments displayed in Appendix A-3).....	112
Table 3-10: NO _x tube deployment sites exceeding the WHO limit value (40 µg/m ³) during the year-long deployment across Manchester to evaluate potential ‘hot-spots’ of NO ₂ , colour-coded by % of exceedance (descending order)	113
Table 3-11: Lichen diversity studies in an ‘urban’ context in the UK/EU and variables that were considered to affect lichen frequency and abundance (by direct air measurements, partially modelled and modelled pollutant concentrations) (Jovan et al., 2012).....	120
Table 3-12: Interfering factors on NO _x diffusion tube measurements, resulting in positive (over-estimation) or negative bias (under-estimation) of NO ₂ concentrations (AEA Energy and Environment, 2008).....	123
Table 3-13: NO ₂ concentrations recorded in urban studies across the UK and Europe (displayed for urban area, reported mean NO ₂ [in µg/m ³ , as two significant figures] and number of deployment sites.....	130
Table 3-14: Monthly temperatures (°C) and total precipitation (Σ mm) for NO _x deployment period (data achieved from the “Whitworth Meteorological Observatory”)	134
Table 3-15: Correlation coefficients Pearson’s r (for NO ₂ concentrations, due to normal distribution of data) related to meteorological data (*significant at the level p<0.05, shaded in yellow; **significant at the level p<0.01, shaded in green)	134
Table 3-16: Pearson's r (for NO ₂) correlation coefficients of NO _x diffusion tube concentrations (N=45) to evaluate effects on spatial variability by urban influencing factors (MR = Distance to major road, RdCl = Road class, TC = Traffic counts, BH = building heights/building density, PS = Distance to (large) point sources and GS = Distance to Greenspace).....	140

Chapter 4

Table 4-1: Number of analysed calibration standards (EDTA 502-092), rice flour and lichen CRM for each analytical batch on the LECO CN analyser	153
Table 4-2: Statistical test (Shapiro-Wilk) outcomes for normal distribution of lichen CNS (wt%) and stable-isotope ratio signatures (δ ¹³ C, δ ¹⁵ N and δ ³⁴ S), to elucidate statistical tests for comparison of datasets; non-normal distributed data shaded in blue, normal distributed data shaded in green.....	156
Table 4-3: Categories applied to potential urban influencing factors used to assess possible controls on the spatial variability of urban <i>X. parietina</i> and <i>Physcia</i> spp. lichen CNS contents and stable-isotope ratios	158
Table 4-4: Identified outliers in analysed lichen CRM and Rice flour for CN analyser batches (N=31 in 6 batches) and analysed lichen CRM by IRMS (N=43 in 3 batches) that were removed before analysis of accuracy and precision; outliers found shaded in yellow (with number and batch the outlier was found), no outliers found shaded in green	160
Table 4-5: Analysed carbon, nitrogen and sulphur contents (wt%) of lichen CRM (No. 482) by CN analyser and IRMS and certified values, displayed with ± 1x standard deviation (Quevauviller et al., 1996) and LECO reference material ‘Rice Flour’ (502-278) for CN analysis (presented as ± 1x standard deviation ; N/A – not measured with CN analyser or IRMS; accuracy 100% ± 5% displayed in green, accuracy 100% ± 10% in yellow and accuracy 100% ± 15% in red	163
Table 4-6: Measured and accepted isotope ratios (mean ± standard deviation) for international isotope standards (USGS40, IAEA-S to S3, MSAG2, M2 and SAAG2) and lichen CRM (N=43) used during IRMS analysis (NA = not applicable, no values available); displayed with overall	

accuracy (%) and precision (%CV); accuracy at 100 ± 5% in green, very low and very high recorded accuracy in red.....	164
Table 4-7: Comparison of carbon and nitrogen contents (wt%) for the sampling periods, to assess potential temporal bias of lichen data; statistical test (paired t-test) to evaluate differences between sampling periods.....	166
Table 4-8: CNS contents (wt%) and stable-isotope-ratio signatures (‰) analysed in rural lichen samples (<i>X. parietina</i> ; N=12); presented as three significant figures; Pearson's r correlation statistics (r-value) to investigate poultry farm influences, *significant at the level p<0.05 presented in bold and green background.....	167
Table 4-9: Descriptive statistics of lichen (<i>X. parietina</i> and <i>Physcia</i> spp.) carbon, nitrogen and sulphur contents (wt%; shown as three significant figures); displayed with mean (N and S wt%) and median value (C wt%). Statistical comparison of CNS contents is also shown (unpaired t-test for N and S contents, Mann-Whitney for C contents, due to normal distribution of N and S and non-normal distribution of C contents), **significance at the level p<0.01 in bold and shaded in green.....	170
Table 4-10: Descriptive statistics of analysed lichen (<i>X. parietina</i> , N=94 and <i>Physcia</i> spp., N=86) stable-isotope ratios ($\delta^{13}\text{C}$, $\delta^{15}\text{N}$ and $\delta^{34}\text{S}$, in ‰) sampled in the urban environment of Manchester (displayed with mean concentrations [\pm 1x standard deviation] for normally distributed data and median concentrations for non-normal distributed data); statistical comparison between lichen species (using unpaired t-test for $\delta^{15}\text{N}$ and Mann-Whitney for $\delta^{13}\text{C}$ and $\delta^{34}\text{S}$) is also shown (significant at the level p<0.01 shown in bold and shaded in green).....	176
Table 4-11: CNS contents (wt%) and stable-isotope-ratio signatures ($\delta^{13}\text{C}$, $\delta^{15}\text{N}$ and $\delta^{34}\text{S}$) ranges of urban and rural lichen samples; displayed with statistical test (Mann-Whitney [MW] and unpaired t-test) to evaluate differences between urban and rural lichens (displayed as p-value; *significant at the level p<0.05: yellow and **significant at the level p<0.01: green).....	184
Table 4-12: Correlation matrix of CNS contents, stable-isotope ratio signatures for <i>X. parietina</i> (N=94; left) and <i>Physcia</i> spp. (N=86; right) together with NO _x tube measurements (N=45; NO ₂ mean - x). Highly significant (p<0.01) relationships are presented in green and bold, significant relationships (p<0.05) are presented in bold and yellow. Spearman ρ correlation coefficients are presented as underlined values, all other represent Pearson's r correlation coefficients.....	187
Table 4-13: Correlation statistics (Pearson's r and Spearman ρ) used to investigate relationships between urban influencing factors and lichen-derived CNS contents (wt%) and stable-isotope-ratio signatures ($\delta^{13}\text{C}$, $\delta^{15}\text{N}$ and $\delta^{34}\text{S}$); underlined values represent Spearman ρ , all other values are presented as Pearson's r, significant values are presented in bold (significance level is indicated by asterisk and coloured; *significant at the level p<0.05: yellow and **significant at the level p<0.01: green); MR = distance to major road, RdCl = road class, TC = traffic counts, BH = surrounding building height, PS = distance to large point source and GS = distance to greenspace.....	189
Table 4-14: Lichen studies which report carbon, nitrogen and/or sulphur contents (wt%) in urban (and anthropogenic influenced) environments, in comparison CNS contents recorded in <i>X. parietina</i> and <i>Physcia</i> spp. examined in Manchester (UK); N/A indicates not analysed C, N and/or S contents (wt%) in the particular study.....	199
Table 4-15: Lichen studies which report carbon, nitrogen and/or sulphur isotope-ratios in urban (and anthropogenic influenced) environments, in comparison to CNS stable-isotope ratio signatures recorded in <i>X. parietina</i> and <i>Physcia</i> spp. examined in Manchester (UK).....	204

Chapter 5

Table 5-1: Methodological development and tested variables for extraction of nitrate and ammonium concentrations from <i>X. parietina</i> (single site; Figure 5-1).....	223
---	-----

Table 5-2: Compounds contained in calibrations standards and ‘Simple Nutrients’ certified reference material (CRM), used for analysis of lichen samples for nitrate and ammonium concentrations (presented in bold) by ion chromatography (Thermo Fisher Scientific, 2018a, 2018b); calibration standards (six-point) and certified reference materials were made up fresh for each analytical run.....	225
Table 5-3: Urban influencing factors (grouped) used to assess spatial variability of nitrate (NO ₃ ⁻) and ammonium (NH ₄ ⁺) concentrations in lichen samples from Manchester	227
Table 5-4: Wilcoxon rank test p-values (*significant at the level p<0.05 presented in bold and shaded in yellow; ** significant at the level p<0.01 presented in bold and shaded in green) to investigate and compare extraction solvents (left) and extraction volumes (right) for nitrate and ammonium concentrations (15% KCl represents 2 M and 7.5% KCl represents 1 M KCl)	230
Table 5-5: Wilcoxon rank test p-values (*significant at the level p<0.05 presented in bold and shaded in green) to investigate and compare extraction solvents (left) and extraction volumes (right) for nitrate and ammonium concentrations	234
Table 5-6: Wilcoxon rank test p-values (*significant at the level p<0.05 presented in bold and shaded in green) to investigate and compare extraction volumes (2 ml and 3 ml) and extraction times (6 and 24 hours) for nitrate and ammonium concentrations; comparison of vortexing and non-vortexing is also shown; N/A indicates not enough valid cases to perform Wilcoxon test for statistical comparison	236
Table 5-7: Certified and measured values of nitrate and ammonium for all analytical batches (N=62), with overall accuracy (%), overall precision (%CV) and lower limits of detection (LLD) ranges	240
Table 5-8: Comparison of nitrate (NO ₃ ⁻) and ammonium (NH ₄ ⁺) concentrations [in mg/kg] in <i>X. parietina</i> (N=17) for different sampling periods undertaken in 2016/17 (1) and same sites revisited in 2018 (2) to investigate temporal bias.....	241
Table 5-9: Nitrate and ammonium concentration (in mg/kg) ranges of <i>X. parietina</i> and <i>Physcia</i> spp., displayed with median (<i>x</i>) values due to non-normality of data (values are shown as three significant figures)	242
Table 5-10: Mann-Whitney test statistics (p-value, two-tailed) for nitrate and ammonium, recorded in <i>X. parietina</i> and <i>Physcia</i> spp.; ** significant at the level p<0.01 in bold and shaded in green)	242
Table 5-11: Rural lichen (<i>X. parietina</i> , N =12) nitrogen contents (wt%), δ ¹⁵ N (‰) and nitrate (NO ₃ ⁻) and ammonium (NH ₄ ⁺) concentrations, displayed as three significant figures; N/A – not assessed by IC analysis	249
Table 5-12: Comparison of urban and rural samples of <i>X. parietina</i> concentration ranges (min. to max.) of nitrate (NO ₃ ⁻) and ammonium (NH ₄ ⁺) [in mg/kg] and statistical test (Mann-Whitney) to compare concentrations; ** significant at the level p<0.01 bold and shaded in green....	254
Table 5-13: Correlation coefficient (Spearman <i>ρ</i> ; non-parametric) of nitrate (NO ₃ ⁻) and ammonium (NH ₄ ⁺) concentrations with urban influencing factors (i.e. MR = distance to major road, BH = surrounding building heights, TC = traffic count and PS = distance to point source and GS = greenspace) to investigate spatial distribution in the City of Manchester; highly significant (at the level p<0.01) relation in bold (and green), significant (at the level p<0.05) relation underlined (and yellow)	256

Chapter 6

Table 6-1: Target metals of primary interest, due to their presence in urban environments (i.e. sourced from vehicular wear and exhaust emissions) and their potential health impacts...278	278
--	-----

Table 6-2: Microwave (CEM Mars Xpress 5) digestion programme (five step programme: temperature ramp up – digestion step I – temperature ramp up – digestion step II and cool down phase).....	281
Table 6-3: Elements determined by ICP-OES and ICP-MS, including the measured wavelengths and isotopes (latter indicated if analysed with helium collision cell by [He]) and lower limits of detection (LLD) ranges for all analytical batches; key target metals shaded in grey.....	283
Table 6-4: Calibration standards for ICP-OES and ICP-MS measurements, as well as signal drift monitors, made from ESSLAB-910B for ICP-OES analysis and multi-elemental standards for ICP-MS (Esslab, 2017; Agilent Technologies, 2019)	284
Table 6-5: Urban environmental variables with potential influences on lichen metal concentrations in the City of Manchester, with associated data groupings.....	286
Table 6-6: Key target metals analysed in lichen CRM by batch (number displayed in table) and statistical test outcomes (Grubb’s test) for outliers that were excluded before further testing for accuracy and precision; no significant outliers found by Grubb’s test shaded in green, significant outliers found in yellow, with number of outliers	288
Table 6-7: Sample batch accuracy (expressed in %) of lichen CRM (N=23) metal concentrations measured by ICP-OES and ICP-MS, compared to: (a) certified values and (b) values measured using a HNO ₃ /H ₂ O ₂ digestion, along with overall precision (%CV); N/A – not recorded by sources (Quevauviller et al., 1996; Baffi et al., 2002)	290
Table 6-8: Measured (this study – mean values ± standard deviation; for all CRM measurements; N=23) and certified (and indicative) lichen CRM-482 elemental concentrations [µg/g] for different acid digestion methods (Quevauviller et al., 1996; Baffi et al., 2002).....	291
Table 6-9: Wilcoxon test statistics to compare metal concentrations recorded in <i>X. parietina</i> (N=17) for the two sampling periods (in 2016/17 and in 2018) to assess potential temporal bias superimposed on spatial analysis, displayed with p-values and significance levels (*p<0.05, shaded in yellow and **p<0.01, shaded in green); key target metals presented in bold	293
Table 6-10: Descriptive statistics ($\bar{x} \pm 1x$ SD, for normal distributed data) for metal concentrations (in µg/g; determined by ICP-OES and ICP-MS) in <i>Xanthoria parietina</i> samples collected from a rural area; As, Pb and Zn concentrations were not normally distributed concentrations are expressed as medians (\bar{x})	297
Table 6-11: Mann-Whitney test statistics (between grouped poultry farm distances; due to different outcomes for normal distribution) for key target metal concentrations recorded in rural <i>X. parietina</i> samples, to assess whether there is a significant difference in metal concentrations with distance to poultry farm (<500m and >500m).....	299
Table 6-12: Concentration ranges (minimum and maximum) and median concentrations (\bar{x}) for analysed metal concentrations (by ICP-OES and ICP-MS) in <i>Xanthoria parietina</i> and <i>Physcia</i> spp. [in µg/g], sampled during an initial sampling period in 2016/17; S was normally distributed for both lichen species and As and Zn for <i>Physcia</i> spp. and are presented as mean (\bar{x}) ± 1x standard deviation; target metal concentrations shaded in light grey.....	302
Table 6-13: Wilcoxon test (due to different outcomes of Shapiro-Wilk normality test) for comparison of metal concentrations in <i>X. parietina</i> and <i>Physcia</i> spp. sampled from the same sites (N=15), displayed with significance levels *p<0.05, shaded in yellow and **p<0.01, shaded in green; key target metals presented in bold	305
Table 6-14: Mann-Whitney test output to assess whether there is a statistically significant difference between metal concentrations in urban (N=84) and rural (N=12) <i>X. parietina</i> samples; displayed as two-tailed p-value and significance levels (*p<0.05 and shaded in yellow; **p<0.01 and shaded in green); key target metals presented in bold (and shaded in grey)	319
Table 6-15: Spearman ρ correlation coefficients of ‘target’ metals recorded in urban <i>X. parietina</i> (N=84); displayed with significance levels (p-values; two-tailed; values presented in bold:	

significance level $p < 0.01$, shaded in green; underlined values: significance level $p < 0.05$; shaded in yellow)325

Table 6-16: Comparison of target metal concentrations (concentrations ranges) [in $\mu\text{g/g}$] recorded in this study and urban biomonitoring studies, using *X. parietina* and *Physcia* spp., displayed with lichen species and location the study was undertaken; additionally the study undertaken by Vingiani et al. (2015) using *Pseudevernia furfuracea* and *Parmelia sulcata* actively deployed in London (UK) was included; N/A represents that elements were not measured/reported in the particular study331

Table 6-17: Spearman ρ correlation coefficients and significance levels (* significant at the level: $p < 0.05$, shaded in yellow; ** significant at the level: $p < 0.01$, shaded in green) of lichen-derived metal concentrations and urban influencing factors to investigate potential controls on urban metal concentrations (MR = distance to major road, RdCl = Road class, TC = traffic counts, BH = mean surrounding building height; GS = distance to greenspace and PS = distance to large point source); key target metals in bold338

Table 6-18: Goodness of Fit (R^2 -value) for GWR modelled metal concentrations, to investigate spatial distribution of metal concentrations by including urban factors.....346

Chapter 7

Table 7-1: Classification of 16 EPA PAHs, based on their carcinogenic risk by the IARC (2010) that are adapted in legislations of the European Union (Lerda, 2011); 'Not classified' is used for PAHs which have not been assigned to a specific group by the IARC (2010), a classification different to 'Group 3' because the latter includes PAHs with inadequate evidence of carcinogenicity in humans (and inadequate or limited in experimental animals)356

Table 7-2: Sites re-sampled for lichens for PAH determinations across Manchester (Site ID; Figure 7-3) displayed with lichen N (wt%; Chapter 3) and target metals (Pb, Cd, Cr, Ni, Mn and Zn; Chapter VI) content, as well as rationale for sampling (MR = major road; GS = greenspace; RES = residential, with average annual daily traffic counts, where applicable; DfT, 2017); data values are displayed as three significant figures; * represents sites that have been sampled for both lichens, i.e. *X. parietina* and *Physcia* spp.361

Table 7-3: Summary of other studies that have solvent extracted PAHs from lichens using the ultrasonication technique, including geographical sampling area, extraction solvent (CYCLO = cyclohexane; DCM = dichloromethane) and volume, lichen mass and ultrasonication time 363

Table 7-4: SPE clean-up test for solvents/solvent mixtures spiked with 2 ng/ml PAH Mix [triplicates for each solvent/solvent mixture] and obtained recovery rates (mean $\% \pm 1$ standard deviation as %) by GC-MS analysis; #indicates that only one of three samples obtained PAHs365

Table 7-5: Solvent/solvent mixtures, lichen masses [g], solvent volumes and ultrasonication times used to test for optimal PAH extraction from lichen material.....366

Table 7-6: Three deuterated PAH standards (no. of rings, molecular weight and structure) used for spiking of lichen samples before extraction, clean-up and GC analysis; deuterated standards were used for quantification of similar PAHs (i.e. phenanthrene-d₁₀ for PAHs with 2- or 3-rings).....367

Table 7-7: GC-APCI-TQ-MS/MS analytical conditions (adapted and changed from EPA TO-13A; EPA, 1999)371

Table 7-8: PAH calibration standards (CS) prepared from 16 EPA PAH Mix for analysis by GC-APCI-TQ-MS/MS (in $\text{pg}/\mu\text{l}$ and $\text{ng}/\mu\text{l}$)372

Table 7-9: Average recovery rates (%), LODs and LOQs (in pg – picogram) and coefficient of variation (CV%) for 16 EPA PAH compounds determined in spiked lichen samples (N=4, TCL PAH mix) and standard solutions (NAP= naphthalene; ACY= acenaphthylene; ACN= acenaphthene; FLU= fluorene; PHE= phenanthrene; ANT= anthracene; FLT= fluoranthene; PYR= pyrene; BaA= benz[a]anthracene; CHRY= chrysene; BbF= benzo[b]fluoranthene; BkF=

benzo[k]fluoranthene; BaP= benzo[a]pyrene; IcdP= indeno[1,2,3-cd]pyrene; DahA= dibenzo[a,h]anthracene; BghiP= benzo[g,h,i]perylene)	373
Table 7-10: Urban influencing factors and associated categories used to assess potential controls on the spatial variability of PAH concentrations.....	374
Table 7-11: PAH concentrations (summarised by ring numbers) recorded in <i>X. parietina</i> and <i>Physcia</i> spp. to investigate species-specific uptake abilities of PAHs	375
Table 7-12: PAH concentration ranges [in ng/g] of most toxic PAHs (group 1, 2A, 2B) and 'traffic-related' PAHs recorded in <i>X. parietina</i> (N=20) and <i>Physcia</i> spp. (N=3) across Manchester; colour-coded by toxicity potential (red-orange and yellow) and traffic-related emissions ((green)).....	377
Table 7-13: Mann-Whitney test p-values presented for focus PAHs (target PAHs, including carcinogenicity groups 1, 2A and 2B) analysed in <i>X. parietina</i> and <i>Physcia</i> spp.....	380
Table 7-14: Spearman ρ correlation coefficient of PAH concentrations (target PAHs, Σ PAHs by ring structure) to investigate potential influences by the urban structure of Manchester (MR = distance to major road, TC = traffic counts, GS = distance to greenspace, PS = distance to point sources and BH = mean of surrounding building heights); *significant at the level $p < 0.05$ (underlined values; shaded in yellow), **significant at the level $p < 0.01$ (bold values ; shaded in green)	388
Table 7-15: Mann-Whitney test for grouped data, to investigate differences between PAHs concentrations with distance to road and traffic count groups (distance to major road < 100 m and > 100 ; traffic counts $< 20,000$ vehicles and $> 20,000$ vehicles); significance differences presented in bold ($*p < 0.05$, shaded in yellow; $**p < 0.01$ shaded in green).....	389
Table 7-16: Overview of PAH concentrations recorded in lichens in urban and traffic-related pollution studies to investigate differences between cities [shortened: excluding studies on landfill and mining sites; Augusto et al., 2016]	394
Table 7-17: PAH profile of <i>X. parietina</i> and <i>Physcia</i> spp. sampled across Manchester, for comparison with other urban studies.....	395
Table 7-18: PAH ratios applied in lichen biomonitoring studies to address major pollution sources (ANT= anthracene; PHE= phenanthrene; FLT= fluoranthene; PYR= pyrene; BaA= benzo[a]anthracene and CHRY= chrysene).....	405
Table 7-19: Site-IDs displayed with analysed diagnostic PAH ratios to evaluate PAH sources/origin; N/A – not calculated due to no data for anthracene (ANT) at both sites.....	406
Table 7-20: Toxic Equivalent Factors for 16 EPA PAHs (Nisbet and LaGoy, 1992) and Σ BaP _{eq} for each PAH.....	419

Abbreviations

Atmospheric pollutants, compounds and elements

C:	carbon
CO:	carbon monoxide
CO₂:	carbon dioxide
N:	nitrogen
NO:	nitric oxide/nitrogen oxide
NO₂:	nitrogen dioxide
NO_x:	nitrogen dioxide (combining NO and NO ₂)
NO₃⁻/NH₃/NH₄⁺:	nitrate/ammonia/ammonium
PAHs:	polycyclic aromatic hydrocarbons
PM:	particulate matter
S:	sulphur
SO₂:	sulphur dioxide

Masses and units

M:	molar
MΩ:	megaohm
mM:	millimolar
mm:	millimetre
mg:	milligram
mg/kg:	milligram per kilogram
mg/L:	milligram per litre
µg/m³:	microgram per cubic meter
kt:	kilo tonnes
%:	per cent
‰:	per mille

Analytical Instrumentation

CN analyser:	Carbon and nitrogen analyser
IC:	Ion Chromatography
ICP-AES:	Inductively Coupled Plasma – Atomic Emission Spectroscopy
ICP-OES:	Inductively Coupled Plasma – Optical Emission Spectroscopy
ICP-MS:	Inductively Coupled Plasma – Mass Spectrometry
IRMS:	Isotope Ratio Mass Spectrometry
GC-MS:	Gas Chromatography – Mass Spectrometry

Solvents and chemicals

ACE:	Acetone
CYCLO:	Cyclohexane
DCM:	Dichloromethane
HEX:	Hexane
METH:	Methanol
TEA:	Triethanolamine

Miscellaneous

GIS:	Geographic Information System
GWR:	Geographically Weighted Regression
OLS:	Ordinary Least Square
LGV:	Light Good Vehicles
HGV:	Heavy Good Vehicles

Chapter 1-

Introduction

This initial chapter introduces and outlines this study's scientific background, i.e. the significance of urban atmospheric pollution, the lichen biomonitoring approach and the necessity for undertaking the research project in the City of Manchester (UK). Aims, objectives and the thesis structure are also described to set the framework for this research project. Further, chapter contents and project justification are presented.

1.1 Scientific rationale

Urban air pollution and degraded air quality is a major concern worldwide (Fenger, 1999; Gulia et al., 2015). Urban populations are becoming increasingly exposed to a large number of airborne pollutants, which can contribute to lung and cardiovascular diseases and lead to approximately 7 million and 40,000 annual premature deaths globally and in the UK, respectively (Brunekreef and Holgate, 2002; Brauer, 2016; The Royal College of Physicians, 2016; WHO, 2018). Airborne pollutants include particulate matter (PM_{2.5} and PM₁₀), gases (including nitrogen oxides, together expressed as NO_x), metals (e.g. Cd, Ni and Pb) and organic compounds (i.e. polycyclic aromatic hydrocarbons – PAHs). For example, long term exposure to nitrogen dioxide (NO₂) was found to reduce life expectancy by an average of 5 months in the UK (DEFRA, 2017b). A reduction of 1 µg/m³ of NO₂ was estimated to save about 1.6 million life years in the UK over the next 106 years (COMEAP, 2018).

Within urban agglomerations ambient air pollution and poor air quality is a major, and arguably increasing, problem for the environment and human health, due to increased emissions of chemical contaminants from anthropogenic activities, i.e. increased road-traffic numbers, industrial manufacturing, energy production and heating (Fenger, 2009; EEA, 2015; The Royal College of Physicians, 2016). Poor air quality caused by air pollution also is associated with additional financial and societal costs, i.e. impact on hospital admissions, school attendance and business activities by affecting worker productivity (Bener et al., 2007; Zivin and Neidell, 2012; Dijkema et al., 2016; Regan, 2018).

Exposure to air pollutants is beyond the control of individuals and therefore needs to be controlled by public authorities, regionally, nationally and internationally (WHO, 2013b). UK monitoring programmes and improvement plans for air pollution are based on “The Air Quality Standards Regulations [2010]” (DEFRA, 2010). Continuous UK urban air quality measurements are undertaken by a small number of automated instrumented monitoring stations, e.g. on Oxford Road and at Piccadilly Gardens within the City of Manchester (UK), but these are small in number and thus record only air quality local to each monitoring station.

The Greater Manchester conurbation comprises 2.7 million inhabitants (GMCA, 2018), with 530,300 within the City of Manchester, the centre of the conurbation (Manchester City Council, 2016a). Consequently, the two instrumented air quality monitoring stations cannot characterize airborne pollutants and air quality in all of the places in which these ca. half a million individuals live and work. Because current instrumented air quality monitoring stations are restricted in number, it is becoming increasingly important to identify and apply environmental monitoring methods that can provide a finer detail of the spatial variability of air pollution and air quality within urban areas. Such an approach also avoids the need for installation of additional costly technical equipment, i.e. stationary air quality monitoring stations (Kienzl et al., 2003; Kot-Wasik et al., 2007; Blasco et al., 2008; Forbes et al., 2015).

To document and assess airborne pollutants and air quality, one low-cost approach is by the use of natural biomonitors, organisms that are already part of an urban ecosystem, a technique that is termed passive biomonitoring. Biomonitors (also called bioindicators) are sedentary organisms that are used to record airborne pollution within their ambient environment, because they reflect their habitats environmental conditions and can provide quantitative data through analysis of accumulated compounds (Zierdt, 1997; Kirschbaum and Wirth, 2010; Forbes et al., 2015).

Lichens are proven biomonitors for studying atmospheric pollution, because they are sedentary and absorb and/or adsorb airborne compounds and particulates within or on their biological tissues (Blasco et al., 2008). Due to lichen morphology, i.e. lacking roots and cuticle, lichens are reliant on atmospheric deposition for mineral nutrition and water supply. Consequently, lichens accumulate atmospheric pollutants via wet (i.e. chemicals dissolved in rainwater) and dry (i.e. gaseous and/or particulate) deposition pathways (Zierdt, 1997; Guidotti et al., 2003; Vingiani et al.,

2015). Historically, lichen biomonitoring studies focussed on elevated SO₂ concentrations related to lichen growth, vitality and ‘species’ (a lichen actually is a symbiotic relationship between a fungus and an algae and/or cyanobacteria) distribution in urban and industrial areas (Nimis and Purvis, 2002; Wadleigh, 2003; Dobson, 2011). Due to declining sulphur emissions, lichen communities are recolonising and increasing in urban environments and a wide range of ‘new’ airborne pollutants, i.e. metals, ammonia/ammonium, radionuclides and hydrocarbons are now monitored worldwide (Rose and Hawksworth, 1981; Nimis and Purvis, 2002; Purvis et al., 2003; Forbes et al., 2015).

The absence and occurrence of different lichen ‘species’ is dependent on air quality (Garty, 2001; Nash III, 2008; Van der Wat and Forbes, 2015). For example, it is well documented that high atmospheric SO₂ concentrations are associated with the disappearance of several lichens, e.g. *Usnea*, *Ramalina* and *Parmelia* spp. (Bartholomeß and John, 1997; Nash III, 2008). For Manchester, Grindon (1859) first attributed lichen species decline to air pollution (Grindon, 1859; Hawksworth, 1970). Some lichen species are able to cope with considerable amounts of airborne nitrogenic compounds (lichens that are termed as “nitrophytes”), i.e. *Xanthoria parietina*, *Phaeophyscia orbicularis*, *Physcia adscendens* and *Physcia tenella* (Van Herk, 1999; Davies et al., 2007; Gadsdon et al., 2010; Kirschbaum and Wirth, 2010; Dobson, 2011), while others are affected negatively by excessive amounts of nitrogen (e.g. *Lecanora conizaeoides*; Van Herk, 2003; Sutton et al., 2004).

Due to the potential for high concentrations of airborne pollutants within urban areas, it is necessary for any lichen biomonitoring study to utilise lichen species that can withstand urban atmospheric pollutant loadings. These organisms also need to be spatially distributed across the entire area where the air quality monitoring will be undertaken (Kirschbaum and Wirth, 2010; Forbes et al., 2015).

The *Xanthoria* and *Physcia* lichens that are the focus of this study are particularly suitable urban air quality recorders because they satisfy the aforementioned criteria and due to their perennial nature (i.e. collection during any season is possible), their longevity and their ability to take up higher concentrations of pollutants than other lichens (Augusto, Máguas, et al., 2013). Vehicle exhaust emissions are considered a main source of airborne pollution in urban areas, with nitrogen oxides (including NO and NO₂) primary pollutants (Air Quality Expert Group, 2007; Kobza and

Geremek, 2017). Within the UK and Manchester, 80% of NO_x emissions are related to vehicle emissions and particularly diesel vehicles (TfGM, 2016; Regan, 2018). Vehicular ammonia (NH₃) and subsequently ammonium (NH₄⁺) emissions, due to use of three-way catalysts in cars, are also influencing urban nitrogen pollution (Cape et al., 2004). Both lichens (*X. parietina* and *Physcia* spp.) are usually found in urban areas because of their nitrophilous nature, i.e. they are organisms preferring habitats rich in nitrogen (Wirth, 1995; Kirschbaum and Wirth, 2010; Dobson, 2011; Schaefer, 2012; Paoli et al., 2015).

1.2 Aims & Objectives

1.2.1 Aims

This PhD project aimed to document and assess the spatial variability of air quality in the City of Manchester (UK) by applying a lichen biomonitoring method, with a focus on carbon, nitrogen, sulphur contents, stable-isotope-ratio signatures, and metal and polycyclic aromatic hydrocarbon (PAH) concentrations. The biomonitoring approach was, in part, ground-truthed by passive air sampling methods (to monitor NO_x). Potential factors that influence the urban air pollution and air quality, as recorded in the lichen samples and passive monitoring devices, were investigated and modelled using numerical GIS-based geospatial analyses.

1.2.2 Objectives

a) Completion of a field survey, consisting of epiphytic (growing on trees) lichen identification and sampling from the twigs and branches of urban street trees, to compile a lichen pollutant chemistry database that is interpreted in relation to air pollution and air quality in the research area. Lichen-derived pollutant loadings were used to inform the passive air sampling deployments, i.e. across a range of sites with good and poor air quality, in order to “ground-truth” lichen NO_x measurements, to validate lichen loadings and further document spatial variability of these important and significant pollutants. Temporal variability of air quality, especially NO₂, was documented by monthly repeated passive sampling over a 12-month time period.

- b) Completion of laboratory analyses of field-collected lichen samples utilizing CN analyser (total C and N contents), IRMS (stable-isotope-ratio signatures, expressed as $\delta^{13}\text{C}$, $\delta^{15}\text{N}$ and $\delta^{34}\text{S}$ values), IC (ammonium and nitrate concentrations), ICP-OES and ICP-MS (S and metals concentrations) and GC-MS (PAHs) to quantify lichen pollutant loadings. Also, laboratory analyses of passive air sampling media using the aforementioned equipment for NO_2 concentrations (NO_x tubes; IC).
- c) Geostatistical modelling of lichen and passively derived chemical data to assess, interpret and simulate spatial pollution patterns across the urban area of the City of Manchester. GIS software (ESRI ArcGIS and QGIS), statistical tests and spatial statistics (i.e. correlation and regression) were used to distinguish between different influences (e.g. building heights, road classes and traffic volume) on the spatial variation of lichen-hosted pollutant signatures and associated air quality inferences.

1.3 Thesis outline, chapter content, project justification and predictions

Following this introductory chapter, Chapter 2 is a literature review that describes human health impacts of atmospheric pollution, lichen biomonitoring for specified pollutants and passive monitoring devices. The City of Manchester (UK) research area, as well as the methodological framework (for lichen sampling and geo-statistical analysis) are also outlined, which will be further described in the analytical chapters. Atmospheric pollutants of main interest are carbon, nitrogen and sulphur compounds, associated with their stable-isotope ratio signatures ($\delta^{13}\text{C}$, $\delta^{15}\text{N}$ and $\delta^{34}\text{S}$ values), as well as nitrogen compounds i.e. nitrate and ammonia/ammonium, airborne metal pollutants and polycyclic aromatic hydrocarbons (PAHs). Passive monitoring devices with a focus on 'NO_x diffusion tubes' (for atmospheric NO₂) are also explicitly described. Figure 1-1 illustrates the thesis structure and chapter contents, including connections between chapters and analytical data.

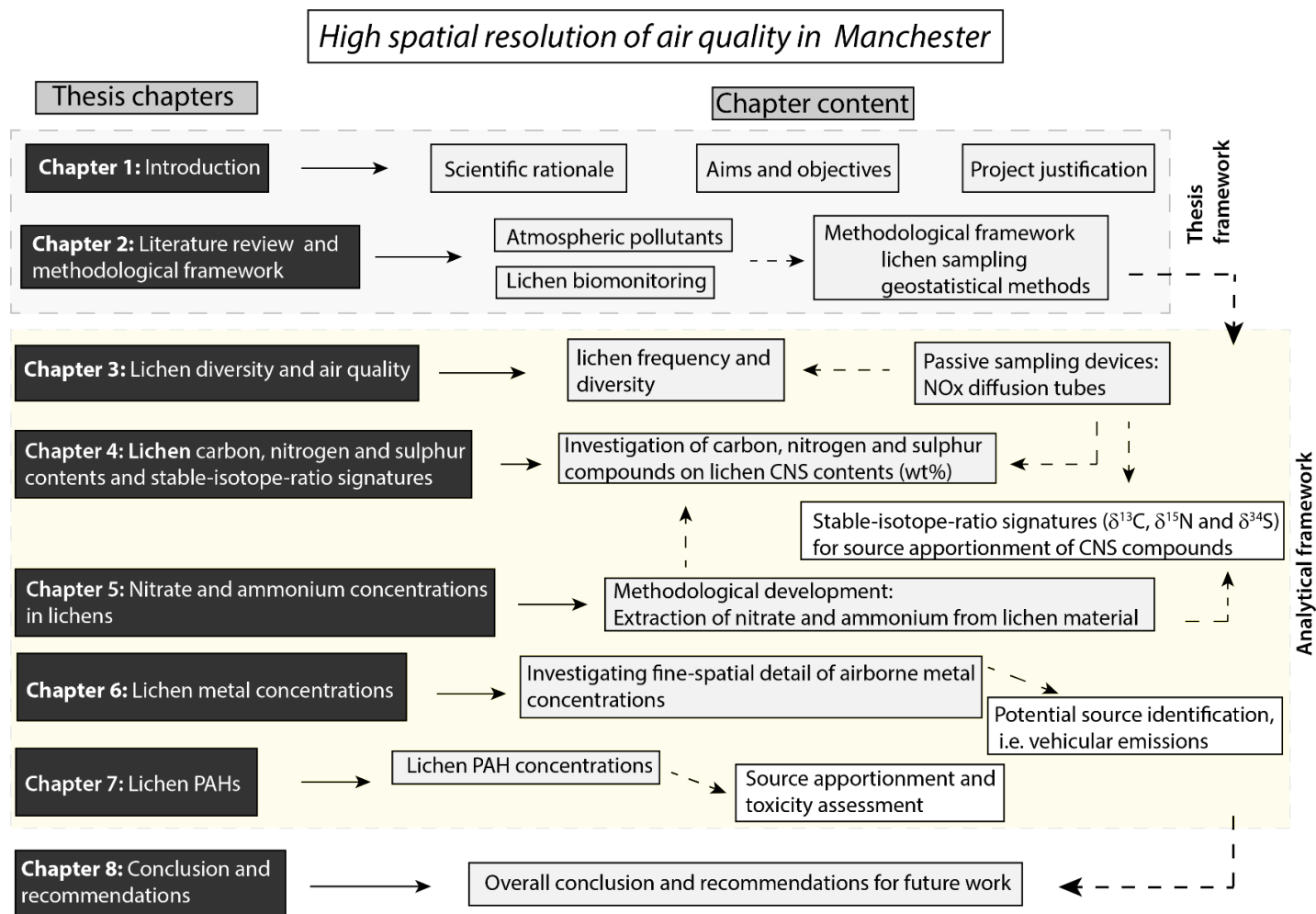


Figure 1-1: Schematic thesis outline and chapter contents to assess high-spatial resolution of air quality in Manchester, dashed arrows indicate linkages between chapters and analytical data (e.g. NO_x diffusion tube measurements in relation to lichen nitrogen contents (N wt%) and stable-nitrogen isotope-ratios ($\delta^{15}\text{N}$))

The following chapters include the measured lichen-derived pollutant loading data and their assessment and interpretation in relation to air quality in the City of Manchester. Chapter 3 focuses on lichen 'species' diversity and air quality, in combination with NO_x diffusion tube measurements. Chapters 4 and 5 present lichen carbon, nitrogen and sulphur contents and stable-isotope ratio signatures ($\delta^{13}\text{C}$, $\delta^{15}\text{N}$ and $\delta^{34}\text{S}$ values), and nitrate and ammonium concentrations, respectively. Lichen metal concentrations are the focus of Chapter 6, while Chapter 7 presents analysed polycyclic aromatic hydrocarbon (PAH) concentrations in lichens. Chapter 8 (Conclusion and recommendations) summarises the main findings of the applied biomonitoring approach in relation to the spatial variability of air quality in the City of Manchester, as detailed in the previous chapters. In addition, recommendations, based on the findings of this study, and further research possibilities, i.e. application of additional air quality monitoring approaches (e.g. tree bark, tree leaves and mosses) are outlined.

Project justification and predictions

Lichen biomonitoring studies are applied worldwide and allow assumptions on air quality (for specific pollutants) over large geographical areas. However, the majority of studies undertaken lack high spatial resolution to address spatial variability within urban environments and their influencing factors (i.e. building heights, major roads and traffic counts). Lichens, *X. parietina* and *Physcia* spp. that are potentially affected by several air pollutants (i.e. NO_x, PAHs and metals) were sampled in an area of approximately 20 km². Lichen-derived pollutant data were, in part, ground-truthed with passive sampling devices, i.e. NO_x diffusion tubes.

Combining lichen chemical data with passive air sampling measurements for NO_x will enable testing the veracity of the lichen datasets. A high spatial resolution lichen biomonitoring will contribute to a better insight into the variability of urban air quality and air pollution within the City of Manchester. The biomonitoring approach, including analytical methods used (i.e. methodological development to extract nitrate and ammonium), could then be applied to other comparable urban environments. Potential source apportionment, by using lichen isotope-ratio signatures, metal and PAH concentration ratios could identify pollutant sources and provide beneficial information for local authorities and organisations such as Manchester City of Trees, to identify areas requiring practical implementation of measures such as tree planting initiatives to improve air quality. City of Trees is a charity to re-invigorate Greater Manchester's landscape (restoring and planting trees), driven by the fact that trees are essential for a healthier, more resilient and prosperous city (City of Trees, 2018). Furthermore, the outcomes of this study will be related to health concerns, i.e. by nitrogen compounds, airborne metal and atmospheric PAH concentrations and contribute to urban planning and development to identify areas of particular health concern within the City of Manchester that need improvement to face the air quality/pollution problem.

Therefore, this study addressed spatial variability of air quality following the main question (and subsequent objective related sub-hypotheses):

Are lichens a useful bio-monitoring tool to monitor air quality at a high spatial resolution for the City of Manchester?

The **third chapter** focuses on lichen diversity, in combination with NO_x diffusion tube measurements. Diversity of lichens can be used to evaluate air quality and identify primary compounds (especially nitrogen and sulphur) and associated effects on lichen occurrence and species diversity. Moreover, NO_x diffusion tubes were deployed at 45 sites (sampled for lichens *X. parietina* and *Physcia* spp.) for a year long period, to ground-truth lichen derived pollutant loadings (further addressed in Chapter 4) and assess spatial and temporal variability of NO₂ across Manchester.

Hypotheses: Lichen frequency and diversity are influenced by recorded NO₂ concentrations across Manchester and provide details on impaired air quality. Moreover, NO₂ concentrations (by passive monitoring devices) could further improve high spatial resolution of NO₂ across the city of Manchester, which is not recorded by automated air quality monitoring stations. It is expected that lichen diversity is related to atmospheric pollutants, in particular NO₂.

The **fourth chapter** addresses carbon, nitrogen and sulphur contents in connection with stable-isotope ratio signatures measured in lichen samples. Lichen-derived N contents were further analysed with NO₂ measurements (by NO_x diffusion tubes) to ground-truth the veracity of the lichen data. Moreover, stable-isotope-ratios ($\delta^{15}\text{N}$, $\delta^{13}\text{C}$ and $\delta^{34}\text{S}$) were investigated for source apportionment of CNS compounds across Manchester. Urban lichen samples of *X. parietina* were compared to rural samples (of *X. parietina*) for CNS compounds and stable-isotope ratio signatures.

Hypotheses: Lichen CNS, associated with their stable-isotope ratio signatures, could provide insights into specific carbon, nitrogen and sulphur sources across the City of Manchester. In return, NO₂ concentrations (analysed by passive devices) could indicate influences on lichen CNS and stable-isotope ratios and indicate specific sources, i.e. vehicular NO_x emissions. Lichen CNS contents and stable-isotope ratios are expected to reflect air pollution and specific sources.

Nitrogen contents (bulk concentrations) in lichens provide information of potential sources in the urban environment, but does not distinguish between different nitrogen compounds that can be taken up by and affect lichens, in particular nitrate (NO_3^-) and ammonium (NH_4^+). The **fifth chapter** elucidates the method development of NO_3^- and NH_4^+ extraction of lichen material and evaluates spatial variability of nitrogen compounds across the urban environment of Manchester. Comparison to rural samples (*X. parietina*) were used to assess the relative importance of nitrate and ammonium to the atmospheric nitrogen loadings in contrasting areas. Nitrogen speciation and extraction of both nitrogen compounds (NO_3^- and NH_4^+) has not been reported for an urban study so far, illustrating the novelty of this study.

Hypotheses: Nitrate (NO_3^-) and ammonia (NH_4^+) are important compounds influencing bulk nitrogen contents of lichens and could be used to assess atmospheric nitrogen compound loadings in the City of Manchester. Nitrate and ammonium are expected to influence lichen nitrogen contents and potentially stable-isotope ratio signatures.

The **sixth chapter** focusses on airborne metal concentrations, analysed in lichen samples (*X. parietina* and *Physcia* spp.) from Manchester and a rural 'control' site (only *X. parietina*). Urban influences affecting lichen metal concentrations were further investigated to assess the degree of spatial (and temporal) variability of airborne metal pollution in Manchester. Airborne metal pollution is not recorded by automated monitoring stations, showing the need for additional methods to assess airborne metals.

Hypotheses: Determination of metal concentrations in lichens could provide fine-spatial detail of airborne metal pollution across Manchester. Metals of health concern (i.e. Pb and Cd) and their spatial variability could further provide detail of deteriorated air quality and areas of health concern. However, airborne metals are expected to be related to urban sources (i.e. vehicular emissions and industrial emissions) resulting in impaired air quality.

Chapter seven elucidates the extraction of polycyclic aromatic hydrocarbons (PAHs) from lichen material, using ultrasonic-assisted extraction and subsequent analysis for 16 EPA priority PAHs. Potential sources of PAHs were further investigated using PAH diagnostic ratios, together with assessment of the PAH compounds toxicity.

Hypotheses: PAHs analysed in lichens provides an insight into PAH pollution across the City of Manchester, which is not continuously monitored by automated monitoring stations. PAH concentrations are expected to be related to specific sources (i.e. vehicular and industrial sources) in the urban surrounding of Manchester. Subsequently, **chapter eight** will present a synthesis of the work undertaken and summarizes further research possibilities.

Chapter 2-

Literature review

This chapter aims to set the framework for this study, by initially describing air pollutants that are of particular interest within the UK and are ascribed to deleterious human health impacts. Atmospheric pollutants, which are the primary focus of this study, including carbon, nitrogen and sulphur compounds and their stable-isotope ratio signatures are described.

Nitrogen compounds, i.e. nitrate (NO_3^-) and ammonia/ ammonium ($\text{NH}_3/\text{NH}_4^+$) are separately described, due to their importance in atmospheric chemistry (i.e. formation of particulate matter). Airborne metals and atmospheric polycyclic aromatic hydrocarbons are also considered. Following, biomonitoring with lichens, including a detailed description of 'species' used for this study is outlined. Furthermore, current knowledge of lichen biomonitoring studies of focus pollutants is investigated. Passive sampling devices are examined, with focus on diffusion tubes for nitrogen dioxide (NO_2). The literature review will be concluded, followed by an outline of the case study area – the City of Manchester. Additionally, the methodological framework, comprising of the lichen sampling approach and spatial modelling of lichen-derived pollutant loadings, is described and will exemplify the foundation of data analysis in following chapters.

2.1 Air Quality, air pollution and health impacts in urban environments

Air pollution and deteriorated air quality in urban areas has been a long recognised problem and is considered an important environmental and social issue, with very complex challenges, i.e. management and mitigation of harmful pollutants (Fenger, 2009; Guerreiro et al., 2016). Pollutant emissions are a local, regional and international problem, which directly or indirectly (e.g. via chemical reactions in the atmosphere) negatively impact ecosystems and human health (DEFRA, 2017e).

Clean air is a basic human need and essential for good human health and every citizen has a right to it (Andrews, 2014). Different pollutants are emitted into the air and have different effects on human health, including, for example cancer, cardiovascular illnesses and strokes (DEFRA, 2018c). The European Union (EU) is responsible for setting air quality legislation through EU Directives (current: *Air Quality Directive 2008/50/EC*; DEFRA, 2014; Miranda et al., 2014) which establish, pollutant limit values as pertaining to human health risk. These airborne pollutants include $\text{PM}_{2.5}$ and PM_{10} , SO_2 , NO_2 , Benzene, lead and CO (Andrews, 2014).

Table 2-1 illustrates the pollutants included in the current EU Air Quality Directive 2008/50, which are implemented into UK legislations. Thirteen pollutants are included in UK ambient air quality standards (Table 2-1) and five damaging air pollutants have been identified (i.e. PM_{2.5}, NH₃, NO_x, SO₂ and non-methane volatile organic compounds - NMVOCs) and included in the UK emission reduction commitments (DEFRA, 2018c).

Table 2-1: UK ambient air quality standard pollutants, pollutant definitions and potential sources with EU limit values and average periods (Sutton et al., 2000; Bourguignon, 2018; Defra, 2018a; European Commission, 2018; NAEI, 2018c)

Pollutant	Definition and source	EU limit values
PM _{2.5} /PM ₁₀	Particulate Matter (PM) of aerodynamic diameter 2.5 and 10 µm, consisting of organic and inorganic compounds	25 µg/m ³ (PM _{2.5} – 1 year average)
		40 µg/m ³ (PM ₁₀ – 1 year average)
SO ₂	Sulphur dioxide, emitted by combustion of sulphur containing materials and fuels	125 µg/m ³ (24 hours average)
		350 µg/m ³ (1 hour average)
NO _x	Nitrogen oxides, i.e. nitrogen monoxide (NO) and nitrogen dioxide (NO ₂)	40 µg/m ³ (1 year average)
		200 µg/m ³ (1 hour average)
NH ₃	Ammonia, emitted from vehicle exhausts (among others)	No limit value for atmospheric concentrations
PAHs	Polycyclic aromatic hydrocarbons, major sources: coal, oil and oil shale (incomplete combustion)	1 ng/m ³ (expressed as concentration of Benzo[a]pyrene)
Lead (Pb)	Trace metal, was used as an additive to petrol	0.5 µg/m ³ (1 year average)
Cadmium (Cd)	Toxic metallic element, main sources: energy production, non-ferrous metal production, iron and steel manufacturing	5 ng/m ³ (1 year average)
Arsenic (As)	Toxic element, emitted in the form of particulate matter, largest source was coal combustion; recently wood preservatives treated with As	6 ng/m ³ (1 year average)
Nickel (Ni)	Toxic metallic element, released from oil and coal combustion, metal processes and manufacturing	20 ng/m ³ (1 year average)
CO	Carbon monoxide, emitted by motor vehicles	10 mg/m ³ (maximum daily 8 hour mean)
O ₃	Ozone, secondary pollutant (produced by sunlight + NO _x and VOCs) from vehicles and industry	120 µg/m ³ (maximum daily 8 hour mean)
C ₆ H ₆	Benzene, domestic and industrial combustion processes and road transport	5 µg/m ³ (1 year average)
C ₄ H ₆	1,3-butadiene, emitted from fuel combustion, i.e. petrol and diesel vehicles and industrial processes	2.25 µg/m ³ (1 year average)

Humans are exposed to air pollutants via inhalation, ingestion and to a minor extent through skin contact (Kampa and Castanas, 2008). Studies focussing on NO_x/NO₂ reported impacts on the respiratory system (i.e. lung inflammation and asthma), risk of low birth weights, dementia, DNA alteration, skin aging, skin surface changes and disturbance of epidermal barrier function (Eberlein-König et al., 1998; Lee et al., 2003; Kampa and Castanas, 2008; Peled, 2011; Laumbach and Kipen, 2012; WHO, 2013b; Pedersen et al., 2013; Winckelmans et al., 2015; Ribeiro et al., 2016; Walton et al., 2016; Hüls et al., 2016; Barth et al., 2017; Chen et al., 2017; Koohgoli et al., 2017; Bowatte et al., 2018).

About one third of EU inhabitants are affected by airborne pollutants, with around 400,000 premature deaths in 2010 in the EU and 40,000 deaths in the UK (Andrews, 2014; Brauer, 2016; The Royal College of Physicians, 2016; WHO, 2018). Within the UK, exposure to NO₂ is responsible for reduced life expectancy by an average of 5 months and approximately 23,500 deaths per year (DEFRA, 2017b; COMEAP, 2018). The 'UK Clean Air Acts' were initiated in 1956 and 1968, and led to a reduction in emissions from industrial and domestic fossil fuels and to the belief that air pollution problems were solved (DEFRA, 2007; The Royal College of Physicians, 2016). From the 1960s, however, other important pollutant emissions occurred related to increasing use of motor vehicles and types of traffic (e.g. growth in freight transport) using petrol and diesel fuels (The Royal College of Physicians, 2016).

Studies (both short- and long-term) were undertaken to link pollutants to several health effects, e.g. the World Health Organisation MONICA project related cardiovascular diseases to air pollution and a Swiss study associated high PM₁₀ concentrations with decreased lung function and elevated NO₂ and SO₂ with bronchitis (Brunekreef and Holgate, 2002). There is also evidence that air pollutants (i.e. NO₂) influences male and female reproductive capacities (Carré et al., 2017). Moreover, Maher et al. (2016) described iron-rich magnetite [Fe₃O₄], alongside Ni, Co and possibly Cu, particles in human brains, identifying a possible Alzheimer's disease risk factor. Magnetite is emitted from brake pads through high-temperature frictional heating, as well as from road vehicle's diesel fuels and combustion processes, e.g. power generation (Abdul-Razzaq and Gautam, 2001; Gómez et al., 2001; Jordanova et al., 2006; Kukutschová et al., 2011; Maher et al., 2016).

Heavy vehicles (i.e. lorries and buses) have always been powered by diesel, but today almost all light goods vehicles are powered by diesel too, illustrating an increase in diesel vehicles and hence emission of pollutants, such as NO_x and PAHs (EEA, 2015; Henschel et al., 2016; The Royal College of Physicians, 2016). Studies of PAHs emitted from diesel fuels indicated a carcinogenic effect on rats and hinted to an increased risk for exposed populations to lung cancer (International Programme on Chemical Safety (IPCS), 1996; Farmer, 1997; International Agency for Research on Cancer (IARC), 2014). Exposure to large amounts of diesel vehicle exhaust emissions increased the risk of lung, bladder and liver cancer for high risk groups, e.g. bus drivers and garage mechanics (Farmer, 1997).

In addition to physical effects of air pollution being reported, mental health can also be affected by poor air quality, such as causing depression and anxiety (Regan, 2018). Moreover, recent studies suggest the influence of air pollution on the circadian rhythm (human sleep-wake cycle or 'internal clock') and even might trigger suicide (by PM₁₀ or O₃; Casas et al., 2017; Haberzettl, 2018). For PAHs in particular, it was reported that prenatal exposure contributes to cognitive and behavioural (i.e. attention deficit/hyperactivity disorder) disturbances (Peterson et al., 2015). Exposure to air pollution during pregnancy is related to low birth-weights and pre-term births (Pedersen et al., 2013; Winckelmans et al., 2015; The Royal College of Physicians, 2016). Furthermore, nitrogen dioxide was linked with spontaneous pregnancy loss during short-term exposure of elevated NO₂ levels (Leiser et al., 2018). Figure 2-1 illustrates effects of air pollutants the human body.

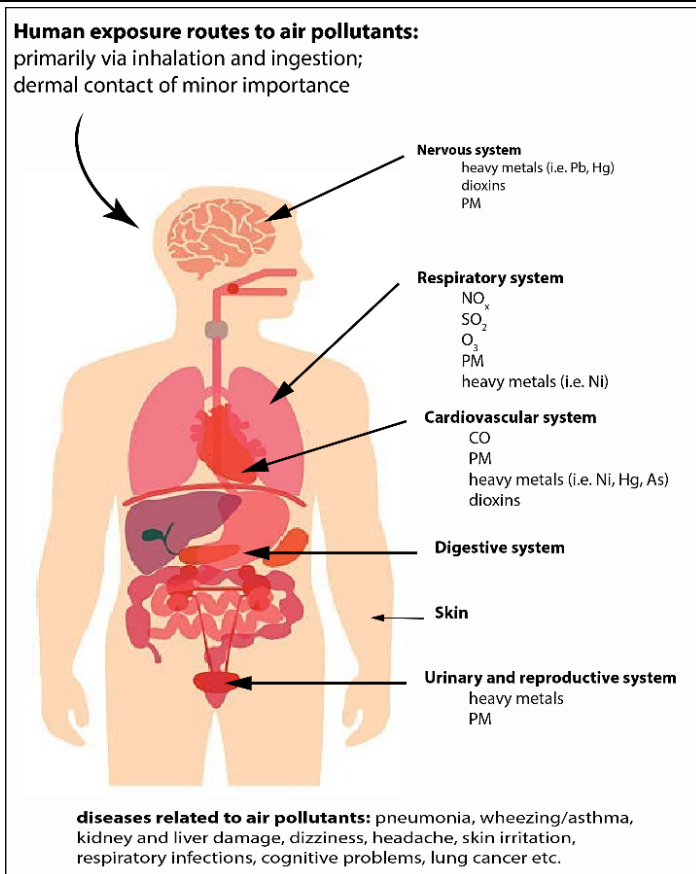


Figure 2-1: Effects of air pollutants (specified for some) on the human system, with pollution related diseases (pollutant impacts summarized from Kampa and Castanas, 2008; Regan, 2018)

2.2 Atmospheric pollutants

Air quality in the UK has significantly improved since the 1970s, i.e. UK NO_x emissions declined by 70% between 1970 and 2015, but continues to pose a significant threat to human health (WHO, 2006; DEFRA and DfT, 2017). This section focusses on pollutants of interest for this study, including carbon, nitrogen and sulphur compounds, nitrate, ammonia/ammonium, airborne metals and PAHs. Due to decreasing SO₂ emissions within urban areas through the use of low sulphur content fuels (i.e. natural gas and oil instead of coal), other atmospheric pollutants are now more important, including nitrogen oxides (NO_x: NO and NO₂), ammonia (NH₃) and PAHs (Fenger, 1999; Augusto, Máguas, et al., 2013; Munzi et al., 2014; Paoli et al., 2015). The geography and topography of the city, pollutant emission density and meteorological parameters all contribute to spatial and temporal variability in urban air pollution (Berkowicz, 2000; Hertel and Goodsite, 2009). Urban air pollution results from local, as well as distant, pollution sources and local anthropogenic activities, such as road traffic, heating and smaller industries that add to ground level pollution within urban areas (Hertel and Goodsite, 2009).

Increased road vehicle numbers and exhaust emissions, mainly nitrogen oxides, volatile organic compounds (e.g. PAHs) and photochemical oxidants, are the main present sources of airborne pollutants by human activities (Brunekreef and Holgate, 2002; Baird and Cann, 2008; Fenger, 2009; Gulia et al., 2015).

2.2.1 Atmospheric carbon, nitrogen and sulphur compounds

Atmospheric pollution with carbon and sulphur compounds, such as carbon monoxide (CO), carbon dioxide (CO₂) and sulphur dioxide (SO₂), is closely linked to fossil fuel combustion (EPA, 2008; WHO, 2018). Nitrogen oxides (NO_x) combining nitric oxide (NO) and nitrogen dioxide (NO₂), are released into urban environments from combustion processes, heating, energy production, road traffic and atmospheric long-range transport (Brunekreef and Holgate, 2002; Hertel and Goodsite, 2009; Boltersdorf et al., 2014; Munzi et al., 2014). CO and SO₂ concentrations in the UK declined considerably since 1990, with combustion of sulphur containing compounds (e.g. coal, heavy oils and petroleum coke) currently being major pollution sources (DEFRA, 2011; NAEI, 2018e, 2018g). CO is of concern due to its effects on human health, since it replaces oxygen in haemoglobin, causing damage to the nervous and cardiovascular system (Kampa and Castanas, 2008; Alvi et al., 2018; NAEI, 2018e). Road transport was the major source of CO emission in the UK, but declined since 1990, with the residential (combustion) sector being responsible for over a quarter of UKs CO emissions (NAEI, 2018e). In recent years (2000 to 2016) the UKs total CO emissions decreased from 4,144 kilo tonnes [kt] to about 1,580 kilo tonnes, with road traffic contributing to about half the total UK emissions in 2000 to about 1270 kilo tonnes in 2016. CO emissions from combustion processes (combined as industrial, commercial and residential) were consistent from 2000 to 2016 (Figure 2-2a).

Sulphur dioxide (SO₂) has long been a key pollutant of interest, due to its role in forming winter-smog, acid rain and effects on the human respiratory system, i.e. coughing, nose and throat irritation, bronchoconstriction and dyspnoea (Balmes et al., 1987; Kampa and Castanas, 2008; DEFRA, 2011; NAEI, 2018g; WHO, 2018). UK SO₂ emissions are dominated by combustion of sulphur containing compounds, such as coal, heavy oils and petroleum coke. Since 1990, SO₂ emissions have declined by 95% due to a reduced use of coal and oil and technological improvements, i.e. flue-gas desulphurisation (DEFRA, 2011; NAEI, 2018g). Since 2000, emissions of SO₂ from all UK sources have declined by 18% from around 1,400 kt to 260 kt in 2016 (Figure 2-2b). Combustion processes were responsible for more than half the UK's SO₂ emissions, while road transport only accounted for 0.22% to 0.50% of total sulphur dioxide emissions, and road transport SO₂ emissions between 2000-2016 declined from 6.56 kt to 1.30 kt (Figure 2-3).

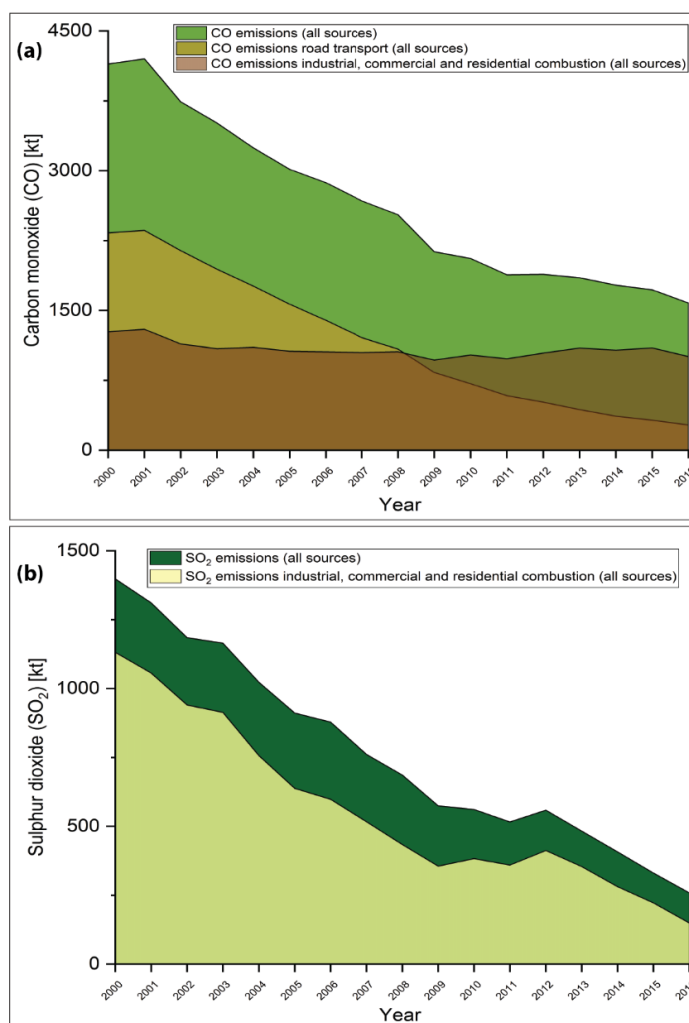


Figure 2-2: UK (a) carbon monoxide (CO) emission in kilo tonnes [kt] for all sources, industrial, commercial and residential combustion and road transport and (b) sulphur dioxide (SO₂) emissions in kilo tonnes [kt] for all sources and industrial, commercial and residential combustion (NAEI, 2018a); sources not stacked

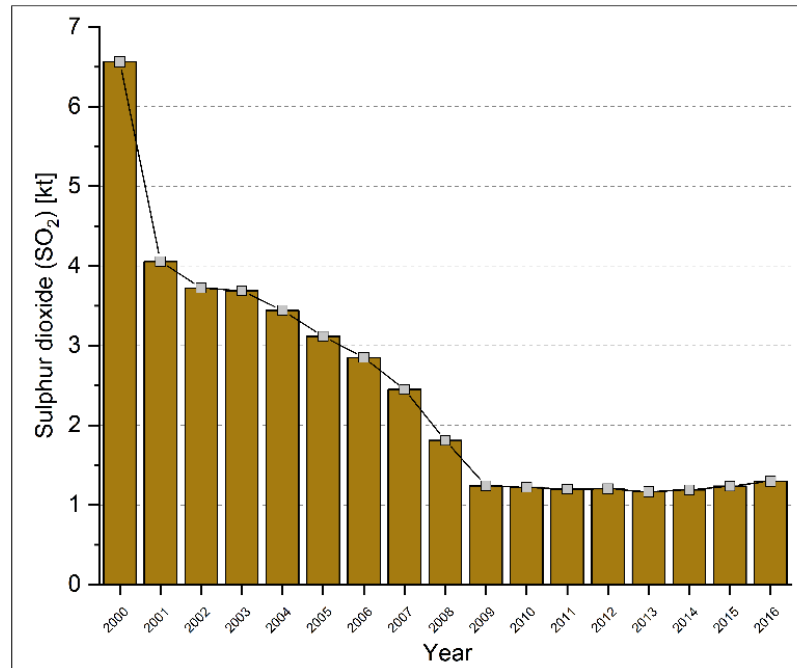


Figure 2-3: Road traffic SO₂ emissions in kilo tonnes [kt] for the years 2000 to 2016 (NAEI, 2018a)

Current air quality research includes a focus on NO_x and NH₃, with NO₂ as main anthropogenic pollutant, through combustion of fuels, for heating, energy generation and road traffic (Brunekreef and Holgate, 2002; Munzi et al., 2014), long-range atmospheric transport is also possible (Hertel and Goodsite, 2009; Boltersdorf et al., 2014). As an airborne pollutant, NO₂ can have a variety of impacts on human health over short or long time periods, such as asthma, respiratory disorder, reduced lung function, bronchitis and cancer. There is also evidence that high NO₂ levels also can impair neurodevelopment (sensory, motor and psychomotor function) in children (WHO, 2006, 2013a; Salem et al., 2009; Moldanová et al., 2011; The Royal College of Physicians, 2016). Within the UK, long-term NO₂ exposure is responsible for reduced life expectancy by an average of 5 months and approximately 23,500 deaths per year (DEFRA, 2017b; COMEAP, 2018). Historically NO_x was emitted at chimney height, but recently it is emitted at ground level (Davies et al., 2007). Within urban environments, vehicle exhaust emissions of nitrogen oxides (NO_x) are major inputs for atmospheric nitrogen (Gombert et al., 2003).

UK NO_x emissions also decreased during the 1990s and 2000s (Figure 2-4), due to reduced emissions from road transport and power stations and technical improvements (i.e. three-way catalysts) and were predicted to decline further by 55% in 2020 and 73% in 2030 (compared to 2005 baseline) (Air Quality Expert Group, 2004; DEFRA and DfT, 2017; DEFRA, 2019a).

For road transport in particular, implementation of three-way catalysts in petrol cars is a strict European regulation to reduce NO_x emissions (Air Quality Expert Group, 2004). The use of the three-way catalyst, however, leads to increasing emissions of ammonia (NH₃) from vehicle exhausts (Cape et al., 2004). 34% of the NO_x emissions in the UK are still related to road transport (DEFRA, 2018c). However, NO₂ concentrations have not decreased, but increased instead, due to the use of oxidation catalysts and particle filters in diesel automobiles (Henschel et al., 2016). Diesel vehicles are responsible for emissions of primary NO₂, especially when moving slowly (Air Quality Expert Group, 2004). In Manchester, the majority (80%) of NO_x emissions are associated with (diesel) vehicle emissions (TfGM, 2016; Regan, 2018). Emissions of NO_x at ground levels is of particular interest in narrow streets and major street junctions, due to impeded dispersion (Davies et al., 2007).

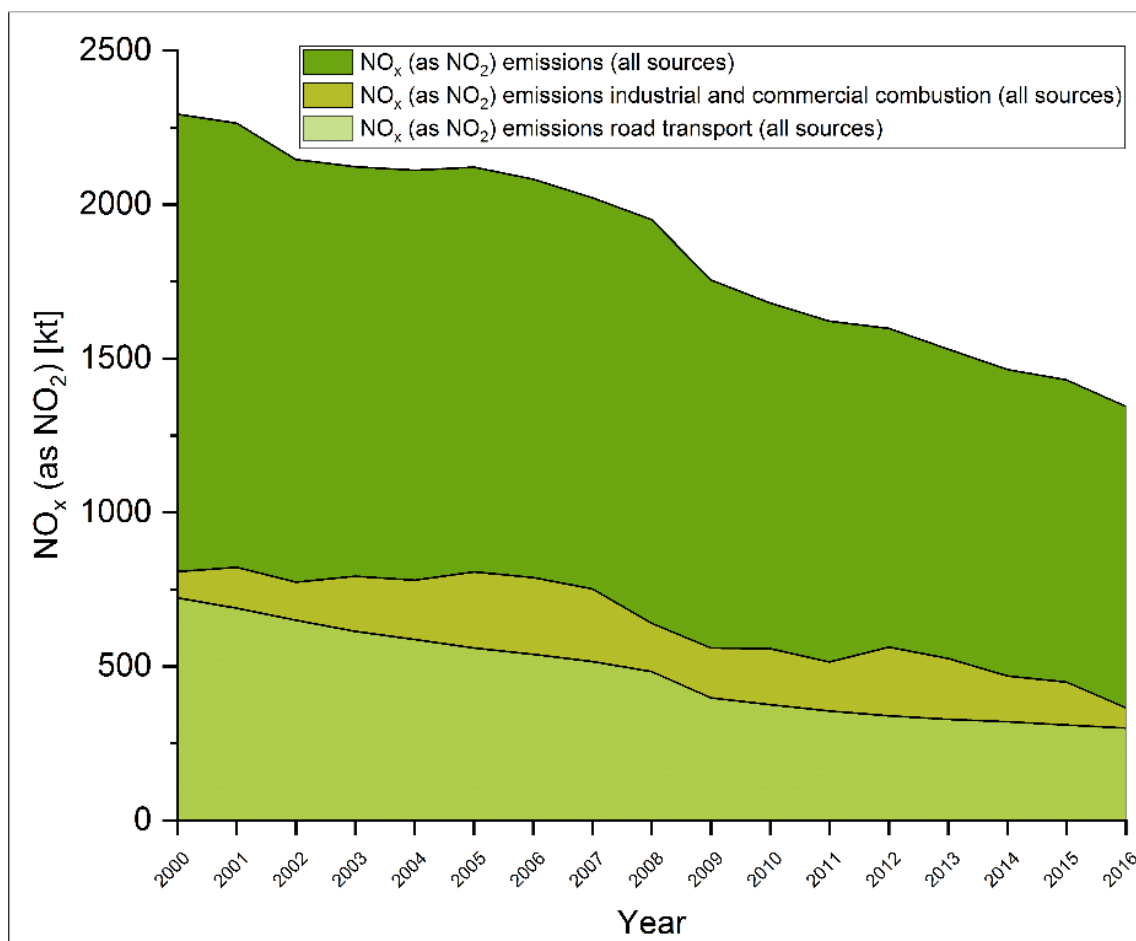


Figure 2-4: UK nitrogen dioxides - NO_x (as NO₂) emissions in kilo tonnes [kt] for all sources, industrial, commercial combustion and road transport from 2000 to 2016 (NAEI, 2018b); sources not stacked

2.2.2 Atmospheric nitrate, ammonia and ammonium

Reactive nitrogen in the atmosphere comprises nitrogen oxides (NO_x) and reduced nitrogen compounds (NH_x), which originate from many different sources, including fossil fuel combustion and agricultural processes (Sutton et al., 2004; Hall et al., 2006; Olsen et al., 2010). Nitrate (NO_3^-), a product of the atmospheric oxidation of NO_x , is an important atmospheric oxidant during the night, but is usually considered insignificant during daytimes due to rapid photolysation (Seinfeld and Pandis, 1997; Geyer et al., 2003; Khan et al., 2015).

Anthropogenic emissions of ammonia (NH_3) into the atmosphere are mainly derived from animal waste, chemical fertilizers and biomass burning, accounting for 55% of total nitrogen emissions into the atmosphere, which is rapidly deposited within 4 to 5 km of its source, but can be converted to ammonium (NH_4^+) in the atmosphere and then be transported distances of 100-1,000km (Olivier et al., 1998; Van Herk, 2001; Krupa, 2003; Webb et al., 2005; Gadsdon and Power, 2009; Hauck, 2010). Road traffic exhaust emission release both nitrate and ammonia compounds (Olivier et al., 1998; Sutton et al., 2000; Gadsdon and Power, 2009; Hauck, 2010). Geyer et al. (2003) reported increased levels of NO_3^- in the afternoon (even higher before sunset) with a significant role for daytime oxidation of hydrocarbons (e.g. alkanes, alkenes and aromatics). Urban NO_3^- concentrations in the UK vary significantly during daytime, with higher concentrations in the early mornings and late afternoons and variability throughout the seasons (Khan et al., 2015).

Both compounds (NO_3^- and NH_4^+) are constituents of particulate matter (PM) and may seriously affect human health and reduce visibility (Watson, 2002; Schnelle-Kreis et al., 2007; Lei and Wuebbles, 2013). Health impacts induced by nitrate and ammonium specifically were reported to impact on the cardiovascular and respiratory system (Atkinson et al., 2010; Kim et al., 2012; Son et al., 2012; WHO, 2013b). Ammonia emissions (total) in 2016 were 13% lower compared to 1980, with 104.43 kt emitted from livestock and 148.62 kt directly from agricultural soils (Figure 2-5). Combustion and production processes account for 12.96 kt ammonia emissions in 2016 (NAEI, 2018d). Other than NO_x and other pollutants (e.g. SO_2 and PM_{10}), ammonia emissions have increased (by 10%) in the UK since 2013 of which 88% are attributed to agricultural emissions. Moreover, under current scenarios, emission reduction targets for ammonia will not be met in the UK by 2030, contributing to nitrogen deposition in habitats (DEFRA, 2018c; Environment Agency, 2018).

For instance, 95% of nitrogen sensitive habitats in the UK receive more nitrogen than they can tolerate and are adversely affected by nitrogen deposition (DEFRA, 2018c; Environment Agency, 2018).

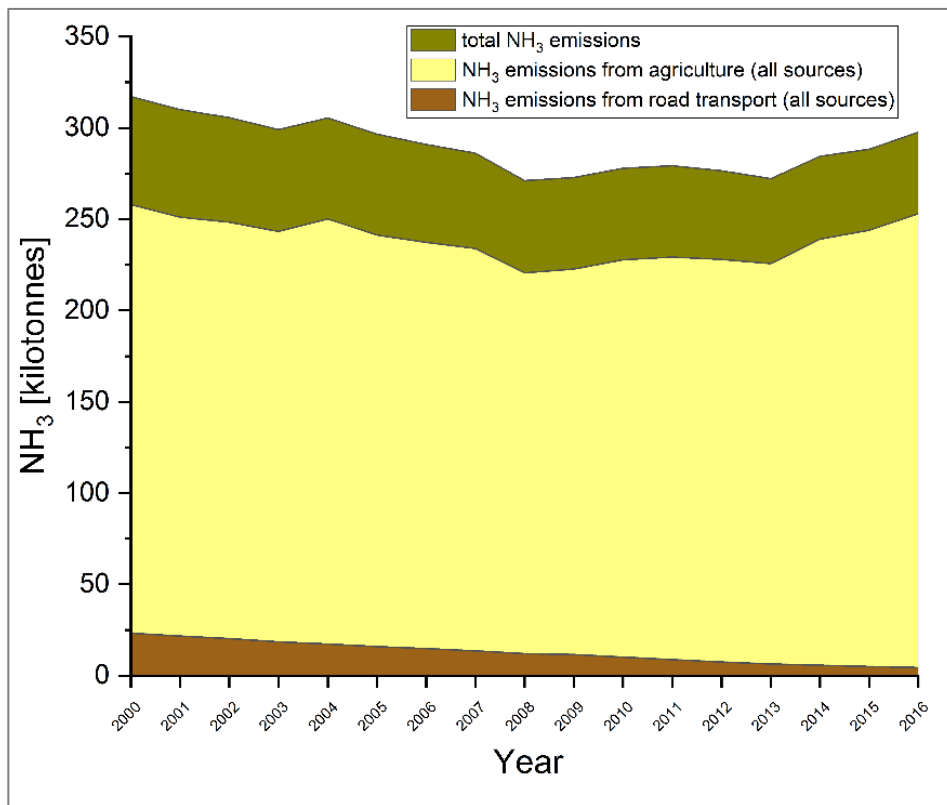


Figure 2-5: UK emissions of NH₃ [in kilotonnes] (total NH₃ including industrial and commercial combustion and road transport; NH₃ including agriculture and road transport) from 2000 to 2016 (NAEI, 2016); sources not stacked

2.2.3 Atmospheric stable-isotope-ratios ($\delta^{13}\text{C}$, $\delta^{15}\text{N}$ and $\delta^{34}\text{S}$)

'Isotopes' comprise of atoms, whose nuclei contain the same number of protons but a different number of neutrons and can be divided into stable and unstable (radioactive) species (Hoefs, 2009). Stable isotopes do not undergo radioactive decay (stable isotopes comprise of <10% of all known isotopes), are abundant (Table 2-2), are not all hazardous to human health since they occur naturally in the human body (Fry, 2006). Table 2-2 shows the most abundant isotopes for carbon, nitrogen and sulphur.

Table 2-2: CNS isotopes (low – ‘light’ and high – ‘heavy’ mass) and natural abundance (Fry, 2006; Sharp, 2017)

Element	Isotope abundance (%)			
	Light isotope	Heavy isotope	Light isotope	Heavy isotope
Carbon	¹² C	¹³ C	99.89%	1.11%
Nitrogen	¹⁴ N	¹⁵ N	99.64%	0.36%
Sulphur	³² S	³⁴ S	95.02%	4.21%

Elements such as carbon, nitrogen and sulphur circulate in compartments of the Earth (i.e. atmosphere and biosphere) and processes (fractionation and mixing) create unique isotope characteristics (Fry, 2006). For example, photosynthesis in plants follows different pathways (i.e. C₃ and C₄; ~95% of plants use C₃-pathway) to obtain energy from atmospheric CO₂, resulting in different $\delta^{13}\text{C}$ values of -18‰ and -4‰ (relative to CO₂ with an average of -8‰) for C₃-plant and C₄-plants, respectively (Hoefs, 2009; Sharp, 2017).

Nitrogen in the atmosphere (as N₂) is constant at 0‰ and most parts of the biosphere also have isotopic compositions near 0‰ (from -10‰ to +10‰), while anthropogenic emissions are related to more negative values (i.e. ammonium and nitrate; Fry, 2006).

Sulphur has four stable isotopes, with ³²S being (~95%) and ³⁴S (~4%) being the most abundant, while ³³S and ³⁶S only make up a small proportion (0.76% and 0.02%, respectively; Hoefs, 2009). Within all spheres of the Earth (i.e. biosphere, lithosphere and atmosphere), sulphur is an important constituent and has broad applications in environmental studies (Sharp, 2017).

Figure 2-6 illustrates representative values (δ) and distribution of stable isotope signatures for different ecosystem compartments (Fry, 2006). Relative differences in isotopic signatures are given in δ -values for isotope ratios of heavy/light isotope, i.e. ¹⁵N/¹⁴N ($\delta^{15}\text{N}$), ¹³C/¹²C ($\delta^{13}\text{C}$) and ³⁴S/³²S ($\delta^{34}\text{S}$), expressed as per-mille (‰). Delta (δ) values are denoted as a difference measurement relative to standards used during analysis and is calculated by:

$$\delta^{\text{YX}} = [(R_{\text{sample}}/R_{\text{standards}} - 1)] * 1000$$

with Y being the heavy isotope mass of element X and R being the ratio (Fry, 2006; Sharp, 2017). Analysing stable-isotope-ratios can aid to ‘fingerprint’ specific sources, i.e. $\delta^{34}\text{S}$ values <10‰ represent anthropogenic sources (e.g. coal and fossil fuel; Wadleigh, 2003; Wadleigh and Blake, 1999; Wiseman and Wadleigh, 2002).

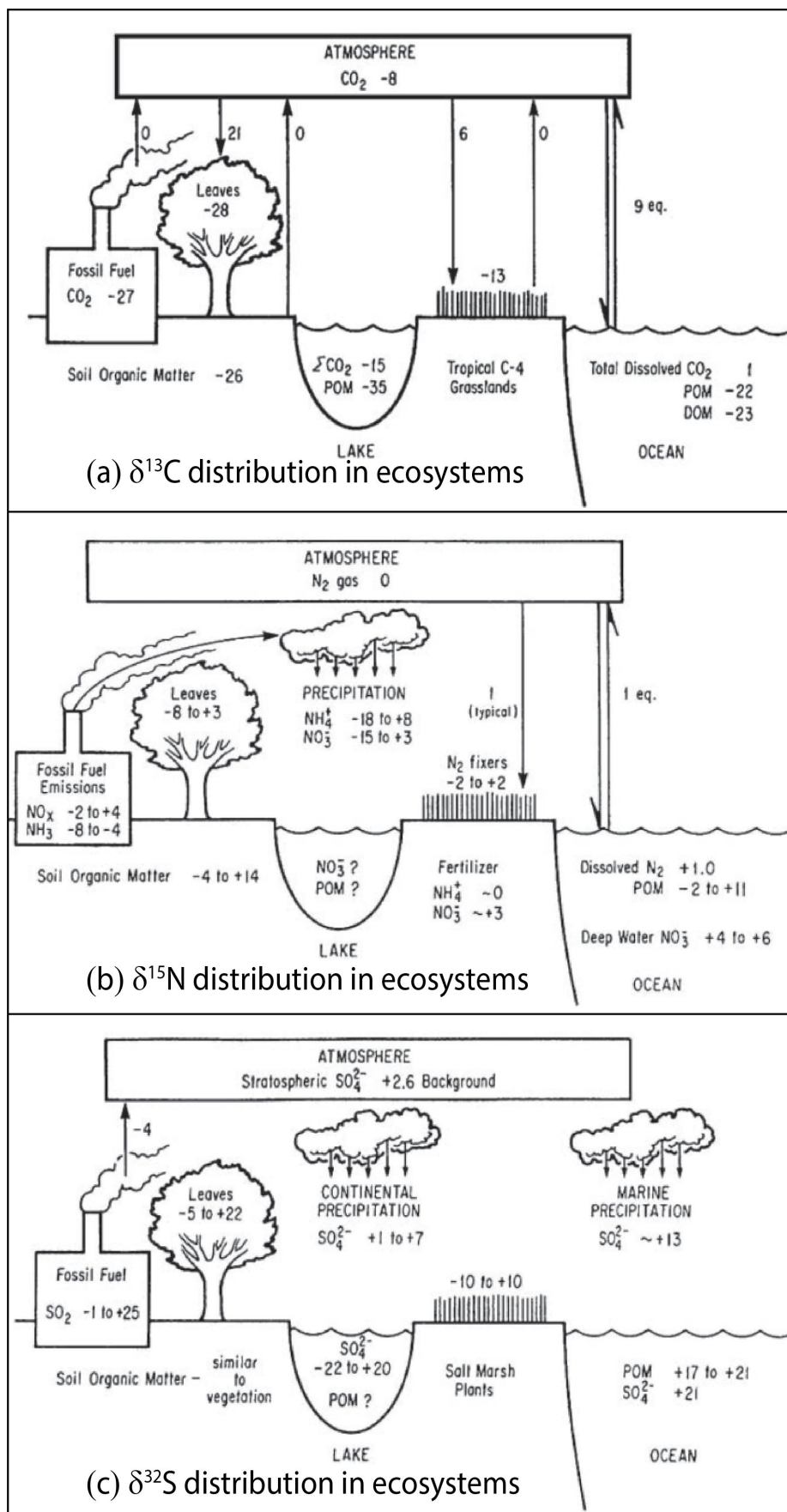


Figure 2-6: Representative δ -values of CNS isotopes in natural systems (taken from Fry (2006); *Annual Review of Ecology and Systematics*, Volume 18, copyright 1987 by Annual Reviews: www.annualreview.org); numbers next to arrows represent δ -values of carbon, nitrogen and sulphur; single arrows represent fluxes, double arrows represent an equilibrium isotope fractionation

2.2.4 Airborne metals

Metals are non-degradable and accumulative in nature, with the potential to enrich in environmental compartments (i.e. soils) and human exposure via inhalation, ingestion and dermal contact (Mielke, 1997; Mielke and Reagan, 1998; Boyd et al., 1999; Mielke et al., 1999; Wong et al., 2006). Toxicity of metals is a problem for ecological, evolutionary, nutritional and environmental reasons and emission of metals derive from various natural and human sources, e.g. erosion, weathering, mining and industrial activities (Nagajyoti et al., 2010; Morais et al., 2012; Jaishankar, Mathew, et al., 2014; Jaishankar, Tseten, et al., 2014). Metals are divided into two groups: crustal and non-crustal. The former include aluminium (Al) and iron (Fe), the latter cadmium (Cd), chromium (Cr), copper (Cu), zinc (Zn) and lead (Pb). Lead has long been and still is a major element of concern, due its severe health impacts (Wong et al., 2006). Cadmium (Cd), Cr, Ni, Pb, Mn, Pd, Pt and Zn (among others; Table 2-3; more in Chapter 6) are potentially toxic elements of concern for environmental human health studies (Järup, 2003; Wong et al., 2006; Kampa and Castanas, 2008).

Some metals, are essential to maintain human metabolism, but higher concentrations (and accumulation) in the human body can have toxic effects (Järup, 2003; Kampa and Castanas, 2008). Pb and Cd can originating from traffic and industry and are hazardous to human health, causing detrimental effects on neural development in children and kidney damage (Pb), pulmonary effects, kidney damage and skeletal damage (Cd) (Järup, 2003; Aksu, 2015; WHO, 2015; The Royal College of Physicians, 2016). Human health impacts of metals are presented in Table 2-3.

Table 2-3: Metals present in the environment, their sources and potential human health impacts

Element	Sources of exposure (anthropogenic)	Health impacts
Aluminium (Al)	Drinking water, food, beverages and drugs	Cell damage (i.e. nervous cells) (Barabasz et al., 2002; Jaishankar, Tseten, et al., 2014)
Arsenic (As)	Paints, dyes, soap, semi-conductors, drugs and fertilizers	Carcinogenic (i.e. lung, bladder and skin cancer) (Jaishankar, Tseten, et al., 2014)
Beryllium (Be)	Alloys, airplane and construction material	Lung damaging, carcinogenic (Hirner et al., 2000)
Cadmium (Cd)	Mining, smelting, Zinc production (by-product), fertilisers, waste incineration and tobacco smoke	Carcinogenic, kidney and lung damage/diseases, osteoporosis, disturbs zinc metabolism, decreases haemoglobin and haematocrit, leads to anaemia (Järup, 2003; Jaishankar, Tseten, et al., 2014)
Chromium (Cr)	Protective metal coatings, alloys, paint, rubber, cement, wood preservatives, metal plating	DNA damage (i.e. chromosomal aberrations), ulcer formation (O'Brien et al., 2001; Matsumoto et al., 2006; Martin and Griswold, 2009; Jaishankar, Tseten, et al., 2014)
Cobalt (Co)	Food and beverages, alloys, paints and tool production	Lung and heart effects, dermatitis and liver and kidney damage (ATSDR, 2004b)
Copper (Cu)	Wire, plumbing pipes and sheet metal, wood, leather and fabric preservative	Throat and nose irritation, liver and kidney damage (very high doses can cause death; (ATSDR, 2004c)
Iron (Fe)	Food and beverages	DNA mutation and malignant transformations, heart, liver and brain effects
Lead (Pb)	Mining, smelting, paint, battery production, glass industry, food	Reduced foetal growth, congenital malformations, impairment in cognitive abilities, kidney damage (Järup, 2003; Bellinger, 2005; Garza et al., 2006; Kampa and Castanas, 2008)
Manganese (Mn)	Steel production, gasoline additive	Nervous system impacts (ATSDR, 2012a)
Nickel (Ni)	Alloys, steel production, battery production	Allergic reactions, cardiovascular disease, carcinogenesis, DNA alteration (Costa et al., 2003; Kampa and Castanas, 2008)
Palladium (Pd)	Dental and electrical appliances, chemical catalysts, automotive catalysts	Allergic reactions, skin and eye irritation (Kielhorn et al., 2002)
Platinum (Pt)	Automotive catalysts, chemical catalysts, electrical industry, dentistry and medicine	Mutagenic, inhibition of DNA synthesis (WHO, 2000a)
Titanium (Ti)	Used in nanotechnology, alloys, hardener, catalytic converters	Titanium dioxide (TiO ₂) related to lung tumours (Farmer, 1997)
Vanadium (V)	Ceramics, catalytic converters, superconductive magnets, fossil fuel combustion, food and beverages	Lung damage, increased blood pressure, decreasing number of red blood cells (potentially carcinogenic; (ATSDR, 2012b)
Zinc (Zn)	Food and water/beverages, construction and painting, mining, smelting, manufacturing, automobiles	Skin irritation, zinc induced 'metal fume fever', anaemia, nausea (ATSDR, 2005, 2018)

The *National Atmospheric Emissions Inventory* (NAEI) provides information on UK emissions for several pollutants, including metals (NAEI, 2018c). Metal emissions (i.e. Cd, Pb, Ni and Zn) have shown varied declines since 1990 within the UK (Figure 2-7), e.g. lead emissions declined by 98% and nickel by 73%. Cadmium (in 2016) was mainly emitted from residential and industrial sources, while road transport (i.e. tyre/break ware and diesel/petrol fuels) contributed to a consistent amount (~0.5 tonnes) since 2000. Road transport was responsible for 36% of UKs Zinc (Zn) emissions in 2016. Lead (Pb) and Nickel (Ni) emissions have significantly declined due to reduced use of coal and fuel oil since 1990. Steelmaking (32%), fireworks (13%) industrial combustion of waste oils (10%) are the major sources of lead emissions in the UK. Nickel was mainly emitted by combustion processes (i.e. petroleum coke, heavy fuel oil) from the residential and industrial sectors (72% ;NAEI, 2018c).

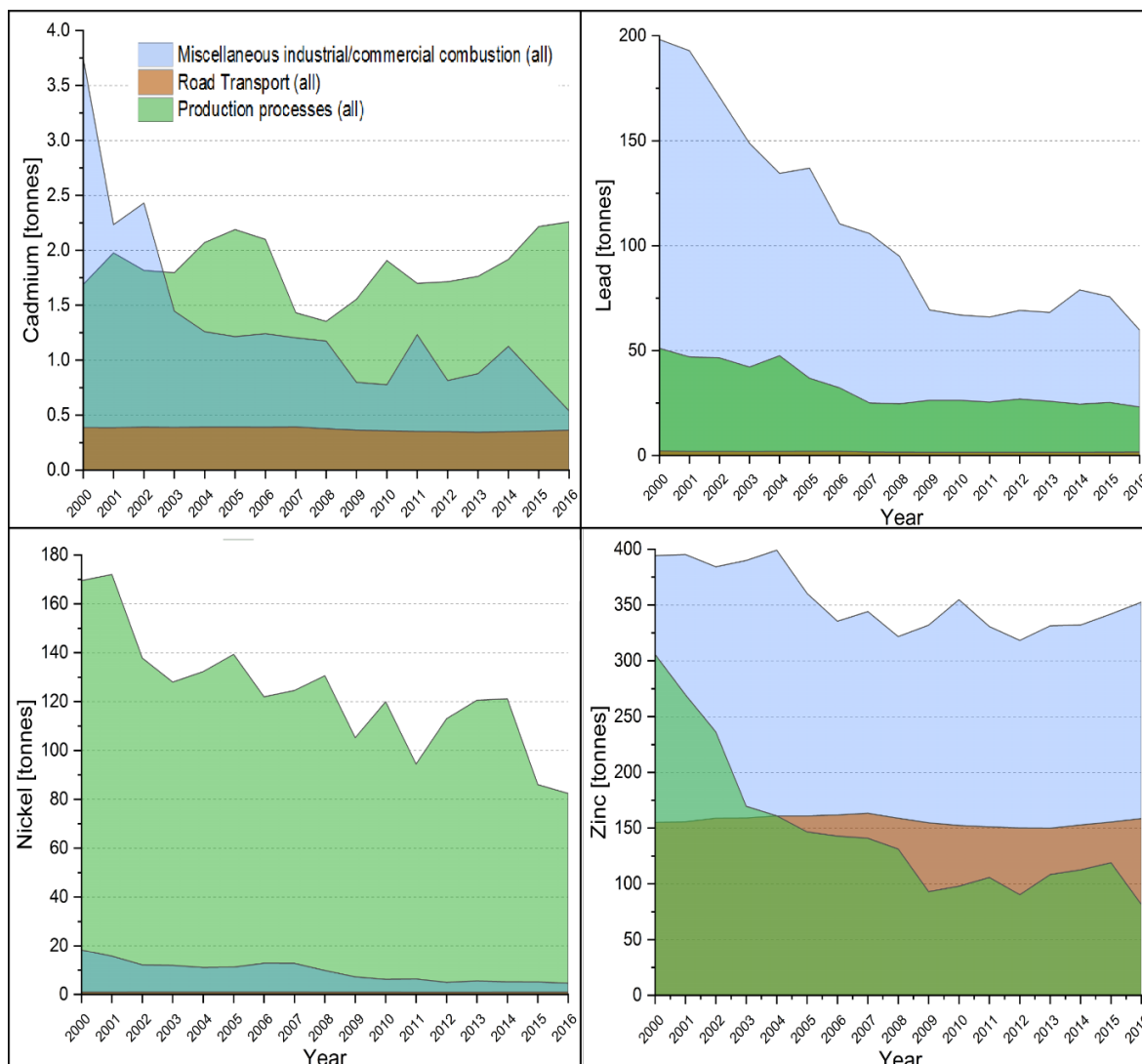


Figure 2-7: UK emissions of Cd, Pb, Ni and Zn between 2000 and 2016 (NAEI, 2018c) by major anthropogenic sources (i.e. industrial/ commercial combustion, production processes and road traffic); sources not stacked

2.2.5 Atmospheric polycyclic aromatic hydrocarbons (PAHs)

Polycyclic aromatic hydrocarbons (PAHs) are produced by incomplete combustion and pyrolysis of organic material and can be found in soils, water and air (Baird and Cann, 2008; Satya et al., 2012). They are considered ubiquitous, persistent, highly liposoluble, semi-volatile, highly carcinogenic and mutagenic toxic compounds, with deleterious effects on human health (Harvey, 1998; WHO, 2000b, 2013b; Ravindra, Sokhi, et al., 2008; Kim et al., 2013).

The molecular structure of PAHs is defined by two adjacent fused, six-membered benzene rings and most PAHs are characterized by their plane structure/geometry, with single- or double-bonds and one or more five-membered rings (Baird and Cann, 2008). PAHs occur in gaseous form and as adsorbents on particles and they tend to persist in the environment for a long time, due to their stable molecular structure and slow photochemical decomposition and degradation (Blasco et al., 2006; Nascimbene et al., 2014). Emission sources can be either natural, e.g. volcanic eruptions and forest fires, or anthropogenic, such as vehicle exhaust emissions, re-suspended contaminated soils, power plants and refineries, i.e. chemical manufacturing, petroleum cracking and incineration (Kaya et al., 2012; Augusto, Máguas et al., 2013; Augusto et al., 2015).

Organic compounds, such as polycyclic aromatic hydrocarbons (PAHs) are atmospheric pollutants emitted by incomplete combustion processes. Approximately 90% of PAH emissions (due to incomplete combustion) are related to vehicles emission that are distributed in the air in vapour- and particle-phase (Augusto et al., 2010; Shukla et al., 2012; Sarigiannis et al., 2015). Concentrations of PAHs in air vary seasonally, with highest concentrations during winter, due to low temperatures (high atmospheric pressure), and low concentrations in summer, due to high evaporation and volatilization (Augusto et al., 2009; Shukla et al., 2012; Augusto, Pereira et al., 2013; Garrido et al., 2014). The spatial distribution of PAHs in air is also dependent on factors such as the size of particles they are adsorbed to, their hydrophilic character (water solubility) and the nature of the emission source (point or non-point) (Augusto et al., 2009). Organic pollutants can be deposited to lichens by dry (gaseous) and wet and dry particle-bound deposition, indicating the importance of physico-chemical properties of PAHs (Augusto et al., 2013; Ravindra et al. 2008).

PAH emissions, affecting air quality in urban environments are related to industrial, commercial, residential and vehicular sources (Kim et al., 2013). Different PAHs are associated with different sources, e.g. naphthalene is emitted by light vehicles, benzo[a]pyrene by automobiles (with and without catalytic converters) and benzo[a]anthracene and chrysene by diesel and natural gas combustion (Rogge et al., 1993; Khalili et al., 1995; Guidotti et al., 2003; Blasco et al., 2006). Road traffic, especially light vehicular traffic, is a major PAH source, thereby contributing to poor air quality in urban areas. The U.S. Environmental Protection Agency (EPA) has identified 16 PAHs of primary interest (Table 2-5; Blasco and Domeño, 2006; Blasco et al., 2008, 2011). Within the EU (Table 2-5) additional PAHs are being monitored (Lerda, 2011).

The UK 'Polycyclic Aromatic Hydrocarbon Network' currently monitors ambient PAH concentrations at 31 sites across the country, by analysing PAHs in particulate and deposition samples (DEFRA, 2018d). Measured PAH concentrations include the 16 EPA priority PAHs (Table 2-5) and EU-PAHs. It has been reported that methylation, a chemical substitution process, adding a methyl group [-CH₃] by replacing a hydrogen atom, is affecting PAHs carcinogenic activity (Braga et al., 1999; Mumtaz and George, 1999; Lam et al., 2018). Methylated and additional PAHs are measured in the UK PAH network, illustrated in Table 2-4 (DEFRA, 2018d).

Table 2-4: Additional considered PAHs and methylated PAHs in the UK PAH network

Methylated PAHs			
1-methyl naphthalene	1-methyl anthracene	1-methyl phenanthrene	retene (1-methyl-7-isopropylphenanthrene)
2-methyl naphthalene	2-methyl anthracene	2-methyl phenanthrene	
	9-methyl anthracene	4.5-methylene phenanthrene	
Further considered PAHs: anthanthrene, benzo[c]phenanthrene, benzo[b]naph[2,1-d]thiophene, benzo[e]pyrene, coronene, cholanthrene, dibenzo[ac]anthracene and perylene			

Table 2-5: List of identified European Union (EU) and U.S. Environmental Protection Agency (EPA) PAHs (Lerda, 2011; National Center for Biotechnology Information, 2018; Royal Society of Chemistry, 2018)

Compound name and molecular formula	Structure	List – EU/US-EPA
Naphthalene C ₁₀ H ₈		
Acenaphthylene C ₁₂ H ₈		
Acenaphthene C ₁₂ H ₁₀		
Fluorene C ₁₃ H ₁₀		
Phenanthrene C ₁₄ H ₁₀		
Anthracene C ₁₄ H ₁₀		
Fluoranthene C ₁₆ H ₁₀		
Pyrene C ₁₆ H ₁₀		
Benz[a]anthracene C ₁₈ H ₁₂		
Chrysene C ₁₈ H ₁₂		
Benz[b]fluoranthene C ₂₀ H ₁₂		
Benz[k]fluoranthene C ₂₀ H ₁₂		
Benzo[a]pyrene C ₂₀ H ₁₂		
Indeno[123-cd]pyrene C ₂₂ H ₁₂		
Benzo[ghi]perylene C ₂₂ H ₁₂		
Dibenz[ah]anthracene C ₂₂ H ₁₄		
Benzo[j]fluoranthene C ₂₀ H ₁₂		
Benzo[c]fluorene C ₁₇ H ₁₂		
Cyclopenta[cd]pyrene C ₁₈ H ₁₀		
5-Methylchrysene C ₁₉ H ₁₄		
Dibenzo[ae]pyrene C ₂₄ H ₁₄		
Dibenzo[ah]pyrene C ₂₄ H ₁₄		
Dibenzo[ai]pyrene C ₂₄ H ₁₄		
Dibenzo[al]pyrene C ₂₄ H ₁₄		

2.3 Biomonitoring with Lichens

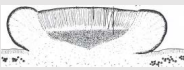



Nimis et al. (2002) describe monitoring as periodical surveillances to identify variations from expected norms and preset standards. Monitoring methods can be divided into sub-groups, such as specific and unspecific, sensitive, accumulative, and active and passive. For example, a specific indication means that one single environmental factor is responsible for a specific reaction of the indicator, e.g. purple discolouration of plant leaves caused by ozone (O₃) (Zierdt, 1997).

Biomonitors are living organisms used to obtain quantitative and qualitative information, reflecting environmental conditions (de Bruin, 1990; Forbes et al., 2015). These organisms react to pollution by their occurrence or absence and/or by accumulating the pollutant within or onto their tissues (Blasco et al., 2008; Kirschbaum and Wirth, 2010). Accumulating mechanisms include the entrapment of particulates, stomata gas exchange and surface ion exchange. Biomonitors are commonly used where costly technical apparatus cannot be afforded. Regarding air pollution, selection of an applicable biomonitor is crucial since it needs to be widely distributed and abundant across the area of interest (Forbes et al., 2015). Furthermore, the targeted biomonitoring organisms should be able to accumulate the specific pollutant (Forbes et al., 2015).

Lichens have been extensively used for biomonitoring studies and as ecological indicators for air pollution (Nimis et al., 1991; Giordani et al., 2002; Giordani, 2007; Pinho et al., 2012). Lichens are symbiotic organisms, between fungal (mycobiont) and photosynthetic (photobiont) partners (Figure 2-8). The photobiont can be either an alga and/or cyanobacteria (Nash III, 2008). Recent research suggests that a third partner is included within this symbiosis; a yeast fungus was found in 52 lichens and is treated as an inherent symbiotic partner (Spribille et al., 2016). Moreover, it was found that that lichen of the genus *Letharia* ('wolf lichens') are associated with another fungal partner (basidiomycete: *Tremella*), which is found on a wide range of lichen genera, raising new questions about lichen symbiosis functions (Lawrey and Diedrich, 2018; Tuovinen et al., 2018).

The symbiotic nature is not entirely correct and lichens can be described as mutualism or controlled parasitism, because the fungal partner gains more benefits, i.e. carbon nutrition via the photobiont, from the cohabitation and several fungi can co-exist alongside with the primary (or dominant) mycobiont (Nash III, 2008). A glossary of terms used to describe lichens is included Table 2-6.

Table 2-6: Definitions of Lichen-related terms (Wirth, 1995; Kirschbaum and Wirth, 2010; Shukla et al., 2014; Cole, 2015)

Term	Definition
 apothecium (plural apothecia) <u>picture:</u> section of apothecium	fruiting body (sexual reproduction); discoidal to patelliform or hemispheric structure with various colours
cilium (plural cilia)	compact strands of hyphae; short, eyelash-like hair; outgrowth from the margin or upper surface of lobes
forniciform	helmet-/dome-like shape
 isidium (plural isidia); <u>picture:</u> coralline shaped isidia of <i>P. elegantula</i>	minute outgrowth of the thallus; pencil, clubbed to coralline shape; contains mycobiont and photobiont
medulla	internal layer of fungal hyphae (marrow); below algal layer
 rhizine(s) <u>picture:</u> rhizines of <i>Physconia grisea</i>	holdfast/ anchoring of the thallus; cord of hyphae (lower cortex); black to light brown
 soralium (plural soralia) <u>picture:</u> fissured soralia	decorticate area or body of thallus where soredia are produced
soredium (plural soredia)	microscopic group of algal and loosely woven hyphae; finely powdery to coarsely granular; vegetative reproduction
thallus (plural thalli)	habit ("lichen body"); see Figure 2-9

Three different morphological groups of lichens are described (Nash III, 2008; Shukla et al., 2014):

- Crustose – tightly attached to substrate (adherent crust), no lower cortex and often without a distinctive or true upper cortex.
- Foliose (exemplary: Figure 2-8) – leaf-like, flat, partially attached to substrate; develop a great range of thallus size and thallus diversity.
- Fruticose – bear-/hair-like, strap-shaped or shrubby, bushy lobes (flat or cylindrical); stand out from substrate.

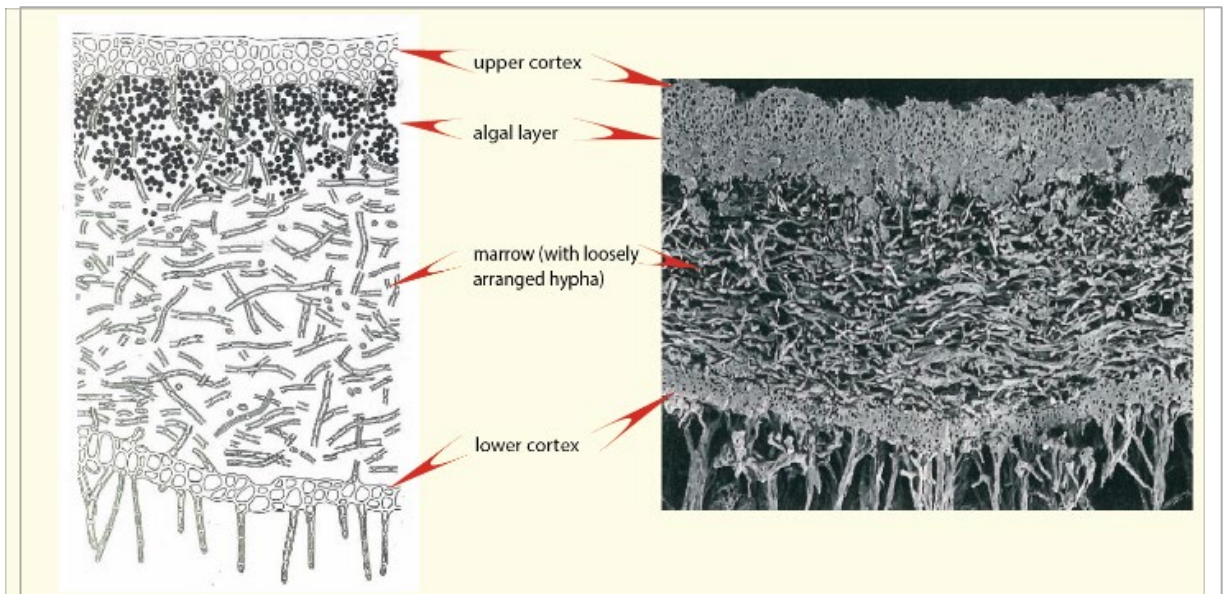


Figure 2-8: Semi-schematic profile of a foliose lichen (left) and SEM-profile (160x) of the foliose lichen *Lobaria scrobiculata* (layered structure) (right) (modified illustration after Wirth, 1995; Kirschbaum and Wirth, 2010)

Compared to higher plants, lichens lack roots, cuticle and stomata, and obtain their mineral and water supplies from the surrounding air (Sloof and Wolterbeek, 1993; Markert et al., 2003; Wolterbeek et al., 2003; Käffer et al., 2012), resulting in uptake of contaminants (gases and particulates) over the entire organisms surface (Conti and Cecchetti, 2001; Blasco et al., 2008; Käffer et al., 2012). Hawksworth and Rose (1970) and Hawksworth (1970) correlated lichen presence or absence to atmospheric SO₂ concentrations in urban areas, leading to method development based on epiphytic indicator species (Hawksworth, 1970; Nash III, 1973; Zierdt, 1997; Van Herk et al., 2003; Sutton et al., 2004; Blasco et al., 2008; Munzi et al., 2014).

Numerous studies have shown the use of lichens as biomonitors for different pollutants, e.g. sulphur dioxide (SO₂), nitrogen dioxide (NO₂) (e.g. Frati et al., 2006; Boltersdorf and Werner, 2014; Paoli et al., 2015) and hydrofluoric acid, as well as other organic pollutants, such as polycyclic aromatic hydrocarbons (PAHs) (e.g. Guidotti et al., 2003; Blasco and Domeño, 2006; Augusto et al., 2010), and inorganic contaminants, i.e. metals (Blasco et al., 2006; Bačkor and Loppi, 2009; Forbes et al., 2015). Nimis et al. (1989) described lichens as a “permanent control system” for air pollution (Nimis et al., 1989; Conti and Cecchetti, 2001). In many countries, e.g. The Netherlands, France, Germany, Italy and United States, lichens are used for monitoring purposes (Nimis and Purvis, 2002). Reasons for using lichens as biomonitoring organisms are (as described by Nimis and Purvis (2002):

- Ubiquitous distribution and currently increasing (in number and diversity) in many urban areas, due to decreased atmospheric SO₂ concentrations.
- No cuticle, thereby absorbing nutrients and pollutants from aerial sources.
- Perennial, i.e. sampling is possible throughout the year.
- Many lichen species are able to accumulate high metal contents, without damage, permitting biomonitoring over wide areas.
- Different lichen monitoring methods existing (e.g. passive and active).
- Vulnerability of instrumented monitoring stations to theft and vandalism.

Within environments where high pollutant loadings occur, lichens may experience reduced growth and altered morphology (Hauck et al., 2002; Forbes et al., 2015). Furthermore, it was shown, that mosses may be a better choice to biomonitor atmospheric deposition of metals (Coskun et al., 2009; State et al., 2012; Sujetovienė and Galinytė, 2016). In contrast, lichens were found to reflect local nitrogen deposition (Boltersdorf et al., 2014; Sujetovienė and Galinytė, 2016). However, lichens were used in environmental pollution studies, pointing out their suitability for biomonitoring studies. Lichens cannot replace the technical equipment used for air pollution measurements and long-term air quality monitoring, but they are extremely useful for providing a rapid overview of larger geographical areas and can act as alarms for onset of air pollution (Nimis and Purvis, 2002). Therefore, lichens, in particular epiphytic lichens, i.e. those growing on other plants, such as trees, without harming or benefiting from them, are useful tools to indicate air pollution (Bartholomeß and John, 1997).

Nitrogen-loving species, such as *Xanthoria parietina*, *Physcia adscendens* and *Physcia tenella* are widespread throughout the UK (Nimis et al., 2009; Dobson, 2011). These lichen species have been used in environmental pollution studies for several pollutants (Gombert et al., 2003; Frati et al., 2007; Pisani et al., 2009; Paoli et al., 2015; Parzych, Zdunczyk, et al., 2016; Kurnaz and Cobanoglu, 2017). They are common in urban areas and tolerate high-levels of nitrogen (Gombert et al., 2003; Gadsdon et al., 2010). Therefore, both lichen species are useful biomonitors to investigate air pollution in the City of Manchester. Utilised lichen species are described in more detail hereafter.

2.3.1 *Xanthoria parietina*

The lichen *Xanthoria parietina* (Figure 2-9) is a foliose, lobate and yellow to orange, grey in shade, coloured lichen with apothecias and lacking isidia and soredia (Kirschbaum and Wirth, 2010). It occurs at eutrophic, nutrient-rich sites (i.e. trees) with high bark pH values, often closely to agricultural properties housing livestock, e.g. poultry farms (Kirschbaum and Wirth, 2010). *Xanthoria parietina* is considered to be resistant to airborne SO₂ and nitrogen pollution and is widely distributed across the British Isles, including urban centres (Dobson, 2011). The species-name “parietina” is related to the orange anthrachinon pigment ‘parietin’ (extracellular crystals in the upper cortex), which protects the photobiont against UV-radiation (Nash III, 2008).



Figure 2-9: *Xanthoria parietina* [left] and *Physcia tenella* and *Physcia adscendens* (socialized) [right] (author [left]; Kirschbaum and Wirth, 2010:154 [right])

2.3.2 *Physcia* spp.

The genus of the lichen *Physcia* includes different species that often co-occur on the same substrate (i.e. trees), namely *Physcia tenella* and *Physcia adscendens* (Kirschbaum and Wirth, 2010). Both are combined here as *Physcia* spp., because both species are rather resistant to air pollution and can advance into urban environments and often occur together and grow on top of each other (Bartholomeß and John, 1997; Kirschbaum and Wirth, 2010). Both lichens have *Trebouxia* spp. as algal partner, suggesting similarities in chemistry, i.e. primary and secondary compounds. *Physcia tenella* is a grey-white, small and narrow lobed foliose lichen, characterised by its cilia and lip-shaped lobe ends (Figure 2-9). The thallus is composed of numerous small lobes evenly distributed over the substratum, often covering larger areas. Lobes are small (width: 0.4-1.0 mm) and (more or less) shallow, elongate and 3 to 5 mm long. Young specimens have loosely adpressed lobes, while older lobes are pointing upward. At the end of the lobes are bright, rhizine-like, up to 2 mm long cilia, which can be absent due to high eutrophication.

The lichens upper side is grey-white coloured and dull, while the lower side is light brown to whitish, with bright rhizines. *Physcia tenella* prefers eutrophic, dust impregnated bark of deciduous trees. Its range increases with a reduction in SO₂ and an increase of nitrogenous compounds (Kirschbaum and Wirth, 2010; Dobson, 2011). The very similar looking lichen *Physcia adscendens* (Figure 2-9) is also grey-white in colour, being a small and narrow-lobed foliose lichen with cilia but, different to *P. tenella*, its lobe ends are hood-shaped and bulgy. Its thallus is about 3 cm (rarely >5 cm diameter) in size or several thalli are interleaved into each other, with an off-white to grey dull colour. The lobes are narrow (width: up to 1 mm), ascending at the ends (dome/helmet-like) and characterized by its forniciform soralia. The lobe ends exhibit bright, rhizina-like cilia (up to 2 mm long). The lichens lower surface is bright, with fewer and lighter coloured rhizines. *Physcia adscendens* has the same ecological preferences as *Physcia tenella* (Kirschbaum and Wirth, 2010; Dobson, 2011).

Within Britain *Physcia* lichens are commonly distributed on rocks and tombstones, asbestos-cement, wood and on nutrient-enriched bark of trees (Nimis et al., 2009; Dobson, 2011). Distinguishing both *Physcia* species can be difficult, due to eroded forniciform soralia of *Physcia adscendens* or younger specimens of *Physcia tenella*, but these can be distinguished from other grey *Physcia* species due to their long cilia (Kirschbaum and Wirth, 2010). *Xanthoria parietina* and both *Physcia* lichens frequently grow together, or grow together with other lichens on the same substratum, e.g. *Xanthoria polycarpa* and other *Physcia* species, and are considered to be toxitolerant (*Physcia tenella* slightly more so and on less eutrophic, more acidic locations) and able to colonise urban ecosystems (Wirth, 1995).

2.4 Lichens and air quality

Human activities and their influence on lichen abundance has been discovered long before regular application of them as biomonitors for air pollution. In 1790, Erasmus Darwin, the grandfather of Charles Darwin observed the effects of mining and smelting on surrounding vegetation, including lichens (Kricke and Loppi, 2002). About a century later, Grindon (in 1859) determined differences in the lichen flora of Manchester compared to other less industrialised cities (Grindon, 1859; Zierdt, 1997). Urban centres are often referred to as “lichen desert” with no lichen species present, due to high pollutant loading (Zierdt, 1997; Endlicher, 2012).

Lichens have been shown to be extremely useful organisms for biomonitoring of atmospheric pollution and air quality. Distribution of specific lichen species, may reflect varying levels of atmospheric pollution, as different lichens (i.e. crustose, foliose and fruticose) exhibit differential sensitivity to specific air pollutants (Nash III, 2008; Dobson, 2011; Shukla et al., 2014). Several methods have been developed and applied to quantify environmental conditions using lichens as indicators, such as the 'Index of Atmospheric Purity (IAP)' and the 'Index of Poleotolerance (IP)' that have been modified and further developed in different countries, including Switzerland, Germany, France, and Japan (Kricke and Loppi, 2002; Van Haluwyn and Van Herk, 2002). Using lichens as indicators (i.e. IAP and IP), can be classified as "quantitative" and/or "qualitative", the latter also called "community approach" (Van Haluwyn and Van Herk, 2002). Quantitative assessments of air quality are related to lichen compositions of sample plots, reduced to a single value expressing air quality. Qualitative approaches use whole lichen communities or species groups to assess air quality (Van Haluwyn and Van Herk, 2002).

Most early lichen air quality studies were related to sulphur dioxide (SO₂), as it was considered the main factor causing the loss of lichen vegetation in urban and industrialised areas, with Hawksworth and Rose (1970) being one of the first to correlate mean SO₂ concentrations to lichen vegetation (Hawksworth and Rose, 1970; Kricke and Loppi, 2002). Different lichen zones, i.e. "lichen desert" and "struggling zone" and SO₂ scales were introduced to characterise lichen communities and abundance (Sernander, 1926; Pearson and Skye, 1965; Zierdt, 1997; Kricke and Loppi, 2002). Following the reduction in (urban and industrial) SO₂ concentrations, increases in lichen diversity and re-colonisation of the 'lichen desert' were recorded across Europe (Sutton et al., 2004; Berglen et al., 2007; Gerdol et al., 2014). However, air quality improvements in SO₂ were partly counteracted by increased atmospheric nitrogen deposition rates (Galloway et al., 2008; Gerdol et al., 2014). Lichen species changes (i.e. return of acidophytic species; preferring acid substrate) did not follow spatial and temporal SO₂ changing patterns and increases in nitrophytic species, i.e. lichens preferring nitrogen-rich habitats, such as *Xanthoria parietina*, *Phaeophyscia orbicularis* and *Physcia adscendens* has been recognised (Van Herk, 1999).

In Britain and other European countries, a shift towards nitrogen tolerant species in rural areas has been observed, linking agriculture and lichen communities (Van Herk, 1999; Sutton et al., 2004). Epiphytic lichens, lichens growing on woody plants, are highly responsive to changes in air quality, due to morphological characteristics and subsistence on atmospheric moisture and nutrients (Nash III, 2008; Jovan et al., 2012). Recent research focusses on atmospheric nitrogen (N) compounds, i.e. ammonia (NH_3), ammonium (NH_4^+), nitrogen dioxides (NO_x) and nitrate (NO_3^- ; Van Herk, 1999, 2001, 2003; Frati et al., 2007; Wolseley et al., 2009; Gadsdon et al., 2010; Jovan et al., 2012).

2.4.1 Lichens and CNS

Nitrogen is a common element in the environment and is essential for life (by being involved in protein and nucleic acids synthesis; Seaward, 2003; Nash III, 2008; Shukla et al., 2014). Limited availability constraints growth and productivity in lichens (Crittenden, 1994; Nash III, 2008).

Lichens are mainly exposed to nitrogen in form of NO_x , NH_3 and its cation NH_4^+ (Andersen and Hovmand, 1999; Miller and Brown, 1999; Ruoss, 1999; Gaio-Oliveira et al., 2004; Gadsdon and Power, 2009). For instance, *Xanthoria parietina* is flourishing in nitrogen-rich habitats, i.e. from NO_x and NH_3 , showing less sensitivity to nitrogen compounds (Søchting, 1995; Van Dobben and Ter Braak, 1998; Van Herk, 1999; Van Herk et al., 2003; Sparrius, 2007; Pinho et al., 2008, 2009; Hauck, 2010; Dobson, 2011). Increases in airborne nitrogen compounds, particularly in urban areas from traffic emissions, nitrogen contents of lichens can reflect airborne nitrogen loads from anthropogenic impacts (Gombert et al., 2003; Frati et al., 2006, 2007; Gadsdon et al., 2010; Olsen et al., 2010; Bermejo-Orduna et al., 2014; Boltersdorf et al., 2014).

The *Xanthoria* and *Physcia* lichens that are the focus of this study are nitrophytes, i.e. they are able to tolerate high concentrations of nitrogenous pollutants and are abundant in urban areas (Gombert et al., 2003; Gadsdon et al., 2010). Lichen studies focussing on total nitrogen (N) contents (as weight percentage, wt%) have investigated influencing factors such as road traffic counts and distance from highways and farmland areas. Gombert et al. (2003) reported a significant positive relationship between lichen N content (*Ph. adscendens*) and traffic density in Grenoble (France), whilst Bermejo-Orduna et al. (2014) reported N content influences on *L. vulpina* in proximity to a major highway in the Sierra Nevada (USA).

Fрати et al. (2007) related accumulated N contents in *X. parietina* and *F. caperata* to NH₃ concentrations around a pig farm in Italy, which is in accordance with Olsen et al. (2010) who reported significant correlation between atmospheric ammonia concentrations and N content of *X. parietina* around a pig farm in Denmark. Some studies attributed an increase to nitrophytic species in urban areas to NO_x, with *X. parietina* being unharmed by high traffic emissions (Silberstein et al., 1996a, 1996b; Davies et al., 2007).

2.4.2 Lichens and stable-isotope ratios of carbon, nitrogen and sulphur

Lichen stable-isotope-ratio signatures have not been analysed to the same extent as soil, groundwater, precipitation and mosses in pollution studies (Russell et al., 1998; Sutton et al., 2004; Widory, 2007). However, prior studies reported the influence on lichen $\delta^{13}\text{C}$ values from urban sources (i.e. street dust PM₁₀ and soot from diesel and gasoline vehicle exhausts) indicating the use of $\delta^{13}\text{C}$ values to characterise lichen CO₂ sources (Batts et al., 2004; López-Veneroni, 2009). Sulphur is an essential nutrient for epiphytic lichens and sulphur-isotope ratio signatures are related to its close surrounding atmosphere (Wadleigh and Blake, 1999; Wadleigh, 2003; Batts et al., 2004). Thus, $\delta^{34}\text{S}$ values can be used to fingerprint anthropogenic sulphur sources (e.g. coal and oil; Wadleigh, 2003; Wadleigh and Blake, 1999; Wiseman and Wadleigh, 2002). Boltersdorf and Werner (2014) further used $\delta^{15}\text{N}$ values (i.e. nitrogen stable-isotope ratios; $^{15}\text{N}/^{14}\text{N}$), combined with nitrogen contents of *X. parietina* and *Physcia* spp. to identify the source and quantity of atmospheric nitrogen loads across different land-use types (e.g. urban agglomeration Rhine-Ruhr) in Germany. NO_x has high $\delta^{15}\text{N}$ values (enriched in ^{15}N) and lichens in urban areas also are characterised by an enrichment of ^{15}N , making them a useful tool to distinguish between nitrogen sources (in addition to N content) (Boltersdorf and Werner, 2014; Boltersdorf et al., 2014). Lichen stable-isotope ratios ($\delta^{13}\text{C}$, $\delta^{15}\text{N}$ and $\delta^{34}\text{S}$) can be used to fingerprint urban sources and influences on lichen isotopic signatures.

2.4.3 Lichens and nitrate and ammonium

Atmospheric nitrogen (N₂) is not readily utilised by lichens (except some cyanolichens) and nitrate (NO₃⁻) and ammonia (NH₃) are critical for survival and growth of green-algal lichens (Nash III, 2008). Ammonia contributes to eutrophication, causing severe impacts on ecosystems, i.e. decreased biodiversity, species composition changes and dominance (Asman et al., 1998; Paoli et al.,

2015). Ammonia release is an important factor influencing epiphytic lichens (growing on trees), increasing nitrophytes (preferring ammonia rich conditions with high bark pH) and reducing acidophytes (favouring low N conditions and naturally acidic bark), by contributing to the deposition of eutrophicating chemicals (Sutton et al., 2004; Frati et al., 2006; Paoli et al., 2015). Generally, NH_3 concentrations decrease exponentially with distance from the emission source (Pinho et al., 2012; Paoli et al., 2015). About 25% of emitted NH_3 can reach distances 100 to 1,000 km from the source, as ammonium (NH_4^+), which is largely wet deposited but has no effect on bark pH. Deposition of NH_3 favour communities of nitrophytic lichens. If NH_4^+ is nitrified to nitrate (NO_3^-), e.g. on mossy trunks, it might add to acidification, which affects acidophytic lichen distributions (Van Herk et al., 2003). Abundance of nitrophytes in urban areas show a positive correlation with basic dust pollution, with nitrate as an important constituent (originating from NO_x) and ammonia (NH_3) (Van Herk et al., 2003). Frati et al. (2007) related accumulated N contents in *X. parietina* and *F. caperata* to NH_3 concentrations around a pig farm in Italy, which is in accordance with Olsen et al. (2010) who reported significant correlation between atmospheric ammonia concentrations and N content of *X. parietina* around a pig farm in Denmark.

There is limited knowledge about preferences of different lichens for various nitrogen forms, but lichens are able to take up ammonia and nitrate, with regard to associated photobionts in green-algal lichens (Smith, 1960; Lang et al., 1976; Shapiro, 1984; Crittenden, 1996, 1998; Dahlman et al., 2004). Pavlova and Maslov (2008) studied the nitrate uptake of the lichen green-algal (*Trebouxia* sp.) lichen *Parmelia sulcata* and reported that the mycobiont is responsible for nitrate assimilation in the lichen symbiosis. Under laboratory conditions, uptake of nitrate in lichens was found to be less effective than ammonium uptake (Dahlman et al., 2002, 2004; Gaio-Oliveira, Dahlman, Palmqvist, Martins-Loução, et al., 2005; Palmqvist and Dahlman, 2006; Hauck, 2010).

Naeth and Wilkinson (2008) extracted nitrate (NO_3^-) and ammonium (NH_4^+) applying a 1:5 water extraction on lichen species *Flavocetraria cucullata*, *Flavocetraria nivalis* and *Cladina arbuscula* sampled around a diamond mine. They reported higher lichen NH_4^+ concentrations in close proximity to the mine. NO_3^- concentrations were reported to be inconsistent for all sites, but NO_3^- and NH_4^+ concentrations being affected by sampling location and direction. Sims et al. (2017) reported urban nitrate (NO_3^-) influences on lichen species in the Los Angeles Valley

(USA). Furthermore, they suggested influences on lichen NO_3^- uptake by atmospheric metal concentrations, i.e. copper and chromium, affecting algal photosynthetic functions and inhibiting growth rate (Kumar et al., 2009; Hauck et al., 2013; Sims et al., 2017).

Site-specific influences, including environmental surroundings, meteorology and topography (EEA, 2015) could potentially affect urban lichens' nitrate concentrations (spatial variability). Levia (2002) reported that lichen nitrate uptake from stem flow was influenced by meteorological conditions (precipitation and temperature). Higher nitrate concentrations in urban lichens could be related to NO_x emission from traffic and industrial activities in the area.

2.4.4 Lichens and airborne metals

Urban lichen biomonitoring studies for metals have been undertaken in Europe and worldwide, e.g. in Argentina, Brazil, Peru and India (Carreras and Pignata, 2002; Majumder et al., 2013; Klimek et al., 2015; Vingiani et al., 2015; De La Cruz et al., 2018; Koch et al., 2018), reporting elevated metal concentrations in lichens sampled or deployed in an urban environment. In particular, *X. parietina* and *Physcia adscendens* have been used to determine metal concentrations in lichens from urban areas in Italy, Turkey and Poland (Owczarek et al., 2001; Doğrul Demiray et al., 2012; Parzych, Zdunczyk, et al., 2016; Kurnaz and Cobanoglu, 2017), illustrating the suitability of these species for airborne metal biomonitoring studies. Lichens are reliable biomonitors of airborne metal pollution, even when present at very low concentrations (Kularatne and De Freitas, 2013). Metals tend to affect lichens in species-specific ways, with different bioaccumulation properties for particular lichens (Brown and Beckett, 1983; Branquinho, Brown and Catarino, 1997; Branquinho, Brown, Máguas, et al., 1997; Bergamaschi et al., 2007; Nash III, 2008; Guidotti et al., 2009; Gauslaa et al., 2016).

Metal accumulation within lichens is a complex and dynamic physiochemical process, influenced by many different factors, including tree bark pH, climatic and topographic factors (Garty, 2001). The rate of absorption, adsorption and accumulation of metals is dependent on lichen's thalli morphological features and emission source intensity (Garty, 2001). Metal-containing particles can be deposited on the lichen thallus (i.e. outer surface), by cation exchange of soluble cations and/or entrapped intra-/ intercellularly within the medulla (Garty et al., 1979; Garty, 2001; Bačkor and Loppi, 2009; Conti and Tudino, 2016).

Paoli, Vannini, Monaci, et al. (2018) reported potentially different behaviour of metals in *X. parietina*, e.g. more toxic metals (Pb and Cd) are preferentially stored extracellular, while others (i.e. micronutrients Zn and Cu) are present intracellular. Due to rain “washing-off” effects, on-thallus particulate metals tend to be higher in concentration during the summer and lower in winter (Bačkor and Loppi, 2009; Kularatne and De Freitas, 2013). Seasonal variations of trace elements in lichen thalli have also been reported for studies undertaken in Italy (Corapi et al., 2014; Vannini et al., 2017).

Lichens are able to cope with the stresses induced by metal pollution through different adaptive mechanisms, i.e. sequestration, complexation and detoxification. These processes include oxalates, extracellular phenols, lichen substances (chelation), cation binding by carboxyl, phosphate, amine and hydroxyl groups, exclusion (by the cell walls of both biotics) and intracellular accumulation within the plasmalemma. The mycobiont, which makes up 90% of total lichen biomass, is able to accumulate most metals, without being affected too seriously in relation to the photobiont (Bačkor and Loppi, 2009). Lichens are capable of producing unique lichen specific substances of which more than 800 aliphatic, cycloaliphatic, aromatic and terpenic compounds are known, which are involved in binding (or chelation) of heavy metals (Hauck and Huneck, 2007). For example, for *Xanthoria parietina*, Kalinowska et al. (2015) reported that the pigment ‘parietin’ protects the photobiont cells from cadmium excess, acting as a cortex barrier for Cd²⁺-ions. Lead (Pb) exposure further seems to impact lichen chlorophyll content and increases the production of usnic acid (in *Cladonia convulata*), which is important in detoxification/tolerance in lichens (Gurbanov and Unal, 2019). However, lichens that have been exposed to higher metal concentrations (i.e. around a landfill or around a copper smelter) recover and recolonise “lichen deserts” over a considerable time (Mikhailova, 2017; Paoli, Vannini, Fačkovcová, et al., 2018).

Moreover, metal competition for binding sites on the lichen surface might result in underestimation of some elements measured in biomonitoring studies (Paoli, Vannini, Monaci, et al., 2018). Reis et al. (1999) further introduced the “remembrance time” effect in lichens, in the sense that transplanted lichens have “memory” of elemental concentrations, which are related to atmospheric concentrations of the element and the health status of the lichen (Godinho et al., 2008, 2011; Paoli, Vannini, Fačkovcová, et al., 2018). The relationship between lichen morphology and elemental acquisition is still poorly understood and additional

factors, i.e. pH, temperature and elevation play a role in metal accumulation (Nieboer et al., 1976; Král et al., 1989; Bačkor and Loppi, 2009). For instance, decreased pH can increase the bioavailability of metals, whereas temperature and altitude increases also increase the metal uptake in lichens (Nieboer et al., 1976; Král et al., 1989; Bačkor and Loppi, 2009). These issues need to be taken into consideration when interpreting data, for example, if lichen sampling is undertaken during different times of the year.

2.4.5 Lichens and PAHs

The utilisation of the accumulative nature of lichens is advantageous compared to direct air sampling, because large volumes (over a long period of time, i.e. >24h) are necessary to detect trace-level concentrations of organic pollutants (Van der Wat and Forbes, 2015). Moreover, lichens provide an integrated value of organic pollutant levels, provide a simple and cheap sampling method and can be used where additional equipment (e.g. high-volume samplers, electricity and site access) is not practicable, e.g. remote areas (Blasco et al., 2008; Van der Wat and Forbes, 2015). Lichens have been recently used as biomonitors for atmospheric PAHs, thus biomonitoring of PAHs with lichens is less advanced than metal-related studies (Blasco et al., 2008; Shukla and Upreti, 2008; Augusto et al., 2010; Shukla et al., 2012).

Due to recent interest in persistent organic pollutants in the environment, numerous PAH related lichen studies have been undertaken in urban areas and to monitor traffic pollution around the world (e.g. India, Italy, Spain, Portugal and France) either using native species or transplanted lichens (Owczarek et al., 2001; Guidotti et al., 2003, 2009; Blasco et al., 2006; Domeño et al., 2006; Shukla and Upreti, 2009; Augusto et al., 2010; Shukla et al., 2012; Nascimbene et al., 2014; Kodnik et al., 2015).

To date, only a few studies focus on the effects of PAHs on lichen species. One of the main reason is the existence (gas-phase or bound to particles) of PAHs. Low-molecular weight PAHs (2- and 3- ring) only exist in gas phase, while 5- and 6- ring PAHs are bound to particles (high-molecular weight), PAHs with a 4-ring structure can exist in both states (Augusto et al., 2016). Augusto et al. (2015) exposed thalli of *Xanthoria parietina* (foliose lichen) to fluoranthene and benzo[a]pyrene over a period of 16 days and found migration of both PAHs into the lichen algal layer. Kummerová et al. (2006) and Kummerová et al. (2007)

demonstrated that fluoranthene is damaging the photobiont of foliose lichens *Lasallia pustulata* and *Umbilicaria hirsuta* (Augusto et al., 2016).

Lichens are useful biomonitors for atmospheric (gas-phase) PAH pollution and are able to respond quickly to increasing PAH concentrations in the atmosphere, i.e. caused by pollutant events (Owczarek et al., 2001; Blasco et al., 2006; Augusto et al., 2015). For example, PAH concentrations in *Parmelia sulcata* around a tunnel in the Central Pyrenees (France/Spain) suggested a strong traffic influence on PAH contamination (Blasco and Domeño, 2006). Guidotti et al. (2009) further showed that *Pseudevernia furfuracea* accumulates PAHs proportional to traffic density and stated that lichens (irrespective of lichen 'species') accumulate PAHs compounds of all sizes, both those bound to particulate matter and from the gas phase. Two-, three- and four-ring PAHs are primarily found in lichen PAH studies, with naphthalene (2-ring), phenanthrene (3-ring), fluoranthene and benzo[a]anthracene (both 4-ring) usually found in highest concentrations (Guidotti et al., 2009; Van der Wat and Forbes, 2015). Urban and industrial areas are characterized by high PAH deposition in lichens, with four-ring PAHs mainly in urban areas and five- to six-ring PAHs in industrial areas (Augusto et al., 2009; Shukla et al., 2012, 2014). Domeño et al. (2006) recorded 12 of the 16 EPA identified PAHs in Zaragoza (Spain), with highest concentrations recorded for benz[a,h]anthracene and benz[k]fluoranthene, followed by benz[a]anthracene, chrysene and fluorene, suggesting traffic related sources, because these PAHs are emitted from catalytic converter and non-catalytic converter vehicles (Domeño et al., 2006). *Physcia adscendens* was used in a study Rieti (Italy) around different traffic influenced areas, which concluded a correlation between total PAH concentrations in lichens and vehicular traffic levels and metal concentrations (Owczarek et al. 2001).

Shukla et al. (2012) reported a predominance of fluoranthene, acenaphthylene, and phenanthrene in lichens, indicating anthropogenic sources, namely traffic, due to dominance of low-molecular weight PAHs in Haridwar (India). Moreover, traffic was identified as main source of PAHs in biomonitoring related studies (Blasco et al., 2008; Nascimbene et al., 2014). Studies report that lichens are able to accumulate the majority of the 16 EPA-PAHs from the atmosphere, especially vapour-phase PAHs (e.g. phenanthrene, anthracene and pyrene), indicating atmospheric pollution from combustion processes (i.e. domestic heating) and vehicle traffic in urban areas and can be used for research related data

comparison (Blasco et al., 2006, 2008, 2011; Shukla and Upreti, 2009; Augusto et al., 2010; Shukla et al., 2012).

The higher ability of lichens to accumulate low molecular weight PAHs (two, three- and four-ring) is due to the higher volatility of these PAH molecules in the gasous phase and their relatively higher solubility in water and subsequent wet deposition. Lichen accumulation mechanisms for higher molecular weight PAHs are associated with PAHs adsorbed to particles and thus dry deposition (Blasco et al., 2011).

Whilst there have been a lot of PAH-related biomonitoring studies undertaken in India and Spain, France and Portugal, just one study focuses on an urban area in the UK, using transplants of the lichen *Pseudevernia furfuracea* (Vingiani et al., 2015). Additionally, just one study uses the lichen *Xanthoria parietina* and one *Physcia adscendens* to assess PAH pollution in urban areas (Owczarek et al., 2001; Domeño et al., 2006). These studies highlighted the beneficial use of lichens to monitor PAHs, with regard to potential influences (e.g. traffic emissions) and potential limitations, i.e. urban structure and climatic conditions, when comparing different urban environments (Owczarek et al., 2001; Vingiani et al., 2015).

2.5 Passive sampling devices

Air monitoring methods can be classified into four generic types, including active and passive samplers, and automatic analyser and remote sensors (WHO, 1999). For the scope of this study, only active and passive methods will be discussed hereafter. Advantages and disadvantages of both methods are displayed in Table 2-7.

Table 2-7: Advantages and disadvantages of monitoring approaches, applicable for air quality monitoring studies, with major differences outlined in detail (WHO, 1999; Tuduri et al., 2012; Pienaar et al., 2015)

	Active	Passive
Advantages	Low cost; easy to operate; reliable operation and performance	Very low cost; very simple, no electrical dependencies; deployable in large numbers; useful for screening studies
Disadvantages	Provide daily averages; labour intensive (sample collection and analysis); slow data throughput; need electricity, maintenance and trained operators; noisy and bulky equipment	Unproven for some pollutants; only provide monthly and weekly averages; labour intensive (deployment and analysis) slow data throughput
Timescale of sampling	5 min to 1 h average	1 day to 1 month average
Requirements	Electric power, shelter, security (major requirements)	No power, no field infrastructure
Network suitability	Individual monitoring site	Regional air quality survey
Human health assessment	Acute and chronic exposure	Chronic exposure

Active sampling (i.e. high-volume samplers) is the method of choice in environmental studies, applying pumps, filters (particulates) and adsorbents (gas-phase) to trap compounds of interest (Tuduri et al., 2012). In contrast, passive sampling devices usually comprise of low-cost material, do not need additional maintenance and electricity and are widely used in environmental pollution studies (Cape, 2005; Kot-Wasik et al., 2007; Zabiegała et al., 2010). In particular, they are useful for regional air quality studies to assess spatial patterns (and ‘hotspots’), which can provide guidance for continuous monitoring sites, such as automated monitoring sites (Krupa and Legge, 2000; Pienaar et al., 2015).

Different passive sampling devices are available, chosen depending upon the study scope and pollutant of interest, and include passive badge sampler, Ogawa passive sampler, cartridge-type sampler, and diffusive devices for volatile organic compounds (Krupa and Legge, 2000; Pienaar et al., 2015). ‘Palmes-type’ diffusion tubes have been widely applied in the UK, to assess variability of nitrogen dioxide (NO_2) concentrations (Cape, 2005). These will be further explored within the next section.

NO_x diffusion tubes

Passive samplers used for ambient air quality monitoring were developed in the 1970s, for instance ‘Palmes Tubes’ for nitrogen dioxide (NO_2) measurements (Palmes et al., 1976; Pienaar et al., 2015). These tubes consist of a simple closed-end acrylic tube, containing two stainless-steel grids (coated with Triethanolamine – TEA; Figure 2-10), where NO_2 is trapped as nitrate (NO_3^-) and reduced to nitrite (NO_2^-) that can be measured by spectrophotometry or Ion Chromatography (IC; (AEA Energy and Environment, 2008; Pienaar et al., 2015).



Figure 2-10: ‘Palmes Tube’ diffusion sampler (schematic overview, with dimensions) [left] and sampling tube components [right]

Palmer diffusion samplers have been widely used in the UK to measure ambient nitrogen dioxide (NO₂) since 1976 (Cape, 2005; AEA Energy and Environment, 2008). As previously presented (section 2.2.1) a general downward trend in NO_x concentrations has been recorded across Europe since the 1990s.

Within EU urban areas, the reduction of NO₂ levels is a key challenge, especially close to major roads (Casquero-Vera et al., 2019). In particular, the UK aims to reduce NO₂ emissions by 55% by 2020 (and by 73% by 2030), against the 2005 baseline (DEFRA, 2018c). However, fine-spatial variability of NO₂ concentrations in urban areas is not continuously measured, but to supplement air quality monitoring stations and to investigate if air quality targets are being met (GMCA and TfGM, 2019). The use of passive samplers can provide high quality data, in both screening and spatial mapping of air quality (Pienaar et al., 2015). However, limitations include environmental effects (i.e. temperature, wind and air humidity) impacting on analyte uptake and the full potential of passive samplers has not yet been achieved (Kot-Wasik et al., 2007).

2.6 Conclusion

Air pollution is a serious threat to public health and exposure to air pollution is linked to severe health impacts, i.e. lung cancer, stroke and heart diseases (The World Bank and Institute for Health Metrics and Evaluation, 2014; DEFRA, 2017b). Legislations and legal limits are in place to protect human health, but evidence suggests that severe health effects can still occur below these limits and improvements in air quality will have positive health consequences (WHO, 2013b; DEFRA, 2017b). Automated air quality monitoring stations are proven, high-performance methods to monitor atmospheric pollution, but in return require high skills and are costly to maintain (WHO, 1999). Furthermore, automated air quality monitoring stations are restricted in number and in fixed positions, record selected pollutants (i.e. metals and PAHs are not continuously monitored at most sites) and therefore only record local air quality. Consequently, air pollutant loadings over a larger urban area are not recorded. Urban environments and air quality are complex systems with various factors influencing spatial pollutant distribution (e.g. building heights and density, traffic counts and meteorological conditions; Endlicher, 2012; Mayer, 1999; Salmond and McKendry, 2009), showing stringent necessity to apply additional methods to achieve finer spatial detail of air quality. Easy and cost-effective methods include the use of biomonitors (e.g. lichens) and passive air sampling devices (e.g. NO_x diffusion tubes).

For instance, lichens have been used in numerous pollutant related biomonitoring studies around the world, to obtain information (quantitative and qualitative) on ecosystem characteristics (Shukla et al., 2014; Forbes, 2015). Some air pollution studies do not use a high spatial resolution approach and only focus on particular pollutants, i.e. PAH or metal concentrations (Blasco et al., 2008; Augusto et al., 2009; Dođrul Demiray et al., 2012; Kularatne and De Freitas, 2013).

This study aimed to apply a high-spatial resolution biomonitoring approach using lichens (*X. parietina* and *Physcia* spp.) sampled across the city centre of Manchester. A high spatial resolution lichen biomonitoring will contribute to a better insight into the variability of urban air quality and air pollution within the City of Manchester. This study's outcomes will be related to health concerns and can contribute to urban planning and development following identification of areas of improvement within the city of Manchester. For example, high spatial detail of deteriorated air quality can be used by local associations, i.e. Manchester's Red Rose Forest, to identify areas requiring improvement in air quality. Red Rose Forest (now: City of Trees) is an innovation to re-invigorate Greater Manchester's landscape (restoring and planting trees), with the opinion that trees are essential for a healthier, more resilient and prosperous city (City of Trees, 2018). Lichen-derived pollutant data will, in part, be ground-truthed with passive sampling devices, i.e. NO_x diffusion tubes. Combining lichen chemical data with passive air sampling measurements for NO₂ concentrations will enable testing of the veracity of the lichen datasets and assess spatio-temporal variability of NO₂ across Manchester.

2.7 The case study area – the City of Manchester (UK)

For the first half of the 19th century Manchester was one of the most polluted and overpopulated cities in England, with ~77,000 inhabitants in 1801, increasing to 544,000 in 1901, illustrating its rapid growth and importance (Williams, 1996). Around 1880 Manchester achieved fame for 'dirt, smoke and gloom' (Douglas et al., 2002:246) illustrating the historic air pollution in this area. In the following years, smokeless zones were set up and the UK's 'Clean Air Act' came into power in 1956. Decreasing levels of smoke and SO₂ helped to achieve cleaner air in Greater Manchester, ascribed as due to a decline of heavy metal industry and the use of electricity, gas and oil instead of coal burning (Douglas et al., 2002).

Increased road traffic volume within the city centre, however, resulted in an increase in lead in airborne dusts, which peaked in 1989 even though lead-free petrol legislation had been introduced in 1986. Subsequently, (suspended) particulate matter ((S)PM) and nitrogen oxides (NO_x) became the airborne pollutants of most interest in Manchester, illustrating changing air pollution issues through time (Douglas et al., 2002).

In 2016 the City of Manchester had 549,000 inhabitants, covering an area of about 11,564 hectares (Manchester City Council, 2016b, 2017), with a large population thus facing air pollution problems, i.e. associated to NO_x, metals and PAHs. About 53% of the City of Manchester's area is identified as built-up area, mainly medium density residential areas (Gill et al. 2008). Within the very complex land-use pattern of Manchester, tree cover varies between (and within) each land-use type. Industrial areas and the city centre are mainly characterized by <10% tree cover, while residential areas have a tree cover between 7-26% and parks the highest cover of 14-28% (Gill et al., 2008).

2.7.1 Air quality in the City of Manchester

European member states are obligated to establish and implement 'Air Quality Plans' (AQPs) to improve air quality in urban agglomerations, where air quality limit values have been exceeded (EU, 2008; Silveira et al., 2016). Within the UK, urban agglomerations, especially large metropolitan areas (with a population of >1.5 million) are monitoring air quality (DEFRA, 2009; OECD, 2019). These five large urban areas include, Glasgow, Leeds, London, the West Midlands urban area and Manchester (OECD, 2019), which record pollutants within automated and non-automated networks (DEFRA, 2019b).

In particular, the urban conurbation of Greater Manchester has prepared the 'Greater Manchester Air Quality Plan 2016 to 2021', by the 'Greater Manchester Combined Authority' (GMCA) and 'Transport for Greater Manchester' (TfGM) to address local air pollution and deteriorated air quality (TfGM, 2016; Greater Manchester Combined Authority (GMCA), 2018). The 'Automatic Urban and Rural (AURN) Monitoring Network' includes five locations of automated air quality monitoring stations across Greater Manchester.

Within the city centre of Manchester, two automated air quality monitoring stations (at Manchester Piccadilly Gardens and on Oxford Road; Figure 2-11) continuously record air pollution. Different air pollutants are monitored at these two stations: NO_x (NO and NO₂) and PM₁₀ at Oxford Road and NO₂, SO₂, O₃, PM_{2.5} and PM₁₀ at Piccadilly Gardens (DEFRA, 2018b, 2018a).

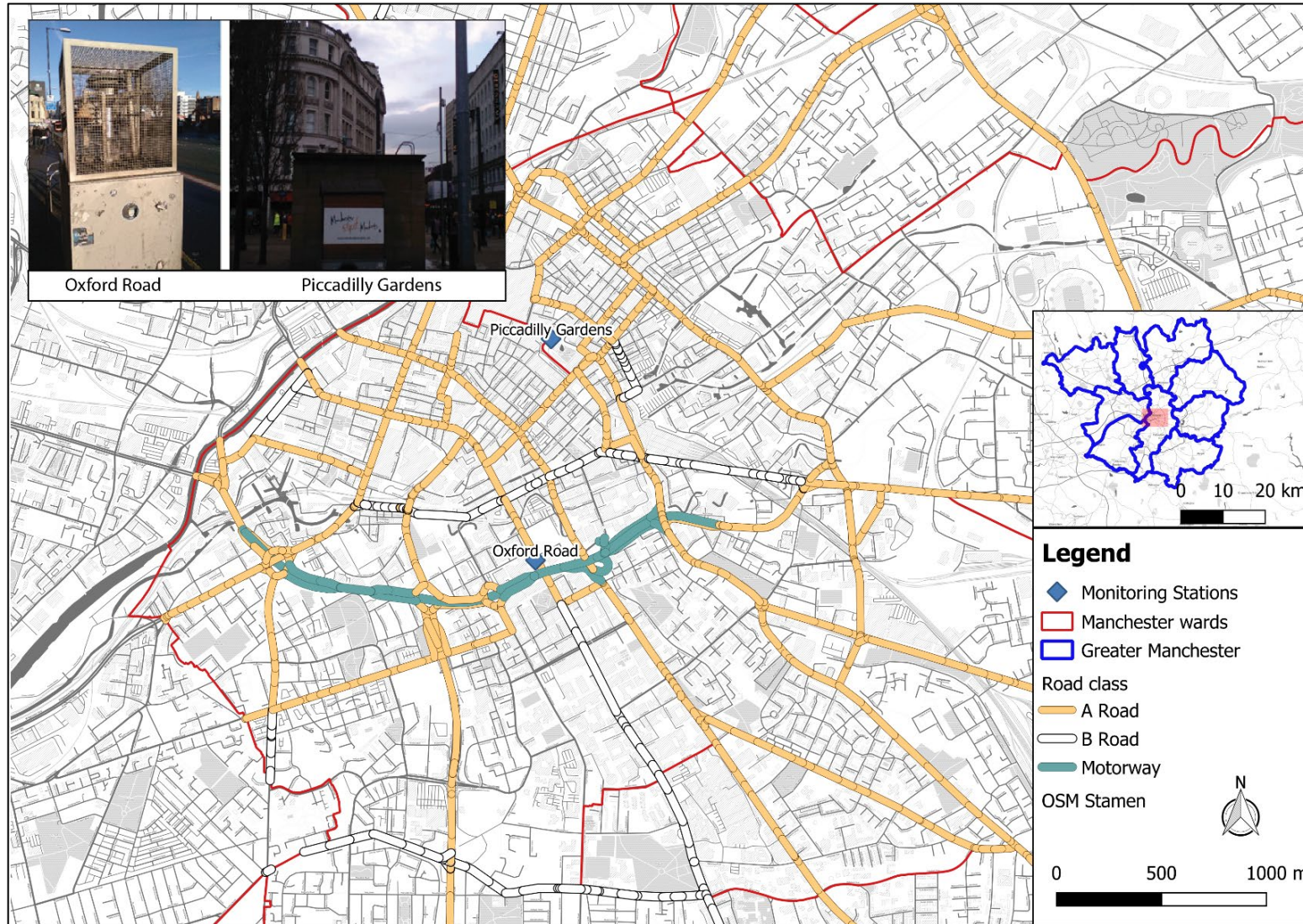


Figure 2-11: The case study area, together with automated air quality monitoring stations (Oxford Road [left] and Piccadilly Gardens [right]) and major road network in the city centre of Manchester; the study area location within Greater Manchester (inset map; blue lines represent the metropolitan boroughs) is also shown

The Oxford Road station notably exceeded the NO₂ annual limit value (40 µg/m³ EU/UK limit value) continuously from 2007 to 2019, with a 2018 annual mean NO₂ concentration of 62 µg/m³. Piccadilly Garden was below the critical value in 2018, but exceeded the limit between 2010 and 2012 (2010: 45 µg/m³; 2012: 41 µg/m³). Recent NO₂ measurements show high concentrations for both monitoring stations, e.g. 73 µg/m³ at Oxford Road and 45 µg/m³ at Piccadilly Gardens in January 2019. (Figure 2-12). Automated air quality monitoring stations are restricted in number and in fixed positions, record selected pollutants (i.e. metals and PAHs are not monitored) and therefore only record local air quality. Consequently, air pollutant loadings over the whole area of the city of Manchester are not recorded.

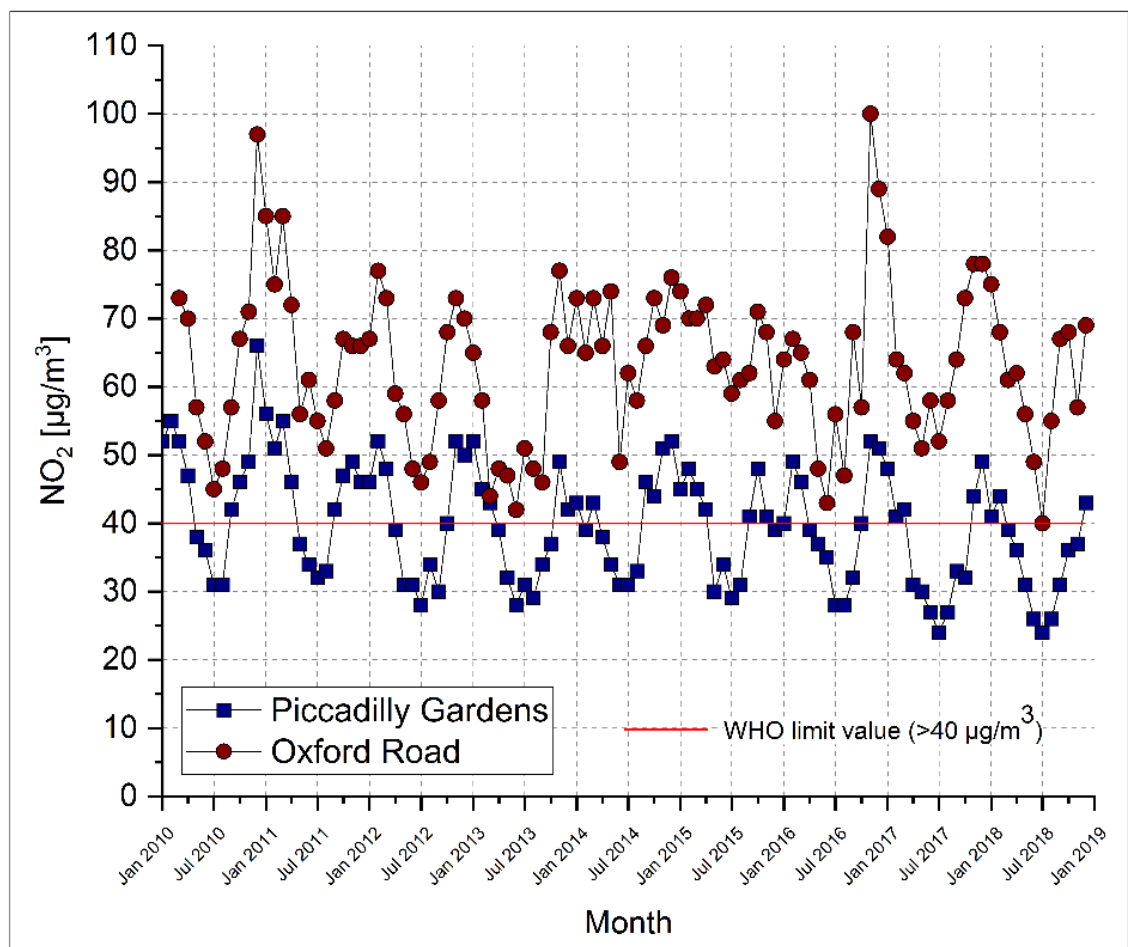


Figure 2-12: Monthly mean NO₂ [µg/m³] at monitoring stations on Oxford Road and at Piccadilly Gardens (2010 to 2018; King et al., 2016; Air Quality England, 2018b, 2018a); the WHO limit value (40 µg/m³) is also shown

Air pollution background data (removed local sources, but including transported pollutants into area) for total NO_x (as NO₂) [µg/m³] were obtained from UK Air (UK Air: background mapping for local authorities, reference year 2017, (DEFRA, 2017d) for the wards of Manchester, in a 1x1km resolution (Figure 2-13).

Background maps provide estimates of background concentrations for specific pollutants, including NO_x, NO₂, PM_{2.5} and PM₁₀ (by source sector, i.e. transport industry and domestic), which include meteorological and ambient monitoring data. (DEFRA, 2014a, 2017d). They can be used in air quality assessments for a better understanding of the contribution of local sources to total pollutant concentrations.

Total NO_x for 2017 includes all source sectors and emission projections of NO_x for road transport, NO_x emission assumptions for EURO 5 and 6 vehicles and light-goods vehicles (LGVs) and assumptions for road transport forecasts (DEFRA, 2014a, 2017c). NO_x data for 2017 was entered into geographic information system (GIS); points were converted to a grid (rasterized, 1x1km size), to create a NO_x pollution map (Figure 2-13). Total NO_x pollution throughout the city of Manchester varies between 9.5 to 52 µg/m³ (2017), with highest pollution around the city centre and the airport). Surrounding Greater Manchester districts, e.g. Salford, Rochdale and Trafford are included on the map and might influence NO_x pollution in Manchester. The annual mean concentrations of NO₂ of 40 µg/m³ was set by the World Health Organization to protect the public from health effects of (gaseous) NO₂ (WHO, 2006). Within the city centre of Manchester this value is exceeded (Figure 2-13). To analyse the distribution of NO_x for Manchester at a high resolution, sampling across a range of NO_x concentrations with focus on the city centre area is undertaken, to address spatial variability.

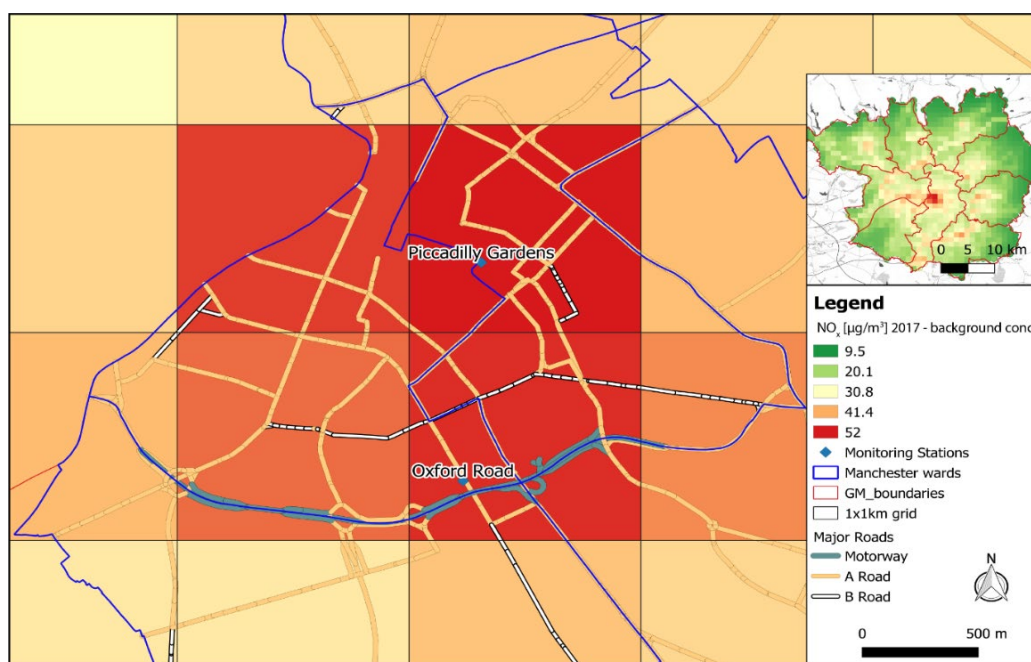


Figure 2-13: Total NO_x [µg/m³] pollution map (sum of all sectors for 2017) for the City of Manchester (and bordering districts) – displayed as 1x1km raster data (QGIS 3.4.2; DEFRA, 2017b)

For PAHs, Lohmann et al. (2001) have shown that, even on a local UK urban scale, atmospheric PAH concentrations (and mixtures) are extremely heterogeneous, resulting from numerous and varied PAH sources in urban environments. Between 1991 and 1995 PAH concentrations (using high-volume air samplers, with glass fibre filters and two polyurethane foam plugs) in the City of Manchester decreased (Figure 2-14), due to controls on domestic fossil fuel and coal use (Halsall et al., 1993; Coleman et al., 1997; Howsam and Jones, 1998).

Recent measurement at 'Manchester Law Courts' (Easting/Northing: 383375, 398260; UK Air ID: UKA00185) of PAH concentrations by 'PAH Andersen sampler' are available for the quarter (Q) of 2010, 2011 and 2013 to 2014 (only Q1; Figure 2-15). 3-ring PAHs (i.e. acenaphthylene, fluorene and anthracene) represent major PAHs measured in Manchester, of which phenanthrene was present at highest concentrations ranging from >1 ng/m^3 to 11 ng/m^3 for the analysed years. PAHs, consisting of 4-rings ranged from 1.66 ng/m^3 to 4.42 ng/m^3 (Σ 4-rings) and were present at higher concentrations in Manchester. 5- and 6-ring PAHs were measured at lower concentrations (<1 ng/m^3) for all quarterly measurements. Figure 2-15 illustrates that PAHs are present in Manchester air, even at low concentrations. However, no further published data are available for more recent years such that monitoring of more recent airborne PAH concentrations is necessary as part of a contemporary air pollution and air quality study.

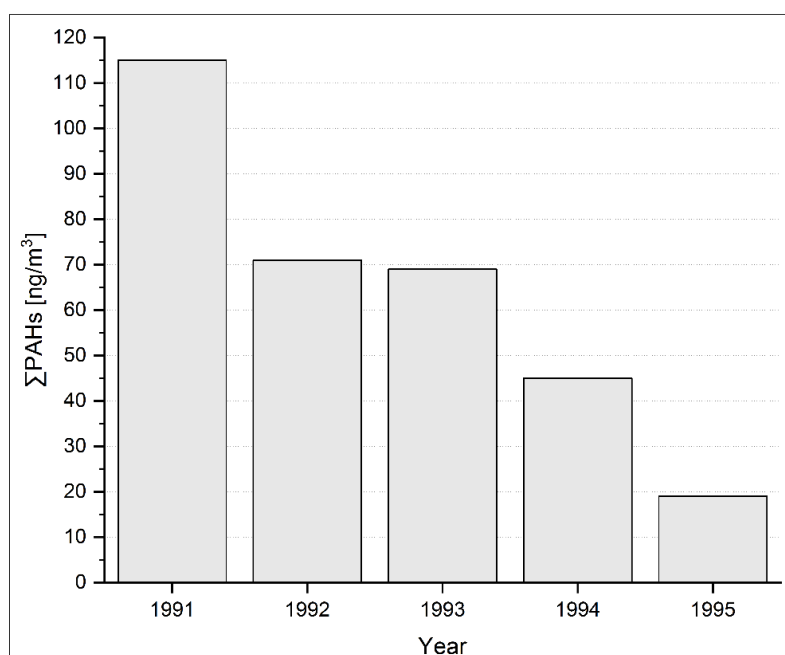


Figure 2-14: Σ PAH concentrations in air for the urban centre of Manchester (measured at Manchester Law Courts') for the years 1991 to 1995 (Coleman et al., 1997; Howsam and Jones, 1998)

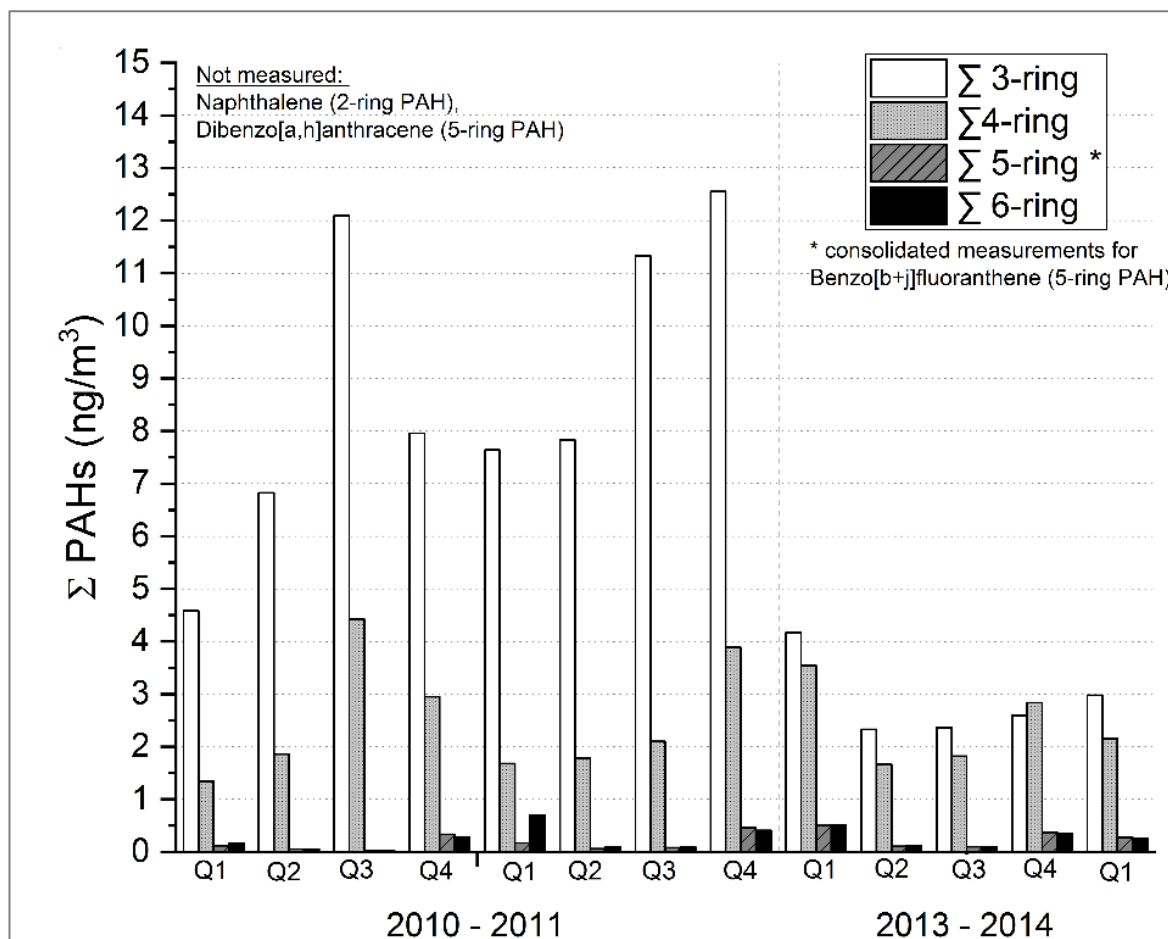


Figure 2-15: Recent quarterly measurements (Q) of PAH concentrations (particulate- and gaseous-phase) at Manchester Law Courts for the years 2010 to 2011 and 2013 to 2014; PAHs have been classified by number of rings; naphthalene and dibenzo[a,h]anthracene were not measured, benzo[b]fluoranthene is included with benzo[j]fluoranthene (DEFRA, 2014b)

As the City of Manchester continues to fail to meet the EU NO_x limits and ammonia is still a widespread problem, it is necessary to obtain more information on the distribution and spatial and temporal variation of different nitrogen compounds throughout the city, using different monitoring approaches, including lichen biomonitoring (for N contents and nitrogen speciation) and passive air sampling methods (NO_x diffusion tubes).

Within the city centre of Manchester, the occurrence of lichen species (i.e. *X. parietina* and *Physcia* spp.) indicates “better” living conditions for lichens, but also indicates an influence of nitrogen compounds due to the nitrophilous nature of the lichen species. The lichens used for this study (*X. parietina* and *Physcia* spp.; see section 2.3) are common and can be found in urban environments, because of their toxitolerance concerning specific pollutants and their preferred habitats. Therefore, both lichens are useful biomonitors for the study of air pollution in the city of Manchester.

This study will contribute to evaluate spatial variability of air quality across Manchester. To assess the influence on both, lichen species and human health, it is necessary to monitor NO_x concentrations in and around the city centre at a high spatial resolution. For instance, Vingiani et al. (2004) and Watmough et al. (2014) reported nitrogen accumulation in lichens (in the urban area of Naples, Italy and Ontario, Canada), due to NO_x/NO₂ and NH₃ pollution. Davies et al. (2007) found similar influences of NO_x on lichen abundance in the urban environment of London. Atmospheric NH₃ concentrations are also considered to effect epiphytic lichen vegetation (i.e. abundance and distribution) ;Van Herk, 1999; Frati et al., 2006), as high concentrations (of NO₂ and NH₃) can be toxic to biota (Camargo and Alonso, 2006; EU, 2008; Watmough et al., 2014).

High nitrogen contents in lichens may reflect higher ambient NO₂ concentrations and reflect long-term concentrations at the particular site, allowing the use of NO_x diffusion tubes to ground-truth lichen data. Within urban environments, pollutant concentrations change temporarily, but toxictolerant (or resistant) lichens (i.e. *Xanthoria parietina* and *Physcia* spp.) have extensive geographical ranges, allowing pollution gradient studies over large areas (Shukla et al., 2014). Further lichen samples were analysed for N-contents, nitrogen isotope ratios, ammonia and nitrate, to obtain a spatial distribution of nitrogenous compounds across Manchester. NO₂ and NH₃ are declining rapidly from the source (i.e. road transport) and sampling across a range of distances from road is necessary to display variability in nitrogen pollution throughout Manchester.

Airborne metal concentrations are not continuously monitored across Manchester, but several sources have been identified in urban environments, especially related to vehicular sources, i.e. petroleum and coal combustion (for Pb), tyre and engine wear (for Zn, Mn, Cd, Cr and Ni), vehicular abrasion and corrosion (for Zn, Cd and Fe), brake linings, lubricating oils and alloys (for Zn, Cd, Cu, Mn and Cr; Taylor, 2006). Lichen have been proven and reliable biomonitors for airborne metal concentrations (section 2.4.4) and could provide additional information on spatial variability throughout Manchester, identifying areas of particular health concern.

PAH concentrations in Manchester are not continuously measured, illustrating the necessity of applying additional methods, i.e. lichen biomonitoring. Lichen PAH concentrations could provide additional information on spatial variation of PAH concentrations in Manchester (section 2.4.5). Further, PAH ratios can be used for potential source apportionment of PAH concentrations affecting lichen pollutant loadings. Moreover, the lichen PAH profile can be used to assess the toxicity of PAHs recorded across Manchester and provide beneficial information on potential health impacts.

2.7.2 Meteorology and weather in (Greater) Manchester

The Northwest of England is characterised by distinct geographical regions, with plain areas (<150 m) west of the Pennines. Manchester, as one of the major population centres is located close to the Pennines, rising to about 600 m, forming a natural barrier in the East. Thus climatic conditions of great variety can be found in the NW of England, including the coldest and wettest place in England (Met Office, 2015).

Annual mean temperatures vary between 9°C to 10.5°C in the region, with January usually being the coldest month and July the warmest. May is the sunniest and December the dullest month in the NW, while sunshine hours vary between 1,200 to 1,500 hours (annual average sunshine duration) in the NW of England. Precipitation is associated with Atlantic depressions (westerly maritime air masses), which are more vigorous in autumn and winter, thus most of the rain falls in these seasons. Manchester often referred to as ‘the wet city’ has an average annual of 830 mm each year (Met Office, 2015). The NW of England is among the more wind exposed parts of the UK, due to its proximity to the Atlantic and large upland areas. Wind directions are also related to Atlantic depressions (similar to precipitation) that typically blow from the south or southwest, later from north to north-west as the air masses move. Spring winds tend to blow from the north-east, while summer tend to have frequent winds from north-west or west (Met Office, 2015).

Dispersion and removal of atmospheric pollutants is governed by local meteorological conditions (Hertel and Goodsite, 2009). Manchester’s urban climatic conditions are influenced by its urban structure, i.e. ‘fresh air corridors’ such as rivers and large roads, building structures (e.g. height and density), building materials and urban green (Salmond and McKendy, 2009; Endlicher, 2012; Trees & Design Action Group, 2012; Salmond et al., 2013).

Therefore, air quality and atmospheric pollution may vary spatially (and temporally) across the research area, which might be reflected by lichen pollutant loadings and passive monitoring devices.

Sampling altitude (geographical variation) in combination with additional factors (i.e. meteorology, local pollution and soil dust; Shukla and Upreti, 2014) also might affect lichen pollutant loadings and stable-isotope ratio (Batts, 2004; Shukla et al. 2013). This was not considered here, as the research area was focussing on the city centre area with a 'flat' extent and meteorological data as well as the urban surrounding (section 2.7.4) being considered more influential on air quality across Manchester.

Climatic data for Manchester (i.e. temperature [$^{\circ}\text{C}$], total precipitation [mm], wind direction [$^{\circ}$] and wind speed [m/s]) was obtained from the 'Whitworth Meteorological Observatory' (Longitude: N53.467374, Latitude: W2.232006, Altitude: 43m), with permission from Dr Michael Flynn (personal communication: January 2018), located at the University of Manchester (Whitworth Meteorological Observatory - Data Archive, 2018). Data was obtained for July 2017 (01/07/2017) to June 2018 (30/06/2018), as this was deployment period for NO_x diffusion tubes and wind, precipitation and temperature may influence passive monitoring devices performance (Heal et al., 2000; Kirby et al., 2000, 2001; Cape, 2005; AEA Energy and Environment, 2008). Temperatures for the NO_x tube deployment period varied from 3.50°C (February 2018) to 16.94°C (July 2018; Figure 2-16). The lowest recorded temperature was recorded on the 28th of February 2018 while the highest temperature was recorded on the 26th of June 2018 (Figure 2-18). Precipitation [mm] and sunshine duration [hours] were diverse throughout the months of deployment. Most precipitation (total mm) fell in September 2017 (with 124 mm), December 2017 (with 111 mm) and January 2018 (with 115 mm). The driest months were May and June, with 29 mm and 14 mm, respectively (Figure 2-16). Sunshine hours ranged from 10.17 hours in December 2017 to 221.82 in May 2018 (Figure 2-16). Mean wind speeds [m/s] recorded at the Whitworth Observatory varied between 2.50 m/s (9 km/h) for May 2018 to 4.01 m/s (14 km/h) for October 2017. Major winds during the deployment time arrived from south-westerly, westerly and north-westerly directions, and to a minor extent from north-east to east (Figure 2-17).

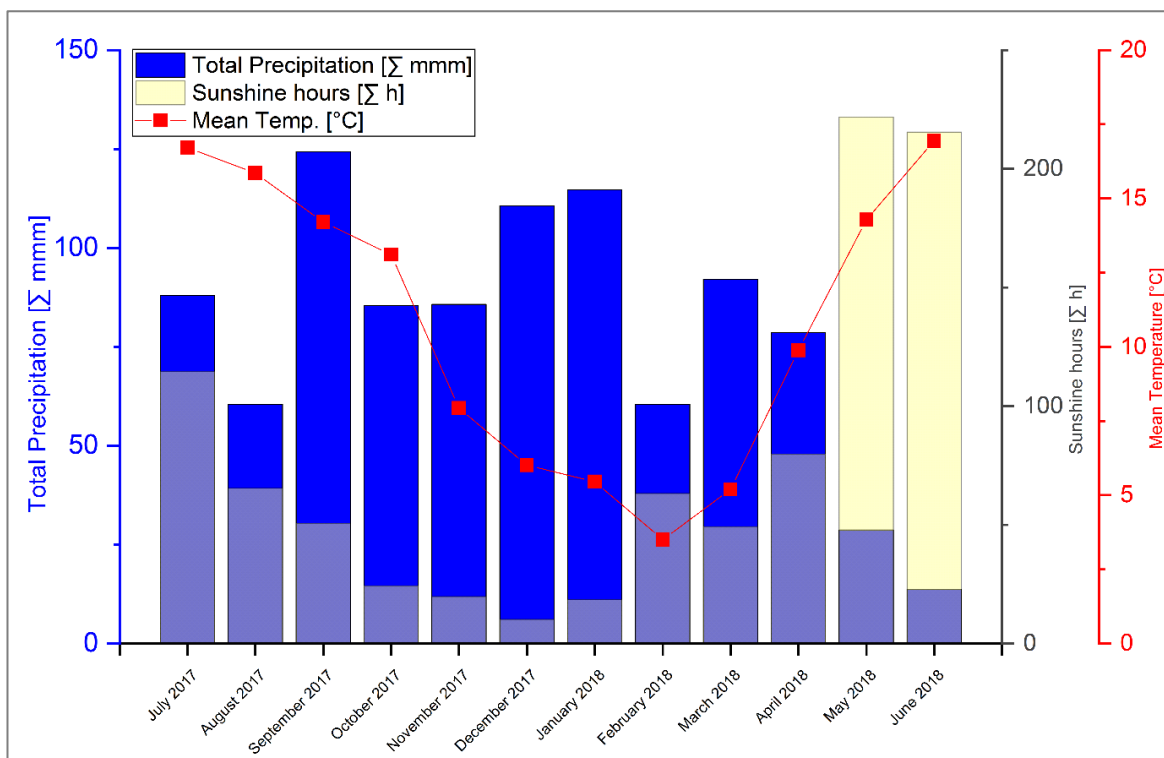


Figure 2-16: Monthly mean temperature [°C], total precipitation [Σ mm] and sunshine hours [Σ hours] for the NO_x deployment period of NO_x diffusion tubes in Manchester, obtained from the Whitworth Meteorological Observatory

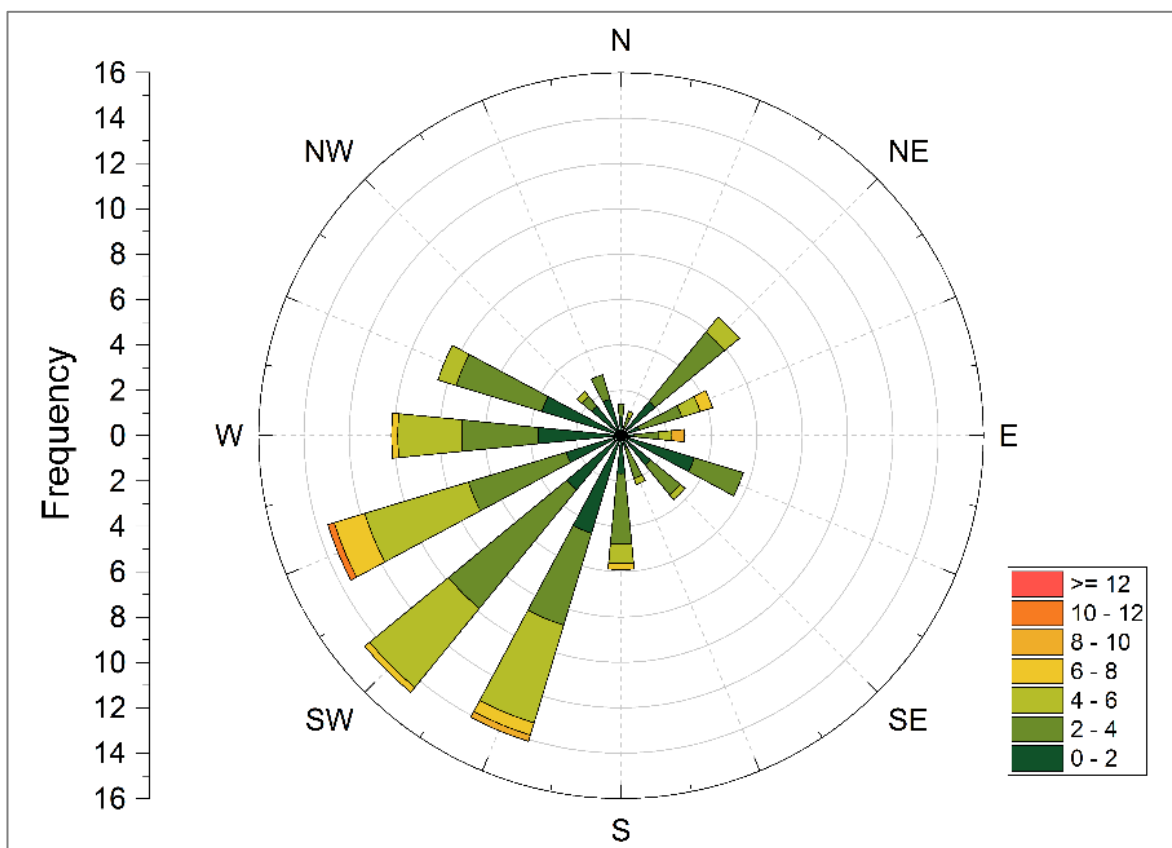


Figure 2-17: Mean wind direction (frequencies) for Manchester during the NO_x deployment period (01/07/2017 to 01/07/2018)

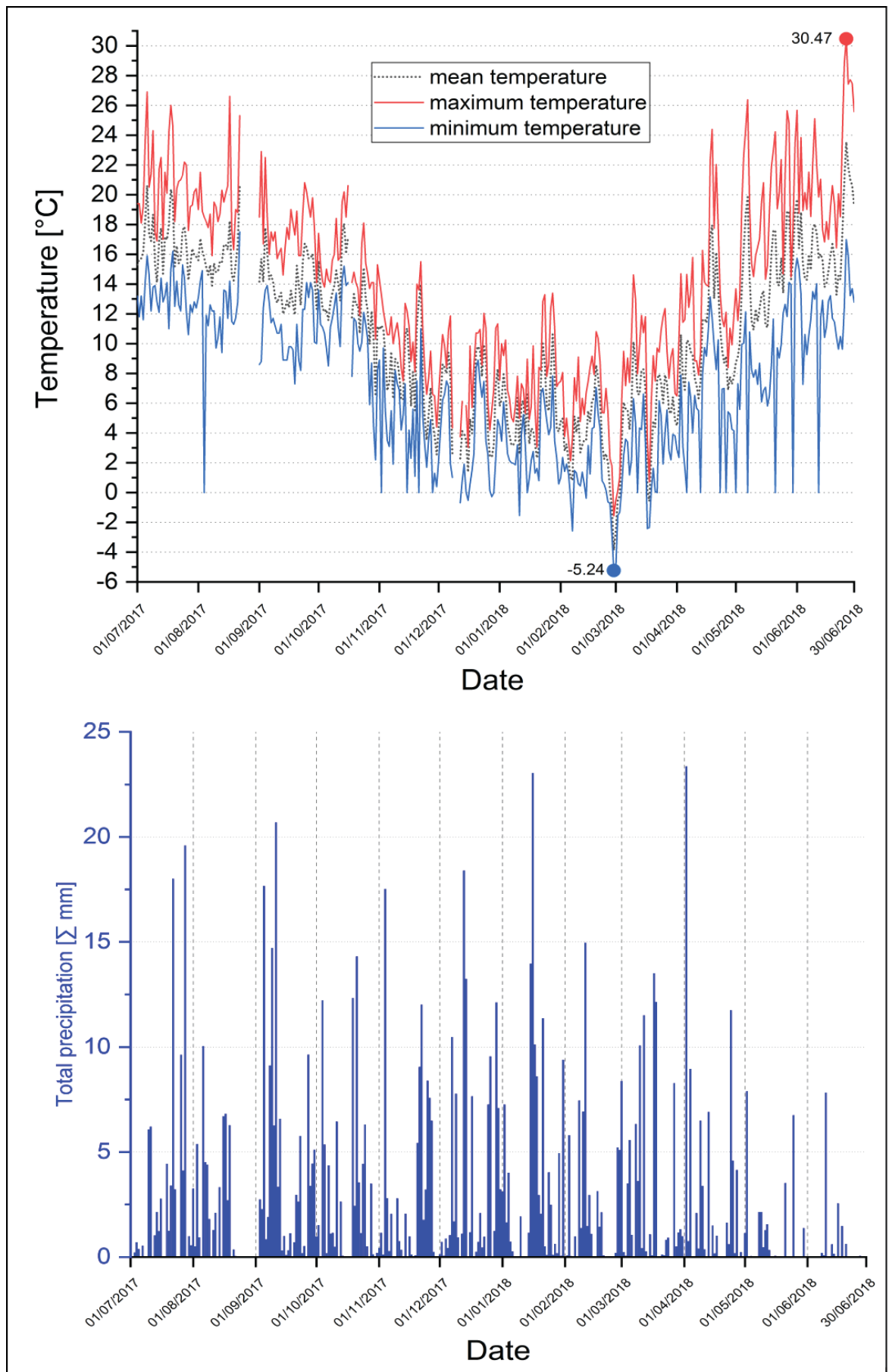


Figure 2-18: Temperature [$^{\circ}\text{C}$] (minimum, maximum and mean; with lowest and highest temperatures) and total precipitation [Σ mm] displayed as day-by-day data for the NO_x deployment period

2.7.3 Population and health characteristics of the City of Manchester

Manchester, as the centre of the Greater Manchester conurbation is characterised by diverse demographic characteristics (e.g. inhabitants, population density and age structure), built structures (i.e. buildings density and heights) and road networks (i.e. motorways, A- and B-roads). Population growth in Manchester has been mainly concentrated within the city centre and surrounding wards, which is expected to increase in the next five years, indicating additional residential developments and potential factors influencing and impairing air quality (Manchester City Council, 2017). Air pollutants affect the whole population of Manchester, but infants, children and older people are particularly identified as populations at high risk (Peled, 2011). Achakulwisut et al. (2019) reported that 19% of childhood asthma within the UK is related to air pollution (especially by NO₂).

Manchester has the highest national rate (per 100,000; compared to national average) of premature deaths regarding cardiovascular diseases (about 1.9 times higher), cancer (about 1.6 times higher) and respiratory diseases (about 2.5 times higher) in England (Manchester City Council, 2017; Regan, 2018). Moreover, childhood hospital admissions for asthma (1st rank in England) and emergency 'Chronic Obstructive Pulmonary Disease (COPD)' hospital admissions (ranked 4th in England; over twice the national rate) illustrate major public health issues in Manchester (Regan, 2018), that are closely linked to poor air quality. Additionally, Manchester Oxford Road (location of an automated monitoring station; Figure 2-11) is one of the busiest bus routes in Europe and NO₂ distribution in Manchester is mainly associated with arterial roads leading into the city centre (Martin et al., 2011; Office for National Statistics, 2013; Manchester City Council, 2016a; Regan, 2018).

Although, many people travel into the city centre of Manchester, to work, shop and/or other leisure activities and are exposed to air pollutants in that area and their 'home wards'. Main bus routes, tram and railway lines are leading into the city centre of Manchester contributing to additional pollution, with Piccadilly Gardens as the main bus station. Close to the bus station, an automated monitoring station (Figure 2-11) is located, recording NO₂, SO₂, O₃, PM_{2.5} and PM₁₀, but no PAHs and airborne metals are recorded. Thus indicating the necessity for additional approaches.

2.7.4 Building and road structures within the City of Manchester

Manchester's building structures, especially building height is diverse throughout the city; with the highest buildings usually found in the city centre (Figure 2-19). The so called 'urban core' is characterised by high density built environment and hard surfaces (James and Bound, 2009). Urban design (e.g. building heights and construction materials) affects the urban microclimate, resulting in increased atmospheric surface temperatures (urban heat island, UHI), alteration of wind regimes (e.g. velocity and direction) and transport and dispersion of local (and regional) air pollution (Salmond and McKendry, 2009; Endlicher, 2012; Abd Razak et al., 2013). Especially at pedestrian-level, wind plays a major role in the dispersion of traffic-related pollutants and is dependent on the surrounding building configuration, i.e. height, width, building arrangements and density (Kubota et al., 2008).

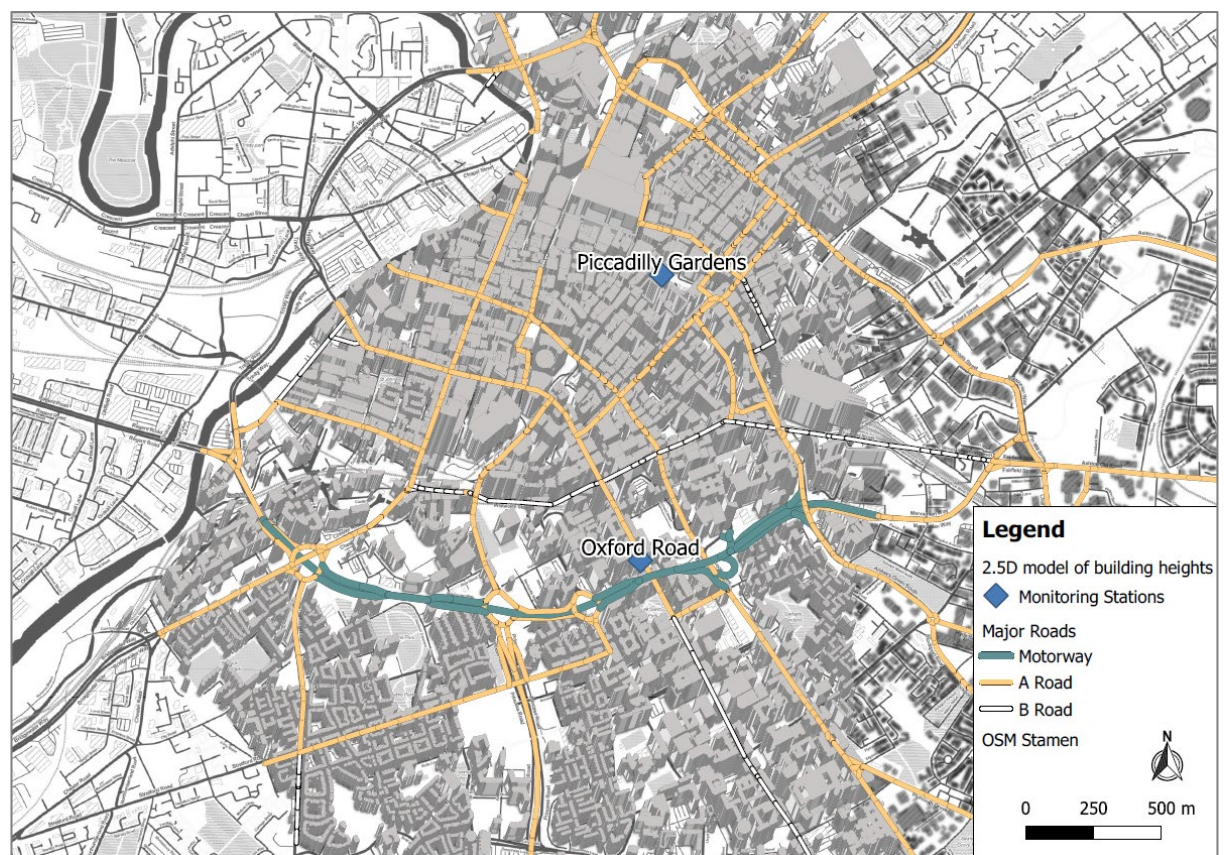


Figure 2-19: 2.5D model of building heights (OS Building Heights; Digimap - Ordnance Survey, 2017) across Manchester, displayed with automated monitoring stations and major road network

Dispersion of pollutants in urban agglomerations is determined by complex transport and mixing processes in the street network. Street canyons, roads bounded by parallel buildings, influence the urban climate and in particular the dispersion of air pollutants (Dobre et al., 2005; Eliasson et al., 2006).

Wind flows in street canyons are affected by the orientation (wind direction and solar radiation), height-to-width ratio, lengths (distance between road intersections) and symmetry of the canyon, resulting in different distribution patterns of airborne pollutants (Dobre et al., 2005; Salmond and McKendry, 2009).

Road classes in the study area include motorways (M), A roads (A), B roads (B) and unclassified (U) roads (UK Department of Transport, 2012). Vehicle counts in the presented area (Figure 2-11) are characterised by high counts on the Mancunian Way (A57(M) - motorway), ranging from approx. 36,000 (East slip road) to 93,500 (close to Oxford Road monitoring station) and 49,000 (West slip road). These numbers indicate the importance of the 'Mancunian Way' as connection road within the city of Manchester. Another Hotspot of vehicle counts (all vehicles) is located in the northern part of the centre around (A road; Greater Ancoats Street) and other A-roads (i.e. Oldham Road, Rochdale Road) leading into the city centre, with an annual daily traffic flow between approximately 20,000 to 35,000 vehicles (DfT, 2017a). Piccadilly Gardens is a major transport hub for buses and trams and work, travel and leisure for a large amount of people in Manchester, it is necessary to assess air quality in this area for further health relevant pollutants (i.e. PAHs and metals), additionally to the already recorded pollutants by automated monitoring station. The bus station at Piccadilly Gardens is the main meeting point for most bus routes leading into Manchester, with about 3,700 buses daily and about 208.5 million customers each year (2015/16) (Manchester City Council, 2016a; DfT, 2017a). Buses are responsible for 14% of NO_x emissions in Greater Manchester (TfGM, 2016), with regard to used fuel (i.e. diesel or natural gas) and filtering technology, e.g. diesel particulate filter or hybrid diesel-electric (Cooper et al., 2014). Since 2009 ('Green Bus Fund') the bus fleet composition in Manchester was altered with 298 low-emission vehicles, primarily hybrid diesel-electric, with continuing improvements planned (TfGM, 2016).

Other important factors regarding vehicle emissions include traffic lights and (average) traffic speed in the research area, resulting in idling or congested traffic and therefore altered pollutant emissions (EPA, 2008; Hu et al., 2009; Alam and Hatzopoulou, 2014). Figure 2-20 illustrates average vehicle speed during the AM and PM peak in the city centre area of Manchester, to indicate diurnal episodes of potentially elevated pollutant concentrations.

This in connection with the idling traffic emissions display possibly increased emissions of vehicular traffic, especially during rush-hour times in the morning and evening. Table 2-8 indicates the emissions of different vehicle types during idling, e.g. on traffic lights or during congestion. Especially diesel-fuelled vehicles are responsible for high amounts of NO_x emissions during idling traffic, compared to other vehicle and fuel types (EPA, 2008).

Table 2-8: Idling traffic emissions by pollutant and vehicle type (extract) (EPA, 2008)

Pollutant	Units	LDGV	LDGT	HDGV	LDDV	LDDT	HDDV
VOC	g/hr	2.68	4.04	6.50	1.37	2.72	3.46
	g/min	0.05	0.07	0.11	0.02	0.05	0.06
THC	g/hr	3.16	4.84	7.26	1.35	2.68	3.50
	g/min	0.05	0.08	0.12	0.02	0.05	0.06
CO	g/hr	71.23	72.73	151.90	7.02	5.85	25.63
	g/min	1.19	1.21	2.53	0.12	0.10	0.43
NO_x	g/hr	3.52	4.07	5.33	2.69	3.71	33.76
	g/min	0.06	0.07	0.09	0.05	0.06	0.56

VOC = volatile organic compounds
THC = total hydrocarbons
CO = carbon monoxide
NO_x = nitrogen oxides

LDGV = light-duty gasoline-fuelled vehicles
LDGT = light-duty gasoline-fuelled trucks
HDGV = heavy-duty gasoline fuelled vehicles
LDDV = light-duty diesel vehicles
LDDT = light-duty diesel trucks
HDDV = high-duty diesel vehicles

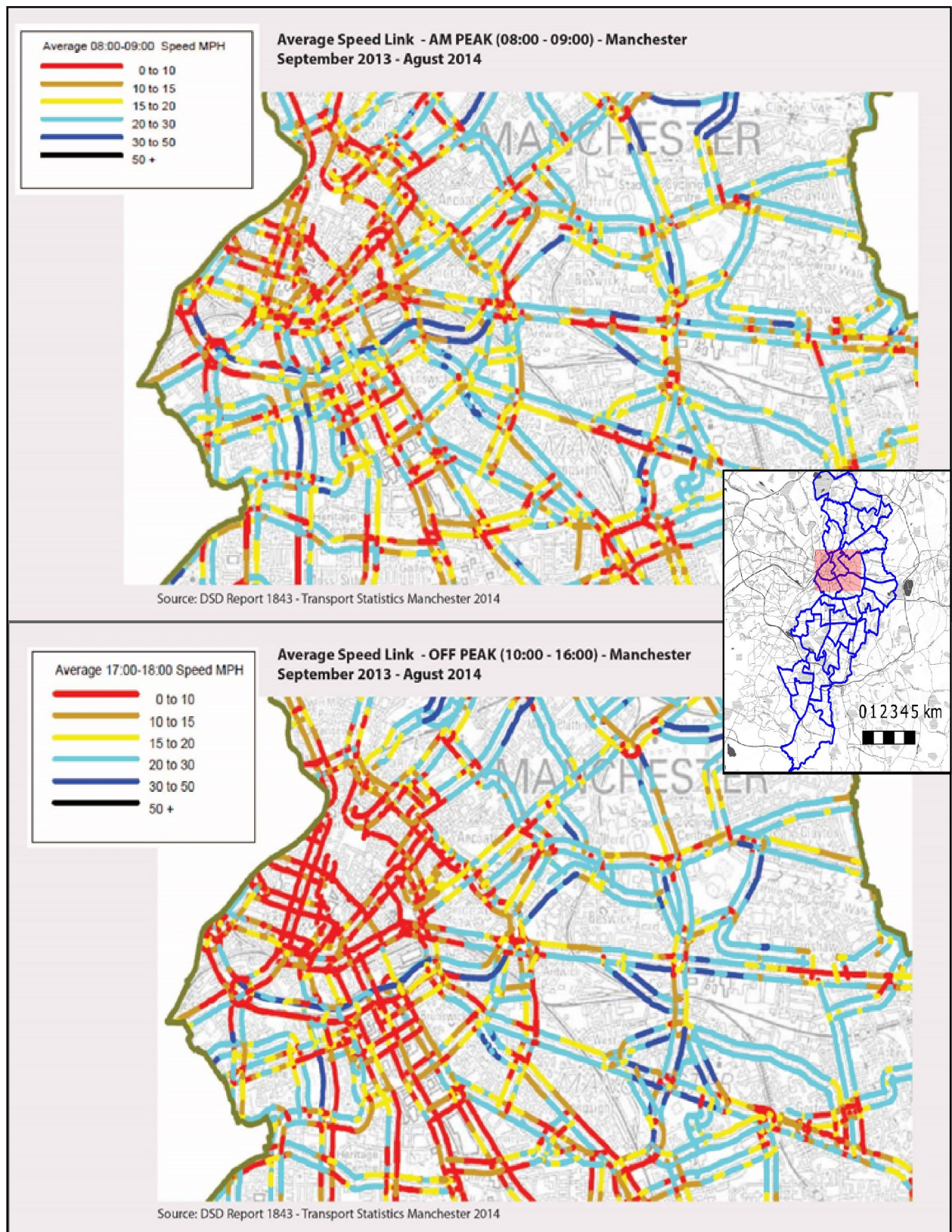


Figure 2-20: Average traffic speed – AM and PM peak (Sept. 2013 to Aug. 2014) on the primary road network in Manchester, indicating potentially high traffic emissions (Highway Forecasting and Analytical Services, 2015); inset map shows the wards belonging to the Manchester City Council

In the UK, motor vehicles are responsible for >50% of NO_x emitted into the atmosphere and account for 80% in Manchester alone, particularly diesel light duty vehicles, i.e. cars and vans (Air Quality Expert Group, 2004; Cape et al., 2004; TfGM, 2016; Regan, 2018). Given the information of traffic hotspots as well as slow-moving traffic (Figure 2-20), it is shown, that the city centre of Manchester is influenced by traffic-related emissions, such as: carbon, nitrogen (including NO_x and ammonia/ammonium) and sulphur compounds, metals and PAHs (Air Quality Expert Group, 2004; Cape et al., 2004; Kirchner et al., 2005; Davies et al., 2007).

The increased amount of traffic, including public transport (i.e. buses, trams and trains) within the city centre, indicate its importance for Manchester. Automated monitoring stations are located within the city centre area, but only provide 'local' air quality information. Elevated pollution levels are expected to occur within the complex area of the city centre that need further investigation. Furthermore, emitted pollutants are affected by meteorological, mixing and transportation conditions, making it necessary to monitor pollutants at a finer scale in order to relate it to possible health impacts. Figure 2-21 displays the identified sampling area, based on the input data (i.e. NO_x 2017 [$\mu\text{g}/\text{m}^3$]), with point sources (including main pollutant) and road types (excluding traffic counts). The identified sampling area depicts a SW - NE transect across central Manchester, including different land-use types (e.g. town centre, residential areas, manufacturing and open green spaces) and availability of trees for sampling.

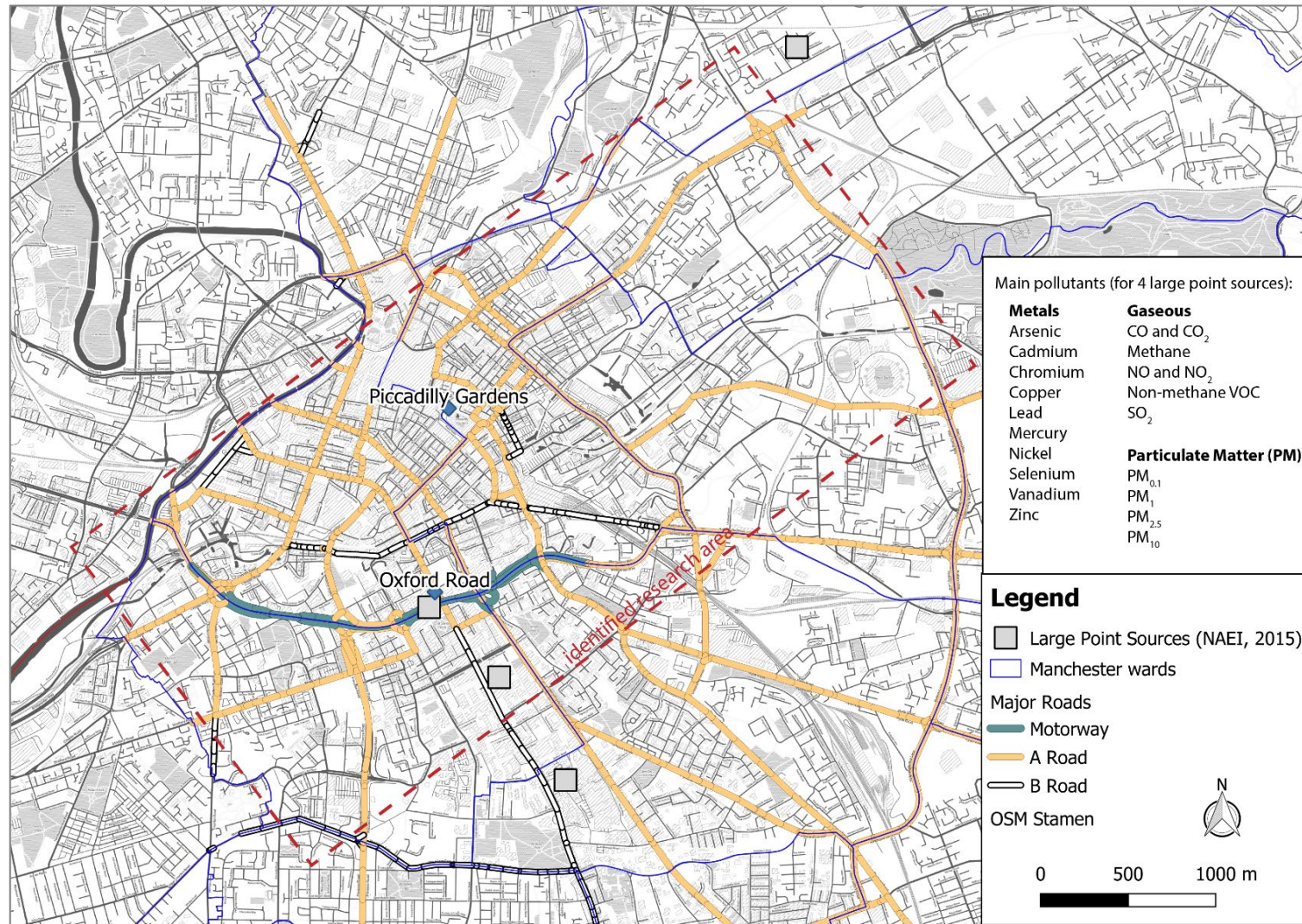


Figure 2-21: Identified research area for the city centre of Manchester, including point sources (and main pollutant; NAEI, 2013) and major roads (including A- and B-roads and motorways; UK Department of Transport, 2012)

2.8 Methodological Framework – sampling site identification, lichen sampling and geo-statistical modelling approach

The identified research area was described and sampling sites had to be identified within the city centre. This section aims to illustrate the methodology used to assess air quality in Manchester, using a high-spatial resolution biomonitoring approach. Figure 2-22 illustrates the methodological framework, including a schematic outline of the lichen sampling and analysis process, as well as the use of secondary datasets (i.e. major road network, traffic counts, building heights, large point sources and greenspaces) that were used to investigate urban influences on spatial variability of air quality.

The following sections outline the sampling site identification (section 2.8.1) lichen sampling procedure (section 2.8.2) prior to chemical analysis and geospatial modelling approaches (section 2.8.3), including used datasets and justification of data classification for analysis. Further statistical and spatial analysis will be described and discussed in the relevant pollutant chapters.

High spatial resolution of air quality in Manchester

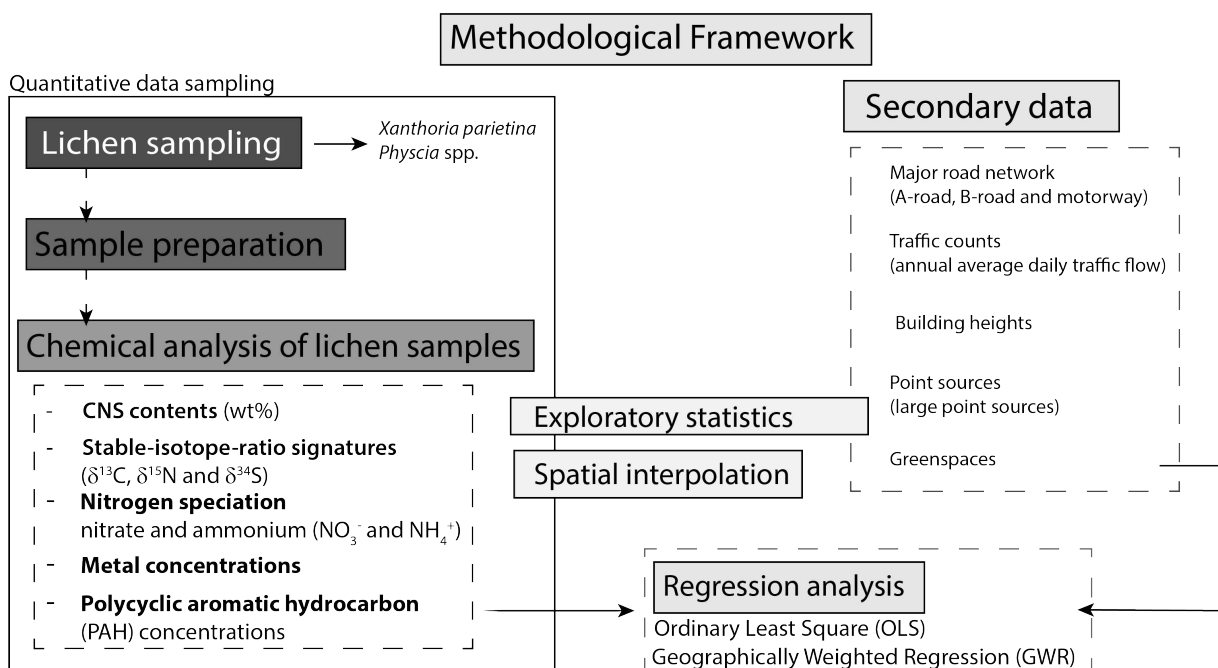


Figure 2-22: Methodological framework to assess high spatial resolution of air quality of Manchester, including the sampling procedure (schematic) and the use of secondary data to explore spatial variability of lichen-derived pollutant loadings

2.8.1 Identification of sampling sites within the city centre of Manchester

This section presents the framework on how potential sampling sites for lichens (*X. parietina* and *Physcia* spp.) were identified. Two information sources were used to identify suitable air pollution sampling sites, NO_x air pollution background maps (for 2017; section 2.7.1, Figure 2-13) and street tree locations (with potentially available lichen species – *X. parietina* and *Physcia* spp.), upon which a random stratified sampling method was based to select sampling sites.

Additional datasets were obtained from public domain sources to understand the urban context, including traffic volumes and road classes, as well as building heights, greens paces and large point sources (Table 2-9). Data was used to further investigate spatial distribution of lichen pollutant loadings, which is described in more detail in section 2.8.3.

Table 2-9: Datasets used to investigate the urban context of Manchester, including source for each dataset; data was used for geo-spatial modelling (further presented in section 2.8.3)

Category	Dataset
Major road classes	Major road class – A- and B-roads and motorways (Digimap - Ordnance Survey, 2016)
Traffic counts	Annual Average Daily Traffic Flow (AADF) 2017 (DfT, 2017a) – all vehicles
Large point sources	National Atmospheric Emission Inventory (NAEI) – Emissions from large pollution sources (commercial and industrial; NAEI, 2015)
Greenspace	OS Greenspaces (Digimap - Ordnance Survey, 2018)
Tree database	Manchester City Council/City of Trees (City of Trees, 2018)
Building heights	OS Building Heights (Digimap - Ordnance Survey, 2017)
Height/Width ratio	Street width measured using Google Earth
Street canyon	Ratio between mean building height and street width

The tree database is used by permission of Manchester City Council/City of Trees. The dataset is available as percentage of trees in a specific urban morphology type (UMT)/ land-use type throughout the City of Manchester (Figure 2-23b). Moreover, tree audits (Phase one and 2) undertaken by the organisation Red Rose Forest (now City of Trees) provide information about tree coverage across Manchester wards (Figure 2-23a).

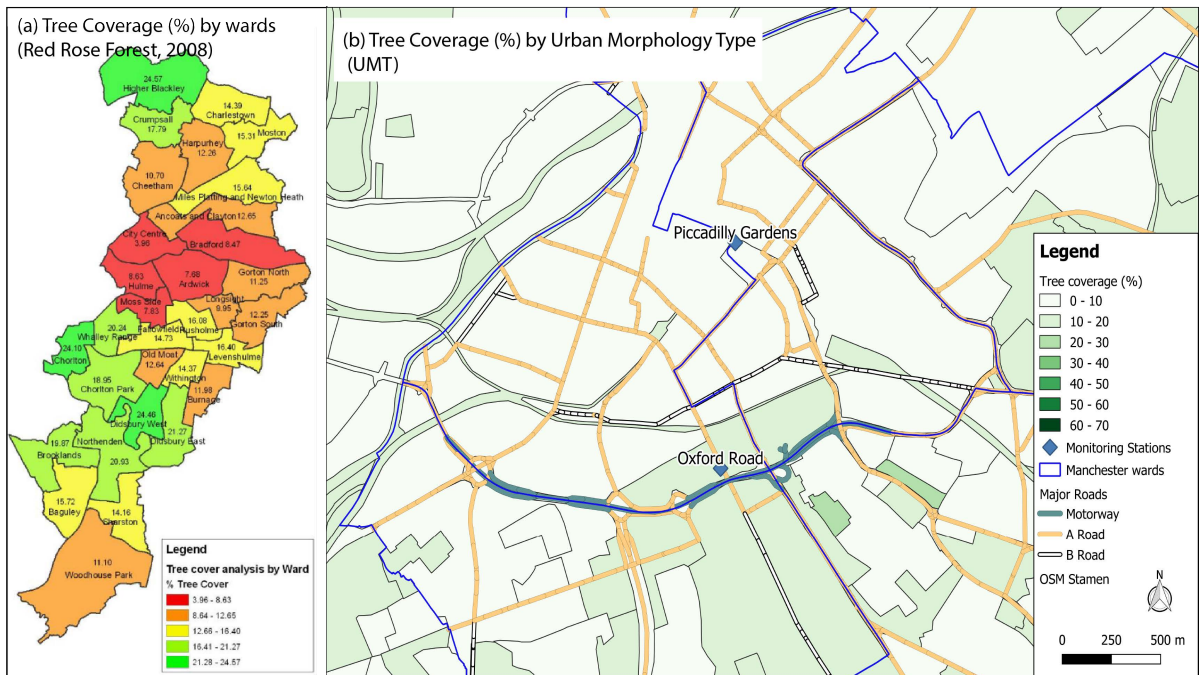


Figure 2-23: Tree coverage (%) per ward (a; ‘Tree Audit Phase 2’ Red Rose Forest, 2008) and per Urban Morphology Type (UMT) across the city centre (b), displayed with major roads and monitoring stations

The NO_x pollution map and the tree cover database were combined to identify possible sampling areas. Tree coverage (in %) varies throughout the Manchester wards (e.g. city centre wards; Figure 2-23) and no minimum percentage threshold was set for sampling site identification. Especially city centre wards, with their specific urban and building structure (i.e. building heights and major road) are seemingly most influenced by higher pollutant concentrations, due to elevated traffic loads (section 2.8.4) and in comparison show the least tree coverage.

Consequently assessing air quality at a high resolution is crucial to further understand spatial variability of air quality. Therefore, the city centre area (and adjacent wards) is of main interest for lichen sampling and subsequent analysis of air quality and lichen pollutant loadings.

2.8.2 Lichen sampling across Manchester

As previously mentioned, tree cover in the city centre is usually low (<10%) compared to more residential areas. Therefore, possible (epiphytic) lichen habitats are spatially limited and depend on the specific land-use type and occurrence of trees. Tree data was not available as “point data” and did not include further information, e.g. tree species, age and height. Consequently, in order to gain more information about the street trees, it was necessary to record species, height and girth (used to estimate the age of a particular tree) of trees during lichen sampling.

Lichens *X. parietina* and *Physcia* spp. were sampled from available trees, which have been identified during a reconnaissance period in May 2016. Lichen species (*Xanthoria parietina* and *Physcia* spp.) have been sampled across Manchester’s city centre (Deansgate and Piccadilly ward) and adjacent wards: Ancoats and Beswick, Ardwick, Cheetham, Hulme and Miles Platting & Newton Heath. The city centre is one of the main areas in the Greater Manchester conurbation, where people live, commute to, work and spend their free time.

A tree pruner was used to sample twigs and smaller branches, having high lichen coverage, from the identified trees across the research area. Twigs and smaller branches represent the younger parts of a tree and lichens growing on these compartments are therefore considered as ‘young’ specimen (due to their slow growth) and provide an early “warning” system about changes, as lichen colonization and succession on twigs are influenced by local environmental conditions (Lambley and Wolseley, 2003; Larsen Vilsholm et al., 2009). Sampling height was set between 2 and 4 metres (Figure 2-24a) at cardinal direction closest to the road. Depending on lichen coverage on individual trees, one or more (rotating clockwise, e.g. “North to South”, including the direction closest to road) cardinal directions were used for sampling and combined into a single sample. Sampled materials were placed into paper bags, marked with ID/site name, sampling direction(s), tree species and sampling date. GIS coordinates, identified lichen species, distance from adjacent street/road, as well as tree species, height and girth (using a measuring tape at about 1.50 m above ground level) and characteristics of the surroundings were recorded. Tree height was estimated using a clinometer and trigonometry (Figure 2-24a). Photographs of the sampled trees were taken. Sampling date and weather conditions (i.e. sunny or cloudy) were also recorded.

Sampled twigs were taken into the laboratory and processed for chemical analysis. Lichens were scraped off twigs using a stainless-steel scalpel and forceps, avoiding contamination of lichen samples by bark. An illuminated magnifying glass was used to maximise processing integrity and also aided the identification of lichen species (Figure 2-24b). After scraping the lichens off the twig, the lower part of the lichen was examined further to confirm other detritus and/or bark was not taken into further processing steps. Lichen materials for individual species, i.e. *X. parietina* and *Physcia* spp., were ground into an homogeneous powder using an agate mortar and pestle (cf. Blasco and Domeño, 2006; Domeño et al., 2006; Guidotti et al., 2009; Forbes et al., 2015). Ground lichen samples then were weighed and stored in glass vials, marked with the name/ID of the sample, the specific lichen species and the processing date, and well as its particular weight (Figure 2-24b). Between each sample, the agate pestle and mortar, as well as other equipment, i.e. plastic spoons and scoops, were wiped with dry and wet paper towels, washed using ultrapure water (18.2 M Ω) and oven dried.

Lichens for PAH analysis were scraped off the twigs (on the day of collection), detritus was removed, ground to a fine powder (using an agate pestle and mortar), stored in glass vials, freeze dried on a 'Buchi L-200 Freeze Dryer' at 0.03 mbar and -55°C for 12h (overnight) and freezer stored (at -18°C) until analysis.

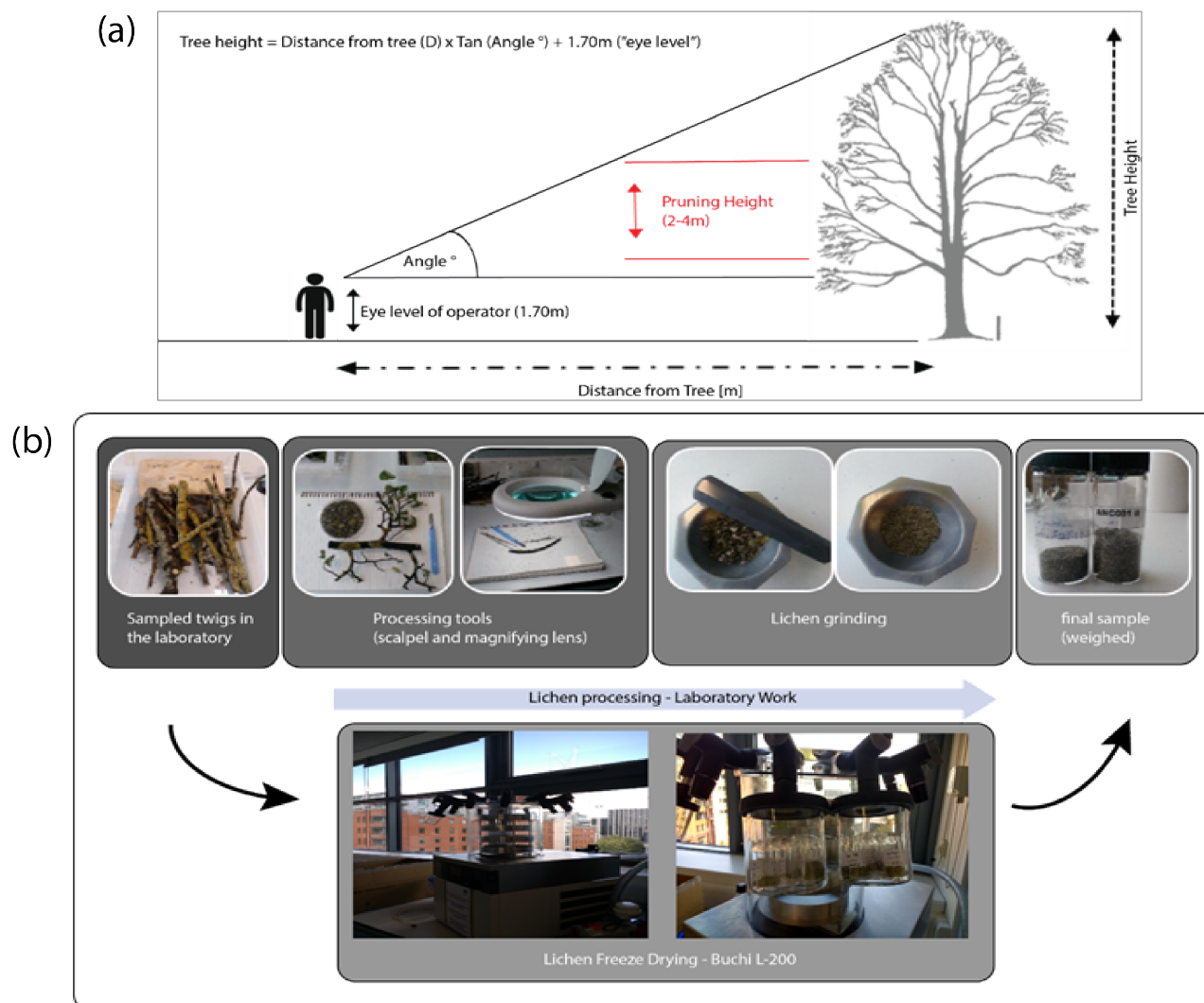


Figure 2-24: Lichen sampling procedure (a), including tree height estimation and processing procedure (b), including freeze drying step (on Buchi L-200) for PAH analysis

2.8.3 Geospatial modelling to assess spatial variability of air quality across Manchester

Environmental measurements (i.e. quantitative or descriptive measurements) usually have spatio-temporal references, determined by location (i.e. XY-coordinates), elevation (aboveground height), and time of measurement (i.e. year, month and day; Hengl, 2009). Several techniques are available for spatial prediction models, for instance Li and Heap (2008) list more than 40 spatial prediction model techniques. Generally, they can be classified as (1) deterministic models (e.g. Thiessen polygons and inverse distance interpolation), (2) linear statistical models (e.g. Kriging and Bayesian-based models) and (3) expert-based systems (e.g. machine learning algorithms and neural networks; Hengl, 2009). Geostatistical techniques, such as 'Kriging' are used to estimate analyte concentrations at and between sampling locations to predict values at unobserved locations, based on data from the surrounding area (Journel and Huijbregts, 1978; Rendu, 1978; Clark, 1979; Krige, 1984; Isaaks and Srivastava, 1989; Paustenbach, 2000; Clark and Harper, 2007b, 2007a, 2008; Demetriades, 2011). It can be used to produce maps of optimal predictions and prediction errors (variances) from incomplete and potentially noisy spatial data, using a variogram, to express spatial variation (Romary et al., 2011; Parzych, Astel, et al., 2016).

Environmental studies, assessing air quality and atmospheric pollution applied kriging methods to datasets derived from passive and active monitoring programmes, i.e. NO_x diffusion tubes and automated monitoring stations (Romary et al., 2011; Beauchamp et al., 2012; Pannullo et al., 2015). Other studies applied kriging methods to assess spatial variation and patterns in soil contamination (Cattle et al., 2002; Lin et al., 2002; Largueche, 2006; Liu et al., 2006; Astel et al., 2011; Parzych, Astel, et al., 2016). Ordinary Kriging, is one of the most frequent used kriging model, assuming a constant trend and a spatially homogenous variation of air pollution (Webster and Oliver, 2007; Ribeiro et al., 2016). It has been successfully applied in environmental epidemiological studies, i.e. assessing human exposure to PAHs using lichens as biomonitors (Augusto et al., 2012). Interpolation methods (i.e. kriging and inverse-distance weighing) are limited by the number of available locations, e.g. by the number of automated monitoring stations (or sampling locations), thus, do not effectively represent small scale spatial variability (Oiamo et al., 2015).

Webster and Oliver (2007) stated that at least 100 data points are needed to compute variograms of significant information value (Parzych, Astel, et al., 2016). Parzych, Astel, et al. (2016) applied kriging to lichen derived metal concentrations in the urban environment of Słupsk (Poland) on only 10 to 19 sampling points. Some authors reported the limitations of (ordinary) kriging for interpolation at an urban and local scale, as it tends to over-smooth predictions in an environment with abrupt concentration changes at short distances (Aguilera et al., 2008; Gulliver et al., 2011; Ribeiro et al., 2016). However, this study aimed to evaluate air quality on a high spatial resolution with sufficient lichen material sampled across the research area, making kriging a favourable method to use.

As previously described, Manchester's characteristics (i.e. building heights, road classes, greenspace distribution and traffic density patterns) are diverse throughout the research area, requiring the incorporation of urban influencing factors on dispersion and distribution of air pollutants derived from lichen dataset. Regression analysis tools are available in 'Geographic Information System' (GIS) software to quantify spatial statistics and relationships (ESRI, 2019). Ordinary Least Square (OLS) is a technique, commonly used to quantify the effects of independent variables on one dependent variable (Yoo and Ready, 2016; Yang et al., 2017). OLS provides a "global" model of the variable that is modelled to evaluate relationships between two or more attributes (ESRI, 2019). It assumes that variables are stationary over space and can lead to biased estimations if spatial correlations are ignored (Yang et al., 2017). In contrast, geographically weighted regression (GWR) is used to examine spatial variation and non-stationarity for a continuous surface of parameters at a regional scale (Fotheringham et al., 2002; Yang et al., 2017). GWR is commonly used in geographical sciences, providing a "local" model of the variable modelled. Both regression techniques can provide powerful and reliable statistics for the examination and estimation of (linear) relationships (ESRI, 2019). Based on the statistical outcomes of the OLS model (OLS model report, provided by the software), potential further modelling of variables using GWR was implemented on lichen-derived pollutant loadings in relation to urban influences.

Urban influences (e.g. building heights, road structures and green space/tree cover), as well as meteorological influences (i.e. temperature, precipitation and humidity) are affecting airborne pollutants distribution and dispersion (Seinfeld and Pandis, 1997; Mayer, 1999; Endlicher, 2012; Kuttler, 2013). Based on pollutant properties (i.e. chemical and physical stability) they can be transported, dispersed and deposited close or further away to its specific source (non-uniformly distributed; Gulia et al., 2015). For example, NO_x has been reported to decline within 200 m of the highway (Gilbert et al., 2003), while other studies reported a steep NO_x decline within the first 0 to 150 m off a major highway (Laffray et al., 2010; Bermejo-Orduna et al., 2014). Nitrogen dioxide (NO₂) was reported to decrease rapidly within 15 to 30 m away from roads, while ammonia (NH₃) declines within 10 m (Air Quality Expert Group, 2004; Cape et al., 2004; Davies et al., 2007; Watmough et al., 2014). To assess urban influences on lichen derived pollutant loadings and subsequent spatial (and temporal) variability of air quality, obtained data was further investigated and classified, based on available literature and reported decline of pollutants, i.e. NO₂.

Figure 2-25 illustrates the methodological framework for datasets used to classify and investigate spatial differences in air quality, applied within each analytical chapter. Figure 2-26 outlines the categorisation of sampling sites for statistical and geostatistical analysis of lichen pollutant loadings. Categorisation was informed by literature reporting decline of pollutants. For instance, distance to major road (including motorways, A- and B-roads) was subdivided by declines of NO_x and NO₂ concentrations from major roads, i.e. within the first 200 m (Gombert et al., 2003; Laffray et al., 2010; Bermejo-Orduna et al., 2014). Traffic data, as annual daily traffic flow (for 2017), are produced for each junction to junction link on a major road (as vehicles per day; DfT, 2017). To include the road segment as a whole (up and down the 'measured' point, as traffic moves dynamically on roads), a 500 m buffer was used to include surrounding trees (sampled for lichens). Dispersion of pollutants, i.e. NO_x from point sources has been reported to range between 100 m (upwind) and 500 m (downwind) of and around the source's perimeter (Leith et al., 2005). Britter and Hanna (2003) reported different scales, ranging from up to 200 km (regional scale) down to street-level (<100 to 200 m). A "neighbourhood" (up to 1 to 2 km) scale was chosen for this study, as emissions from (large) point sources can be transported further into and away from the source due to emission at larger heights (Britter and Hanna, 2003).

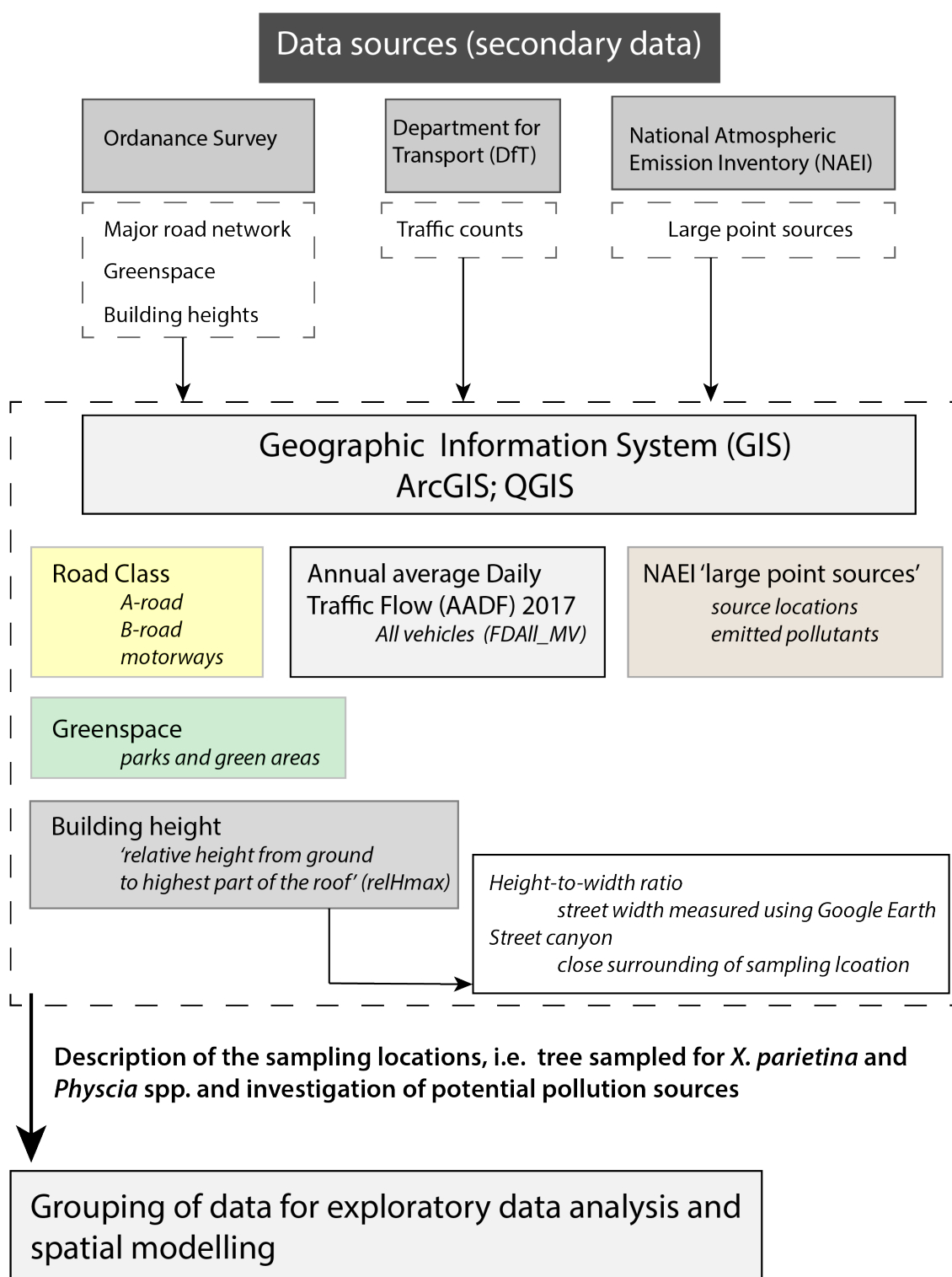
Distance of sampling location to greenspace was measured within GIS, whereas 'amount of green' around a sampling site was calculated using a 50 m buffer (around the sampling location). The amount was calculated within the buffer using GIS (area in m²), under the assumption that vegetation can have a positive impact on air quality and reduce pollution (Salmond et al., 2013; Janhäll, 2015). Classifications were based on human health studies, reporting decreased impacts of air pollution within the first 30 m and 500 m of greenspaces (Dadvand, de Nazelle, et al., 2012; Dadvand, Sunyer, et al., 2012; Browning and Lee, 2017).

Building heights were analysed including 'relative height from ground level to highest part of the roof (relHMax)', of the building heights dataset (Table 2-9). Again, the 50 m buffer (around the sampled tree) was used to depict the close surrounding of the sampling point. The building height was calculated using the average of 'relHMax' of all surrounding buildings (within the pre-set buffer).

Street Canyons are characterised by the presence of tall buildings on both sides of the street, affecting the 'vortex flow' of pollutants that can result in ten-times higher pollutant concentrations in street canyons (Hertel and Goodsite, 2009). High-density urban forms affect flow patterns (i.e. ventilation), causing poor air quality and influence pedestrian health (Britter and Hanna, 2003; Hertel and Goodsite, 2009; Buccolieri et al., 2010; Lo and Ngan, 2015; Shen et al., 2017).

Urban studies usually apply uniform heights and/or widths to model wind fields, turbulences and dispersion of pollutants (Eliasson et al., 2006; Fu et al., 2017; Shen et al., 2017). Building height was additionally used, together with street widths (measured with Google Earth; Google, 2018) to obtain a *height-to-width ratio* for the sampling sites. A 50 m buffer around the sampling sites was used and each cardinal direction was investigated for its building height and related to its street width (H/W-ratio). Oke (1988) reported H/W-ratios ranging from 0.75 to 1.75 for Europe, which is in accordance with analysed ranges for Manchester (0 to 2.60).

Incorporated datasets might not represent the sampling sites surrounding in detail (e.g. measured distances on a '2D-basis' within a 3D environment), and meteorological data could provide additional information. However, datasets were considered useful to identify potential pollutant sources and investigate dispersion and variability of pollutants within the urban environment of Manchester.



Chapter 3: Lichen diversity and air quality

Chapter 4: Carbon, nitrogen and sulphur contents and stable-isotope-ratio signatures

Chapter 5: Extraction of nitrate and ammonium concentrations from lichen material

Chapter 6: Spatial variability of airborne metal pollution

Chapter 7: Lichen PAHs for atmospheric source apportionment and toxicity assessment

Figure 2-25: Secondary datasets used for description of the close surrounding of the sampling sites, which were included into spatial regression methods within each analytical chapter

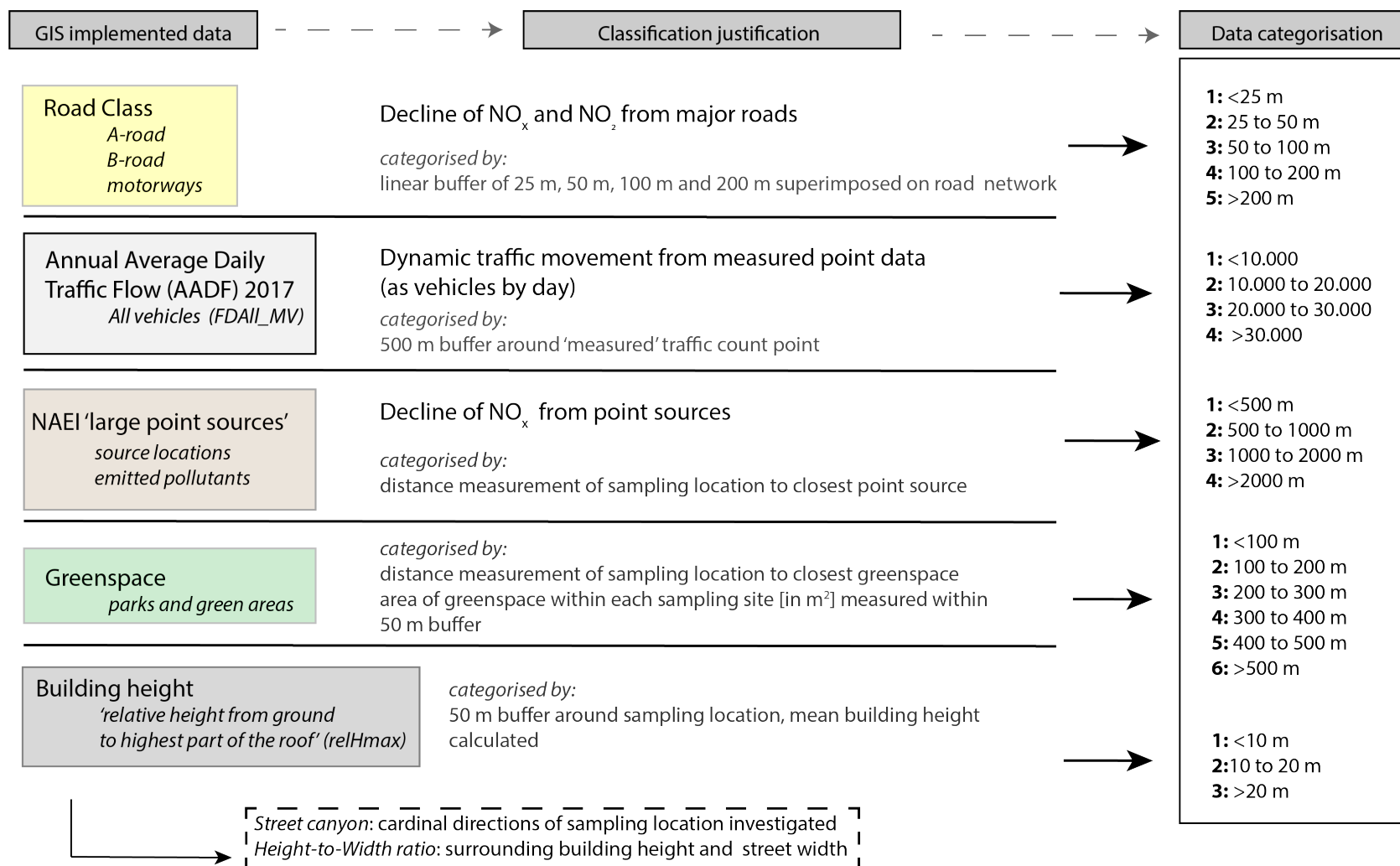


Figure 2- 26: Categorisation of datasets for spatial analysis of chemically analysed lichen pollutant loadings; urban factors datasets were implemented into GIS and sampling sites were categorised/grouped based on literature informed pollutant declines (i.e. NO_x); distances were measured from the specific sampling location

Chapter 3-
Epiphytic lichen
diversity and air
quality in Manchester

3.1 Introduction – Lichen diversity and NO_x diffusion tubes

The occurrence of different lichen species is dependent on air quality (Garty, 2001; Nash III, 2008; Van der Wat and Forbes, 2015). Historically, lichen biomonitoring studies focussed on elevated SO₂ concentrations and lichen growth, vitality and distribution in urban and industrial areas (Kricke and Loppi, 2002; Nimis and Purvis, 2002; Wadleigh, 2003; Dobson, 2011). SO₂ scales of tolerance for lichen communities were developed and widely used across Europe (Kricke and Loppi, 2002). Due to declining SO₂ concentrations and increased emissions of nitrogen compounds (i.e. NO_x and NH_x), these compounds and their impact on epiphytic lichen species have become of recent interest (Van Herk, 1999, 2003; Van Dobben et al., 2001; Van Herk et al., 2003).

In general, crustose lichens (i.e. lichens closely attached to the substrate; see chapter 2.3) are more tolerant to pollutants than foliose lichens, and foliose lichens are more tolerant than fruticose ones (Bartholomeß and John, 1997). Some lichens are more sensitive to pollution than others, which leads to a reduction, or absence, of a particular lichen within an environment (Hawksworth and Rose, 1970; Nash III, 2008). For example, Dongarrà and Varrica (1998) recorded absence of *Parmelia* spp. in close proximity to a volcano, due to emitted gases (e.g. SO₂ and H₂S) and high amounts of trace metals (e.g. Pb and Cu), whilst other lichens, e.g. *Parmelia sulcata* and *Xanthoria parietina*, can withstand higher levels of atmospheric pollutants (Dongarrà and Varrica, 1998; Forbes et al., 2015). Thus, the potential high concentrations of atmospheric pollutants (i.e. SO₂, NO_x and CO) in urban environments (Fenger, 1999; Gulia et al., 2015), could determine lichen presence and diversity in cities/ urban environments. Atmospheric pollutants in Manchester are measured at automated monitoring stations, one on Oxford Road and one at Piccadilly Gardens. For instance, NO and NO₂ is measured on Oxford Road, while O₃, SO₂ and CO are additionally recorded at Piccadilly Gardens (DEFRA, 2018b, 2018a). Monitoring stations provide continuous measurements of pollutants and provide long-term trends of air quality.

Nonetheless, both automated monitoring stations are located within the city centre of Manchester and thus only provide local air quality. Spatial variability, dispersion and distribution of pollutants are not fully recorded across the city centre. Making it therefore necessary to apply additional methods to obtain fine spatial detail of air quality. For instance by using biomonitors, such as lichens and passive sampling devices.

Passive monitors, relying on the passive diffusion of air pollutants onto a sorbent can be applied, where it is impractical to use 'active' methods, i.e. continuously measurements, using pumps and electricity (Pienaar et al., 2015). Within the UK, Palmes-type diffusion tubes are regularly applied to monitor ambient NO₂ concentrations, e.g. at 1200 monitoring sites in 330 local authorities (UK Nitrogen Dioxide Network; Bush et al., 2001). Diffusion tubes have been widely used as an inexpensive method to measure ambient nitrogen dioxide (NO₂) as they provide long-term concentrations (e.g. the annual mean) and are able to represent spatial distribution (Bush et al., 2001; Cape, 2005; Pienaar et al., 2015). Main advantages are that they comprise of low-cost material, do not need electrical power, can be analysed by simple procedure(s) and provide an absolute air concentration (Cape, 2005). Hence, using NO_x diffusion tubes across the urban environment of Manchester, in combination with epiphytic lichen diversity, could provide fine spatial detail of air quality (not measured by automated monitoring stations) and potential influences on lichen communities.

This chapter aims to relate lichen diversity to air quality in Manchester. Additionally, NO_x diffusion tube measurements for NO₂ are presented and related to lichens species recorded across Manchester, with specific focus on nitrogen dioxide (NO₂). Research methodologies will describe the assessment of lichen diversity and the preparation, deployment procedure and analysis of NO_x diffusion tubes. Results are presented separately for lichen diversity and NO_x diffusion tubes, which will be interpreted and discussed subsequently. NO_x diffusion tube measurements will be related to lichen diversity, to potentially identify influences on lichen communities. However, NO_x tube measurements were primarily used to ground-truth lichen chemical data, which will be further discussed in the following chapter (Chapter 4: Lichen carbon, nitrogen and sulphur contents and stable-isotope ratio signatures).

3.2 Research methodology – Lichen frequency and diversity

3.2.1 Epiphytic lichen diversity to assess ‘environmental conditions’ in Manchester

The primary aim of this study was to chemically analyse lichen samples for elemental composition, which will be further presented in subsequent chapters. Lichens (*X. parietina* and *Physcia* spp.) were sampled off street trees (twigs and small branches; 2 to 4 m height; detailed sampling described in chapter 2) across Manchester, focussing on carbon, nitrogen, sulphur contents and stable-isotope ratio signatures ($\delta^{13}\text{C}$, $\delta^{15}\text{N}$ and $\delta^{34}\text{S}$), nitrogen speciation, as well as metal and polycyclic aromatic hydrocarbon (PAHs) concentrations. However, lichen diversity and frequency on tree trunks were used to investigate influences of atmospheric pollutants (i.e. NO_x and NH_x) and thus a potential shift in lichen community to a nitrophilous (i.e. lichens preferring nitrogen-rich habitats; Van Herk, 2003) taxa in the urban environment of Manchester, which is presented in this chapter. Mapping lichen diversity provides an indication of biological impacts of air pollution, allows a quick and inexpensive method to indicate potential human health impacts and can provide information of air quality changes in urban areas over time (Cislaghi and Nimis, 1997; Loppi et al., 1997; Paoli et al., 2012).

In the 1960s a method has been developed to quantify environmental conditions, using lichens as bioindicators (De Sloover and LeBlanc, 1968; Kricke and Loppi, 2002), which has been modified by researchers in different countries, i.e. Estonia, Germany, Switzerland and Italy (Kricke and Loppi, 2002). Several approaches were proposed, to biomonitor with lichens focussing on abundance or cover of species and different sampling areas (Barkman, 1963; De Sloover and LeBlanc, 1968; Hawksworth and Rose, 1970; Nimis et al., 1989; Nimis and Bargagli, 1999; Castello and Skert, 2005). The different approaches, i.e. using different sampling grid sizes, grid location and the selection of trees made it difficult to compare data and were criticised being too subjective (Castello and Skert, 2005).

More recently a strongly standardised methodology, to allow easier comparison throughout Europe was proposed, as an indicator of general environmental quality (Asta, Erhardt, et al., 2002; Gombert et al., 2004). It is largely based on the German ‘Lichen Mapping Guideline’ (VDI, 1995) and Italian guideline (Nimis and Bargagli, 1999) and has been modified regarding sampling location, selection of trees and positioning of the sampling grid on the trunk (Asta, Erhardt, et al., 2002; Asta,

Ferretti, et al., 2002). The high level of standardisation of the lichen monitoring guideline by Asta, Erhardt, et al. (2002), which was agreed on during a 'NATO Advanced Research Workshop on Lichen Monitoring' (Pier Luigi Nimis et al., 2002) was used to investigate diversity and frequency (occurrence) of lichens across the city centre of Manchester. On a local level, this method could produce reliable results even with a reduced set of species (VDI, 1995; Asta, Erhardt, et al., 2002). Thus, potential influences by atmospheric pollutants on lichen communities could provide additional information on air quality in Manchester.

Lichen sampling across Manchester focussed on the city centre area, to assess spatial variability of atmospheric pollution on a high spatial scale. In total 94 sites were sampled off street trees for *X. parietina* and *Physcia* spp. across Manchester for further chemical analysis (N=94). Of those sampling sites, 58 trees were suitable (i.e. tree species, girth and trunk inclination; described hereafter) to assess the lichen diversity on tree barks, to supplementary assess potential air quality effects on lichens in Manchester (Figure 3-1).

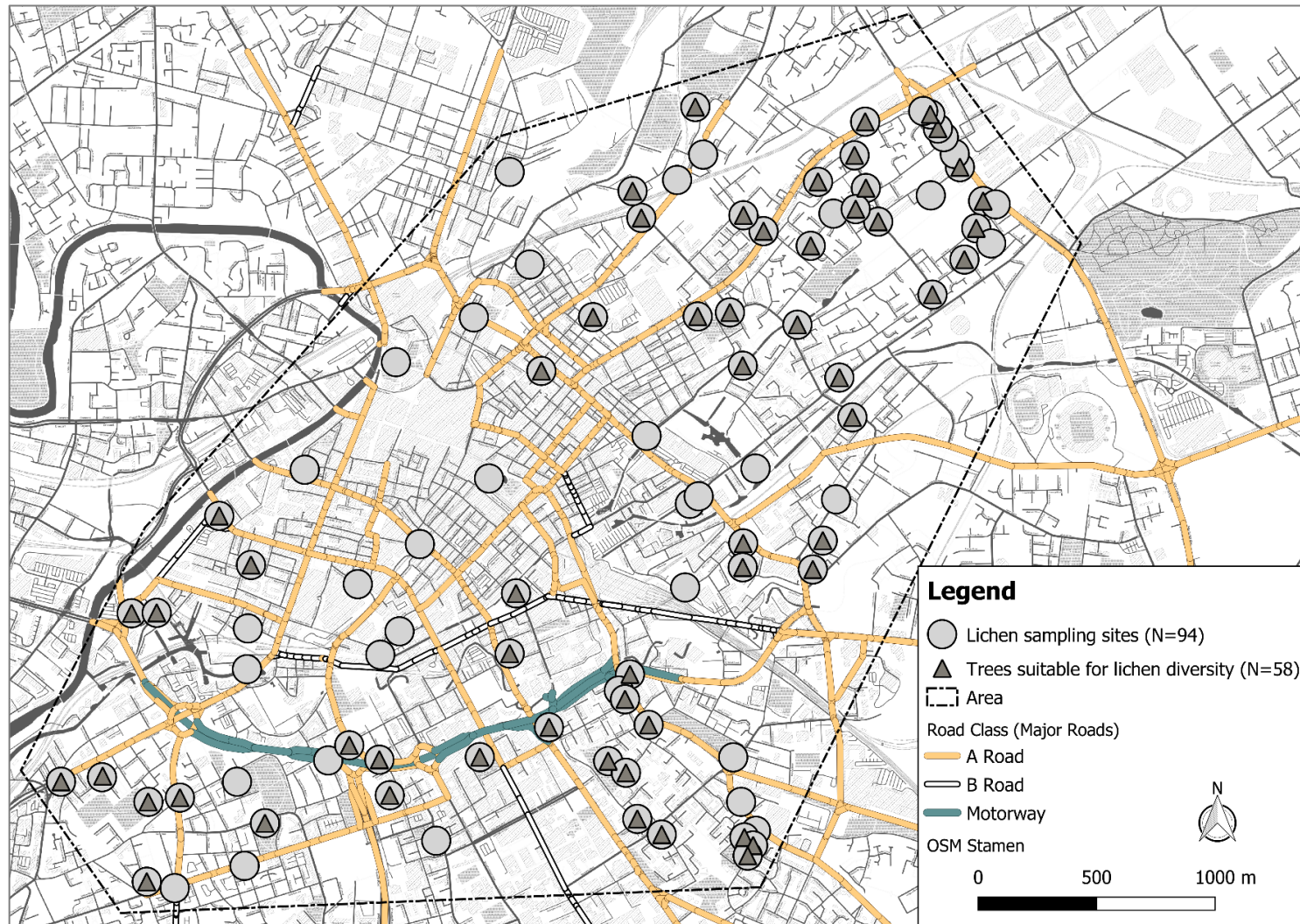


Figure 3-1: Lichen sampling sites (grey circles; N=94) sampled for *X. parietina* and *Physcia* spp. off street tree twigs and small branches to chemically analyse elemental composition and trees that were suitable to assess lichen frequency and diversity on bark (dark grey triangle; N=58)

3.2.2 Lichen species identification growing on street tree trunks across Manchester

Lichen identification guides and identification keys in Kirschbaum and Wirth (2010) 'Flechten erkennen – Umwelt bewerten' and Dobson (2011) 'Lichens – An Illustrated Guide to British and Irish Species' and 'Open Air Laboratories (OPAL)' lichen-ID guides and Nimis et al. (2009) 'A key to common lichens on trees in England' were used for lichen identification on tree trunks. Identification was supported by magnifying glasses (25x and 40x magnification), with additional illumination (40x) to closely examine upper and lower lichen parts. Most common UK lichen species can be visually identified with the naked eye or hand-lenses (10x magnification; Nimis et al., 2009). Chemical reactions of the lichen thallus (called spot tests), using different chemicals (i.e. KOH, Ca(ClO)₂ or NaClO and/or C₆H₈N₂) could be used to aid lichen identification (Nimis et al., 2009; Kirschbaum and Wirth, 2010). However, lichen diversity was additionally used to assess a 'general' overview of air quality and evaluate potential influences on the lichen community across Manchester. Therefore, visual identification was considered sufficient for this study.

Identified lichen species were categorised into reference species and eutrophication species (Table 3-1). Eutrophication species are lichens which are related to nutrient-rich emissions (especially nitrogen; Bartholomeß, n.d.). All other lichen species identified on a tree, are termed "reference species" (oligotrophic species; Table 3-1; Upreti et al., 2015). Additionally, *Xanthoria ucrainica*, also recoded across Manchester, was treated as an "eutrophication species", because it is frequent in Britain and is abundant in nutrient-rich habitats, e.g. trees and walls (Dobson, 2011). Lichens of the genus *Xanthoria*, main differences for identification and 'typical' habitats are illustrated in Figure 3-2. Therefore, specific 'habitat demands' by different lichen species indicate potential influences at particular sites. Lichen species, as illustrated in Table 3-1, were investigated on tree trunks across the city centre of Manchester. The methodology applied is described hereafter.

Table 3-1: Reference and eutrophication species that have been used to analyse lichen diversity across Manchester (adapted from Bartholomeß (n.d.) and modified by species mentioned by Wolseley et al. (2009), shaded in yellow, to include common British lichen species (Smith et al., 2009; Sutcliffe, 2009)

Reference Species (oligotrophic species, negatively correlated with eutrophication)	Eutrophication species
<i>Candelariella reflexa</i>	<i>Caloplaca citrina</i>
<i>Lecidella elaeochroma</i>	<i>Caloplaca holocarpa</i>
<i>Ramalina farinacea</i>	<i>Lecanora dispersa</i>
<i>Lepraria lobificans</i>	<i>Lecanora hagenii</i>
<i>Melanohalea exasperatula</i>	<i>Lecanora muralis</i>
<i>Parmelia sulcata</i>	<i>Phaeophyscia nigricans</i>
<i>Physcia aipolia</i>	<i>Phaeophyscia orbicularis</i>
<i>Lepraria incana</i>	<i>Physcia adscendens</i>
<i>Lecanora expallens</i>	<i>Physcia caesia</i>
<i>Lecanora chlorotera</i>	<i>Physcia dubia</i>
<i>Flavoparmelia soredians</i>	<i>Physcia tenella</i>
<i>Amandinea punctata</i>	<i>Physconia grisea</i>
<i>Evernia prunastri</i>	<i>Rinodina spp.</i>
<i>Flavoparmelia caperata</i>	<i>Xanthoria candelaria</i>
<i>Hypogymnia spp.</i>	<i>Xanthoria parietina</i>
<i>Plastimatia glauca</i>	<i>Xanthoria polycarpa</i>
<i>Pseudevernia furfuracea</i>	<i>Xanthoria ucrainica</i>
<i>Usnea and/or Bryoria species</i>	<i>Hyperphyscia adglutinata</i>

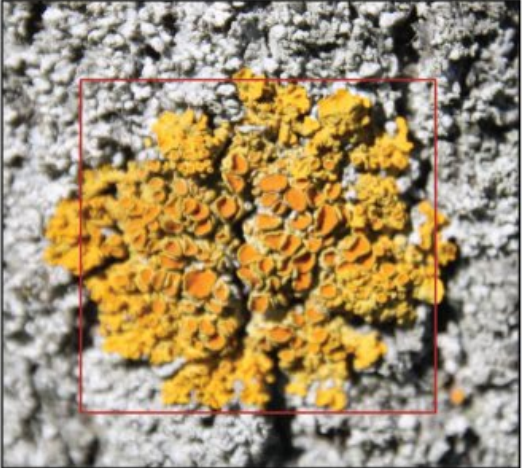


		
<p><i>Xanthoria parietina</i></p>	<p><i>Xanthoria polycarpa</i> (Kirschbaum & Wirth, 2010)</p>	<p><i>Xanthoria ucrainica</i> (Dobson, 2011)</p>
<ul style="list-style-type: none"> - thallus to 15 cm diameter - greenish grey in shade - bright orange in strong sunlight 	<ul style="list-style-type: none"> - thallus orbicular, up to 2 cm diam. - greenish grey to yellow-orange - numerous, stalked apothecia 	<ul style="list-style-type: none"> - thallus lemon-yellow to yellow-green - flattened lobes, up to 1 mm wide and 1.5 mm tall
<p><u>Habitat:</u> very common on nutrient-rich trees, rocks and walls; one of the most resistant foliose species to SO₂ and nitrogen pollution</p>	<p><u>Habitat:</u> common on nutrient-rich trees, especially twig angles; rapidly returning to cities (due to declining SO₂)</p>	<p><u>Habitat:</u> common on nutrient-enriched trees (especially deciduous), walls and fences and especially bird-perching sites; most frequent member (of this group) in Britain</p>

Figure 3-2: Comparison of lichens of the genus *Xanthoria*, including *X. parietina*, *X. polycarpa* and *X. ucrainica*; their main identification characteristics and habitats (Dobson, 2011)

3.2.3 Methodology to assess lichen frequency and diversity on tree trunks of street trees

Lichen frequency of occurrence can be used to estimate diversity and the degree of environmental stress within an (urban) environment, based on the fact that epiphytic lichen diversity is impaired by air pollution (Asta, Ferretti, et al., 2002). The lichen frequency and diversity approach used for Manchester was based on 58 trees, which were also sampled for *Xanthoria parietina* and *Physcia* spp. across the city centre area of Manchester (Figure 3-1), to assess environmental quality (i.e. eutrophication and anthropization; Asta, Erhardt, et al., 2002; Asta, Ferretti, et al., 2002).

Tree species were chosen according to similar bark characteristics (i.e. roughness and acidity) and girth (Asta, Erhardt, et al., 2002; Kirschbaum and Wirth, 2010). They were free-standing, with girths >70 cm and near straight trunks (inclination <10°), while damaged or disturbed trees (i.e. by liming and fertilizing) were avoided (Asta, Erhardt, et al., 2002; Kirschbaum and Wirth, 2010). Suitable tree species to investigate lichen diversity are displayed in Table 3-2. Trees present in Manchester were identified during an initial reconnaissance in May 2016.

Table 3-2: Trees applicable for the lichen diversity index, based on bark properties and girth at 150 cm height (adopted by Kirschbaum and Wirth, 2010; tree translations from: Sterry, 2007)

Group I: tree bark with sub-neutral conditions [natural conditions]	Group II: tree bark ± acid conditions [natural conditions]
Norway Maple (<i>Acer platanoides</i>) (70-280cm)	Common Alder (<i>Alnus glutinosa</i>) (70-280cm)
Ash (<i>Fraxinus excelsior</i>) (70-280cm)	Silver Birch (<i>Betula pendula</i>) (70-280cm)
Elm (<i>Ulmus spec.</i>) (70-280cm)	Wild Cherry (<i>Prunus avium</i>) (70-280cm)
Common Walnut (<i>Juglans regia</i>) (70-280cm)	Plum (<i>Prunus domestica</i>) (70-280cm)
Manna Ash (<i>Fraxinus ornus</i>) (70-280cm)	Pedunculate Oak (<i>Quercus robur</i>) (70-280cm)
Hybrid Black-poplar (<i>Populus x canadensis</i>) (70-280cm)	Sessile Oak (<i>Quercus petraea</i>) (70-280cm)
Sycamore (<i>Acer pseudoplatanus</i>) (70-280cm)	Common Pear (<i>Pyrus communis</i>) (70-160cm)
Cultivated Apple (<i>Malus domestica</i>) (70-160cm)	Small-leaved Lime (<i>Tilia cordata</i>) (70-280cm)
Common Pear (<i>Pyrus communis</i>) (70-160cm)	Large-leaved Lime (<i>Tilia platyphyllos</i>) (70-280cm)
Small-leaved Lime (<i>Tilia cordata</i>) (70-280cm)	
Large-leaved Lime (<i>Tilia platyphyllos</i>) (70-280cm)	

The number of analysed trees is dependent on the geographical scale of the study and area characteristics (Asta, Erhardt, et al., 2002; Kirschbaum and Wirth, 2010). In this study, a 1x1 km grid was superimposed to the research area (see Figure 2-21) and trees (according to Table 3-2) within the grid were analysed for lichen frequency and diversity. According to Kirschbaum and Wirth (2010) and the German lichen diversity approach (included in the guideline 'VDI-Richtlinie 3957, Blatt 13') 6 to 12 evenly distributed trees should to be analysed to describe the air quality in a 1x1 km grid (Kirschbaum and Wirth, 2010). More condensed grids can be applied to research areas, i.e. 0.5 x 0.5 km (>4 trees) or 0.25 x 0.25 km (>3 trees).

Lichen diversity across Manchester, was used to evaluate influences on lichen communities by atmospheric pollution. Moreover, frequency and diversity of lichens across the research area provides information on pollutants (i.e. nitrogen compounds) affecting the lichen community. Therefore, lichen diversity was considered a useful tool to investigate air quality in areas, not continuously monitored and to identify potential areas with impacts on human health.

All present lichen species on the trunk (of a particular tree) were recorded following this procedure Bartholomeß (n.d.), Asta et al. (2002) and Kirschbaum and Wirth (2010):

- 1) Attaching a sampling ladder on each cardinal direction between 1.00 to 1.50 m height, so that the lower edge is 1 m above the highest point of the ground (sampling ladder = five contiguous quadrats, each 10x10 cm)

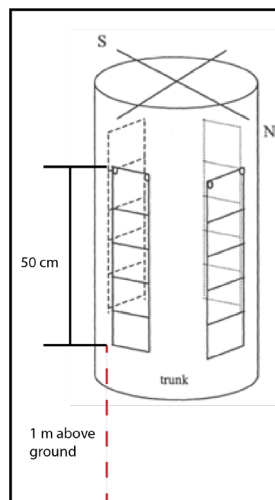


Figure 3-3: Sampling grid ('lichen ladder') attached to the tree trunk between 1.00 to 1.50 m height at each cardinal direction (Asta, Erhardt, et al., 2002)

- 2) Recording all lichen species frequencies on each cardinal direction on a tree. The frequency is determined by the number of occurrence of a species in a sample grid (e.g. presence of a species in a quadrat = 1), so the maximum frequency of a species is 5 for a cardinal direction and 20 for a tree.
 - Lichen species were categorised into reference (=respond negatively to eutrophication) and eutrophication species (Table 3-1; Kirschbaum and Wirth, 2010)
 - The sum of frequency (SF) is calculated for each tree (t) according to the cardinal point, i.e. four sums of frequencies for each tree: SF_{tN} , SF_{tE} , SF_{tS} , SF_{tW} (e.g. SF_{tN} = sum of frequency for tree (t) at cardinal direction north (N); Table 3-3)
- 3) Then SF_{tN} , SF_{tE} , SF_{tS} , SF_{tW} are summed up individually by summarizing reference and eutrophication species, for a given sample unit (Table 3-3).
 - Sampling unit = area for which the lichen diversity was calculated (in this study 1x1km grid)
- 4) Calculating \bar{x} (mean) for each of the cardinal sites and trees
 - $\bar{x} = (SF_{t1N} + SF_{t2N} \dots + SF_{txN}) / n_t$
- 5) Summarizing arithmetic means for the cardinal points
 - $\sum \bar{x}_N + \bar{x}_E + \bar{x}_S + \bar{x}_W =$ lichen diversity value for reference and eutrophication species
- 6) Using the lichen diversity value obtained on the colouring matrix to evaluate air quality and influence of eutrophication compounds in a sampling unit (Figure 3-4).

To illustrate the AQI methodology, five trees are used as an example (Table 3-3). The lichen diversity value then can be used to describe the air quality and the influence of eutrophication compounds, as illustrated on Figure 3-4.

Table 3-3: (a) Five recorded trees as an example to illustrate the calculation of the AQI; lichens found divided into reference and eutrophication species; numbers display frequencies of the species found at a cardinal site (max. 5); summed up frequencies for reference and eutrophication species per tree and cardinal site; (b) summed up frequencies for each tree and cardinal direction (for reference and eutrophication species), mean for the sampling area and 'Lichen Diversity Value (LDV)' of the sampling unit, with colour coding following Figure 3-4

(a)	Tree	Lichen	Reference Species				Eutrophication species			
			N	E	S	W	N	E	S	W
	1	Species 1					0	0	5	3
	1	Species 2					4	3	5	5
	1	Species 3					1	5	4	2
	1	Species 4	2	0	0	0				
	1	Species 5	0	0	0	1				
	1	∑ of frequencies	2	0	0	1	5	8	14	10
	2	Species 1					0	1	5	0
	2	Species 2					4	4	4	4
	2	Species 3	0	0	0	0				
	2	Species 4	0	1	1	1				
	2	Species 5	3	1	0	3				
	2	∑ of frequencies	3	2	1	4	4	5	9	4
	3	Species 1					0	1	2	1
	3	Species 2					0	0	4	0
	3	Species 3					1	2	5	4
	3	Species 4	1	1	0	0				
	3	Species 5	1	1	0	0				
	3	∑ of frequencies	2	2	0	0	1	3	11	5
	4	Species 1					5	3	1	4
	4	Species 2					1	2	2	2
	4	Species 3					5	5	4	4
	4	∑ of frequencies	0	0	0	0	11	10	7	10
	5	Species 1					1	2	1	1
	5	Species 2					0	0	1	1
	5	Species 3					1	0	2	1
	5	Species 4	2	3	2	1				
	5	Species 5	1	2	2	2				
	5	Species 6	1	0	1	1				
	5	∑ of frequencies	4	5	5	4	2	2	4	3

(b)	Tree	Lichen	Reference Species				Eutrophication species			
			N	E	S	W	N	E	S	W
	1	∑ of frequencies	2	0	0	1	5	8	14	10
	2	∑ of frequencies	3	2	1	4	4	5	9	4
	3	∑ of frequencies	2	2	0	0	1	3	11	5
	4	∑ of frequencies	0	0	0	0	11	10	7	10
	5	∑ of frequencies	4	5	5	4	2	2	4	3
	Mean ∑ of frequencies of the sampling area		2.2	1.8	1.2	1.8	4.6	5.8	9	6.4
	Lichen Diversity Index (LDI) of the sampling unit		7				25.8			
	Using Evaluation Matrix (Figure 3-2): y-axis: 7 and x-axis: 25.8		3.3							

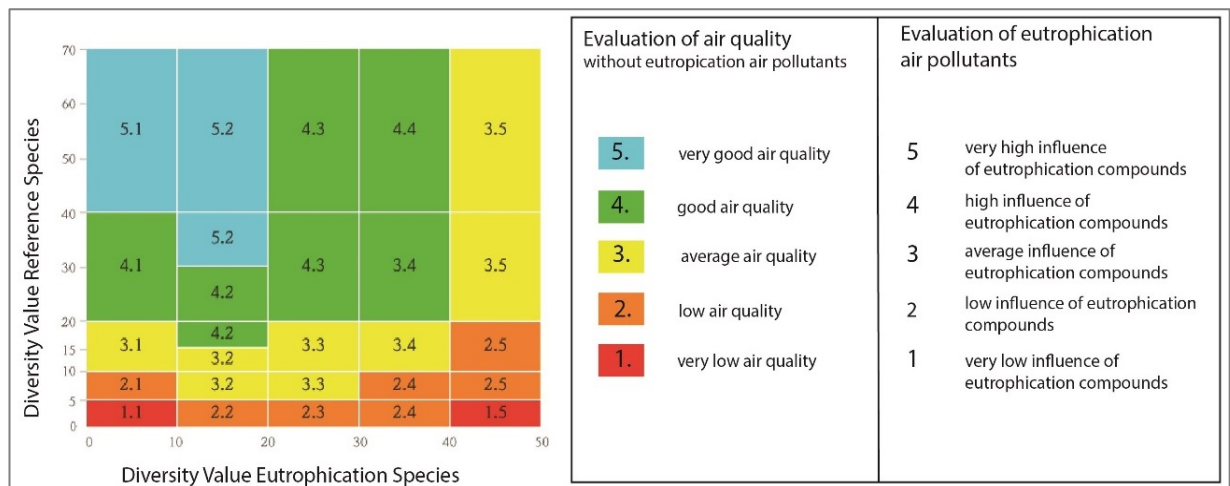


Figure 3-4: Evaluation matrix used to colour-code air quality across Manchester, based on lichen diversity (i.e. red illustrating deteriorated air quality) on 58 analysed trees (the evaluation matrix was adopted from Kirschbaum and Wirth, 2010)

Due to number of trees and spatial inconsistencies of tree distribution, the lichen diversity approach was further elaborated by applying a “by-tree” classification to achieve high spatial resolution. Lichen diversity per tree was calculated for reference and eutrophication species (summarised at each tree; step 2 in aforementioned procedure). The ratio between reference divided by eutrophication species was used to rate the influence of eutrophication compounds at the particular site.

Highly nitrogen polluted areas showed a decline in many lichen species, whereas nitrogen-preferring or eutrophication-tolerant species increase (Van Dobben and Ter Braak, 1998; Van Herk, 1999; Hauck, 2011). Nitrogen compounds that are likely to affect epiphytic lichens are ammonia (NH_3) and ammonium (NH_4^+), nitrogen oxides (NO_x), nitrate (NO_3^-) and basic dust from traffic and industry (Van Herk, 2003). These compounds have been reported to increase the bark pH and/or increase the nitrogen content of the bark (Van Herk, 2003). Comparable to the approach used within the ‘evaluation matrix’ (Figure 3-4) a classification into five categories was used to describe the influence of eutrophication compounds. It was considered, that a low ratio of <0.5 (between eutrophication species and reference species) indicates a dominance of eutrophication species and eutrophication compounds at the particular site. In contrast, a ratio of >2.0 was considered to suggest very low influences of eutrophication compounds, due to dominance of reference species at the particular site. Ratio increments are displayed in Table 3-4.

Table 3-4: Suggested 'per tree' lichen species ratios that potentially indicate influences of eutrophication compounds on lichen diversity; colour-coded by influence of eutrophication compounds (i.e. NO_x and NH_x)

Ratio between reference/ eutrophication species (Σ) at each tree	Influence of eutrophication species
<0.5	Very high influence of eutrophication compounds
0.5 to 1.0	High influence of eutrophication compounds
1.0 to 1.5	Moderate influence of eutrophication compounds
1.5 to 2.0	Low influence of eutrophication compounds
>2.0	Very low influence of eutrophication compounds

The ratio approach was applied, to obtain fine-spatial detail of air quality affecting lichen diversity on tree trunks. Therefore suggesting potential site-specific influences of atmospheric pollutants, i.e. by NO_x and NH₃ on lichen communities.

3.3 Research Methodology – NO_x diffusion tubes

3.3.1 NO_x diffusion tube deployment procedure

Passive sampling devices can be used where 'active' (i.e. the use of continuous samplers, requiring electricity and maintenance) sampling is impractical (Pienaar et al., 2015). 'Palmer-type' diffusion tubes have been widely applied in the UK, to assess variability of nitrogen dioxide (NO₂) concentrations (Cape, 2005). NO_x diffusion tubes were used to ground-truth lichen data, in particular chemical data, i.e. nitrogen contents (wt%) and stable nitrogen isotope ratios ($\delta^{15}\text{N}$), presented in the chapter hereafter (Chapter 4). Furthermore, NO_x tubes were used to obtain a spatio-temporal overview of nitrogen pollution across the city centre of Manchester. NO₂ concentrations were considered to affect epiphytic lichen diversity (discussed in section 3.8.2).

It is recommended that tubes should be exposed in replicates (ideally three tubes; Cape, 2005). There might still be systematic bias, i.e. caused by turbulence and in-tube chemistry, consequently not guaranteeing accuracy (Cape, 2005). More precise results can be obtained using three or more tubes per side (rather than single tubes; AEA Energy and Environment, 2008). However, multiple tube exposure is not essential, if good precision is demonstrated (AEA Energy and Environment, 2008). Diffusion tubes are particularly useful, where simple, indicative techniques will suffice, highlight areas of high NO₂ and provide an indication of long-term average (mean) NO₂ concentrations (Loader, 2006).

Due to high spatial resolution (N=45 sites), biweekly change (fieldwork workload), analysis procedure (laboratory time and IC analysis) and costs, only one tube was deployed per site.

NO_x diffusion tubes were deployed at 45 sites that have been sampled for lichens (N=94; Figure 3-5) to ground-truth lichen data on a high spatial scale. Tube locations were informed by analysed lichen N wt% (data not shown here; Appendix A-1) to cover lower and higher N contents, thus indicating varying NO₂ influences. In return, this can be related to lichen diversity at analysed locations.

Tube deployment followed the 'Department for Environment, Food & Rural Affairs (DEFRA)' guidelines and recommendations:

- Deployment height of 2 to 2.50 m above ground (to avoid vandalism of equipment) on the tree (AEA Energy and Environment, 2008), facing the closest road.
- Diffusion tube was held vertically (open end pointing downwards) during the sampling period (two-weeks deployment)
- NO_x diffusion tubes were secured and fixed on site with plastic straps (re-usable), mounting clips and a spacer block (Figure 3-6a). A 'deployment tag' was attached to the equipment, including project contact details.

Deployment started on the 3rd of July 2017 and tubes were changed on a biweekly cycle over a 12-months period until the end of June 2018 (28/06/2018; 361 days). NO_x tube deployment started during a second lichen sampling period in 2017, illustrating a potential temporal bias. Paoli et al. (2018) transplanted *Flavoparmelia carperatea* thalli from polluted sites to unpolluted sites and reported elemental concentrations and physiological parameters changes in the lichen after 12 months. Lichens therefore reflect environmental conditions over time (due to longevity; Shukla et al., 2014). High nitrogen contents (wt%) in lichens may reflect higher ambient NO₂ concentrations and reflect long-term concentrations at the particular site. Biomonitors, such as lichens provide spatial and temporal distribution of pollutants deposition (Sujetovienė and Galinytė, 2016). The comparative use of NO_x diffusion tubes and lichen diversity in Manchester could identify areas of high N loads and potential impacts on human health.

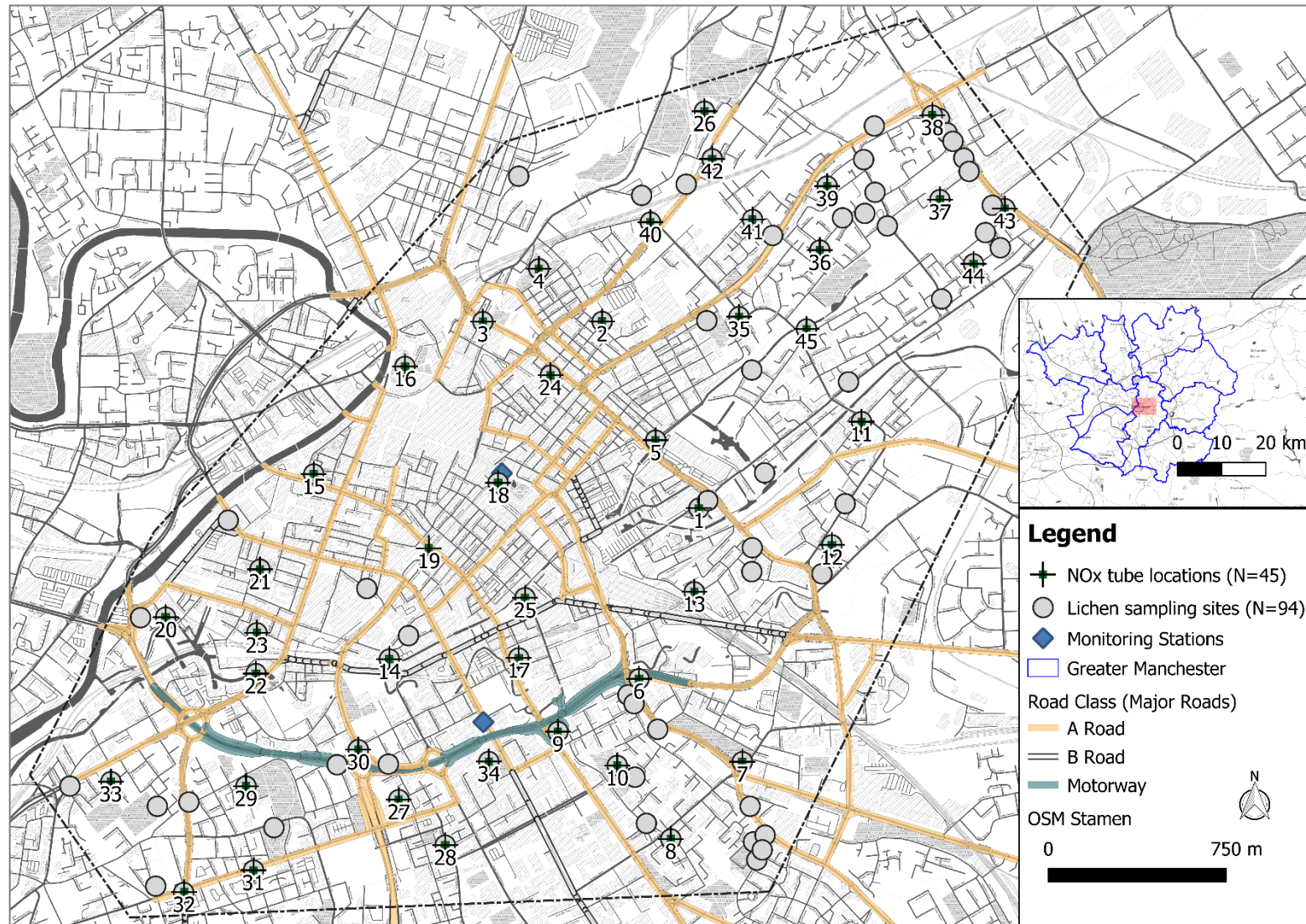


Figure 3-5: Lichen sampling sites for analysis of CNS contents, stable-isotope ratios and metal concentrations, together with NO_x diffusion tubes locations (N=45; and site ID) across Manchester; displayed with automated monitoring stations (Oxford Road and Piccadilly Gardens) within the city centre and location within Greater Manchester (inset map).

During NO_x tube deployment, some sites were vandalised (deliberately cut down) and/or equipment was missing, i.e. the tube and/or the fixation equipment. Missing equipment was replaced and a new tube was placed on-site. The majority of sites (29 out of 45) were not affected by tube loss and/or missing equipment. Eleven sites were missing once and only three sites were missing twice. Sites ID: 32 and ID: 33 in the southwest of the research area (Figure 3-5) were missing three times during the deployment period. No site was missing more than three times, illustrating continuously high data capturing for NO_x tube deployment. Figure 3-6 illustrates the used NO_x diffusion tubes, including components and deployment at locations.

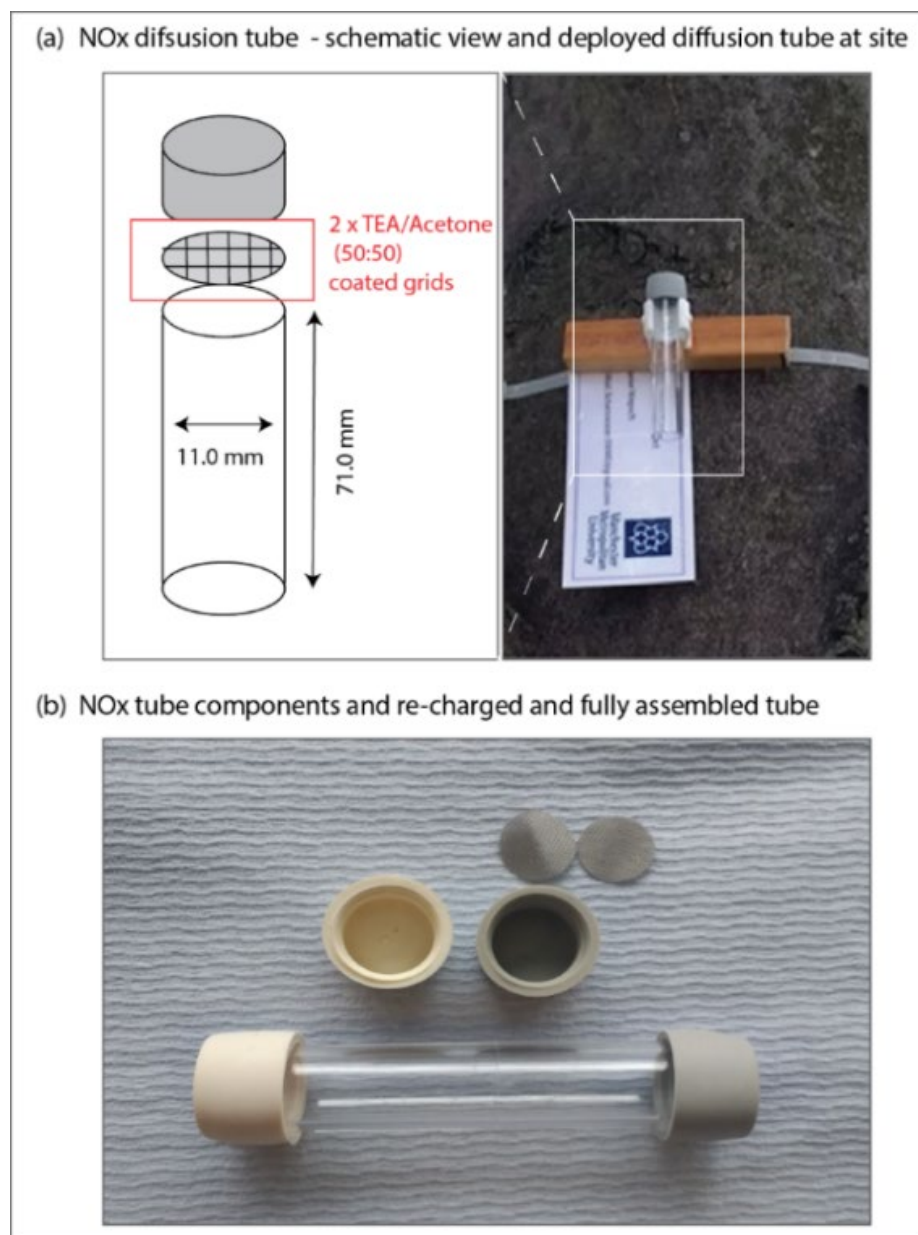


Figure 3-6: (a) NO_x diffusion tube - schematic view of NO_x diffusion tubes with dimensions and deployed tube at sampling site (with spacer block and information tag) (b) NO_x tube components and re-charged and fully assembled tube

3.3.2 Preparation and extraction of NO_x diffusion tubes before analysis

Diffusion tube (Palmes-type) samplers, coated with Triethanolamine (TEA) allow to determine NO₂ concentrations in ambient air (Kasper-Giebl and Puxbaum, 1999; Plaisance et al., 2002; Buzica and Gerboles, 2008). NO_x diffusion tubes (Gradko international, UK) were prepared and handled according to the DEFRA guidelines (AEA Energy and Environment, 2008).

- (1) Triethanolamine (TEA)/Acetone (v/v: 50/50) solution was used to re-charge the tube meshes. Meshes were soaked in the TEA/Acetone solution for 1h, excess solution was discarded and meshes were dried on paper towel (for 15 minutes). All work was undertaken in a fume cupboard.
- (2) Two (dried and impregnated) grids per tube were put into the grey cap and diffusion tube was finally assembled and fridge stored until deployment (expiry date: 4 months).
- (3) Deployed NO_x tubes were fridge stored in zip-lock bags until further analysis via ion chromatography (IC).
- (4) Extraction and IC analysis of NO_x tubes was undertaken in the same week the tube was retrieved from the field. Before tube extraction, dirt and insects/residues were carefully removed from the tubes inside (if necessary), with avoiding touching the grids before extraction.
- (5) Tubes were put into racks, with meshes at the bottom of the tube (grey cap); 3 ml of ultrapure water (18.2 MΩ) were added and tubes were cautiously agitated and extracted for 30 minutes (stopwatch controlled). Extracted tubes were filtered through 0.2µm nylon filters (Fisherbrand™ Non-sterile Nylon Syringe Filter) into IC vials. Filters were pre-cleaned with 10 ml of ultrapure water. About 1.5 ml of extracted tube solution were discarded and ~1 ml was filtered into vials and analysed for Anions by IC for nitrite, sulphate and nitrate on a Thermo Scientific (Dionex) ICS-5000 ion chromatography (IC) system.

Analysed tubes were cleaned and meshes were re-charged using the following procedure: stainless steel meshes were washed using cleaning agent “Decon 90” and ultrasonication for 15 minutes. Secondly, meshes were washed in diluted hydrochloric acid (HCl – 1 mol) for 30 minutes, rinsed with ultrapure water (18.2 MΩ) and oven dried at 100°C.

Acrylic tubes and caps were washed with cleaning agent (Decon90), cotton-tipped brushes and ultrasonication (15 min). Cleaned meshes and tubes were prepared as described above and fridge stored in zip-lock bags until analysis.

3.3.3 NO_x diffusion tube analysis by ion chromatography (IC)

Ion chromatography (IC) is a well-established technique to monitor ions (anions and cations) in different environmental compartments (i.e. water and air; (Michalski et al., 2012). In this study, IC provided a fast and easy method to simultaneously analyses NO_x diffusion tube extracts for NO₂⁻.

Anions were analysed using an AG18 guard column (2 mm x 50 mm) and an AS18 (IonPac™) separation column (2 mm x 250 mm). A potassium hydroxide eluent gradient was generated electrolytically using a EGC III KOH cartridge starting at 18 mM KOH with a slope of 1.96 mM/min for 16 minutes. Signals were measured using suppressed conductivity.

'Laboratory blanks', prepared in the same way, but not deployed (left within zip-lock bags in laboratory fridge), were included during each NO_x tube extraction, handled in exactly the same way as deployed tubes. Laboratory blanks (N=3, for each analytical run) were used for subtraction before further data analysis. Travel blanks, prepared tubes that are carried when deploying and collecting NO_x diffusion tubes (but were not exposed), were included as well but not used for blank subtraction, but to highlight possible preparation contamination issues (DEFRA, 2009). Filter blanks (N=1, for each analytical run) were used to check for possible contamination from the filter material (0.2µm nylon filters).

Calibration standard 'Dionex™ Seven Anion Standard II' (supplied by Thermo Scientific; specifications: Table 3-5) was made up fresh for each IC run. A six point calibration was used for each run, using following concentrations (Table 3-5).

Table 3-5: Calibration concentrations NO_x tube analysis made from 'Dionex™ Seven Anion Standard II'

Nitrite and Nitrate [100mg/l]	
Calibration "zero"	
	0.05 mg/l
	0.01 mg/l
	0.5 mg/l
	1.0 mg/l
	2.0 mg/l

Certified Reference Material 'Simple Nutrients – Whole Volume (QC3198)' (supplied by Sigma-Aldrich) was used to check for accuracy and precision throughout IC runs. Initial concentrations of the CRM were too high for IC equipment and needed to be diluted with ultrapure water (18.2 MΩ, dilution factor 1:5). Following IC analysis and data processing, i.e. blank subtraction and linear calibration check, NO₂ concentrations were calculated.

3.3.4 NO_x diffusion tube calculations for NO₂ in ambient air

Calculations for nitrite concentrations in air followed the DEFRA guidelines (AEA Energy and Environment, 2008) using the following equations:

$$(1) C = \frac{1}{\text{'sampling rate'}}$$

$$(2) \text{'sampling rate'} = \frac{D_{NO_2} * a}{l}$$

With C being the concentration of NO₂ in the atmosphere (µg/m³), m as the mass of nitrite in tube (µg) and t as exposure time (h). The 'sampling rate' (in equation 2) was calculated by using the diffusion coefficient of NO₂ through air (D) the cross sectional area (a) and the length of the tube (l), shown in Table 3-6. For tubes exposed in the UK the diffusion coefficient D equals 1.46×10^{-5} m²/s, the cross sectional areas $a = 9.503 \times 10^{-5}$ m² and the length $l = 0.071$ m (AEA Energy and Environment, 2008).

The calculated 'sampling rate' for the NO_x diffusion tubes was calculated as 70.2×10^{-6} m³/h. To compare the values with EU limit values, measured concentrations must be reported in mass units (µg/m³) at a temperature of 293K (20°C), making it necessary to apply a correction factor to the equation.

The 'sampling rate' and the correction factor of 0.969 (for 284K to 293K) can be incorporated into equation (1), resulting in equation (3).

$$(3) C = 0.969 * 14245 * \frac{m}{t}$$

Table 3-6: Specifications for calculations of NO₂ concentrations from NO_x diffusion tubes; diffusion coefficients for NO₂ in air, together with tube dimensions and correction factor for EU comparability

Parameter	NO ₂
Diffusion coefficient (D) in air for the UK	1.46×10^{-5} m ² /s (at 11°C) #1
NO _x diffusion tube dimensions <ul style="list-style-type: none"> • tube cross sectional area (a) • tube length (l) 	9.503×10^{-5} m ² 0.071 m
Calculated 'sampling rate' for NO _x diffusion tubes deployed in Manchester	70.2×10^{-6} m ³ /h
EU temperature correction (at 20°C; 293K) for comparability	0.969 #2

#1: typical mean UK ambient temperature at 284K (11°C) (AEA Energy and Environment, 2008)

#2: correction from 284K to 293K (AEA Energy and Environment, 2008)

3.4 Statistical data analysis

Statistical analysis was undertaken using 'SPSS Statistics 25' and 'GraphPad Prism 7'. Data visualisation was undertaken using Origin 2018.

Normal distribution of data, obtained for lichen diversity (i.e. reference and eutrophication species) and NO_x diffusion tubes (i.e. NO₂), was tested with a Shapiro-Wilk test. Shapiro-Wilk is considered a stronger statistical test for normality, compared to other tests (e.g. Kolmogorov-Smirnoff), regardless of sample size and distribution (Mendes and Pala, 2003; Razali and Wah, 2011).

Lichen reference species were not drawn from a normal distribution ($p < 0.05$), whereas eutrophication species were drawn from a normal distributed population, favouring the use of non-parametric tests (i.e. Kruskal-Wallis) and parametric test (i.e. ANOVA), respectively. NO₂ concentrations recorded with NO_x diffusion tubes were drawn from a normal distribution. Statistical relationships for NO₂ concentrations (with lichen diversity) were analysed using Pearson's r correlation (parametric test).

Grouping of data for statistical analysis of urban environmental variables (Table 3-7) was described in detail in chapter 2, i.e. classification of distance to major road based on NO_x decline within the first 200 m distance from major roads (i.e. highways; Gilbert et al., 2003; Laffray et al., 2010; Bermejo-Orduna et al., 2014). Road class and traffic counts were based on traffic count statistics (available for major roads; DfT, 2017a) and the UKs 'primary route network' (including major roads: A-roads, B-roads and motorways; UK Department of Transport, 2012). Surrounding building heights were calculated using the close surrounding of the tree (50 m buffer around the sampling location), using the dataset 'OS building heights – alpha' (Digimap - Ordnance Survey, 2017). Classification of 'distance to large point sources' was based on potential pollutant distribution at greater distances (Britter and Hanna, 2003; NAEI, 2015). Distances to greenspace (using 'OS – Open Greenspace' (Digimap - Ordnance Survey, 2018) classifications were based on human health studies, reporting decreased impacts of air pollution within the first 30 m and 500 m of greenspaces (Dadvand, de Nazelle, et al., 2012; Dadvand, Sunyer, et al., 2012; Browning and Lee, 2017).

Table 3-7: Urban environmental variables [grouped] with potential influences on lichen diversity and NO₂ concentrations in the City of Manchester

Environmental variable	Data grouping
Distance to major road (including A-roads, B-roads and motorway)	1: <25 m 2: 25-50 m 3: 50-100 m 4: 100-200 m 5: >200 m
Traffic counts (annual average daily traffic flow)	1: <10.000 2: 10.000 to 20.000 3: 20.000 to 30.000 4: >30.000
Building heights	1: <10 m 2: 10 to 20 m 3: >20m
Distance to (large) point source	1: <500 m 2: 500 to 1000 m 3: 1000 m to 2000 m 4: >2000m
Distance to greenspace	1: <100 m 2: 100 to 200 m 3: 200 to 300 m 4: 300 to 400 m 5: 400 to 500 m 6: >500 m

Climatic data for Manchester (i.e. temperature [°C], total precipitation [mm], wind direction [°] and wind speed [m/s]) was obtained from the 'Whitworth Meteorological Observatory', with permission from Dr Michael Flynn (personal E-mail communication: January 2018), located at the University of Manchester (*Whitworth Meteorological Observatory - Data Archive*, 2018). Data was obtained from July 2017 (01/07/2017) to June 2018 (30/06/2018), as this was deployment period for NO_x diffusion tubes. Wind, precipitation and temperature may influence passive monitoring devices performance (Heal et al., 2000; Kirby et al., 2000, 2001; Cape, 2005; AEA Energy and Environment, 2008).

3.5 Geospatial data analysis

Geographic Information Software (GIS; ArcMap 10.5 and QGIS 3.4.2 – 'Madeira') was used for geospatial analysis and mapping of NO_x tube data. Environmental studies, assessing air quality and atmospheric pollution applied kriging methods to datasets derived from passive and active monitoring programmes, i.e. NO_x diffusion tubes and automated monitoring stations (Romary et al., 2011; Beauchamp et al., 2012; Pannullo et al., 2015).

Ordinary Kriging is one of the most frequent used kriging model assuming a constant trend and a spatially homogenous variation of air pollution (Webster and Oliver, 2007; Ribeiro et al., 2016). It has been successfully applied in environmental epidemiological studies, i.e. assessing human exposure to pollutants (i.e. PAHs) using lichens as biomonitors (Augusto et al., 2012). Ordinary Kriging (OK) was applied to NO₂ data from NO_x diffusion tubes to investigate spatial patterns.

As previously described (Chapter 2), Manchester's characteristics (i.e. building heights, road classes, greenspace distribution and traffic counts; Table 3-7) are diverse throughout the research area. To further investigate small-scale variability and include urban influencing factors (Table 3-7) on pollutant distribution and dispersion, geospatial statistics were applied. Geographically weighted regression (GWR) is commonly used in geographical sciences, providing reliable statistics (for estimation of relationships) and a "local"/regional scale of the variable modelled (Fotheringham et al., 2002; Yang and Wang, 2017; ESRI, 2019). Modelling was undertaken for NO₂ concentrations, due to primary focus of this study. NO₂ concentrations (mean concentrations) were used as 'dependent variable' and urban influencing factors were used as 'explanatory variables' within the GIS (ArcMap 10.5 default setting input features: fixed Kernel type; Bandwidth method: 'Akaike Information Criterion' - AICc; number of neighbours: 30).

3.6 Results – Lichen diversity across Manchester

The lichen diversity was evaluated at 58 trees across the city centre of Manchester. Recorded lichen species for specific sites are displayed in the Appendix A-2.

The main lichen families, accounting for 52.3% of families found across the research area, are *Teloschistaceae* (Genus: *Xanthoria* spp.; 23.87%; Figure 3-7) and *Physciaceae* (Genera: *Physcia* spp. and *Phaeophyscia* spp.; 28.40%; Figure 3-7), which belong to eutrophication species (excluding *Physcia aipolia*). Reference species families that were recorded are *Candelariaceae* (Genus: *Candelariella* spp.; 14.50%), *Calciaceae* (Genus: *Buellia* spp.; 9.06%) and *Lecanoraceae* (Genus: *Lecanora* spp.; 9.06%). *Arthoniaceae* (Genus: *Arthonia* spp.) and *Stereocaulaceae* (Genus: *Lepraria* spp.) account for 2.72% and 4.83% respectively. Only 0.6% of lichens recorded belong to the family of *Ramalinaceae* (Genus: *Lecania* spp.) and

1.81% to *Parmeliaceae* (Genera: *Evernia* spp., *Flavoparmelia* spp., *Parmelia* spp., *Parmelina* spp. and *Melanohalea* spp.).

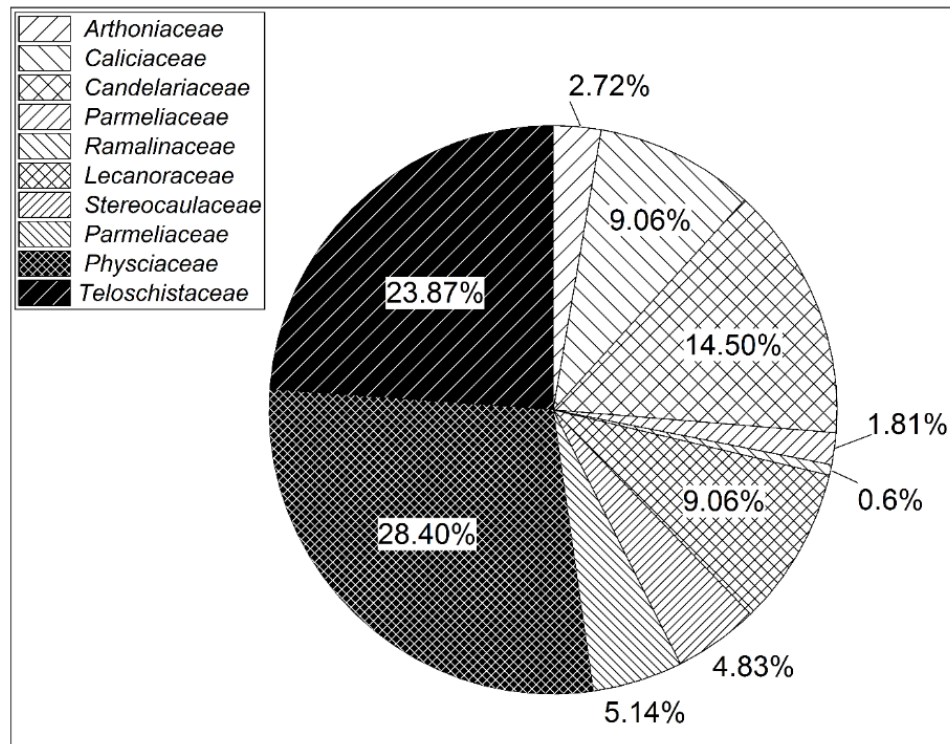


Figure 3-7: Pie chart of lichen families recorded on examined trees to assess lichen diversity across Manchester; reference species are displayed as white patterns, eutrophication species as black patterns

A 1x1 km grid, that is usually used for cities (Kirschbaum and Wirth, 2010), was applied to the wards of Manchester city centre that were analysed for lichen diversity. Trees included within a grid square were used for AQI calculations, following the aforementioned procedure (section 3.2.3). Figure 3-8 illustrates the grid, analysed trees and Lichen Diversity Index (LDI; according to section 3.2.3 and procedure described in (Table 3-3) for reference and eutrophication species (a) and subsequently colour coding (b) according to the evaluation matrix (Figure 3-8). Figure 3-8(a) highlights that eutrophication species, i.e. *Xanthoria* spp. and *Physcia* spp., are dominant across Manchester (except in M09) in the analysed areas. Lichen Diversity Indices (LDI) for eutrophication species range from 3.5 to 17.8, while the LDI for reference species range from 4.00 to 31.25, indicating higher abundance of reference species (referring to Table 3-1) in Manchester. In general, air quality in Manchester can be classified as 'average air quality' (3.) with 'low to high influences' (.2 to .4) of eutrophication, i.e. nitrogen compounds (Figure 3-8b). Figure 3-9(a) illustrates the 'by-tree approach', with the majority of sites belonging to 'very high' (26 trees) and 'high' (15 trees) eutrophication (according to Table 3-4). Eight analysed trees were classified as 'very low eutrophication'.

Figure 3-9(b) displays the lichen frequency, classified as reference and eutrophication species. Most frequent reference species recorded in the research area are *Candelariella reflexa* (48 trees) and *Buellia punctata* (also called *Amandinea punctata*, 30 trees). Rare lichens recorded were *Punctelia subrudecta*, *Parmelina tiliacea* and *Flavoparmelia soredians* (all recorded only once). *Evernia prunastri*, a fruticose lichen, was recorded at four sites. Eutrophication species, that were mostly recorded are: *Physcia tenella* (57 trees), *Xanthoria ucrainica* and *Xanthoria parietina* at 43 and 36 trees, respectively. *Phaeophyscia orbicularis* and *Physcia adscendens* were recorded at 21 and 14 trees in Manchester, respectively. Predominance of eutrophication species, i.e. nitrogen preferring lichen species (e.g. genus *Xanthoria* and *Physcia*) indicates influences of nitrogen compounds on lichen diversity across Manchester. Lichen species classified as 'reference' species (e.g. *Candelariella reflexa* and *Buellia punctata*) occur on nutrient-enriched substrates (Nimis et al., 2009) and point towards deteriorated air quality by nitrogen compounds. However, rare lichen findings indicate site-specific influences on lichen diversity, i.e. sunlight and rain run-off, bark pH, microclimatic conditions, local effects, i.e. street canyons.

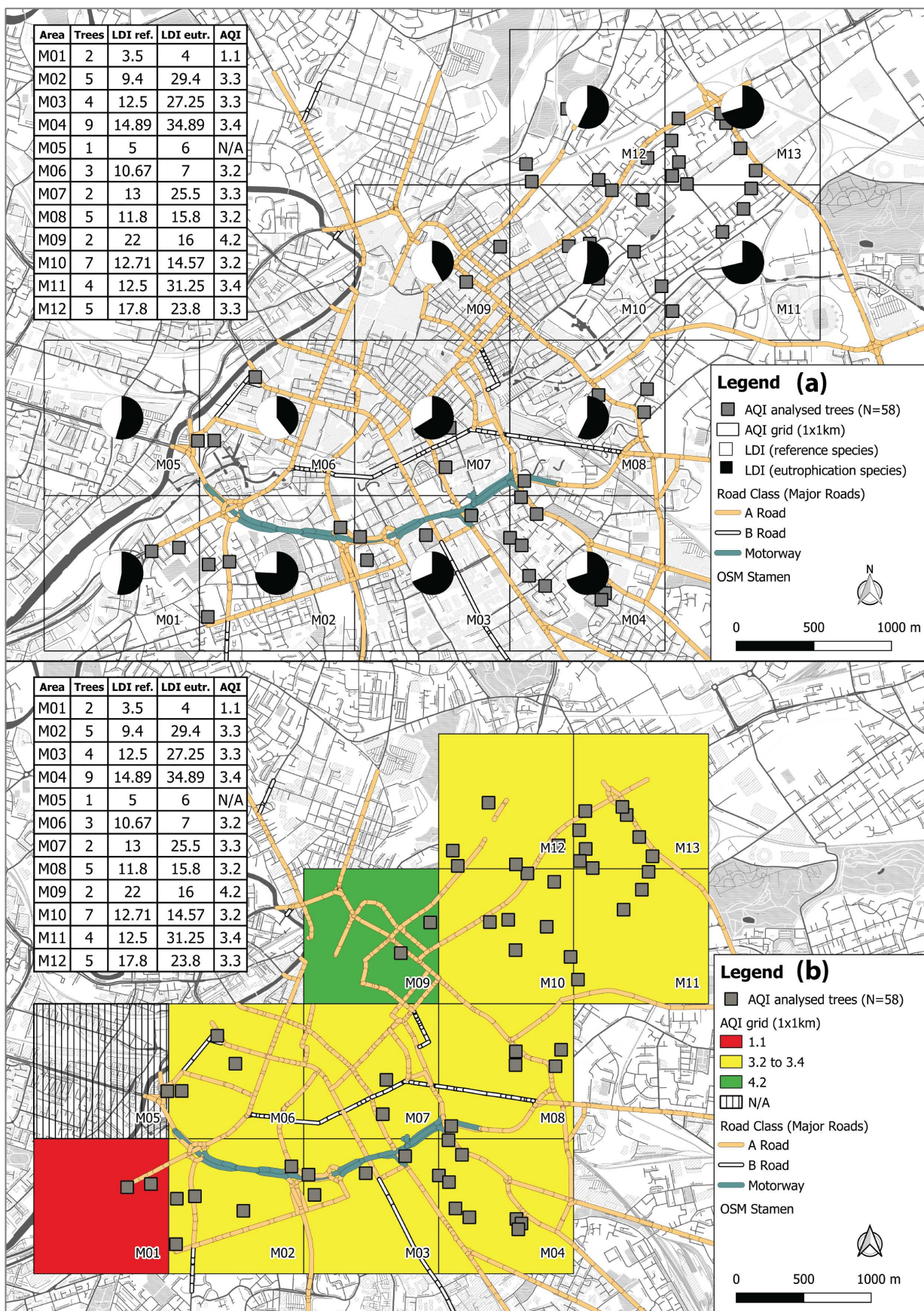


Figure 3-8: Lichen diversity map – (a) 1x1 km grid, included analysed trees (N=58), LDI for reference and eutrophication species and (b) 1x1 km grid colour codes according to Figure 3-4 (evaluation matrix) and AQI for each area (N/A – one tree analysed, no evaluation matrix used); displayed with major road classes and attribute table

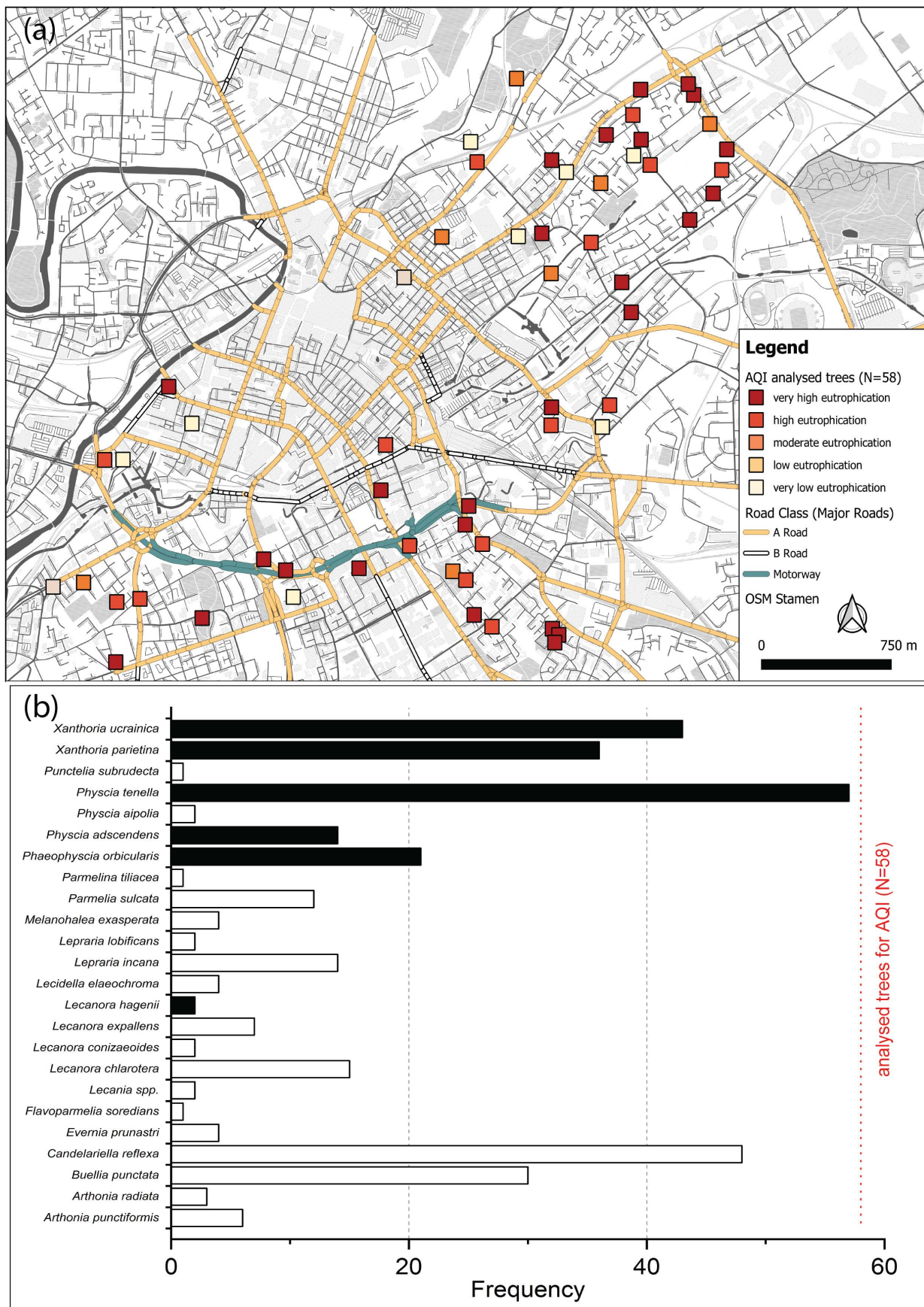


Figure 3-9: Lichen diversity – (a) by tree approach, classified as ratio between reference and eutrophication species (colour-coded according to Table 3-4), major road classes and frequencies of recorded lichen species (b)

To investigate potential influences of distance to (major) road (i.e. A-, B-road and motorway) and traffic counts, correlation statistics (and group differences; ANOVA for eutrophication species and Kruskal-Wallis for reference species) were analysed. No statistical significance was found between lichen diversity and distance to major road and traffic counts (Figure 3-10). Therefore, additional factors are suggested, such as urban climatic factors that may influence epiphytic lichen diversity.

However, vehicular emitted NO₂ is potentially higher along highly trafficked roads, where predominance of eutrophication species was recorded (see Figure 3-9). To further investigate NO₂ concentrations across Manchester (and assess potential influences on lichen diversity) NO_x diffusion tubes were deployed across Manchester. Diffusion tubes were deployed over a 12-months period, between June 2017 and July 2018, to ground-truth lichen chemical data and assess spatio-temporal variability of air quality across the City of Manchester. However, potential influences on lichen diversity were suggest at sites close to highly trafficked roads.

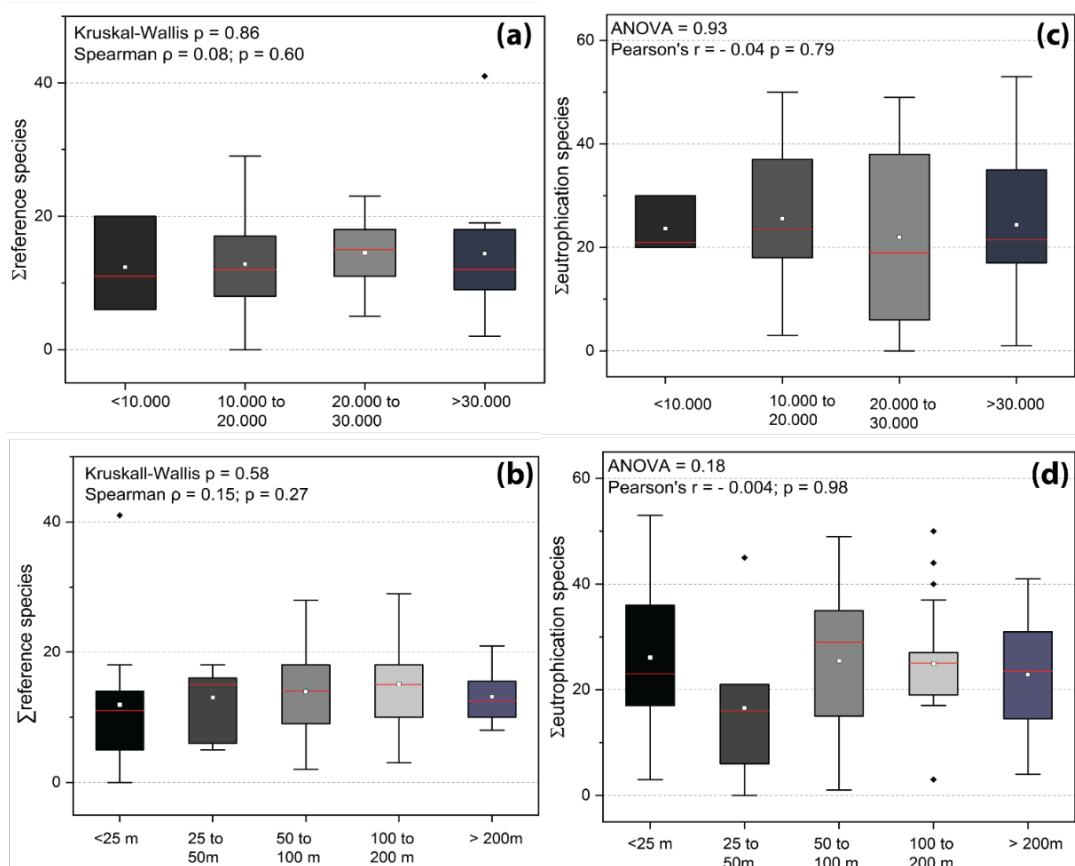


Figure 3-10: Box-Whisker plots (25th to 75th percentile) of (a) reference species and traffic counts (grouped, N=46), (b) reference species and distance to major road (grouped, N=46), (c) eutrophication species and traffic counts (grouped, N=58) and (d) eutrophication species and distance to major road (grouped, N=58); Pearson's r and ANOVA p -values are displayed for eutrophication species (normally distributed); Spearman ρ and Kruskal-Wallis p -values are displayed for reference species.

3.7 Results – NO_x diffusion tubes

3.7.1 Assessment of accuracy and precision of NO_x diffusion tube analysis by IC

NO_x diffusion tube analysis was accompanied by analysis of 'certified reference material' (CRM) for all analytical runs on the IC (24 times). Analysed NO₂⁻ in CRM for all batches was below the nitrite reference value (NO₂⁻: 2.95 mg/l; Sigma-Aldrich, 2017). Figure 3-11a illustrates the variability of measurements (N=230) for all analysed batches (within the 95% confidence interval), whereas Figure 3-11b shows analysed mean concentrations of NO₂⁻ for each analytical batch. Only few measurements were found outside the 95% confidence interval and were not considered as 'outliers' and kept for analysis of accuracy and precision.

Friedman's two-way ANOVA was used to analysed CRM concentrations for differences between analysed batches, due to non-normality of data. Significant ($p < 0.05$) differences were found between batches. However, batch correction was not undertaken, due to already underestimation of nitrite concentrations analysed in NO_x tube extracts. Moreover, calibrations (linear) were checked before data processing and R² showed very good results for all calibrations (R² > 0.98) run with the same method parameters on the IC for each analytical NO_x tube analysis run. Calibration standards and CRM solutions was freshly prepared for each analytical run, indicating potential errors (i.e. pipetting errors and/or dilution errors).

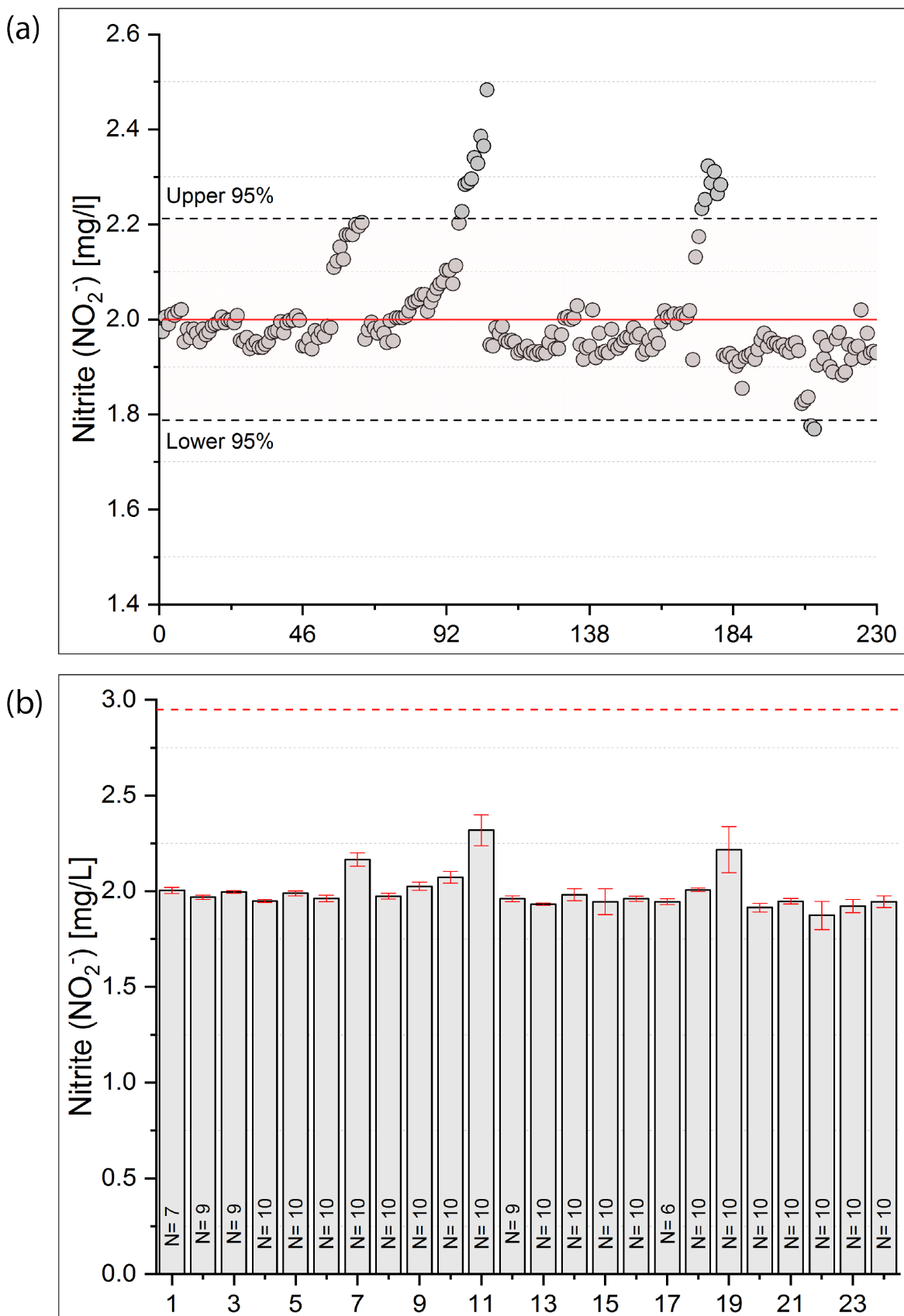


Figure 3-11: (a) Analysed nitrite concentrations (N=230) in certified reference material (CRM Simple Nutrients – Whole Volume QC3198; with upper and lower 95% confidence interval) and (b) mean nitrite concentrations (in CRM) by batch (red dashed line illustrates the certified value 2.95; error bars presented as 1x standard deviation of repeated CRM measurements for each analytical batch); CRM was prepared fresh before each run, instrumental variability can be seen throughout analytical runs, potentially related to instrument components, (i.e. capillary pressure and suppressor)

Analytical accuracy of CRM measurements (N=230) for nitrite was 67.80%, with batch-to-batch accuracy varying between 63.49% to 78.64%. LLDs were determined using ultrapure-water (18.2 MΩ) analysed throughout the IC run (analysed every five samples) within each analytical batch (N=265) and were calculated as three times the standard deviation. Nitrite was consistently lower as the certified reference value for each analysed batch, which could be related to IC analysis specifications. The quality of results is mostly dependent on the type of stationary phase, cross-linking, exchange capacity, eluent type and eluent flow rate (Michalski et al., 2012). For instance, Lee et al. (1998) reported the use of 2.0 mM Na₂CO₃ and 2.5 mM NaHCO₃ as an eluent and a flow-rate of 0.5 ml/min to obtain optimal results for seven anions (including NO₂⁻, NO₃⁻ and SO₄²⁻).

However, this study used a KOH for analysis of anions eluent, which provides highest detection sensitivity and low noise, resulting in lower detection limits on the IC (Pohl and Saini, 2014). Repeatability of measurements (5% for NO₂⁻; Table 3-8) show the suitability of the analytical method for the extracted NO_x diffusion tubes.

Table 3-8: Certified Reference Material – certified values and for IC analysis of NO_x diffusion tubes for nitrite and nitrate (N=230; in mg/l) (Sigma-Aldrich, 2017)

	Certified Value¹	Mean values (analysis)	Accuracy (%) - overall	Precision (%CV) - overall	Lower limit of Detection (LLD) [mg/L]
Nitrite	2.95 ± 0.0536	2.00 ± 0.108	67.80	5.42	0.078
Nitrate	10.5 ± 0.187	10.023 ± 1.477	95.45	14.74	0.063

3.7.2 Nitrogen dioxide (NO₂) concentrations in the City of Manchester

NO_x diffusion tubes at lichen sampling sites (N=45; Figure 3-6), to in part, ground-truth lichen data (i.e. N wt% and δ¹⁵N values) and to analyse spatio-temporal variability of NO₂ concentrations across Manchester. The EU/UK limit values for NO₂, which has been implemented into UK legislations since 2010, is 40 µg/m³ to protect human health (WHO, 2013b; European Commission, 2018; Casquero-Vera et al., 2019). Individual site concentrations of NO₂ ranged from 2.26 to 84.05 µg/m³ for the full yearlong deployment period (Table 3-9).

Table 3-9: NO₂ concentrations recorded at deployment sites (N=45), displayed as minimum - maximum range (mean \pm 1x standard deviation, due to normal distribution of data) to illustrate spatial variability across Manchester (data for 24 biweekly deployments displayed in Appendix A-3)

ID	NO ₂ [$\mu\text{g}/\text{m}^3$]	ID	NO ₂ [$\mu\text{g}/\text{m}^3$]	ID	NO ₂ [$\mu\text{g}/\text{m}^3$]
1	28.45 - 68.54 (43.95 \pm 10.73)	16	23.30 – 52.91 (33.44 \pm 8.10)	31	2.26 – 54.92 (30.25 \pm 11.61)
2	18.79 - 52.50 (33.09 \pm 8.95)	17	23.96 – 61.59 (41.55 \pm 9.49)	32	32.23 – 84.05 (45.70 \pm 11.65)
3	21.99 - 60.07 (39.54 \pm 10.18)	18	29.36 – 53.75 (39.51 \pm 7.67)	33	13.71 – 49.89 (25.23 \pm 8.66)
4	17.08 - 48.94 (28.91 \pm 8.24)	19	26.85 – 61.63 (41.79 \pm 8.21)	34	20.27 – 56.26 (33.21 \pm 8.75)
5	20.09 - 59.09 (37.37 \pm 10.74)	20	14.48 – 55.58 (30.4 \pm 9.09)	35	17.16 – 79.79 (31.33 \pm 12.90)
6	31.05 – 62.63 (43.81 \pm 9.03)	21	19.18 – 46.01 (28.04 \pm 6.72)	36	15.34 – 51.25 (27.25 \pm 8.95)
7	23.91 – 54.92 (35.67 \pm 8.32)	22	7.35 – 54.74 (33.76 \pm 10.04)	37	14.69 – 44.24 (26.68 \pm 8.50)
8	14.69 – 43.60 (27.94 \pm 8.45)	23	22.59 – 47.02 (32.64 \pm 6.81)	38	17.96 – 66.27 (31.26 \pm 10.38)
9	21.01 – 65.27 (41.43 \pm 10.29)	24	25.92 – 56.26 (36.30 \pm 7.77)	39	16.13 – 53.25 (28.01 \pm 9.09)
10	16.55 – 41.59 (29.35 \pm 7.76)	25	24.22 – 64.15 (41.70 \pm 9.76)	40	15.69 – 56.26 (33.42 \pm 8.95)
11	18.75 – 45.24 (29.58 \pm 8.60)	26	10.65 – 39.73 (23.28 \pm 8.96)	41	12.88 – 47.74 (25.40 \pm 9.75)
12	11.96 – 48.24 (28.16 \pm 10.67)	27	22.50 – 63.46 (35.24 \pm 10.21)	42	18.82 – 53.75 (32.41 \pm 8.79)
13	24.05 – 62.30 (40.18 \pm 9.38)	28	16.92 – 48.39 (29.68 \pm 8.30)	43	8.16 – 68.78 (30.75 \pm 13.31)
14	21.37 – 47.67 (32.08 \pm 6.42)	29	13.43 – 44.87 (26.66 \pm 8.00)	44	11.51 – 56.76 (27.01 \pm 10.71)
15	25.57 – 58.93 (37.61 \pm 9.33)	30	30.87 – 68.98 (50.00 \pm 9.90)	45	13.84 – 51.75 (27.56 \pm 9.46)

Analysed NO₂ concentrations varied throughout the year, and all sites, except one, exceeded the limit value at least once. About 47% of all deployment sites exceeded 40 $\mu\text{g}/\text{m}^3$ less than 5 times. Of 45 sites, 13 sites (29%) were above the limit value between 5 to 10 times. Exceeding the limit value more than 10 times occurred at 10 sites, of which one exceeded it 22 times.

Table 3-10 displays the amount of sites that exceeded the EU/UK limit value during the deployment time (in %), with one site exceeding the WHO value of 40 $\mu\text{g}/\text{m}^3$ for more than 75% of the 24 bi-weekly deployment periods. In contrast, only one site did not exceed the limit value during this time.

Table 3-10: NO_x tube deployment sites exceeding the EU/UK NO₂ limit value (40 µg/m³) during the year-long deployment across Manchester to evaluate potential 'hot-spots' of NO₂, colour-coded by % of exceedance (descending order)

Exceedance of 40 µg/m ³	Number of sites
>75%	1
75% to 50%	5
25% to 50%	14
<25%	25
0%	1

Limit value (40 µg/m³) exceedance at deployment sites are displayed in Figure 3-12, colour coded as percentage and displayed with number of times above the limit value. Exceedances of the 40 µg/m³ were predominantly recorded along major roads (especially the motorway; Figure 3-12) and within the city centre (close to Piccadilly Gardens automated monitoring station). Exceedances of less than 25% were recorded in the northeast and southwest of the area and sites further away from major roads (A and B roads).

Exceedances, primarily occurring within the city centre area (and along the major road network; Figure 3-13) indicate vehicular emissions as primary source of NO₂. Moreover, higher NO₂ suggests potential human health impacts within the city centre of Manchester.

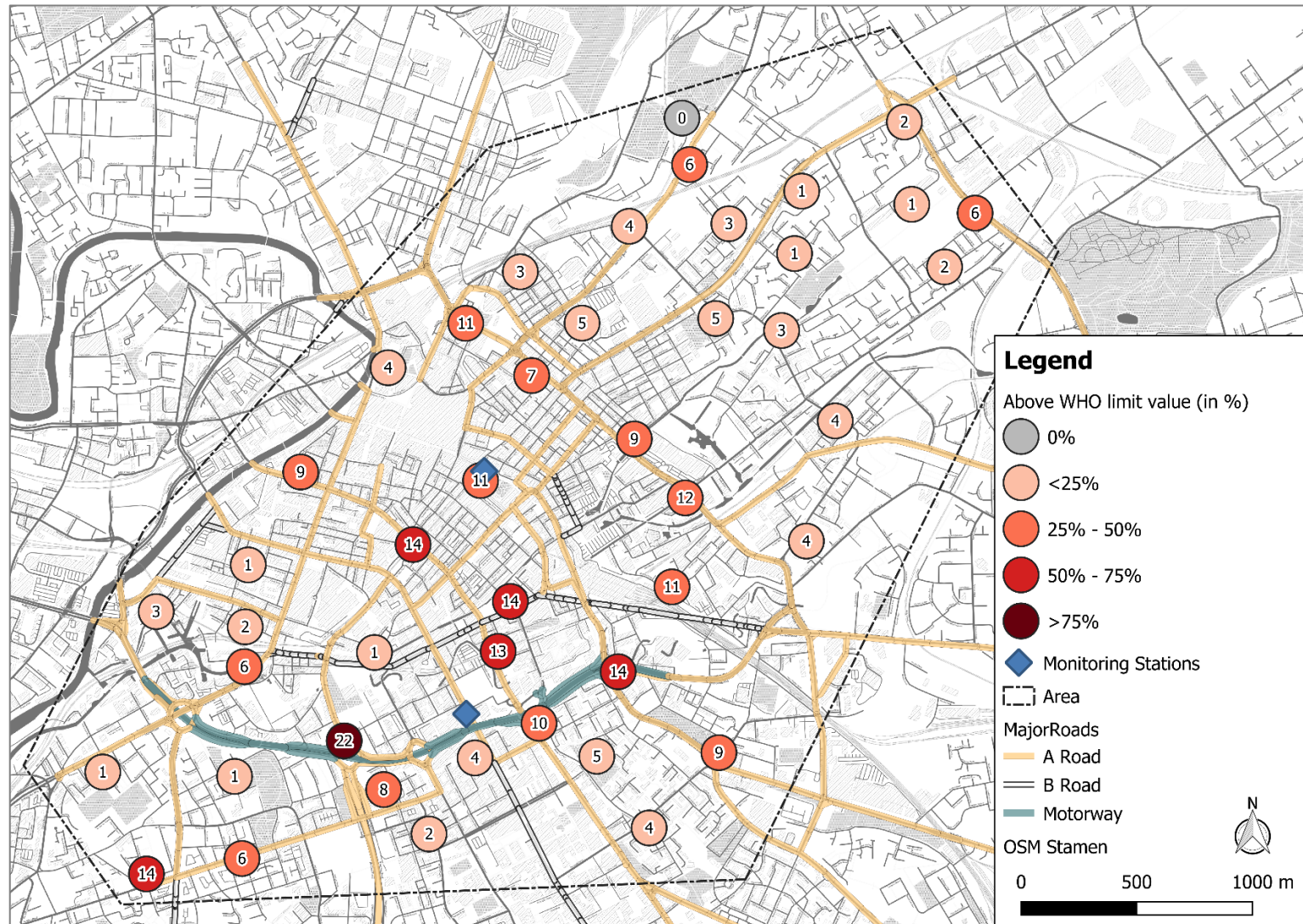


Figure 3-12: NO_x tube deployment sites that exceeded the WHO limit value of 40 µg/m³ (colour coded by percentage of exceedance), displayed with number of exceedance out of 24 bi-weekly deployments; one site was recorded (grey circle) with no exceedance for the deployment period

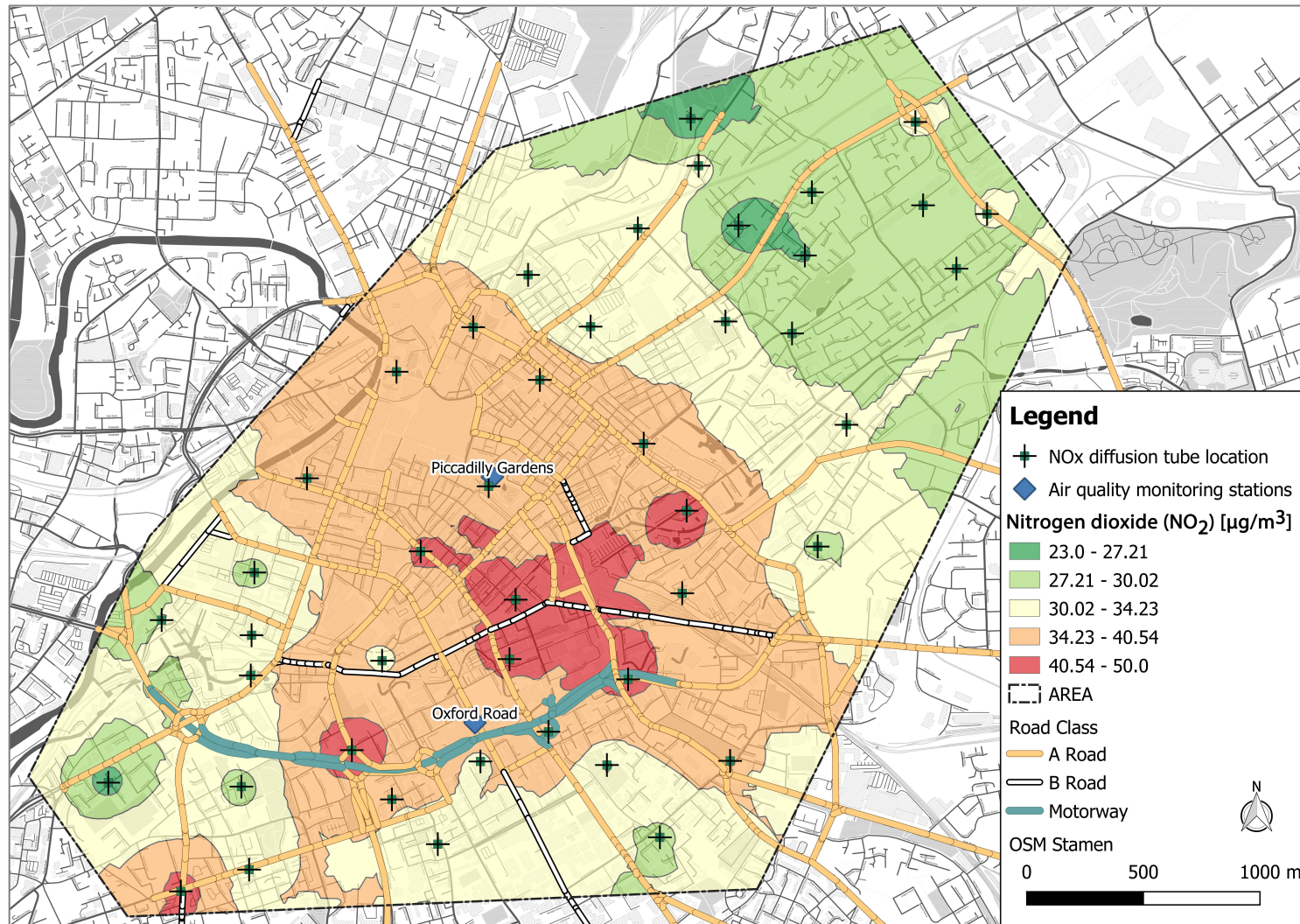


Figure 3-13: Analysed mean concentrations [in $\mu\text{g}/\text{m}^3$] of NO₂ concentrations for all deployment sites (N=45) between the 03/07/2017 and the 28/06/2018; no influencing factors (i.e. building heights, distance to road etc.) were used for spatial interpolation of data (mean NO₂ values were interpolated by ordinary kriging; kriging error map is displayed in the Appendix A-4)

3.8 Interpretation and discussion

3.8.1 Lichen diversity across Manchester in relation to air quality

Lichen diversity across Manchester (evaluated on 58 street tree trunks) was used to obtain an overview of atmospheric pollutants (i.e. nitrogen compounds) and a potential influence on lichen communities. Dominant lichen families in Manchester were *Teloschistaceae* and *Physciaceae*, including both lichen species sampled for further chemical analysis (*X. parietina* and *Physcia* spp.).

'Eutrophication' species, i.e. *Physcia tenella* (98%), *X. ucrainica* (74%) and *X. parietina* (62%) were most frequent at analysed sites across Manchester. *Xanthoria* and *Physcia* lichens are considered as nitrogen-tolerant species ('nitrophytic'; Van Herk, 1999; Kirschbaum and Wirth, 2010; Dobson, 2011) and dominance of these species and families suggest influences of nitrogen compounds in the urban environment of Manchester.

NO_x and NH₃, both part of vehicular emissions, could influence lichen diversity recorded in Manchester (Sutton et al., 2000; Degraeuwe et al., 2017). Moreover, NO_x was considered to prevent colonisation of *Parmelia saxatilis*, preferring acid-rich bark, at trees in proximity to roads (Batty et al., 2003; Davies et al., 2007; Kirschbaum and Wirth, 2010). A decline in oligotrophic species (i.e. requiring low nitrogen) was reported with proximity to anthropogenic influences, e.g. higher NO₂ concentrations in urban areas, whereas nitrophytic species thrive with increasing N loads (Pinho et al., 2008). For instance increased nitrogen contents in *Physcia adscendens*, with proximity to highly trafficked roads were reported, whereas such a relationship was not found for *Hypogymnia physodes* (Gombert et al., 2003; Davies et al., 2007).

X. parietina was found to be present at sites with high nitrogen loads, i.e. around a nitrogen fertiliser plant (Lithuania) and a highly trafficked area (in Spain) with increasing lichen diversity with distance from pollution sources (Blasco et al., 2008; Kostryukova et al., 2017; Sujetovienė, 2017). Therefore, vehicular emissions of NO_x could influence lichen communities, i.e. by promoting the growth of nitrogen-tolerant species, within the urban environment of Manchester.

On the contrary, increases in ammonia concentrations increase the pH of the substrate, i.e. tree bark, which could explain occurrence of nitrogen-tolerant lichen species that are able to withstand elevated levels of ammonia (Olsen et al., 2010). Moreover, *X. parietina* was reported to be positively related to wet deposition of NH_x , i.e. ammonium (NH_4^+ ; Seed et al., 2013), indicating its high tolerance towards N-elevated environments.

In contrast, acidophytic species, such as *H. physodes*, are negatively affected by high NH_3 concentrations, resulting in disappearance of those species (Søchting, 1995; Olsen et al., 2010). Hence, primarily nitrogen-preferring lichens on tree trunks could indicate ammonia influences on bark pH. Mechanisms trying to explain increases in 'nitrophytic' lichens include: (1) a potential upward trend of bark pH, due to decreased SO_2 , (2) preference of high bark pH by nitrophytic species, (3) higher sensitivity of nitrophytic species towards SO_2 and (4) rapid response of nitrophytic species to sudden decrease in SO_2 , suggesting a more rapid colonisation by nitrophytes than other lichen species (Van Dobben and Ter Braak, 1998; Krupa, 2003). In contrast, reference species, which are generally negatively affected by high nitrogen loads, found in Manchester were *Candelariella reflexa* and *Buellia punctata* (also *Amandinea punctata*). Both lichen species can grow on nutrient-enriched bark and are common across the UK (Kirschbaum and Wirth, 2010; Dobson, 2011). *A. punctata* is less affected by air pollution and is often present at sites with *C. reflexa*, *Physcia adscendens* and *Ph. tenella*, showing its wide ecological amplitude (Wirth, 1995; Kirschbaum and Wirth, 2010). For London, Davies et al. (2007) reported lichen families *Candelariaceae*, *Physciaceae* and *Teloschistaceae* where NO_x was highest, which is comparable with findings presented. Presence of 'reference' lichens that also prefer nutrient-enriched bark further suggest nitrogen influences across Manchester, due to potentially increased bark pH by nitrogen compounds and rapid colonisation of these lichen species.

Rare recorded lichen species (e.g. *Flavoparmelia soredians*, *Punctelia subrudecta* and *Evernia prunastri*) are more sensitive towards atmospheric pollution (Dobson, 2011). For instance, *F. soredians* is considered as 'intermediate' species, i.e. can be found under clean and polluted conditions and appears to be tolerant to nitrogen (Nimis et al., 2009; OPAL, 2015b). In contrast, *E. prunastri* is sensitive considered towards nitrogen pollution (Nimis et al., 2009).

NO_x rapidly declines with distance to the emission source, i.e. major roads (Cape et al., 2004) and *E. prunastri* was found at sites further away from major roads. However, *E. prunastri* was found as solitary individual on trees, suggesting bark surface roughness, bark pH and the urban microclimate as potential influencing factors (Wolseley and Pryor, 1999; Käffer et al., 2011; Munzi et al., 2014). Moreover, dispersion and removal of pollutants is governed by local meteorological conditions (Hertel and Goodsite, 2009) and solitary individuals could be growing on 'less polluted' parts of the tree, i.e. shaded from high pollutant effects.

For Manchester in particular, urban climatic conditions and air quality are influenced by its urban structure, i.e. 'fresh air corridors', building structures and materials and urban greenspaces (Salmond and McKendry, 2009; Trees & Design Action Group, 2012; Salmond et al., 2013; Janhäll, 2015). For instance, Longley et al. (2004) highlighted the complexity of wind direction and street canyon effects, and subsequent dispersion of pollutants within the city centre of Manchester. In consequence, this could also affect lichen diversity at particular locations and at cardinal directions on the tree.

A predominance of eutrophication species (i.e. *X. parietina* and *Physcia* spp.) across Manchester suggests that high nitrogen loads may be favouring the growth of these lichen species. In particular, locations close to major roads (Figure 3-9) showed higher frequencies of nitrophytic species. Faster colonisation abilities of nitrogen-tolerant lichens, compared to sensitive species, could also be responsible for predominantly 'nitrophytic' lichen communities recorded across Manchester (Van Dobben and Ter Braak, 1998; Krupa, 2003).

However, sites with increasing distance from major roads (Figure 3-9) showed an increase in 'reference species' including sensitive lichen species, suggesting a rapid decline of nitrogen compounds with increasing distance to major roads. Nevertheless, locations within residential or industrial/manufacturing surroundings, i.e. the north-east and south-east of the research area (Figure 3-9), also showed presence of 'eutrophication' species. Additional influences, i.e. bark pH, water, light and nutrient status, urban climate (Spier et al., 2010; Munzi et al., 2014; Shukla et al., 2014), as well as specific emissions (NO_x, SO₂ and other compounds) of its close surrounding are suggested, i.e. energy production, residential and industrial combustion (NAEI, 2018f, 2018g).

Lichen growth may vary between regions, due to ecological and climatic, as well as floristic differences and should be critically interpreted according to the specific region (Asta, Ferretti, et al., 2002). A UK-wide 'Open Air Laboratory (OPAL)' volunteering lichen biomonitoring study was undertaken between 2009 and 2011 across England, analysing presence/absence of lichen species on tree trunks in Greater Manchester (Seed et al., 2013; OPAL, 2015a). However, only 3 analysed trees were located within the area for this study, with no species-specific data available. Additionally, the 'Greater Manchester Ecology Unit' provides datasets on lichens across Greater Manchester (GMUE, 2017; NBN, 2019). Again, no data for the specified research area in this study is available. Therefore, no detailed comparison between this study and other data was possible, highlighting the beneficial use of lichen diversity to extend these datasets and extend the lichen survey on atmospheric pollution across Manchester.

The method applied in this study to evaluate lichen diversity was based on the standardised method presented by Asta, Erhardt, et al. (2002). However, analysed trees were not evenly distributed across the 1x1 km grid superimposed onto the city centre of Manchester (Figure 3-8), as suggested by (Asta, Erhardt, et al., 2002; Kirschbaum and Wirth, 2010). Supplemental analysis of tree trunks within each grid could provide finer spatial detail of air quality and lichen diversity, indicate potential future research potential. Moreover, it is suggested to analyse tree twigs for lichen growth, to assess recent air quality impacts (especially by NH_3), due to rapid response by younger lichens on younger bark substrate (Wolseley et al., 2006; Seed et al., 2013).

In this study, the main aim was to sample lichens from twigs and small branches of street trees for chemical analysis of pollutant loadings, to assess recent air pollution. It is important to state, that atmospheric transformation processes (e.g. organic compounds and increased toxicity of reaction products), gaseous pollutants (i.e. CO, SO_2) and trace elements (such as As, Cr, Cd, Mo and Zn) could negatively affect lichen vegetation (Jeran et al., 2002; Giordani, 2007; Blasco et al., 2008; Biazrov, 2010; Augusto et al., 2016; Kostryukova et al., 2017). Moreover, urban microclimatic conditions (i.e. rainfall and temperatures), substrate characteristics and anthropogenic interferences, as well as urban layouts, can play an important role when using lichens as bioindicators (Gombert et al., 2004; Frati and Brunialti, 2006; Wolseley et al., 2006, 2009; Davies et al., 2007; Giordani, 2007; Gadsdon et al., 2010).

Therefore, a complex mixture of pollutants of gaseous (e.g. NO₂ and SO₂) and particulate-bound (e.g. airborne metals and PAHs), especially in urban environments, could additionally influence lichen diversity across Manchester. Chemical analysis of lichens could therefore aid to better evaluate spatial variability of specific pollutants in Manchester, which will be presented in the following chapters.

Findings presented suggested an influence of NO_x compounds (among others) on lichen diversity. NO₂ concentrations, recorded by diffusion tubes, were spatially variable across Manchester. Therefore, potential positive and/or negative impacts on lichen diversity were further investigated.

3.8.2 Lichen species diversity and NO_x tube-derived NO₂ concentrations

Several studies used lichens as bioindicators for air quality across urban environments in Europe (Table 3-11), reporting NH₃, bark pH, NO_x (including NO and NO₂) and SO₂ as influencing factor on lichen diversity and distribution (Van Herk, 1999; Gombert et al., 2004; Wolseley et al., 2006, 2009; Davies et al., 2007; Sparrius, 2007; Larsen Vilsholm et al., 2009; Gadsdon et al., 2010), whereas others related lichen diversity to tree species and climatic conditions (Spier et al., 2010; Munzi et al., 2014).

Table 3-11: Lichen diversity studies in an ‘urban’ context in the UK/EU and variables that were considered to affect lichen frequency and abundance (by direct air measurements, partially modelled and modelled pollutant concentrations) (Jovan et al., 2012)

Authors	Location	Analysed variables
Gadsdon et al. (2010)	Epping Forest (~ 25 km ² , Greater London, UK)	NH ₃ , bark pH, NO ₂
Wolseley et al. (2009)	UK-wide	NH ₃ , bark pH
Davies et al. (2007)	London, UK	NO _x , NO ₂
Sparrius (2007)	Southeast Friesland, NL (~150 km ²)	NH ₃
Wolseley et al. (2006)	Thetford and North Wyke, UK	NH ₃ , bark pH
Gombert et al. (2004)	Grenoble, FR	SO ₂ , NO ₂ , NO

Studies reported the influence of NO_x on lichen communities composition, frequency and declining lichen populations (Van Dobben et al., 2001; Giordani, 2007; Larsen et al., 2007). In contrast, no clear association between epiphytic lichen diversity and air pollutants (i.e. NO, NO₂ and SO₂) was reported in other studies (Gombert et al., 2004; Frati et al., 2006). Manchester’s lichen diversity (i.e. eutrophication and reference species) were related to NO₂ measurements by NO_x diffusion tubes. Significant negative correlation (Spearman $\rho = -0.43$; $p < 0.05$; Figure

3-14) was found between reference species and mean NO₂ concentrations, suggesting potentially toxic effects on non-nitrogen preferring lichens (Figure 3-14).

A UK based study (undertaken in London) associated epiphytic lichen distribution and diversity with NO_x and abundance of eutrophication species. Furthermore, phytotoxic effects for NO_x concentrations >70 µg/m³ and NO₂ concentrations >40 µg/m³ were suggested for species decline (Davies et al., 2007). Diffusion tube measurements across Manchester showed concentrations >40 µg/m³ at some sites (one site in particular was above >40 µg/m³ for 22 times). Therefore, high NO₂ concentrations recorded could indicate toxic effects on 'nitrogen-sensitive' lichen species, whereas N-tolerant lichens, such as *X. parietina* and *Physcia* spp. are able to withstand high NO₂. However, the influence of NO_x on particular lichen species is difficult to identify, even though a general influence on lichen communities seems to be established (Gombert et al., 2003).

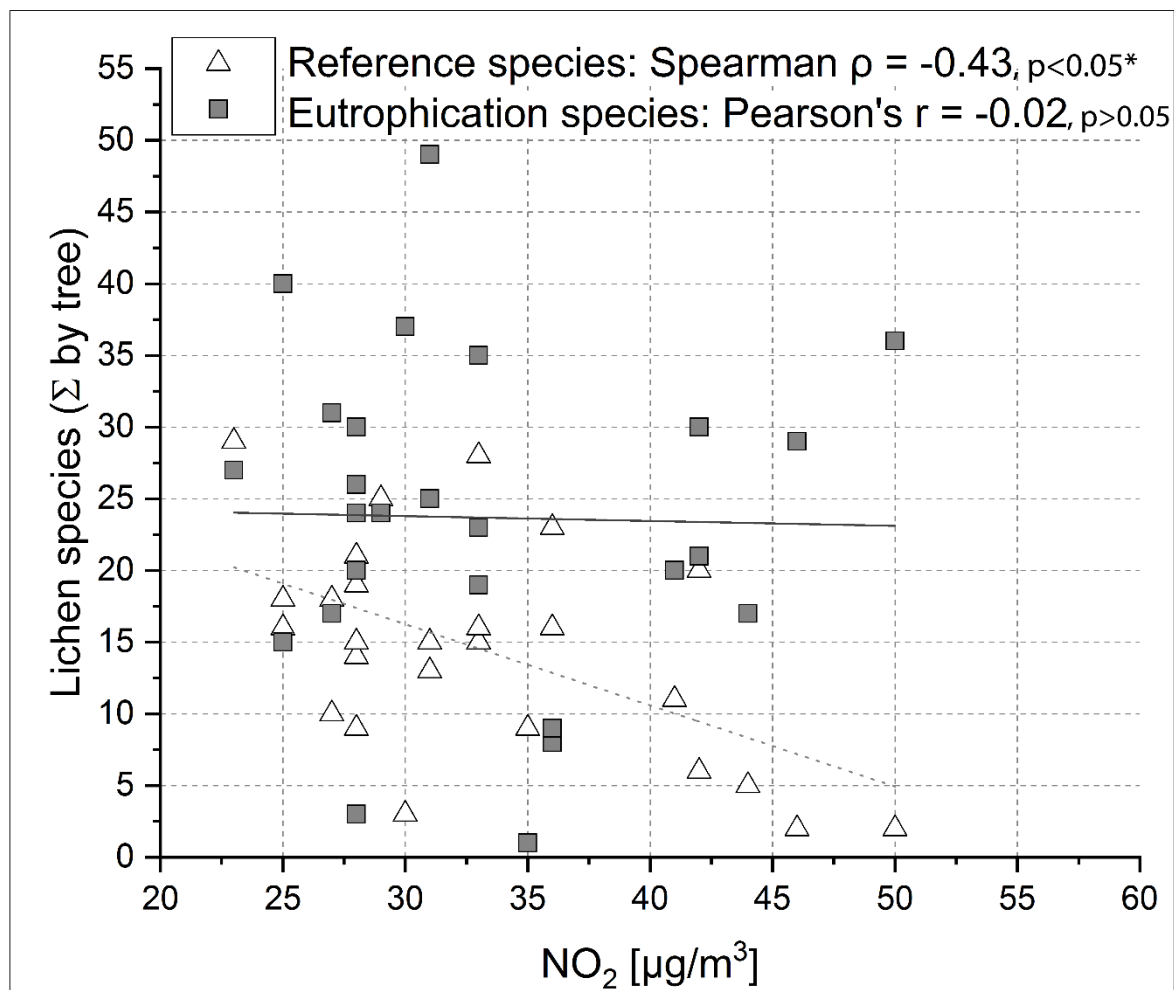


Figure 3-14: Reference and eutrophication species (summarised by tree) with mean NO₂ concentrations for sites where NO_x diffusion tubes were located and that were analysed for lichen diversity (N=26)

Mean NO₂ concentrations for a yearlong deployment period at 45 sites display spatial and temporal variability in Manchester. Consistently high NO₂ concentrations at analysed sites (see Table 3-9) could additionally indicate phytotoxic effects (Hawksworth and Rose, 1970; Richardson, 1993; Giordani and Brunialti, 2015) on more sensitive lichen species and explain the shift towards predominant taxa of eutrophication species in Manchester. Moreover, additional nitrogen compounds (i.e. nitrate and ammonia) could influence the bark pH and thus be related to decline in lichen species, i.e. preferring acid bark (e.g. *Lecanora conozaeoides*), which have become less widespread as it used to be, due to decline in sulphur dioxide concentrations (Nimis et al., 2009).

However, further investigation of spatial variability of nitrogen compounds (i.e. nitrate, ammonia and ammonium) on epiphytic lichens in Manchester needs further investigation. Nitrogen contents and nitrogen speciation in lichens (*X. parietina* and *Physcia* spp.) will be presented and discussed in the following chapters, i.e. chapter 4 and chapter 5.

Measurements for NO₂ provided additional insights on air quality (and lichen diversity) in Manchester, whereas potential influences on NO_x tube performance needs to be further investigated, which is presented hereafter.

3.8.3 Discussion of influencing factors resulting in over- or underestimation of NO_x diffusion tube measurements

NO_x diffusion tubes are considered as “indicative” measurements, because they do not offer the same precision and accuracy as EU implemented reference methods, i.e. chemiluminescence analysers, but are ideal for screening studies or identification of high concentrations (AEA Energy and Environment, 2008). Influencing factors, resulting in over- or under-estimation (positive or negative bias) of NO₂ concentrations are reported in Table 3-12.

Table 3-12: Interfering factors on NO_x diffusion tube measurements, resulting in positive (over-estimation) or negative bias (under-estimation) of NO₂ concentrations (AEA Energy and Environment, 2008)

Positive bias	Negative bias
Shortening of diffusive path length, by turbulence at the open tube end caused by wind	Increasing exposure period (average of four consecutive one-week, or two consecutive two-week exposures is systematically greater than one four-week exposure)
Blocking of UV light by the tube material (reduction of NO ₂ photolysis)	Insufficient nitrite extraction from grids
Interference of peroxyacetyl nitrate (PAN) – pollutant associated with vehicle emissions	Tube preparation with a 50% (v/v) solution of TEA in water (may affect NO ₂ uptake)
	Photochemical degradation of TEA-nitrite complex by light
(Atkins et al., 1986; Campbell et al., 1994; Heal et al., 2000; Kirby et al., 2000; Laxen and Wilson, 2002)	

Positive bias by wind has been addressed (i.e. wind speed and turbulences), but was reported to not affect tube performance under field conditions (Cape, 2005). Wind speeds of 1.0 to 4.5 m/s and 2.3 to 4.5 m/s were reported to have no effect on NO_x diffusion tube sampling rates. Small effects of higher wind speed, of up to 6.5 m/s were reported in prior studies (Atkins et al., 1986; Hargreaves, 1989; Gair and Penkett, 1995; Hangartner, 2001; Kirby et al., 2001; Cape, 2005).

Monthly mean wind speeds in Manchester did not exceed 4.01 m/s (or 14 km/h). Highest wind speed was recorded on the 3rd of January 2018 with 11.51 m/s that could have influenced performance of NO_x diffusion tube. Hence, wind speed and potential increased uptake rates (Palmes et al., 1976; Cape, 2005) were considered of minor importance.

Extreme temperatures and relative humidity may have an effect on sampling rates, especially during winter (Buzica et al., 2003). Constant uptake rates of diffusion tubes were reported for temperatures between -8 to 45° C, using TEA as absorbent, and were considered small and predictable (Moschandreas et al., 1990; Hansen et al., 2001; Cape, 2005). However, another study found no temperature dependence (Hangartner, 2001). Humidity is potentially the most important variable affecting NO_x diffusion tube performance (when using TEA; Cape, 2005). Boleij et al. (1986) reported an 18% change in uptake rate between 20 and 80% relative humidity, which has been confirmed by a more recent study, which reported a 23% change in NO₂ uptake between 20 and 80% (at 20 °C; Gerboles et al., 2005). Temperatures during this study (deployment between July 2017 to July 2018) varied between -5.24°C to 30.47°C (Figure 2-18), being in the reported range of constant uptake.

Mean relative humidity of 100% (each day) was reported for the first six months (01/07/2017 to 05/12/2017; 'Whitworth Meteorological Observatory - Data Archive', 2018) of deployment and was not further considered due to insufficient data. Therefore, temperature and relative humidity were considered not to influence uptake rates of diffusion tubes, indicating reliable NO₂ concentrations throughout the deployment period.

Blocking of UV light and therefore reducing NO₂ photolysis by the material can be excluded, because tubes were not marked or covered (i.e. by labels or stickers). However, chemical reactions during sampling, i.e. reaction between NO and O₃ (to give NO₂) within the tube could affect NO₂ concentrations (Atkins et al., 1986; Cape, 2005). This has to be taken into consideration, especially at locations where NO concentrations are high, i.e. close to roads, which is reportedly a major source of uncertainty using Palmes-type diffusion tubes (Heal and Cape, 1997; Heal et al., 2000; Cape, 2005). Tubes in this study were deployed on urban trees, at different distances to roads (and different road classes, e.g. A- and B-roads, motorways and unclassified). Potential in-tube reactions, in particular at sites close to highly trafficked roads, cannot be fully excluded. Potential vegetation influence, by being fixed to an urban tree, could have blocked UV light, thus influencing tube NO₂ uptake (Cape, 2005; Fantozzi et al., 2015).

Interferences by peroxyacetyl nitrate (PAN) cannot be fully excluded, as it is quantitatively converted to NO₂⁻ on TEA (Cape, 2005). However, no measurements are available to compare PAN with analysed NO₂ concentrations. Moreover, under UK conditions, interferences from PAN are likely to be very small (Cape, 2005; McFadyen and Cape, 2005).

Negative bias, i.e. exposure periods, extraction and tube preparation could influence diffusion tube performance and therefore reported NO₂ concentrations (Table 3-9). Analysed concentrations are systematically greater with shorter exposure periods (and tube changes), due to potential nitrite degradation (Heal et al., 2000). This study applied a bi-weekly exposure and under-estimation by exposure time was considered minimal.

Insufficient extraction is also considered of minor influence, as tubes were (manually) agitated and extraction consisted 30 minutes (stop-watch controlled) to ensure efficient extraction. Moreover, photochemical degradation is minimised due to opaque caps (grey; Figure 3-6). Tube preparation could be the most possible factor influencing NO₂ uptake, as tube components were cleaned and meshes were

independently re-charged. TEA/Acetone was used for grid preparation, ruling out TEA/water influences. The lowest analysed NO₂ concentration was ~2 µg/m³ which could be related to preparation issues, i.e. grid not fully covered with TEA-mixture and/or insufficient extraction of nitrite (NO₂⁻).

In conclusion, potential influencing factors in this study, i.e. wind, temperature and peroxyacetyl nitrate (PAN) were considered minimal to affect NO₂ uptake. However, potential in-tube chemistry should be further considered and additional co-deployment with O₃ samplers could benefit a potential bias assessment. Although there are limitations of Palmes-type diffusion samplers, they provided a useful tool to assess spatial (and temporal) variability of NO₂ concentrations across Manchester. Potential interferences on NO_x diffusion tube performance was discussed. Measured NO₂ concentrations were further compared to automated monitoring stations (located in the city centre of Manchester).

3.8.4 Comparison of NO_x diffusion tube measurements with automated air quality monitoring stations in Manchester to evaluate reliable performance of tubes

Diffusion tubes have been widely used by local authorities (including Manchester City Council; McLean and Drabble, 2015) for air quality monitoring studies, including required co-location studies (comparison of diffusion tubes with automated monitoring stations), to evaluate positive or negative bias of NO_x diffusion tube measurements (i.e. over- or underestimation concentrations DEFRA, 2003; AEA Energy and Environment, 2008). Recorded NO₂ concentrations, in this study, were compared with automated monitoring stations to investigate NO_x diffusion tube performance and reliability.

Co-location studies should expose tubes (in triplicates) alongside with automated chemiluminescence analysers for at least nine months (AEA Energy and Environment, 2008). NO_x tube locations, close to the two automated monitoring stations were used to compare NO₂ concentrations to measured values of automated air quality monitoring stations, as a direct deployment of NO_x tubes at the samplers was not possible (due to additional necessary permissions). Monthly mean nitrogen dioxide concentrations (NO₂ in µg/m³) at automated monitoring stations ranged from 24 µg/m³ to 56 µg/m³ (at Manchester Piccadilly Gardens) and 49 µg/m³ to 78 µg/m³ (at Manchester Oxford Road) for the deployment period (Figure 3-15).

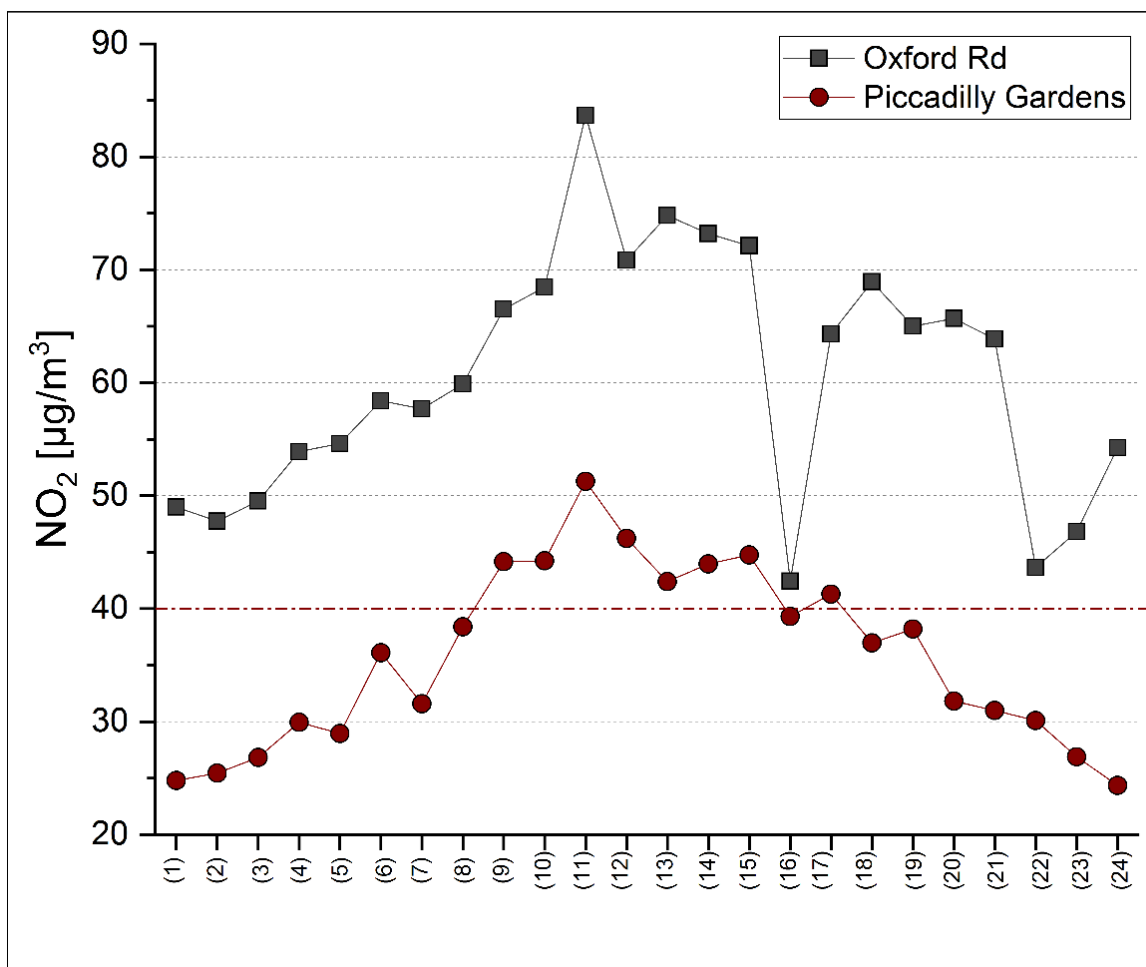


Figure 3-15: Bi-weekly (mean) concentrations of NO₂ in µg/m³ measured at Manchester Piccadilly Gardens (red circle) and Oxford Road (grey square) between June 2017 and June 2018 (displayed with WHO limit value – red dotted line); numbers (1) represent a bi-weekly deployment period

Analysed NO₂ concentrations of NO_x diffusion tubes were compared with automatically measured concentration for both monitoring stations. For Manchester Piccadilly Gardens one site ID: 18 (CC009), which was located on a tree about 7 m away from the monitoring station, was taken into consideration.

Manchester Oxford Road is located next to Manchester's (and Europe's; Leavy, 2009; Martin et al., 2011) busiest bus route and no trees are in close proximity and direct deployment on the automated measuring station was not possible. Therefore two trees, closest to the monitoring station (up and down the road) were considered ID: 17 (CC008) and ID: 34 (HUL027).

Bi-weekly concentrations of both, automated monitoring stations and NO_xdiffusion tubes in close proximity are displayed in Figure 3-16. NO₂ concentrations (by diffusion tubes) follow a comparable trend, indicating their beneficial use for this study.

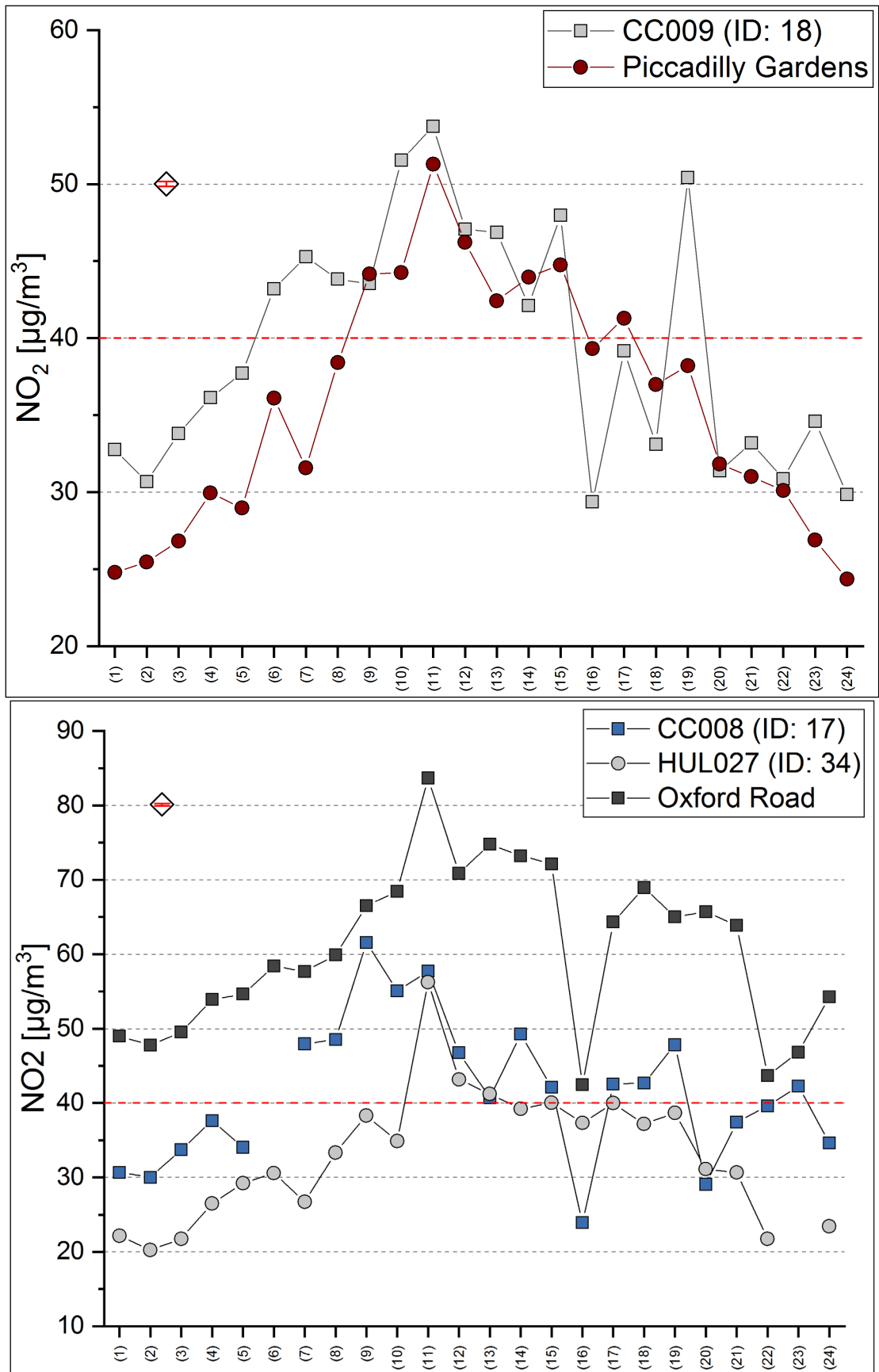


Figure 3-16: Biweekly NO₂ concentrations at ‘co-located’ sites recorded for 24-weeks (361 days); dummy value (white diamond) with CRM-derived nitrite value, as 1x standard deviation (±0.108) and WHO limit value (red dotted line); numbers (1) represent a bi-weekly deployment period; missing values for ID: 17 indicate missing tubes

To further investigate the performance of NO_x diffusion tubes in comparison to automated monitoring stations, recorded NO₂ concentrations were plotted against each other. Figure 3-17a illustrates that NO₂, recorded at 'Oxford Road' monitoring station showed consistently higher values compared to closest NO_x diffusion tubes. This could be related to the position of the NO_x tubes further away from the site of the automated monitoring station (and further away from Oxford Road; indicating a decline of NO₂ with distance to road).

In contrast, concentrations recorded at 'Piccadilly Gardens' and closest site showed higher concentrations recorded with NO_x tubes (Figure 3-17b). Additionally, significantly strong positive correlation (presented as Pearson's *r*) between values at automated monitoring stations and NO_x diffusion tube locations indicate the viability of measured NO₂ values.

In conclusion, it can be stated that 'co-location' of NO_x diffusion tubes showed a comparable pattern of NO₂ concentrations throughout the deployment period. Therefore, providing beneficial information on spatial and temporal variability of NO₂ concentrations. Lanzafame et al. (2016) highlighted the beneficial use of passive sampling devices in combination with automated monitoring stations, for sites, that are not regularly covered by measurements.

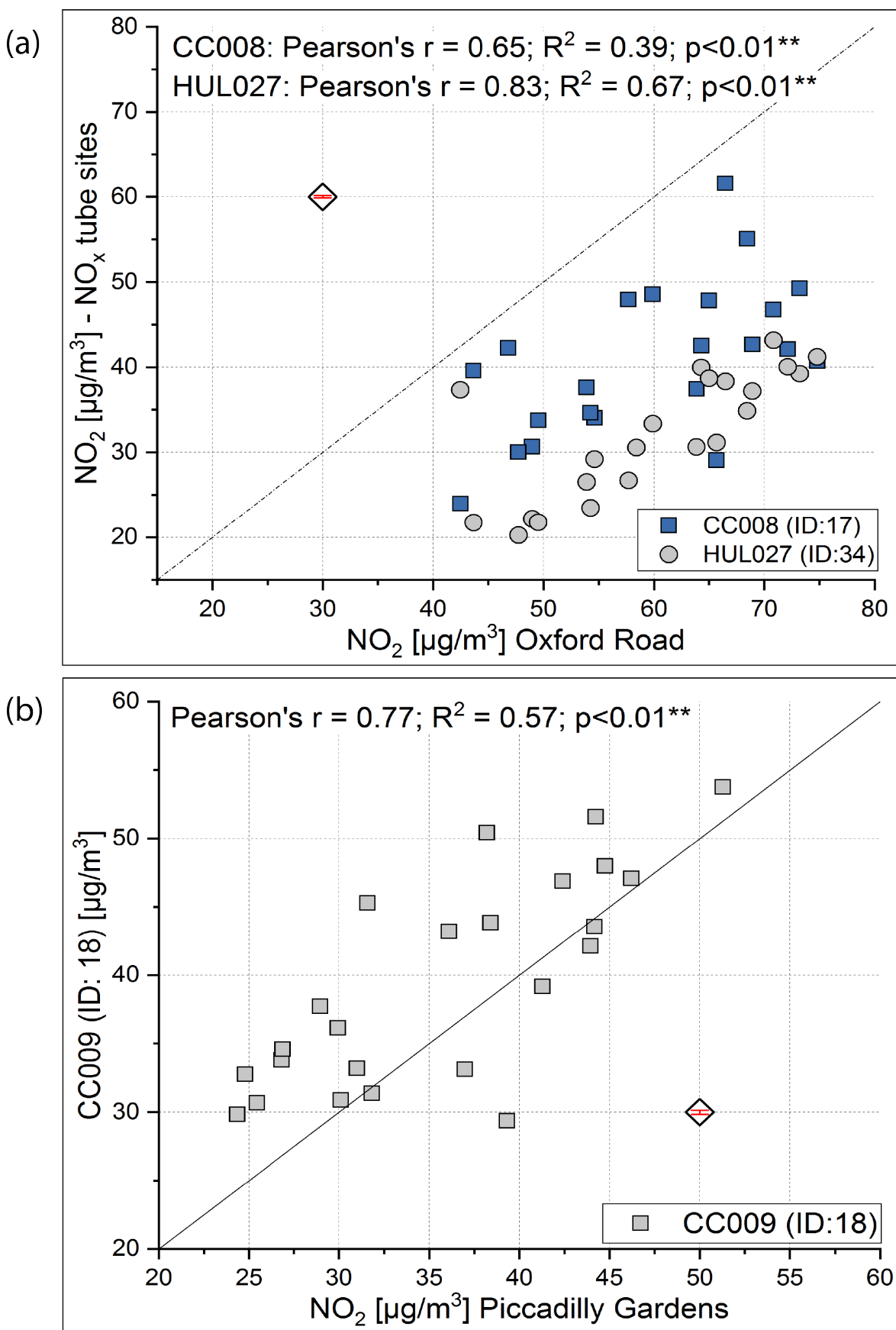


Figure 3-17: Automatically measured NO₂ concentrations at (a) Manchester Oxford Road and (b) Manchester Piccadilly Gardens with closest NO_x diffusion tube (ID: 17 and ID: 34 for Oxford Road; ID: 18 for Piccadilly Gardens and); error bars are presented as 1x Std. Dev. On 'dummy value' (CRM by IC analysis: ±0.108)

Within the city centre, the two automated monitoring stations exceeded the EU limit value of $40 \mu\text{g}/\text{m}^3$ (for the NO_x deployment period; Figure 3-15) with recordings at 'Oxford Road' being particularly high, illustrating potential health impacts by elevated NO_2 .

NO_2 concentrations varied across Manchester, with higher NO_2 within the city centre and close to major roads and the motorway ('Mancunian Way, M56'). The northwest and southwest of the city, consisting mainly of residential areas, are characterised by lower NO_2 concentrations. Findings suggest traffic emissions as primary source of NO_2 .

Results obtained with NO_x diffusion tubes in this study were comparable to automated air quality monitoring stations throughout the deployment period. Therefore, diffusion tube measurement in this study were considered useful to assess a spatio-temporal overview of NO_2 concentrations across Manchester. Comparison with other urban studies could further provide insights into the importance of NO_2 in urban environments.

3.8.5 Comparison of NO_2 concentrations across Manchester with other urban studies

Comparison with other urban studies, which applied passive monitoring devices, could indicate potential changes in NO_2 concentrations across urban areas over time and provide information of the potential importance to further monitor and tackle elevated NO_2 concentrations. Urban studies, undertaken within the UK and Europe using diffusion tubes are illustrated in Table 3-13 and Figure 3-18.

Table 3-13: NO_2 concentrations recorded in urban studies across the UK and Europe (displayed for urban area, reported mean NO_2 [in $\mu\text{g}/\text{m}^3$, as two significant figures] and number of deployment sites)

	Geographic location	NO_2 concentration	Number of sites	reference
(1)	Manchester (city centre)	34 ± 11	45	This study
(2)	Greater London	55	27	
(3)	Greater Manchester	43	20	(Bower et al., 1991)
(4)	Merseyside	39	18	
(5)	Glasgow	35	16	
(6)	Lancaster (city centre)	63 ± 24	12	(Hewitt, 1991)
(7)	Birmingham (roadside)	43	13	(Vardoulakis et al., 2011)
(8)	Elche (ESP)	32 ± 12	79	(Caballero et al., 2012)

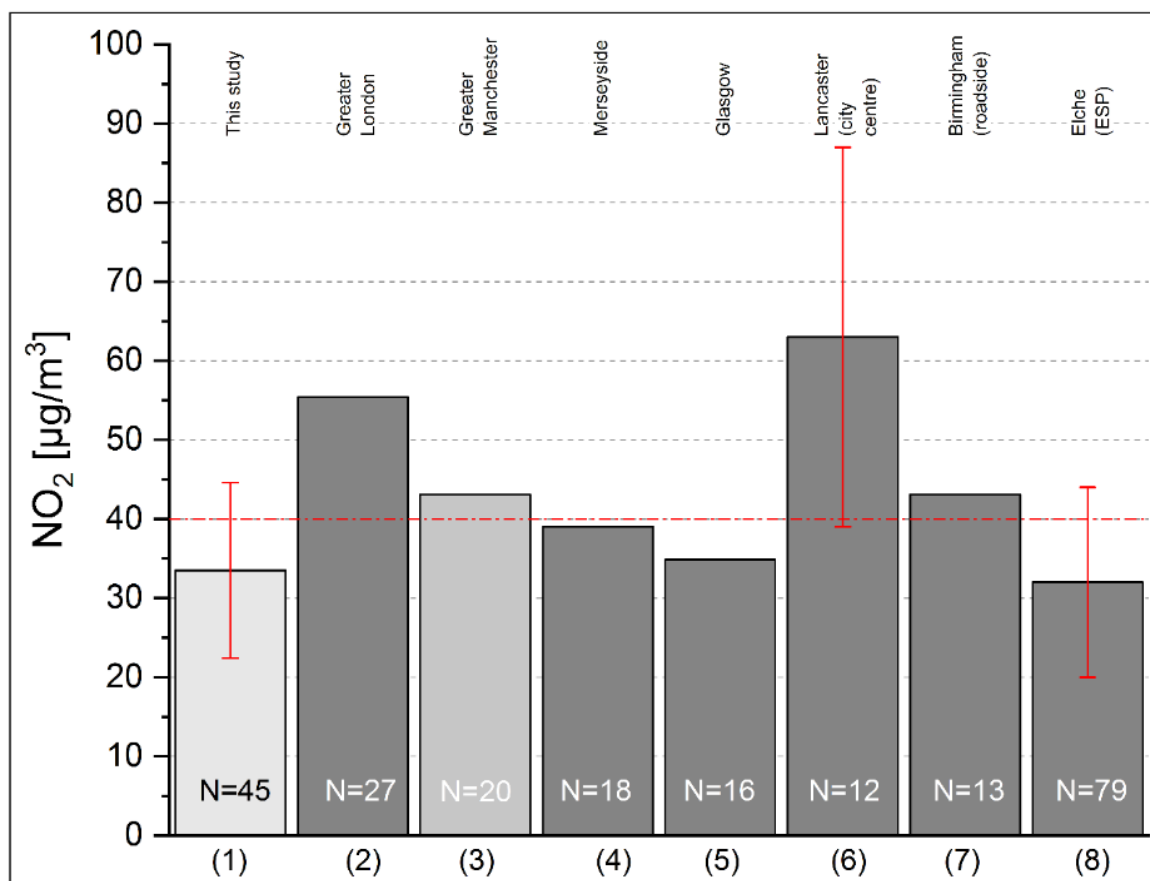


Figure 3-18: Bar graphs of urban mean NO₂ concentrations [in µg/m³] (following Table 3-13) reported for UK and European studies to compare recorded NO₂ in Manchester (with error bars, as 1 x Std. Dev. where applicable); WHO limit value of 40 µg/m³ displayed as dashed-dotted line.

Mean nitrogen for 45 sites across Manchester were found at 34 (±11) µg/m³ for a yearlong deployment period, which is comparable to results reported by Bower et al. (1991) for Greater Manchester (and other UK conurbations, i.e. Greater London, Merseyside and Glasgow; Figure 3-18). However, these studies were undertaken about 30 years ago and findings presented here indicates, to date, the considerable importance of NO₂ in Manchester. Within Manchester, 80% of NO₂ emissions are related to vehicular emissions, especially diesel vehicles (Regan, 2018). Traffic was named the primary source of NO₂ in urban areas, being particularly high in urban centres and at roadsides across the UK (Bower et al., 1991; Hewitt, 1991; Vardoulakis et al., 2011; Caballero et al., 2012).

Individual site NO₂ concentrations (in Manchester) ranged between 2.26 to 84.05 µg/m³ (individual mean NO₂ between 23 µg/m³ to 50 µg/m³). Highest mean concentrations were found around the highly trafficked 'Mancunian Way' (at site ID: 30) with 50 µg/m³ and about 59,400 vehicles daily (DfT, 2017a). This site exceeded the WHO limit value (40 µg/m³) 22 times, strongly suggesting traffic-emitted NO₂.

Moreover, diffusion tubes deployed along the Mancunian Way (i.e. ID: 6 and ID: 9) and other major roads (i.e. ID: 1 and ID: 3) show higher NO₂ (mean) concentrations for time of exposure, from 41 µg/m³ to 44 µg/m³. However, Bower et al. (1991) reported NO₂ concentrations of 67 µg/m³ for a site further away from a major road in Manchester, indicating additional influences (i.e. power stations and industrial emissions; Air Quality Expert Group, 2004) at particular sites.

A more recent study, undertaken in 2014, by the Manchester City Council, reported elevated NO₂ (>44 µg/m³) within the city centre and along the major road network (TfGM, 2016). This is comparable to results presented here. Moreover, sites outside the city centre exceeded the WHO limit value of 40 µg/m³ (see Figure 3-12), indicating site-specific influences and dispersion and distribution of NO₂ across the area. 'Clean Air Greater Manchester' provides a network of 38 NO_x tube locations across the city centre of Manchester (total 272 sites across Greater Manchester), of which 15 were located within the research area investigated in this study (GMCA and TfGM, 2019). Mean concentrations (for 2017) at these sites ranged between 34.4 to 58.5 µg/m³, which is comparable with results presented here. Moreover, especially 'urban traffic' sites (i.e. locations close to major roads) did not achieve the target of NO₂ <40 µg/m³ (GMCA and TfGM, 2019). NO₂ concentrations recorded here, when compared to previous studies (i.e. (Bower et al., 1991; TfGM, 2016; GMCA and TfGM, 2019), still show particular problems regarding (traffic emitted) NO₂ within the urban area of Manchester that, in return, is potentially related to its major public health issues (Regan, 2018). Moreover, findings presented suggest the importance of high spatial coverage of NO₂ concentrations across the urban environment of Manchester, in areas that are not covered by automated monitoring stations.

Spatial and temporal variability of NO₂ concentrations across Manchester were presented for co-located sites and when compared to other urban studies. Meteorological influences on nitrogen concentrations were further considered and are discussed hereafter.

3.8.6 'Seasonal' variability of NO₂ concentrations for a yearlong deployment period across Manchester

Temporal variation of NO₂ concentrations were reported to be lower in summer and higher in winter, due to changing meteorological conditions, i.e. temperature and solar radiation (Vardoulakis et al., 2011; Caballero et al., 2012). Temporal (i.e. between bi-weekly measurements) variability of NO₂ concentrations was observed during the deployment period. To examine "seasonal" variation of NO₂ concentrations throughout the 12-month duration deployment period, the mean value of six diffusion tube measurements (summarising 3 months) has been used to represent a season.

Meteorological seasons are classically defined as spring (March, April and May), summer (June, July and August), autumn (September, October and November) and winter (December, January and February; Met Office, 2018). In this study, deployment of NO_x diffusion tubes started in July 2017 and ended in June 2018, therefore a directly aligned meteorological season subdivision was not possible. Seasonal variability was analysed in relation to temperature, precipitation, wind speed and sunshine hours (Table 3-14). Correlation between measured NO_x tube variables and meteorological data is displayed in Table 3-15). Figure 3-22 illustrates 'seasonal' correlations of NO₂ and meteorological data.

Table 3-14: Monthly temperatures (°C) and total precipitation (Σ mm) for NO_x deployment period (data obtained from the “Whitworth Meteorological Observatory”)

Month	Temperature (°C) – monthly mean	Total Precipitation (Σ mm)	Wind speed (m/s)- monthly mean	Sunshine hours (Σ hours)	Season
July 2017	16.71	88.04	2.57	114.59	1 ‘Summer’
August 2017	15.86	60.49	3.20	65.40	Figure 3-22(a)
September 2017	14.20	124.32	2.64	50.71	
October 2017	13.11	85.44	4.01	24.37	2 ‘Autumn’
November 2017	7.94	85.75	2.70	19.79	Figure 3-22(b)
December 2017	6.01	110.69	2.63	10.17	
January 2018	5.46	114.65	3.99	18.47	3 ‘Winter’
February 2018	3.50	60.42	3.00	63.19	Figure 3-23(c)
March 2018	5.19	92.00	3.50	49.26	
April 2018	9.88	78.58	2.97	79.77	4 ‘Spring’
May 2018	14.28	28.74	2.50	221.82	Figure 3-23(d)
June 2018	16.94	13.65	2.55	215.53	

Table 3-15: Correlation coefficients Pearson’s r (for NO₂ concentrations, due to normal distribution of data) related to meteorological data (*significant at the level $p < 0.05$, shaded in yellow; **significant at the level $p < 0.01$, shaded in green)

	NO ₂ (Pearson’s r)
Temperature	-0.69*
Precipitation	0.63*
Wind speed	0.27
Sunshine	-0.80**

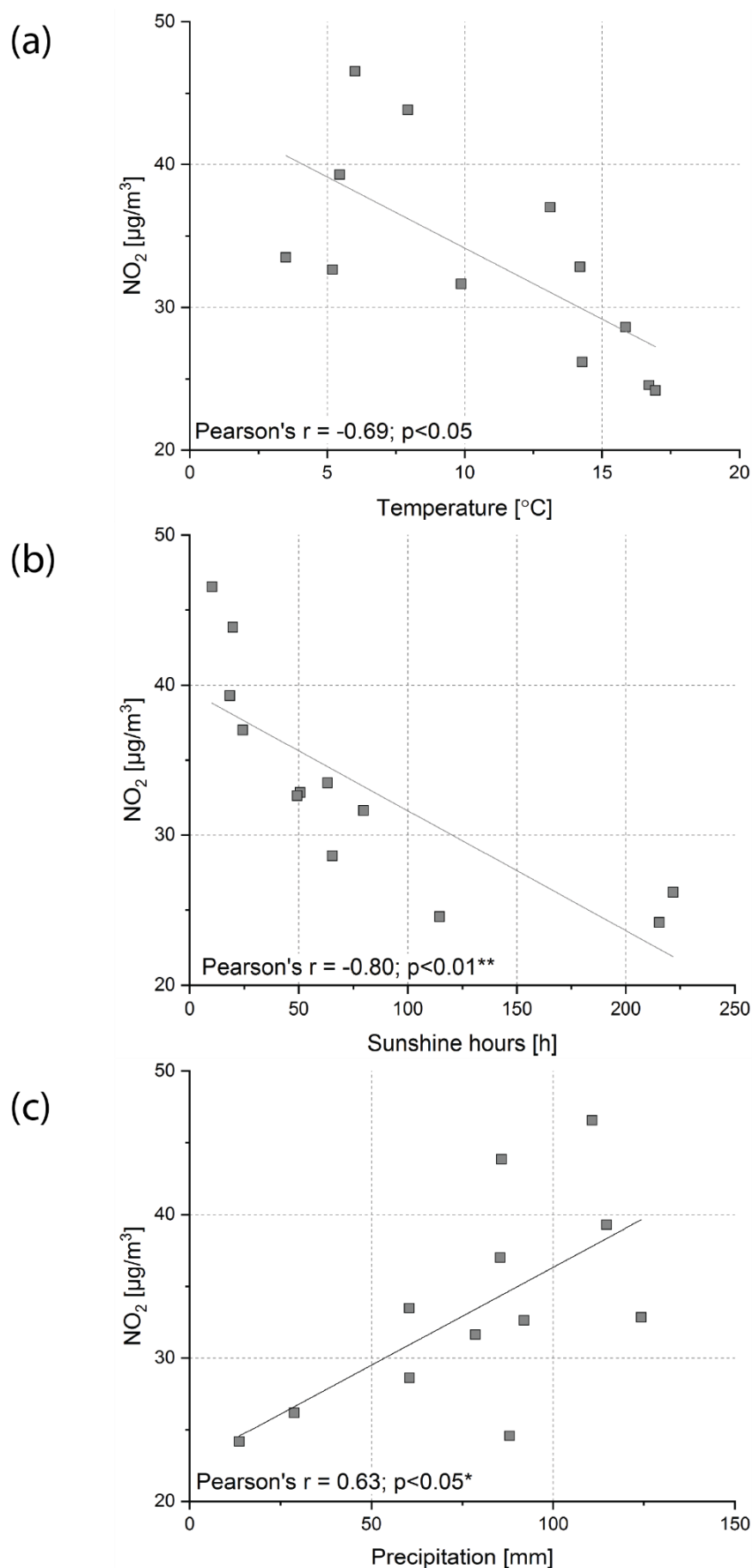


Figure 3-19: 'Seasonal' NO₂ concentrations and meteorological data, to assess influences of (a) temperature [°C], (b) sunshine hours [Σhours] and (c) precipitation [Σmm] on NO₂ concentrations

A seasonal trend of NO₂ concentrations was recorded for the yearlong deployment period, with highest NO₂ concentrations during the colder months (i.e. autumn and winter; Figure 3-20 and Figure 3-21). This is usually ascribed to anthropogenic emissions and weather conditions (Heidorn and Yap, 1986; Fantozzi et al., 2015). Furthermore, potential uptake of NO₂ by tree leaves is hindered during winter (Desyana et al., 2017). Similar seasonality of NO₂ has been reported in studies worldwide, i.e. Italy, China, Spain and Canada (Parra et al., 2008; Wheeler et al., 2008; Boersma et al., 2009; Meng et al., 2010; Bigi and Harrison, 2012; Caballero et al., 2012).

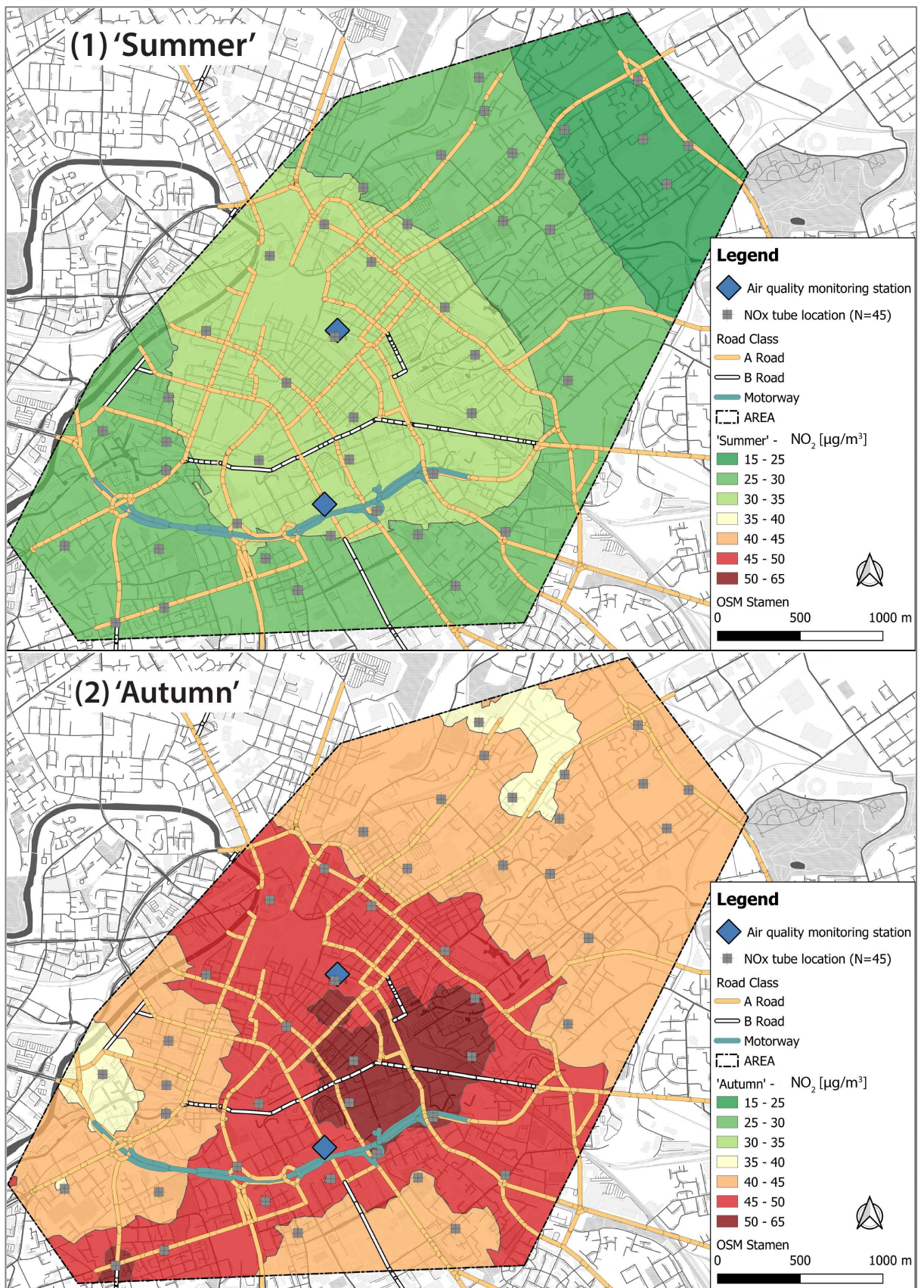


Figure 3-20: Seasonal variation of NO₂ concentration in Manchester (1) 'Summer' and (2) 'autumn; interpolated by Ordinary Kriging (OK), colour-coded by NO₂ concentration

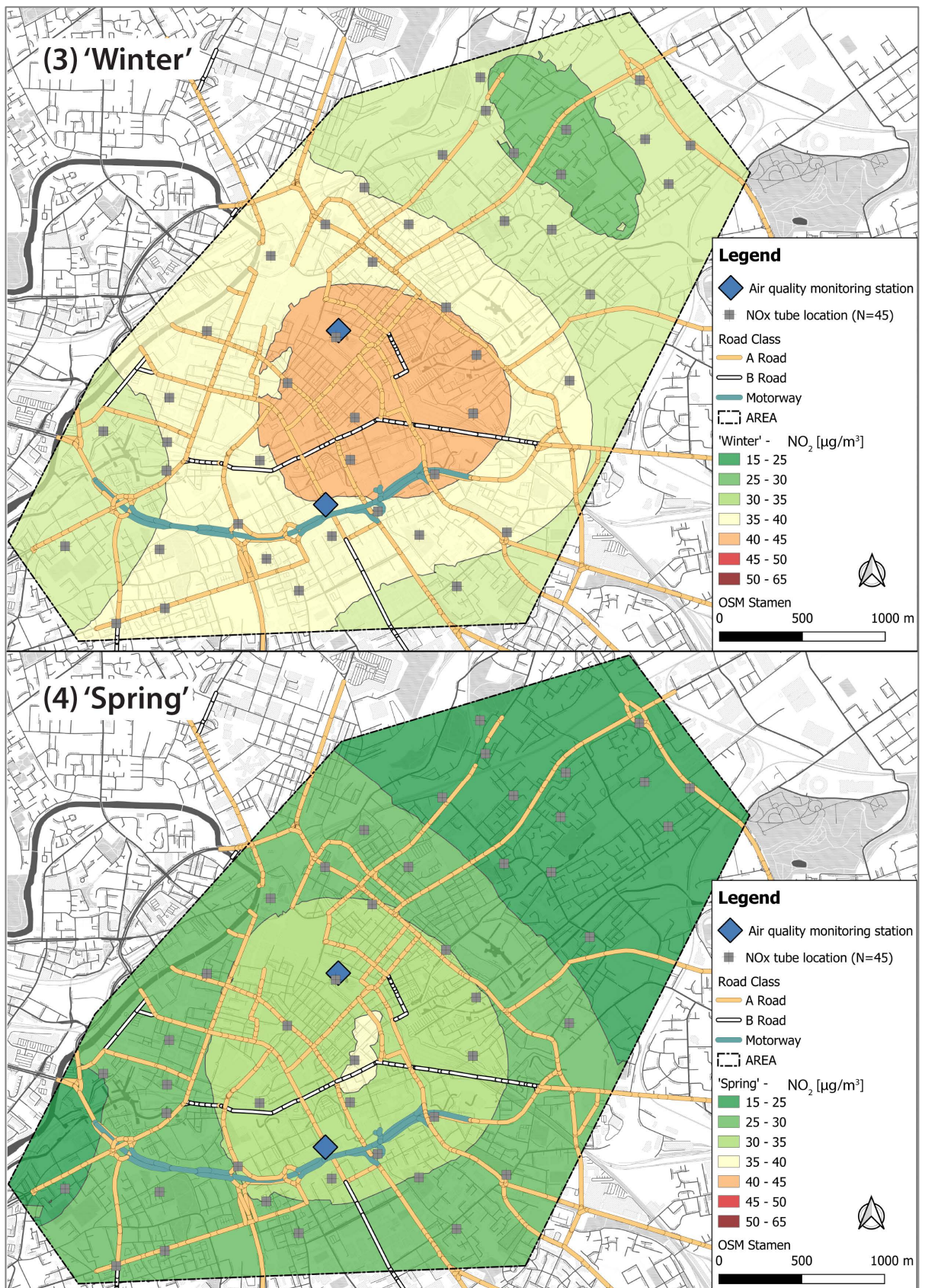


Figure 3-21: Seasonal variation of NO₂ concentration in Manchester (3) 'Winter' and (4) 'Spring; interpolated by Ordinary Kriging (OK), colour-coded by NO₂ concentration'

Low NO₂ concentrations are generally related to higher rainfall, temperatures and increased wind speeds (Heidorn and Yap, 1986; Fantozzi et al., 2015). Temperature and sunshine hours were negatively correlated (Table 3-15 and Figure 3-19) with NO₂ concentrations recorded. Higher temperatures in summer and solar radiation increase the photochemical oxidation rate of NO₂ to NO₃⁻ (Kadowaki, 1986; Caballero et al., 2012). In contrast, Kwak et al. (2017) reported influences of rainfall on pollutant concentrations, e.g. NO₂, with increasing pollutant concentrations due to increased traffic volume, combined with decreased vehicle speed during rainfall events.

The city centre area of Manchester consistently showed higher NO₂ concentrations during all 'seasons' (especially during 'autumn' with concentrations of up to 53 µg/m³), which was also recorded by automated air quality monitoring stations (Figure 3-16). However, additional factors, such as building-structure, ventilation effects, urban green and meteorological data could influence NO₂ distribution and dispersion (James and Bound, 2009; Vardoulakis et al., 2011; Caballero et al., 2012; Gómez-Baggethun and Barton, 2013; Fu et al., 2017; Shen et al., 2017; Kurppa et al., 2018).

Nonetheless, diffusion tubes results (during 'autumn' and 'winter' in particular) showed deteriorated air quality over a wider area, where no monitoring station is located. Adverse health effects (i.e. increases in all-cause mortality, respiratory and cardiovascular diseases) of NO₂ have been linked to short- and long-term exposure (Faustini et al., 2014; Mills et al., 2015; Barrett et al., 2017). Within the city centre area, NO₂ concentrations were consistently higher than 30 µg/m³, indicating increased exposure (short- and long-term) for people travelling, commuting into the city centre for leisure activities and work. Therefore, arrangements for the city centre in particular (i.e. vehicular taxes and bus/taxi fleet improvement; TfGM and GMCA, 2016) should be considered to reduce NO₂ concentrations and minimise additional health impacts on local population and commuters. Variability of NO₂ concentrations across Manchester were related to meteorological conditions, which did not include potential urban factors (i.e. street canyon effects). Potential effects of the urban structure of Manchester are subsequently discussed.

3.8.7 Assessment of potential influences of Manchester's urban structure on recorded NO₂ concentrations

Urban environments are complex systems (i.e. building structures and urban green), resulting in interferences of pollutant dispersion and dilution (Salmond and McKendry, 2009; Salmond et al., 2013).

Dore et al. (2008) reported traffic as major source of total UK pollution emissions for nitrogenous pollutants. In Manchester, 80% of NO_x emissions are related to vehicular emissions, particularly from (light duty) diesel vehicles (TfGM, 2016; Regan, 2018). High NO₂ concentrations and exceedances of the WHO limit value (40 µg/m³) occurred alongside the major road network (A-, B-roads and the motorway) and within the city centre (Figure 3-12). Table 3-16 illustrates the correlation coefficients of NO₂ concentrations with urban influencing factors (as stated in Table 3-7).

Table 3-16: Pearson's *r* (for NO₂) correlation coefficients of NO_x diffusion tube concentrations (N=45) to evaluate effects on spatial variability by urban influencing factors (MR = Distance to major road, RdCl = Road class, TC = Traffic counts, BH = building heights/building density, PS = Distance to (large) point sources and GS = Distance to green space); ** indicates significance level *p*<0.01

	MR	RdCl	TC	BH	PS	GS
NO ₂ (mean)	-0.61**	-0.05	0.17	0.20	-0.05	0.17

NO_x was reported to decline within the first 200 m off a major road, while NO₂ was reported to decline within the first 30 m (Cape et al., 2004; Davies et al., 2007; Laffray et al., 2010; Bermejo-Orduna et al., 2014; Watmough et al., 2014). Findings showed a decline of NO₂ concentrations with distance to major road (>100 m; Figure 3-22). High NO₂ concentrations at traffic sites were also reported for Madrid and Barcelona (Spain), with primary NO₂ (from diesel-fueled vehicles) significantly contributing to total NO₂ concentrations (Casquero-Vera et al., 2019). Especially Euro 5 and Euro 6 diesel vehicles have been reported to have real-world emissions up to 5-times and 4-20-times higher than allowed emission levels (Fontaras et al., 2014; Hagman et al., 2015; Barrett et al., 2017; European Environment Agency, 2018), strongly suggesting vehicular emissions as primary NO₂ source and research potential in analysing the vehicular fleet (i.e. cars and busses) across Manchester.

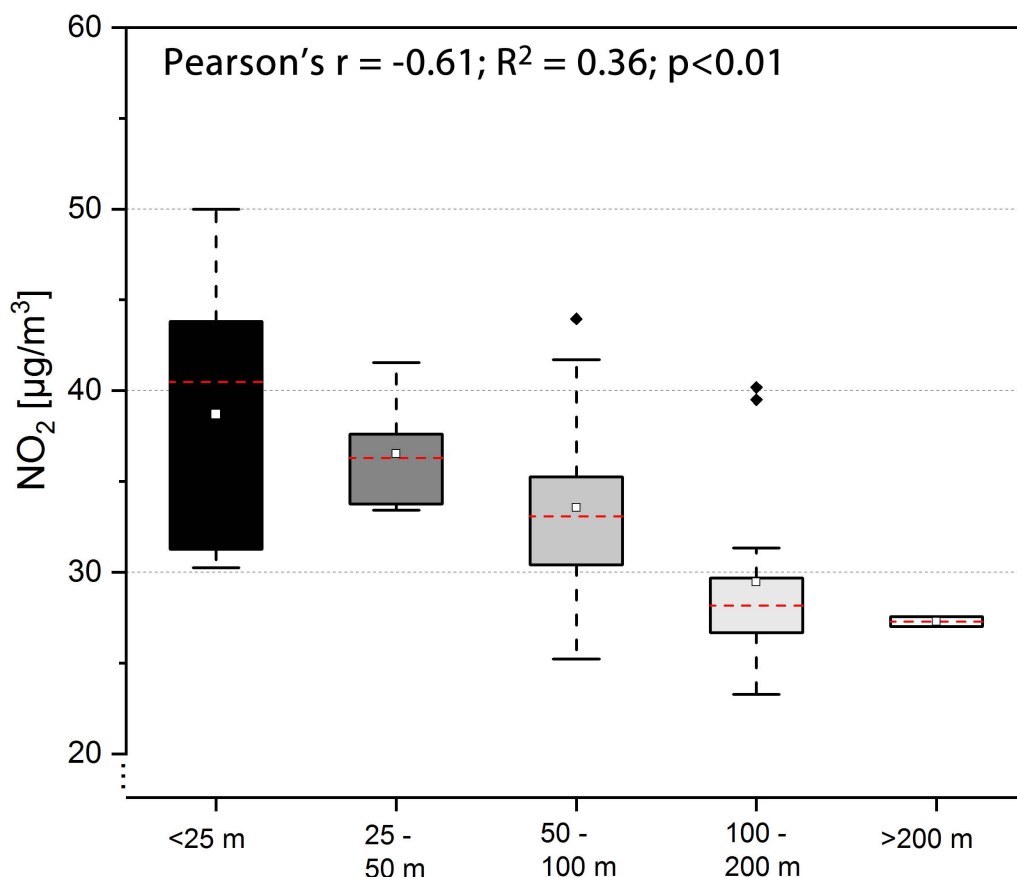


Figure 3-22: Nitrogen dioxide (NO₂) concentrations with distance to major road distance (displayed with correlation coefficient Pearson's r , for normal distributed NO₂)

NO₂ concentrations (mean) were modelled, using urban influencing factors (although not significantly influencing recorded concentrations; except major road distance). Distribution and dispersion of pollutants is influenced by geographical, topographical, meteorological and 'urban street' characteristics (Hertel and Goodsite, 2009; Salmond and McKendry, 2009). GWR was applied to NO₂ concentrations and results are illustrated in Figure 3-23.

Modelled NO₂ (from diffusion tubes), illustrates that both automated monitoring stations are located at 'hot-spots' of high NO₂ concentrations, illustrating their suitability at these locations. Moreover, additional influences from the surrounding council boroughs (i.e. Trafford and Salford City Council) could be indicated by elevated concentrations within southwest of the research area. However, GWR only accounted for 29% of variability of recorded NO₂ concentrations including urban influencing factors. As previously described (chapter 2: section 2.8.3), urban variables might not represent the 'real-world' of pollutant variability across Manchester, but were considered to affect dispersion and distribution. Furthermore, NO₂ concentrations are further influenced by meteorology, i.e. precipitation and temperature.

Temperature, sunshine data and precipitation were found to influence NO₂ concentrations, but were not included into the GWR due to potential differences in NO_x tube location microclimate and atmospheric reactions with other pollutants (i.e. O₃), potentially affecting NO₂ concentrations.

Elevated NO₂ concentrations were recorded within the city centre as a whole and expanding into the more residential surroundings (i.e. southwest and northeast). Therefore, the full extent of NO₂ concentrations (and dispersion into surrounding areas) might be underestimated by both monitoring stations. NO_x diffusion tubes provide an easy-to-use and cost effective approach to assess areas of high NO₂ and potential health concerns. Additional, measurements of pollutants closely linked with NO₂ (i.e. O₃; Clapp and Jenkin, 2001) could be further used to estimate public health impacts.

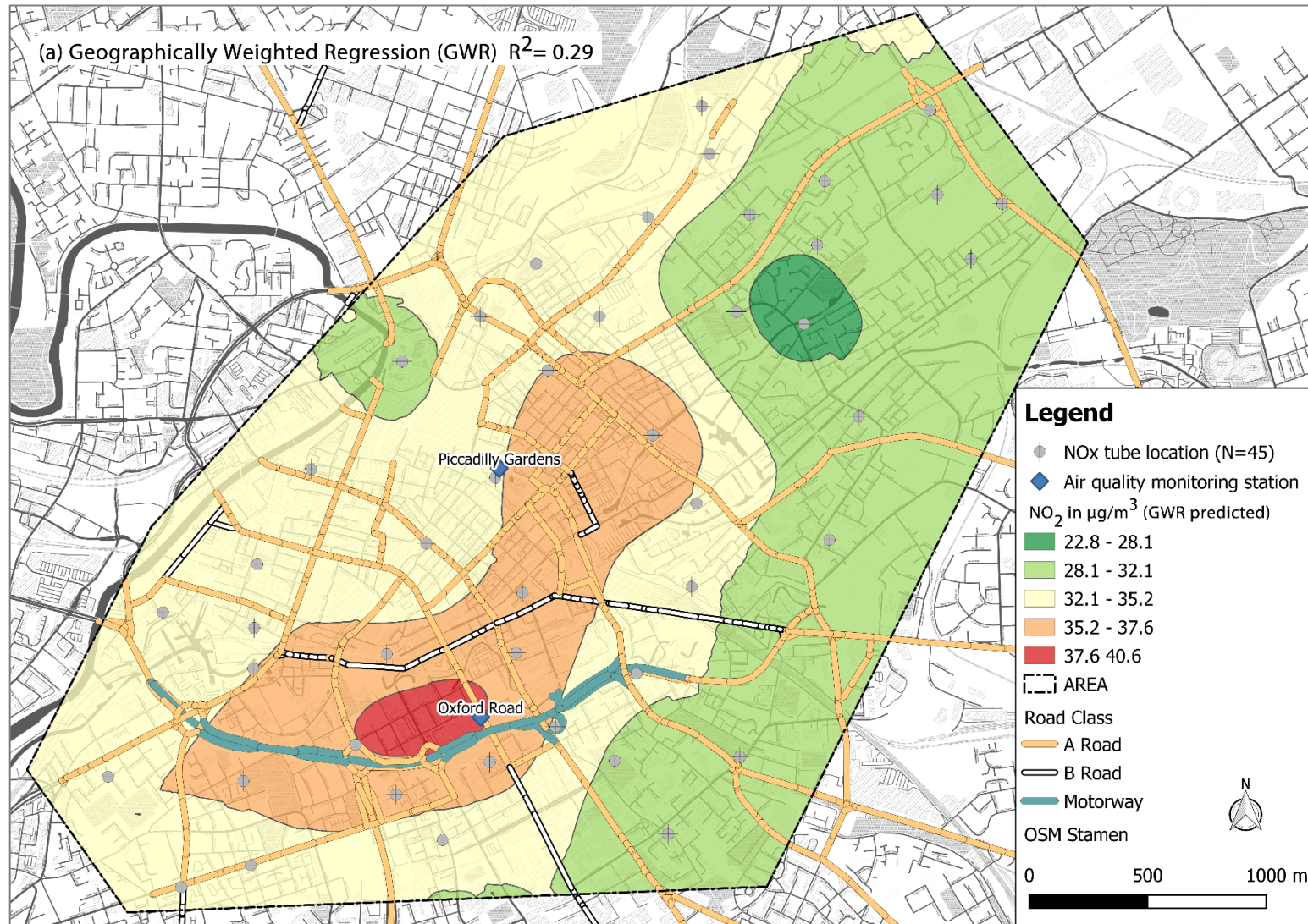


Figure 3-23: Modelled NO₂ concentrations (mean concentrations) to investigate potential urban influences of Manchester's urban structure on NO₂ concentrations, using Geographically Weighted Regression (GWR)

3.9 Conclusion

Using lichen diversity provides a rapid and low-cost approach to define zones of environmental quality, with information on eutrophication, anthropization and climate change and possible long-term effects of air pollution (Asta, Erhardt, et al., 2002; Shukla et al., 2014). Repetition at the same sites may permit to monitor environmental changes and environmental quality (Asta, Erhardt, et al., 2002; Loppi, 2019).

It is well known that epiphytic lichens respond to atmospheric pollution, but cannot evaluate environmental conditions, i.e. complex pollutants mixture and their combined effects on lichen vegetation, on its own (Nimis and Bargagli, 1999; Van Dobben and Braak, 1999; Falla et al., 2000; Kricke and Loppi, 2002). Therefore, the importance of automated stations to continuously measure pollutant concentrations cannot be replaced by biomonitoring methods (Kricke and Loppi, 2002). However, using lichen frequency as a bio-indication method has evolved over the past decades and has shown to be a useful and widely applied tool in European countries (e.g. Switzerland, Germany and Italy; Kricke and Loppi, 2002).

For Manchester, eutrophication species were primarily recorded across the city centre, suggesting spatial variability of N compounds at areas not continuously measured by automated monitoring stations. Additionally NO₂ concentrations, recorded by diffusion tubes showed spatial and temporal variability throughout the deployment period. NO₂ was found to affect lichen species (i.e. a decline in nitrogen-sensitive species) further suggesting elevated nitrogen levels favouring the growth of nitrogen-tolerant species. By implication, deteriorated air quality due to elevated nitrogen levels, at sites not continuously measured, suggests potential health impacts across the City of Manchester. Moreover, traffic appeared to be the primary source of NO₂ across the city centre of Manchester, indicating the necessity to improve bus and car fleets, reduce vehicular emissions and subsequently improve the population's health.

Additional influences on lichens, e.g. from other toxic substances (i.e. polycyclic aromatic hydrocarbons – PAHs; (Blasco et al., 2008), cannot be ruled out and chemical analysis of lichens sampled from the urban area is necessary to further evaluate fine-spatial detail of air quality in Manchester by using lichen pollutant loadings.

Chemical analysis of lichen samples (*X. parietina* and *Physcia* spp.) for pollutant loadings (i.e. CNS contents, stable-isotope-ratio signatures, metal and PAH concentrations) are presented in the following chapters. Further investigating air quality by chemically analysing lichens for potential harmful pollutant loadings will provide an insight into fine-spatial detail of air quality in Manchester. The following chapter will focus on lichen-derived pollutant loadings, i.e. carbon, nitrogen and sulphur in combination with their stable-isotope-ratio signatures, to further investigate air quality (and potential health impacts) in Manchester. Lichen chemical data, in particular nitrogen contents (wt%) and stable-nitrogen-isotope ratios ($\delta^{15}\text{N}$), when combined with NO_x diffusion tube measurements can potentially further identify pollutant sources.

Chapter 4-
Assessing urban air
quality in Manchester
(UK) at high spatial
resolution using lichen
carbon, nitrogen and
sulphur contents and
stable-isotope ratio
signatures

4.1 Introduction

Atmospheric pollutants, such as carbon monoxide/dioxide (CO and CO₂), sulphur dioxide (SO₂) and nitrogen oxides (NO_x; including nitric oxide – NO and nitrogen dioxide NO₂) have deleterious impacts on human health, i.e. respiratory and cardiovascular diseases (Fenger, 1999; Brunekreef and Holgate, 2002; Gulia et al., 2015). Within the UK about 40,000 premature deaths are linked to air pollution each year, with 7 million such deaths globally (Brauer, 2016; The Royal College of Physicians, 2016; WHO, 2018).

Atmospheric pollution by carbon and sulphur compounds, such as CO, CO₂ and SO₂, is closely linked to fossil fuel combustion (EPA, 2008; WHO, 2018). Nitrogen oxides (NO_x) are released into urban environments from fossil fuel combustion processes (for heating, energy production and from road traffic) and via atmospheric long-range transport (Brunekreef and Holgate, 2002; Hertel and Goodsite, 2009; Boltersdorf et al., 2014; Munzi et al., 2014). Diesel vehicles are responsible for emissions of primary NO₂, especially when moving slowly (Air Quality Expert Group, 2004). In the City of Manchester (UK), the majority (80%) of NO_x emissions are associated with (diesel) vehicle emissions (TfGM, 2016; Regan, 2018).

Two automated air quality monitoring stations record pollutants (i.e. O₃, NO, NO₂, NO_x, SO₂ and PM₁₀ and PM_{2.5}) within central Manchester, i.e. at Piccadilly Gardens and on Oxford Road (Figure 4-1). Although these monitoring stations generate continuous records of air quality, they are high cost infrastructures and thus are restricted in number, therefore only recording localised air quality. Urban environments and associated air quality are, however, complex systems with various factors (e.g. building heights and density, road traffic counts and meteorological conditions) influencing spatial pollutant distribution (Endlicher, 2012; Mayer, 1999; Salmond and McKendry, 2009), highlighting the necessity to apply additional methods to achieve finer spatial scale assessment of urban air quality.

Lichens have been shown to be excellent organisms to (bio)monitor atmospheric pollution and air quality, where the high cost of technical air quality measurement equipment cannot be afforded, due to their morphology (i.e. lacking roots and cuticle) and ability to take up and accumulate airborne pollutants (and required nutrients) (Zierdt, 1997; Garty, 2001; Wolterbeek et al., 2003; Forbes, 2015; Forbes et al., 2015).

Only a few prior studies have used lichen carbon (C) and sulphur (S) contents in air quality monitoring studies, while a greater number used lichens as indicators and/or monitors for airborne nitrogen compounds in (urban) environments (Hawksworth, 1970; Tynnyrinen et al., 1992; Vingiani et al., 2004; Beck and Mayr, 2012; Boltersdorf and Werner, 2014; Boltersdorf et al., 2014; Gerdol et al., 2014; Pinho et al., 2017). Specifically, lichen nitrogen contents can reflect airborne nitrogen loads originating from anthropogenic impacts, particularly in urban areas (Fрати et al., 2006; Gadsdon et al., 2010; Boltersdorf et al., 2014).

Lichen stable-isotope ratio signatures have not been analysed to the same extent as it has been done for soil, groundwater, precipitation and mosses in pollution studies (Russell et al., 1998; Sutton et al., 2004; Widory, 2007). However, prior studies reported urban carbon sources (i.e. street dust, PM₁₀ and soot from diesel and gasoline vehicle exhausts) to influence lichen $\delta^{13}\text{C}$ values, indicating the use of $\delta^{13}\text{C}$ values to characterise lichen CO₂ sources (Batts et al., 2004; López-Veneroni, 2009). Sulphur is an essential nutrient for epiphytic lichens (i.e. those living on plant surfaces) and lichen sulphur-isotope ratio signatures are related to the close surrounding atmosphere (Wadleigh and Blake, 1999; Wadleigh, 2003; Batts et al., 2004). Thus, $\delta^{34}\text{S}$ values can be used to fingerprint anthropogenic sulphur sources (e.g. coal and oil; Wadleigh, 2003; Wadleigh and Blake, 1999; Wiseman and Wadleigh, 2002). Atmospheric nitrogen compounds have different $\delta^{15}\text{N}$ signatures (atmospheric N₂ is 0‰), with NO_x having positive $\delta^{15}\text{N}$ values (Laffray et al., 2010; Felix et al., 2012; Felix and Elliott, 2014; Pinho et al., 2017). Lichen nitrogen-isotope ratio signatures ($\delta^{15}\text{N}$ values) thus are able to reflect predominant environmental nitrogen sources (Russow et al., 2004; Tozer et al., 2005; Fogel et al., 2008; Lee et al., 2009; Boltersdorf and Werner, 2013; Boltersdorf et al., 2014). Epiphytic lichens can uptake nitrogen from different sources (such as nitrate and ammonia, or ammonium) and therefore exhibit a wide range of $\delta^{15}\text{N}$ ratios (Beck and Mayr, 2012). $\delta^{15}\text{N}$ values are reported to be more positive (i.e. are more ¹⁵N enriched) where NO_x concentration is high (such as in urban areas) and more negative in rural areas, the latter primarily due to a greater contribution of reduced nitrogen from agricultural sources (Pearson et al., 2000; Sutton et al., 2004; Boltersdorf et al., 2014).

This chapter presents the analysis of *X. parietina* and *Physcia* spp. lichens, sampled from the City of Manchester urban environment, for carbon, nitrogen and sulphur contents and their stable-isotope ratios (expressed as $\delta^{13}\text{C}$, $\delta^{15}\text{N}$ and $\delta^{34}\text{S}$ values) in order to assess air quality at a high spatial scale than is possible with high cost instrumented air quality monitoring stations. Stable-isotope ratio signatures are assessed in terms of whether they can be used to identify and 'fingerprint' major pollution sources in the Manchester urban environment.

Passive sampling NO_x tube measurements, as described in Chapter 3, will also be used to ground-truth lichen N contents, i.e. in relation to atmospheric NO_2 concentrations, and to investigate if elevated NO_x concentrations correspond to more positive $\delta^{15}\text{N}$ values. Moreover, rural environment 'control' lichen samples were also analysed for their CNS contents and stable-isotope ratios, to investigate the magnitude of differences between an assumed less polluted rural situation and an urban environment experiencing lower air quality. Temporal variability of lichen carbon and nitrogen contents also is discussed in relation to implications for lichen biomonitoring studies.

Following description of the analytical research methodologies, results for both rural and urban environments are described. A comparison of rural and urban lichen CNS contents and stable-isotope ratios is then presented, as well as a brief description of NO_x diffusion tube measurements. Spatial analysis of the variability of lichen CNS contents and stable-isotope ratio signatures is undertaken, with regard to site-specific urban influences, i.e. distance to major road, road traffic counts, surrounding building heights, and distances to large potential pollutant point sources and greenspaces. Final conclusions on the utility of lichens to biomonitor spatial variability of airborne CNS compounds, as well as the potential for 'fingerprinting' potential airborne pollutant sources using lichen isotopic signatures, will be drawn.

4.2 Research Methodology

4.2.1 Lichen sampling and preparation

Urban lichen samples of *X. parietina* (N=94; Figure 4-1) and *Physcia* spp. (N=86; Figure 4-1) were sampled from street trees situated across the City of Manchester (as described in Chapter 2), between the end of June 2016 to end of October 2017 (site specifics, i.e. tree species and XY-coordinates can be found in Appendix B-1). A detailed description of lichen sampling procedure, transport and preparation for analysis was described in chapter 2.

A second lichen sampling period was undertaken in 2018 (N=15; Figure 4-1), to assess the scale of any temporal variability of CNS contents and stable-isotope ratio signatures in urban lichen samples, since evidence for temporal variability on lichen chemistry will impact on the analysis and interpretation of spatial variability.

Lichen rural environment 'control' samples were sampled to evaluate whether urban lichen CNS contents and stable-isotope ratios are diagnostic for an urban environment with poorer air quality. Rural lichen samples (*X. parietina*, N=12; Figure 4-2) were collected from oak (*Quercus* spp.) and hawthorn (*Crataegus* spp.) trees distributed around a poultry farm in Shrewsbury (UK) in May 2018, following the same procedure described above. Lichen sampling was undertaken in close proximity to (i.e. between 50 to 500 m) and on a general south-west transect (i.e. between 1 to 3 km) away from the poultry farm, as defined by accessibility of sampling sites, i.e. fenced and hedged agricultural fields and private property.

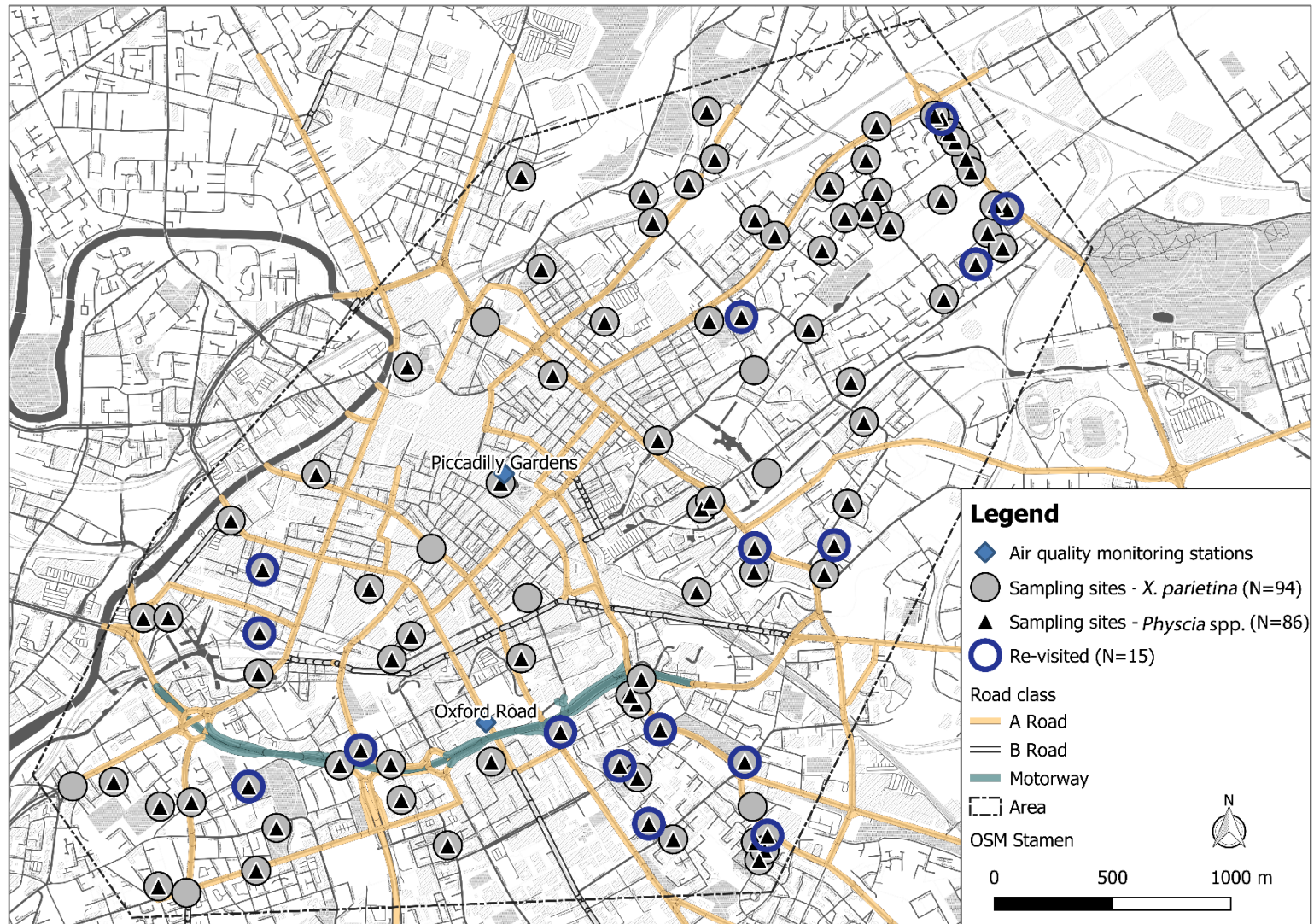


Figure 4-1: Lichen sampling sites (*X. parietina*: grey circle; *Physcia* spp.: black triangle and re-visited sampling sites in 2018: blue outline) across Manchester city centre; two automated instrumented air quality monitoring stations and major roads (motorway, A and B-roads) are also shown



Figure 4-2: Rural lichen sampling sites (*X. parietina*; N=12) distributed around a poultry farm in Shrewsbury, UK (sampled in May 2018); displayed with location of poultry farm in relation to Greater Manchester (upper left corner, red square); background map: Google Maps - Satellite (map data 2018 - Google)

4.2.2 Lichen analysis for total carbon and total nitrogen contents – by CN analyser

Total carbon and total nitrogen, expressed as percentage by weight (wt%), were measured using a 'Leco TruSpec[®]' CN analyser. About 0.15 g of each lichen sample was weighed into a tin foil, as well as 0.15 g of the calibration standard 'Ethylenediaminetetra-acetic acid' (EDTA 502-092), rice flour (LECO calibration material), and 'Certified Reference Material (CRM) No. 482' (BCR – Trace elements in lichen *Pseudevernia furfuracea*, sample identification No. 594), for each analytical run (Table 4-1). EDTA was used to calibrate the CN analyser, while the lichen CRM and rice flour were used to check accuracy and precision. Before measuring the samples, blanks (Helium carrier gas only) were used to zero the CN analyser. Lichen CN contents were analysed in batches and batch-to-batch variability was investigated using 'Rice Flour' and lichen CRM run throughout analysis (after every five lichen unknowns, one sample each of rice flour and CRM were run). Batch-to-batch bias analysis is addressed in section 4.3.1.

Table 4-1: Number of analysed calibration standards (EDTA 502-092), rice flour and lichen CRM for each analytical batch on the LECO CN analyser

	EDTA	Rice Flour	Lichen CRM
Batch 1	5	7	7
Batch 2	5	6	6
Batch 3	5	5	5
Batch 4	5	4	4
Batch 5	5	6	6
Batch 6	5	4	4
Total	30	32	32

4.2.3 Lichen analysis for stable-isotope ratios – by IRMS

Lichen samples were analysed for CNS (wt%) and stable-isotope ratios (i.e. $\delta^{15}\text{N}$, $\delta^{13}\text{C}$ and $\delta^{34}\text{S}$ values, as defined below) simultaneously by Isotope Ratio Mass Spectrometry (IRMS) using an Elementar Pyrocube elemental analyser (EA) interfaced with a VISION isotope ratio mass spectrometer (IRMS) at the Scottish Universities Environmental Research Centre (SUERC) in East Kilbride/Glasgow. About 7 mg lichen samples were weighed into tin capsules (6 x 4 mm), handled and closed with tweezers and stored in 1.5 ml centrifuge tubes until analysis. International reference standards, USGS40 (glutamic acid) for $\delta^{13}\text{C}$ and $\delta^{15}\text{N}$ and silver sulphides (IAEA-S1, S2 and S3) for $\delta^{34}\text{S}$, were analysed with lichen samples.

Three internal laboratory standards, MSAG2 (methanesulfonamide/gelatin), M2 (methionine, gelatine, glycine and ^{15}N -enriched alanine) and SAAG2 (sulphanilamide, gelatine and ^{13}C -enriched alanine), were used to check for “change” (drift; automatically corrected by IRMS software) in $\delta^{15}\text{N}$, $\delta^{13}\text{C}$ and $\delta^{34}\text{S}$ values through time for each experimental batch. Isotopic composition data are not available for the lichen CRM (BCR No. 482), but this reference material was measured throughout each run, to compare individual datasets and to check for potential analytical bias. Three batches of lichen samples were analysed, including 43 CRM samples in total (batch 1: N= 7, batch 2: N=32 and batch 3: N=4).

Stable-isotope ratios are expressed as ‘delta’-values (δ), denoting the difference of measurements made relative to an international standard reference frame (Eq. 1; Fry, 2006; Sharp, 2017).

$$\text{(Eq. 1) } \delta^y\text{X} = \left(\frac{R_{\text{sample}}}{R_{\text{standard}}} - 1 \right) \times 1000$$

Delta (δ) values are reported in per mille (‰), or ‘parts per thousand’, with y being the heavy isotope of element X (e.g. ^{13}C) and R as the ratio of abundance of the heavy to light isotope, for the sample (R_{sample}) and the standard (R_{standard}). In this study R is either $^{13}\text{C}/^{12}\text{C}$ ($\delta^{13}\text{C}$), $^{15}\text{N}/^{14}\text{N}$ ($\delta^{15}\text{N}$) or $^{34}\text{S}/^{32}\text{S}$ ($\delta^{34}\text{S}$). A positive δ value means that the ratio of the heavy to light isotope is higher in the sample compared to the standard, and the opposite for negative δ -values. For example, a sample with a $\delta^{15}\text{N}$ value of -5.0‰ has a $^{15}\text{N}/^{14}\text{N}$ ratio that is -5.0 per mille (or -0.5%) lower than that of the standard (Sharp, 2017).

4.2.4 NO_x diffusion tube analysis

NO_x diffusion tubes were deployed at 45 sites in the City of Manchester (that had been sampled for lichens) between the 3rd of July 2017 and the 28th of June 2018 (changed on a bi-weekly cycle over a 12-month period; 361 days) to ground-truth the lichen dataset. See chapter 3 for detailed deployment and analysis procedures, as well as for description of the spatial variability of measured NO_2 . Figure 4-3 displays the location of the NO_x diffusion tubes together with the lichen sampling sites considered in this chapter. Site-specific CNS contents (wt%) and $\delta^{15}\text{N}$, $\delta^{13}\text{C}$ and $\delta^{34}\text{S}$ signatures, where NO_x diffusion tubes were deployed, are shown in Appendix B-2.

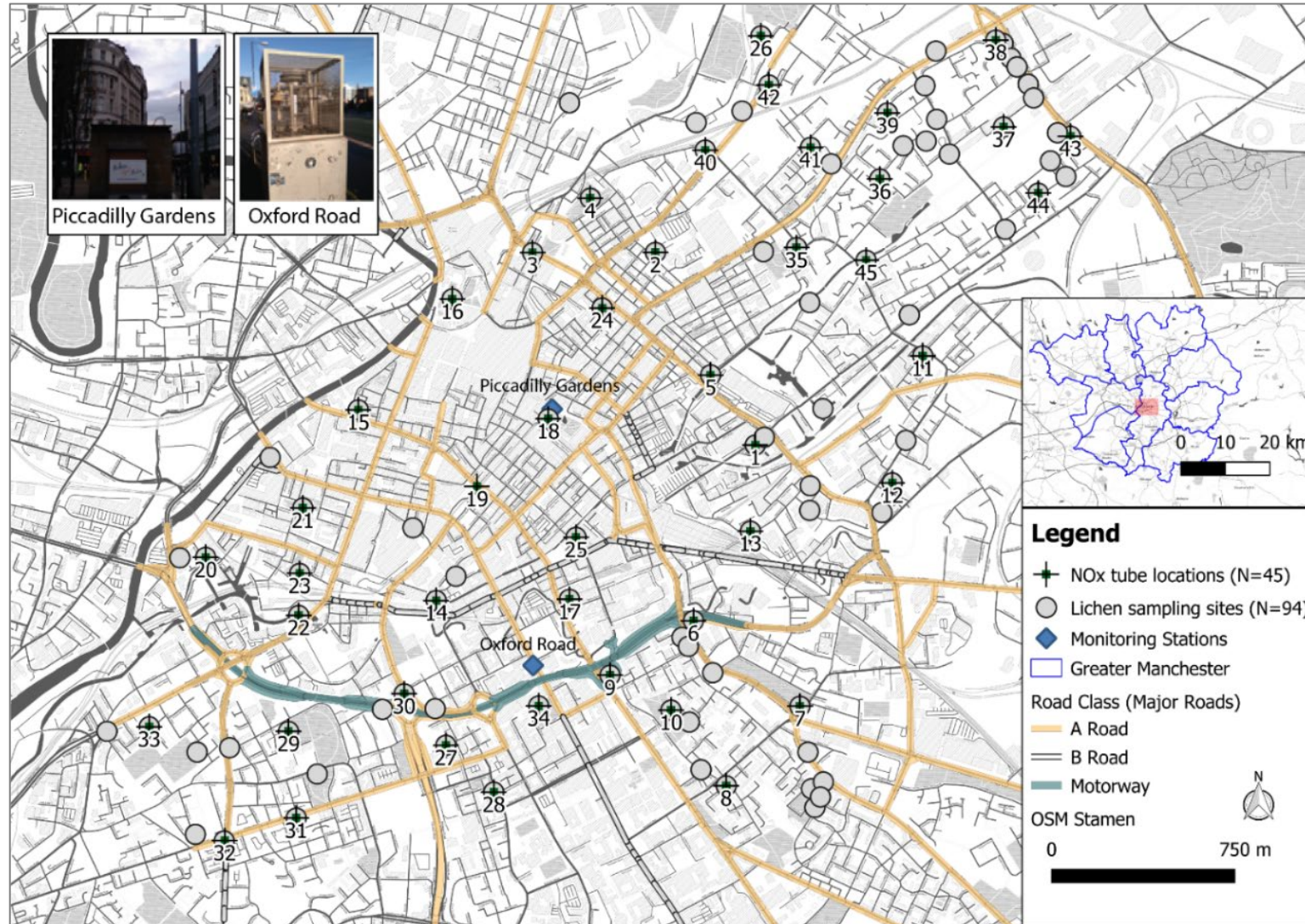


Figure 4-3: NO_x tube deployment sites (N=45; with site IDs), displayed with two automated instrumented air quality monitoring stations (pictures displayed in the upper left corner) and lichen sampling sites (N=94)

4.2.5 Statistical data analysis

Statistical analysis was completed using 'SPSS Statistics 25' and 'GraphPad Prism 7' statistical software. Data visualisation was undertaken using 'Origin 2019'. Lichen CNS content and stable-isotope ratio datasets were tested for normality using Shapiro-Wilk tests. Shapiro-Wilk is considered a stronger statistical test for normality, compared to other tests (e.g. Kolmogorov-Smirnoff), regardless of data distribution and sample size (Mendes and Pala, 2003; Razali and Wah, 2011). Table 4-2 displays test outcomes for normal distribution of data. Shapiro-Wilk test outcomes were used to inform statistical analysis of datasets. For instance, comparison of lichen species CNS contents was undertaken using a Mann-Whitney (C contents; non-parametric) and unpaired t-tests (N and S contents; parametric).

To analyse relationships between these lichen data and potential urban influencing factors, correlation statistics, i.e. Pearson's r (parametric) and Spearman ρ (non-parametric) were used. Stable-isotope ratios in urban lichens were compared using Mann-Whitney (for $\delta^{13}\text{C}$ and $\delta^{34}\text{S}$ values) and t-test ($\delta^{15}\text{N}$ values) statistics. Comparison of urban and rural lichen CNS contents was undertaken using unpaired t-tests for N and S contents, whereas C contents were compared by Mann-Whitney test statistics, due to non-normal distribution of urban C contents. Stable-isotope ratios between urban and rural *X. parietina* lichen samples was undertaken using unpaired t-tests for $\delta^{13}\text{C}$ and $\delta^{15}\text{N}$ values, whereas $\delta^{34}\text{S}$ values were compared using a Mann-Whitney statistical test. Relationships of CNS data and stable-isotope ratios with distance to poultry farm were analysed using Pearson's r (parametric test), due to normal distribution of data.

Table 4-2: Statistical test (Shapiro-Wilk) outcomes for normal distribution of lichen CNS (wt%) and stable-isotope ratio signatures ($\delta^{13}\text{C}$, $\delta^{15}\text{N}$ and $\delta^{34}\text{S}$), to elucidate statistical tests for comparison of datasets; non-normal distributed data shaded in blue, normal distributed data shaded in green

	<i>X. parietina</i> (urban, N=94)	<i>Physcia</i> spp. (urban, N=86)	<i>X. parietina</i> (rural, N=12)
Carbon wt%	Non-normal	Non-normal	Normal
Nitrogen (wt%)	Normal	Normal	Normal
Sulphur (wt%)	Normal	Normal	normal
$\delta^{13}\text{C}$	Normal	Non-normal	Normal
$\delta^{15}\text{N}$	Normal	Normal	Normal
$\delta^{34}\text{S}$	Non-normal	Non-normal	Normal

The NO_x diffusion tube dataset was normally distributed for NO₂ concentrations. Thus, statistical relationships were tested with Pearson's *r* for airborne NO₂ with lichen N wt% and δ¹⁵N values.

The rationale for the grouping of sampled sites for statistical analysis of lichen CNS contents in relation to potential urban influences (i.e. distance to major roads, traffic counts and building heights; Table 4-3) were described in detail in chapter 2. For instance, classification of distance to major road based on airborne NO_x decline within the first 200 m distance from major roads (Gilbert et al., 2003; Laffray et al., 2010; Bermejo-Orduna et al., 2014). The UK's primary route network includes A-roads, B-roads and motorways (UK Department of Transport, 2012), which were included for analysis with distance to road. Road traffic counts are based on traffic count statistics, i.e. annual average daily traffic flow (DfT, 2017a). Building heights surrounding each sampling location were calculated by applying a 50 m buffer around each tree, using 'OS building heights – alpha' (Digimap - Ordnance Survey, 2017). Classification of 'distance to large potential pollutant point sources' (e.g. industrial and commercial combustion) was based on potential emissions at greater distances that might be transported across the research area (Britter and Hanna, 2003; NAEI, 2015). Distances to urban greenspace (using 'OS – Open Greenspace' (Digimap - Ordnance Survey, 2018) classifications were based on human health studies that report decreased impacts of air pollution within 30 to 500 m of greenspaces (Dadvand, de Nazelle, et al., 2012; Dadvand, Sunyer, et al., 2012; Browning and Lee, 2017).

Rural lichen sample data were compared with distance to poultry farm and classified accordingly, being located in close proximity (<500 m) and further away (>500 m) from the poultry farm.

Table 4-3: Categories applied to potential urban influencing factors used to assess possible controls on the spatial variability of urban *X. parietina* and *Physcia* spp. lichen CNS contents and stable-isotope ratios

Environmental variable	Categories
Distance to major road (including A-, B- road and motorway)	1: <25 m 2: 25-50 m 3: 50-100 m 4: 100-200 m 5: >200 m
Road class (major roads)	M – motorway A - A-road B - B-road U - Unclassified
Road traffic count (annual average daily traffic flow)	1: <10,000 2: 10,000 to 20,000 3: 20,000 to 30,000 4: >30,000
Building heights	1: <10 m 2: 10 to 20 m 3: >20m
Distance to (large) potential pollutant point source	1: <500 m 2: 500 to 1000 m 3: 1000 m to 2000 m 4: >2000m
Distance to urban greenspace	1: <100 m 2: 100 to 200 m 3: 200 to 300 m 4: 300 to 400 m 5: 400 to 500 m 6: >500 m

4.2.6 Geospatial data analysis

Geographic Information System Software (GIS; ArcMap 10.5 and QGIS 3.4.2 – ‘Madeira’) was used for geospatial analysis and mapping of lichen CNS contents (wt%) and $\delta^{13}\text{C}$, $\delta^{15}\text{N}$ and $\delta^{34}\text{S}$ values. Other environmental studies that have assessed spatial variation and patterns of air quality and atmospheric pollution have applied kriging methods to produce prediction maps (Romary et al., 2011; Beauchamp et al., 2012; Pannullo et al., 2015; Parzych, Astel, et al., 2016). In this study, ordinary Kriging (OK) was applied to lichen CNS contents and stable-isotope ratios to investigate spatial patterns of lichen pollutant loadings in Manchester. Ordinary kriging was not applied to rural samples due to smaller sample size (N=12).

'Geographically Weighted Regression' (GWR) has been applied in several fields, such as geographical and environmental sciences, providing a 'local' model of spatial relationship between a modelled variable (i.e. pollutant) and predictors (i.e. building heights and traffic counts; Fotheringham et al., 2002; Warsito et al., 2018). Spatial relationships were modelled using GWR using ArcMap 10.5. 'spatial statistics' tool (ESRI, 2016), to assess what factors have the strongest influence on lichen chemistry and thus air quality and to be able to predict concentrations over a larger spatial scale (where lichens have not been sampled). Specific lichen 'pollutant' loadings (i.e. CNS contents and $\delta^{13}\text{C}$, $\delta^{15}\text{N}$ and $\delta^{34}\text{S}$ values) were used as dependent variables, while potential urban influencing factors (Table 4-3) were used as explanatory variables in the GWR modelling approach. The ArcMap 10.5 'spatial statistics' tool was used with default input features: fixed Kernel type; Bandwidth method: 'Akaike Information Criterion' - AICc; number of neighbours: 30 to model spatial relationships between urban influences that might affect pollutant loadings recorded in lichen samples. For instance, a sampling site closer to a highly trafficked road may have elevated pollutant levels, indicating the potential relationship. GWR can be used to predict pollutant loadings at un-sampled site, taking the effect of the location into the predictor (Fotheringham et al., 2002; Warsito et al., 2018)

4.3 Results – Lichen CNS in urban and rural environments

4.3.1 Assessment of accuracy and precision of CNS and stable-isotope analysis

Analytical accuracy and precision was investigated for both analytical instruments (CN analyser and IRMS) and results (specifically carbon and nitrogen contents) were compared. Sulphur contents (wt%) by IRMS were compared with ICP-OES measurements (sulphur in $\mu\text{g/g}$).

'Outliers' are data points that deviate markedly from others and can be caused by experimental errors (Motulsky and Brown, 2006; Aguinis et al., 2013). Lichen CRM datasets (i.e. CNS contents and stable-isotope ratios), analysed by CN analyser (N=31 in 6 analytical batches) and IRMS (N=43 in 3 analytical batches) were investigated for potential outliers (by visual interpretation of boxplots and subsequently by statistical analysis, using 'Grubbs outlier test; Grubbs, 1969; Tuckey, 1977; Aguinis et al., 2013) that were removed before analysis of accuracy and precision. Table 4-4 shows number of outliers identified that were removed before analysis.

Table 4-4: Identified outliers in analysed lichen CRM and Rice flour for CN analyser batches (N=31 in 6 batches) and analysed lichen CRM by IRMS (N=43 in 3 batches) that were removed before analysis of accuracy and precision; outliers found shaded in yellow (with number and batch the outlier was found), no outliers found shaded in green

N=32 (in 6 batches)	CRM	Rice Flour
Carbon (wt%)	Yes (1 Outlier, batch 1)	Yes (1 Outlier, batch 1)
Nitrogen (wt%)	No	No

N=43 (in 3 batches)	IRMS		
Carbon (wt%)	Yes (1 Outlier, batch 1)	$\delta^{13}\text{C}$	No
Nitrogen (wt%)	Yes (1 Outlier, batch 1)	$\delta^{15}\text{N}$	No
Sulphur (wt%)	No	$\delta^{34}\text{S}$	No

Figure 4-4 illustrates the batch-to-batch N wt% and C wt%, recorded in lichen CRM, showing analytical results in agreements with certified values. To analyse for batch-to-batch variability, Friedman's test (two-way analysis of variance; non-parametric) was used, due to varying CRM numbers run with the analytical instrument in each batch. No significant differences ($p > 0.05$) were found for nitrogen and carbon contents (in lichen CRM) between analytical batches.

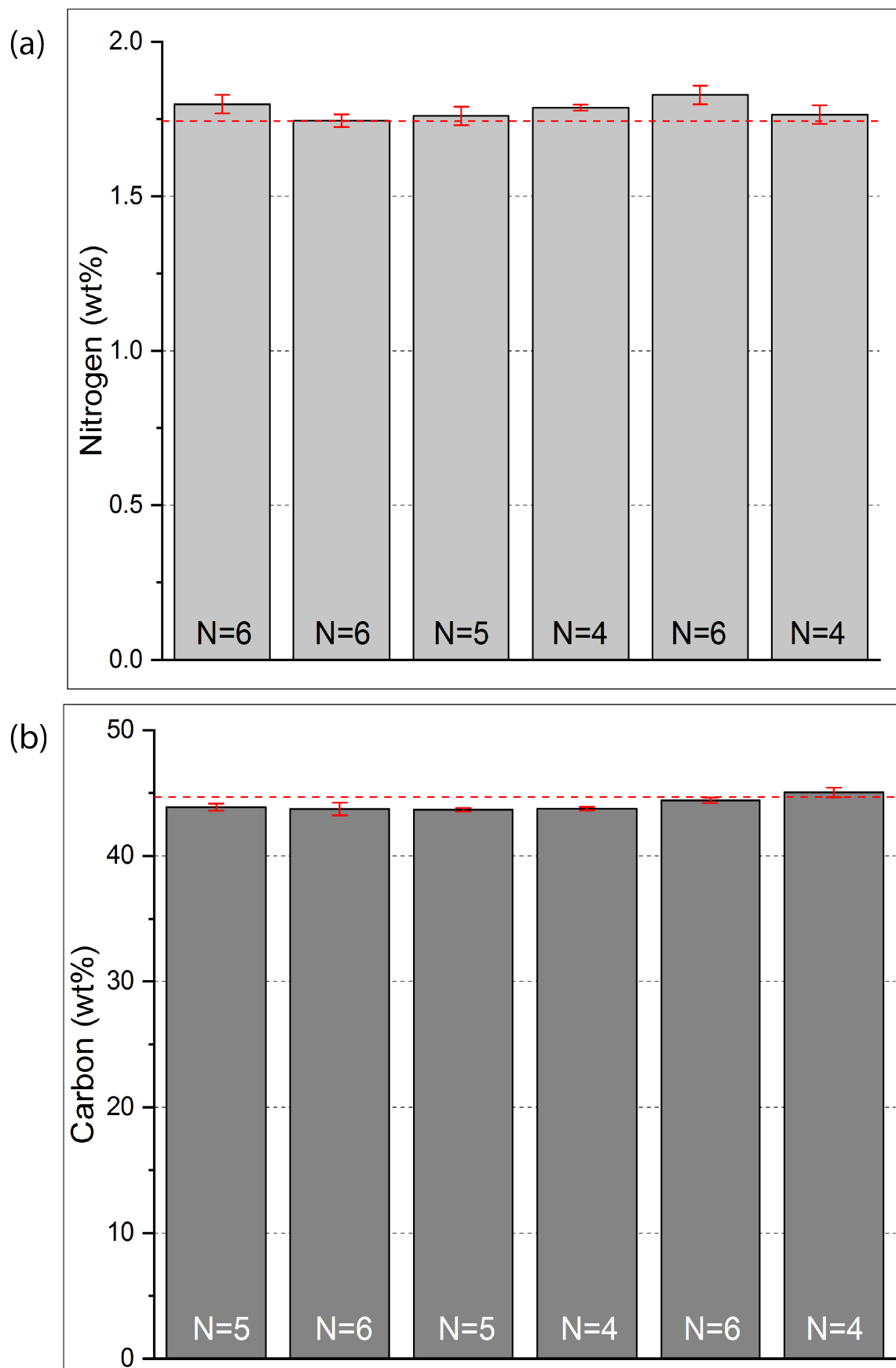


Figure 4-4: Mean concentrations (presented as bar plots with 1x standard deviation) of recorded (a) nitrogen and (b) carbon contents (in wt%) in lichen CRM (No. 482) for each analytical batch using a CN analyser (with number of individual samples run; dashed lines represent certified values, N wt%: 1.743 and C wt%: 44.7)

Lichen CRM analysis for carbon and nitrogen contents using a LECO CN analyser gave analytical accuracy of 102% for nitrogen and 98.6% for carbon contents (Table 4-5) and overall precision of 2.19% (%CV; calculated as ratio between standard deviation and mean) for nitrogen and 1.25% (%CV) for carbon, respectively. Batch-to-batch accuracy varied between 100.98% and 104.89% for N wt% and between 97.70% to 102.4% for C wt%. Rice flour, analysed during CN analysis, accuracy was found between 83.89% to 90.13% for nitrogen contents and 91.27% to 93.26% for carbon contents. Certified and measured values for lichen CRM and 'Rice Flour' are presented in Table 4-5.

CNS contents in lichen samples were simultaneously analysed with stable-isotope-ratio signatures, using an IRMS. Lichen CRM (No. 482) was also analysed during the IRMS evaluation, but no certified isotope values are available. IRMS analysis of lichen CRM gave 107% analytical accuracy for nitrogen (wt%), 101% (C wt%) for carbon and 85% for sulphur contents (Table 4-5). Comparison of analysed carbon and nitrogen contents by CN analyser and IRMS is displayed in the Appendix B-3. Measured lichen CRM (N=43) precision (%CV) was 2.4% ($\delta^{13}\text{C}$), 2.9% ($\delta^{15}\text{N}$) and 11% ($\delta^{34}\text{S}$) for stable isotopes and 13.15% (± 0.02 wt%; Table 4-5) for sulphur contents (S wt%). Accuracy of IRMS analysis varied between 98.3% to 101.96% for international and internal reference material. Only SAAG2 (for $\delta^{34}\text{S}$) and IAEA-S1 measurements were very different from accepted values (Table 4-6). Figure 4-5 illustrates CNS contents and $\delta^{13}\text{C}$, $\delta^{15}\text{N}$ and $\delta^{34}\text{S}$ values recorded in lichen CRM for each analytical batch by IRMS.

Results of both, CN analyser and IRMS showed accuracy of ~100% ($\pm 10\%$) of C and N contents in lichen CRM, illustrating the viability of analytical results in this study. Accuracy of sulphur contents, analysed by IRMS was found at 85%, indicating potential underestimation of sulphur in lichen CRM. Sulphur concentration in the CRM have been measured by 'Inductively Coupled Plasma – Atomic Emission Spectrometry' (ICP-AES) and 'X-Ray Fluorescence' (XRF) and are reported as 'indicative values' in Quevauviller et al. (1996).

Table 4-5: Analysed carbon, nitrogen and sulphur contents (wt%) of lichen CRM (No. 482) by CN analyser and IRMS and certified values, displayed with $\pm 1x$ standard deviation (Quevauviller et al., 1996) and LECO reference material 'Rice Flour' (502-278) for CN analysis (presented as $\pm 1x$ standard deviation ; N/A – not measured with CN analyser or IRMS; accuracy 100% \pm 5% displayed in green, accuracy 100% \pm 10% in yellow and accuracy 100% \pm 15% in red)

	CN analyser	IRMS	Certified value	Accuracy (%) CN	Precision (%CV) CN	Accuracy (%) IRMS	Precision (%CV) IRMS
Measured values							
Nitrogen (wt%)	1.78 \pm 0.04	1.87 \pm 0.15	1.743 \pm 0.025	102	2.19	107	8.3
Carbon (wt%)	44.05 \pm 0.55	45.48 \pm 5.16	44.7 \pm 0.700	99	1.25	102	11.3
Sulphur (wt%)	N/A	0.18 \pm 0.02	0.2166 \pm 0.029	N/A	N/A	85	13.5
LECO reference material – Rice Flour (CN analysis)							
Nitrogen (wt%)	0.99 \pm 0.04	N/A	1.13	88	3.85	N/A	N/A
Carbon (wt%)	40.95 \pm 0.41	N/A	44.46	92	1.00	N/A	N/A

Table 4-6: Measured and accepted isotope ratios (mean \pm standard deviation) for international isotope standards (USGS40, IAEA-S1 to S3, MSAG2, M2 and SAAG2) and lichen CRM (N=43) used during IRMS analysis (NA = not applicable, no values available); displayed with overall accuracy (%) and precision (%CV); accuracy at $100 \pm 5\%$ in green, very low and very high recorded accuracy in red.

Reference Material	Measured Values			Accepted Values			Accuracy (%)			Precision (%CV)		
	$\delta^{15}\text{N}$	$\delta^{13}\text{C}$	$\delta^{34}\text{S}$	$\delta^{15}\text{N}$	$\delta^{13}\text{C}$	$\delta^{34}\text{S}$	$\delta^{15}\text{N}$	$\delta^{13}\text{C}$	$\delta^{34}\text{S}$	$\delta^{15}\text{N}$	$\delta^{13}\text{C}$	$\delta^{34}\text{S}$
USGS40 (N=8)	-4.61 ± 0.00	-26.32 \pm 0.00	NA	-4.52 \pm 0.06	-26.39 \pm 0.04	NA	102	99.7	N/A	<0.0	<0.0	N/A
IAEA-S1 (N=11)	NA	NA	-0.07 ± 0.12	NA	NA	-0.3	N/A	N/A	24.7	N/A	N/A	161
IAEA-S2 (N=11)	NA	NA	22.23 ± 0.35	NA	NA	22.62 \pm 0.20	N/A	N/A	98.3	N/A	N/A	1.6
IAEA-S3 (N=11)	NA	NA	-32.44 ± 0.26	NA	NA	-32.49 \pm 0.20	N/A	N/A	99.9	N/A	N/A	0.8
MSAG2 (N=121)	2.28 ± 0.03	-21.30 ± 0.03	6.27 ± 0.13	2.24 ± 0.09	-21.23 ± 0.12	6.18 \pm 0.43	100.8	99.8	101.6	1.1	0.1	2.1
M2 (N=78)	32.70 ± 0.00	-34.21 ± 0.01	14.23 ± 0.39	32.70 ± 0.27	-34.28 \pm 0.11	14.43 \pm 0.46	100	100.1	101.3	<0.01	<0.05	2.7
SAAG2 (N=73)	4.52 \pm 0.08	-5.72 \pm 0.02	0.58 ± 0.58	4.55 \pm 0.06	-5.78 \pm 0.12	0.04 \pm 0.36	98.9	100.6	>1000	1.8	0.3	101
Lichen CRM 482	-7.95 \pm 0.23	-25.04 \pm 0.61	5.58 ± 0.62	NA	NA	NA	N/A	N/A	N/A	2.9	2.4	11.0

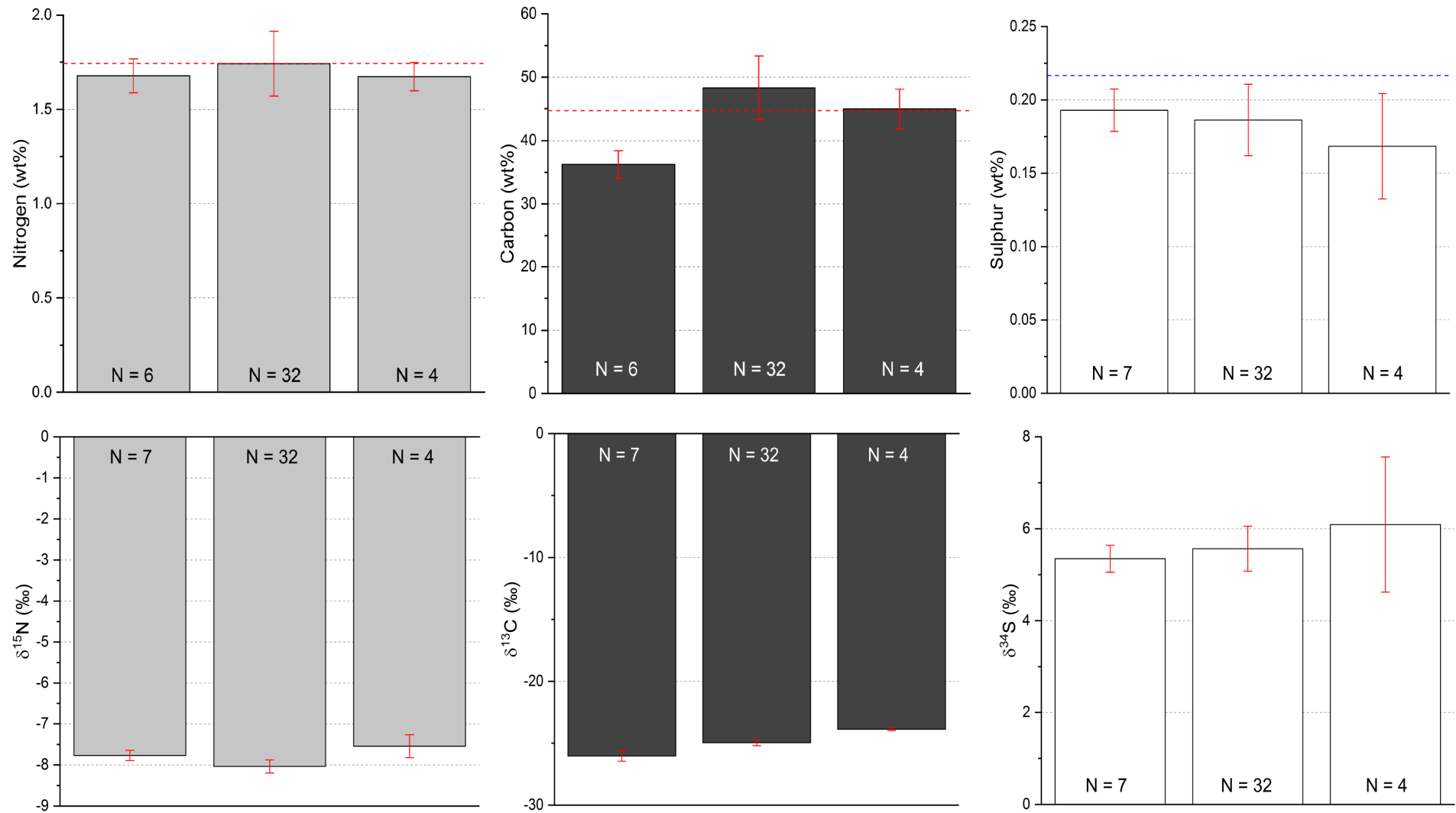


Figure 4-5: CNS contents (wt%; above) and stable-isotope-ratio signatures (‰; below) recorded for analytical batches recorded in lichen CRM (No. 482) using IRMS; dashed red lines presents certified values, blue dashed line represents indicative values for sulphur contents (wt%; Quevauviller et al., 1996); no certified values available for stable-isotope ratios in lichen CRM

4.3.2 Assessment of temporal variability of CNS contents (wt%) in urban *X. parietina* samples

Urban lichens (*X. parietina*) have been re-sampled during a second sampling period in 2018 (May to October), of which 15 sites were re-analysed for their CN contents (wt%) following the described procedure by CN analyser (section 4.2.2). Re-sampling was undertaken to evaluate a potential temporal bias, superimposed on spatial variability. Comparison of C and N contents for both sampling periods is displayed in Table 4-7. A paired t-test (due to normal distribution of C and N contents for re-sampled sites) was used to assess differences between sampling periods (Table 4-7 and Figure 4-6). Significant differences between the sampling periods were found for carbon contents only (Table 4-7). A temporal bias on spatial variability of lichen carbon contents cannot be ruled out and should be considered. Potential influences on lichen C contents are further discussed in section 4.4.1

Table 4-7: Comparison of carbon and nitrogen contents (wt%) for the sampling periods, to assess potential temporal bias of lichen data; statistical test (paired t-test) to evaluate differences between sampling periods; ** indicates significance at $p < 0.01$

<i>X. parietina</i> (N=15)	Sampling period (1)	Sampling period (2)	
Carbon (wt%)	38.82 – 41.5	41.59 – 45.60	
Nitrogen (wt%)	2.18 – 3.60	2.15 – 3.76	
Sulphur (wt%)	0.329 – 0.544	0.314 – 0.553	
Paired t-test	Carbon wt% <0.01**	Nitrogen wt% 0.13	Sulphur wt% 0.53

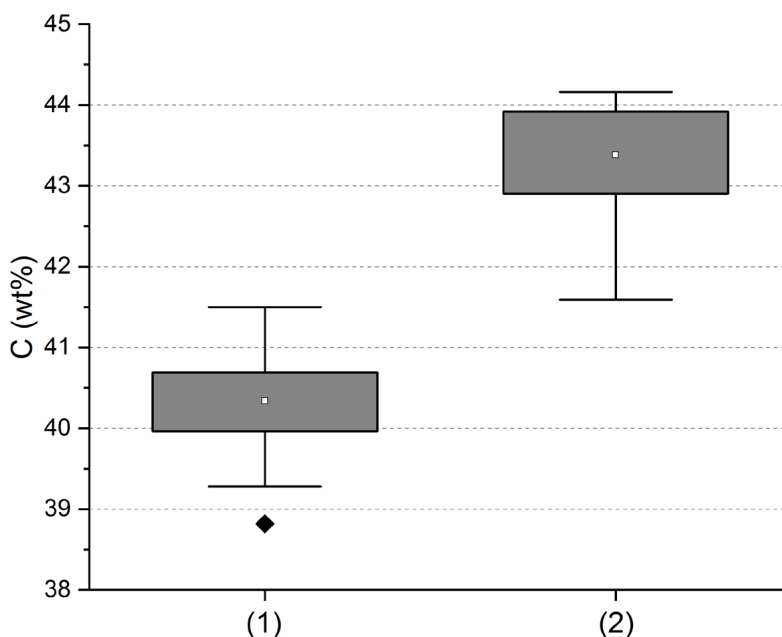


Figure 4-6: Box-Whisker plots (25th to 75th percentile) of carbon contents (C wt%) recorded in *X. parietina* for sampling periods (undertaken during 2016/17 displayed as (1) and in 2018, as (2)), displayed with mean value: white square and extreme values (black diamond)

4.3.3 Carbon, nitrogen and sulphur contents (wt%) and stable-isotope-ratios in rural *X. parietina* samples

X. parietina (sampled around a poultry farm; Figure 4-2) were used to compare urban and rural lichens, to evaluate differences in CNS contents (wt%) and stable-isotope-ratio signatures in these contrasting environments. Analysed CNS contents and stable-isotope-ratio signatures for rural samples are displayed in Table 4-8. Lichens were sampled at different locations around the poultry farm and Pearson's *r* was used to investigate a potential relationship with distance to the poultry farm and CNS contents and stable-isotope-ratios. Nitrogen content (wt%) were found to decrease with distance to poultry farm, while $\delta^{34}\text{S}$ values increased with proximity to the farm area (Figure 4-7).

Especially, nitrogen contents and $\delta^{15}\text{N}$ could indicate potential sources (i.e. agricultural areas and poultry farm emissions) in the rural environment, as displayed in Figure 4-8. A comparison of urban and rural *X. parietina* samples is provided hereafter. Interpretation and discussion is presented in section 4.4.2.

Table 4-8: CNS contents (wt%) and stable-isotope-ratio signatures (‰) analysed in rural lichen samples (*X. parietina*; N=12); presented as three significant figures; Pearson's *r* correlation statistics (*r*-value) to investigate poultry farm influences, *significant at the level $p < 0.05$ presented in bold and green background

Site	C (wt%)	N (wt%)	S (wt%)		$\delta^{13}\text{C}$ (‰)	$\delta^{15}\text{N}$ (‰)	$\delta^{34}\text{S}$ (‰)
1	43.3	3.44	0.353		-23.4	-6.36	9.44
2	42.8	3.34	0.332		-23.0	-8.09	10.9
3	42.0	4.22	0.420		-23.1	4.44	8.42
4	41.5	3.81	0.521		-22.8	0.03	9.96
5	41.4	3.95	0.515		-22.0	-2.69	12.8
6	42.2	3.87	0.453		-22.3	-1.05	11.0
7	42.8	3.51	0.427		-22.8	-6.59	13.4
8	42.7	3.21	0.403		-22.6	-7.61	14.2
9	42.0	3.39	0.235		-22.4	-2.67	11.0
10	42.2	3.42	0.400		-22.1	-5.95	14.1
11	43.0	3.09	0.342		-22.5	-10.1	12.7
12	42.6	3.40	0.462		-22.6	-6.76	13.5
Pearson's <i>r</i> correlation statistics with distance to poultry farm							
	0.23	-0.61*	-0.48		0.40	-0.46	0.60*

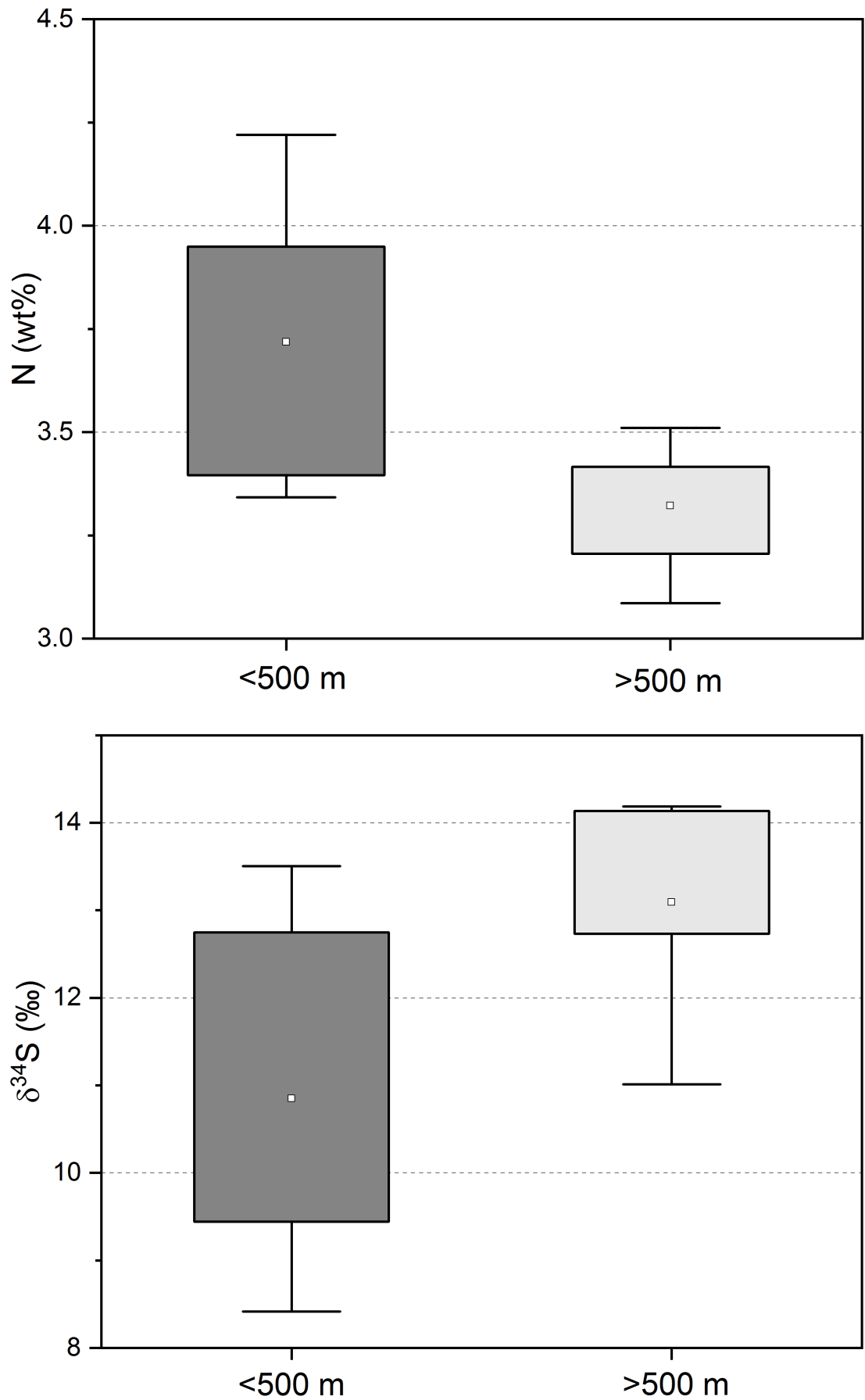


Figure 4-7: Comparison of nitrogen (wt%) [above] and $\delta^{34}\text{S}$ (‰) [below] in rural *X. parietina* samples, with distance to poultry farm (<500 m and >500 m)



Figure 4-8: (a) Nitrogen contents (wt%) and (b) $\delta^{15}\text{N}$ (‰) values recorded in *X. parietina*, sampled around a poultry farm (in Shrewsbury, UK); displayed with sampling area and poultry farm location

4.3.4 Spatial variability of carbon, nitrogen and sulphur contents (wt%) in lichens (*X. parietina* and *Physcia* spp.) sampled across the City of Manchester

Lichen samples across the City of Manchester were analysed for their carbon, nitrogen (by CN analyser) and sulphur contents (by IRMS) to investigate variability of atmospheric CNS compounds in the City of Manchester, and to evaluate potential species-specific differences. CNS contents (wt%) descriptive statistics are displayed in Table 4-9.

Carbon contents in *X. parietina* (N=94) were less variable, compared to *Physcia* spp. (Figure 4-9a and d). Nitrogen contents in *Physcia* spp. were marginally higher, when compared to *X. parietina* (Figure 4-9b and e). In contrast, sulphur contents were found more variable in *X. parietina*, compared to *Physcia* spp. (Figure 4-9c and f). Due to non-normality of carbon contents, Mann-Whitney test was used to compare C wt% in *X. parietina* and *Physcia* spp. In contrast, unpaired t-test was used for N and S contents (normal distribution of data; Table 4-9). Carbon and sulphur contents were significantly ($p < 0.01$) different between *X. parietina* and *Physcia* spp.

Table 4-9: Descriptive statistics of lichen (*X. parietina* and *Physcia* spp.) carbon, nitrogen and sulphur contents (wt%; shown as three significant figures); displayed with mean (N and S wt%) and median value (C wt%). Statistical comparison of CNS contents is also shown (unpaired t-test for N and S contents, Mann-Whitney for C contents, due to normal distribution of N and S and non-normal distribution of C contents), **significance at the level $p < 0.01$ in bold and shaded in green

	<i>X. parietina</i> (N=94)	<i>Physcia</i> spp. (N =86)
Carbon (C wt%)	36.07 – 41.56% $\tilde{x} = 40.29\%$	11.73 – 50.14% $\tilde{x} = 42.48$
Nitrogen (N wt%)	1.01 – 3.77% $\bar{x} = 2.75 \pm 0.479\%$	0.804 – 4.19% $\bar{x} = 2.79 \pm 0.631\%$
Sulphur (N wt%)	0.272 – 0.727% $\bar{x} = 0.474 \pm 0.0894$	0.0508 – 0.492% $\bar{x} = 0.321 \pm 0.0778$
Statistical comparison (unpaired t-test: N and S contents; Mann-Whitney: C contents)		
Carbon (C wt%)	<0.01**	
Nitrogen (N wt%)	0.63	
Sulphur (N wt%)	<0.01**	

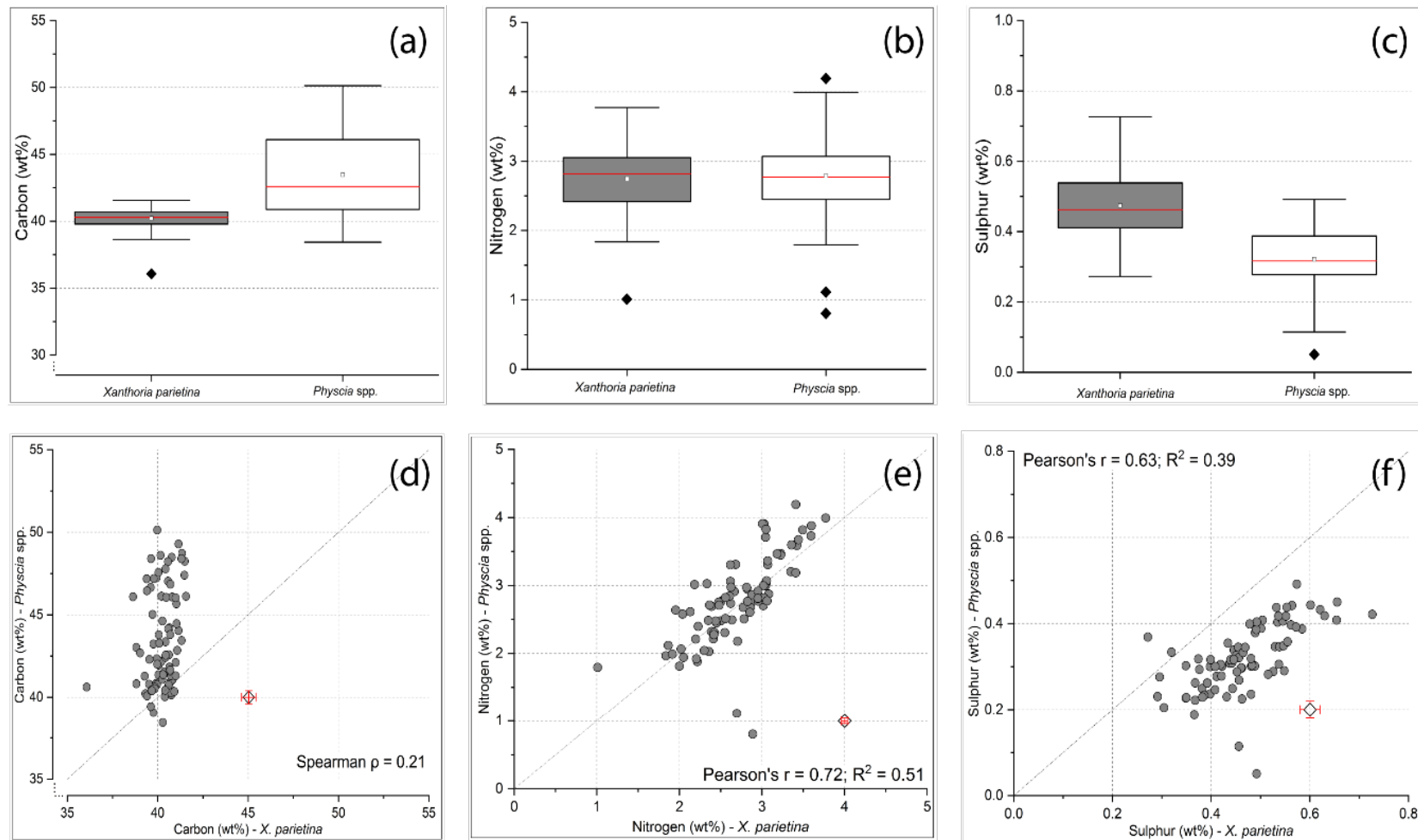


Figure 4-9: Comparison of urban *X. parietina* and *Physcia* spp. samples for (a) carbon, (b) nitrogen and (c) sulphur contents, presented as Box-Whisker plots (with mean value: white square, median line and extreme values: black diamond) and scatter-plots for (d) carbon, (e) nitrogen and (f) sulphur contents to illustrate species-specific differences (with correlation statistics; error bars are presented on dummy value C wt%: ± 0.55 ; N wt%: ± 0.04 and S wt%: ± 0.02 ; two significant outliers (identified by Grubbs test, $p < 0.05$) in (d) *Physcia* spp. at 11.73 wt% and 18.37 wt% not shown)

Carbon contents were found spatially variable across the research area (Figure 4-10a) with C wt% primarily >38 wt%. In contrast, majority of sites sampled for *Physcia* spp. showed C contents >40.0 wt%. Two sites showed C contents below 40 wt% (38.43 wt% and 39.43 wt%) and two were found <20 wt% (18.37 wt% and 11.73 wt%); Figure 4-10b). The latter could be related to 'dying-off' of the lichens (i.e. destruction of carbon skeleton) which was not (yet) visible during sampling/preparation.

Lichen nitrogen contents for both species (*X. parietina* and *Physcia* spp.) vary across Manchester, with highest N wt% (>3.50 wt%) in the city centre area and north and east of the city centre (Figure 4-11a). Elevated N contents were also recorded across the whole research area, illustrating spatial variability of N contents in *X. parietina*. A similar pattern was found for *Physcia* spp. (Figure 4-11b), with elevated (>3.0 wt%) across the whole research area. Comparable to nitrogen contents (in both lichen species), sulphur contents were found spatially variable across the city centre of Manchester (Figure 4-12a and b). Ordinary kriging (OK) maps of CNS contents and stable-isotope ratio signatures in *X. parietina* and *Physcia* spp. can be found in the Appendix B-4 (together with kriging error maps).

Lichen nitrogen and sulphur contents showed spatial variability (in both lichen species) across Manchester, while carbon contents were less variable in *X. parietina*, compared to *Physcia* spp., suggesting species-specific differences for C compounds. Sulphur contents were recorded higher in *X. parietina*, additionally suggesting species-specific differences. However, elevated N and S contents in both lichens could indicate site-specific sources, which will be discussed later (section 4.4.3) and further investigated including urban influencing factors in Manchester. Stable-isotope-ratio signatures of lichens might aid to identify specific sources in the urban environment, which are presented hereafter.

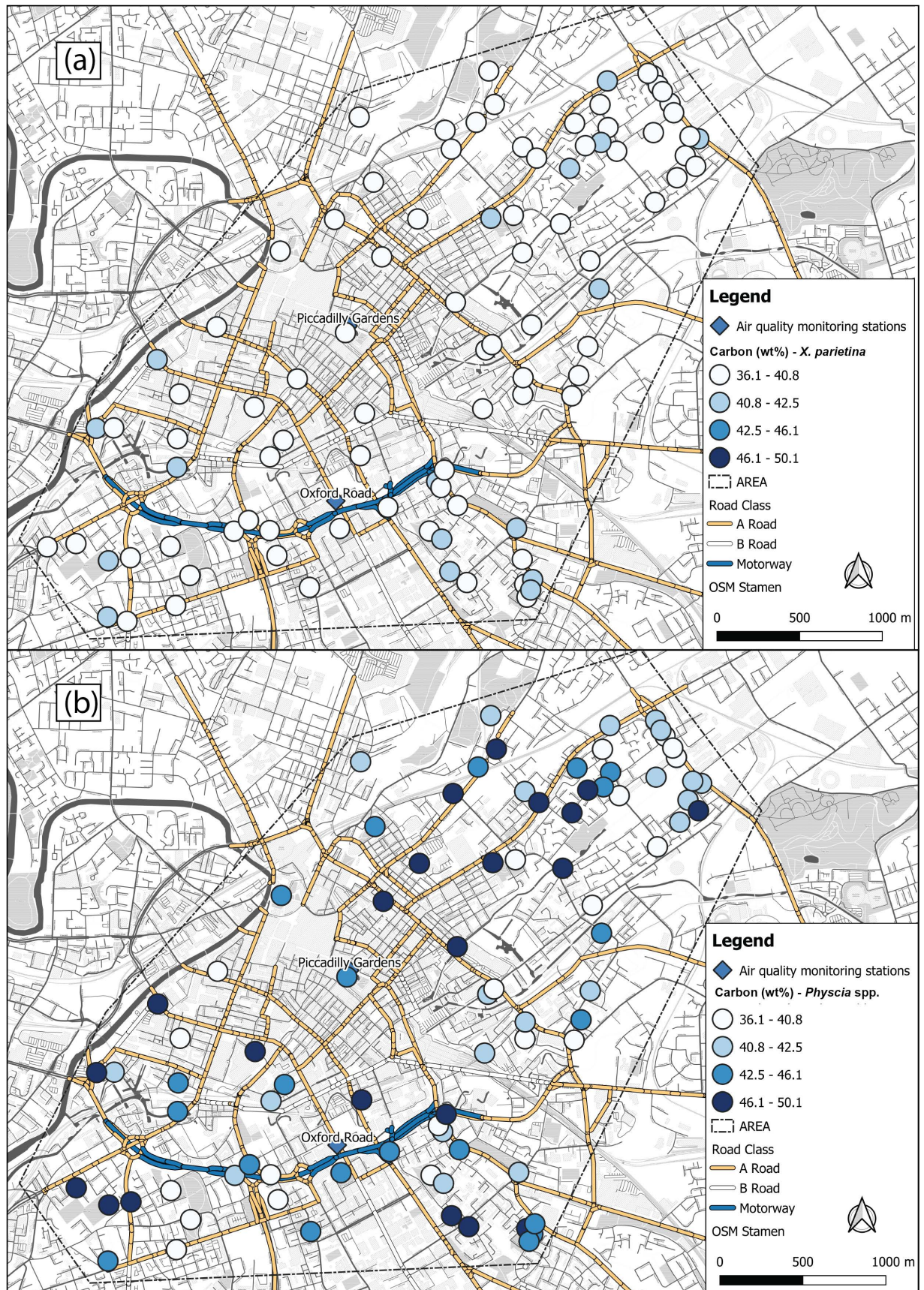


Figure 4-10: Carbon contents (C wt%) in (a) *X. parietina* and (b) *Physcia* spp. (colour-coded, low to high) across the City of Manchester; displayed with automated air quality monitoring stations

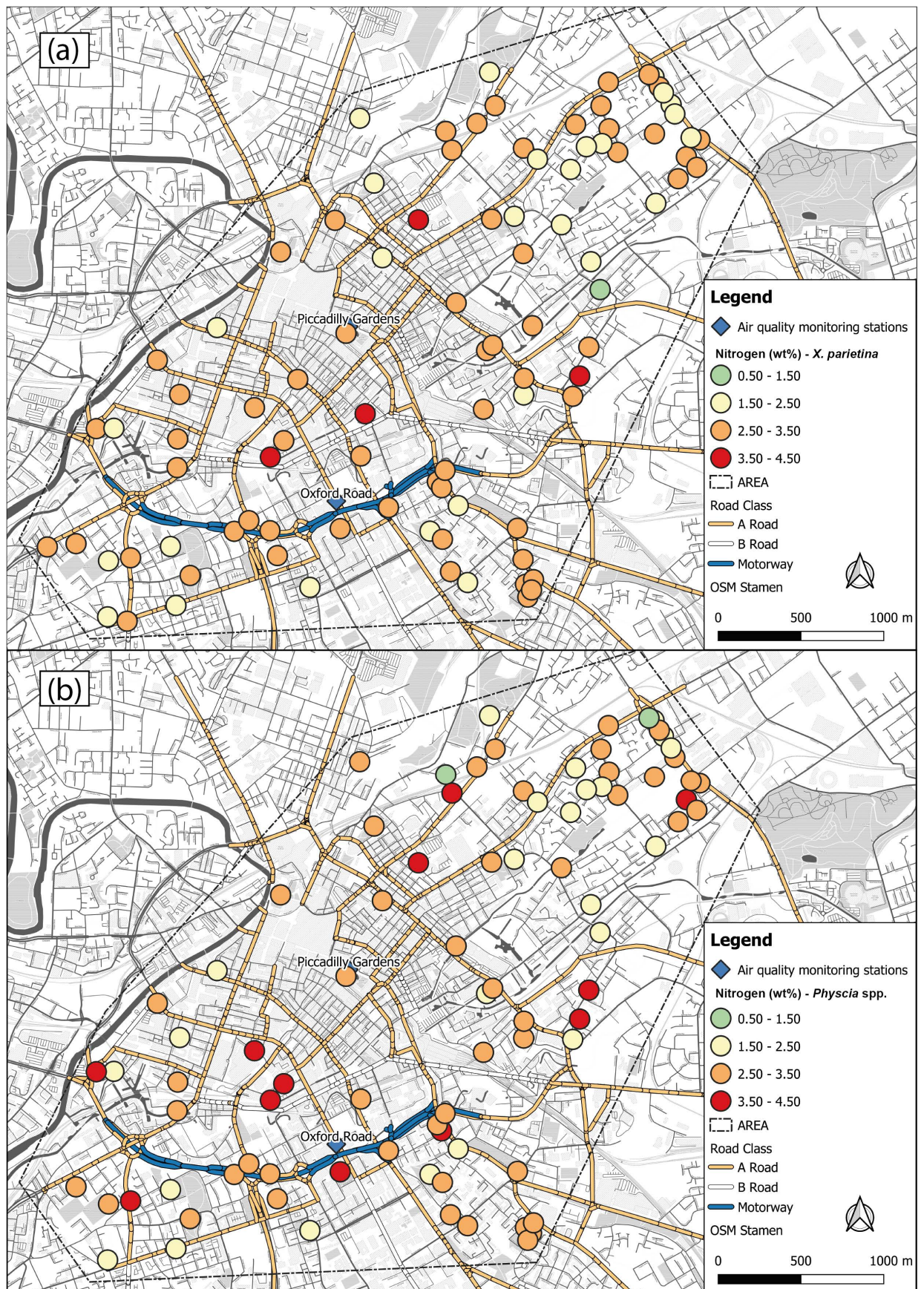


Figure 4-11: Nitrogen contents (N wt%) in (a) *X. parietina* and (b) *Physcia* spp. (colour-coded, low to high) across the City of Manchester; displayed with automated air quality monitoring stations

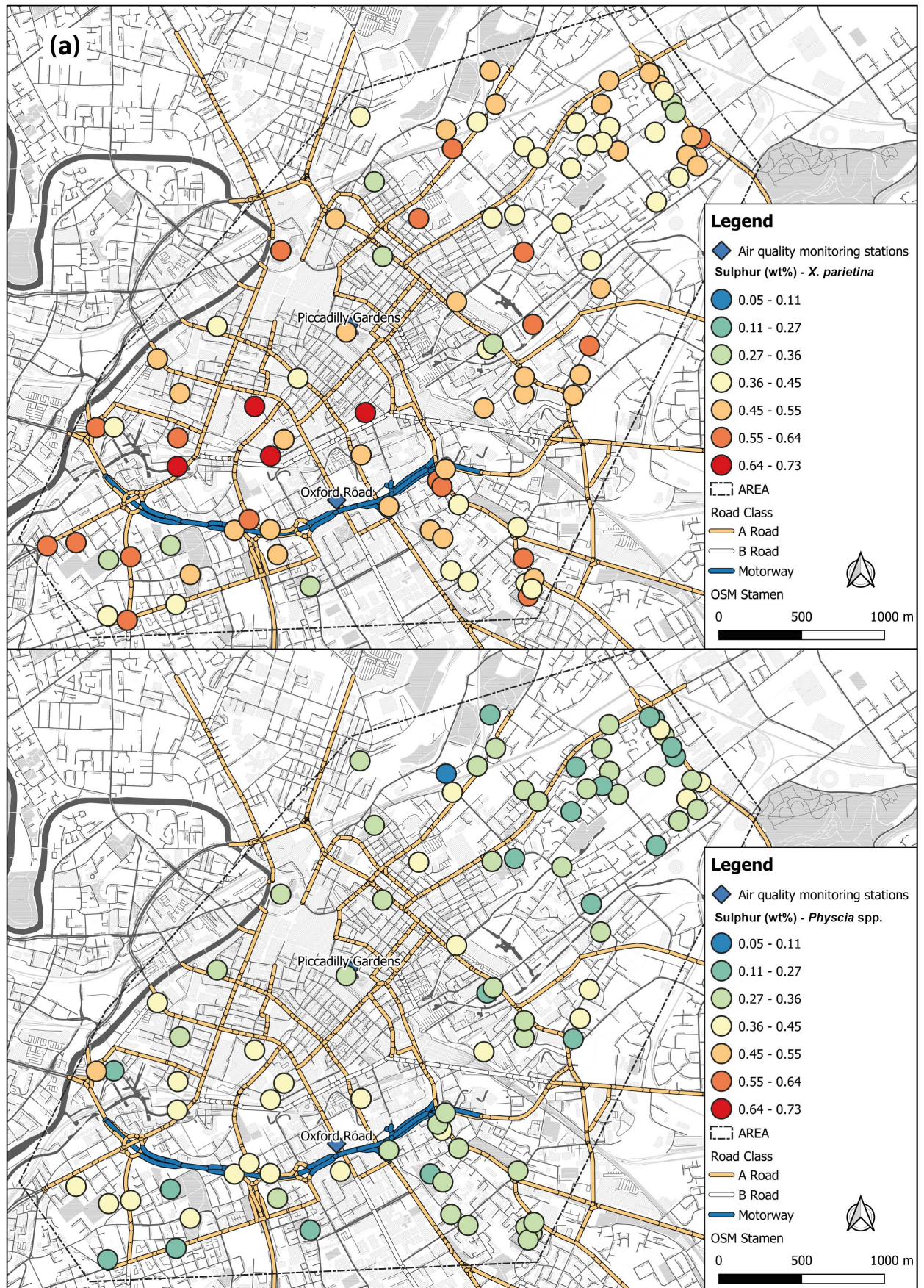


Figure 4-12: Sulphur contents (S wt%) in (a) *X. parietina* and (b) *Physcia* spp. (colour-coded, low to high) across the City of Manchester; displayed with automated air quality monitoring stations

4.3.5 Spatial variability of stable-isotope ratio signatures ($\delta^{13}\text{C}$, $\delta^{15}\text{N}$ and $\delta^{34}\text{S}$) in lichens (*X. parietina* and *Physcia* spp.) sampled across the City of Manchester

Variability of stable-isotope ratios in lichens could be used to identify and 'fingerprint' particular sources within the urban environment of Manchester. Moreover, species-specific differences, also presented for CNS compounds, could indicate the applicability of lichen species *X. parietina* and *Physcia* spp. for air quality related biomonitoring studies.

$\delta^{13}\text{C}$, $\delta^{15}\text{N}$ and $\delta^{34}\text{S}$ values recorded in both lichen species are displayed in Table 4-10. To compare lichen species stable-isotope ratio signatures, an unpaired t-test was used for $\delta^{15}\text{N}$ (due to normal distribution of data in both lichens); $\delta^{13}\text{C}$ and $\delta^{34}\text{S}$ were compared using Mann-Whitney tests (non-normal distribution; Table 4-10). Statistical significant differences (at the level $p < 0.01$) between *X. parietina* and *Physcia* spp. were found for $\delta^{13}\text{C}$ and $\delta^{15}\text{N}$ values. Figure 4-13 illustrates the comparison of both lichen species for their stable-isotope ratio signatures as box-whisker and scatter-plots.

Table 4-10: Descriptive statistics of analysed lichen (*X. parietina*, N=94 and *Physcia* spp., N=86) stable-isotope-ratios ($\delta^{13}\text{C}$, $\delta^{15}\text{N}$ and $\delta^{34}\text{S}$, in ‰) sampled in the urban environment of Manchester (displayed with mean concentrations [$\pm 1 \times$ standard deviation] for normally distributed data and median concentrations for non-normal distributed data); statistical comparison between lichen species (using unpaired t-test for $\delta^{15}\text{N}$ and Mann-Whitney for $\delta^{13}\text{C}$ and $\delta^{34}\text{S}$) is also shown (significant at the level $p < 0.01$ shown in bold and shaded in green)

	$\delta^{13}\text{C}$	$\delta^{15}\text{N}$	$\delta^{34}\text{S}$
<i>X. parietina</i> (N=94)	-26.67 - -22.44‰ $\bar{x} = -24.70 \pm 0.78\%$	-13.62 - -1.58‰ $\bar{x} = -7.42 \pm 2.13\%$	1.34 – 10.56‰ $\tilde{x} = 7.97\%$
<i>Physcia</i> spp. (N=86)	-27.59 - -23.55‰ $\tilde{x} = -25.10\%$	-14.2 – -2.03‰ $\bar{x} = -8.25 \pm 2.05\%$	1.48 – 9.55 $\tilde{x} = 7.85\%$
Statistical comparison (unpaired t-test: $\delta^{15}\text{N}$; Mann-Whitney: $\delta^{13}\text{C}$ and $\delta^{34}\text{S}$ contents contents)			
	$p < 0.01^{**}$	$p < 0.01^{**}$	$p > 0.05$

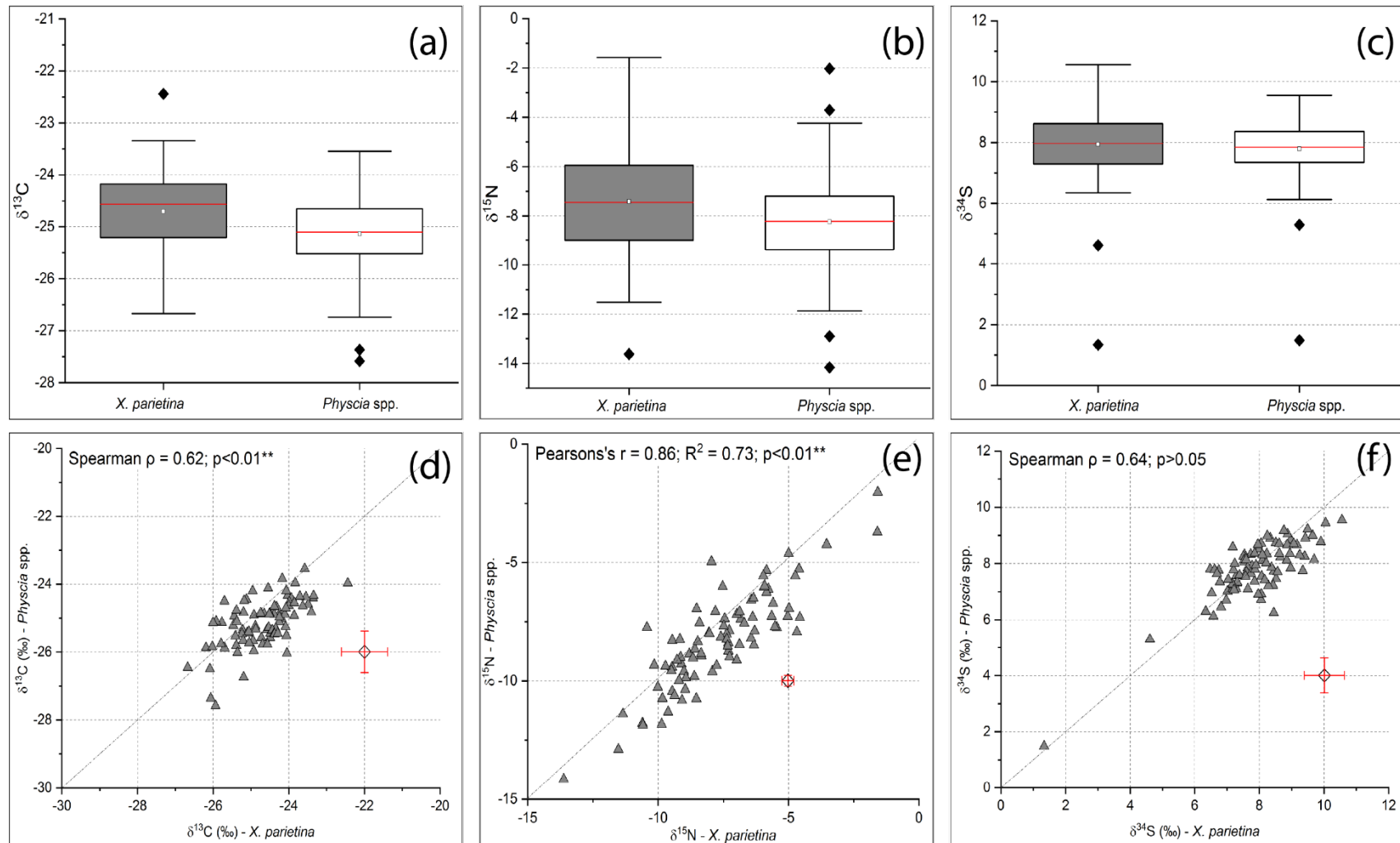


Figure 4-13: Comparison of urban *X. parietina* and *Physcia* spp. samples for (a) $\delta^{13}\text{C}$, (b) $\delta^{15}\text{N}$ and (c) $\delta^{34}\text{S}$, presented as Box-Whisker plots (with mean value: white square, median line and extreme values: black diamond) and scatter-plots for (d) $\delta^{13}\text{C}$, (e) $\delta^{15}\text{N}$ and (f) $\delta^{34}\text{S}$ to illustrate species-specific differences (with correlation statistics; error bars are presented on dummy value $\delta^{13}\text{C}$: $\pm 0.61\text{‰}$; $\delta^{15}\text{N}$: $\pm 0.23\text{‰}$ and $\delta^{34}\text{S}$: $\pm 0.62\text{‰}$)

Spatial variability of $\delta^{13}\text{C}$ and $\delta^{34}\text{S}$ values was comparable in both lichen species, even though significantly different for $\delta^{13}\text{C}$ (Figure 4-14 and Figure 4-15). In contrast, ^{15}N values were marginally enriched in *X. parietina*. Less depleted $\delta^{15}\text{N}$ (in both lichen species) was recorded within and around the city centre. Least depleted $\delta^{15}\text{N}$ values was recorded at two sites close to the motorway ('Mancunian Way'; Figure 4-16) in both lichen species.

Figure 4-17 illustrates the relationships (by correlation statistics, using Pearson's r and Spearman ρ) between CNS contents (wt%) and stable-isotope-ratios in *X. parietina* and *Physcia* spp. Carbon contents in *X. parietina* were not related to $\delta^{13}\text{C}$ values, while a significant ($p < 0.05$) negative relationship was found for *Physcia* spp. In contrast, increasing N wt% were highly significant ($p < 0.01$) correlated with an enrichment in ^{15}N in both lichen species. Increasing sulphur contents in lichens were significantly accompanied by decreasing $\delta^{34}\text{S}$ values in *X. parietina* ($p < 0.01$) and *Physcia* spp. ($p < 0.05$).

Stable-isotope ratio signatures vary between lichen species ($\delta^{13}\text{C}$ and $\delta^{15}\text{N}$) and displayed spatial variability across Manchester, in particular for $\delta^{15}\text{N}$. Therefore, influences of nitrogen compounds in the urban environment are suggested to influence lichen nitrogen isotope signatures. Potential influences on lichen N contents, as well as $\delta^{15}\text{N}$ could be relate to atmospheric NO_2 concentrations. NO_x diffusion tubes were deployed across Manchester and measurements in relation to lichen-derived data is presented in section 4.3.7. The following section will compare rural lichen samples with urban counterparts.

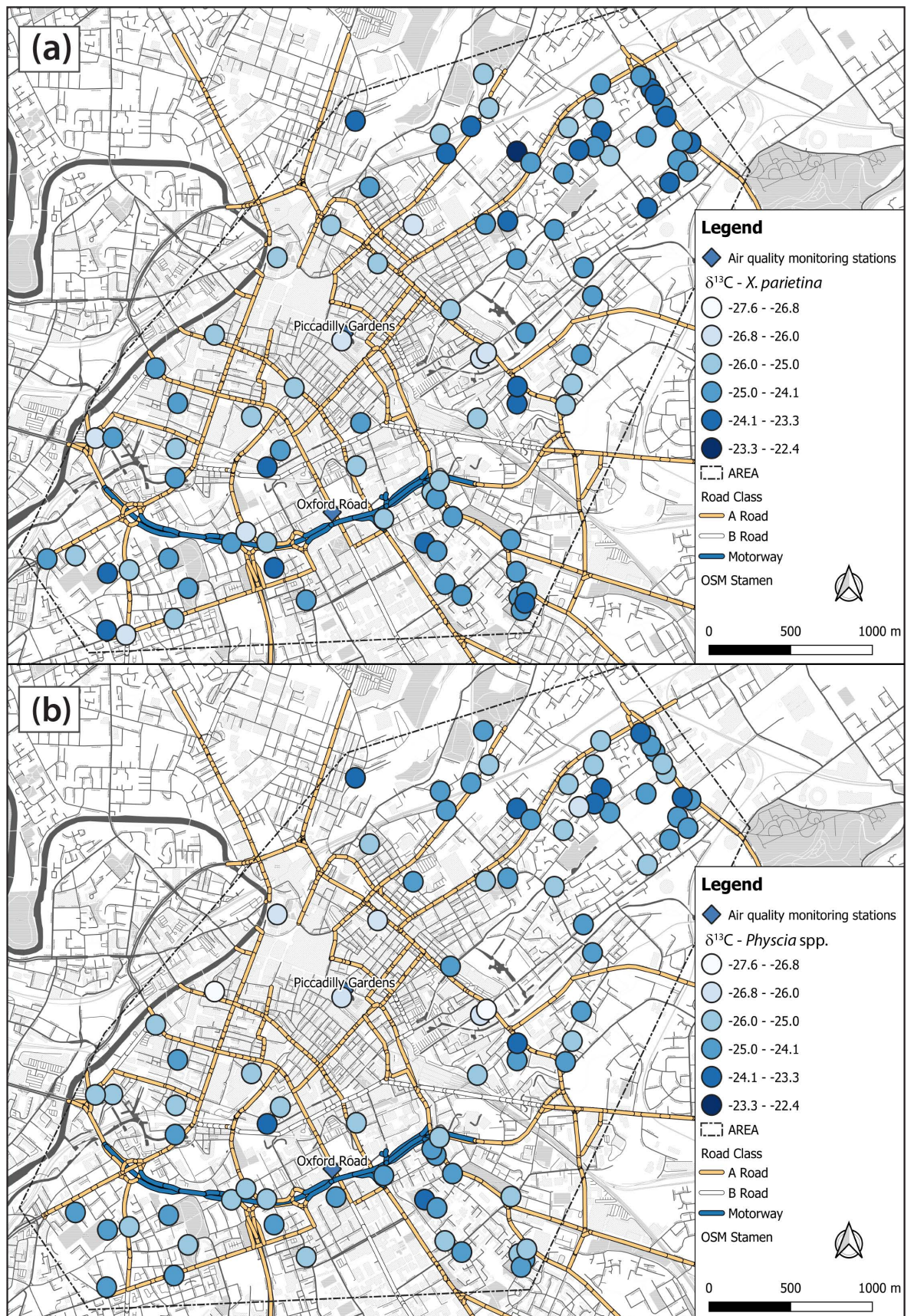


Figure 4-14: $\delta^{13}\text{C}$ values of (a) *X. parietina* and (b) *Physcia* spp. (colour-coded, low to high) across the City of Manchester; displayed with automated air quality monitoring stations



Figure 4-15: $\delta^{34}\text{S}$ values of (a) *X. parietina* and (b) *Physcia* spp. (colour-coded, low to high) across the City of Manchester; displayed with automated air quality monitoring stations

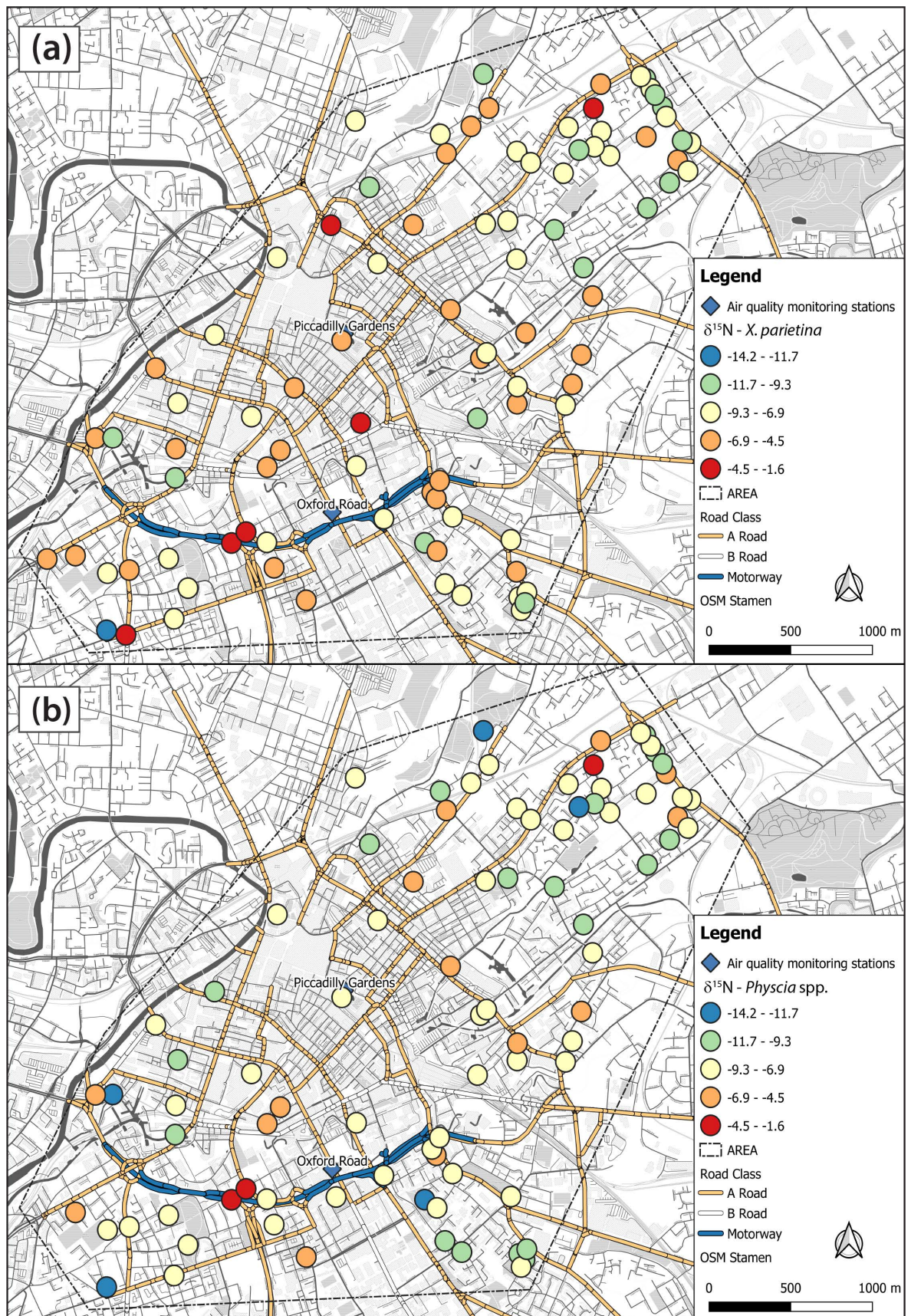


Figure 4-16: $\delta^{15}\text{N}$ values of (a) *X. parietina* and (b) *Physcia* spp. (colour-coded, low to high) across the City of Manchester; displayed with automated air quality monitoring stations

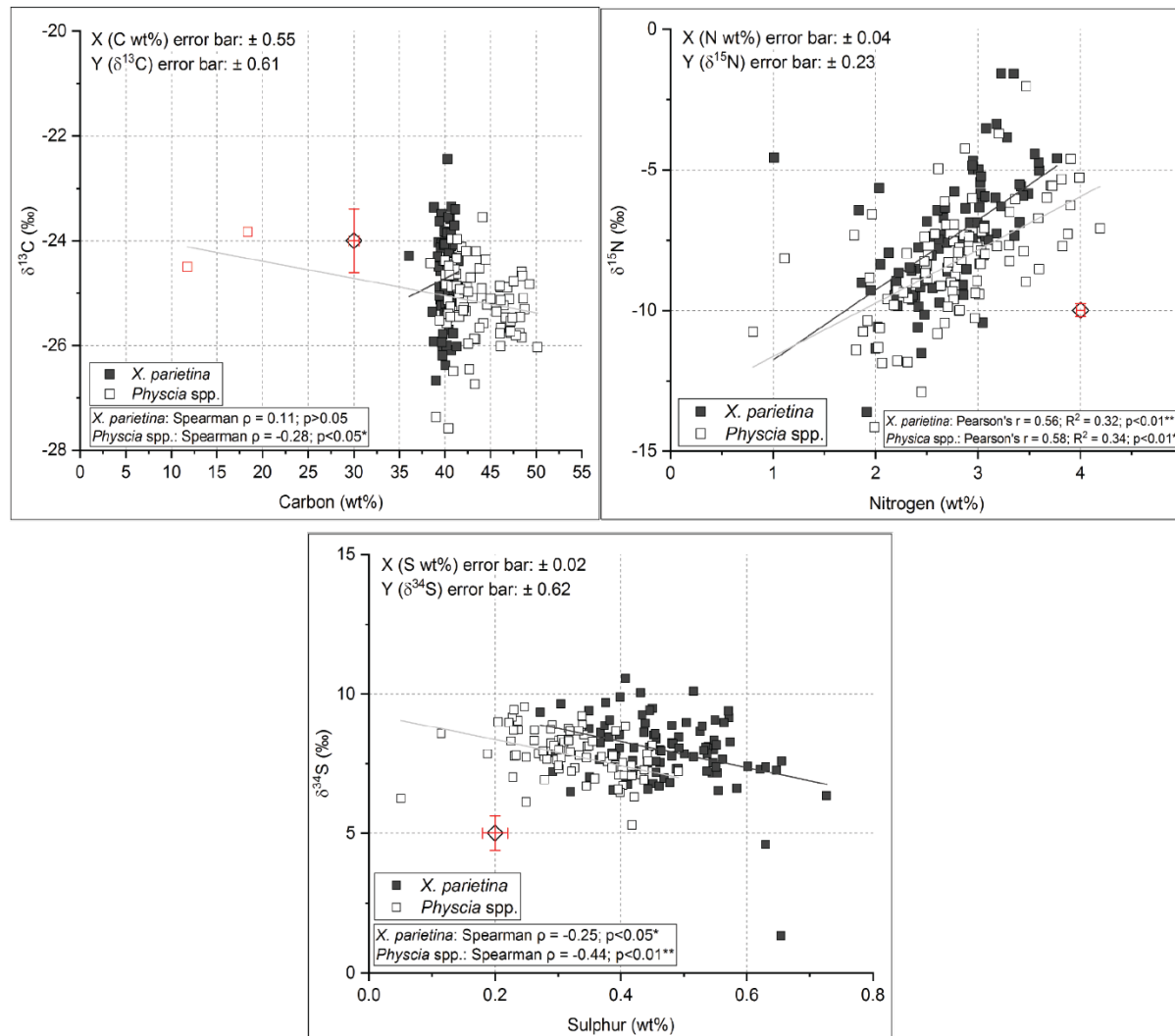


Figure 4-17: Scatter-plots of lichen CNS contents and stable isotope signatures ($\delta^{13}\text{C}$, $\delta^{15}\text{N}$ and $\delta^{34}\text{S}$) with correlation coefficients (Pearson's r and Spearman ρ); lichen CRM (No. 482) derived error bars are presented as \pm one standard deviation (on dummy value); lines (dark grey: *X. parietina*, light grey *Physcia* spp.) represent correlation slopes; red squared (in upper left panel) represent outliers for *Physcia* spp. (Cwt%)

4.3.6 Comparison of rural and urban *X. parietina* samples

Lichen samples (*X. parietina*) from two contrasting environments were analysed (for CNS contents and their stable-isotope-ratio signatures) to evaluate potential differences (and/or similarities) in urban and rural environments.

Comparison of analysed CNS (wt%) and stable-isotope-ratio (‰) are displayed in Table 4-11. Recorded carbon and nitrogen contents in rural *X. parietina* samples were higher and less variable compared to urban *X. parietina*. Stable-isotope-ratio signatures in rural lichen samples were enriched in ^{13}C and ^{15}N and less depleted in ^{34}S . On the contrary, sulphur contents were found higher and more variable in urban samples.

To investigate differences between both environment, Mann-Whitney (non-parametric; C wt% and $\delta^{34}\text{S}$) and unpaired t-test (N wt% and S wt%; $\delta^{13}\text{C}$ and $\delta^{15}\text{N}$) were used. Highly statistical significant ($p < 0.01$) differences were found for carbon and nitrogen contents, as well as stable-isotope-ratio signatures ($\delta^{13}\text{C}$, $\delta^{15}\text{N}$ and $\delta^{34}\text{S}$; Table 4-11). Sulphur contents recorded in *X. parietina* were significantly different ($p < 0.05$) in the urban and rural environment (Table 4-11). Figure 4-18 illustrates recorded CNS contents and stable-isotope-ratio signatures in urban and rural *X. parietina* samples (displayed as box-whisker plots).

Significant differences between rural and urban *X. parietina* samples for analysed CNS contents and stable-isotope ratio signatures indicate specific influences in both environments. Potential source apportionment for contrasting environments is discussed later (section 4.5.2)

Table 4-11: CNS contents (wt%) and stable-isotope-ratio signatures ($\delta^{13}\text{C}$, $\delta^{15}\text{N}$ and $\delta^{34}\text{S}$) ranges of urban and rural lichen samples; displayed with statistical test (Mann-Whitney [MW] and unpaired t-test) to evaluate differences between urban and rural lichens (displayed as p-value; *significant at the level $p < 0.05$: yellow and **significant at the level $p < 0.01$: green)

	C (wt%)	N (wt%)	S (wt%)	$\delta^{13}\text{C}$ (‰)	$\delta^{15}\text{N}$ (‰)	$\delta^{34}\text{S}$ (‰)
Urban (N=94)	36.07 – 41.56	1.01 – 3.77	0.272 – 0.727	-26.67 to - 22.4	-13.62 to -1.58	1.34 – 10.56
Rural (N=12)	41.39 – 43.30	3.09 – 4.22	0.235 – 0.521	-23.42 to - 22.0	-10.09 to 4.44	8.42 – 14.19
Statistical tests for comparison of urban and rural X. parietina samples (p-value)						
	MW (two-tailed)	Unpaired t-test (two-tailed)		Unpaired t-test (two-tailed)		MW (two-tailed)
urban vs rural	<0.01	<0.01	<0.05	<0.01	<0.01	<0.01

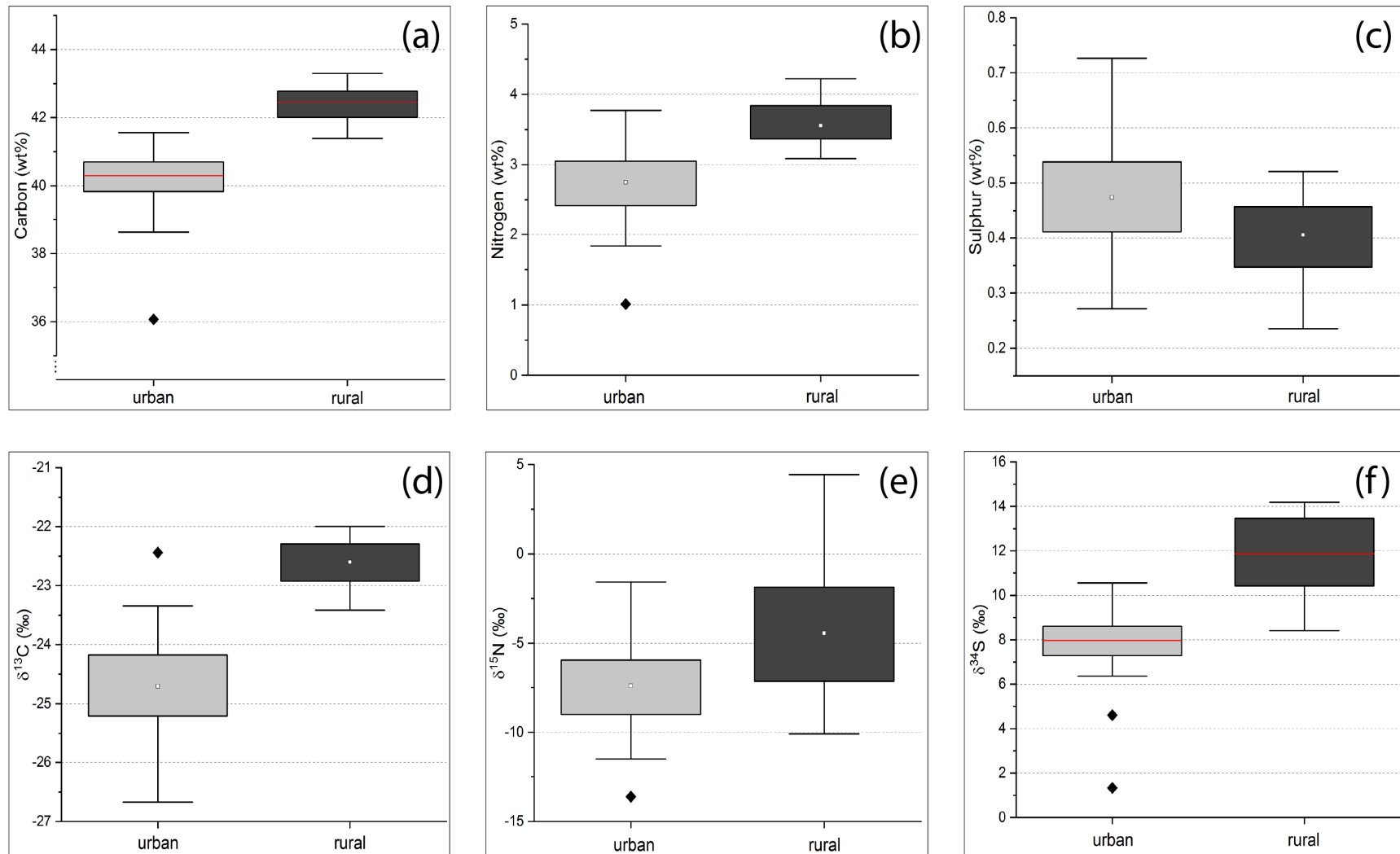


Figure 4-18: Box-Whisker plots (25th to 75th percentile; displayed with mean: white square for normally distributed data, median line for non-normally distributed data; extreme values: black diamond) for (a) carbon, (b) nitrogen, (c) sulphur contents (in wt%) and (d) $\delta^{13}\text{C}$, (e) $\delta^{15}\text{N}$ and (f) $\delta^{34}\text{S}$ values (in ‰) in urban (left) and rural (right) *X. parietina* samples

4.3.7 Urban NO_x diffusion tube measurements in relation to analysed lichen CNS contents (wt%) and stable-isotope-ratio-signatures ($\delta^{13}\text{C}$, $\delta^{15}\text{N}$ and $\delta^{34}\text{S}$)

NO_x diffusion tubes were deployed at 45 sites in and around the city centre of Manchester (Figure 4-3), at sites that have been sampled and analysed for CNS contents and stable isotope ratios ($\delta^{15}\text{N}$, $\delta^{13}\text{C}$ and $\delta^{34}\text{S}$). Diffusion tubes were used to ground-truth lichen dataset and assess a spatio-temporal variability of NO₂. Site-specific NO₂ and CNS (wt%) and δ -values are displayed in the Appendix B-2. Mean NO₂ concentrations of the yearlong deployment period range from 23 $\mu\text{g}/\text{m}^3$ to 50 $\mu\text{g}/\text{m}^3$ at all sites. For detailed description of analysis and discussion of NO₂ concentrations see Chapter 3.

To investigate potential influences on lichen CNS contents and $\delta^{15}\text{N}$, $\delta^{13}\text{C}$ and $\delta^{34}\text{S}$ by recorded NO₂ concentrations across Manchester, correlation statistics were used, i.e. Pearson's r (parametric test) and Spearman ρ (non-parametric test). Results are displayed in Table 4-12. Recorded NO₂ concentrations were specifically related to lichen N contents and $\delta^{15}\text{N}$ values (Figure 4-19a and b), to potentially identify NO₂ sources. NO₂ concentrations were significantly positive correlated with N wt% ($r= 0.34$; $p<0.05$) and $\delta^{15}\text{N}$ values ($r= 0.54$; $p<0.01$) in *X. parietina*. In *Physcia* spp., only $\delta^{15}\text{N}$ values were significantly correlated with NO₂ concentrations (Pearson's $r= 0.37$; $p<0.01$), while N wt% were not. In contrast, NO₂ concentrations might have additional influences on CNS contents and stable-isotope-ratios in lichens (Table 4-12), which will be further discussed later in this chapter (section 4.4.5).

Table 4-12: Correlation matrix of CNS contents, stable-isotope ratio signatures for *X. parietina* (N=94; left) and *Physcia* spp. (N=86; right) together with NO_x tube measurements (N=45; NO₂ mean - \bar{x}). Highly significant (p<0.01) relationships are presented in green and bold, significant relationships (p<0.05) are presented in bold and yellow. Spearman ρ correlation coefficients are presented as underlined values, all other represent Pearson's r correlation coefficients

<i>X. parietina</i> and <i>Physcia</i> spp. together with NO _x tube measurements (N=45)							
	<i>Physcia</i> spp.	C (wt%)	S (wt%)	$\delta^{15}\text{N}$	$\delta^{13}\text{C}$	$\delta^{34}\text{S}$	NO ₂ (\bar{x})
<i>X. parietina</i>	N (wt%)	0.54**	0.92**	0.59**	-0.21	-0.24*	0.21
C (wt%)	-0.08	C (wt%)	0.59**	0.086	<u>-0.28*</u>	<u>-0.04</u>	<u>0.04</u>
S (wt%)	0.70**	-0.06	S (wt%)	0.51**	-0.19	<u>-0.44**</u>	0.28
$\delta^{15}\text{N}$	0.56**	-0.10	0.51**	$\delta^{15}\text{N}$	-0.10	<u>-0.21</u>	0.37**
$\delta^{13}\text{C}$	-0.23*	0.11	-0.156	-0.32*	$\delta^{13}\text{C}$	<u>0.21</u>	<u>-0.40*</u>
$\delta^{34}\text{S}$	-0.27*	<u>0.19</u>	<u>-0.25*</u>	<u>0.37</u>	<u>0.17</u>	$\delta^{34}\text{S}$	<u>-0.57**</u>
NO ₂ (\bar{x})	0.34*	<u>-0.32</u>	0.29	0.54**	-0.48*	<u>-0.47*</u>	

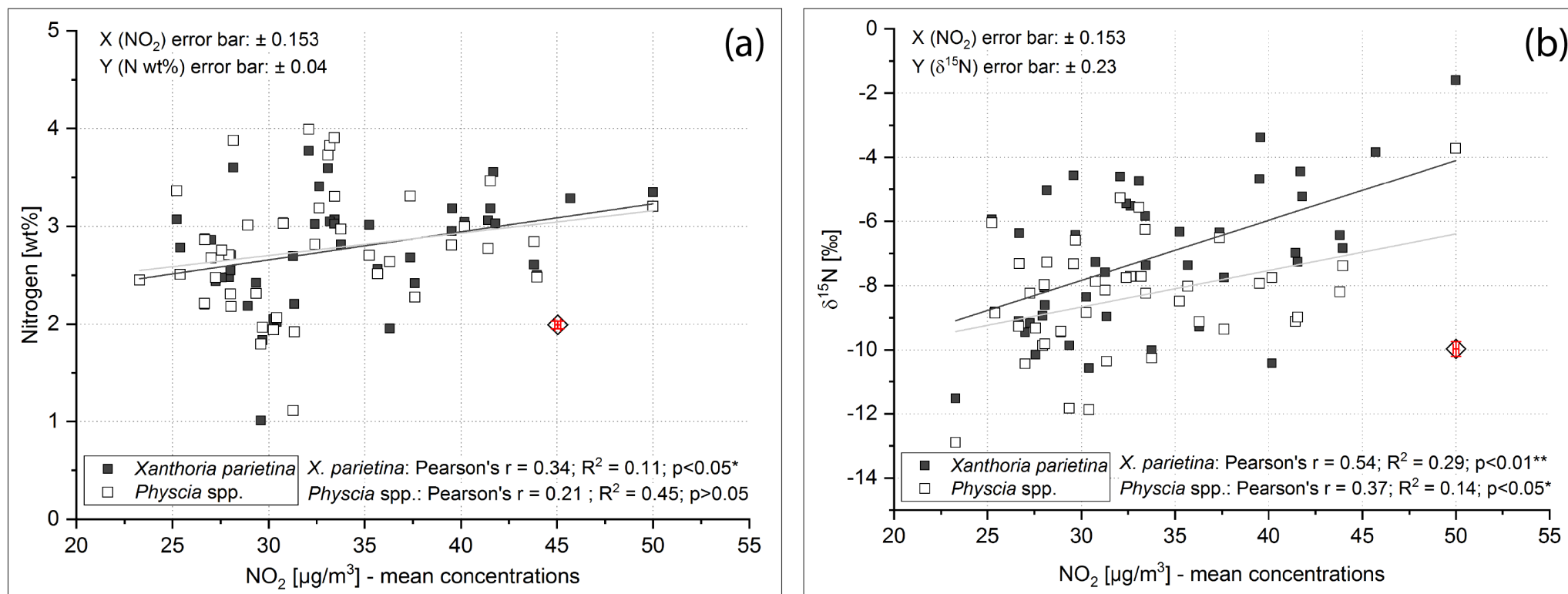


Figure 4-19: Scatter plots of NO_2 concentrations (NO_2 mean concentration in $\mu\text{g}/\text{m}^3$) and lichen (a) N wt%, and (b) $\delta^{15}\text{N}$ with correlation coefficients (Pearson's r , R^2 and significance level; **significant at the level $p < 0.05$, **significant at the level $p < 0.01$); error bars on dummy value derived from lichen CRM (No. 482; N contents and δ -values, displayed in figure) and IC-CRM (QC3198; nitrite concentrations); lines (dark grey: *X. parietina*, light grey: *Physcia* spp.)

4.3.8 Urban influences on spatial variability of CNS contents and stable-isotope-ratio signatures recorded in *X. parietina* and *Physcia* spp. in Manchester (UK)

The urban environment of Manchester has been described in chapter 2, including building height and road structures (and traffic counts) that potentially affect pollutant dispersion. Recorded CNS contents and stable-isotope ratio signatures were related to urban influencing factors (Table 4-13), to evaluate spatial variability and dispersion of CNS compounds in the City of Manchester. Grouping of data was described in section 4.2.5 and will be discussed later (section 4.4.6). Correlation statistics (Pearson's r and Spearman ρ) of urban influencing factors, with lichen CNS contents and stable-isotope ratio signatures are displayed in Table 4-13. Highly significant ($p < 0.01$) relationships were recorded between urban influences, i.e. distances to major roads, road class and $\delta^{15}\text{N}$ values, while nitrogen and sulphur contents in *X. parietina* seemed to be influenced by surrounding building heights at the sampling location (which are displayed Figure 4-20). In contrast, traffic counts primarily appeared to impact N and S contents and $\delta^{15}\text{N}$ and $\delta^{34}\text{S}$ values in *Physcia* spp. whereas distance to major road appeared to influence $\delta^{15}\text{N}$ and $\delta^{34}\text{S}$ values.

Table 4-13: Correlation statistics (Pearson's r and Spearman ρ) used to investigate relationships between urban influencing factors and lichen-derived CNS contents (wt%) and stable-isotope-ratio signatures ($\delta^{13}\text{C}$, $\delta^{15}\text{N}$ and $\delta^{34}\text{S}$); underlined values represent Spearman ρ , all other values are presented as Pearson's r , significant values are presented in bold (significance level is indicated by asterisk and coloured; *significant at the level $p < 0.05$: yellow and **significant at the level $p < 0.01$: green); MR = distance to major road, RdCl = road class, TC = traffic counts, BH = surrounding building height, PS = distance to large point source and GS = distance to greenspace

	MR	RdCl	TC	BH	PS	GS
<i>X. parietina</i>						
Carbon	<u>0.11</u>	<u>-0.02</u>	<u>-0.12</u>	<u>-0.17</u>	<u>-0.08</u>	<u>-0.07</u>
Nitrogen	-0.17	-0.15	0.07	0.30**	-0.19	0.17
Sulphur	-0.13	-0.11	0.11	0.30**	-0.18	0.12
$\delta^{13}\text{C}$	0.21*	0.22*	-0.07	-0.20	0.01	-0.21*
$\delta^{15}\text{N}$	-0.28**	-0.28**	0.22*	0.25*	-0.18	0.20
$\delta^{34}\text{S}$	<u>0.15</u>	<u>-0.06</u>	<u>-0.14</u>	-0.22*	0.24*	<u>-0.08</u>
<i>Physcia</i> spp.						
Carbon	<u>-0.03</u>	<u><-0.005</u>	<u>-0.11</u>	<u>-0.02</u>	<u>0.002</u>	<u><-0.002</u>
Nitrogen	-0.14	-0.05	0.24*	0.15	-0.12	0.16
Sulphur	-0.19	-0.06	0.25*	0.16	-0.15	0.16
$\delta^{13}\text{C}$	<u>0.20</u>	<u>0.11</u>	<u>-0.13</u>	<u>-0.08</u>	<u>0.02</u>	<u>-0.15</u>
$\delta^{15}\text{N}$	-0.26*	-0.17	0.26*	0.09	-0.11	0.27*
$\delta^{34}\text{S}$	0.22*	<u>-0.04</u>	-0.29*	<u>-0.21</u>	<u>0.18</u>	<u>-0.10</u>

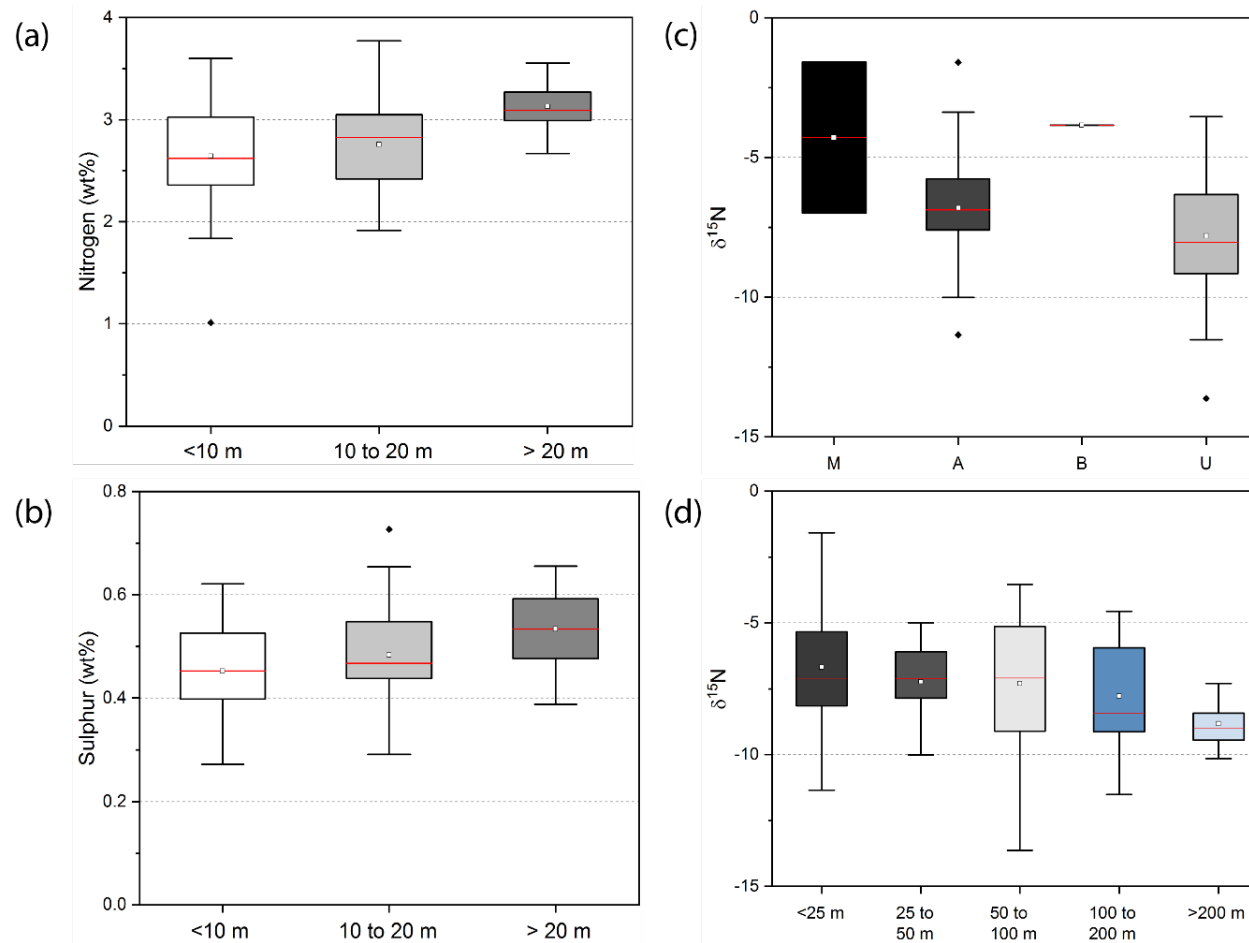


Figure 4-20: Box-Whisker plots (25th to 75th percentile, displayed with mean: white square, median line and extreme values: black diamond) of urban influencing factors and (a) nitrogen contents (wt%) with surrounding building heights, (b) sulphur contents (wt%) with surrounding building heights, (c) $\delta^{15}\text{N}$ values (‰) with road class (M = motorway, A = A-road, B = B-road and U = unclassified) and (d) $\delta^{15}\text{N}$ values (‰) with distance to major road (including motorway, A- and B-roads) recorded in *X. parietina* (see Table 4-12)

GWR was used to model spatial distribution of lichen-derived pollutant loadings and study local difference in response to input variables (i.e. urban influences). Nitrogen contents (wt%) and $\delta^{15}\text{N}$ values were of particular interest, due to previously described high spatial variability and potential influences (Table 4-13). Figure 4-21 illustrates modelled distribution of N wt% and $\delta^{15}\text{N}$ in *X. parietina* (GWR modelled *Physcia* spp. N wt% and $\delta^{15}\text{N}$ can be found in Appendix B-6).

Elevated N contents (wt%) are found within the city centre and the north-east of the research area (Figure 4-21a). Enrichments in ^{15}N in lichens is found along the motorway ('Mancunian Way') (Figure 4-21b) and at locations within the north and north-east of the city centre (at comparable locations that are elevated in N wt%). In contrast, locations around the city centre showed lower N contents and depleted $\delta^{15}\text{N}$ in *X. parietina*.

Modelling outcomes were able to explain 16% (for N wt%) and 34% (for $\delta^{15}\text{N}$) of variability, based on urban factors, suggesting additional influences (i.e. microclimatic conditions) on distribution and dispersion of lichen N contents and $\delta^{15}\text{N}$ values. Higher modelling outcomes for $\delta^{15}\text{N}$ values could indicate that urban factors (used in this study) are able to better explain spatial variability recorded in lichens, with regard to specific influences, i.e. distance to major road (including road class; Table 4-13 and Figure 4-20), compared to nitrogen (wt%).

Site-specific influences on lichen nitrogen and sulphur contents, as well as stable-isotope ratio signatures, in particular $\delta^{15}\text{N}$ and $\delta^{34}\text{S}$ are suggested by findings presented. Especially, *X. parietina* seemed to reflect site-specific influences, with regard to road class, traffic counts, distance to a particular road and surrounding building heights. Spatial distribution and dispersion of pollutants recorded in *X. parietina* therefore illustrate areas of increased pollutant loadings across Manchester, which are not continuously measured by air quality monitoring stations.

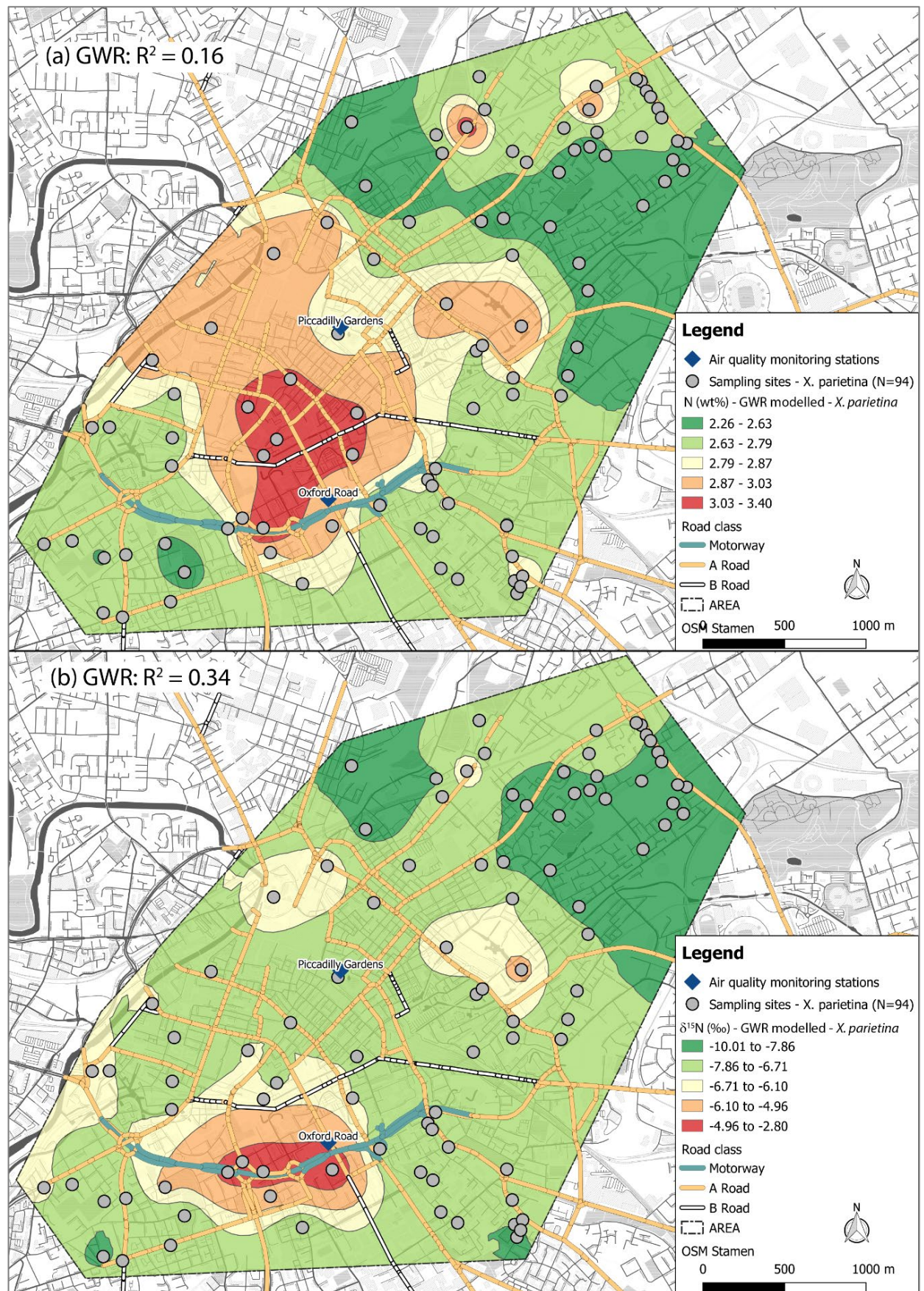


Figure 4-21: Geographically Weighed Regression (GWR) used to model urban influencing factors (as described in Table 4-10) of (a) N wt% and (b) $\delta^{15}\text{N}$ (‰) recorded in *X. parietina* (less negative $\delta^{15}\text{N}$ values indicate potential NO_x influences)

4.4 Interpretation and Discussion

4.4.1 Temporal variability of carbon, nitrogen and sulphur contents (wt%) in urban *X. parietina* samples

Lichen sampling in the urban environment and around the poultry farm were undertaken during different times of the year and a longer period of time (for urban samples, June 2016 to October 2017).

This factor needs to be taken into account when interpreting and comparing both contrasting environments and spatial data in the urban environment. Urban lichen samples have been re-sampled (in 2018) to assess temporal variability of CNS contents that might be superimposed on spatial variability. Results showed a significant increase in carbon contents in *X. parietina* between the two sampling periods. In contrast, nitrogen and sulphur contents did not show a significant increase. Uptake and release of elements in lichens are reversible processes, influenced by thallus morphology, lichen age, physiological status, pH, duration of exposure, microclimatic conditions and concentrations and types of pollutants present in the environment (Bargagli, 1998; Paoli, Vannini, Fačkovcová, et al., 2018). Here, presumably young lichen species (off twigs and small branches) were sampled and were considered to reflect recent atmospheric pollution.

Lichens produce genus-specific sugar alcohols (photosynthetic products) that are used by the mycobiont, who makes up the bulk of the lichen thalli (Brown, 1996). Increased carbon contents could therefore be related to fungal metabolism, induced by (high) availability of nutrients (i.e. nitrogen and sulphur). However, additional investigation of lichen chlorophyll contents, amino acids and secondary products could further provide insights into increases in carbon contents (due to increased photosynthetic activity; Gaio-Oliveira et al., 2005; Hauck, 2010) and explain temporal variability. Microclimatic conditions as well as bark pH and CO₂ concentrations across Manchester could be investigated to further evaluate influences on lichen carbon contents.

For this study, non-significant differences in nitrogen contents indicate high N-loads in the urban environment of Manchester and potential 'equilibrium' state of *X. parietina* with its surrounding environment (Paoli, Vannini, Fačkovcová, et al., 2018). Lichen sulphur concentrations were also found similar for both sampling periods. Non-significant changes in urban lichen samples could therefore indicate low influences of sulphur compounds in Manchester. Due to their slow growth,

lichens can be used as long-term biomonitors for air pollution, i.e. summarizers of environmental conditions (Loppi and De Dominicis, 1996; Loppi et al., 2004). Therefore, temporal variability (of N and S contents) was considered not to affect spatial variability of both, N and S contents in lichens.

Lichen biomonitoring is often used to integrate instrumental data on atmospheric pollution and developing forecasts in connection to human health impacts (Nimis et al., 1990; Cislighi and Nimis, 1997; Giordani et al., 2002, 2018; Pinho et al., 2004; Giordani, 2007). Potential differences between contrasting environments, i.e. rural and urban, could identify particular sources within each environment. A comparison of CNS contents (wt%) and stable-isotope ratios is discussed hereafter.

4.4.2 Comparison of rural and urban lichen samples and the applicability of rural *X. parietina* as 'control samples'

Rural *X. parietina* samples were analysed for CNS contents and stable-isotope ratios to evaluate differences between the contrasting environments. Moreover, potential emissions from the surrounding agricultural area and the poultry farm were considered to influence lichen (*X. parietina*) CNS and stable-isotope ratio signatures. C and N contents were higher in rural lichen samples, while S contents were lower, compared to urban lichen samples, suggesting additional influences (by C and N compounds) on rural *X. parietina*.

Several factors influence C contents in lichens, i.e. light and water ability, CO₂ release from bark and soil (Vingiani et al., 2004; Beck and Mayr, 2012; Máguas et al., 2013). Moreover, elevated atmospheric N compound concentrations (and thus increased N wt% in rural *X. parietina*) could be related to increased biomass and net gain from CO₂ (Dahlman et al., 2002; Johansson et al., 2010). However, carbon contents were reported to vary within (and between species), depending on CO and CO₂ concentrations in air and potential CO₂ uptake from the lichen substrate (i.e. bark; Vingiani et al., 2004; Beck and Mayr, 2012; Máguas et al., 2013). Additional measurements, i.e. CO₂ concentrations and release of carbon compounds from bark (and in particulates, i.e. from soil) need to be further investigated in both environments. Therefore, carbon contents were considered not to be a useful tool to compare contrasting environments.

Nitrogen contents recorded in rural *X. parietina* samples were higher compared to urban *X. parietina*. Pinho et al. (2017) reported elevated N wt% in lichens (*Parmotrema hypoleucinum*) in intensive agricultural areas of Portugal, which has also been reported for lichens in Germany (Franzen-Reuter, 2004; Boltersdorf and Werner, 2013) and around livestock farming areas (Ruoss, 1999; Gaio-Oliveira et al., 2001; Frati et al., 2007). Higher N contents in lichens sampled close to the poultry farm suggest N emissions from the poultry farm, e.g. from poultry manure and fertilizers (Nahm, 2005; AQEG, 2018). Studies reported that an increase in nitrogen levels showed increasing chlorophyll contents and increasing photosynthetic capacity in *Xanthoria parietina* and *X. aureola* (Palmqvist et al., 1998; Gaio-Oliveira, Dahlman, Palmqvist and Máguas, 2005; Nybakken et al., 2009; Hauck, 2010). Therefore, elevated N wt% in rural lichens could be related to increased photosynthetic activity, due to high availability of N compounds and potentially less influences by shade (on photosynthesis; Larsen Vilsholm et al., 2009; Gauslaa, 2014) from its surrounding environment (i.e. tree canopies and buildings, such as in urban environments). In return, this could explain higher carbon contents in rural lichens (i.e. increased photosynthetic activity; Dahlman et al., 2003; Johansson et al., 2010).

Measuring NO_x concentrations around the poultry farm could be used to evaluate potential influences on lichen N wt%. However, nitrogen contents in rural and urban *X. parietina* samples allowed comparison between the two environments, with regard to its specific surrounding.

Sulphur is an essential lichen nutrient (Wadleigh, 2003), which could explain comparable sulphur contents in rural and urban environments. Sulphur enters the atmosphere from a number of different sources, natural (e.g. sea spray and biogenic sources) and anthropogenic (combustion of sulphur containing fuels, e.g. coal and oil) and SO₂ can be widely distributed (Pinho et al., 2008; Dämmgen et al., 2011). Within the UK, SO₂ emissions from agriculture only accounted for small amount (11.70 kt in 2016) compared to other anthropogenic sources, i.e. combustion for energy production (66.82 kt in 2016), manufacturing (38.70 kt in 2016), residential and commercial combustion (45.73 kt in 2016) and transport (16.21 kt in 2016; NAEI, 2018). However, urban *X. parietina* S wt% ranges were higher compared to rural samples, suggesting additional sources, i.e. from combustion SO₂, which will be further discussed (section 4.4.3).

Stable-isotopes ratio signatures ($\delta^{13}\text{C}$, $\delta^{15}\text{N}$ and $\delta^{34}\text{S}$) in rural *X. parietina* were highly significant ($p < 0.01$) different from urban samples. Moreover, rural lichens were enriched in ^{13}C , ^{15}N and ^{34}S , when compared to urban counterparts. Rural *X. parietina* $\delta^{13}\text{C}$ is potentially related to uptake and assimilation, metabolism and biochemical processes (i.e. biosynthesis and isotopic fractioning; Batts et al., 2004; Hoefs, 2009; Biazrov, 2012). As reported by Lee et al. (2009) lichens of the same species can vary considerably in $\delta^{13}\text{C}$ signatures. Additionally, meteorological influences (i.e. rainfall) could be related to ^{13}C enrichments (Krouse and Herbert, 1996; Batts et al., 2004). Potential influencing factors were not considered for this study and are not discussed in detail. Therefore, $\delta^{13}\text{C}$ in lichens was considered not to be a useful tool to evaluate anthropogenic (and/ or agricultural) influences.

$\delta^{15}\text{N}$ values are reported to be less negative (i.e. are more ^{15}N enriched) where NO_x concentration is high (urban areas) and more negative in rural areas, the latter primarily due to a greater contribution of reduced nitrogen from agricultural sources (Pearson et al., 2000; Sutton et al., 2004; Boltersdorf et al., 2014). Interestingly, $\delta^{15}\text{N}$ values in rural lichens were more positive, compared to urban samples, especially close to the poultry farm (Figure 4-8). Thus, rural lichen samples indicate NO_x influences rather than expected NH_x influences (i.e. from the poultry farm). Within the UK, nitrogen in agriculture is primarily applied as ammonium nitrate (NH_4NO_3) (AQEG, 2018). Moreover, main contributors to secondary aerosols are NO_3^- , SO_4^{2-} and NH_4^+ , with NO_3^- being the dominant species (NH_4^+ only comprises between a few to 20%; AQEG, 2012, 2018; Twigg et al., 2015), with potential influences on lichen $\delta^{15}\text{N}$. Here, it was unknown which fertilizers were applied in the surrounding agricultural area. Poultry farm emissions might also be isotopically different, compared to pig stock farms as reported by Liu et al. (2016). For instance, poultry NO_2 $\delta^{15}\text{N}$ was reported at -8.5‰ (Felix and Elliott, 2014) that could explain less depleted $\delta^{15}\text{N}$ in rural lichen samples.

However, no clear distinction in $\delta^{15}\text{N}$ values between the diverse environments was found. Interestingly N contents and $\delta^{15}\text{N}$ in rural *X. parietina* were higher and less depleted, respectively, when compared to urban samples. Passive sampling methods could be used to improve isotopic composition of nitrogen compounds in the rural environment and influences on lichen $\delta^{15}\text{N}$ values.

In contrast, $\delta^{34}\text{S}$ in urban samples were less positive, compared to rural samples, with $\delta^{34}\text{S} < 10\text{‰}$ suggesting anthropogenic (i.e. combustion sources; Wadleigh 2003) as primary source in Manchester. Different from urban *X. parietina* samples, $\delta^{34}\text{S}$ did not decrease with increasing S wt% in rural samples, suggesting a mixture of sulphur compound influences in the rural environment (i.e. from distant sources and sulphur-containing particulates). However, $\delta^{34}\text{S}$ (as well as S wt%) in rural samples might reflect the 'background/natural' SO_2 in the environment, not particularly affected by anthropogenic sources.

Sampled sites around a poultry farm might not represent the 'best' sites for comparison with an urban environment, regarding lichen CNS contents. Stable nitrogen isotope-ratios ($\delta^{15}\text{N}$) interestingly showed NO_x influences on rural lichens, which were expected to be potentially highly influenced by NH_x compounds.

A clear differentiation between an urban and rural environment was therefore not possible, when using $\delta^{15}\text{N}$. In contrast, stable sulphur isotopic signatures ($\delta^{34}\text{S}$) suggested additional anthropogenic sulphur emissions in the urban environment of Manchester. Findings suggest that more remote lichen samples (i.e. not influenced by agricultural emissions) should be used for comparison of $\delta^{15}\text{N}$ values and fingerprint potential sources. Further investigating isotope-ratio signatures, i.e. in lichens with increasing distance to agricultural areas and of atmospheric sources, around the poultry farm could improve the source identification of nitrogen compounds within the rural environment.

4.4.3 Comparison of carbon, nitrogen and sulphur contents (wt%) in lichens (*X. parietina* and *Physcia* spp.) with other urban studies and the relation to air quality in the City of Manchester

Atmospheric measurements of pollutant concentrations is undertaken by two automated monitoring stations across Manchester. Continuous measurements provide temporal variability of pollutant concentrations, but do not provide spatial variability of C, N and S compounds across the city of Manchester. Carbon, nitrogen and sulphur contents showed spatial variability across the city centre of Manchester. Nitrogen (N wt%) and sulphur (S wt%) contents showed higher variability compared to C contents.

Nitrogen contents tend to be higher in the city centre and along major roads leading into the city (see Figure 4-11), suggesting traffic-related influences and accumulation of N compounds in lichens. Especially nitrogen contents in lichens potentially reflect anthropogenic nitrogen loads in Manchester. Lichen sulphur contents do not show a distinct pattern across the research area, indicating site-specific influences and S compound accumulation. Table 4-14 displays lichen-derived carbon, nitrogen and/or sulphur contents recorded in lichens from an urban (or anthropogenic influenced) environment.

Table 4-14: Lichen studies which report carbon, nitrogen and/or sulphur contents (wt%) in urban (and anthropogenic influenced) environments, in comparison CNS contents recorded in *X. parietina* and *Physcia* spp. examined in Manchester (UK); N/A indicates not analysed C, N and/or S contents (wt%) in the particular study

Author(s)	Location	Lichen species	C wt%	N wt%	S wt%
This study	Manchester (UK)	<i>X. parietina</i>	36.07 – 41.56	1.01 – 3.77	0.271 – 0.727
This study	Manchester (UK)	<i>Physcia</i> spp.	38.43 – 50.14	0.805 – 4.19	0.051 – 0.492
Pinho et al. (2017)	Alentejo Litoral region (Portugal)	<i>Parmotrema hypoleucinum</i>	N/A	0.87 – 1.46	N/A
Boltersdorf and Werner (2014)	West Germany (urban, industrial and agricultural areas)	<i>X. parietina</i> <i>Physcia</i> spp.	N/A	0.98 – 4.28	N/A
Bermejo-Orduna et al. (2014)	Sierraville (USA)	<i>Letharia vulpina</i>	N/A	0.76 – 2.0	N/A
Beck and Mayr, (2012)	South Germany	<i>X. parietina</i>	N/A	1.2 – 3.8	N/A
(Gaio-Oliveira, Dahlman, Palmqvist and Máguas, 2005)	Cities and country-sides (Portugal)	<i>X. parietina</i>	N/A	1.1 – 4.3	N/A
Vingiani et al. (2004) *active deployment*	Naples (Italy)	<i>Pseudevernia furfuracea</i>	35.08 -41.85 (10 weeks) 35.71 – 41.77 (17 weeks)	9.83 – 16.20 (10 weeks) 7.87 – 12.47 (17 weeks)	2.03 – 6.72 (10 weeks) 1.05 – 5.20 (17 weeks)
(Franzen-Reuter, 2004)	Urbanised and agricultural areas (Germany)	<i>X. parietina</i>	N/A	2.06 - 3.61	N/A
Gombert et al. (2003)	Grenoble (France)	<i>Hypogymnia physodes</i> <i>Ph. adscendens</i>	N/A	1.21 – 3.75 1.75 – 4.21	N/A
(Wadleigh, 2003)	Newfoundland (Canada)	<i>Alectoria sarmentosa</i>	N/A	N/A	<0.04 – 0.11
Carreras and Pignata (2002)	Cordoba (Argentina)	<i>Usnea amblyclada</i>	N/A	N/A	0.08 – 0.2
Wiseman and Wadleigh (2002) *active deployment*	Newfoundland (Canada)	<i>A. sarmentosa</i>	N/A	N/A	0.023 – 0.041
Wadleigh and Blake (1999)	Newfoundland (Canada)	<i>A. sarmentosa</i>	N/A	N/A	0.005 – 0.115
González et al. (1996)	Cordoba (Argentina)	<i>Ramalina ecklonii</i>	N/A	N/A	0.025 – 0.181
Tynnyrinen et al. (1992)	Central Finland	<i>H. physodes</i>	N/A	0.8 - 3.1	0.19 – 0.28
Addison and Puckett (1980)	Alberta (Canada)	<i>H. physodes</i> <i>Evernia mesomorpha</i>	N/A	N/A	– >0.25 0.15 - >0.3

Carbon contents in lichens, recorded in Manchester, were less variable in both lichen species, compared to N and S contents. Presented findings are in accordance with results presented by Vingiani et al. (2004) for *Pseudevernia furfuracea* actively deployed in Naples (Italy) urban area (\bar{x} = 43.78 wt% and 42.87 wt% after 10 and 17 weeks of deployment). In contrast, lichen carbon contents from King George Island (Antarctic), away from possible urban influences, ranged from 21.48 wt% and 47.11 wt% (\bar{x} = 39.92 \pm 5.71 wt%; Lee et al., 2009), illustrating minor influences on lichen carbon contents in urban environments.

Carbon variability in lichens could be related to respiratory uptake and release of CO₂ (from bark and soil), water and light availability and additional uptake of organic carbon from the substrate (Vingiani et al., 2004; Beck and Mayr, 2012; Máguas et al., 2013). Moreover, these factors also could be related to shifts in $\delta^{13}\text{C}$ values (Beck and Mayr, 2012), which will be discussed later.

Differences in both lichen species (and within species) could be related CO₂ fixation from different ecosystem components, i.e. soil, tree bark and leaves; Máguas et al., 2013). Elevated CO and CO₂ concentrations in air, as well as organic contaminants (i.e. particulates) have been reported to increase C contents in urban tree leaves (Mamane and Dzubay, 1988; Wong, 1990; Cipollini et al., 1993; Freer-Smith et al., 1997; Vingiani et al., 2004), which could have also affect lichen C wt%. In Manchester, 31% of CO₂ is emitted by road traffic (TfGM and GMCA, 2016), which could be related to increased C contents in lichens. Additionally, carbon contents of *Physcia* spp. in this study, have been found to be positively correlated ($p < 0.001$) with N and S contents (Table 4-12), indicating interrelationship of CNS contents for this particular lichen. Increased N loads (and thus increased biomass and net CO₂ gain; Dahlman et al., 2003; Johansson et al., 2010) might explain increased C contents in *Physcia* spp. and the positive relationship between C, N and S contents. Temporal variability was recorded in *X. parietina*, suggesting a potential bias of recorded C contents superimposed on the initial sampling period (in 2016/17). Species-specific differences in C wt% were also recorded, indicating that lichen C contents might not provide a beneficial tool to assess spatial variability of carbon in urban environments.

Nitrogen (wt%) recorded in *X. parietina* and *Physcia* spp. were found spatially variable across Manchester (Figure 4-11). In both lichen species N wt% were found higher along the major road network (i.e. A- and B-roads and motorways; Figure 4-11). Lichen N contents have been reported to be influenced by traffic in urban areas and at highly trafficked roads (e.g. motorways) (Gombert et al., 2003; Bermejo-Orduna et al., 2014). In contrast, Pinho et al. (2017) did not find such a relationship for *Parmotrema hypoleucinum* in urban areas of Portugal.

Within Manchester, 80% of NO_x emissions are related to vehicular emissions (Regan, 2018) and increased N contents for *X. parietina* and *Physcia* spp. are comparable to prior studies (Table 4-14), suggesting influences by vehicular emissions at sampling sites close to roads. However, spatial variability of nitrogen in lichens (*X. parietina* and *Physcia* spp.) suggest site-specific influences across Manchester (i.e. vehicular emissions and the close urban surrounding, such as building heights – ‘street canyon effect’), which are not recorded by urban monitoring stations.

N contents of *X. parietina* were positively correlated ($p < 0.001$) with S contents, but not with C contents (see Table 4-12). Nitrogen and sulphur in (urban) air consist of different compounds (i.e. nitrogen dioxide, ammonia and nitrous oxides for N and hydrogen sulphide and sulphates for S; Olivier et al., 1998; Vingiani et al., 2004) and positive correlation of N and S in lichens is presumably a consequence of nitrogen and sulphur compound deposition (wet and dry) and uptake by the lichen.

Lichen sulphur contents, in Manchester were found higher in *X. parietina* samples, compared to *Physcia* spp. Sulphur is also an essential nutrient in lichens (Wiseman and Wadleigh, 2002), and increased contents in *X. parietina* could be related to species-specific uptake abilities and sensitivity towards sulphur compounds. Studies, using lichen S contents (Table 4-14) reported increased contents with regard to traffic emissions in Cordoba, Argentina González et al., 1996; Carreras and Pignata, 2002) and point sources, i.e. industrial emissions in Canada; (Addison and Puckett, 1980; Wadleigh and Blake, 1999). Influences from sea spray (sea salt sulphate) have also been reported (Wadleigh and Blake, 1999; Wiseman and Wadleigh, 2002; Wadleigh, 2003). Lichen S contents (*X. parietina* and *Physcia* spp.) in Manchester were higher, compared to these studies, which is potentially related to different geographic regions and specific regional pollution sources, as well as sulphur contents of coal and fuel oil used.

Sulphur dioxide (SO₂) in the UK from vehicular sources (i.e. diesel cars) have decreased since 1990 (by 91%; NAEI, 2018). Coal and fuel oil use also decreased since 1990, representing 34% and 10% of total UK emissions in 2016 (NAEI, 2018g). In contrast, the use of petroleum coke (for energy production, industrial processes and residential fuel) has increased since 1990 (2016: 26% of SO₂ emissions; NAEI, 2018). Sources of SO₂ in Manchester are primarily related to industrial processes (Manchester City Council, 2018). Anthropogenic sources (i.e. combustion from energy and transformation industry) are potentially influencing lichen S contents across Manchester. Moreover, residential combustion could be related to elevated S in both lichen species. Investigating the S content of potential sulphur sources (e.g. petroleum coke) could further define potential sulphur influences on lichens.

In conclusion, nitrogen and sulphur contents, recorded in urban lichen species indicate potential anthropogenic sources (i.e. vehicular and industrial emissions) across Manchester. In contrast, carbon contents in lichens could not be related to sources and were potentially affected by temporal variability of C compounds. Increases in N contents are most likely to represent additional NO_x emissions from traffic, while S contents seemed to be influenced by industrial (and residential) combustion processes. Analysing additional lichen samples in more residential surroundings and within industrial areas could indicate 'land-use' specific variation in lichen N and S contents.

Both lichen species provide useful information on spatial distribution on nitrogen and sulphur across Manchester and indicated deteriorated air quality not analysed by automated monitoring stations. Therefore, potential health impacts along major roads (for nitrogen) and within residential areas (for sulphur) are potentially underestimated by automated measurements. However, lichen-derived carbon, nitrogen and sulphur contents may not be 'good' indicators for potential sources on their own. Therefore, lichen stable-isotope-ratio signatures ($\delta^{13}\text{C}$, $\delta^{15}\text{N}$ and $\delta^{34}\text{S}$) could provide additional information on influences on lichen CNS contents and could be used to 'fingerprint' potential sources in the City of Manchester.

4.4.4 Comparison of stable-isotope ratio signatures in lichens (*X. parietina* and *Physcia* spp.) with other urban studies and the relation to air quality in the City of Manchester

Lichen stable-isotope ratio signatures have not been analysed to the same extent as soil, groundwater, precipitation and mosses in pollution studies (Russell et al., 1998; Sutton et al., 2004; Widory, 2007). However, studies reported the use of $\delta^{13}\text{C}$, $\delta^{15}\text{N}$ and $\delta^{34}\text{S}$ in lichens, to characterise specific sources, which are presented in Table 4-15.

Green-algae lichens (i.e. *X. parietina* and *Physcia* spp.) follow the C_3 photosynthetic pathway and generally have $\delta^{13}\text{C}$ values of -28‰ (Batts et al., 2004; Fry, 2006; Hoefs, 2009), if the carbon source is ambient atmospheric CO_2 with an average $\delta^{13}\text{C}$ value of -8.0‰ (Fry, 2006). $\delta^{13}\text{C}$ values for both lichens species are slightly different from -28‰ indicating minor influences on carbon isotopic signatures. However, $\delta^{13}\text{C}$ values of lichens sampled across Manchester show comparable isotopic signatures, reported by urban pollution studies (Table 4-15).

Table 4-15: Lichen studies which reporting carbon, nitrogen and/or sulphur isotope-ratios in urban (and anthropogenic influenced) environments, in comparison to CNS stable-isotope-ratio signatures recorded in *X. parietina* and *Physcia* spp. examined in Manchester (UK)

Author(s)	Location	Lichen species	$\delta^{13}\text{C}$ (‰)	$\delta^{15}\text{N}$ (‰)	$\delta^{34}\text{S}$ (‰)
This study	Manchester (UK)	<i>X. parietina</i>	-26.67 to -22.4	-13.62 to -1.58	+1.34 to +10.56
This study	Manchester (UK)	<i>Physcia</i> spp.	-27.58 to -23.55	-14.16 to -2.03	+1.48 to +9.55
Pinho et al. (2017)	Alentejo Litoral region (Portugal)	<i>Parmotrema hypoleucinum</i>	N/A	-13.16 to -9.44	N/A
Boltersdorf and Werner (2014)	West Germany (urban, industrial and agricultural areas)	<i>X. parietina</i> <i>Physcia</i> spp.	N/A	-15.2 to -1.3	N/A
Bermejo-Orduna et al. (2014)	Sierraville (USA)	<i>Letharia vulpina</i>	-26.7 to -24.5	-12.5 to -0.6	N/A
Batts et al. (2004)	Sydney (Australia)	<i>Cladia aggregata</i>	-27.3 to -20.9	N/A	N/A
Wadleigh (2003)	Newfoundland (Canada)	<i>A. sarmentosa</i>	N/A	N/A	+3.7 to +16.6
Wiseman and Wadleigh (2002) *active deployment*	Newfoundland (Canada)	<i>A. sarmentosa</i>	N/A	N/A	+13.3 to +7.0
Teeri (1981)	Michigan (USA)	<i>Cladina rangiferina</i> <i>Cladonia</i> spp. <i>Stereocaulon tomentosum</i>	-24.6 to -21.8	N/A	N/A

Figure 4-22 illustrates $\delta^{13}\text{C}$ values of natural and anthropogenic carbon sources. Lichen $\delta^{13}\text{C}$ values span different pollutant $\delta^{13}\text{C}$ signatures (i.e. particulate matter, tailpipe exhausts and liquid fuels), indicating a complex mixture of potential carbon sources. Additionally, moisture and light are related to $^{13}\text{C}/^{12}\text{C}$ ratio in the lichens, as drivers of photosynthetic activity (Batts et al., 2004). Krouse and Herbert (1996) reported an increase in $\delta^{13}\text{C}$ in lichens (*Ramalina celastri* and *R. subfraxinea*) with increasing rainfall and indicated that an increase annual rainfall of 260 mm resulted in +1‰ $\delta^{13}\text{C}$ changes. Average annual rainfall of 860 mm (Met Office, 2015) in Manchester could potentially influence $\delta^{13}\text{C}$ values of *X. parietina* and *Physcia* spp. and explain slightly less negative $\delta^{13}\text{C}$ from -28‰. Both lichen species were significantly ($p < 0.01$) different in their C contents and $\delta^{13}\text{C}$ values, indicating species-specific differences in uptake of carbon (and resulting assimilation and synthesis of lichen compounds). Moreover, physiological and/or biochemical processes and water-use efficiency could be related to $\delta^{13}\text{C}$ differences in lichens (Batts et al., 1996, 2004; Galimov, 2000; Lee et al., 2009).

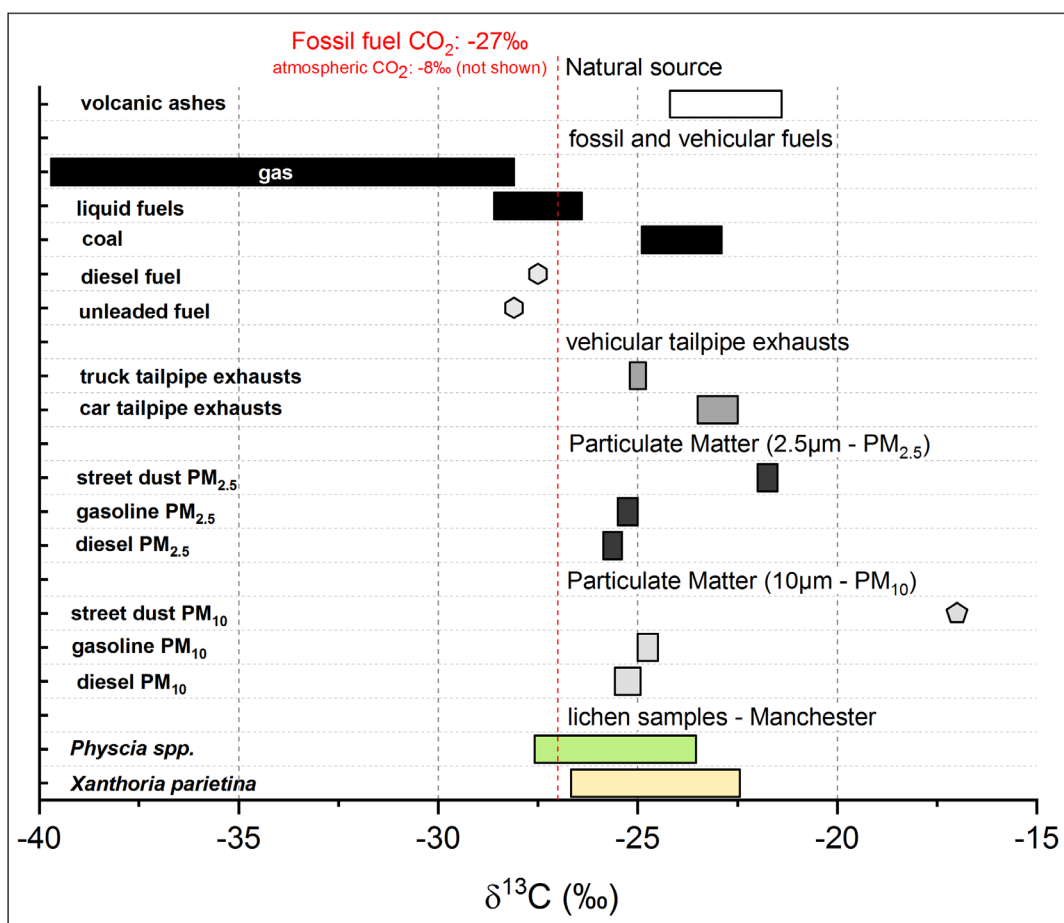


Figure 4-22: $\delta^{13}\text{C}$ values of atmospheric pollutants and pollution sources, reported in carbon isotope studies (Widory, 2006; López-Veneroni, 2009) to identify potential sources, displayed with analysed $\delta^{13}\text{C}$ values for lichen samples (*X. parietina* and *Physcia* spp.) in Manchester

No significant relationship between C content and $\delta^{13}\text{C}$ values of *X. parietina* was found, but significant negative relationships between $\delta^{13}\text{C}$ and N wt% and $\delta^{15}\text{N}$, indicating potential influences of nitrogen compounds on $\delta^{13}\text{C}$ signatures (Table 4-12). In contrast, significant ($p < 0.05$) negative correlation between $\delta^{13}\text{C}$ and C wt% in *Physcia* spp. was found. The total $\delta^{13}\text{C}$ of lichens is dictated by its carbon budget, largely determined by the balance between photosynthesis (algal partner) and respiration (both partners; Batts et al., 2004). Additionally, isotopic fractionation due to uptake and assimilation, metabolism and biosynthesis could affect $\delta^{13}\text{C}$ values recorded (Batts et al., 2004; Hoefs, 2009; Biazrov, 2012).

Carbon contents, together with their stable-isotope ratios do not vary considerably across Manchester, to 'fingerprint' particular sources, which has also been reported by Bermejo-Orduna et al. (2014). Environmental factors additionally seem to influence C contents and $\delta^{13}\text{C}$ values, illustrating the difficulty to distinguish 'urban' from natural impacts. Analysing potential urban sources (i.e. particulate matter or atmospheric CO_2 concentrations) in Manchester for $\delta^{13}\text{C}$ signatures, could contribute to further understand influences on lichen carbon isotope ratio signatures.

$\delta^{15}\text{N}$ values are reported to be less negative (i.e. are more ^{15}N enriched) where NO_x concentration is high, i.e. urban areas (Pearson et al., 2000; Sutton et al., 2004; Boltersdorf et al., 2014). Lichen isotope analysis can therefore aid to identify the predominant N sources in the field (Tozer et al., 2005; Fogel et al., 2008; Boltersdorf and Werner, 2014).

Lichen $\delta^{15}\text{N}$ values were spatially variable across the urban area of Manchester and were found comparable to other (urban) studies (Table 4-15). Enrichment in ^{15}N was primarily found along the major road network (A-, B-roads and motorway) and within the city centre (Figure 4-16), suggesting vehicular emissions (i.e. NO_x) as primary influence. Traffic influences on $\delta^{15}\text{N}$ in lichens (and mosses) was reported for highly trafficked roads (Pearson et al., 2000; Laffray et al., 2010; Bermejo-Orduna et al., 2014). In contrast, Pinho et al. (2017) reported $\delta^{15}\text{N}$ ranges for urban lichen samples, ranging from -13.16‰ to -9.44‰ , but could not identify relationships with urban settings (i.e. roads and industrial areas). Figure 4-23 shows the broad $\delta^{15}\text{N}$ ranges of anthropogenic emitted N-compounds. *Xanthoria parietina* and *Physcia* spp. nitrogen isotope values are found in more positive ranges, compared to highly negative ranges

(e.g. from pig farm NH₃) suggesting urban influences, i.e. from traffic sources (e.g. NO₂, NO_x, NH₃ and NO₃; Figure 4-23). However, a clear distinction of $\delta^{15}\text{N}$ cannot be stated for both lichen species investigated here (*X. parietina* and *Physcia* spp.), due to overlapping $\delta^{15}\text{N}$ signatures with those of pollutant sources.

Comparable to $\delta^{13}\text{C}$ values, $\delta^{15}\text{N}$ in lichens are potentially affected by different sources in the urban environment of Manchester. Moreover, a significant negative relationship between N wt%, $\delta^{15}\text{N}$ and $\delta^{13}\text{C}$ values in *X. parietina*, i.e. more negative $\delta^{13}\text{C}$ values following increasing nitrogen contents and enrichment in ^{15}N was found. Batts et al., (2004) reported decreasing $\delta^{13}\text{C}$ with increasing pollution levels (primarily SO₂), but increased N loads, as suggested by increased N contents in *X. parietina* and *Physcia* spp., could have a similar impact. This will be further discussed with NO_x diffusion tube measurements in the following section (section 4.4.5)

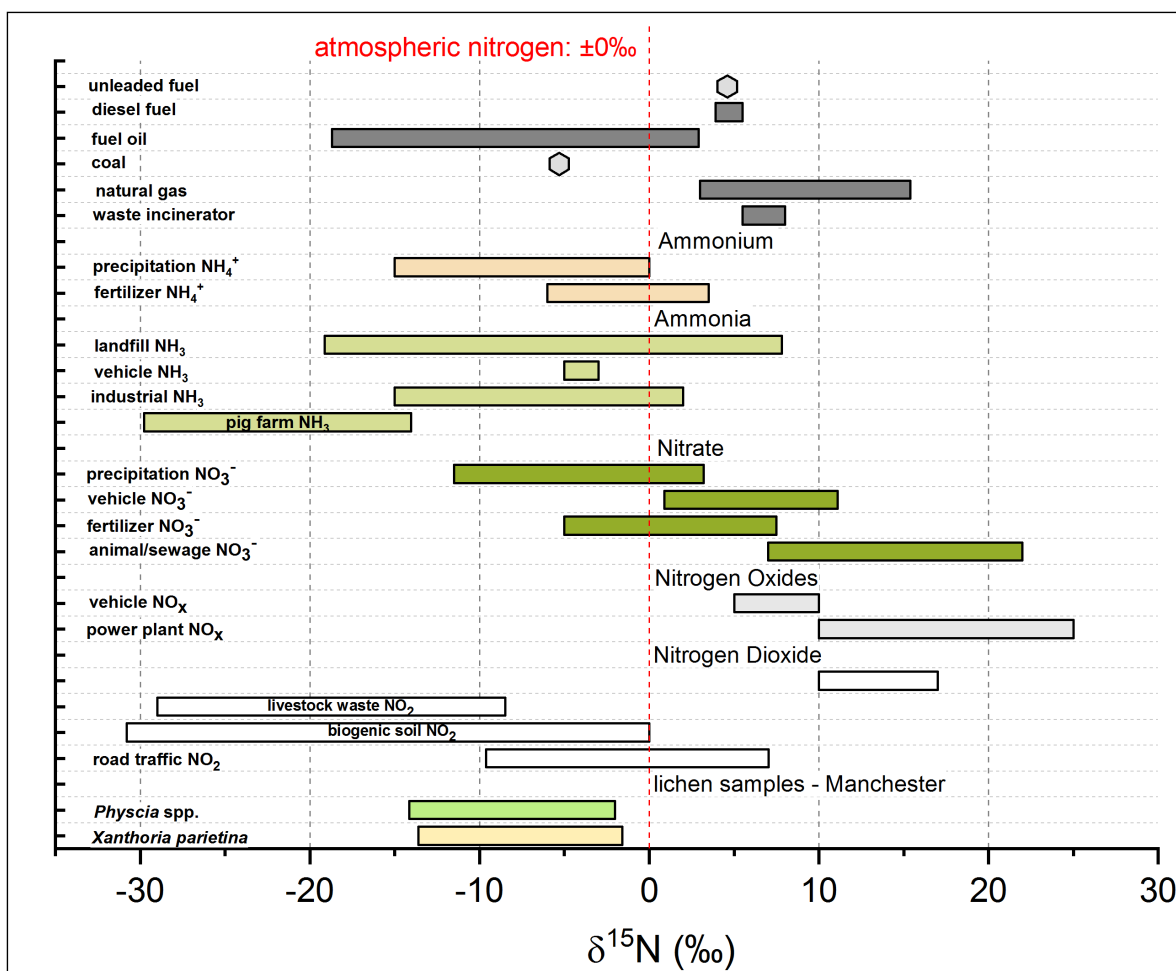


Figure 4-23: $\delta^{15}\text{N}$ values of atmospheric pollutants and pollution sources, reported in nitrogen isotope studies (Heaton, 1986; Elliott et al., 2007; Widory, 2007; Felix et al., 2012, 2013; Felix and Elliott, 2014; Liu et al., 2016) to identify potential sources; displayed with analysed $\delta^{15}\text{N}$ values for lichen samples (*X. parietina* and *Physcia* spp.) in Manchester

Sulphur is an essential nutrient for epiphytic lichens (i.e. living on plant surfaces) and sulphur-isotope ratio signatures are related to its close surrounding atmosphere (Wadleigh and Blake, 1999; Wadleigh, 2003; Batts et al., 2004). Thus, $\delta^{34}\text{S}$ values can be used to fingerprint anthropogenic sulphur sources (e.g. coal and oil; Wadleigh, 2003; Wadleigh and Blake, 1999; Wiseman and Wadleigh, 2002). Lichens convert inorganic sulphur from their surroundings to organic sulphur (by assimilatory sulphate reduction), which has been demonstrated to result in little isotopic fractionation (Mektiyeva et al., 1976; Trust and Fry, 1992; Wiseman and Wadleigh, 2002). Epiphytic lichens therefore represent the isotopic sulphur signatures of their surrounding atmosphere (Evans, 1996; Wadleigh and Blake, 1999; Wiseman and Wadleigh, 2002).

Studies reported influences of $\delta^{34}\text{S}$ values (in *Usnea scabrata* and *Alectoria sarmentosa*) with distance to pollution source (Case and Krouse, 1980; Spiro et al., 2002; Wadleigh, 2003). Moreover, decreasing $\delta^{34}\text{S}$ values were reported with increasing S contents and $\delta^{34}\text{S} < 10\text{‰}$ being related to anthropogenic sulphur sources (Wadleigh and Blake, 1999; Wiseman and Wadleigh, 2002; Wadleigh, 2003). Comparable results have been found for both lichen species (Figure 4-18) in this study, with $\delta^{34}\text{S}$ values decreasing with increasing S wt% in *X. parietina* and *Physcia* spp.

Figure 4-24 shows anthropogenic and natural $\delta^{34}\text{S}$ values, with analysed lichen $\delta^{34}\text{S}$ being in similar ranges as anthropogenic sources (i.e. fossil fuel combustion and vehicular emissions), while natural sources are in the negative (bacterial H_2S) and highly positive range (seawater sulphate; Figure 4-24). Uptake and release of sulphur (and fractionation during sulphur metabolism) from lichens could affect $\delta^{34}\text{S}$ values (Wadleigh, 2003; Hoefs, 2009). Meteorological conditions might affect $\delta^{34}\text{S}$ values (Spiro et al., 2002) in lichens, but were not further considered here.

Decreasing $\delta^{34}\text{S}$ were also accompanied by increases in S contents, further suggesting anthropogenic influences. Lichen sampling around potential S sources (i.e. power plants) across Manchester and subsequent analysis could improve source apportionment. Moreover, analysis of fuel types used across Manchester (for energy production and residential heating) could benefit the insights into sulphur composition across Manchester.

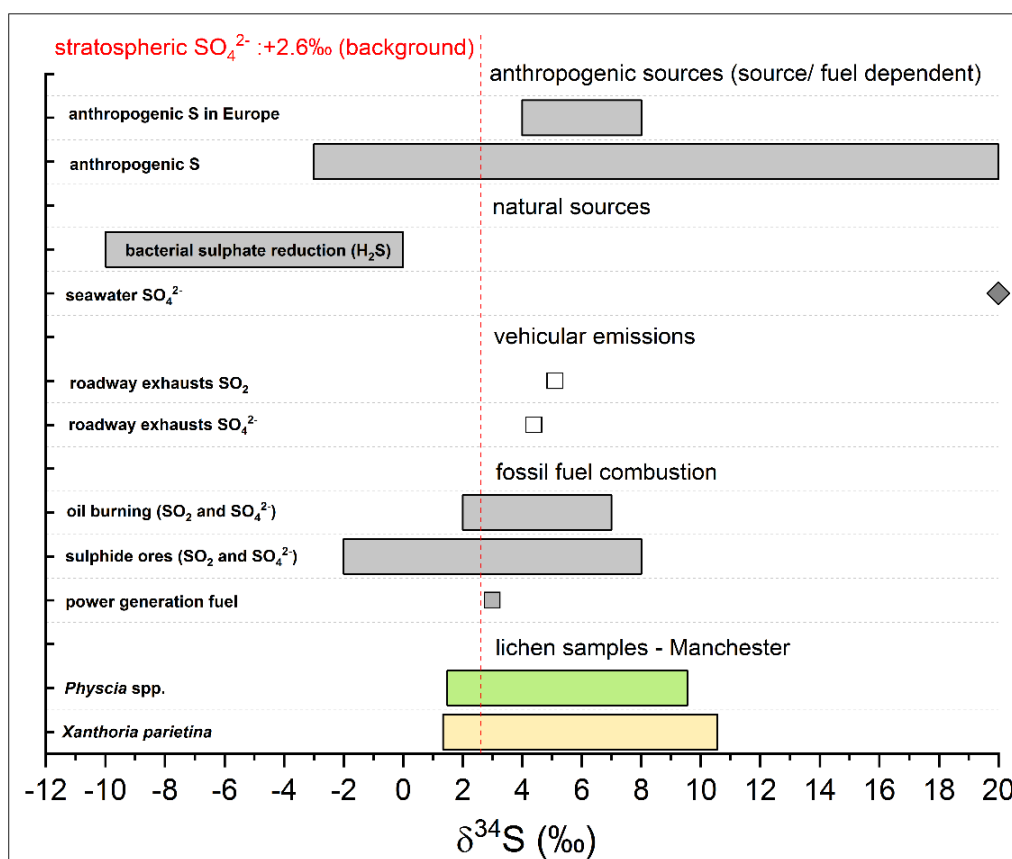


Figure 4-24: $\delta^{34}\text{S}$ values of atmospheric pollutants and pollution sources reported in sulphur isotope studies (Cortecci and Longinelli, 1970; Case and Krouse, 1980; Wadleigh and Blake, 1999; Wadleigh, 2003; Norman, 2004) to identify potential sources, displayed with $\delta^{34}\text{S}$ values of lichens (*X. parietina* and *Physcia* spp.) in Manchester.

In conclusion, lichen $\delta^{13}\text{C}$ and $\delta^{15}\text{N}$ values could not be used to identify particular pollution sources in Manchester. However, $\delta^{13}\text{C}$ seemed to be primarily affected by environmental factors (i.e. precipitation and light), whereas $\delta^{15}\text{N}$ indicate NO_x influences, but additional anthropogenic sources are suggested, due to overlapping $\delta^{15}\text{N}$ values and a mixture of nitrogen-containing compounds are more likely to influence lichen nitrogen isotopes. In contrast, sulphur contents (wt%) and $\delta^{34}\text{S}$ (<10‰) indicate anthropogenic sources in the urban environment of Manchester.

However, anthropogenic emissions of nitrogen and sulphur compounds in the urban environment are responsible for shifts in stable-isotope ratio signatures recorded in lichen samples. A complex mixture of nitrogen compounds (as shown by lichen isotopic signatures) indicate deteriorated air quality by diverse sources across Manchester that need to be further investigated, especially in areas not covered by automated measurements. Sulphur compounds, even though recorded at low concentrations (by automated monitoring stations and in lichens) still seem to be of importance for lichens in urban environments.

Therefore, additional research focussing on stable-isotope ratio signatures, i.e. in particulates and gaseous compounds (passive sampling) could improve source apportionment, especially for $\delta^{15}\text{N}$. Extending the lichen sampling to less 'urban' affected sites could show a more distinct pattern of $\delta^{15}\text{N}$ values. Moreover, nitrogen speciation (i.e. nitrate and ammonium) in lichens could provide additional insights into lichen nitrogen composition and potential influences on $\delta^{15}\text{N}$ signatures. To further investigate a potential traffic-related influence on lichen $\delta^{15}\text{N}$, metal concentrations, i.e. traffic markers such as Pb and Zn were suggested (Pearson et al., 2000; Gerdol et al., 2002; Bermejo-Orduna et al., 2014).

Overall, air quality in Manchester appears to be primarily affected by nitrogen compounds, which can be investigated using lichen N wt%, in combination with stable nitrogen isotope ratios. Poor air quality in Manchester, due to influences of nitrogen compounds was further investigated by analysing NO_2 concentrations, measured with NO_x diffusion tubes to lichen N wt% and $\delta^{15}\text{N}$.

4.4.5 Urban NO_x diffusion tube measurements

NO_x diffusion tubes were used to ground-truth lichen data and to assess a spatio-temporal overview of NO_2 concentrations across the City of Manchester. NO_2 concentrations were found spatially and temporally variable. NO_2 was recorded higher during colder months, whereas concentrations decreased during warm, sunnier weather. Elevated NO_2 concentrations were considered to affect lichen N contents, as well as $\delta^{15}\text{N}$ values.

Positive correlation was found for N wt% in *X. parietina* and $\delta^{15}\text{N}$ with NO_2 in both lichen species (Table 4-12 and Figure 4-19). Higher NO_2 was found close to major roads (A, B- roads and motorway), suggesting vehicular emissions as primary source and influence of highly trafficked roads on lichen $\delta^{15}\text{N}$ (*X. parietina*; Table 4-13 and Figure 4-20). A traffic-related nitrogen-isotope study also reported $\delta^{15}\text{N}$ values as ^{15}N -enriched as -4.10‰ for *Letharia vulpina* (wolf lichen) sampled close to (busy) roads and motorways (Bermejo-Orduna et al., 2014). Interestingly, higher NO_2 concentrations seem to have a negative effect on lichen $\delta^{13}\text{C}$ and $\delta^{34}\text{S}$ values (Table 4-12), which could be related to 'preferences' of lichens (*X. parietina* and *Physcia* spp.) for nitrogen compounds, due to their nitrophilous nature and thus a depletion in carbon and sulphur isotope ratios. This needs to be further investigated, with relation to potential carbon and sulphur compounds, influencing stable-isotope ratio signatures.

However, a mixture of nitrogen compounds is more likely to affect lichen N wt% and $\delta^{15}\text{N}$ signatures in the urban environment than NO_2 influences only (Figure 4-23). In contrast, negative correlation between NO_x concentrations have been reported for $\delta^{13}\text{C}$ (Batts et al., 2004). In this study, moderate negative correlation between increasing NO_2 concentrations and less negative $\delta^{13}\text{C}$ values in lichens was found (Table 4-12), which could explain shifts in $\delta^{13}\text{C}$ signatures in *X. parietina* and *Physcia* spp.

Elevated nitrogen contents in lichens (and less depleted $\delta^{15}\text{N}$ values), appeared to respond to higher NO_2 concentrations and thus indicate potential areas of human health risks. Therefore, lichen N wt% and $\delta^{15}\text{N}$ values can be used to identify 'hot-spots' of nitrogen pollution and identify areas of improvement. However, to potentially 'fingerprint' nitrogen sources, nitrogen compounds (i.e. nitrate and ammonium) and their influence on lichens need further consideration, which will be investigated in the following chapter.

4.4.6 Investigating potential urban influences on spatial variability of CNS contents and stable-isotope ratio signatures recorded in *X. parietina* and *Physcia* spp. in Manchester (UK)

Spatial variability for CNS contents (wt%) and stable-isotope ratio signatures ($\delta^{13}\text{C}$, $\delta^{15}\text{N}$ and $\delta^{34}\text{S}$) in lichens was presented, indicating site-specific influences and impacts by the sampling sites close surrounding.

In this study, lichen CNS contents and stable isotope-ratio-signatures ($\delta^{13}\text{C}$, $\delta^{15}\text{N}$ and $\delta^{34}\text{S}$) were categorised according to the described procedure in section 4.2.6 and categories for urban environmental variables (Table 4-3). Here, distance to major roads and road class (i.e. A- and B-roads and motorways), as well as surrounding building heights primarily influenced spatial distribution and dispersion of nitrogen and sulphur compounds and $\delta^{15}\text{N}$ recorded in *X. parietina* (Table 4-13 and Figure 4-20). However, different relationships with urban factors found for *Physcia* spp. could be related to specific environmental factors (i.e. microclimatic, meteorological and atmospheric conditions), which were not considered here. Obtained datasets i.e. traffic count statistics are available for major roads (i.e. road class: M, A- and B roads). Moreover, distances rely on measurements between the sampling location and the 'nearest' major road, large point source and green space, neglecting structures of urban environments.

However, correlation statistics is a useful tool to evaluate relationships between pollutants and additional variables (affecting air quality) and potentially identify most influential factors or sources of chemical components (Tiwari and Singh, 2014; Zhu et al., 2017; Núñez-Alonso et al., 2019). Moreover, available datasets i.e. traffic counts on minor roads, pollutant distribution from large point sources and interception by urban vegetation (i.e. uptake of gaseous, aerosol and particulate pollutants; Freer-Smith et al., 1997; Gaston, 2010) are scarce. Hence, data classification was based on available studies, reporting the decline of pollutants with distance to road and/or human health related studies (see chapter 2 for a detailed description).

Urban environments are complex systems, affecting distribution and dispersion of atmospheric pollutants (Gaston, 2010; Forman, 2014). Urban areas comprise of rough surfaces, influencing aerodynamic properties of the atmosphere, which are critical for air quality in urban environments (Grimmond and Oke, 1999; Cariolet et al., 2018). Major roads (i.e. motorways and all class 'A' roads) are often the main arteries within urban environments and usually have high traffic flows (DfT, 2017a). Moreover, pedestrian level winds play an important role in the dispersion of traffic-related pollutants, with regard to surrounding building height, width, building arrangements and density (Kubota et al., 2008). For Manchester, westerly winds tend to have consistently low impact on pollutant concentrations, whereas northerly and easterly winds are affecting pollutant variability with seasonal dependence on chemical composition (Martin et al., 2011). However, due to the complexity of urban environments and additional meteorological influences (i.e. daily temperature and rainfall), atmospheric processes (i.e. chemical reactions in the atmosphere) and site-specific influences (i.e. tree species and bark pH) potential (urban) influences on lichen pollutant loadings could be related to these additional factors. GWR was used to investigate variability and explanation of urban variables on lichen pollutant loadings. GWR is often used to study local differences (based on input variables), with focus on explanation of variables, rather than interpolation (Hengl, 2009). Studies applied GWR to model air pollution and air quality data with different influencing variables, i.e. population data, land-use data and meteorological data (Fang et al., 2015; Yang et al., 2017; Warsito et al., 2018).

Modelling outcomes for Manchester showed explanation of spatial variability between 16% and 34% for N wt% and $\delta^{15}\text{N}$ in *X. parietina* (Figure 4-21) by urban influencing factors, respectively. Higher N wt% in lichens and enriched $\delta^{15}\text{N}$ were found close to major roads and within the city centre, suggesting traffic as primary source of NO_x compounds (affecting lichens) and poor distribution and dispersion of emitted pollutants, i.e. due to surrounding building heights. However, further investigating meteorological influences (i.e. micro-climatic) and atmospheric reactions of nitrogen (sulphur and carbon) compounds, could provide additional input into spatial variability of atmospheric pollutants and improve modelling outcomes.

4.5 Conclusion

This study aimed to use lichen CNS contents (wt%) in combination with their stable-isotope-ratio signatures ($\delta^{13}\text{C}$, $\delta^{15}\text{N}$ and $\delta^{34}\text{S}$) to assess high spatial variability of air quality and to identify anthropogenic sources in the urban environment of Manchester.

Lichen carbon contents and $\delta^{13}\text{C}$ values were considered not to be reliable indicators of anthropogenic pollution in the urban environment of Manchester. Indeed, minor variation in carbon contents and $\delta^{13}\text{C}$ values, of both lichen species, are most likely due to local meteorological conditions and variability of NO_2 concentrations. Moreover, a temporal impact on lichen C wt% was found, suggesting shorter sampling periods for spatial (and temporal) studies.

In contrast, elevated nitrogen contents in lichens were found to be accompanied by an enrichment in ^{15}N , pointing towards NO_x influences (i.e. from traffic) on lichen nitrogen and $\delta^{15}\text{N}$ ratios. Urban factors seemed to influence lichen pollutant loadings at specific sampling sites, indicating the necessity to further investigate atmospheric pollution in highly trafficked areas that are not covered by automated monitoring stations. Moreover, elevated NO_2 concentrations (recorded with NO_x diffusion tubes) across Manchester were (potentially) influencing lichen $\delta^{15}\text{N}$ values, further indicating potential NO_x influence on lichens. However, a clear distinction between nitrogen compounds, based on $\delta^{15}\text{N}$ signatures could not be made, suggesting the complexity of nitrogen compounds potentially affecting lichen isotopic signatures.

SO₂ concentrations decreased during the last 30 years in Manchester and are now primarily related to industrial and domestic (heating) emissions. However, depletion in $\delta^{34}\text{S}$ accompanied by an increase of sulphur contents, recorded in lichen samples across Manchester, suggested anthropogenic sources of sulphur. Therefore, $\delta^{34}\text{S}$ accompanied by analysis of sulphur contents can be used to identify sources of sulphur in urban environments.

Extending the lichen sampling, to less urbanised areas could provide additional insights into lichen CNS contents and stable-isotope ratio signatures, further (re-)defining potential sources.

The urban structure of Manchester, additionally influenced dispersion and distribution of pollutants, indicating higher pollutant loadings within densely built-up areas and thus affecting human health, especially within the city centre area.

Further research on potential urban influences (e.g. traffic counts for minor roads) and dispersion of pollutants can contribute to finer spatial resolution of air quality in Manchester. Moreover, meteorological conditions in the urban environment of Manchester could have impacted on lichen CNS contents and stable-isotope ratio signatures that need further investigation.

Findings showed that especially nitrogen contents seemed to reflect increased nitrogen loads in the urban environment of Manchester. Furthermore, $\delta^{15}\text{N}$ values in lichens (even though not related to specific sources) hint towards NO_x influences, but also illustrate the complex mixture of nitrogen compounds affecting the population's health across Manchester. Especially along the major road network and within densely built-up areas (i.e. city centre of Manchester), elevated N loads were recorded, which are not measured by automated measurement stations.

Therefore indicating the beneficial use of lichens to provide spatial overview of atmospheric pollution and suggesting areas of improvement and/or further investigation (in relation to human health impacts). Moreover, both lichen species seemed to reflect their surrounding environmental conditions. However, species-specific differences were found, suggesting the use of a 'single' lichen species, when comparing urban environments.

In conclusion, combining both biomonitoring and a passive sampling approach is a beneficial tool to assess variability of air quality in an urban environment. Lichens could aid to identify hot-spots that can be further investigated by NO_x diffusion tubes, leading to the identification of areas of improvement, i.e. to tackle high nitrogen levels.

Nonetheless, further research on interfering compounds (i.e. nitrate and ammonium) could provide additional information on N contents and $\delta^{15}\text{N}$ signatures, which will be addressed in the following chapter.

Chapter 5-
Development of a
new method to
quantify nitrate and
ammonium in lichens

5.1 Introduction

Increases in airborne nitrogen compounds, particularly in urban areas from traffic emissions, nitrogen contents of lichens can reflect airborne nitrogen loads from anthropogenic impacts (Gombert et al., 2003; Frati et al., 2006, 2007; Gadsdon et al., 2010; Olsen et al., 2010; Bermejo-Orduna et al., 2014; Boltersdorf et al., 2014). Several studies investigated the ability of lichens to take up nitrate and ammonium (Smith, 1960; Lang et al., 1976; Shapiro, 1984; Crittenden, 1996, 1998; Dahlman et al., 2004; Palmqvist and Dahlman, 2006), but availability of different N compounds to lichens, especially in urban areas, has not been studied and little is known about lichen N-species assimilation (Dahlman et al., 2004).

Reactive nitrogen in the atmosphere comprises nitrogen oxides (NO_x) and reduced nitrogen compounds (NH_x), these originating from many different sources, including fossil fuel combustion and agricultural processes (Sutton et al., 2004; Hall et al., 2006; Olsen et al., 2010). Nitrate (NO_3^- , and nitrite, NO_2^-) naturally occur as highly water-soluble ionic species that are part of the global nitrogen biogeochemical cycle. Nitrite is readily oxidised to the more environmentally stable nitrate (NO_3^-), which is a key plant nutrient (ATSDR, 2015). Anthropogenic sources of nitrate include the production and use of fertilisers (ATSDR, 2015). Additionally, atmospheric nitrate is primarily emitted during fossil fuel combustion as nitric oxides (Gadsdon and Power, 2009; Hauck, 2010). Anthropogenic emissions of ammonia (NH_3) into the atmosphere within the UK were dominated by agricultural sources (i.e. nitrogen-based fertilisers and livestock farming), accounting for 82% of total emissions in 2016 (other sources include: direct soil emissions and combustion and production processes (NAEI, 2016, 2018d). Atmospheric ammonia (NH_3) is rapidly deposited within 4 to 5 km of its source, but can be converted to ammonium (NH_4^+) in the atmosphere which then can be transported distances of 100-1,000 km (Olivier et al., 1998; Van Herk, 2001; Krupa, 2003; Webb et al., 2005; Hauck, 2010).

Road vehicle exhaust emissions release both nitrate and ammonia compounds (Olivier et al., 1998; Sutton et al., 2000; Gadsdon and Power, 2009; Hauck, 2010). Recent findings suggest that NH_3 is now the dominant nitrogen species emitted by vehicles in urban environments, due to the increased NO_x reduction efficiency of three-way catalysts, with dependence on road grade (i.e. gradient of the road), driving mode (i.e. traffic speed and potential 'stop-and-go'), and vehicle age (Bishop et al., 2010; Bishop and Stedman, 2015; Stritzke et al., 2015; Sun et al., 2017).

For example, Sun et al. (2014) found that vehicular NH_3 emissions more than double when the gradient of the road increases from 0 to 7%. Nitrogen compounds, such nitrate, ammonia (NH_3) and ammonium (NH_4^+) are not continuously measured with common monitoring stations, due to high spatial heterogeneity and necessity of costly equipment (Pinho et al., 2017). Ammonia can act as precursor for secondary particulate matter formation and growth, especially in urban areas and contribute to related health impacts (i.e. respiratory, skin and eye irritation; ATSDR, 2004; Liu et al., 2015; Sun et al., 2017; NAEI, 2018). Health impacts induced by nitrate and ammonium specifically, were reported to impact on the cardiovascular and respiratory system (Atkinson et al., 2010; Kim et al., 2012; Son et al., 2012; WHO, 2013b). Assessment of atmospheric nitrate and ammonium pollution in the urban environment of Manchester could be related to such health concerns (i.e. respiratory and cardiovascular diseases in Manchester; Regan, 2018).

This chapter presents the development and application of an entirely new method for the extraction and separation of different nitrogen compounds, i.e. nitrate and ammonium, within lichen samples, in order to separate the total nitrogen loading into its constituent parts and thus improve source apportionment studies.

To extract lichen sample nitrate and ammonium, methodological development was undertaken based on established extraction techniques that are applied to soil samples (Bremner and Keeney, 1966; Jones and Willett, 2006). Soil nitrate can be extracted using 2M and 1M potassium chloride (KCl) solutions (Maynard and Kalra, 1993; Jones and Willett, 2006). Methodological development (and experimental design) to extract NO_3^- and NH_4^+ from lichen material will be described in detail hereafter.

The chosen extraction method was then applied to rural and urban lichen samples. Lichens (*X. parietina* and *Physcia* spp.) sampled across the City of Manchester (UK) and, by way of contrast, from around poultry farm (*X. parietina* only) in Shrewsbury (UK) are used.

Extracted nitrate and ammonium concentrations (from rural and urban *X. parietina* samples) were also investigated with bulk nitrogen contents (N wt%) and stable nitrogen isotope signatures ($\delta^{15}\text{N}$), reported in detail in chapter 4, for both contrasting environments. Temporal and spatial variability of both nitrogen constituents will be considered for the urban environment of Manchester in detail.

Interpretation and discussion will focus on the applied extraction method, as well as NO_3^- and NH_4^+ concentrations in rural and urban environments. Moreover, potential influences of both nitrogen species (NO_3^- and NH_4^+) on nitrogen contents and stable isotopes of lichens will be discussed.

Subsequently a conclusion will be drawn, in particular for the urban environment of Manchester, and impacts of NO_3^- and NH_4^+ on its urban air quality and further applications of nitrate and ammonium extraction in biomonitoring studies.

5.2 Research Methodology – Development of an extraction method to enable quantification of lichen nitrate and ammonium concentrations by ion chromatography (IC)

5.2.1 Lichen sampling and preparation

Urban lichen samples of *X. parietina* (N=87; Figure 5-1) and *Physcia* spp. (N=48; Figure 5-1) were sampled off street trees across Manchester (as described in previous chapters, during sampling periods in 2016 and 2017). Due to the long initial sampling period, certain sites (N=17) were re-sampled (same tree) for *X. parietina*. Sampling sites were re-visited based on analysed nitrogen contents (site specific N wt% in Appendix C-1), as lower N wt% in lichens potentially indicate lower N-compound inputs. Collected lichen were stored in paper bags and then carefully scraped off the bark using a stainless-steel scalpel, non-lichen detritus was removed and lichen samples were ground into powder and homogenised using an agate pestle and mortar and stored in glass vials until analysis.

A single lichen sample (*X. parietina*), of which sufficient lichen material (~6.5 g) was sampled, was used for methodological development (Figure 5-1, red hexagon). The 'test site' was located close to a major road ('A road') leading into Manchester's city centre, which is used by ~30,000 vehicles daily (DfT, 2017a), indicating potential NO_3^- and NH_4^+ influences by road traffic.

Lichen 'control' samples were sampled in a rural environment to evaluate differences between the contrasting environments. Rural lichen samples (*X. parietina*, N=12; Figure 5-2) were collected from oak (*Quercus* spp.) and hawthorn (*Crataegus* spp.) trees around a poultry farm in Shrewsbury (UK) in May 2018, following the same procedure described. Lichen sampling was undertaken in close proximity (i.e. between 50 to 500 m) and on a general south-west transect (i.e. between 1 - 3 km) away from the poultry farm, defined by accessibility of potential sampling sites, i.e. fenced and hedged agricultural fields and private property.

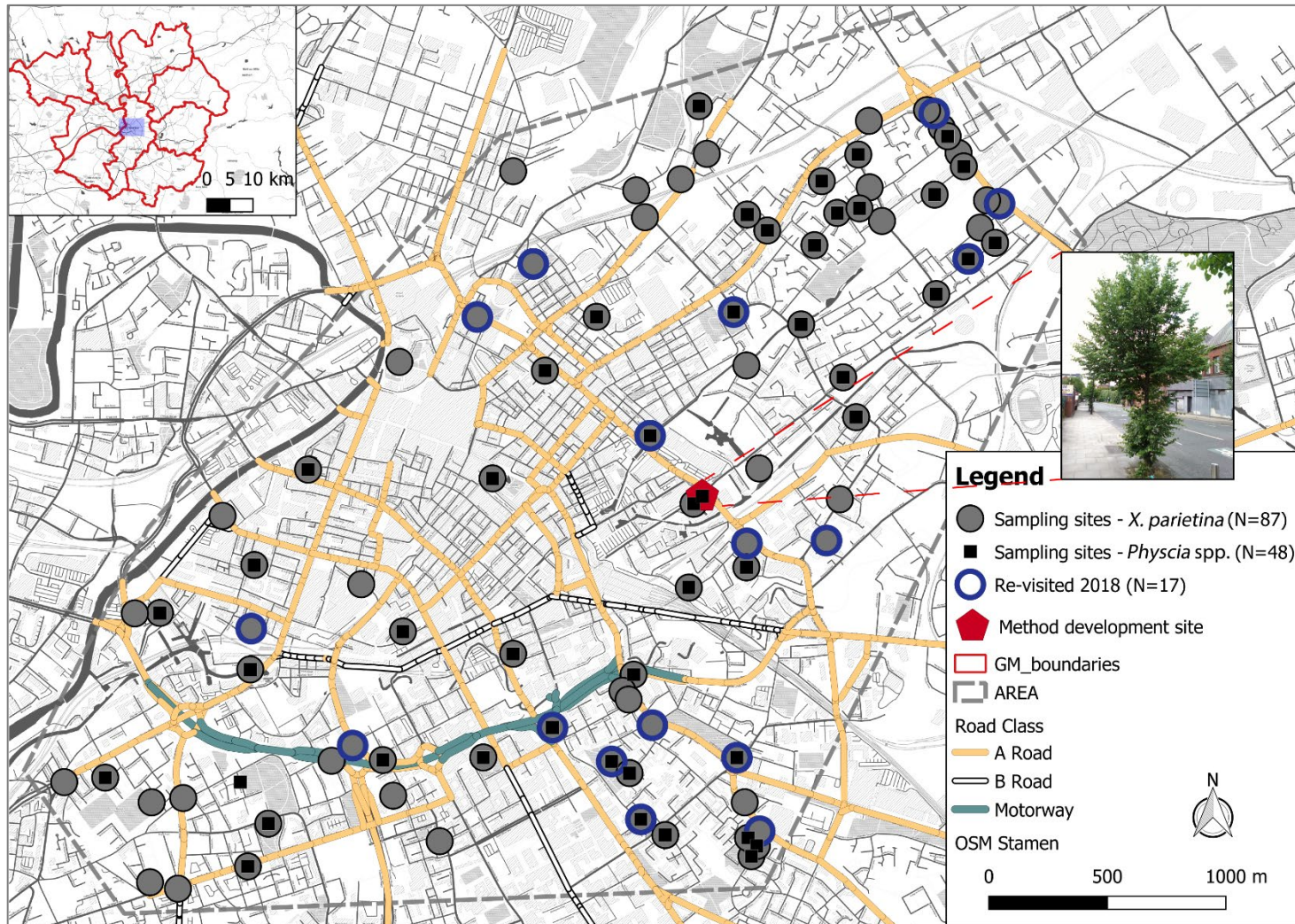


Figure 5-1: Urban lichen sampling sites (*X. parietina*: grey circles, N=87; *Physcia* spp.: black triangles, N=48 and re-visited sites: blue circle, N=17) across the city centre of Manchester, displayed with method development site (red hexagon and picture of sampled tree)



Figure 5-2: Rural lichen sampling sites (*X. parietina*; N=12) around a poultry farm in Shrewsbury, UK (sampled in May 2018); displayed with location of poultry farm in relation to Greater Manchester (upper left corner, red square)

5.2.2 Experimental design to determine lichen nitrate and ammonium concentrations

To assess extractability of nitrate and ammonium from lichen material, methodological development was based on soil studies that applied Potassium chloride (KCl) to extract inorganic nitrogen. A high sample mass-to-extractant ratio (1:100 w/v, to begin methodological development) was chosen to effectively extract NO_3^- and NH_4^+ .

About 0.05 g of lichen (a single sample of *X. parietina*: red hexagon in Figure 5-1) was weighed into 12 ml plastic tubes, in triplicate for each extraction procedure variable tested (solvent strength, solvent volume extraction time and vortexing/non-vortexing) and extraction solvent (1 ml to 5 ml) was added to the tubes. Different solvents were tested; deionised water (DI), 1% KCl, 3% KCl, 6% KCl, 7.5% KCl (1 M) and 15% KCl (2 M). Two leaching times were additionally tested, including 6 hours to simulate a 'laboratory day' and 24 hours, to simulate a 'normal' (used in soil studies) extraction procedure (Keeney and Nelson, 1982; Maynard and Kalra, 1993). Specified variables were adjusted during the experimental setup and is further described in the following sections (i.e. 5.2.3 and 5.2.4).

Extraction times were noted and controlled, and samples were subsequently centrifuged for 20 minutes at 4000 rpm. Supernatant (500 μl) was pipetted out filtered through 0.2 μm nylon filters (into new 12 ml tubes) and more concentrated KCl solutions (i.e. 15%, 7.5%, 6% and 3%) were diluted with ultrapure water (18.2 M Ω) to 1% KCl strength, to avoid built-up of salts in the IC column and subsequently analysed by ion chromatography. Figure 5-3 illustrates the extraction procedure applied to lichen material. Blanks were included and handled exactly as lichen samples (i.e. vortexing and filtering) and used for blank subtraction before further data analysis. Potassium chloride (KCl, $\geq 99\%$, Sigma-Aldrich) extraction solutions were prepared fresh before each sample extraction and for each set of matrix-matched ion chromatography calibration standards.

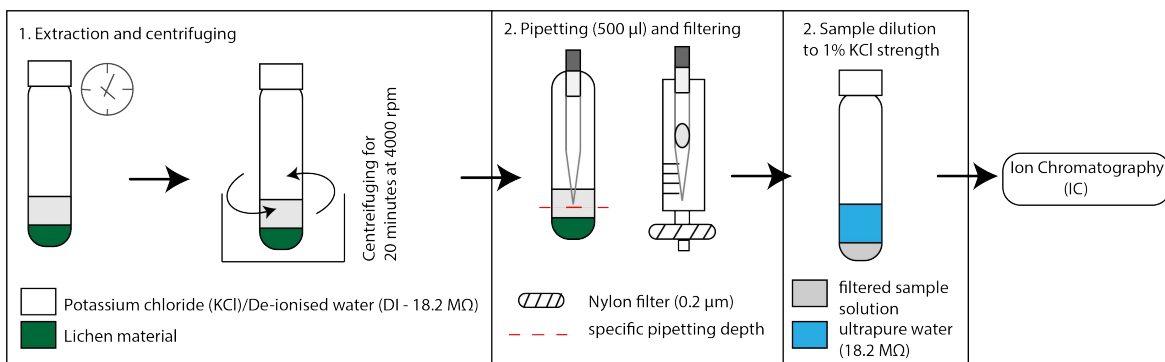


Figure 5-3: Summary of lichen chemical extraction procedure (schematic) for nitrate and ammonium

5.2.3 Detailed testing of different chemical extraction approaches using a single urban lichen sample

Methodological development and experimental setup were based on soil NO_3^- and NH_4^+ extraction studies and tested on a single lichen sample that potentially contained higher concentrations of nitrate and ammonium (Figure 5-1). Experimental setup, with variables for each undertaken experiment are displayed in Table 5-1.

Table 5-1: Methodological development and tested variables for extraction of nitrate and ammonium concentrations from *X. parietina* (single site; Figure 5-1)

Experiment	Variables
Experiment 1	Solvents: DI, 1%, 7.5% and 15% KCl Volume [ml]: 1, 2, 3, 4, 5 Extraction time [hours]: 24 (non-vortexing)
Experiment 2	Solvents: DI, 1%, 3% and 6% KCl Volume [ml]: 1, 2, 3, 4, 5 Extraction time [hours]: 24 (non-vortexing)
Experiment 3	Solvents: 3% KCl Volume [ml]: 2, 3 Extraction time [hours]: 6, 24 (vortexing and non-vortexing)

Potassium chloride (KCl) with the strengths of 2 M (~15%) has been used to extract nitrogen compounds (i.e. NO_3^- and NH_4^+) from soils (Bremner and Keeney, 1966; Maynard and Kalra, 1993; Jones and Willett, 2006). In addition to 7.5% KCl (1 M) was added to the experimental setup, as it also has been applied in soil inorganic nitrogen studies (Keeney and Nelson, 1982; Maynard and Kalra, 1993). Additionally, 1% KCl (~0.1 M) was included to evaluate the potential of KCl that can be directly analysed by IC without further dilution (to minimise potential dilution errors). Solvent volumes were set to 1 ml, 2 ml, 3 ml, 4 ml and 5 ml to investigate

potential saturation and to concentrate NO_3^- and NH_4^+ before IC analysis. Extraction time was kept at 24 hours and samples were cautiously shaken only (non-vortexed).

Extractant strength was adjusted and included 3% KCl (~0.5 M) and 6% (~0.75 M), to further investigate extractability of NO_3^- and NH_4^+ and to reduce errors from dilution of samples (i.e. pipetting errors; SAWG, 2002); DI and 1% KCl were kept. Solvent volumes (including 1, 2, 3, 4 and 5 ml) and extraction time of 24 hours were also kept.

Extraction of NO_3^- and NH_4^+ of lichen material (0.05 g) was investigated for 2 and 3 ml of 3% KCl, representing sample-to-extractant ratio of 1:40 and 1:60, respectively. Additionally, extraction time of 6 hours was added to simulate a 'laboratory day' and achieve same day extraction and analysis by IC. Vortexing was included to thoroughly mix the analytical sample.

5.2.4 Determination of nitrate and ammonium by ion chromatography (IC)

Ion chromatography is commonly used to determine anions (i.e. NO_3^-) and cations (i.e. NH_4^+), and is particularly recommended for speciation analysis, due to simultaneous determination, short time, good reproducibility and high sensitivity (Michalski and Kurzyca, 2014)

Extractants were analysed using a 'Thermo Scientific - ICS5000'. For anions the calibration standard "Dionex™ Seven Anion Standard II" (Thermo Fisher Scientific, UK) was used and "Simple Nutrients - Whole Volume (QC3198)" as certified reference material. CRM was diluted by a factor of 1:5 with ultrapure water (18.2 MΩ) for extractions using DI and with 1% KCl for extractions using KCl to matrix-match with samples. The CRM was used to assess accuracy and precision of nitrate determinations. Calibration standard for cations "Dionex™ Six Cation Standard I" (Thermo Fischer Scientific, UK). Specifications of the used standards and reference material are displayed in Table 5-2. A dilution of the cation calibration standard (to 3.125 mg/l) was used as an ammonium reference material throughout the analytical batches.

Anion IC equipment characteristics are: Thermo Scientific - ICS5000, columns: AG18 (2 mm x 5 mm) guard column, AS18 (2mm x 250mm) separation column; EGC III KOH cartridge (electronically generated elution; Potassium Hydroxide), starting at 18 mM KOH (slope: 1.96 mM/min) for 16 minutes. The signal was measured using suppressed conductivity.

Characteristics for cation analysis (IC) are: Thermo Scientific – ICS5000, columns: CG16 guard column (3 mm x 50 mm) and CS16 separation column (3 mm x 250 mm) were used for analysis. Methanesulfonic acid (MSA) at 39 mM was pumped isocratically during the analysis. Signals were measured using suppressed conductivity.

Table 5-2: Compounds contained in calibrations standards and ‘Simple Nutrients’ certified reference material (CRM), used for analysis of lichen samples for nitrate and ammonium concentrations (presented in bold) by ion chromatography (Thermo Fisher Scientific, 2018a, 2018b); calibration standards (six-point) and certified reference materials were made up fresh for each analytical run

Dionex Seven Anion Standard II	Dionex Six Cation Standard I
Fluoride: 20 mg/L	Lithium: 50 mg/L
Chloride: 100 mg/L	Sodium: 200 mg/L
Nitrite: 100 mg/L	Ammonium: 400 mg/L
Bromide: 100 mg/L	Potassium: 200 mg/L
Nitrate: 100 mg/L	Magnesium: 200 mg/L
Phosphate: 200 mg/L	Calcium: 1000 mg/L
Sulphate: 100 mg/L	
Simple Nutrients – Whole Volume (WP) (CRM)	
Nitrate as N: 10.5 ± 0.187 mg/L	

5.3 Statistical data analysis

Statistical analysis was undertaken using statistical software, such as ‘SPSS Statistics 25’ and ‘GraphPad Prism 7’. Data visualisation was undertaken using ‘Origin 2018’. Normal distribution of data (nitrate and ammonium concentrations) in lichens was tested with Shapiro-Wilk test. Shapiro-Wilk is considered a stronger statistical test for normality, compared to other tests (e.g. Kolmogorov-Smirnoff; Mendes and Pala, 2003; Razali and Wah, 2011).

Different normal-distribution outcomes informed about parametric and non-parametric tests, to compare groups and correlation statistics. For instance, methodological development data was non-normally distributed, and a Wilcoxon test was applied to evaluate differences of testing variables (i.e. solvent, solvent volumes, extraction times and mixing technique). Urban lichen-derived NO₃⁻ and NH₄⁺ concentrations were also not drawn from a normal distribution, therefore Mann-Whitney tests was applied to compare lichen species and correlation statistics (i.e. with N contents and δ¹⁵N values) were undertaken using Spearman ρ.

Comparison between sampling periods was undertaken by using Wilcoxon test statistics for nitrate concentrations, due to different test outcomes for normal distribution, whereas NH_4^+ was compared using a paired t-test (normally distributed data). In contrast, rural concentrations of NO_3^- and NH_4^+ were normally distributed favouring the use of parametric tests (i.e. Pearson's r) to assess relationships between distance to poultry farm, N contents (wt%) and lichen nitrogen isotope signatures ($\delta^{15}\text{N}$).

5.4 Geospatial data analysis

Geographic Information Software (GIS; ArcMap 10.5 and QGIS 3.4.2 – 'Madeira', latter for mapping of data) was used for geospatial analysis and mapping of NO_3^- and NH_4^+ concentrations recorded in lichens. Environmental studies, assessing air quality and atmospheric pollution applied kriging methods to datasets (Romary et al., 2011; Beauchamp et al., 2012; Pannullo et al., 2015). Ordinary Kriging (OK) was applied to nitrate and ammonia data from lichens to investigate spatial patterns in Manchester UK. Due to smaller sampling size ($N=12$) for rural lichens, ordinary kriging was not applied to rural NO_3^- and NH_4^+ concentrations.

To investigate small-scale variability and include urban influencing factors (described in detail in chapter 2; Table 5-3) on spatial distribution and dispersion (of NO_3^- and NH_4^+) geospatial statistics were applied. Regression analysis tools are available in 'Geographic Information System' (GIS) software to quantify spatial statistics and relationships (ESRI, 2019). Ordinary Least Square (OLS) is a technique, commonly used to quantify the effects of independent variables on one dependent variable (Yoo and Ready, 2016; Yang et al., 2017).

Ordinary Least Square (OLS, regression analysis tool) was used to quantify spatial statistics and relationships of lichen NH_4^+ and NO_3^- , and potential influences by urban factors, as displayed in Table 5-3.

The ArcMap 10.5 'spatial statistics' tool was used for OLS, including urban variables (Table 5-3) and lichen-derived NO_3^- and NH_4^+ concentrations of urban *X. parietina* samples, due to higher sampling density (compared to *Physcia* spp). OLS was used due to non-significance of 'Koenker' statistics (informing about potentially non-stationarity, meaning changing relationships across the study area; ESRI, 2019) for modelling of NO_3^- and NH_4^+ concentrations with urban influencing factors. Spatial modelling of NO_3^- and NH_4^+ was not applied to rural lichen samples, due to small sample size ($N=12$) and focus of this study on air quality in Manchester.

Table 5-3: Urban influencing factors (grouped) used to assess spatial variability of nitrate (NO_3^-) and ammonium (NH_4^+) concentrations in lichen samples from Manchester

Environmental variable	Data grouping
Distance to major road (including A-roads, B-roads and motorways)	1: <25 m 2: 25-50 m 3: 50-100 m 4: 100-200 m 5: >200 m
Traffic counts (annual average daily traffic flow)	1: <10.000 2: 10.000 to 20.000 3: 20.000 to 30.000 4: >30.000
Building heights (surrounding sampling location)	1: <10 m 2: 10 to 20 m 3: >20m
Distance to (large) point source	1: <500 m 2: 500 to 1000 m 3: 1000 m to 2000 m 4: >2000m
Distance to greenspace	1: <100 m 2: 100 to 200 m 3: 200 to 300 m 4: 300 to 400 m 5: 400 to 500 m 6: >500 m

5.5 Determination of nitrate and ammonium concentrations extracted from a single lichen sample and analysis by ion chromatography

5.5.1 Experiment 1: Extraction using DI, 1%, 7.5% and 15% KCl

This experimental setup included the use of 'weakest' (DI) and 'strongest' (15% KCl) extractants. Additionally, 7.5% (~1M) and 1% (~0.1) were investigated to minimise dilution errors (7.5% was diluted by a factor of 5 before IC analysis, while 15% was diluted by a factor of 10, both with DI) and to directly run the samples on the instrument, using 1% KCl. Extraction volumes between 1 ml to 5 ml were included, to potentially concentrate $\text{NO}_3^-/\text{NH}_4^+$ and investigate potential solvent saturation.

Results for nitrate showed varying concentrations, using different extractants and volumes Figure 5-4a. Extracted concentrations ranged from 1.03 mg/kg (1 ml of DI) to 94.85 mg/kg (1 ml of 15% KCl). DI showed slight increases of extracted NO_3^- with increased volumes, while 15% KCl showed varying concentrations for all tested volumes. 7.5% KCl also showed varying concentrations, with a general increase of NO_3^- with increasing volumes. In contrast 1% KCl showed vaguely consistent values for NO_3^- (Figure 5-4a). Concentrations of ammonium (NH_4^+) showed a general trend of increasing concentrations by volume and extractant strength (Figure 5-4a). Lowest concentrations were found for 1 ml of 15% KCl (1.14 mg/kg), while highest were found for 5 ml of 7.5% KCl (67.52 mg/kg). However, 15% KCl and 7.5% KCl showed higher variability in NH_4^+ , similar to NO_3^- .

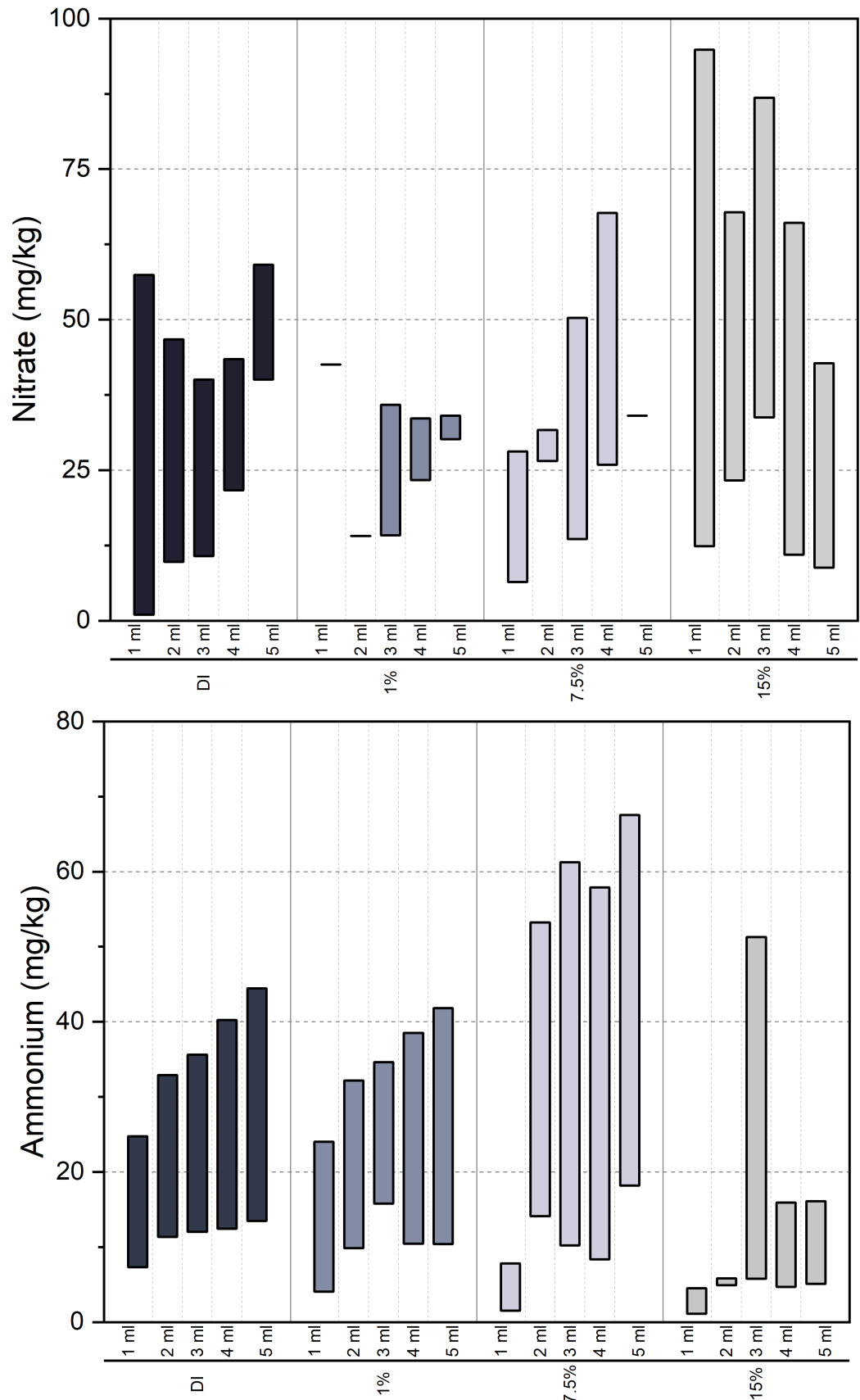


Figure 5-4: Extracted (a) nitrate and (b) ammonium from lichen material (triplicates; in mg/kg) using DI, 1%, 7.5 and 15% KCl, grouped by solvent and solvent volume used [in ml], presented as box-whisker plots (25th to 75th percentile, with mean value: white square and median line)

A Wilcoxon signed rank test (two-tailed; non-parametric) was used to investigate statistical differences of extraction solvents and extractant volumes. Table 5-4 shows the p-values for comparison of volumes of nitrate and ammonium concentrations by extractant (DI and KCl) and volumes (1 ml to 5 ml). Significant differences of nitrate concentrations ($p < 0.05$) were found for deionised water and 1% KCl, as well as between 1% KCl with 7.5%. In contrast, significant differences ($p < 0.05$) for NH_4^+ were found between DI and 15% KCl, as well as 1% and 15% KCl and 7.5% and 15% (Figure 5-5).

Extraction volumes showed no significant differences for NO_3^- . In contrast, extracted ammonium showed significant differences for 1 ml with all other tested volumes and again significant ($p < 0.01$) differences for 2 ml and 5 ml.

Table 5-4: Wilcoxon rank test p-values (*significant at the level $p < 0.05$ presented in bold and shaded in yellow; ** significant at the level $p < 0.01$ presented in bold and shaded in green) to investigate and compare extraction solvents (left) and extraction volumes (right) for nitrate and ammonium concentrations (15% KCl represents 2 M and 7.5% KCl represents 1 M KCl)

Solvents	Nitrate	Ammonium		Volumes	Nitrate	Ammonium
DI vs 1%	0.02*	0.09		1 ml vs 2 ml	0.91	<0.01**
DI vs 7.5%	0.30	0.36		1 ml vs 3 ml	0.30	<0.01**
DI vs 15%	0.15	0.01*		1 ml vs 4 ml	0.43	<0.01**
1% vs 7.5%	0.04*	0.19		1 ml vs 5 ml	0.36	<0.01**
1% vs 15%	0.05	0.04*		2 ml vs 3 ml	0.13	0.11
7.5% vs 15%	0.63	0.02*		2 ml vs 4 ml	0.16	0.15
				2 ml vs 5 ml	0.08	<0.01**
				3 ml vs 4 ml	0.57	0.57
				3 ml vs 5 ml	0.47	0.85
				4 ml vs 5 ml	0.23	0.08

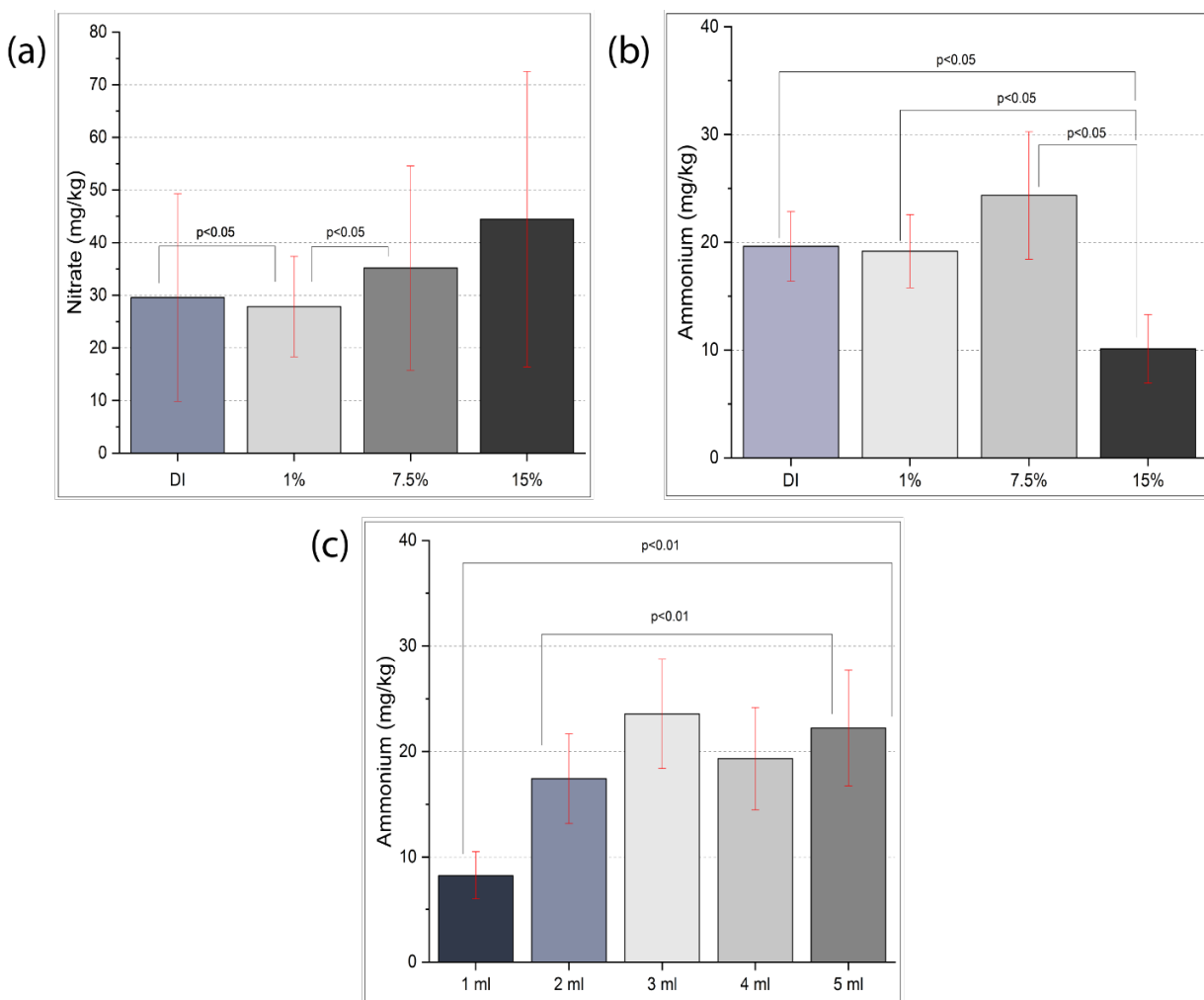


Figure 5-5: Comparison plot of (a) nitrate concentrations by extraction solvent, (b) ammonium by extraction solvent and (c) ammonium by solvent volumes (presented as bar graphs, with 1x standard error of the mean concentration); displayed with statistical significance of differences (as presented in Table 5-5)

Extracted concentrations of nitrate and ammonium for the first experiment showed variability, especially for 15% and 7.5%, indicating that 2 M (15%) and 1 M (7.5%) KCl solutions might be too 'strong' for extraction of lichen material. Additionally, 1 ml of extraction volume appeared to influence the amount of ammonium leached from the lichen material, indicating potential saturation of small volumes.

Therefore, potassium chloride solutions were lowered to 6% (~0.75 M) and 3% (~0.5 M) to further investigate extractability of NO_3^- and NH_4^+ for the next experimental setup (Experiment #2). Extraction volumes, non-vortexing and 24 hours were kept as test variables.

5.5.2 Experiment 2: Extraction using DI, 1%, 3% and 6% KCl

Experimental setup 2 included lowered KCl strengths to 3% and 6% (together with DI and 1% KCl), to evaluate extractability of NO_3^- and NH_4^+ from 'weaker' KCl solutions and to potentially reduce variability of concentrations.

Nitrate and ammonium concentrations, extracted with DI, 1% KCl, 3% KCl and 6% KCl showed varying concentration, again primarily for NO_3^- , with concentrations ranging between 0.98 mg/kg (1 ml of 3%) and 50.45 mg/kg (5 ml of DI; Figure 5-6a). Nitrate extraction using 1% and 6% KCl also showed 'no nitrate' after blank subtraction. Additionally, blanks for 3% KCl were lower, compared to other extractants, with highest for 6% KCl. Furthermore 3% KCl showed the expected 'extraction range' of increasing NO_3^- with increasing volume (Figure 5-6a). Consistent concentrations of nitrate were recorded with 2 ml and 3 ml of KCl solutions, while 3 ml of DI showed lower concentration.

NH_4^+ concentrations varied between 0.88 mg/kg (5 ml of 6%) to 49.93 mg/kg (5 ml of 1% KCl; Figure 5-6b). Procedural blanks were consistently low, resulting in NH_4^+ concentrations recorded in all extractants and volumes. Ammonium concentrations were consistent for 2 ml, 3 ml and 4 ml and KCl solutions (of different strengths), while 3 ml DI and 2 ml 3% KCl showed lower values.

Wilcoxon rank test was applied to NO_3^- and NH_4^+ concentrations, to investigate differences between extraction solvents and solvent volumes. No statistical significance was found for NO_3^- and extraction solvents ($p > 0.05$; Table 5-5). In contrast, all extraction volumes were significantly different (Table 5-5; Figure 5-7) from 1 ml, again indicating saturation of very small volumes.

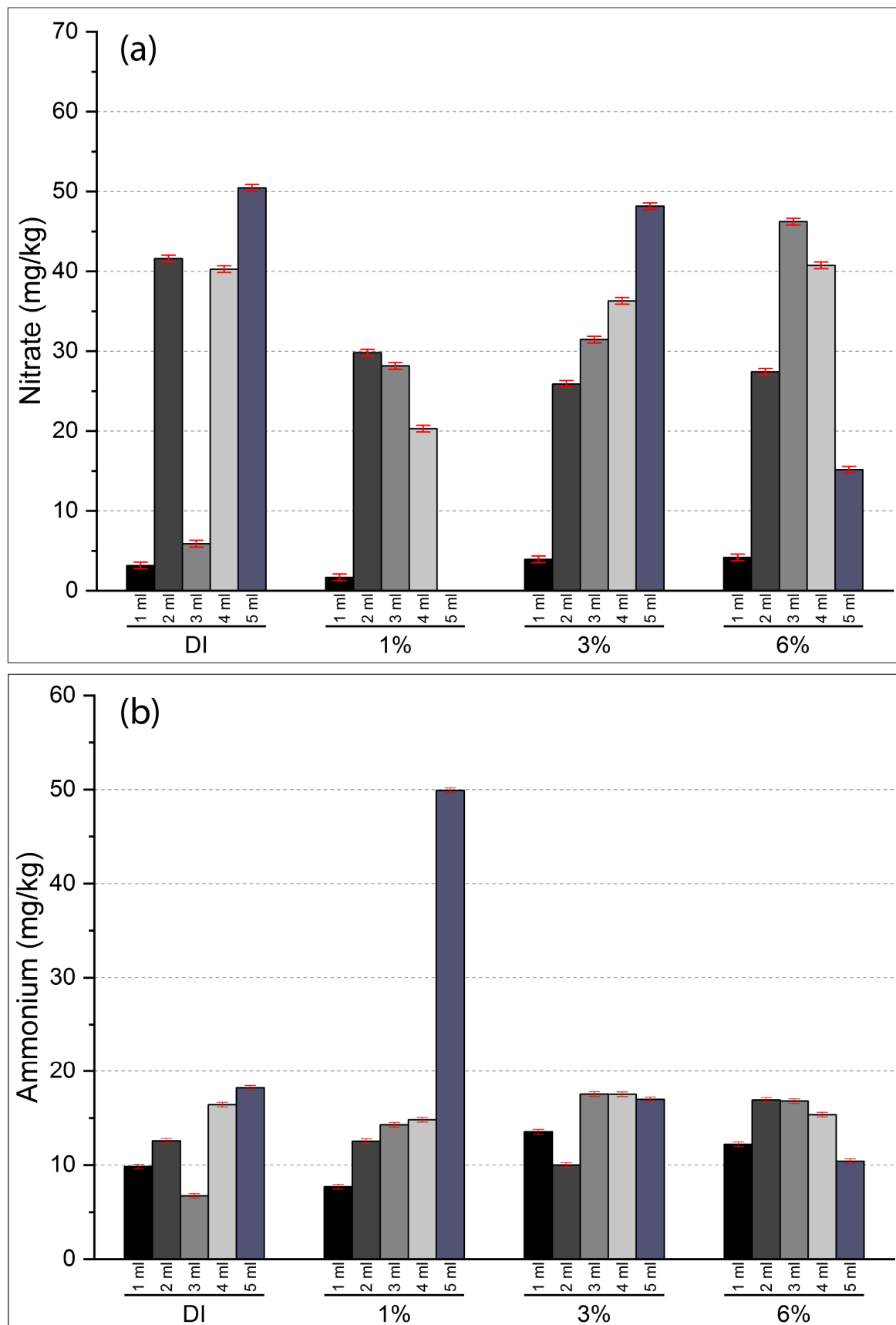


Figure 5-6: Extracted (a) nitrate and (b) ammonium from lichen material (triplicates, in mg/kg) using different solvents KCl, grouped by solvent and solvent volume), error-bars are presented as 1x standard deviation (CRM-derived: NO_3^- 6.42% and NH_4^+ 6.30%)

Table 5-5: Wilcoxon rank test p-values (*significant at the level $p < 0.05$ presented in bold and shaded in green) to investigate and compare extraction solvents (left) and extraction volumes (right) for nitrate and ammonium concentrations

Solvent	Nitrate	Ammonium	Volumes	Nitrate	Ammonium
DI vs 1%	0.88	0.81	1 ml vs 2 ml	0.02*	0.20
DI vs 3%	0.13	0.81	1 ml vs 3 ml	0.02*	0.15
DI vs 6%	0.13	0.44	1 ml vs 4 ml	0.03*	0.06
1% vs 3%	0.25	0.44	1 ml vs 5 ml	0.01*	0.31
1% vs 6%	0.38	>0.99	2 ml vs 3 ml	>0.99	0.95
3% vs 6%	0.31	0.06	2 ml vs 4 ml	0.84	0.55
			2 ml vs 5 ml	0.63	0.74
			3 ml vs 4 ml	0.56	0.84
			4 ml vs 5 ml	0.88	0.64

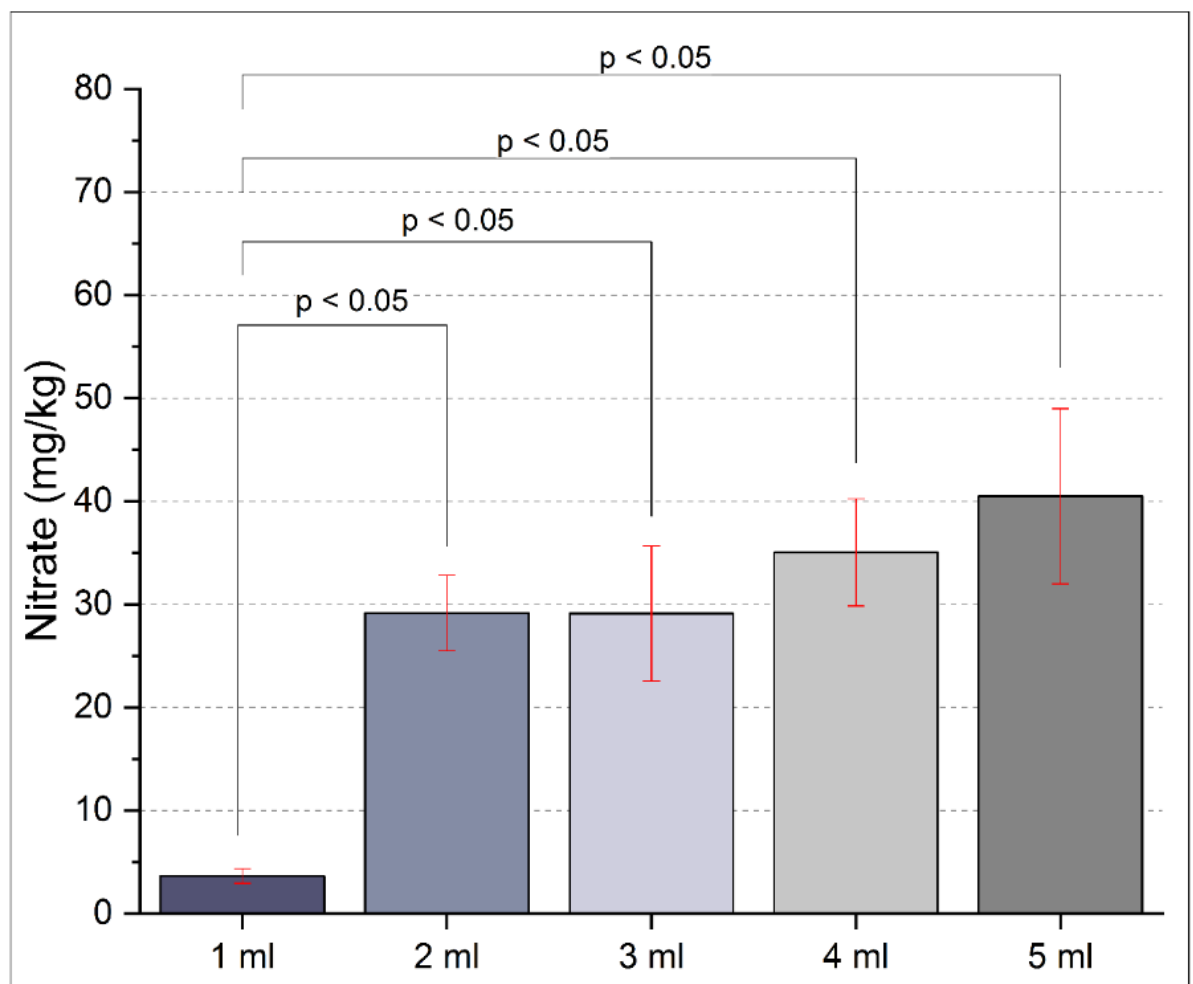


Figure 5-7: Comparison of nitrate with extraction volumes (presented as bar charts with 1x standard error of the mean concentration); displayed with statistical significance of differences (as presented in Table 5-6)

Results suggested that potassium chloride (3%) is able to effectively extract nitrate and ammonium, while higher variability was found for deionised water (18.2 MΩ). Because of the consistent results given for 3% KCl, 2 ml and 3 ml and low analytical blanks for NO₃⁻ and NH₄⁺ (with 3% KCl), further testing using these variables was implemented. 2 ml was chosen over 4 ml (for KCl solutions), because of variability of nitrate for higher volumes used (i.e. 4 ml and 5 ml; Figure 5-4).

Additionally, 6h extraction time was added to simulate a “laboratory day” and to achieve same-day extraction and IC analysis for NO₃⁻ and NH₄⁺. Moreover, reduced extraction times could reduce variability of nitrate and more consistent values for ammonium.

5.5.3 Experiment 3: Extraction using 3% KCl

Extraction of NO₃⁻ and NH₄⁺ from lichens was further tested using 3% KCl (~0.5 M) for 6 hours and 24 hours, only using 2 and 3 ml of extractant. Experiment #3 revealed consistent values for NO₃⁻ for both extraction volumes and 6h extraction time, ranging from 95.7 mg/kg to 105.1 mg/kg. Highest values, for all undertaken experiments, were furthermore achieved using 6 hours extraction and non-vortexing (for both volumes; Figure 5-8). Extracting lichen material for 24 hours with 3% KCl gave low nitrate concentrations (~5 mg/kg). Nitrate in blanks were high for 24 hours extractions, thus resulting in unrecorded concentrations in 2 ml and 3 ml for 24 hours (after blank subtraction). In contrast, 6 hours blanks were consistently low for both volumes. For all extractants, consistent ammonium values have been observed, ranging from 12.8 mg/kg to 18.9 mg/kg. Highest values were achieved for 3 ml and 24h extraction, with 17.4 mg/kg to 18.9 mg/kg (Figure 5-8).

Nitrate extraction, especially for 24 hours showed ‘not enough valid cases’ to statistically compare (by Wilcoxon test; Table 5-6) extracted nitrate concentrations, for solvent volumes and extraction times. In contrast, ammonium concentrations were significantly ($p < 0.05$) different for each test variable (Table 5-6; Figure 5-9). Slightly higher concentrations of ammonium using 24h extraction time were achieved but were negligible in comparison with extracted nitrate concentrations (Figure 5-9).

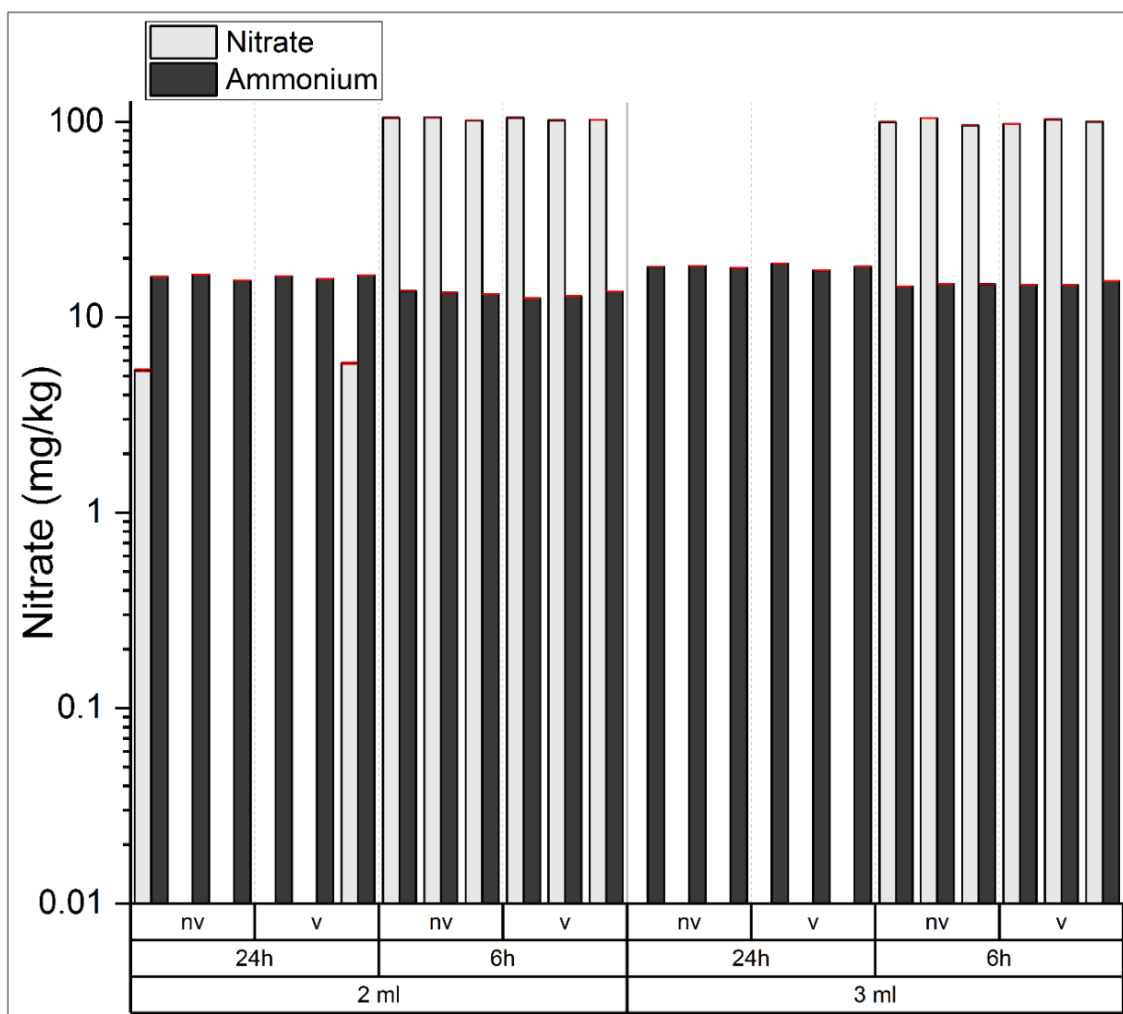


Figure 5-8: Concentrations of nitrate and ammonium (in mg/kg) (\log_{10} scale; bar charts, presented with CRM derived 1x standard deviation of NO_3^- : $\pm 0.91\%$ and NH_4^+ : $\pm 1.07\%$); shown for 3% KCl, with 2 ml and 3 ml, 24 and 6 hours extraction time and vortexting (v) and non-vortexting (nv)

Table 5-6: Wilcoxon rank test p-values (*significant at the level $p < 0.05$ presented in bold and shaded in green) to investigate and compare extraction volumes (2 ml and 3 ml) and extraction times (6 and 24 hours) for nitrate and ammonium concentrations; comparison of vortexting and non-vortexting is also shown; N/A indicates that not enough valid cases to perform Wilcoxon test for statistical comparison

	Nitrate	Ammonium
2 ml (6h) vs 2 ml (24h)	0.18	0.03*
2 ml (24h) vs 3 ml (24h)	N/A	0.03*
2 ml (6h) 3 ml (6 h)	0.09	0.03*
3 ml (6h) vs 3 ml (24h)	N/A	0.03*
Vort. vs non-vort.	0.93	0.97

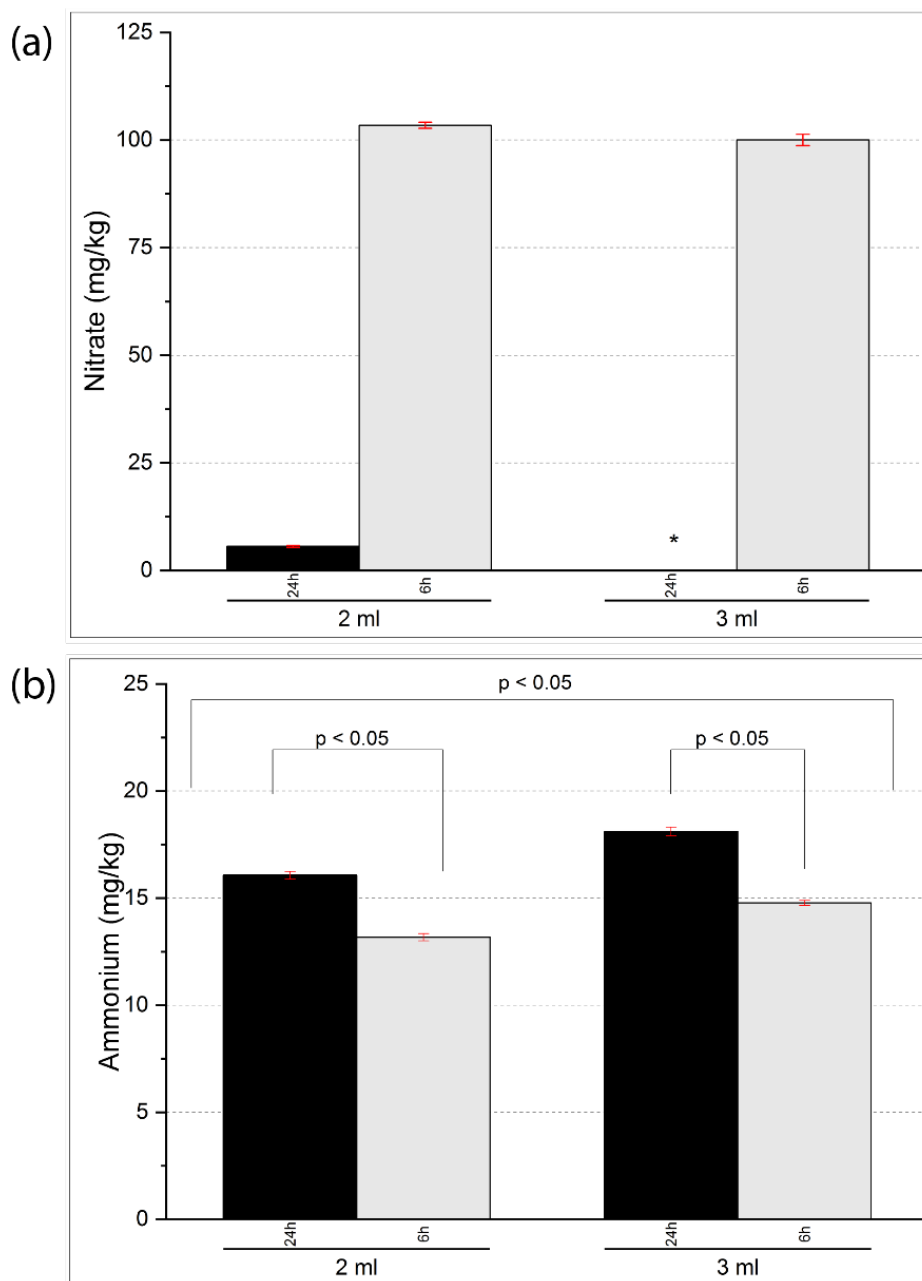


Figure 5-9: Comparison of (a) nitrate and (b) ammonium with extraction volumes (in mg/kg) (presented as bar charts with 1x standard error of the mean); displayed with statistical significance of differences (as presented in Table 5-7); * indicates that no nitrate was extracted (or blank subtraction resulted in negative value)

Methodological development to investigate extractability of nitrate and ammonium from lichen material was based on extraction procedures for inorganic nitrogen of in soils. Application of 2 M (15%) and 1 M (7.5%) KCl solutions showed high variability in comparison to other tested extractants. Moreover, reduced extraction time might have resulted in less microbial activity to reduce NO_3^- (EPA, 2007) within the tube and subsequently lower blanks.

Additionally, 24 hours extraction time obtained very low or negative nitrate values after blank subtraction, favouring the use of 'lab day' extraction and analysis.

Results illustrated the adaption of 6 hours for extraction according to low nitrate and very low ammonium blanks and consistent extracted concentrations (for 3 ml used). The chosen extraction method, described in this section, was therefore applied to rural and urban lichen samples, to compare NO_3^- and NH_4^+ in contrasting environments.

5.5.4 Application of optimised chemical extraction method to urban and rural lichen samples.

Lichen samples, *Xanthoria parietina* and *Physcia* spp., sampled from street trees in the urban environment of Manchester (Figure 5-1) and around a poultry farm (*X. parietina* only, Figure 5-2) were analysed following the determined extraction procedure, using 0.05 g of lichen material with 3 ml (lichen mass-to-extractant ratio 1:60) of 3% potassium chloride (KCl). Samples were extracted for 6 hours ('laboratory day'), filtered through 0.2 μm nylon filters, diluted to 1% KCl strength (1:3 with ultrapure water, 18.2M Ω) and subsequently analysed by IC (same day extraction and analysis; Figure 5-3). Lichen samples were extracted and analysed in batches and datasets were investigated for batch-to-batch bias by analysis of certified reference materials and diluted calibration standard throughout IC analysis.

5.6 Results – nitrate and ammonium in rural and urban lichen samples

5.6.1 Assessment of accuracy and precision of nitrate and ammonium concentrations by ion chromatography (IC)

This section focusses on the accuracy and precision for analytical batches of NO_3^- and NH_4^+ to inform potential data bias. Concentrations of nitrate (in certified reference material) and ammonium (in certified calibration standard, diluted as reference material) were not drawn from a normal distribution (Shapiro-Wilk, $p < 0.05$). Therefore, Friedman's test (two-way analysis of variance; non-parametric test) was used to evaluate differences between analysed batches. Friedman's test of variance showed significant differences ($p < 0.05$) between analysed batches for NO_3^- and NH_4^+ , indicating either preparation (random errors) and/or analytical problems (systematic errors). Extraction solutions (KCl) and analytical (certified) reference solutions were made up freshly each time before analysis, therefore preparation errors (i.e. pipetting, weighing of KCl and dilution) could have influenced recorded NO_3^- and NH_4^+ concentrations.

Nitrate concentrations recorded in CRM were consistently lower than the certified value, while NH_4^+ was more variable. NH_4^+ reference material was made up from a dilution of calibration standard and pipetting and standard preparation errors are most likely to have occurred before IC analysis. However, Figure 5-10 illustrates measured mean values of NO_3^- (Figure 5-10a) and NH_4^+ (Figure 5-10b) for each analytical batch, with batch accuracy found between 83% to 92% (for NO_3^-) and 94% to 115% (for NH_4^+). Overall batch-to-batch precision was <5% for NO_3^- and <8% for NH_4^+ . Accuracy and precision illustrates practicability of IC measurements for nitrate and ammonium, with minor underestimation of nitrate concentrations. However, a batch-to-batch correction was not undertaken, due to consistency of NO_3^- and NH_4^+ for all analytical batches.

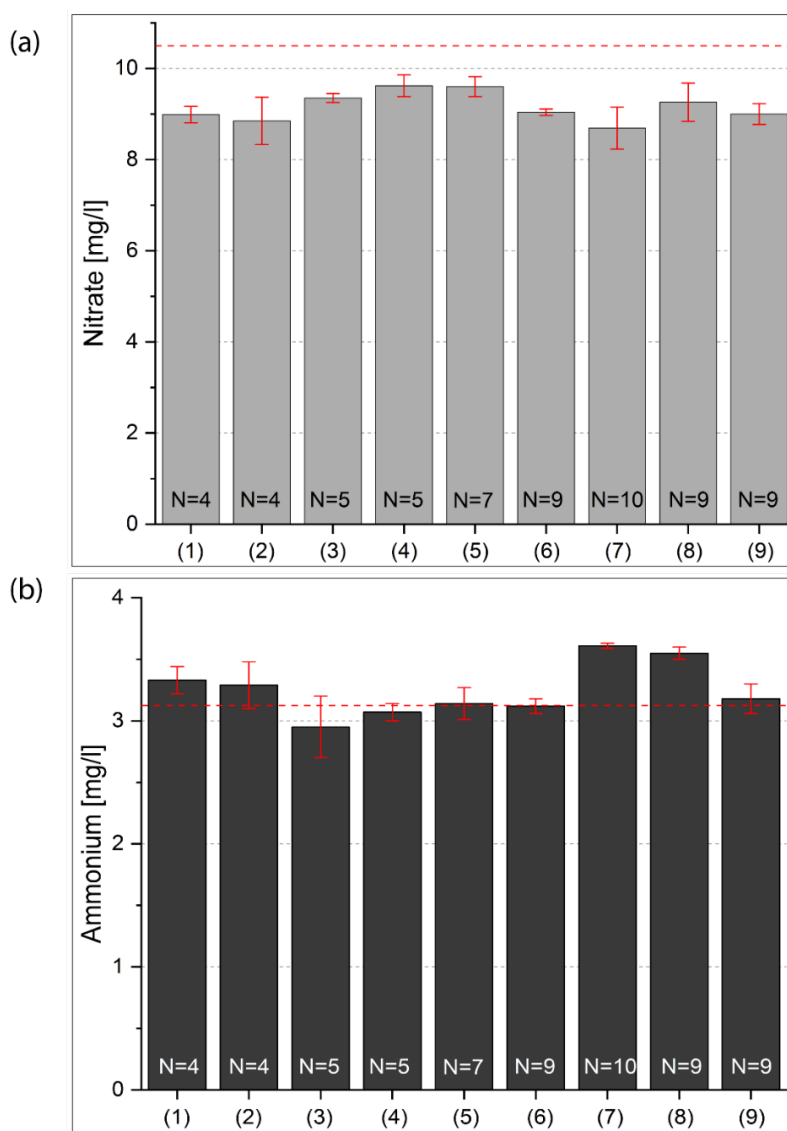


Figure 5-10: (a) Nitrate and (b) ammonium concentrations analysed for each KCl extraction batch (N=62), displayed with number analysed per batch (error bars are presented as 1x standard deviation); dashed line represent certified values (nitrate: 10.5 mg/l and ammonium: 3.125 mg/l)

Table 5-7 displays the certified and measured values of nitrate and ammonium recorded for all analytical batches (N=62). Overall accuracy for NO_3^- and NH_4^+ was found at 87% and 105%, respectively. Precision (overall, %CV) was <5% for nitrate and at 7.5% for ammonium. Lower limits of detection were calculated as three times the standard deviation of the procedural blanks (N=46), calculated separately for each analytical batch (displayed as range).

Procedural blanks were additionally used for blank subtraction (separate for each analytical batch), to exclude contamination from equipment and preparation methodology.

Table 5-7: Certified and measured values of nitrate and ammonium for all analytical batches (N=62), with overall accuracy (%), overall precision (%CV) and lower limits of detection (LLD) ranges

	Certified value [mg/l]	Measured value [mg/l]	Accuracy (%) - overall	Precision (%CV) - overall	LLD [mg/l] (Min-Max)
Nitrate (NO_3^-)	10.50 ± 0.187	9.13 ± 0.42	86.92	4.64	0.09 – 0.41
Ammonium (NH_4^+)	3.125 ±	3.28 ± 0.25	104.93	7.52	0.01 – 0.13

5.3.2 Temporal variability of lichen nitrate and ammonium concentrations

Initial lichen sampling was undertaken between June 2016 and October 2017. To investigate, if nitrate and ammonium concentrations in lichens vary over time, 17 sites were re-visited (in 2018) and NO_3^- and NH_4^+ was extracted according the optimised method (section 5.5.3 – ‘laboratory day’) and analysed by IC. In general, a downward trend in nitrate and ammonium concentrations was found for the second sampling period. However, nitrate concentrations were variable for each re-visited site (Table 5-8). Nitrate concentrations were compared using a Wilcoxon test (non-parametric), whereas ammonium concentrations were compared using a paired t-test. No significant differences between NO_3^- concentrations) was found, whereas NH_4^+ concentrations were significantly different for the sampling periods (Table 5-8). Findings suggest temporal variations of both, nitrate and ammonium concentrations, although not significant for NO_3^- (Figure 5-11). Lichens as organisms might employ both species during their metabolism, which could explain differences over the sampling periods. However, spatial variability of NO_3^- and NH_4^+ could still indicate degraded air quality across Manchester, although temporal variations might occur.

This in return could also be related to the lichen species and their species-specific uptake ability of nitrogen compounds. Spatial variability of nitrate and ammonium concentrations will be presented hereafter. Temporal variability, species-specific uptake of NO_3^- and NH_4^+ , together with implications for spatial variability will be discussed in section 5.5.4.

Table 5-8: Comparison of nitrate (NO_3^-) and ammonium (NH_4^+) concentrations [in mg/kg] in *X. parietina* (N=17) for different sampling periods undertaken in 2016/17 (1) and same sites re-visited in 2018 (2) to investigate temporal bias

	NO_3^- (1)	NO_3^- (2)	NH_4^+ (1)	NH_4^+ (2)
1	100.03	106.88	8.043	2.409
2	35.57	5.944	5.111	2.722
3	64.43	111.9	7.481	2.901
4	49.68	3.357	11.28	2.695
5	88.52	17.59	11.03	2.729
6	109.5	4.431	5.058	1.961
7	5.319	29.07	11.110	3.719
8	75.80	26.93	10.59	4.261
9	91.29	18.52	8.998	3.687
10	46.71	12.44	12.92	2.570
11	37.57	125.62	5.772	3.796
12	36.75	N/A	5.610	1.899
13	45.18	16.48	7.987	3.337
14	85.03	71.81	2.428	2.428
15	27.40	29.26	9.352	3.359
16	50.42	9.85	5.941	1.719
17	94.34	16.24	11.861	3.893
	Wilcoxon (two-tailed) p-value		Paired t-test (two-tailed) p-value	
	p=0.083		p<0.01**	

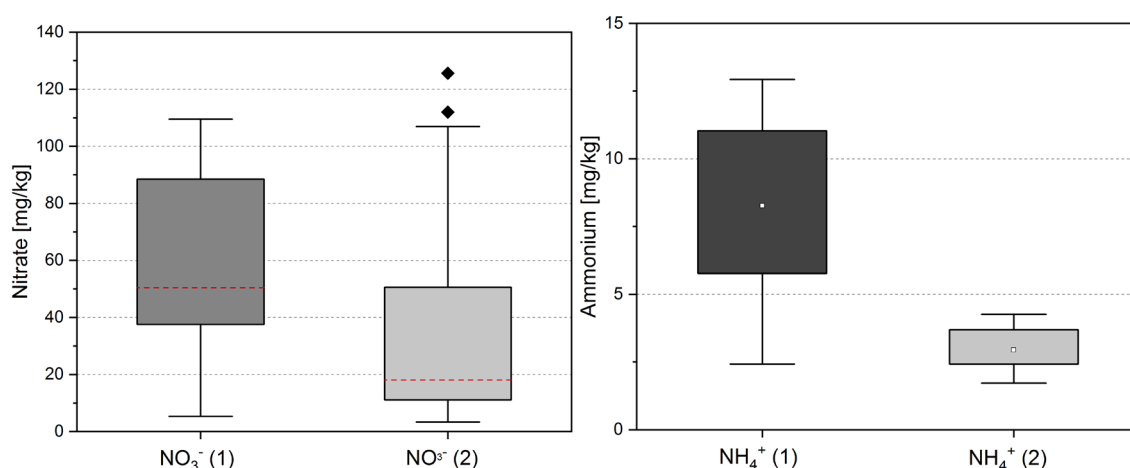


Figure 5-11: Box-Whisker plots (25th to 75th percentile) of nitrate [left] and ammonium concentrations [lower panel] concentrations recorded for sampling periods undertaken in 2016/17 (1) and 2018 at the same site (2); displayed with median line (non-normal distributed data) and mean: whit square (normally distributed data)

5.6.3 Nitrate and ammonium concentrations in urban lichen samples (*X. parietina* and *Physcia* spp.)

Extraction of nitrate and ammonium (using 3 ml of 3% KCl for 6 hours) was applied to urban lichen samples of *X. parietina* (N=87) and *Physcia* spp. (N=48) sampled in 2016/2017. Site-specific data is shown in the Appendix C-2. Species-specific differences in NO_3^- and NH_4^+ were investigated and spatial patterns of across Manchester were further analysed. Table 5-9 shows the recorded concentration ranges of NO_3^- and NH_4^+ in *X. parietina* and *Physcia* spp. Median (\tilde{x}) concentrations (due to non-normality of data) were recorded higher in *X. parietina*, for both, NO_3^- and NH_4^+ .

Table 5-9: Nitrate and ammonium concentration (in mg/kg) ranges of *X. parietina* and *Physcia* spp., displayed with median (\tilde{x}) values due to non-normality of data (values are shown as three significant figures)

	<i>X. parietina</i> (N=87)	<i>Physcia</i> spp. (N =48)
NO_3^-	1.02 to 143 mg/kg ($\tilde{x} = 48.5$ mg/kg)	0.796 to 170 mg/kg ($\tilde{x} = 26.8$ mg/kg)
NH_4^+	3.18 to 27.7 mg/ kg ($\tilde{x} = 9.35$ mg/kg)	2.69 to 15.5 mg/kg ($\tilde{x} = 6.28$ mg/kg)

A Mann-Whitney test was used (non-parametric test) to investigate differences of NO_3^- and NH_4^+ concentrations between *X. parietina* and *Physcia* spp. (Table 5-10). Highly significant ($p < 0.01$) differences were found between both lichen species for nitrate and ammonium concentrations, with higher concentrations in *X. parietina* (Figure 5-12).

Table 5-10: Mann-Whitney test statistics (p-value, two-tailed) for nitrate and ammonium, recorded in *X. parietina* and *Physcia* spp.; ** significant at the level $p < 0.01$ in bold and shaded in green)

Mann-Whitney p-value (two-tailed)	
NO_3^-	0.01**
NH_4^+	<0.01**

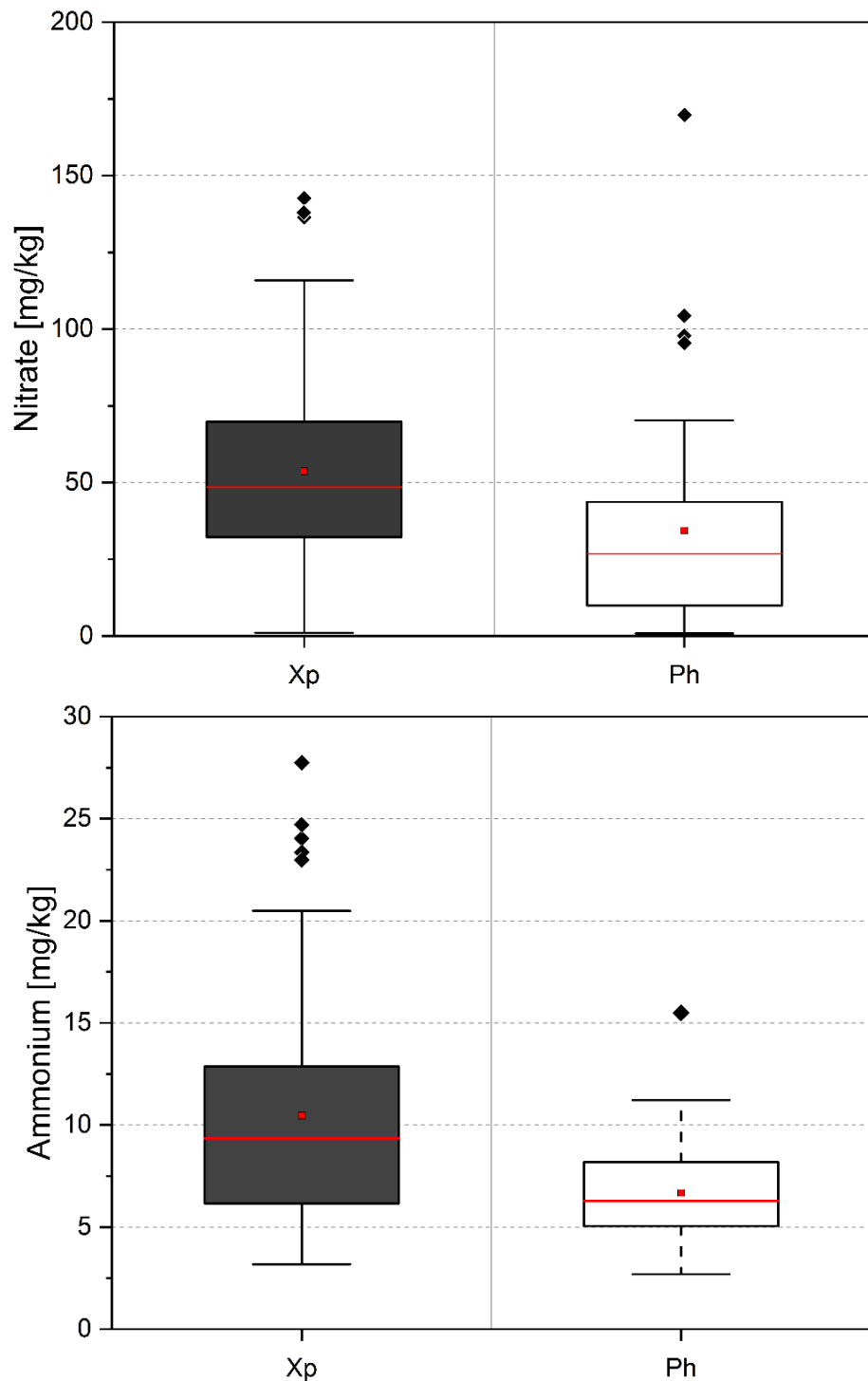


Figure 5-12: Box-whisker plots (25th and 75th percentile, displayed with mean (red square) and median line and extreme values: black diamonds) for comparison of nitrate [above] and ammonium concentrations [below] (in mg/kg) recorded in *X. parietina* (left, N=84) and *Phycia* spp. (right, N=48)

Concentrations of nitrate and ammonium in both lichen species were spatially variable across Manchester. To investigate spatial patterns, ordinary kriging (OK) was applied to lichen-derived NO_3^- and NH_4^+ concentrations. Spatial patterns for NO_3^- are displayed in Figure 5-13a and b. Higher NO_3^- (>68 mg/kg) in *X. parietina* was recorded in samples in the northeast and southeast of the research area, showing distinct 'hotspots' of high NO_3^- (Figure 5-13a).

In contrast, NO_3^- concentrations in *Physcia* spp. (Figure 5-13b) were generally low across the research area. However, elevated concentrations (>34 mg/kg) in NO_3^- (recorded in *Physcia* spp.) were also found in the north-eastern research area, which is comparable to concentrations recorded in *X. parietina*. Ammonium concentrations in both lichen species (Figure 5-14a and b) showed elevated concentrations across the city centre area, with NH_4^+ recorded in *X. parietina* extending across the city centre and primary road network (i.e. A- roads and motorways). A comparable pattern (of NH_4^+) was found for *Physcia* spp. (Figure 5-14b), but in contrast to *X. parietina*, NH_4^+ concentrations in *Physcia* spp. were consistently lower. However, findings suggest elevated NH_4^+ primarily within the city centre of Manchester.

To investigate relationships between recorded NO_3^- and NH_4^+ concentrations on lichen N contents (wt%) and nitrogen isotope-ratios ($\delta^{15}\text{N}$), Spearman ρ correlation was applied (non-parametric, due to non-normal distribution). No statistical significance ($p>0.05$) was found between NO_3^- concentrations and nitrogen contents in *X. parietina* (Figure 5-15a). In contrast, significant negative correlation ($p<0.05$) was found for *Physcia* spp. (Figure 5-15b). Both lichen species showed highly significant ($p<0.01$) positive relationship between ammonium concentrations and N wt% and $\delta^{15}\text{N}$ (Figure 5-16). Effects on lichen N and $\delta^{15}\text{N}$ values by NO_3^- and NH_4^+ are discussed later in this chapter (section 5.4.3).

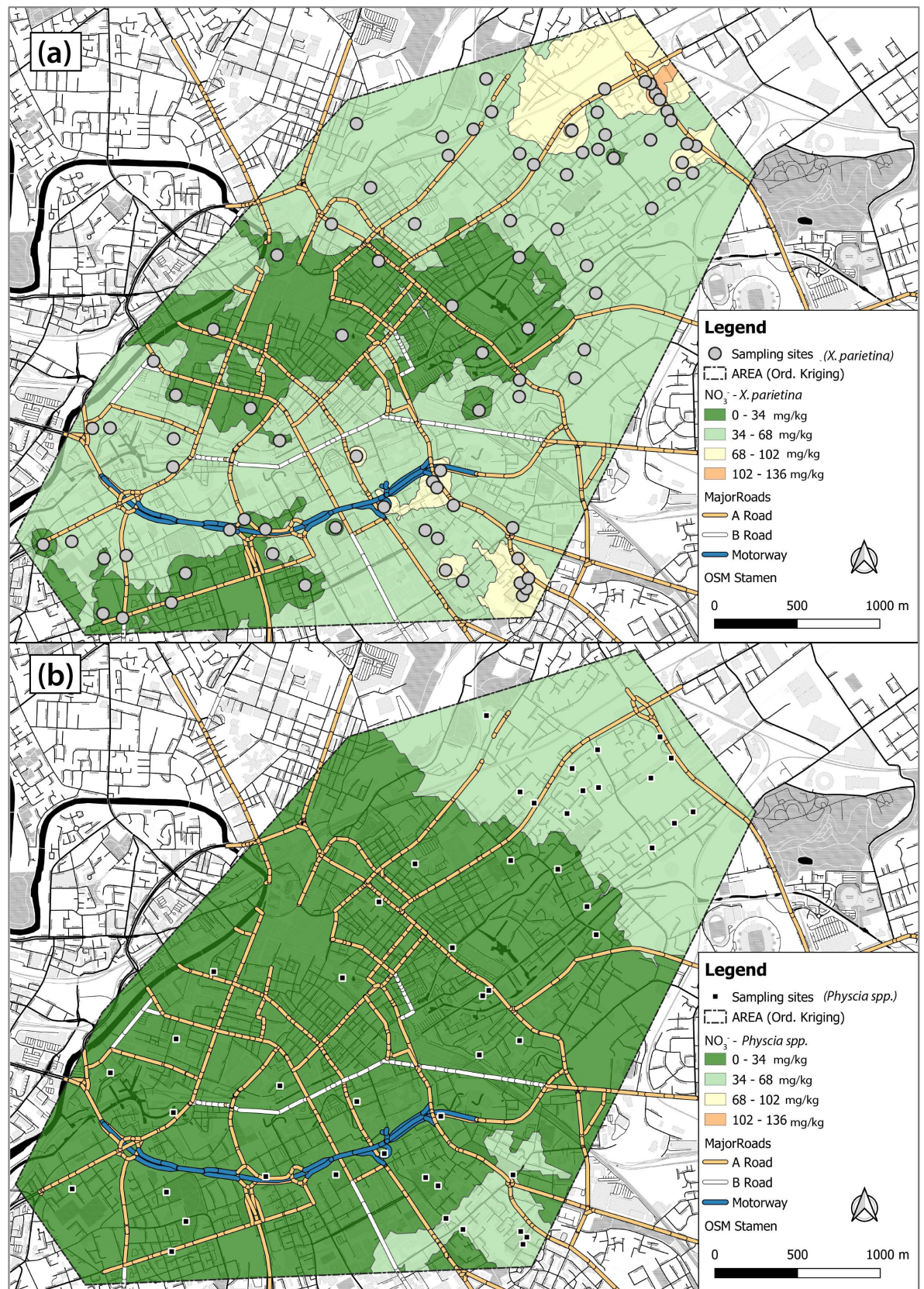


Figure 5-13: Nitrate concentrations (in mg/kg) (interpolated by ordinary kriging) in (a) *X. parietina* and (b) *Physcia* spp. to analyse spatial patterns across Manchester (kriging error maps in Appendix C-4); no NO₃⁻ limit value (in air) available.

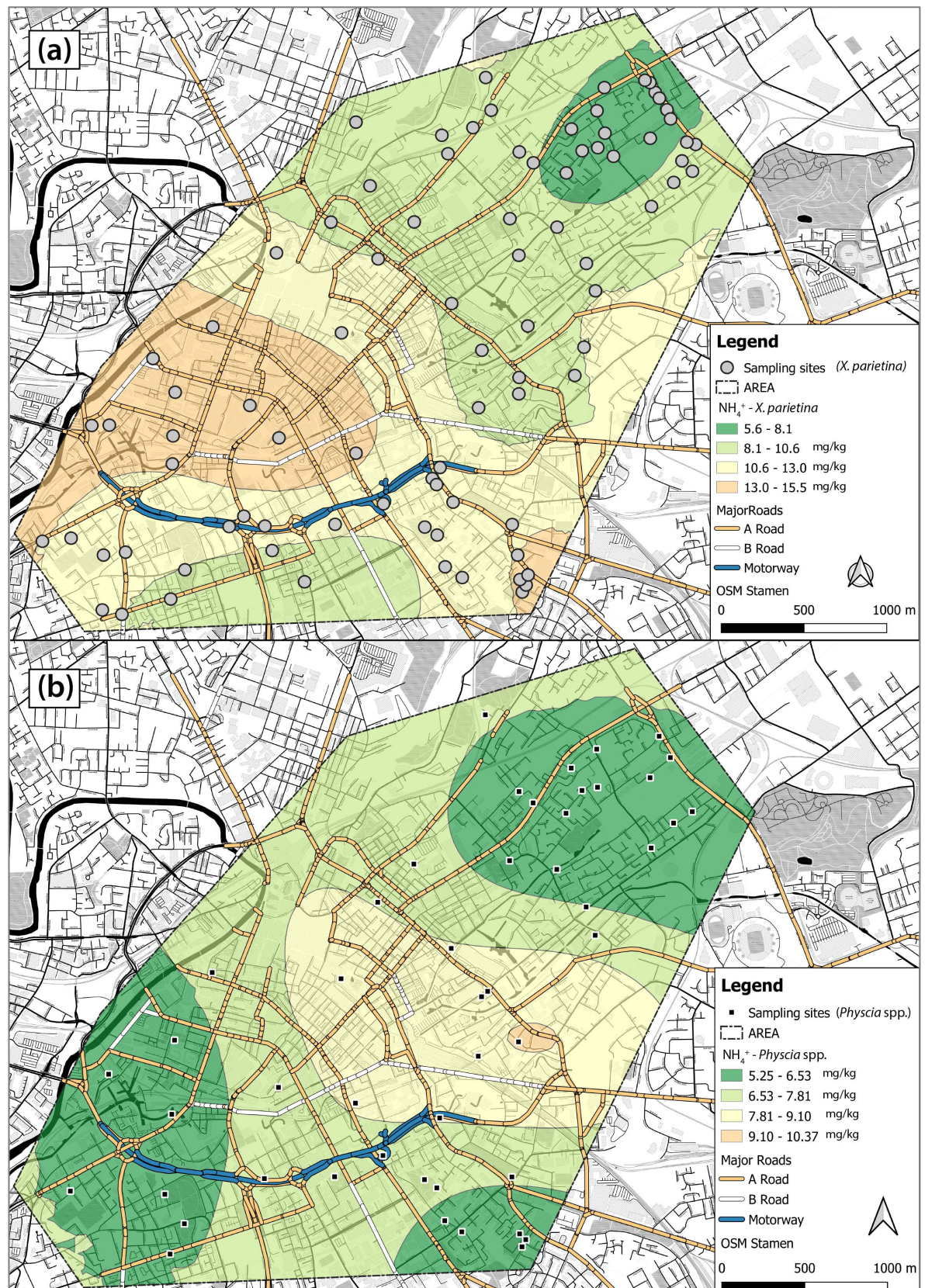


Figure 5-14: Ammonium concentrations (in mg/kg) (interpolated by ordinary kriging) in (a) *X. parietina* and (b) *Physcia* spp. to analyse spatial patterns across Manchester (kriging error maps in Appendix C-5); no NH_4^+ limit value (in air) available; classes not linked between lichen species for NH_4^+ , due to reduction in resolution.

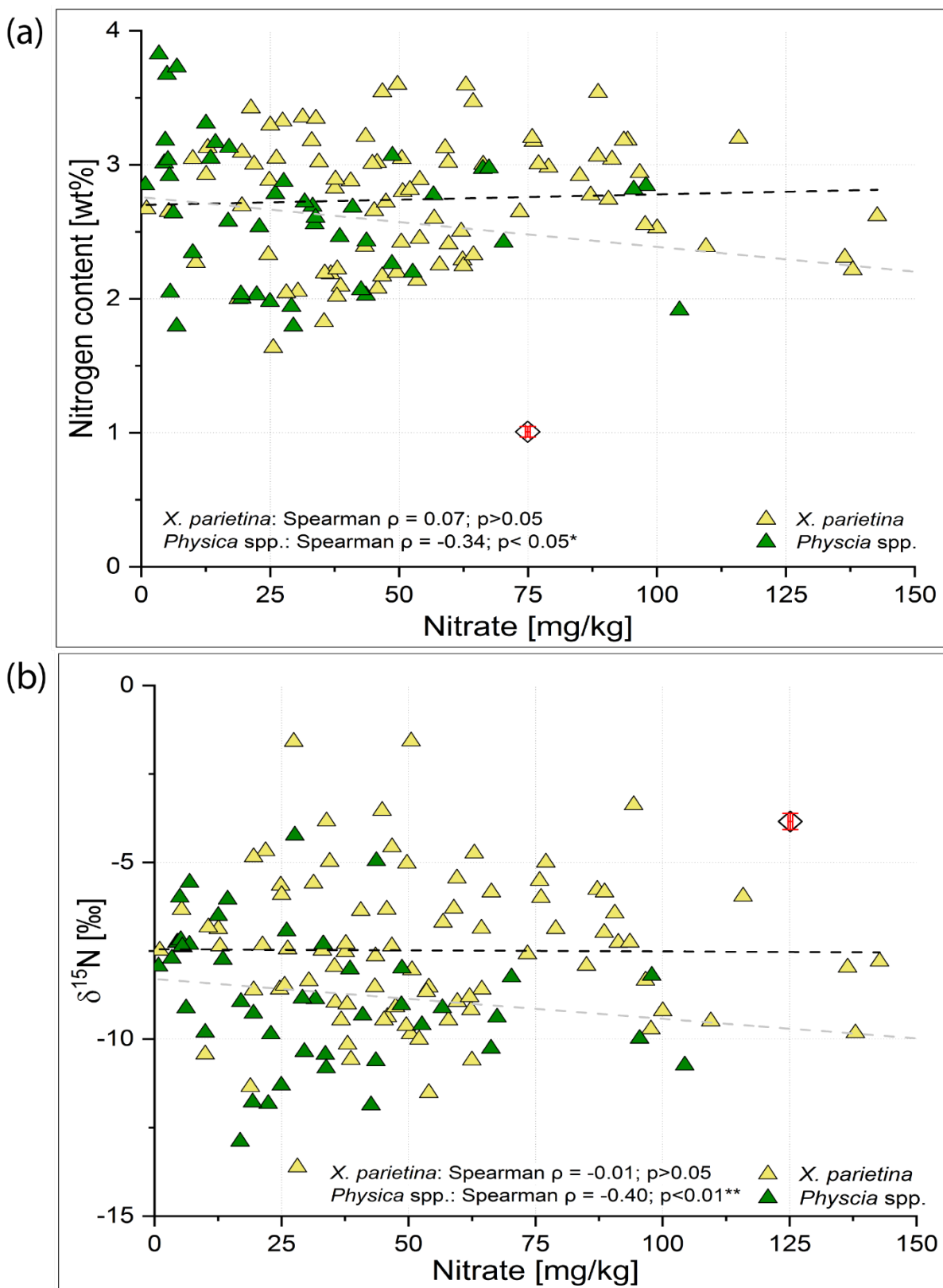


Figure 5-15: Scatterplot of nitrate concentrations (in mg/kg) for comparison with (a) nitrogen contents [wt%] and (b) $\delta^{15}\text{N}$ [‰] in *X. parietina* and *Physcia* spp. (CRM-derived error bars on dummy value: N wt% ± 0.04 ; $\delta^{15}\text{N}$ ± 0.23 ; NO_3^- ± 0.45 and NH_4^+ ± 0.25); displayed with correlation statistics (Spearman ρ ; *significant at the level $p < 0.05$; **significant at the level $p < 0.01$)

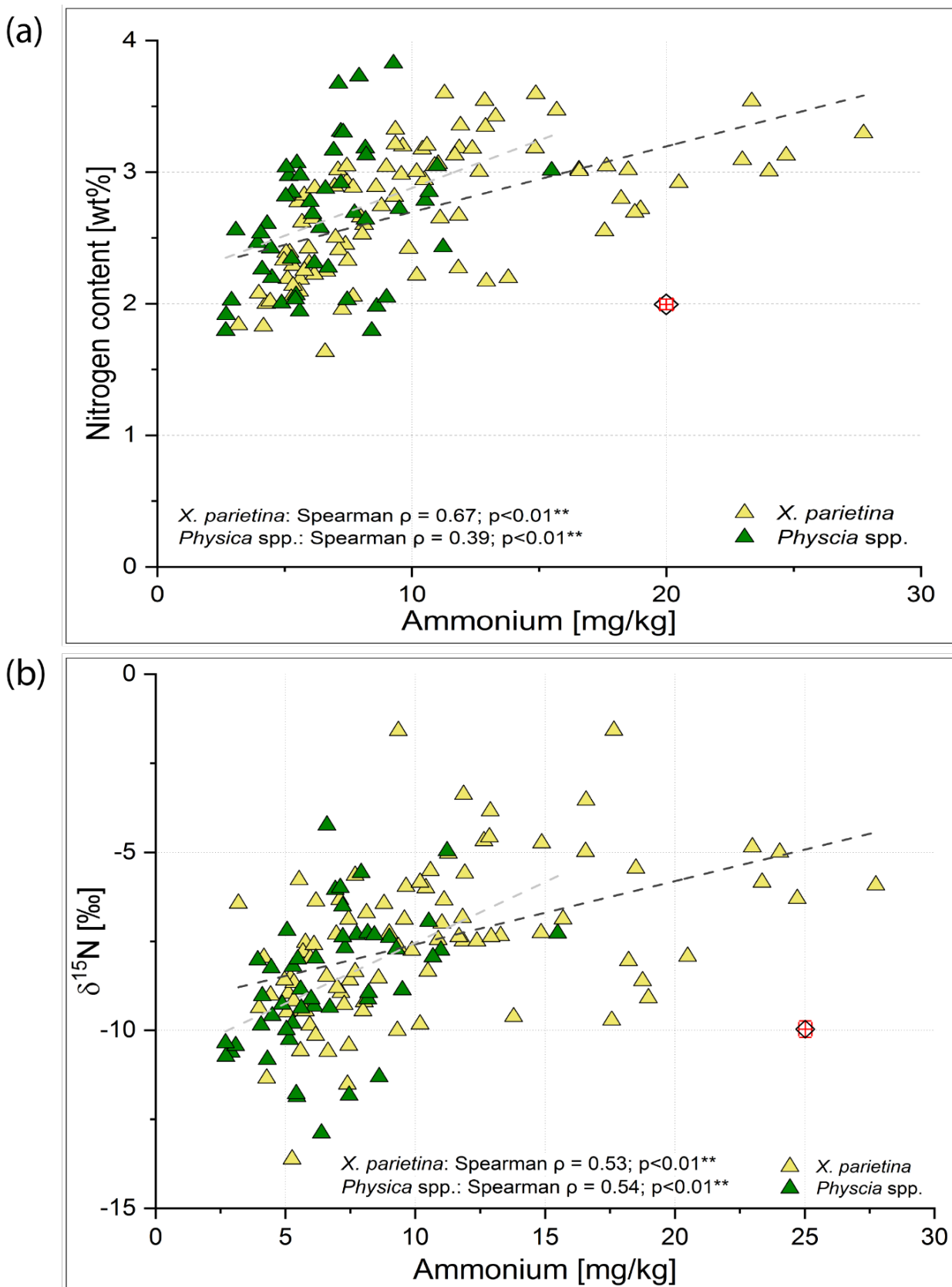


Figure 5-16: Scatterplot of ammonium concentrations (in mg/kg) for comparison with nitrogen contents [wt%] and $\delta^{15}\text{N}$ [‰] in *X. parietina* and *Physcia* spp. (CRM-derived error bars on dummy value: N wt% ± 0.04 ; $\delta^{15}\text{N}$ ± 0.23 ; NO_3^- ± 0.45 and NH_4^+ ± 0.25); displayed with correlation statistics (Spearman ρ ; *significant at the level $p < 0.05$; **significant at the level $p < 0.01$)

5.6.4 Nitrate and ammonium concentrations in rural lichen samples

Rural lichen samples were analysed for their NO_3^- and NH_4^+ concentrations to evaluate potential differences, when compared to an urban environment. Analysed nitrate and ammonium concentrations in rural *X. parietina* samples, together with N contents (wt%) and $\delta^{15}\text{N}$ (‰) are displayed in Table 5-11. Nitrogen contents (wt%) and $\delta^{15}\text{N}$ values were previously described in Chapter 4. Recorded nitrate concentrations were found between 1.07 mg/kg to 46.0 mg/kg (one site did not show NO_3^- ; ID: 11). Concentrations of ammonium were found between 9.18 mg/kg to 13.7 mg/kg (Table 5-11).

Table 5-11: Rural lichen (*X. parietina*, N =12) nitrogen contents (wt%), $\delta^{15}\text{N}$ (‰) and nitrate (NO_3^-) and ammonium (NH_4^+) concentrations, displayed as three significant figures; N/A – not assed by IC analysis

Site-ID	NO_3^- (mg/kg)	NH_4^+ (mg/kg)	N (wt%)	$\delta^{15}\text{N}$ (‰)
1	15.6	9.18	3.44	-6.36
2	5.81	9.46	3.34	-8.09
3	34.8	12.18	4.22	4.44
4	46.0	13.1	3.81	0.0280
5	11.6	13.7	3.95	-2.69
6	38.5	11.4	3.87	-1.06
7	24.9	10.2	3.51	-6.59
8	3.85	9.82	3.21	-7.61
9	9.99	11.6	3.39	-2.67
10	1.07	8.54	3.42	-5.95
11	N/A	8.99	3.09	-10.09
12	11.38	9.41	3.40	-6.68

Figure 5-17a and b illustrate recorded NO_3^- and NH_4^+ concentrations for each sampling site. Additionally Figure 5-17c, shows the percentage of nitrate and ammonium (of the total nitrate and ammonium concentrations) recorded in the lichen. NO_3^- and NH_4^+ ‘percentages’ in lichens also show variability based on location, with majority of sites containing primarily more NO_3^- than NH_4^+ . Figure 5-18 shows the analysed concentrations of nitrate (a) and ammonium (b) in *X. parietina*, colour-coded by recorded concentrations (low to high).

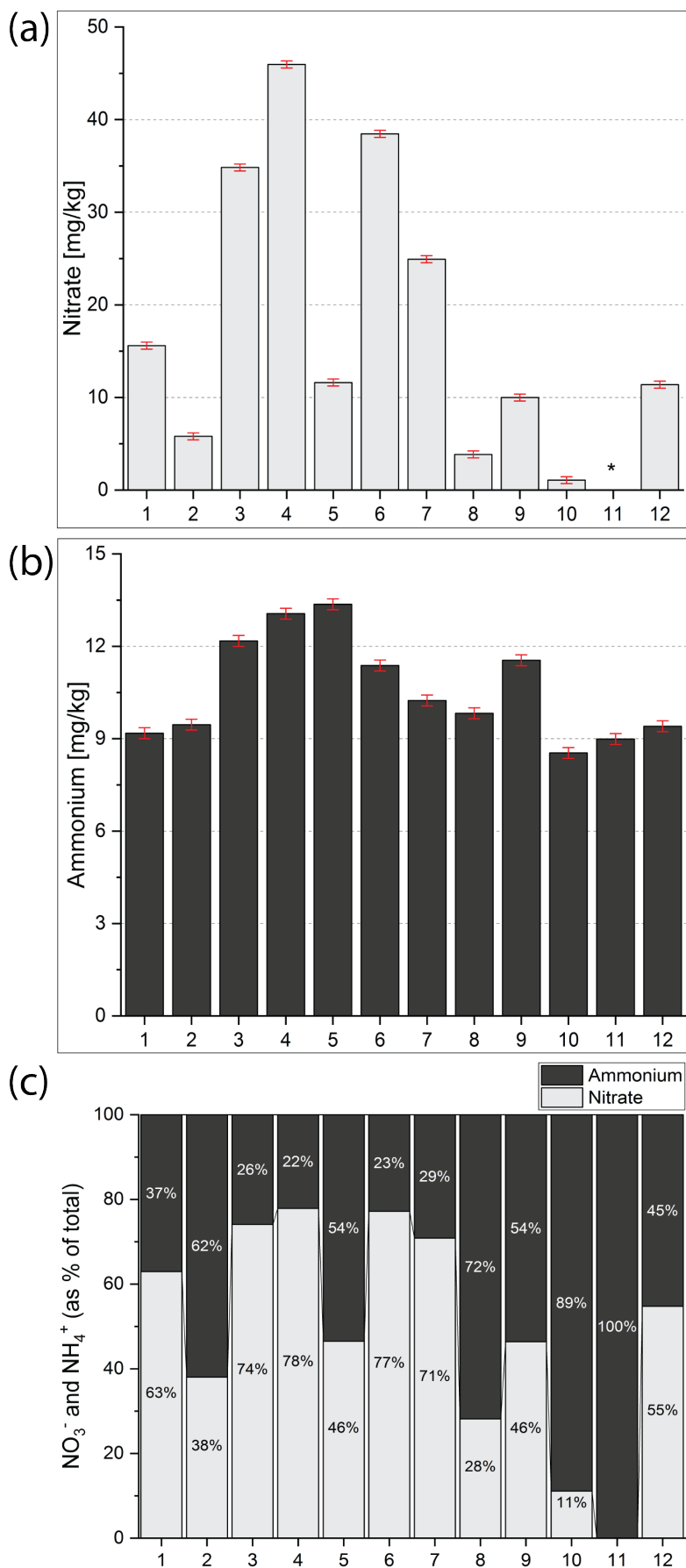


Figure 5-17: (a) Nitrate, (b) ammonium (both in mg/kg) and (c) NO₃⁻ and NH₄⁺ presented as percentage (of total recorded nitrate and ammonium) for each rural sampling site; error bars in (a) and (b) are presented as 1x standard deviation (CRM-derived: NO₃⁻: ±0.42 and NH₄⁺: ±0.25); * indicates missing value (not extractable NO₃⁻)



Figure 5-18: (a) Nitrate and (b) ammonium concentrations (mg/kg) in *X. parietina* around a poultry farm (colour-coded by concentration ranges), displayed with poultry farm, site-ID and sampling area around the farm

Pearson's correlation statistics were used to investigate NO_3^- and NH_4^+ concentrations with distance to poultry farm. However, no significant relationships were found for distance to farm and NO_3^- (Pearson's $r = -0.59$; $p = 0.06$) and NH_4^+ (Pearson's $r = -0.36$; $p = 0.26$) concentration. Figure 5-19 illustrates NO_3^- and NH_4^+ with distance to poultry farm (in ascending order) and indicates influences of poultry farm emissions, in particular for NO_3^- at locations in close proximity (<150 m). Pearson's correlation was further used to investigate relationships between nitrate and ammonium on nitrogen (N wt%) and $\delta^{15}\text{N}$ in rural *X. parietina*. Nitrogen contents were strongly positively correlated with nitrate ($p < 0.05$) and ammonium ($p < 0.05$) in *X. parietina*, as displayed in Figure 5-20. Presented results will be discussed in section 5.5.2.

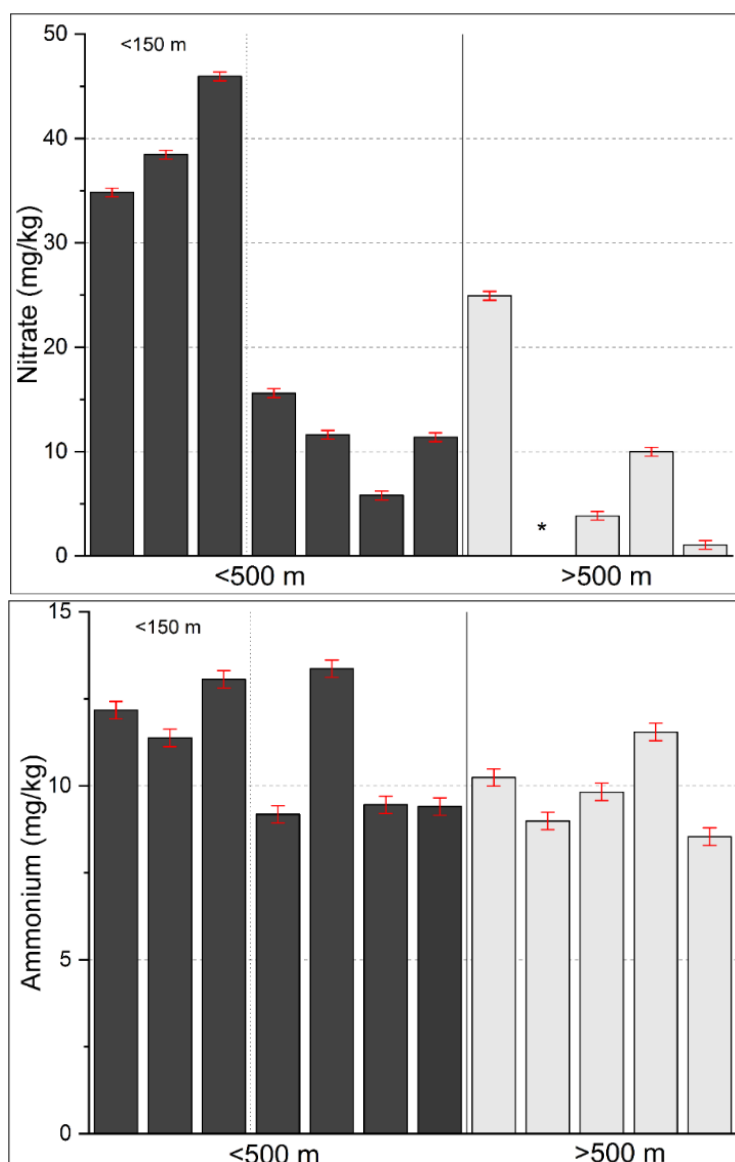


Figure 5-19: Concentrations of nitrate (above) and ammonium (below) in *X. parietina*, displayed with distance to poultry farm (<500 m and >500m), in ascending order; distances below 150 m are also shown (error bars are presented as 1x standard deviation of IC-CRMs, NO_3^- : ± 0.42 and NH_4^+ : ± 0.25)

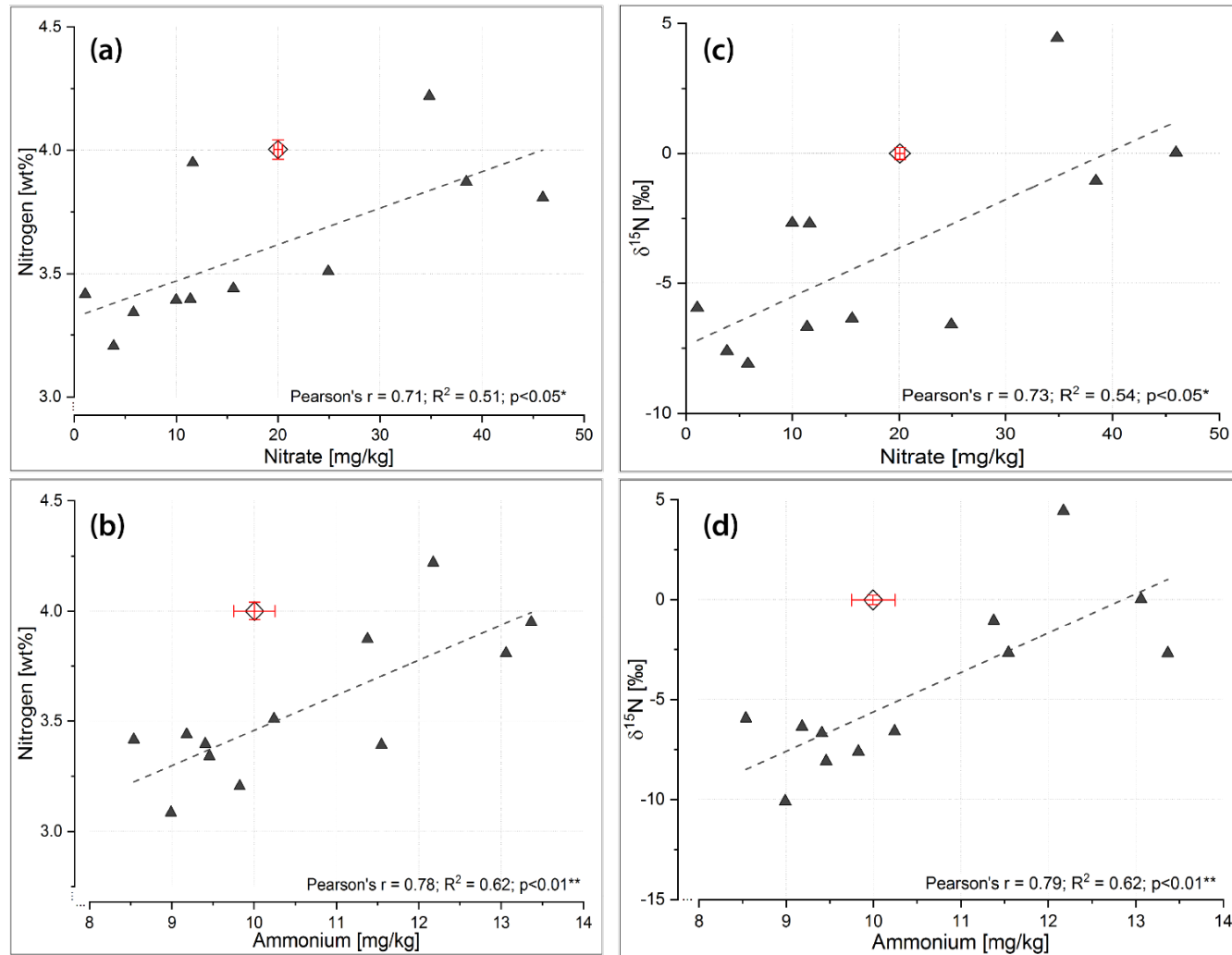


Figure 5-20: Scatter-plots of nitrate and ammonium concentrations recorded in rural *X. parietina* (N=12) samples, with nitrogen contents [wt%] (a) and (b) and $\delta^{15}\text{N}$ [‰] (c) and (d); error bars presented as 1x standard deviation, CRM-derived: N wt% ± 0.04 ; $\delta^{15}\text{N}$ ± 0.23 ; NO_3^- ± 0.42 and NH_4^+ ± 0.25 ; displayed with correlation statistics (Pearson's r , R^2 value and significance level; *significant at the level $p < 0.05$, **significant at the level $p < 0.01$)

5.6.5 Comparison of nitrate and ammonium in urban and rural lichen samples

Comparison of urban and rural lichen samples allowed to assess the variability of NO_3^- and NH_4^+ in contrasting environments and investigate potentially different sources. Nitrate and ammonium recorded in urban and rural samples of *X. parietina* were found variable in both environments (Table 5-12). Concentration ranges in urban samples of *X. parietina* were found higher, compared to rural samples, for nitrate and ammonium.

A Mann-Whitney test was used to evaluate differences in recorded concentrations of NO_3^- and NH_4^+ in rural and urban lichen samples. It was favoured, due to different outcomes in normality of data (i.e. rural: normal and urban: non-normal). Mann-Whitney test only showed statistically significant ($p < 0.01$; Table 5-12) differences for nitrate, but not for ammonium. Figure 5-21 displays the concentrations ranges of urban and rural NO_3^- and NH_4^+ concentrations, as box-whisker plots.

Table 5-12: Comparison of urban and rural samples of *X. parietina* concentration ranges (min. to max.) of nitrate (NO_3^-) and ammonium (NH_4^+) [in mg/kg; with mean and median concentrations] and statistical test (Mann-Whitney) to compare concentrations; ** significant at the level $p < 0.01$ bold and shaded in green

	NO_3^-	NH_4^+
Urban (N=87)	1.02 – 142.73 (\tilde{x} = 48.51 mg/kg)	3.18 – 27.74 (\tilde{x} = 9.35 mg/kg)
Rural (N=12)	1.07 – 45.96 (\bar{x} = 18.50 ± 15.23 mg/kg)	8.54 – 13.37 (\bar{x} = 10.60 ± 1.65 mg/kg)
Mann Whitney p-value (two-tailed)		
Urban vs rural	<0.01**	0.28

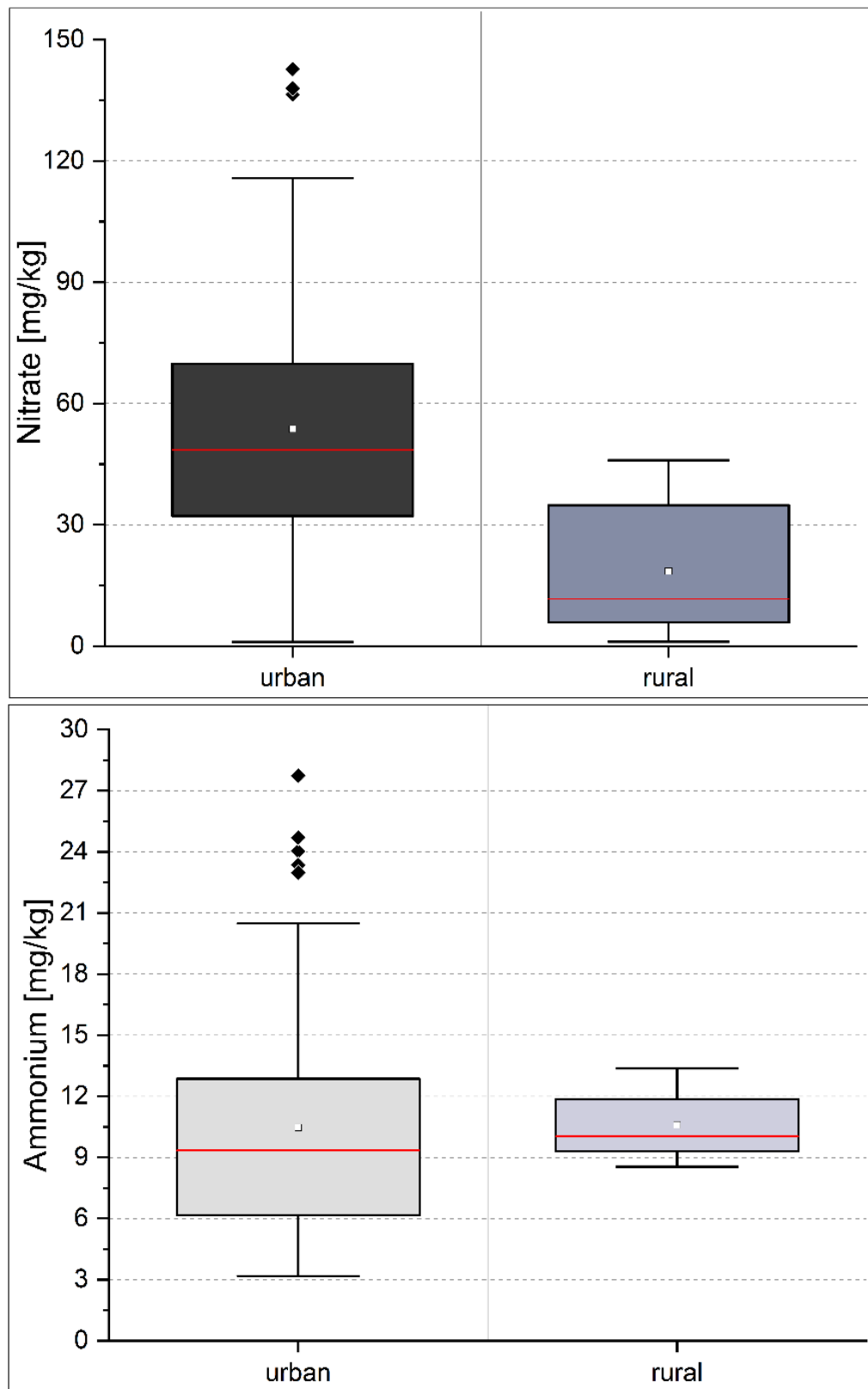


Figure 5-21: Box-whisker plots (25th to 75th percentile, displayed with mean: white square, median line and extreme values: black diamonds) for nitrate [above] and ammonium [below] in urban (N=87) and rural (N=12) *X. parietina* samples

5.6.6 Spatial variability of nitrate and ammonium concentrations recorded in *X. parietina* and *Physcia* spp.

Spatial patterns of NO_3^- and NH_4^+ concentrations in *X. parietina* and *Physcia* spp. across Manchester were previously described (section 5.3.3), with specific identified NO_3^- ‘hotspots’ in the north-east and south of the area (in *X. parietina*). A contrasting pattern was found for *Physcia* spp., with elevated concentrations in the northeast of Manchester. In contrast, NH_4^+ concentrations in both lichen species showed a comparable distribution pattern, with elevated concentrations within the city centre of Manchester.

To investigate spatial distribution and dispersion of nitrate and ammonium across Manchester’s city centre, Spearman ρ correlation (non-parametric) was used to evaluate urban influencing factors (i.e. distance to major roads, traffic counts, surrounding building heights and distances to large point sources and greenspaces; grouped according to Table 5-3) on NO_3^- and NH_4^+ (in both lichen species). Results are presented in Table 5-13.

Significant relationships (for NO_3^- and NH_4^+) were primarily found in *X. parietina* (i.e. distance to major road and large point sources), while traffic counts were significantly correlated with *Physcia* spp. only (Table 5-13). However, surrounding building heights were significantly negative correlated for NO_3^- in both lichen species. On the contrary, significant positive correlation was found for NH_4^+ and surrounding building heights (Table 5-13). Figure 5-22 and Figure 5-23 displays the significant relationships as box-whisker plots (grouped according to Table 5-3)

Table 5-13: Correlation coefficient (Spearman ρ ; non-parametric) of nitrate (NO_3^-) and ammonium (NH_4^+) concentrations with urban influencing factors (i.e. MR = distance to major road, BH = surrounding building heights, TC = traffic count and PS = distance to point source and GS = greenspace) to investigate spatial distribution in the City of Manchester; highly significant (at the level $p < 0.01$) relation in bold (and green), significant (at the level $p < 0.05$) relation underlined (and yellow)

	<i>Xanthoria parietina</i>				
	MR	BH	TC	PS	GS
NO_3^-	-0.32**	<u>-0.21*</u>	-0.02	<u>-0.27*</u>	-0.05
NH_4^+	-0.19	0.30**	<u>-0.27*</u>	-0.08	0.17
	<i>Physcia</i> spp.				
NO_3^-	0.01	-0.55**	0.08	-0.2	-0.28
NH_4^+	0.01	0.44**	-0.002	0.08	0.21
* significant at the level $p < 0.05$; ** significant at the level $p < 0.01$					

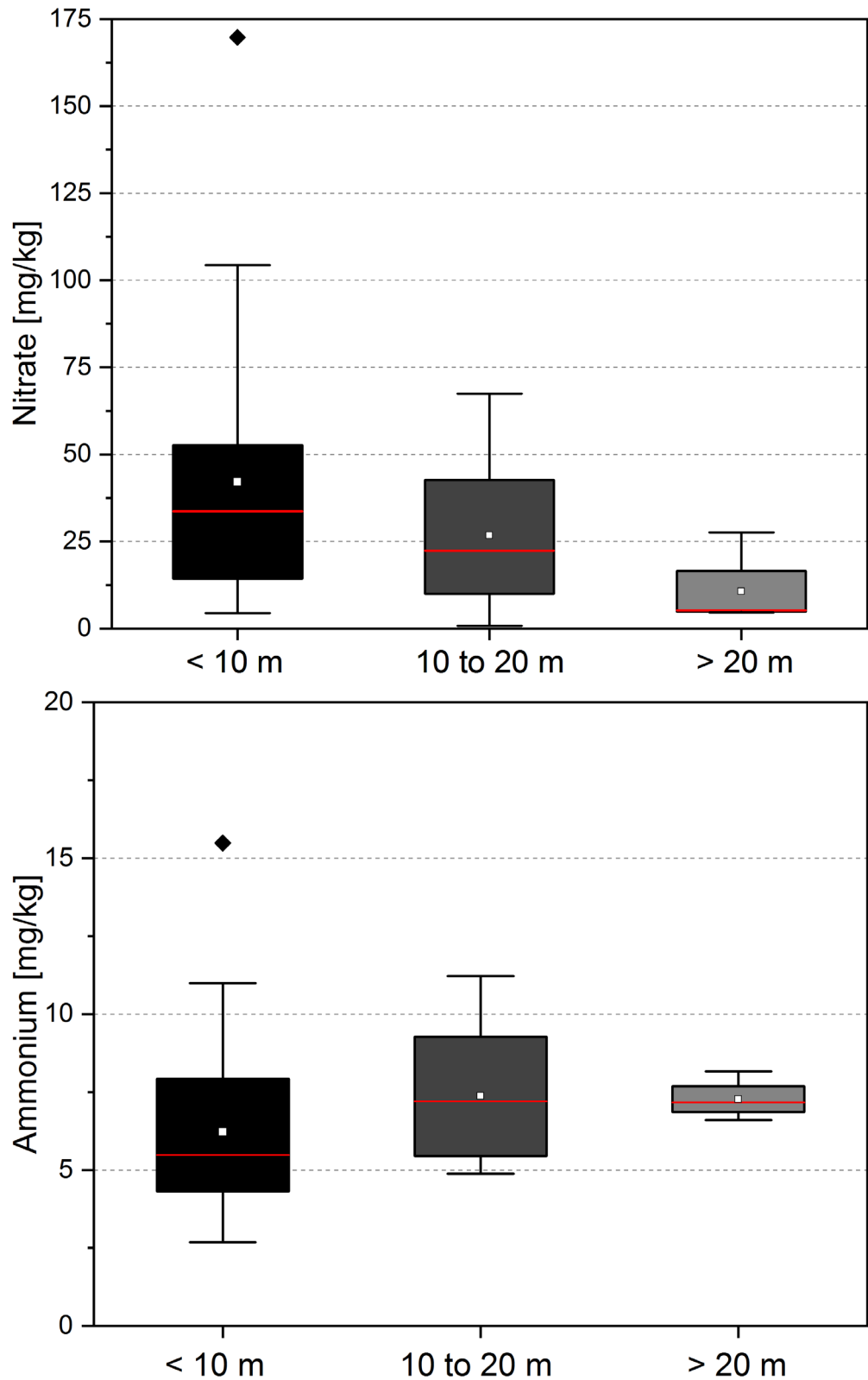


Figure 5-22: Box-Whisker plots (25th to 75th percentile; displayed with mean: white square, median line and extreme values: black diamond) for significant relationships of NO_3^- [upper panel] and NH_4^+ [lower panel] with building heights in *Physcia* spp.

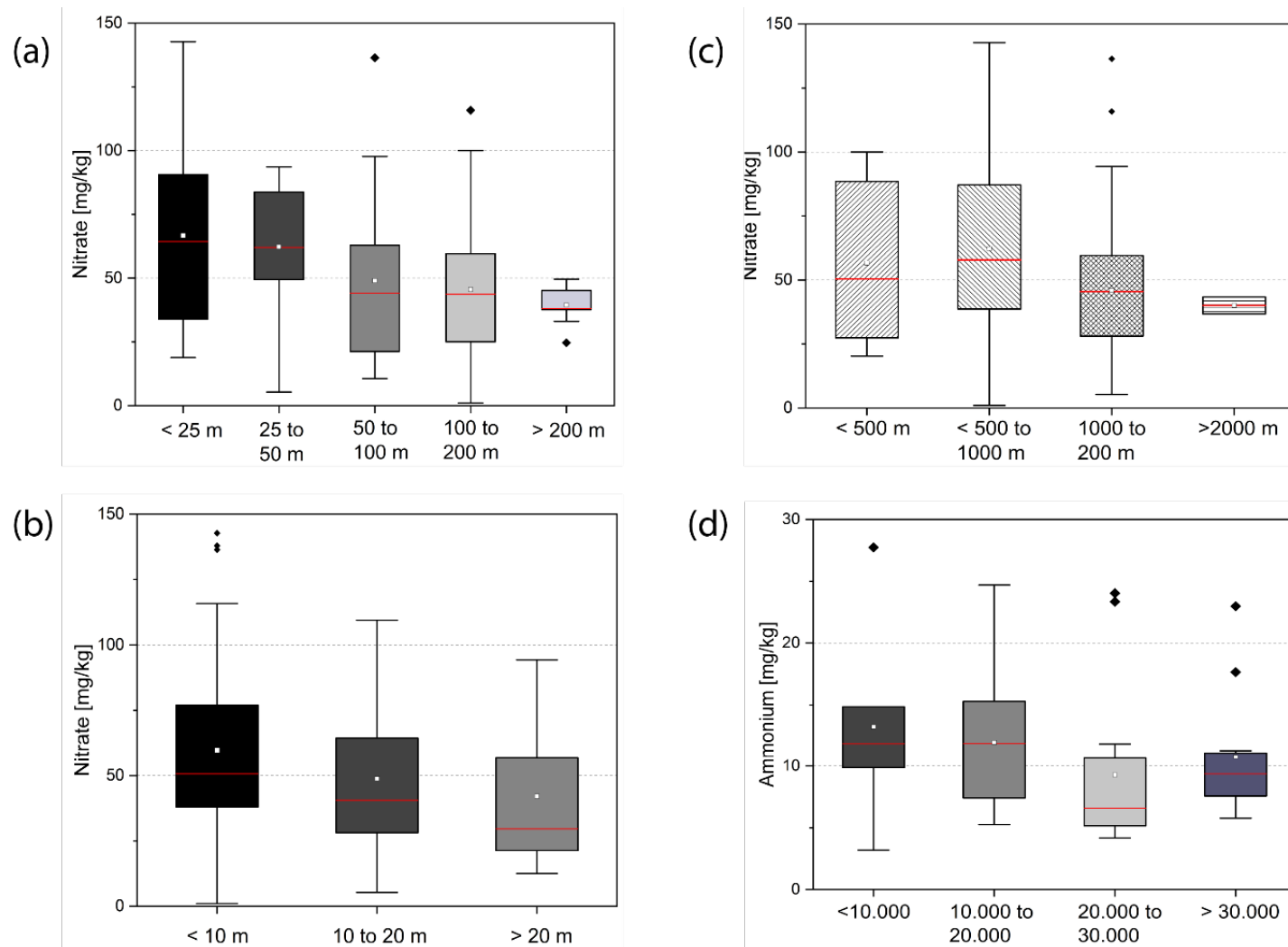


Figure 5-23: Box-Whisker plots (25th to 75th percentile; displayed with mean: white square, median line and extreme values: black diamond) for significant relationships of (a) NO_3^- with distance to major road, (b) NO_3^- with surrounding building heights, (c) NO_3^- with distance to large point sources and (d) NH_4^+ with traffic counts in *X. parietina*

To further investigate and predict spatial distribution of NO_3^- and NH_4^+ concentrations in the urban environment of Manchester, 'urban environmental' variables (i.e. distance to major roads, traffic counts, surrounding building heights and distances to point sources and greenspaces) were included into the modelling approach. Ordinary least square (OLS) was used, combined with urban influencing factors, to assess spatial variability (Figure 5-23). Nitrate and ammonium derived from *X. parietina* was used for modelling, due to higher spatial density of sampling sites, compared to *Physcia* spp. across the research area.

Estimated (modelled) concentrations of NO_3^- and NH_4^+ , with regard to the urban layout of Manchester display spatial variability (in *X. parietina*) across Manchester, with higher values for both in the city centre area and northeast of the research area (Figure 5-23). Distribution of NO_3^- and NH_4^+ appear to be affected by its specific surrounding and urban influences and spatial variability, including modelling outcomes will be discussed later (section 5.4.2).

Concentrations of nitrate and ammonium recorded in rural and lichen samples, as well as in urban samples were found to vary within the specific environment. Moreover, species-specific differences and impacts on dispersion and distribution of NO_3^- and NH_4^+ in the urban environment of Manchester were described. Following, findings will be interpreted and discussed in more detail (sections 5.5.2 to 5.5.3). Initially, methodological development and IC analysis will be discussed.

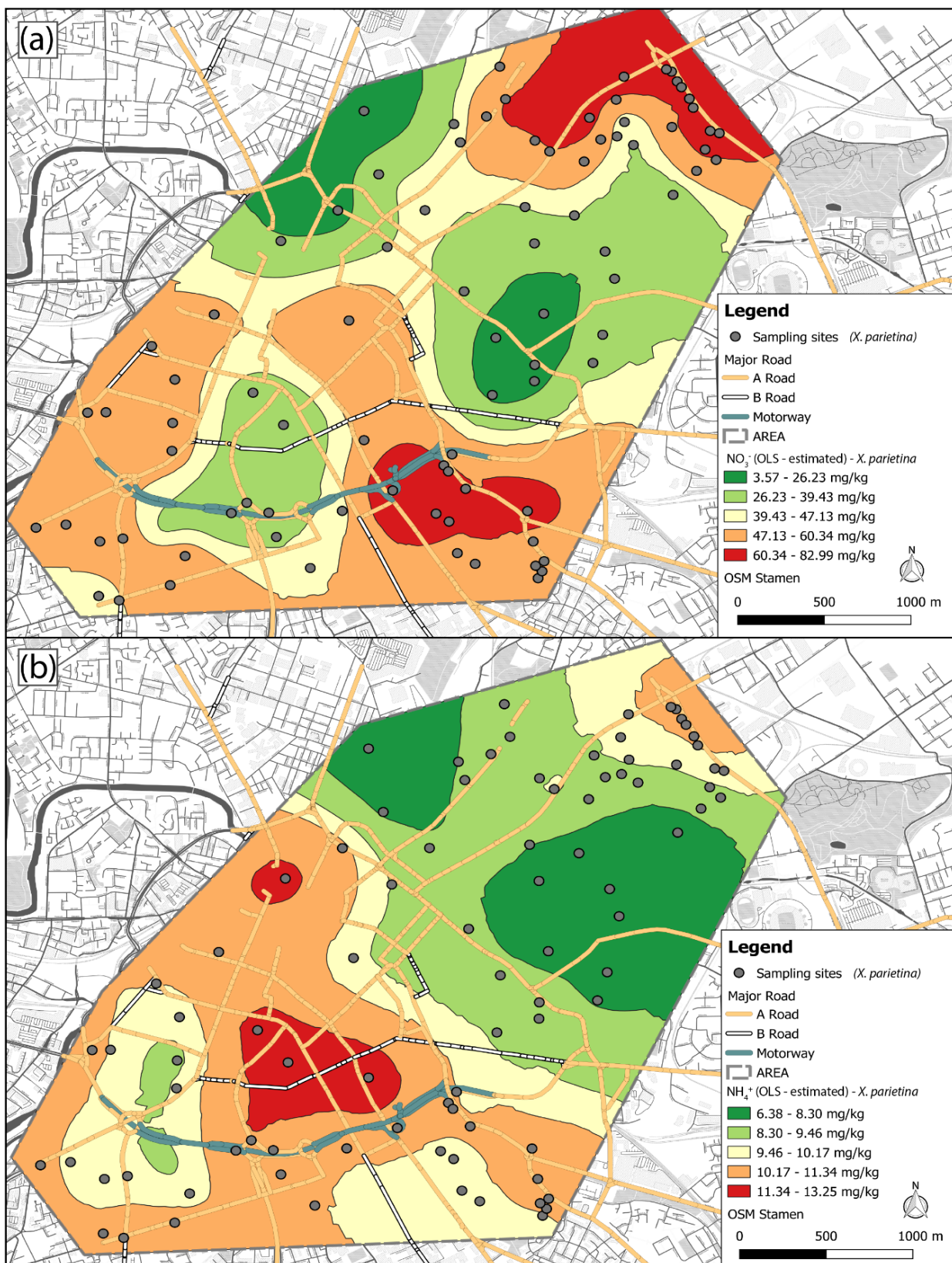


Figure 5-24: Modelled (Ordinary Least Square - OLS) NO₃⁻ and NH₄⁺ concentrations in *X. parietina* based on urban influencing factors (i.e. traffic counts, surrounding building heights, distance to major road, green space and large point source) to evaluate spatial dispersion and distribution

5.7 Interpretation and Discussion

5.7.1 Nitrogen speciation (NO_3^- and NH_4^+) using DI and KCl and subsequent analysis by ion chromatography (IC)

This study aimed to investigate the extractability of NO_3^- and NH_4^+ from lichen material, using different extractants (DI and KCl), different extractant strengths (specifically for KCl, 1% to 15%), different extraction volumes (1 ml to 5 ml) and different extraction times and subsequent analysis by ion chromatography.

Extraction of nitrate and ammonium with potassium chloride is commonly used in soil studies. Methodological development showed that nitrate and ammonium extraction by KCl can be applied to lichen material. Different strengths, extraction times and volumes of KCl indicated varying extraction abilities. In general, nitrate concentrations were more variable than NH_4^+ concentrations, which could be related to bacterial processes during the extraction process (EPA, 2007).

A single lichen sampling site (of *X. parietina*) was used to evaluate the best procedure to extract nitrogen species. Methodological variables (i.e. solvents and solvent volumes) influenced extractability of nitrate and ammonium from lichen material. For instance, Jones and Willett (2006) reported that the extraction methodology for soils (e.g. shaking time and extractant) has an impact on extracted NO_3^- and NH_4^+ . In general, significant differences occurred between DI and KCl of different strength and volumes. In contrast, vortexing (i.e. to achieve cell breakdown and thoroughly mixing) of the sample did not seem to affect the extraction of nitrate and ammonium from lichens.

In soils studies, 24 hours extraction time are usually applied for NO_3^- and NH_4^+ , with gradual increases over time (Maynard and Kalra, 1993; Jones and Willett, 2006). This was also tested for lichen extraction and compared with a considerably reduced extraction time of 6 hours to achieve 'same day extraction and analysis'. A same-day extraction and analysis was considered beneficial, due to bacteria (in organic matter) that utilise NO_3^- as an oxidant causing decreases in NO_3^- concentrations (EPA, 2007).

The EPA method ('9210 A') for potentiometric analysis of nitrate (in aqueous samples) reports the use of boric acid (1M) to preserve samples and prevent bacterial nitrate reduction (EPA, 2007). This could have been taken into consideration, when samples were left to leach for 24 hours.

Deionised (ultrapure, 18.2 M Ω) water (different volumes) was tested in this study and concentrations, specifically nitrate, were variable for undertaken experiments, which is comparable with KCl solutions of high strengths. Deionised water as used by Naeth and Wilkinson (2008) might be insufficient to extract all nitrate and ammonium from lichen material, whereas KCl solutions were shown to increase extraction efficiency. In contrast, Sims et al. (2017) used potentiometric determination of NO₃⁻ in lichen samples, by using a 'Nitrate ion selective electrode (ISE)', which was not available for this study. Results presented illustrated variability of analysed NO₃⁻ and NH₄⁺ for one single lichen samples and therefore indicating that care must be taken, when extracting lichen material (i.e. fully homogenised material and clean equipment).

However, methodological development favoured the use of 3 ml 3% KCl solution for 6 hours, to extract nitrate and ammonium from lichen samples (and subsequent IC analysis) within one day. Ion chromatography is one of the commonly used method to determine anions (i.e. NO₃⁻) and cations (NH₄⁺), and is particularly recommended for speciation analysis, due to simultaneous determination, short time, good reproducibility and high sensitivity (Michalski and Kurzyca, 2014). In this study, nitrate concentrations were slightly underestimated by ion chromatography (regarding NO₃⁻ recorded in CRM), suggesting potential instrumental adjustments, i.e. different eluents (e.g. NaHCO₃ and Na₂CO₃) and eluent flow rates (for specific IC columns) as reported by Michalski et al. (2012). Moreover, NO₃⁻ could have been analysed using colorimetrically (used in soil extraction studies Maynard and Kalra, 1993; Jones et al., 2004). However, the IC analysis and columns used in this study (for anion and cation separation) provided reliable concentrations of NO₃⁻ and NH₄⁺ extracted from lichens, showing good reproducibility (overall %CV) <10% for all analysed batches.

This study was the first to test and apply a KCl extraction to lichen material and analysis by IC. However, only few studies tried to assess lichen NO₃⁻ and NH₄⁺ showing the significant research potential, regarding the testing of additional solvents (i.e. BaCl₂, NaHCO₃ and NH₄Cl also applied in soil studies; Jones and Willett, 2006). No other study has investigated nitrate and ammonium extraction from lichens using KCl solutions, illustrating the novelty of this study.

The selected extraction procedure was further applied to rural and urban lichen samples, to investigate potential influences on NO_3^- and NH_4^+ in these contrasting environments.

5.7.2 What does temporal variability imply for spatial variability of NO_3^- and NH_4^+ across Manchester?

Uptake and temporal variability of NO_3^- and NH_4^+ in lichens

In principle, lichens can use organic nitrogen, nitrate and ammonium to fulfil their nitrogen demand (Hauck, 2010). Under natural conditions, lichens showed high efficiency to simultaneously take up ammonium and nitrate (Smith, 1960; Lang et al., 1976; Shapiro, 1984; Crittenden, 1996, 1998; Dahlman et al., 2004; Hauck, 2010). Findings (section 5.4.2) suggested temporal variation of NO_3^- and NH_4^+ concentrations in *X. parietina*. Assimilation of nitrate, in comparison to ammonium is energetically less attractive (Hauck, 2010). However, nitrate reductase activity, i.e. nitrite to nitrate was reported for the lichen *Lobaria pulmonaria*, with regard to its specific lichen substance (norstictic acid; (Shapiro, 1983, 1985, 1987; Avalos and Vicente, 1985; Shapiro and Nifontova, 1991; Hauck, 2010).

Concentrations of nitrate in *X. parietina* sampled across Manchester varied by individual sites, suggesting potential uptake of NO_3^- by the lichen and/or additional influences, such as (ammonium-)nitrate secondary pollutants and NO_3^- containing particulates (The Royal College of Physicians, 2016; Schraufnagel et al., 2019).

In contrast, it is known that green-algal lichens, i.e. *X. parietina* have a higher affinity for ammonium (Crittenden, 1996; Dahlman et al., 2002, 2004; Gaio-Oliveira et al., 2004). Nitrophytic lichens, such as *X. parietina* increase their photosynthetic capacity even at high ammonium concentrations, due to allocated N to the photobiont (Palmqvist et al., 1998; Gaio-Oliveira, Dahlman, Palmqvist and Máguas, 2005; Palmqvist and Dahlman, 2006; Hauck, 2010). NH_4^+ is cytotoxic and intracellular ammonium should be rapidly converted to amino acids (Neuhauser et al., 2007; Hauck, 2010). Additionally, ammonium assimilation in fungi is also faster than NO_3^- uptake (Smith and Read, 1997; Dahlman et al., 2002).

Lower concentrations of NH_4^+ in the second sampling period, at all sites could be related to reduction of ammonium in the lichen, due to its toxic effects, by oxidizing it to nitrate (non-toxic storage form of N; (Gaio-Oliveira, Dahlman, Palmqvist, Martins-Loução, et al., 2005).

However, NH_4^+ and NO_3^- are major constituents of particulates (Martin et al., 2011; AQEG, 2012) and variability is potentially related to wash-off during precipitation events. Furthermore, lichen samples were not washed before extraction for nitrate and ammonium, indicating a potential interference by entrapped particulates on the lichen surface. Hence, including a sample wash before extraction could remove interferences from entrapped particulates.

Sampling of lichen material was undertaken during different time of the years and seasonal trends for NH_4^+ and NO_3^- (in particulates), in relation to air temperature, atmospheric mixture and traffic intensity were reported (Yamamoto et al., 1988, 1995; Lee et al., 1999; Perrino et al., 2002; Bari et al., 2003; Whitehead et al., 2007). However, little is known about molecular mechanisms of nitrogen metabolism in lichens, whereas literature is available for nitrogen-fixating, free-living (or vascular plant associated) bacteria (Desnoues et al., 2003; Martinez-Argudo et al., 2005; Hauck, 2010). Bacterial communities living on the lichen surface could therefore play a role in nitrogen fixation, as well as the lichen substance produced (for *X. parietina*, i.e. 'parietin') (Shapiro, 1985, 1987; Hauck, 2010).

Further investigations on seasonal and diurnal patterns of NO_3^- and NH_4^+ , as well as particulates could provide additional information and temporal variability of NO_3^- and NH_4^+ in lichens. Therefore, shorter lichen sampling periods are suggested to investigate seasonal patterns, which could be combined with particulate sampling.

NO_3^- and NH_4^+ concentrations in lichens were still considered for spatial variability and to investigate the influence of both nitrogen compounds on bulk nitrogen and $\delta^{15}\text{N}$ values. Spatial variability of NO_3^- and NH_4^+ recorded in lichens and potentially increases in N wt% could suggest areas of higher nitrogen loads within the city, which could then be further investigated by additional sampling, i.e. particulates or $\text{NO}_3^-/\text{NH}_4^+$. Therefore, lichen derived NO_3^- and NH_4^+ concentrations were investigated in relation to the urban layout of Manchester.

Spatial variability of NO_3^- and NH_4^+ in Manchester

Although lichen total N contents can be used to investigate spatial variability in the atmospheric burden of nitrogen compound pollutants, such an approach does not distinguish between the different nitrogen compounds that can be taken up by the lichens, i.e. NO_3^- and NH_4^+ . In this study, lichen-derived NO_3^- and NH_4^+ concentrations were shown to be spatially variable across Manchester.

Urban 'layouts' appeared to influence the dispersion and distribution of pollutants and thus affecting air quality. Traffic is a main source of NO_x (of which NO_3^- is an important constituent), which can be transformed into aerosols and could be deposited in dust particles (dry deposition) or as dissolved NO_3^- (wet deposition) in precipitation (Van Herk, 2003). NO_2 concentrations (analysed by passive Palmes-type diffusion tubes) were shown to be spatially variable across Manchester (chapter 3) that could indicate potentially elevated levels of N compounds, including NO_3^- and (potentially NH_4^+).

NO_x gases act as precursors for (ammonium-)nitrate secondary pollutants and NO_3^- containing particles are emitted by diesel vehicles (The Royal College of Physicians, 2016; Schraufnagel et al., 2019). Nitrate concentrations in *X. parietina* were significantly correlated with distances to major roads. Elevated NO_3^- recorded in lichen species (*X. parietina*) in proximity to major roads suggest vehicular emissions as potential source. However, traffic counts did not have a (significant) impact on lichen NO_3^- , suggesting additional sources and implies the effect of driving conditions (i.e. traffic flow and speed) at the specific sampling site (Bishop et al., 2010; Sun et al., 2014, 2017; Bishop and Stedman, 2015; Stritzke et al., 2015).

Moreover, distance to large point sources (e.g. power stations; DEFRA, 2017) was significantly correlated with NO_3^- in *X. parietina*, suggesting additional NO_x emissions that could affect lichen nitrate concentrations. Emissions by large point sources can be distributed and dispersed over large areas, depending on ambient conditions as well as emission conditions, including height and temperature (EEA, 2015). Elevated NO_3^- concentrations therefore cannot be related to specific 'point sources' (i.e. power plants) within Manchester, but might additionally contribute to NO_3^- (and particulates) into the atmosphere.

Interestingly, surrounding building heights appeared to influence NO_3^- and NH_4^+ concentrations in both lichens (Table 5-13). This could indicate 'street-canyon-effects' that result in poor air quality ventilation (Lo and Ngan, 2015) in densely built-up areas of the city centre of Manchester (with usually higher buildings, see Chapter 2). NO_3^- was significantly negatively correlated with surrounding building heights, while NH_4^+ was positively correlated with surrounding building heights. Nitrate and ammonium form particulates from gaseous precursors (i.e. NO_x ; Limbeck and Puls, 2011) that could be deposited on the lichen. NH_4^+ primarily occurs in fine particles, potentially derived from diesel vehicles (i.e. Euro 2 and Euro 3 ;Finlayson-Pitts and Pitts, 1999; Krupa, 2003; Tzamkiozis et al., 2010) and higher concentrations in more

densely built-up areas could be related to particles being not effectively removed by wind and rain and thus are deposited on the lichen surface. Sampling of particulates (i.e. road dust) and analysis for nitrogen species could therefore benefit the understanding of NO_3^- and NH_4^+ in Manchester and their effect on lichens. However, findings indicate ‘canyoning’ effects of higher NO_3^- and NH_4^+ within the city centre.

Dispersion and distribution of nitrate and ammonium concentrations at sampling sites appeared to be influenced by its specific urban layout. Released substances into the atmosphere are dispersed depending on wind speed, turbulence and atmospheric stability (Seinfeld and Pandis, 1997), but also on presence of buildings (and building heights) and surface roughness (Brunner and Hanna, 2003; Loubet et al., 2009). Wind direction, street canyon layout and urban morphology and occurrence of street trees have been reported to alter pollution dispersion (Kurppa et al., 2018). Computational fluid model (CFD) has been used to assess NO_x distribution in Madrid taking atmospheric conditions into account, showing accurate pollutant concentrations at microscale (which was compared to passive measurements; Sanchez et al., 2017). Spatial distribution modelled with OLS and urban variables only accounted for about 20% for NO_3^- and 6% for NH_4^+ variability in *X. parietina*, respectively. Modelled concentrations (Figure 5-24) were lower compared to recorded concentrations in *X. parietina*, suggesting underestimation of NO_3^- and NH_4^+ by modelled variables (at un-sampled sites). This indicates that additional explanatory variables would improve the modelled spatial variability. For instance, meteorological parameters (i.e. temperature, wind and precipitation), bark pH and bark N contents (that are affected by NO_3^- and NH_4^+ ; Van Herk, 2003) and other pollutants (i.e. SO_4 and particulates containing nitrate and ammonium) could be included to improve spatial modelling.

Ecological indicators, such as lichens are influenced by environmental factors on different spatial scales, i.e. locally and regionally (e.g. land-cover and climate) as well as multiple pollutants (Ribeiro et al., 2013). Meteorological parameters (i.e. wind, temperature and precipitation) were not considered here, but could be applied in further research on spatial distribution of NO_3^- and NH_4^+ . Additionally, atmospheric air pollutant chemistry and dynamics (Kurppa et al., 2018) that occur within the city of Manchester could have an impact on NO_3^- and NH_4^+ concentrations.

The complexity of the urban environment of Manchester and additional influencing factors (i.e. atmospheric chemistry and meteorological data) needs to be further investigated to improve spatial modelling of NO_3^- and NH_4^+ . This in contrast, could lead to increasing amounts of data that might, in return, increase the model complexity. Modelling variables applied in this study might not represent the 'urban layout' in Manchester as a real-world model (i.e. distances and building heights), but were used to investigate potential influencing factors. However, spatial variability of NO_3^- and NH_4^+ was evidenced within Manchester and investigated potential urban influences. Moreover, lichen sampling and analysis could be extended towards the outside of the city centre, into less built-up areas, and could improve the insight into spatial variability of NO_3^- and NH_4^+ .

Rural *X. parietina* samples were also analysed for nitrate and ammonium concentrations and findings will be discussed hereafter, in relation to N wt% and stable-isotope ratio signatures ($\delta^{15}\text{N}$).

5.7.3 Assessment of nitrate and ammonium concentrations in rural *X. parietina* and influences on bulk nitrogen (N wt%) contents and $\delta^{15}\text{N}$ values

Nitrate and ammonium concentrations in rural environments were found less variable, when compared to urban lichen samples (of the same lichen species). Findings presented, indicated significant differences for NO_3^- , but not for NH_4^+ between these environments. Therefore, suggesting additional NO_x influences in urban lichens, whereas NH_4^+ seemed to be of relevance in both environments, with potentially different sources. Moreover, N contents (wt%) and $\delta^{15}\text{N}$ values seemed to be influenced by both nitrogen compounds NO_3^- and NH_4^+ (section 5.3.4; Figure 5-20).

Highest nitrate concentrations were found at locations in proximity to the poultry farm. NO_3^- was especially found high in close proximity (<150 m) of the poultry farm (see Figure 5-19), indicating NO_x emissions from the surrounding. Additionally, poultry manure contains nitrate, that could be (bound to particulates) influencing NO_3^- concentrations (Nahm, 2005; Twigg et al., 2015). In this study, NO_3^- was the main constituent of inorganic nitrogen in rural samples of *X. parietina* (see Figure 5-17c), which is potentially related to the cytotoxic effects of ammonium, which is rapidly converted by the lichen (Neuhauser et al., 2007; Hauck, 2010).

Agricultural activities are major sources for NH_3 and its reaction product NH_4^+ , the latter primarily emitted near the ground level in rural environments (Asman et al., 1998; Sutton et al., 1998; Boltersdorf and Werner, 2013). Only few studies investigated the ammonia/ammonium influence on lichens in rural environments. For instance, Olsen et al. (2010) combined transplants of *X. parietina* around a pig farm and passive ammonia samplers (ALPHA samplers) and highlighted influences on nitrogen contents (by NH_3) of lichens close to the farm, which was in accordance with results reported for *X. parietina* and *Flavoparmelia carperata* by Frati et al. (2007). Extracted NH_4^+ concentrations for rural lichen samples showed less spatial variability, compared to urban lichens and were generally high for all sites (ranging between 8.54 mg/kg to 13.37 mg/kg), suggesting livestock and agricultural effects on *X. parietina*, i.e. from animal waste and chemical fertilisers, e.g. in the form of ammonium nitrate (NH_4NO_3) (Hauck, 2010; AQEG, 2018).

Elevated concentrations in lichen nitrate and ammonium from Shrewsbury could indicate the steady uptake of both, NO_3^- and NH_4^+ , due to availability of high atmospheric concentrations. Thus, leading to increases in nitrogen contents of *X. parietina* around the poultry farm, as reported for ammonium by Gaio-Oliveira, Dahlman, Palmqvist, Martins-Loução, et al. (2005). Moreover, nitrate and ammonium are part of particulate matter (Lei and Wuebbles, 2013) and nitrogenous fertilisers and could additionally influence *X. parietina* in the farmland surrounding. Naeth and Wilkinson (2008) reported influences on NO_3^- and NH_4^+ concentrations with regard to sampling location and direction. This study sampled lichens from around a poultry farm on a south-west transect away from the farm, therefore potentially indicate influences on NO_3^- and NH_4^+ concentrations. Prevailing winds in the UK are south to south-westerly winds (Lapworth and McGregor, 2008; Met Office, 2015), which could indicate distribution of pollutants from distant sources. Site-specific influences, i.e. surroundings (e.g. additional farmland and farms), meteorology and topography (EEA, 2015) could also have an impact on lichen NO_3^- and NH_4^+ . These factors were not considered for rural, due to its focus on spatial variability in an urban environment. However, NO_3^- and NH_4^+ concentrations in rural lichens were investigated in relation to N wt% and $\delta^{15}\text{N}$ values.

Nitrate and ammonium are a significant source of N for lichens (Dahlman et al., 2004) and both appeared to positively influence N contents in *X. parietina*. Lichens are able to take up both forms of inorganic nitrogen, NO_3^- and NH_4^+ , with

NH_4^+ generally being the preferred form (Dahlman et al., 2004; Palmqvist and Dahlman, 2006; Johansson et al., 2010). Nitrogen contents (wt%) and $\delta^{15}\text{N}$ values (‰) of *X. parietina* in rural samples (as presented in Table 5-11) were found higher in rural samples, when compared to urban samples (see chapter 4).

$\delta^{15}\text{N}$ of atmospheric NH_x (i.e. NH_3), from agriculture is usually depleted (Freyer, 1978; Heaton et al., 1997; Boltersdorf and Werner, 2013). Moreover, NO_3^- was a major constituent in rural *X. parietina* (Figure 5-17) and NO_x from atmospheric pollution is usually enriched in $\delta^{15}\text{N}$ (Freyer, 1978; Heaton et al., 1997; Boltersdorf and Werner, 2013). Boltersdorf and Werner (2013) reported differences in $\delta^{15}\text{N}$ values of *X. parietina* affected by agriculture in Germany and Sweden and observed decreasing ^{15}N with increasing NH_4^+ . Here different results were found: increasing $\delta^{15}\text{N}$ with both NO_3^- and NH_4^+ and less depleted $\delta^{15}\text{N}$ values (ranging between -10 to 0.03‰) in *X. parietina*. Nitrogen supply in lichens is dependent on dry and wet deposition, i.e. dry (NH_3) deposition close to local sources and wet (NH_4^+) downwind from the source, which could explain differences in $\delta^{15}\text{N}$ values (Boltersdorf and Werner, 2013). NH_4^+ can be transported over wide distances (Olivier et al., 1998; Van Herk, 2001; Krupa, 2003; Webb et al., 2005; Hauck, 2010) and lichen NH_4^+ concentrations could be related to distant sources (transported into the area).

Moreover, the emissions of NH_3 (and subsequently NH_4^+) in the UK are lower compared to other European countries (i.e. highest in Germany and France; EEA, 2016) and influence of agricultural NH_4^+ on $\delta^{15}\text{N}$ cannot be distinguished unproblematically. Scattered local sources could influence the lichens sampled around the poultry farm, making it difficult to evaluate agriculture-related N deposition (Asman et al., 1998). However, NO_3^- was found to be the primary constituent in rural lichens, suggesting its primary influence on lichen N and $\delta^{15}\text{N}$ values. Further sampling and analysis could provide additional information on total N and $\delta^{15}\text{N}$ signatures in rural samples. Additionally, passive sampling (i.e. ALPHA samplers; Olsen et al., 2010), soil analysis (for nitrogen speciation) and rainwater sampling (and analysis for NH_4^+ and $\delta^{15}\text{N}$) could further provide beneficial insights into atmospheric concentrations of ammonia that potentially influence rural lichen samples. Moreover, more remote sampling sites could further be used to evaluate NO_3^- and NH_4^+ concentrations across non-urban areas.

In contrast, urban lichen samples seemed to be influenced by additional NO_3^- and NH_4^+ sources, indicated by higher spatial variability. This will be further investigated and discussed for both *X. parietina* and *Physcia* spp., again with regard to N wt% and $\delta^{15}\text{N}$.

5.7.4 Comparison of urban lichen samples (*X. parietina* and *Physcia* spp. nitrate and ammonium concentrations in relation to bulk nitrogen and $\delta^{15}\text{N}$ values

This study aimed to investigate nitrogen speciation in urban lichens, to distinguish constituents of bulk nitrogen contents (N wt%; previously described in Chapter 4) and potentially improve source apportionment of nitrogen compounds (using $\delta^{15}\text{N}$ values; Chapter 4). Presented results showed higher variability of NO_3^- and NH_4^+ in *X. parietina*, suggesting species-specific uptake ability and impacts of nitrogen compounds.

Naeth and Wilkinson (2008) analysed lichens (*Flavocetraria cucullata*, *Flavocetraria nivalis* and *Cladina arbuscular*) sampled around a diamond mine (Canada) and reported much lower NO_3^- concentrations, compared to Manchester. This is probably most likely due to the 'nature' of the analysed environments, i.e. mining site and urban environment. In contrast, Sims et al. (2017) reported NO_3^- concentrations between 14 mg/kg to 564 mg/kg in the Los Angeles Valley (USA). Lower concentrations recorded in the urban environment of Manchester could be related to the lichen species uptake abilities and sensitivity (i.e. *Buellia dispersa* – crustose lichen species and *X. parietina* and *Physcia* spp. – foliose lichen species) and specific urban sources (i.e. NO_x from traffic). Furthermore, they suggested influences on lichen NO_3^- uptake by atmospheric metal concentrations, i.e. copper and chromium, affecting algal photosynthetic functions and inhibit growth rate (Kumar et al., 2009; Hauck et al., 2013; Sims et al., 2017). Pavlova and Maslov (2008) and Maslaňáková et al. (2015) found that the mycobiont is absorbing nitrate, and sensitivity towards excessive nitrate is related to the fungal partner, hinting towards species-specific response to elevated NO_3^- (and NH_4^+) levels. These findings are supported by Gaio-Oliveira, Dahlman, Palmqvist, Martins-Loução, et al. (2005), who reported different uptake of nitrate and ammonium in *E. prunastri* and *X. parietina*. Levia (2002) reported higher nitrate uptake in *Parmelia stuppea* and *P. caperata* during mixed-precipitation events and limited uptake during cold temperatures.

This indicates potential meteorological influences on uptake of nitrogen compounds in lichens. Meteorological data was not obtained (for the sampling period of lichens) and therefore not considered during analysis.

High ammonium concentrations in Manchester were found in the city centre and at sites close to major roads (Figure 5-14), suggesting urban influences (i.e. traffic) as source of ammonium. Increases in three-way catalyst cars led to an increase of NH_3 emissions, due to reducing conditions in the converter (Cape et al., 2004) and subsequently ammonium. Ammonium concentrations reported by Naeth and Wilkinson (2008), ranging from 9 mg/kg to 30 mg/kg are comparable to concentrations achieved for *X. parietina* and slightly higher compared to *Physcia* spp. They also reported influences of NH_4^+ by sampling direction, which could also be of importance, especially in urban environments (i.e. with regard dispersion and distribution of pollutants). Green algal lichens (i.e. *X. parietina* and *Physcia* spp.; Wade, 1953; Gaio-Oliveira et al., 2005) have a high affinity for ammonium, which is in accordance with presented spatial patterns of NH_4^+ concentrations recorded in both lichens (see Figure 5-13 and Figure 5-14; Dahlman et al., 2002, 2003; Gaio-Oliveira et al., 2005).

However, *Physcia* spp. NH_4^+ concentrations were lower than recorded in *X. parietina*, suggesting the effective use of both nitrogen species in *X. parietina*. It has been reported that *X. parietina* appears to have the ability to oxidise ammonium surplus into nitrate (Gaio-Oliveira, Dahlman, Palmqvist, Martins-Loução, et al., 2005). Gaio-Oliveira et al. (2005) further hypothesised that the presence of apothecia could function as nitrogen sinks in *X. parietina*. These are not present on *Physcia* spp. (in particular *Ph. adscendens* and *Ph. tenella*), which could be related to different NH_4^+ concentrations.

Under laboratory conditions, uptake of nitrate in lichens was found to be less effective than ammonium uptake (Dahlman et al., 2002, 2004; Gaio-Oliveira, Dahlman, Palmqvist, Martins-Loução, et al., 2005; Palmqvist and Dahlman, 2006; Hauck, 2010). However, carbon skeletons must be available to bind nitrogen and avoid toxic levels (especially of NH_4^+) and subsequent death of the lichen (Hauck, 2010). Palmqvist and Dahlman (2006) reported ammonium being the main N source for *Plastimatia glauca*, followed by glutamine and nitrate. Furthermore, nitrogen concentrations (and photosynthetic capacity) increased with high ammonium concentrations (Hauck, 2010). This could be explained by higher assimilation rates of NO_3^- compared to NH_4^+ (Chapin et al., 1987; Palmqvist and Dahlman, 2006).

This is in accordance with higher plant studies, illustrating the preference of NH_4^+ uptake from an energetic point of view (Salsac et al., 1987; Boudsocq et al., 2012). Analysis of the specific lichen partners (including biont markers, i.e. chlorophyll and ergosterol contents; Gaio-Oliveira et al., 2005) could improve the understanding of NO_3^- and NH_4^+ uptake. However, both lichen species are considered nitrophilous and both seemed to respond similar to available nitrate and ammonium.

Concentrations of NO_3^- and NH_4^+ were found to be spatially variable across Manchester, with higher concentrations recorded in *X. parietina* (compared to *Physcia* spp.). However, findings in this study suggested additional influences of NO_x compounds in the urban area of Manchester, due to elevated NO_3^- . For instance, elevated concentrations of NO_2 were presented in chapter 3 and NO_x influences on lichens are likely to have an impact on NO_3^- .

Lichen N contents (wt%) and stable-isotope ratio signatures showed spatial (and species-specific) variability across Manchester (chapter 4). Elevated nitrogen contents in lichens were found to be accompanied by an enrichment in ^{15}N , pointing towards NO_x influences (i.e. from traffic) on lichen nitrogen and $\delta^{15}\text{N}$ ratios. Findings presented also indicate influences of NO_3^- in *Physcia* spp. N contents, but not in *X. parietina* (Figure 5-15), which could be related to lichen substances in the particular lichens (i.e. 'atranorin' in *Physcia* spp. and 'parietina' in *X. parietina*) and subsequently nitrate reductase (Shapiro, 1985, 1987; Hauck, 2010). This needs to be further investigated to clearly state an impact of NO_3^- on lichen N contents.

In contrast, ammonium positively affects N contents and $\delta^{15}\text{N}$ values in both lichen species (Figure 5-16). This again could be related to a preference of green-algal lichens for NH_4^+ (Dahlman et al., 2004; Gaio-Oliveira, Dahlman, Palmqvist, Martins-Loução, et al., 2005; Palmqvist and Dahlman, 2006; Johansson et al., 2010). Boltersdorf et al. (2014) and Boltersdorf and Werner (2014) used $\delta^{15}\text{N}$ values of lichens to reflect environmental nitrogen (N) sources and were able to relate more positive $\delta^{15}\text{N}$ values to nitrogen oxides (NO_x), whilst more negative $\delta^{15}\text{N}$ signatures were associated with NH_4^+ . Pinho et al. (2017) associated higher nitrogen contents and more negative $\delta^{15}\text{N}$ values agricultural and urban areas, while more positive $\delta^{15}\text{N}$ values (and less N contents) were found sites dominated by oceanic influences. A potential influence of oceanic sources cannot be ruled out completely for Manchester, due to its location about 70 km away from 'Irish Sea' and prevailing

south to south-westerly winds (Lapworth and McGregor, 2008; Met Office, 2015). However, NO₂ concentrations (recorded with Palmes-type diffusion tubes; Chapter 3) were positively correlated with lichen N and δ¹⁵N, indicating NO_x influences in lichens, which is in accordance with comparable urban (and traffic-related) studies (Gombert et al., 2003; Bermejo-Orduna et al., 2014; Pinho et al., 2017).

In this study, results suggest traffic related influences on lichen N concentrations and δ¹⁵N values (see Chapter 4). Vehicular emissions are also a source of NH₃ and NH₄⁺, with δ¹⁵N values of -4.6‰ to -2.2‰ recorded in vehicular NH₃ (Felix et al., 2013). δ¹⁵N values of NH₄⁺ (recorded in rainwater) vary widely, between -20 to +22‰ (Yeatman et al., 2001; Tozer et al., 2005). Therefore, isotopic signatures, influenced by NO₃⁻ and NH₄⁺ recorded in Manchester cannot be related to a specific source and additional measurements of NO₃⁻ and NH₄⁺ (in different compartments, e.g. rainwater and passive sampling) could improve source apportionment of both nitrogen species.

Presented results showed heterogeneity of nitrate and ammonium concentrations across Manchester, with regard to the specific lichen species (i.e. *X. parietina* and *Physcia* spp.). Therefore, one lichen species should be applied in biomonitoring studies, in particular a species that can withstand high atmospheric nitrogen loads, i.e. *X. parietina*, when analysing for NO₃⁻ and NH₄⁺.

5.8 Conclusion

Nitrogen compounds, such nitrate, ammonia (NH₃) and ammonium (NH₄) are not continuously measured with common monitoring stations, due to high spatial heterogeneity and necessity of costly equipment (Pinho et al., 2017).

Although lichen total N contents can be used to investigate spatial variability in the atmospheric burden of nitrogen compound pollutants, such an approach does not distinguish between the different nitrogen compounds that can be taken up by lichens, i.e. NO₃⁻ and NH₄⁺. In order to separate the established lichen total N content measurement into two constituent nitrogen compounds, i.e. nitrate (NO₃⁻) and ammonium (NH₄⁺), as well as quantify the concentrations of the latter, this chapter focussed on the assessment of different chemical extraction methods applied to lichen material.

This study was the first to apply potassium chloride (KCl) solutions, commonly used in soil analysis, to extract nitrogen compounds from lichen material. A preferred extraction method has then been applied to lichen samples collected from urban

(City of Manchester, UK) and rural (poultry farm near Shrewsbury, UK) environments, to assess the relative importance of nitrate and ammonium compounds to the atmospheric nitrogen loading in these contrasting areas. Differences were only recorded for nitrate, indicating additional influences of NO_x compounds (i.e. NO_3^-) in the urban environment of Manchester. NH_4^+ appeared to be a relevant N source for *X. parietina* in both environments.

Temporal variability of NO_3^- and NH_4^+ concentrations in lichen samples was recorded, suggesting short sampling periods when analysing lichens for nitrate and ammonium concentrations. However, lichens are able to oxidise ammonium to avoid toxic levels. Moreover, diurnal and seasonal patterns of NO_3^- and NH_4^+ in urban air have been reported. These facts need to be considered when analysing lichens for nitrate and ammonium concentrations. Potential analysis of atmospheric NO_3^- and NH_4^+ (i.e. in particulates) combined with lichens could improve the understanding of changing concentrations within the lichens.

Therefore, spatial variability was investigated in relation to influence of NO_3^- and NH_4^+ on N wt% and $\delta^{15}\text{N}$. Lichen nitrate and ammonium concentrations (*X. parietina* and *Physcia* spp.) in Manchester showed spatial variability with higher values recorded in *X. parietina*. Both lichen species seemed to respond similarly to available nitrogen compounds, due to their nitrophilous nature, by increasing N contents. In contrast, $\delta^{15}\text{N}$ values hint towards a predominance of NO_x , which is comparable to findings presented in Chapter 4 (CNS contents and stable-isotopic-signatures), but could not be related to specific sources, due to overlapping $\delta^{15}\text{N}$ values. This further suggests the complex mixture of nitrogen compounds within Manchester.

Specific areas with elevated concentrations of NO_3^- and NH_4^+ could indicate potential areas to further investigate atmospheric concentrations, i.e. by passive sampling. Recorded concentrations indicate deteriorated air quality across Manchester by NO_x and NH_x compounds. In particular, NO_3^- and NH_4^+ are involved in the formation of particulate matter, illustrating potential health impacts arising from 'secondary' products of both compounds. Furthermore, nitrate and ammonium displayed spatial variability with effects of the urban surrounding (i.e. surrounding building height and thus 'canyoning' effects), leading to higher concentrations within the city centre area.

However, further investigations regarding the specific urban setup (including meteorological parameters, potential 'canyoning' effects and atmospheric chemistry) should be considered. Findings presented indicated the vast research potential arising from nitrogen speciation in lichens, with regard to refining the technique, to additional sampling and analysis of other environmental compartments (i.e. soils and rainwater) to better identify NO_3^- and NH_4^+ composition in urban environments. However, the developed chemical extraction technique can extend the scope of lichen biomonitoring studies by enabling quantification of different atmospheric nitrogen compounds and their contribution to bulk nitrogen contents in lichens and influences on $\delta^{15}\text{N}$ values in lichens.

Chapter 6-
Lichen
biomonitoring of
spatial variability of
airborne metal
pollution in the City
of Manchester

6.1 Introduction

In addition to gaseous pollutants, urban air quality can be further affected by other chemicals, including airborne metals. Airborne metals in urban environments are derived from combustion, manufacturing and industrial processes, as well as from vehicle exhaust emissions, brake lining material and tyre and body wear (Taylor, 2006; Robertson and Taylor, 2007; Kampa and Castanas, 2008).

Metals, like zinc (Zn) and iron (Fe) in low concentration, are important to maintain human metabolism, but can become hazardous to human health at higher concentrations (Järup, 2003; Kampa and Castanas, 2008). For instance, inhaled airborne Zn can cause 'metal fume fever' and iron-rich particulates ('magnetite') have been found within the human brain, which are potentially linked to Alzheimer's disease (ATSDR, 2005; Maher et al., 2016). Other metals, such as arsenic (As), cadmium (Cd) and lead (Pb), have no beneficial human effects and are also well known for their toxic impacts on human health, these particularly affecting the nervous and urinary systems (Kampa and Castanas, 2008; Morais et al., 2012; Jaishankar, Tseten, et al., 2014). Exposure to toxic metals therefore poses a significant threat to human health (Jaishankar, Tseten, et al., 2014) that needs to be addressed in urban environments. The automated air quality monitoring stations in Manchester (on Oxford Road and at Piccadilly Gardens) record gaseous pollutants (i.e. NO_x) and do not provide information on how air quality is affected by metals.

Lichens readily accumulate airborne pollutants within their thallus, even when present at very low concentrations, these being consistent with atmospheric concentrations, and are thus widely considered reliable biomonitors for monitoring atmospheric metal pollution (Kularatne and De Freitas, 2013). Indeed, the rate of absorption, adsorption and accumulation of metals is dependent on lichen thalli morphological features (which varies by species), as well as the magnitude of the metal emission source (Garty, 2001). Three main lichen metal uptake mechanisms are described in the literature, i.e.: 1) entrapment of metal-containing particulates on the thallus surface; 2) intercellular, intracellular (within the medulla) accumulation, and 3) extracellular cation exchange (see Chapter 2: section 2.4.4.) (Garty, 2001; Bačkor and Loppi, 2009; Conti and Tudino, 2016; Vannini et al., 2017). Various lichen species (e.g., *Hypogymnia physodes*, *Parmelia sulcata*, *Evernia prunastri* and *Pseudevernia furfuracea*) have been employed for airborne metal biomonitoring purposes, being well studied worldwide in relation to their metal

uptake (Loppi et al., 1999; Bačkor and Loppi, 2009; Paoli et al., 2012; Malaspina et al., 2014; Shukla et al., 2014; Conti and Tudino, 2016; Piovár et al., 2017; Paoli, Vannini, Monaci, et al., 2018). For example, *Xanthoria parietina* and *Physcia adscendens* (the two species investigated in this study) have been used to monitor airborne metal concentrations in urban areas in Italy, Turkey, Poland and the UK, i.e. London (Owczarek et al., 2001; Doğrul Demiray et al., 2012; Vingiani et al., 2015; Parzych, Zdunczyk, et al., 2016), making them suitable species to address metal pollution in the City of Manchester.

Health relevant metals (i.e. Pb and Cd), as well as metals related to vehicular wear, i.e. Cr, Ni, Mn and Zn, and vehicular exhaust emissions, i.e. Pt and Pd, are of primary interest in this study (Zereini et al., 1997; Gebel, 2000; Palacios et al., 2000; WHO, 2000a; Kielhorn et al., 2002; Taylor, 2006; Robertson and Taylor, 2007; Barrett et al., 2011). These target metals, together with their potential sources in an urban environment and potential health impacts are displayed in Table 6-1.

Table 6-1: Target metals of primary interest, due to their presence in urban environments (i.e. sourced from vehicular wear and exhaust emissions) and their potential health impacts

Element	Sources in urban environments	Health impacts
Pb	Petrol and coal combustion, paint	Reduced foetal growth, kidney damage and impairment of cognitive abilities
Cd	Tyre wear, vehicle wear, lubricating oils and alloys	Carcinogenic, kidney and lung damage, osteoporosis
Cr	Engine wear, vehicle plating, alloys and road surface wear	DNA damage, ulcer formation, liver and kidney damage
Ni	Engine wear and metal industries	Cardiovascular diseases, carcinogenic, DNA alteration and allergic reactions
Mn	Tyre wear, brake linings	Impacting the nervous system
Pd and Pt	Catalytic convertors	Skin and eye irritation, mutagenic, inhibition of DNA synthesis, allergic reactions
Zn	Tyre wear, vehicle wear, lubricating oils and alloys	Anemia, nausea, skin irritation, 'metal fume fever'

(Costa, 1997; WHO, 2000a; O'Brien et al., 2001; Kielhorn et al., 2002; Bellinger, 2005; Taylor, 2006; Garza et al., 2006; Matsumoto et al., 2006; Kampa and Castanas, 2008; Martin and Griswold, 2009; ATSDR, 2012a; Morais et al., 2012; Jaishankar, Tseten, et al., 2014)

The main focus of this chapter is an assessment of the degree of spatial (and temporal) variability of airborne metal concentrations in the City of Manchester, UK, using *X. parietina* and *Physcia* spp. lichens, as well as investigation of factors that potentially influence lichen metal contents. A comparison between these urban lichen samples and specimens from a rural environment (*X. parietina* lichens sampled from around a poultry farm) has also been undertaken in order to assess the relative magnitude of airborne metal loadings within an urban setting. Following methodological and results sections, the discussion of lichen metal concentrations

will specifically focus on elements that have human health implications, as well as some other trace elements (i.e. Pd and Pt; Table 6-1) sourced from road vehicles. This study's urban and rural lichen metal concentrations also will be interpreted and discussed in relation to comparable (urban) lichen metal biomonitoring studies.

6.2 Research Methodology – metal concentrations by ICP-OES and ICP-MS

6.2.1 Lichen sampling for analysis of metal concentrations

As described previously (chapter 2), the urban lichens were sampled from street trees across the City of Manchester. Lichens were scraped off the twig bark, ground to powder and homogenised, stored in glass vials and subsequently acid digested to determine lichen metal concentrations. Of 94 trees sampled during an initial sampling period (June 2016 to October 2017; Figure 6-1), sufficient lichen material for metals determination was available for *X. parietina* for 84 sites and for *Physcia* spp. for 17 sites (site specific data, i.e. XY-coordinates, tree height and tree species can be found in the Appendix B-1). Lichens absorb constituents (i.e. airborne pollutants) during their entire lifecycle and excretion is negligible, hence providing integrated exposure measurements over time (Carreras et al., 2009; Boamponsem and de Freitas, 2017). However, the long sampling period could indicate temporal changes in lichen metal concentrations.

Therefore, a sub-set of sites were resampled between May and October 2018 (Figure 6-1), in order to assess the magnitude of any temporal variability on lichen metal contents, and lichen material (primarily *X. parietina* N=17; only one site could be sampled for both species, *X. parietina* and *Physcia* spp.) was obtained from the exact same trees originally sampled (Figure 6-1).

Rural lichen samples (*X. parietina*, N=12) were collected from oak (*Quercus* spp.) and hawthorn (*Crataegus* spp.) trees around a poultry farm near to Shrewsbury (UK) in May 2018, following the same procedure described previously (see Chapter 5: Figure 5-5 for sampling locations). Lichen sampling was undertaken in close proximity (i.e. between 50 to 500 m) to, and on a general south-west transect (i.e. between 1 to 3 km) away from, the poultry farm, sampling sites being defined by accessibility in relation to fenced and hedged agricultural fields and private property.

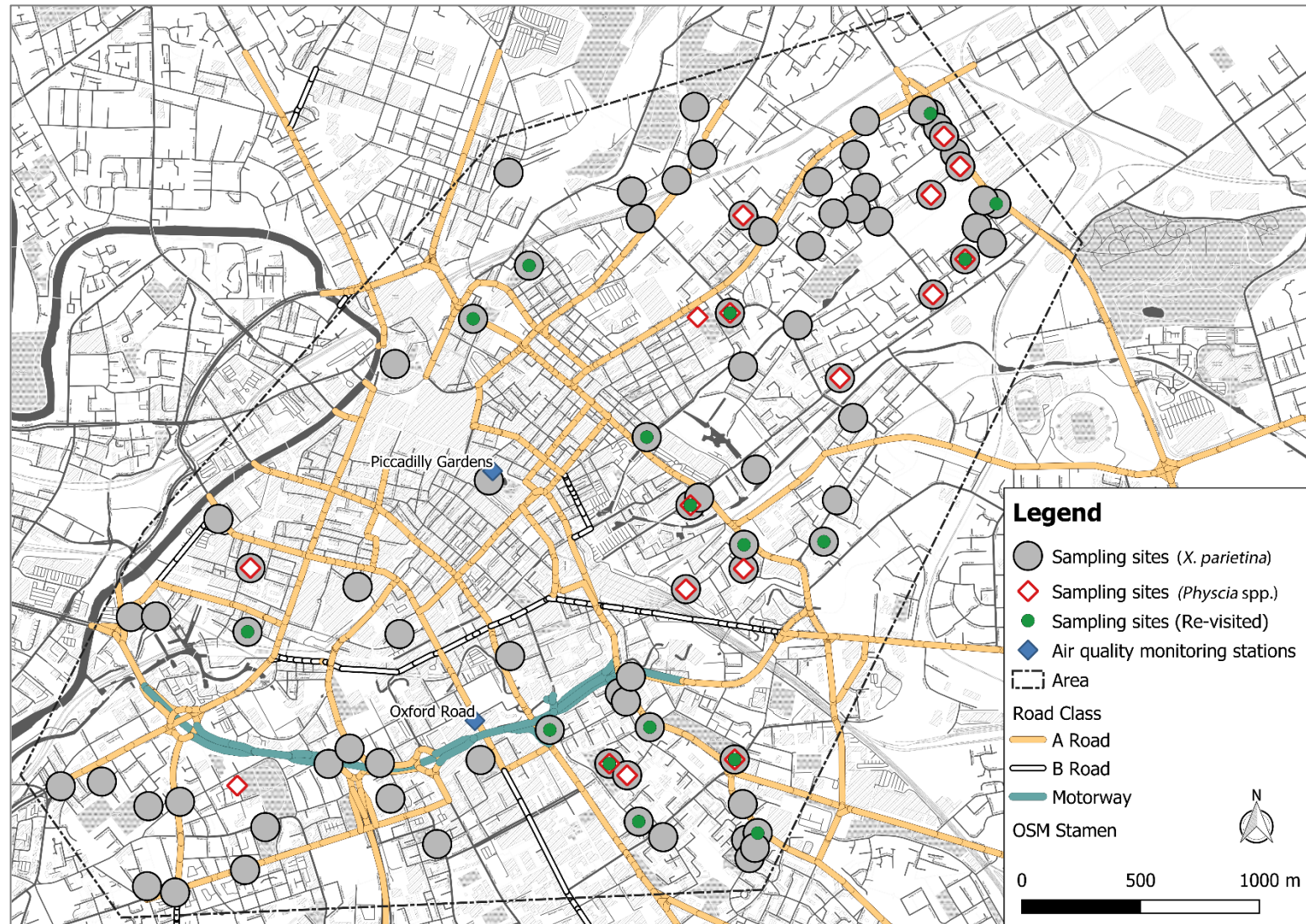


Figure 6-1: Sampling sites (and re-visited sites) for *X. parietina* (N=84) and *Physcia* spp. (N=17) lichens analysed for metal concentrations, with automated air quality monitoring stations also shown (overview map with site ID labels is included in Appendix D-1)

6.2.2 Microwave-assisted acid digestion of lichen material

Microwave-assisted nitric acid digestion and ICP-OES and ICP-MS measurements were used to determine lichen metal contents. PTFE microwave digestion vessels first were pre-cleaned with 7 ml of ultrapure water (18.2 MΩ) and 7 ml nitric acid (69%; VWR Aristar® grade) to minimise carry-over of any metals contaminants from former use. Digestion vessels (with ultrapure water and HNO₃) were processed through a microwave cleaning cycle (CEM Mars Xpress 5: ramping up to 165°C in 10 minutes and hold for 10 minutes at 1200 W), then thoroughly rinsed with ultrapure water and oven dried at 80°C before use.

About 0.25 g of each ground and homogenised lichen sample powder (*X. parietina* N=84; *Physcia* spp. N=17) were weighed into the pre-cleaned PTFE microwave digestion vessels, followed by addition of 2 ml of 18.2 MΩ ultrapure water and 8 ml of nitric acid (69%; VWR Aristar® grade) and subsequently run through a microwave-digestion programme (Table 6-2).

Table 6-2: Microwave (CEM Mars Xpress 5) digestion programme (five step programme: temperature ramp up – digestion step I – temperature ramp up – digestion step II and cool down phase)

Temperature ramp up – Step I
Ramping temperature up to 90°C Time: 10 minutes
Microwave digestion – Step II
Temperature: 90°C Power: 600 W Time: 5 minutes
Temperature ramp up – Step III
Ramping temperature up to 170°C Time: 10 minutes
Microwave digestion – Step IV
Temperature: 170°C Power: 1200W Time: 10 minutes
Cool down phase – Step V
Time: 30 minutes

Replicate procedural blank solutions (N=20; consisting only of 2 ml 18.2 MΩ ultrapure water and 8 ml nitric acid) and replicate lichen reference material (CRM No. 482 – Trace elements in lichen *Pseudevernia furfuracea*) were included within each sample digestion batch (total of N=23 CRMs; N=20 blanks), the CRM to facilitate assessment of the precision and accuracy of the metals dataset. Subsequently, the acid digest solutions were gravity filtered into 50 ml volumetric flasks using 'Whatman®, grade 540, hardened ashless, 110 mm' filter papers

(Sigma-Aldrich), made up to volume with 18.2 MΩ ultrapure water and stored in 50 ml metal-free centrifuge tubes until determination of 12 elements by ICP-OES and 18 elements by ICP-MS (Table 6-3). Several elements (e.g. As, Cd, and Pb) were analysed using both analytical techniques, ICP-OES (Thermo Scientific iCap 6000 series) and ICP-MS (Agilent 7900). Both techniques were used due to certain advantages and disadvantages for each analytical instrument, i.e. higher sensitivity and lower background signals to achieve low detection limits (parts-per-trillion) for ICP-MS compared to ICP-OES (Agilent Technologies, 2006), but higher sample throughput with ICP-OES.

Selection of elements to analyse was based on the US Environmental Protection Agency (EPA) list of priority substances and metals recorded in soils of the European Union (EPA, 2014; Tóth et al., 2016). Moreover, as detailed in the introduction to this chapter, the health implications of metals (i.e. Pb and Cd), specific sources, i.e. road vehicle parts (e.g. Cd, Cr, Mn, Ni, Pd, Pt and Zn) and potential geological sources (e.g. Al, As and Fe) were considered.

6.2.3 Analysis of acid-digested lichen samples by ICP-OES and ICP-MS

Several elements of interest were measured by both instruments, ICP-OES (Thermo Scientific iCap 6000 series) and ICP-MS (Agilent 7900). To discriminate, which metal to report for which analytical instrument a decision matrix (Appendix D-4) based on (polyatomic) interferences (May et al., 1998; Esslab, 2017) and instrument sensitivity was used.

Procedural blanks were used to determine methodological lower limits of detection (LLD), calculated as three times the standard deviation (SD) of the procedural blanks (N=20; for four analysed batches by ICP-OES and ICP-MS), calculated separately for each analytical batch. Procedural blanks were also used for blank subtraction and to exclude contamination from equipment, reagents and preparation methodology. Table 6-3 presents the analysed elements by each ICP instrument, including measured wavelengths (in nm) for ICP-OES and analysed isotopes (with or without helium collision cell [He]) for ICP-MS. LLD ranges for each element (summarized for all batches) also are shown.

Table 6-3: Elements determined by ICP-OES and ICP-MS, including the measured wavelengths and isotopes (latter indicated if analysed with helium collision cell by [He]) and lower limits of detection (LLD) ranges for all analytical batches; key target metals shaded in grey

ICP-OES			ICP-MS		
Elements	Analysed wavelength [nm]	LLD (range: min- max [ng/ml])	Elements	Analysed isotope	LLD (range: min- max [ng/ml])
Aluminium (Al)	167.0	0.005-0.035	Arsenic (As)	75 As [He]	0.001-0.003
Iron (Fe)	259.9	0.006-0.068	Beryllium (Be)	9 Be	0.08-0.15
Manganese (Mn)	257.0	0.0001-0.003	Cadmium (Cd)	111 Cd [He]	0.004-0.006
Nickel (Ni)	231.6	0.001-0.012	Cobalt (Co)	59 Co [He]	0.50-0.90
Lead (Pb)	220.3	0.0006-0.012	Chromium (Cr)	52 Cr [He]	0.007-0.014
Sulphur (S)	182.0	0.005-0.014	Copper (Cu)	63 Cu [He]	0.09-0.40
Zinc (Zn)	206.2	0.008-0.077	Palladium (Pd)	105 Pd	0.005-0.008
			Platinum (Pt)	196 Pt	0.002-0.02
			Titanium (Ti)	47 Ti [He]	0.006-0.01
			Vanadium (V)	51 V [He]	0.001-0.002

ICP-OES calibration standards and signal drift monitors were made from ESSLAB-910B (5% v/v HNO₃) that contained 1000 mg/L Al, Ca, Fe, K and Na, 500 mg/L Cu, Mg, P and S and 200 mg/L Cd, Co, Cr₃, Mn, Mo, Ni, Pb, Zn and As (Table 6-4). ICP-MS calibration standards and signal drift monitors were made up from multi-elemental standards (Agilent Technologies; Table 6-4): 'multi-elemental calibration standard-2A' containing 10 µg/ml of Ag, Al, As, Ba, Be, Ca, Cd, Co, Cr, Cs, Cu, Fe, Ga, K, Li, Mg, Mn, Na, Ni, Pb, Rb, Se, Sr, Ti, U, V Zn (in matrix 5% HNO₃), 'multi-elemental standard-3' containing 10 µg/ml of Sb, Au, Hf, Ir, Pd, Pt, Rh, Ru, Te, Sn (in 10% HCl and 1% HNO₃) and 'multi-elemental standard-4B' containing 10 µg/ml of B, Ge, Mo, Nb, P, Re, S, Si, Ta, Ti, Wi and Zr (in trace HNO₃/trace HF).

Table 6-4: Calibration standards for ICP-OES and ICP-MS measurements, as well as signal drift monitors, made from ESSLAB-910B for ICP-OES analysis and multi-elemental standards for ICP-MS (Esstab, 2017; Agilent Technologies, 2019)

ICP-OES			
Calibration standard	Al, Ca, Fe, K, Na [µg/ml]	Cu, Mg, P, S [µg/ml]	Cd, Co, Cr ₃ , Mn, Mo, Ni, Pb, Zn, As [µg/ml]
I	0.1	0.05	0.02
II	0.16	0.08	0.032
III	1	0.5	0.2
IV	10	5	2
V	20	10	4
VI	40	20	8
Signal drift monitor			
	2	1	0.4
ICP-MS			
Al, As, Be, Cd, Co, Cr, Cu, Fe, Mn, Ni, Pb, Pd, Pt, S, Ti, V, Zn [ng/ml]			
I	10		
II	20		
III	30		
IV	40		
V	50		
Signal drift monitor			
	10		

Signal drift monitors were made up from the same analytical standards for ICP-OES and ICP-MS to check for instrumental changes sensitivity through time (Salit and Turk, 1998). For ICP-OES analyses, a signal drift solution (containing 2 µg/ml, 1 µg/ml and 0.4 µg/ml of the elements of interest; Table 6-4) was analysed after every two acid digested samples. ICP-MS analyses were run with a signal drift solution (containing 10 ng/ml of each element; Table 6-4) after each sample. Acid digested CRM solutions were measured every five acid digested samples for ICP-OES and ICP-MS analytical runs. ICP-OES signal drift solutions showed low variability (<5% RSD) for each analysed element through each analytical batch and no signal drift correction was applied to ICP-OES data. In contrast, ICP-MS signal drifts had to be used for drift correction due to changes in recorded drift solution signals through each analytical run.

To apply ICP-MS signal drift correction, the two signal drift measurements bracketing an unknown sample solution (lichen or CRM) were averaged and related to the initially measured signal drift solution, resulting in a 'correction factor'. This 'correction factor' then was applied to the unknown sample (analysed between the two signal drift solutions) (Figure 6-2).

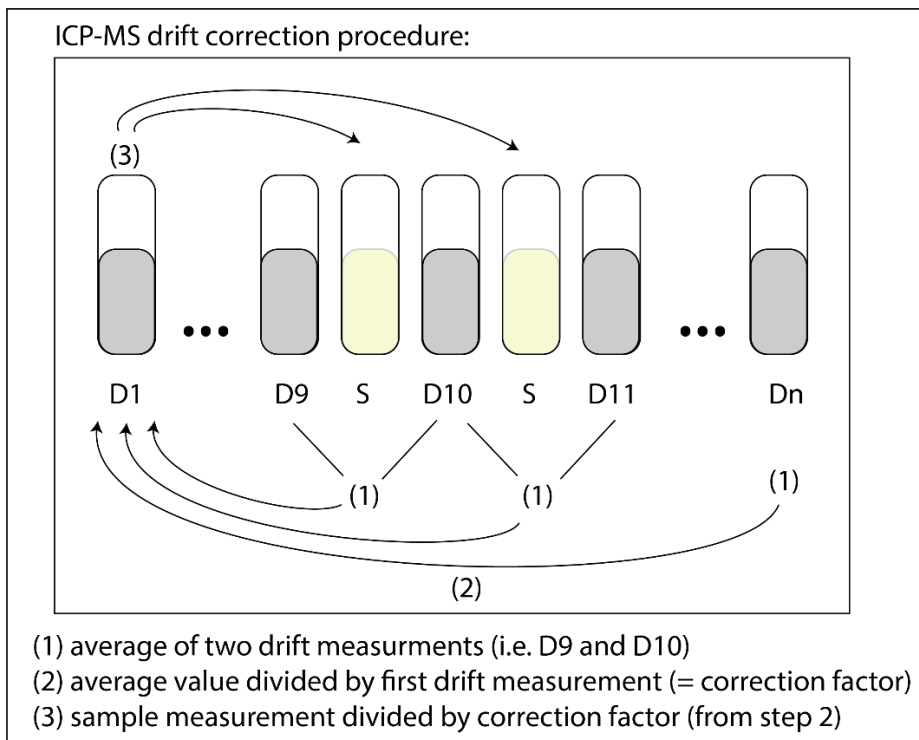


Figure 6-2: ICP-MS signal drift correction procedure, showing calculation steps and application to each analysed unknown solution (lichen sample or lichen CRM)

6.2.4 Statistical analysis

Statistical analysis was carried out using SPSS Statistics 25 and Graph Pad Prism 7. Data visualisation was carried out using Origin 2019. Testing of lichen metals data for statistical normality was performed using a Shapiro-Wilkinson test, because this test has been reported to have higher statistical power regarding sample size and distribution, compared to other statistical tests (i.e. Kolmogorov-Smirnoff and Lillefors; Mendes and Pala, 2003; Razali and Wah, 2011). Correlation statistics are expressed as Pearson's r (normal distributed data) or Spearman's ρ (non-normal distributed data), based on outcomes of testing for normality. Statistical comparisons of metal concentrations was informed by 'normal distribution' outcomes, using either paired/unpaired t-tests (normal data distribution) or Mann-Whitney/Wilcoxon tests (non-normal data distribution).

To investigate similarities within the metals dataset cluster analysis was undertaken, following the methodology described by Doğrul Demiray et al. (2012):

metal concentrations were standardised, by subtracting the mean from each sample concentration (individually for each different metal) and dividing by the standard deviation (z-score) before clustering. Standardisation was applied to compensate different magnitudes in elemental concentrations of lichen samples (Doğrul Demiray et al., 2012). Agglomerative hierarchical clustering, with complete linkage (furthest neighbour) and squared Euclidian distance were used to produce dendrograms of similarities/dissimilarities (Doğrul Demiray et al., 2012).

Comparison of urban lichen metal concentrations with urban environmental variables that may influence lichen metal content, i.e. distance to major road, road traffic counts (AADF), proximal building heights (mean of surrounding building heights), distance to potential pollution point sources and greenspace, followed grouping of data (Table 6-5), which was detailed in chapter 2 (methodological framework). Rural poultry farm lichen samples were only classified based on distance to the farm (1: within 500 m; 2: outside 500 m).

Table 6-5: Urban environmental variables with potential influences on lichen metal concentrations in the City of Manchester, with associated data groupings

Environmental variable	Data grouping
Distance to major road (including A-roads, B-roads and motorway)	1: <25 m 2: 25-50 m 3: 50-100 m 4: 100-200 m 5: >200 m
Road Class (major roads)	M – motorway A - A-road B - B-road U - Unclassified
Traffic counts (annual average daily traffic flow)	1: <10.000 2: 10.000 to 20.000 3: 20.000 to 30.000 4: >30.000
Building heights	1: <10 m 2: 10 to 20 m 3: >20m
Distance to (large) point source	1: <500 m 2: 500 to 1000 m 3: 1000 m to 2000 m 4: >2000m
Distance to greenspace	1: <100 m 2: 100 to 200 m 3: 200 to 300 m 4: 300 to 400 m 5: 400 to 500 m 6: >500 m

6.2.5 Geospatial data analysis

Geographic Information System Software (GIS; ArcMap 10.5 and QGIS 3.4.2 – ‘Madeira’) was used for geospatial analysis and mapping of lichen metals data. To investigate small-scale spatial variability and potential urban influencing factors (Table 6-5) on lichen metal distributions (and thus airborne metals dispersion) geospatial statistics were applied to key target metal concentrations (Table 6-1). Regression analysis tools (i.e. Ordinary Least Square – OLS and Geographically Weighed Regression – GWR) were used to quantify spatial statistics and spatial relationships within ArcMap 10.5

‘Geographically Weighed Regression’ (GWR) has been applied in several fields, such as geographical and environmental sciences, to explore spatial regression relationships, taking location effects for prediction into account (Fotheringham et al., 2002; Warsito et al., 2018). Spatial relationships were modelled using ‘Geographically Weighted Regression (GWR)’ using ArcMap 10.5. ‘spatial statistics’ tool (ESRI, 2016). GWR was only undertaken for *X. parietina* metal concentrations, due to the small sample number of *Physcia* spp., with ‘dependent variable’ being the target *X. parietina* metal concentration and urban influencing factors as ‘explanatory variables’ (input features: fixed Kernel type; Bandwidth method: ‘Akaike Information Criterion’ - AICc; number of neighbours: 30).

6.3 Results – lichen metal concentrations

6.3.1 Assessment of accuracy and precision of metals dataset

Certified (and indicative) metal concentrations for lichen CRM-482 are presented in Table 6-6. The certified concentrations included on the CRM certificate are for a nitric acid (HNO₃)/hydrofluoric acid (HF) digestion. However, this study was only able to apply a HNO₃ acid digestion, due to health and safety issues at MMU regarding use of hydrofluoric acid. In this regard, it would be expected that a simple HNO₃ digestion would result in lower element concentrations than a more aggressive and complete HNO₃/HF digestion, because HF dissolves silicate minerals. Nevertheless, Baffi et al. (2002) applied a HNO₃/hydrogen peroxide (H₂O₂) digestion to lichen CRM-482 and that procedure is more comparable to the nitric acid digestion undertaken in this study (Table 6-6).

Moreover, for environmental airborne pollution biomonitoring studies, dissolving silicate material (i.e. from soil particles) is not important, due to immobilisation of metals attached to silicate structures, which are not available for biological processes (Bettinelli et al., 2002; Kularatne and De Freitas, 2013). Therefore, silicate-bound metals are not taken up by the lichen and do not contribute to the overall metal concentration.

Lichen CRM target metal concentrations per analysed batches (i.e. Cd, Cr, Mn, Ni, Pb, Pd, Pt and Zn) were tested for significant outliers by Grubbs outlier test (Table 6-6). Significant outliers ($p < 0.05$) were excluded from analysis for accuracy and statistical testing for batch-to-batch correction. A Friedman's test (two-way analysis of variance; non-parametric test) was used to analyse for differences between analytical batches and to investigate if batch-to-batch correction was necessary. Due to different CRM numbers within each batch, a non-parametric test was favoured for statistical analysis of batch differences. However, no significant differences between analysed CRMs by batch were found, therefore corrections for batch-to-batch biases in metal concentrations were not necessary. Figure 6-3 illustrates metal concentrations recorded in lichen CRM for each analytical batch (Pd and Pt were not included due to unavailability of certified values).

Table 6-6: Key target metals analysed in lichen CRM by batch (number displayed in table) and statistical test outcomes (Grubb's test) for outliers that were excluded before further testing for accuracy and precision; no significant outliers found by Grubb's test shaded in green, significant outliers found in yellow, with number of outliers

	Cd	Cr	Mn	Ni	Pb	Pd	Pt	Zn
Batch 1 (N=9)	No	No	No	No	No	Yes (N=2)	Yes (N=4)	No
Batch 2 (N=5)	No	No	No	No	No	No	No	Yes (N=1)
Batch 3 (N=6)	No	No	Yes (N=1)	No	No	No	No	No
Batch 4 (N=3)	No	No	No	Yes (N=1)	No	No	No	No

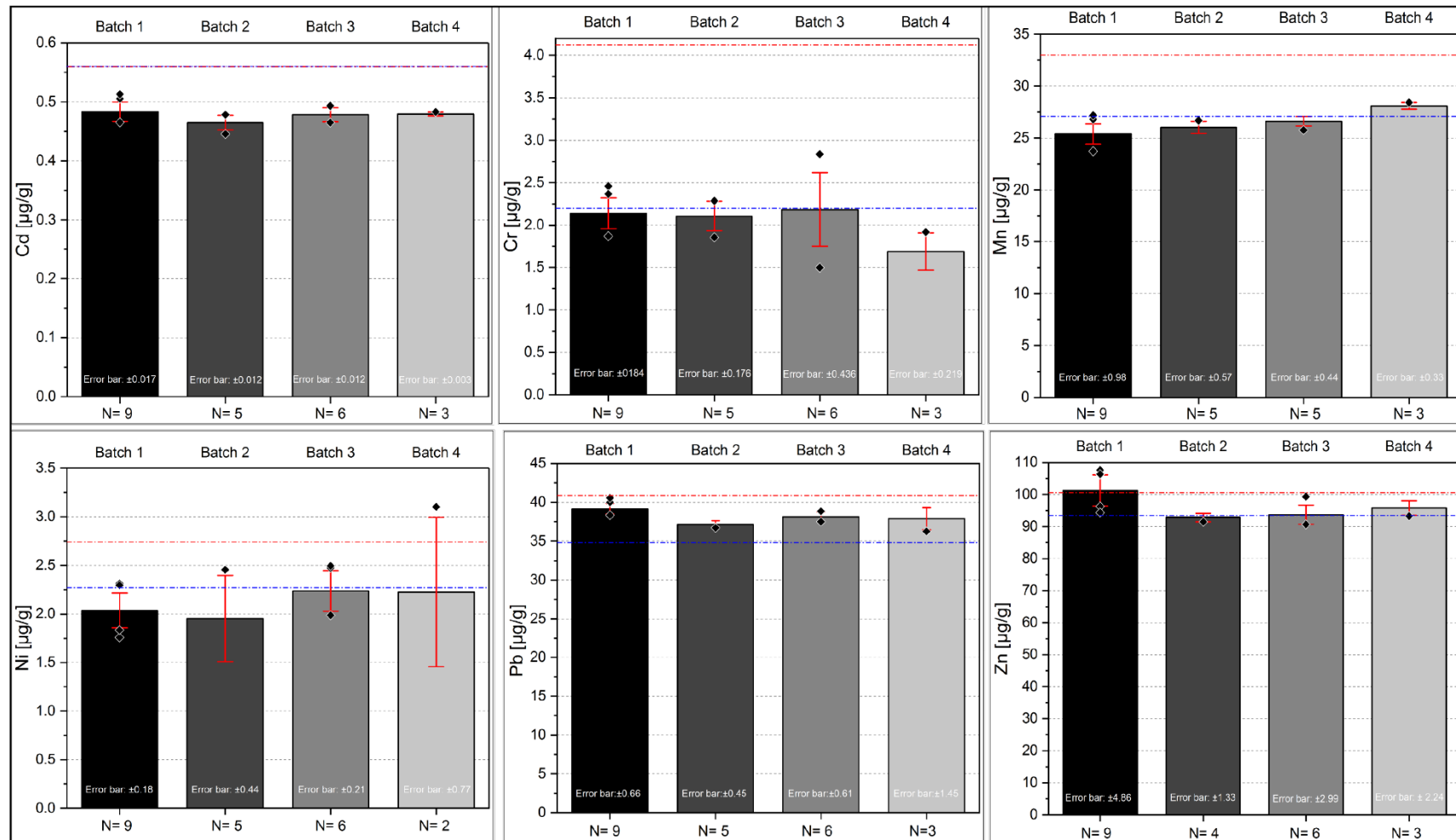


Figure 6-3: Lichen CRM (482) metal concentrations measured per sample batch (N=4, left to right) for Cd (by ICP-MS; upper left), Cr (by ICP-MS), Mn (by ICP-OES) and lower left for Ni (by ICP-OES), Pb (by ICP-OES) and Zn (by ICP-OES). Results presented as mean values with error bars as 1xSD of CRM values measured within a batch; displayed with certified CRM values (red dashed line; Quevauviller et al., 1996), and concentrations reported by Baffi et al. (2002) (blue dashed line). Palladium (Pd) and Platinum (Pt) not shown, due to unavailability of certified values

Individual batch accuracy (expressed in %) for elements measured by ICP-OES and ICP-MS, together with overall precision (coefficient of variation – CV%; calculated as precision for all analysed CRM measurements by standard deviation/ mean*100) are displayed in Table 6-7.

Table 6-7: Sample batch accuracy (expressed in %) of lichen CRM (N=23) metal concentrations measured by ICP-OES and ICP-MS, compared to: (a) certified values and (b) values measured using a HNO₃/H₂O₂ digestion, along with overall precision (%CV); N/A – not recorded by sources (Quevauviller et al., 1996; Baffi et al., 2002)

	Batch 1 (N=9)		Batch 2 (N=5)		Batch 3 (N=6)		Batch 4 (N=3)		Precision (overall)
	(a)	(b)	(a)	(b)	(a)	(b)	(a)	(b)	CV%
Al	61	114	45	84	61	113	53	98	13
As	81	78	81	78	85	83	91	88	5
Be	N/A	1038	N/A	1021	N/A	1053	N/A	1036	8
Cd	86	86	83	83	85	85	85	85	3
Co	82	105	81	103	82	106	83	106	4
Cr	52	97	51	96	53	99	41	77	15
Cu	88	96	87	94	89	97	91	99	2
Fe	74	91	68	83	77	94	53	98	6
Mn	77	94	79	96	81	98	79	96	4
Ni	83	N/A	79	N/A	91	N/A	90	N/A	12
Pb	96	N/A	91	N/A	93	N/A	93	N/A	3
Pd	N/A	N/A	N/A	N/A	N/A	N/A	N/A	N/A	14
Pt	N/A	N/A	N/A	N/A	N/A	N/A	N/A	N/A	33
S	88	N/A	81	N/A	84	N/A	78	N/A	3
Ti	33	69	32	68	35	74	33	69	8
V	75	90	74	90	78	93	77	92	3
Zn	101	108	92	99	93	103	95	103	6

Table 6-8 shows the measured CRM values (overall; N=23) in comparison to certified values that applied a HNO₃/HF acid digestion and a study analysing lichen CRM by HNO₃/H₂O₂ acid digestion (Quevauviller et al., 1996; Baffi et al., 2002). This study's lichen CRM measurements, following digestion only with HNO₃, yielded lower concentrations compared to the more aggressive digestion using HNO₃/HF (Quevauviller et al., 1996); consequently, accuracy when compared to the latter values is between 33% (for Ti) and 97% (for Zn). Nevertheless, the element concentrations determined for the lichen CRM values by this study are in much closer agreement with concentrations reported by Baffi et al. (2002), who also did not use HF, illustrating accuracy between 69% (Ti) and 109% (Co). Overall accuracy for the key target metals that are the focus of this study, in relation to Baffi et al. (2002), is between 81% for Cd and 109% for Pb.

Table 6-8: Measured (this study – mean values ± standard deviation; for all CRM measurements; N=23) and certified (and indicative) lichen CRM-482 elemental concentrations [µg/g] for different acid digestion methods (Quevauviller et al., 1996; Baffi et al., 2002)

Element	Measured values (HNO ₃ digestion – this study) N = 23	Certified values (HNO ₃ /HF digestion) ^(a)	Measured values (HNO ₃ /H ₂ O ₂ digestion) ^(b)	Accuracy* (%)	
				(a)	(b)
Al	635.32 ± 81.51	1103 ± 24	592 ± 43	58	107
As	0.70 ± 0.05	0.85 ± 0.07	0.88 ± 0.44	83	80
Be	0.02 ± 0.002	N/A	0.002 ± 0.001	N/A	1030
Cd	0.45 ± 0.10	0.56 ± 0.02	0.56 ± 0.02	81	81
Co	0.27 ± 0.04	0.32 ± 0.03 [†]	0.25 ± 0.01	85	109
Cr	2.09 ± 0.34	4.12 ± 0.15	2.20 ± 0.51	51	95
Cu	6.88 ± 2.32	7.03 ± 0.19	6.49 ± 0.69	98	106
Fe	629.49 ± 37.45	804 ± 160 [†]	688 ± 54	75	92
Mn	26.19 ± 0.94	33.0 ± 0.5 [†]	27.1 ± 0.98	79	97
Ni	2.11 ± 0.25	2.47 ± 0.07	2.27 ± 0.05	85	93
Pb	38.08 ± 0.96	40.9 ± 1.4	34.8 ± 1.1	93	108
Pd	0.02 ± 0.01	N/A	N/A	N/A	N/A
Pt	0.003 ± 0.004	N/A	N/A	N/A	N/A
S	1829.65 ± 59.11	2166 ± 292 [†]	N/A	85	N/A
Ti	11.29 ± 1.17	34.2 ± 1.1 [†]	16.30 ± 2.6	33	69
V	2.71 ± 0.45	3.74 ± 0.61 [†]	3.11 ± 0.19	72	87
Zn	97.32 ± 5.54	100.6 ± 2.2	93.5 ± 4.11	97	104

^(a) certified concentrations for CRM-482 and ^(b) values measured by Baffi et al. (2002)

* accuracy presented for comparison of this study's concentrations with both digestion methods: first value = comparison to HNO₃/HF digestion; second value = comparison to HNO₃/H₂O₂ digestion

[†] indicative value

Overall the accuracy of ICP-OES and ICP-MS determination of lichen CRM metals is considered good, with minor underestimations for some elements (i.e. Cr, Mn and Ni), while Pb and Zn concentrations were marginally overestimated (Table 6-8). The HNO₃ acid digestion of lichen material was able to achieve valid measurements for this study, when compared to similar acid extraction methods, i.e. using HNO₃/H₂O₂. Repeatability is an expression of the precision of measurements made under the same operating conditions (i.e. extraction method and instrumental conditions; European Medicines Agency, 1995). Overall precision (repeatability expressed as %CV, Table 6-7) for the key target metals (for all batches) is considered good, with %CV ranging from 2.5% (Pb) to 33% (Pt). Unfortunately, no certified values for Pd and Pt are available such that accuracy for these two metals could not be specified.

6.3.2 Temporal variability of metal concentrations in urban lichen samples

Lichen sampling was undertaken between June 2016 and October 2017. The long sampling periods suggest a potential temporal bias on metal concentrations, superimposed on spatial variability. To investigate temporal variability of metal concentrations, a sub-set of sampling sites (N=17; *X. parietina*) that have been sampled during the first sampling period (2016/17), were re-visited in 2018. Samples were subsequently analysed for metal concentrations to investigate temporal variability, which could comprise spatial analysis.

Testing for normal distribution (Shapiro-Wilk test) of metal concentrations in 2018 varied by metal (in *X. parietina*). Different distribution outcomes favoured the use of the Wilcoxon test (non-parametric) to analyse differences in concentrations for the sampling periods (Table 6-9). Highly significant ($p < 0.01$) differences were found for Al, Ti and Pd, whereas significant differences were recorded for Be, Cr, and Pb. Concentrations of Cd, Mn, Ni and Zn were not significantly different for 2016/17 to 2018.

Table 6-9: Wilcoxon test statistics to compare metal concentrations recorded in *X. parietina* (N=17) for the two sampling periods (in 2016/17 and in 2018) to assess potential temporal bias superimposed on spatial analysis, displayed with p-values and significance levels (*p<0.05, shaded in yellow and **p<0.01, shaded in green); key target metals presented in bold

Element	Wilcoxon test p-value (two-tailed)
Aluminium (Al)	0.007**
Arsenic (As)	0.329
Beryllium (Be)	0.110*
Cadmium (Cd)	0.263
Cobalt (Co)	0.207
Chromium (Cr)	0.035*
Copper (Cu)	>0.99
Iron (Fe)	0.12
Manganese (Mn)	0.064
Nickel (Ni)	0.459
Lead (Pb)	0.031*
Palladium (Pd)	<0.0001**
Platinum (Pt)	0.927
Sulphur (S)	0.353
Titanium (Ti)	0.0007**
Vanadium (V)	0.015*
Zinc (Zn)	0.96

Key target metals for this study, i.e. Cr and Pb showed temporal differences (p<0.05) for both sampling periods, whereas Pt showed highly significant differences (p<0.01), indicating a potential bias for these metals.

Lead (Pb) is ubiquitous in the environment and Chromium (Cr) is associated with vehicular sources (Taylor, 2006). Both elements have no beneficial effects in humans and pose a significant risk to human health (Table 6-1; Kampa and Castana). Although there is temporal variability for both target metals, spatial variability will further be presented and discussed, due to significant potential health risks. In contrast, Palladium (Pd) will not be further discussed, due to highly significant differences between sampling periods, and impairment of spatial variability discussion for this particular element.

Accumulations patterns in lichens are dependent on length of exposure and/or age (Coccaro et al., 2000; Garty, 2001). Presumably, young lichens (*X. parietina*) were sampled off street tree twigs and small branches to assess recent air quality. Due to the lichens morphology, they are accumulating metals over a period of time (i.e. extracellularly, inter- and intracellularly).

A highly significant difference for Pd was therefore considered to undermine a potential spatial trend for this element in Manchester. Comparison of metal concentrations for both sampling periods (presented as box-whisker plots) are displayed in Figure 6-4 (for Cd, Cr, Mn, Ni, Pb and Pd) and Figure 6-5 (for Pt and Zn). Site-specific (N=17; *X. parietina*) metal concentrations, recorded for both sampling periods (in 2016/17 and re-visited in 2018), are displayed in the Appendix D-3.

A general trend of increases in metal concentration ranges was observed for Cd, Cr, Mn, Ni and Pd (Figure 6-4a, b, c, d and f). In contrast, Pb was recorded at lower concentrations in 2018, compared to the first sampling period (Figure 6-4e). Platinum (Pt) was found at comparable ranges, with concentrations between 0.001 to 0.006 µg/g in 2016/17 and 0.002 to 0.007 µg/g in 2018, indicating a slight increase in overall Pt concentrations (Figure 6-5, upper panel). Zinc concentrations for both sampling periods was comparable (Figure 6-5, lower panel)

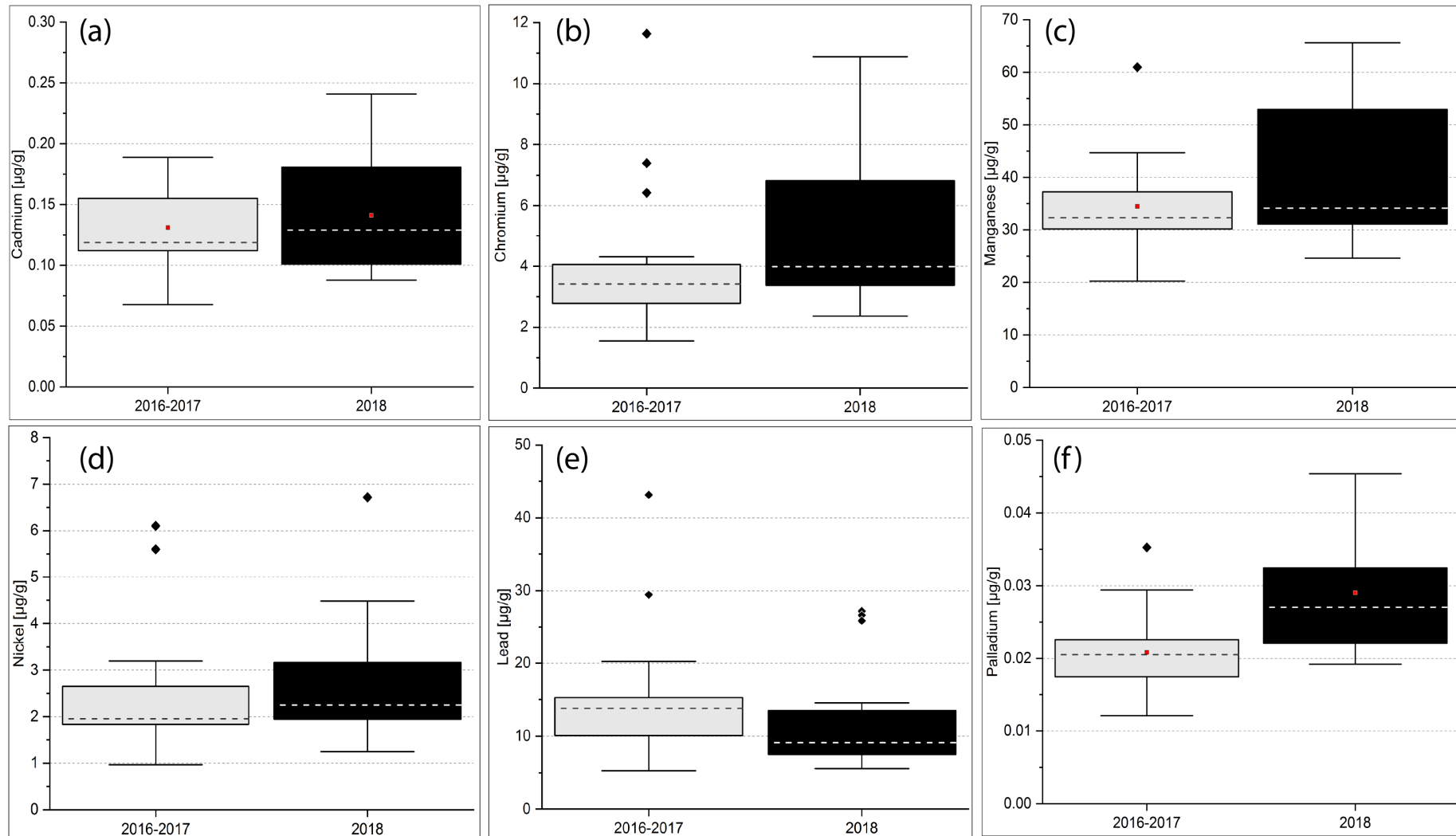


Figure 6-4: Box-Whisker plots (25th to 75th percentile, displayed with mean: red square, for normally distributed metal concentrations; median line for non-normally distributed metal concentrations; extreme values: black diamond) of target metal concentrations in *X. parietina* for both sampling periods 2016/17 and 2018, for (a) Cd, (b) Cr, (c) Mn, (d) Ni, (e) Pb and (f) Pd

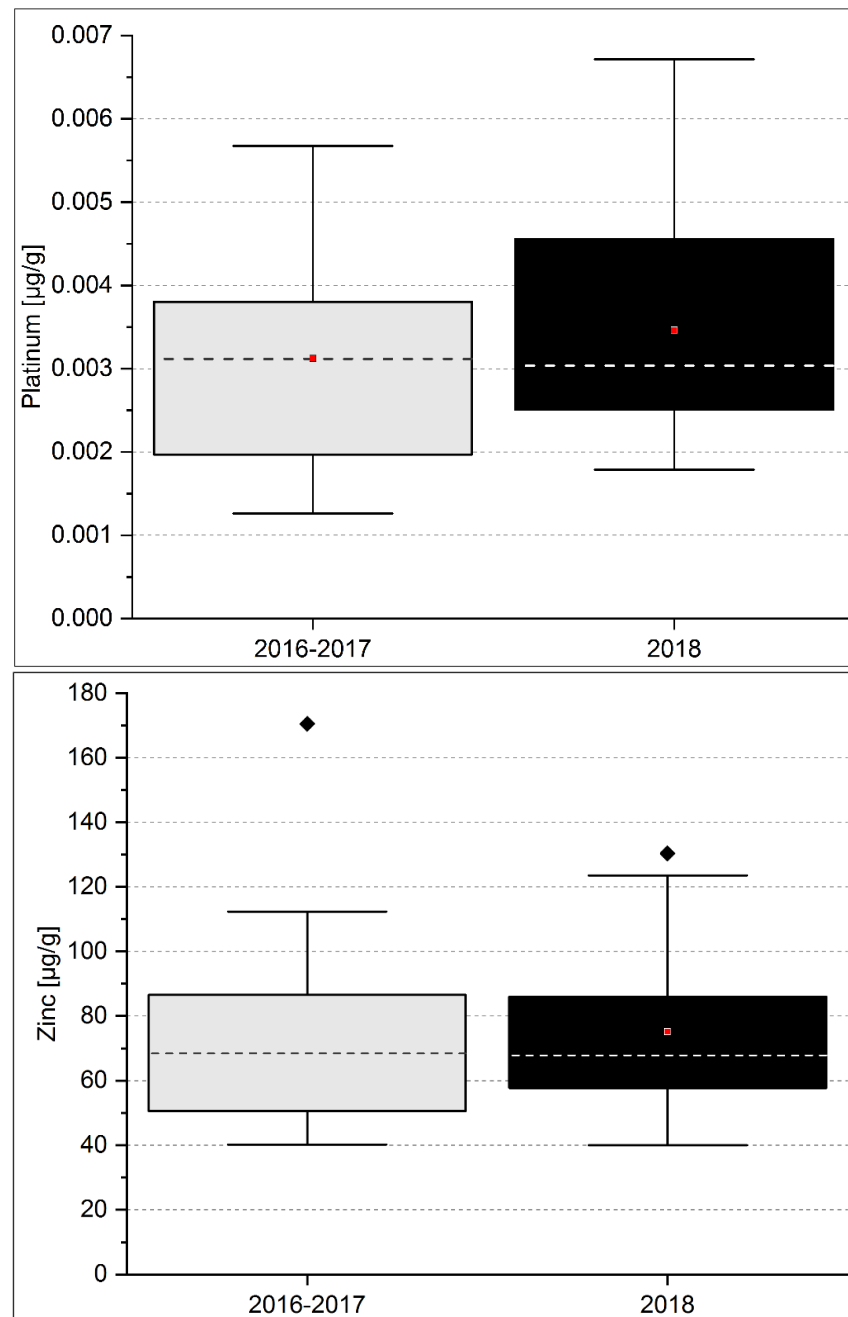


Figure 6-5: Box-Whisker plots (25th to 75th percentile, displayed with mean: red square for normally distributed metal concentrations; median line for non-normally distributed metal concentrations; extreme values: black diamond) of target metal concentrations in *X. parietina* for both sampling periods 2016/17 and 2018, for Pt (upper panel) and Zn (lower panel)

A temporal influence on analysed lichen metal concentrations was found for key target metals, i.e. Cr, Pb and Pd, whereas other metals (i.e. Cd, Mn, Ni, Pt and Zn) did not show a potential bias superimposed on spatial variability. Cr and Pb were further considered for spatial variability analysis due to severe health impacts, whereas Pd was excluded (due to highly significant differences). Influences on temporal variation in metal concentrations will be discussed in section 6.4.1

6.3.3 Metal concentrations in rural *X. parietina* samples

Rural *X. parietina* (N=12) were analysed for metal concentrations for comparison with urban counterparts. Metal concentrations in rural lichen samples are displayed in Table 6-10. Most element concentration were normally distributed (Shapiro-Wilk; $p > 0.05$), except Pb, Zn and As. Figure 6-6a illustrates the metal concentrations (note: y-axis presented on a \log_{10} scale) recorded in *X. parietina* sampled around the poultry farm, with highest concentrations found for Al and Fe (Table 6-10). Target metals Mn and Zn were also recorded at relatively high concentrations in rural *X. parietina*, while Pd and Pt were recorded at low concentrations (Figure 6-6b and Table 6-10).

Table 6-10: Descriptive statistics ($\bar{x} \pm 1 \times \text{SD}$, for normal distributed data) for metal concentrations (in $\mu\text{g/g}$; determined by ICP-OES and ICP-MS) in *Xanthoria parietina* samples collected from a rural area; As, Pb and Zn concentrations were not normally distributed and their average concentrations are expressed as medians (\tilde{x})

Element	<i>X. parietina</i> (N=12)	
	Range (minimum – maximum)	Mean \pm 1 standard deviation (or median #)
Aluminium (Al)	175.35 – 535.11	321.18 \pm 86.23
Arsenic (As)	0.23 – 1.76	0.44 #
Beryllium (Be)	0.007 – 0.02	0.01 \pm 0.002
Cadmium (Cd)	0.05 – 0.11	0.07 \pm 0.02
Cobalt (Co)	0.08 – 0.25	0.15 \pm 0.04
Chromium (Cr)	0.50 – 1.05	0.77 \pm 0.15
Copper (Cu)	3.88 – 8.93	5.80 \pm 1.49
Iron (Fe)	212.16 – 595.79	369.92 \pm 94.75
Manganese (Mn)	22.23 – 52.06	33.67 \pm 8.39
Nickel (Ni)	0.19 – 0.96	0.52 \pm 0.21
Lead (Pb)	0.67 – 5.50	1.55 #
Palladium (Pd)	0.01 – 0.02	0.02 \pm 0.003
Platinum (Pt)	0.001 – 0.004	0.002 \pm 0.0008
Sulphur (S)	2152.1 – 4730.1	3766.1 \pm 789.4
Titanium (Ti)	2.89 – 11.20	6.69 \pm 2.28
Vanadium (V)	0.43 – 1.02	0.76 \pm 0.17
Zinc (Zn)	24.9 – 121.3	33.8 #

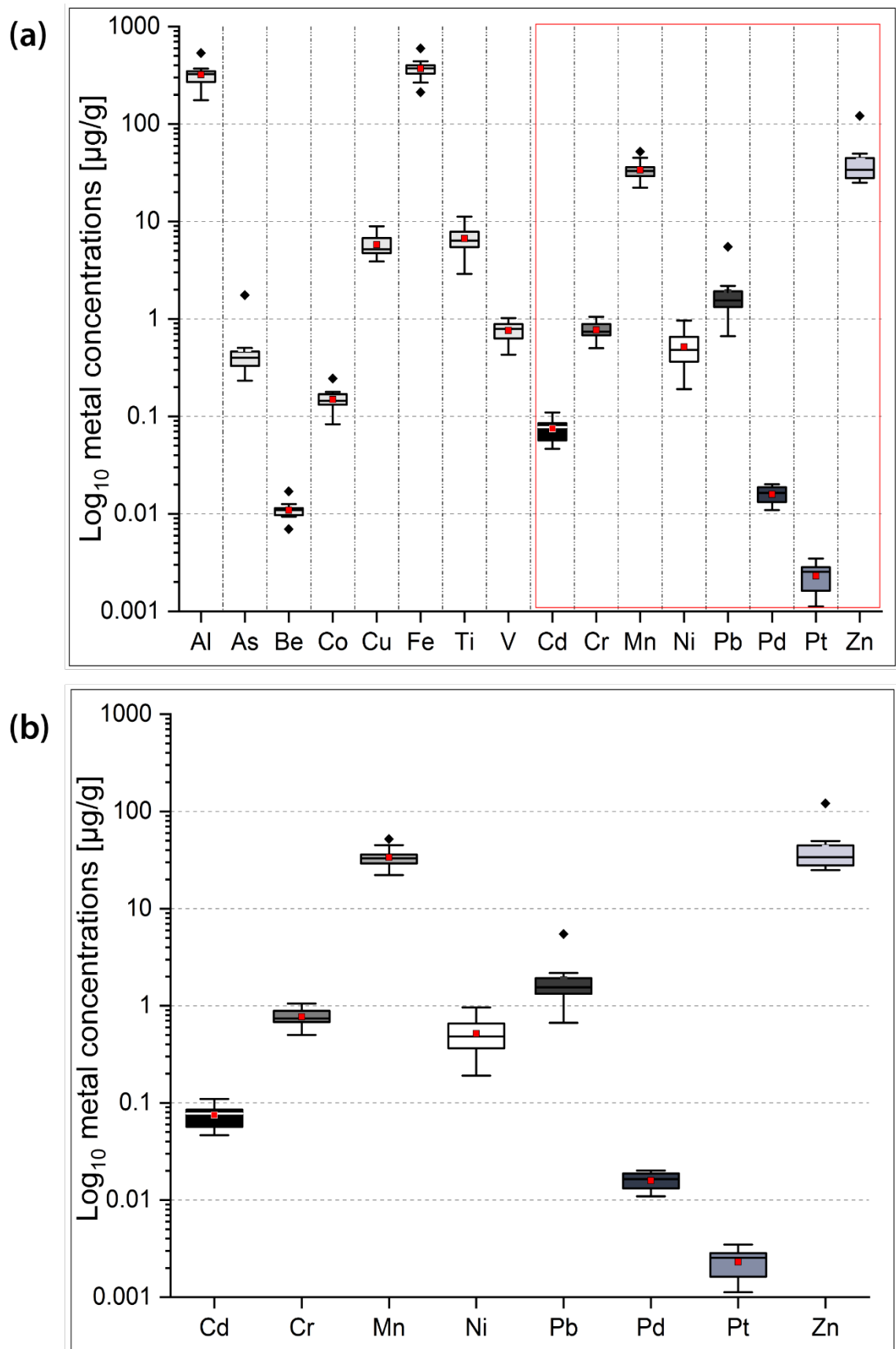


Figure 6-6: Box-Whisker plots (25th to 75th percentile, displayed with mean: red square for normally distributed metal concentrations; median line for non-normally distributed metal concentrations; extreme values: black diamond) of metal concentrations (y-axes presented as log₁₀-scale) in rural samples of *X. parietina* (N=12), for all analysed metals (a) and for the key target metals that are the focus of this study (b)

Different outcomes of the Shapiro-Wilk test for normal distribution (of grouped key target metal concentrations with distance to poultry farm) favoured the use of non-parametric statistical tests for comparison of distance groups (<500 m and >500 m), to assess whether lichen metal concentrations vary in relation to distance from this potential source of metal pollution and to distinguish what 'true' background rural metal concentrations would be. Figure 6-7 illustrates metal concentrations for samples grouped by distance to poultry farm (1: <500 m and 2: >500 m) for the key target metals. Except for Zn ($p < 0.05$), no significant differences between distance to poultry farm and metal concentrations was found (Table 6-11). This analysis indicates that for all elements apart from Zn, all *X. parietina* samples can be combined to yield rural background metal concentrations, whereas the poultry farm appears to be a source of Zn pollution, such as only the samples from >500 m distances should be used to determine a rural Zn concentration.

Table 6-11: Mann-Whitney test statistics (between grouped poultry farm distances; due to different outcomes for normal distribution) for key target metal concentrations recorded in rural *X. parietina* samples, to assess whether there is a significant difference in metal concentrations with distance to poultry farm (<500m and >500m)

Target elements	Mann-Whitney test p-value (two-tailed)
Cadmium (Cd)	0.15
Manganese (Mn)	0.78
Nickel (Ni)	0.43
Lead (Pb)	>0.99
Palladium (Pd)	0.79
Platinum (Pt)	0.92
Zinc (Zn)	0.02*

* significant difference between sample distance groups at the level $p < 0.05$

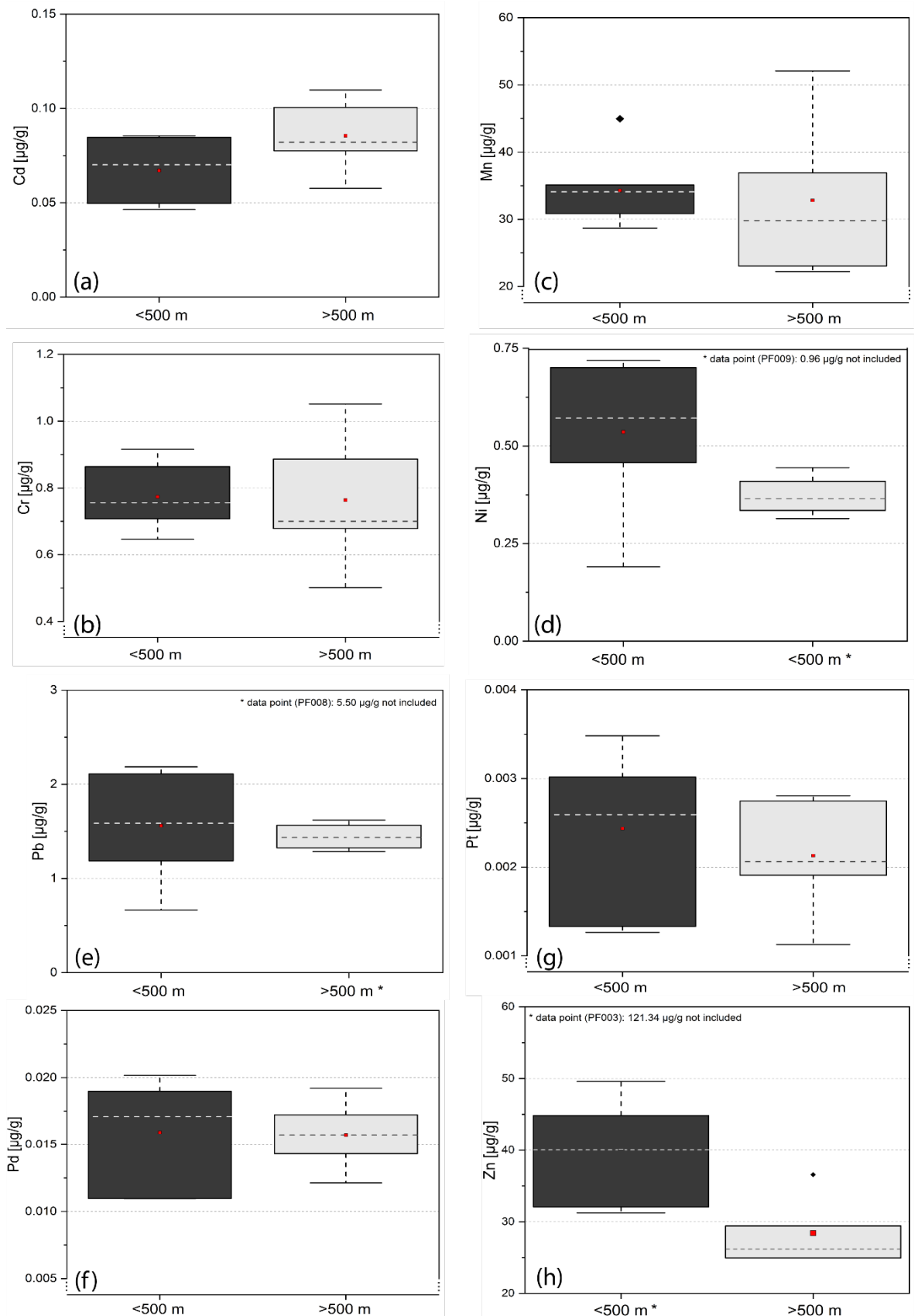


Figure 6-7: Box-whisker plots (25th and 75th percentile) of rural *X. parietina* metal concentrations against distance to poultry farm (<500m and >500 m), displayed with mean values (red square; for normally distributed group data) and median line (dashed line; for non-normally distributed group data)

6.3.4 Comparison of metal concentrations in *X. parietina* and *Physcia* spp. sampled across Manchester

Lichen samples, *X. parietina* and *Physcia* spp., were obtained during an initial sampling period in 2016/2017 and subsequently analysed for their metal concentration, with particular focus on key target metals (Table 6-1). Due to temporal variation of Pd (section 6.3.2), when compared to a second sampling period, spatial variability results were not further included.

Concentrations of target metals, i.e. Cd, Cr, Mn, Ni, Pt and Zn were not normally distributed for *X. parietina*, while Zn was normally distributed in *Physcia* spp. (Table 6-12). Descriptive statistics for additional metal concentrations are presented in Table 6-12, as minimum to maximum (range) and median ($\tilde{}$) concentrations, due to metals concentration data not being normally distributed for most analysed metals. Highest target metal concentrations in *X. parietina* and *Physcia* spp. were recorded for Manganese (Mn) and Zinc (Zn), followed by Lead (Pb), Nickel (Ni), Chromium (Cr) and Cadmium (Cd) in decreasing order (Figure 6-8 and Figure 6-9; note: y-axis presented on a \log_{10} scale).

Lichen sulphur was analysed by ICP-OES (in $\mu\text{g/g}$) and by IRMS (in wt %) and analytical instruments were compared, with similar results for both analytical procedures ($R^2=0.83$; Appendix D-7). Sulphur (S) content in lichens was previously addressed in detail within chapter 3 and is displayed for reasons of data integrity.

Table 6-12: Concentration ranges (minimum and maximum) and median concentrations (\bar{x}) for analysed metal concentrations (by ICP-OES and ICP-MS) in *Xanthoria parietina* and *Physcia* spp. [in $\mu\text{g/g}$], sampled during an initial sampling period in 2016/17; S was normally distributed for both lichen species and As and Zn for *Physcia* spp. and are presented as mean (\bar{x}) \pm 1x standard deviation; target metal concentrations shaded in light grey

Element	<i>Xanthoria parietina</i> (N=84)		<i>Physcia</i> spp. (N=17)	
	Range (min – max)	Median (\bar{x})	Range (min – max)	Median (\bar{x})
Aluminium (Al)	218.2 – 1231.1	530.8	243.2 – 967.4	410.2
Arsenic (As) †	0.23 – 1.56	0.62	0.49 – 1.42	0.89 \pm 0.29
Beryllium (Be)	0.008 – 0.05	0.02	0.01 – 0.04	0.02
Cadmium (Cd)	0.06 – 0.39	0.13	0.11 – 0.48	0.19
Cobalt (Co)	0.16 – 1.19	0.41	0.19 – 0.79	0.29
Chromium (Cr)	0.88 – 11.64	3.36	1.00 – 6.56	2.23
Copper (Cu)	8.00 – 61.55	16.12	6.21 – 38.08	13.02
Iron (Fe)	438.1 – 4349.4	1200.15	422.2 – 2410.6	869.6
Manganese (Mn)	12.57 – 73.41	29.33	19.10 – 48.04	25.98
Nickel (Ni)	0.62 – 13.68	2.13	0.80 – 3.29	1.43
Lead (Pb)	4.37 – 90.60	11.12	4.79 – 29.42	8.74
Palladium (Pd)	0.01 – 0.04	0.02	0.01 – 0.05	0.02
Platinum (Pt)	0.001 – 0.008	0.003	0.001 – 0.007	0.002
Sulphur (S) #	2953.6 – 5878.7	4412.9 \pm 693.7	2008.3 – 3433.0	2685.2 \pm 428.5
Titanium (Ti)	4.8 – 33.6	13.14	5.02 – 22.68	8.85
Vanadium (V)	0.46 – 4.05	1.39	0.65 – 2.75	1.06
Zinc (Zn) †	31.56 – 199.73	64.12	59.95 – 125.36	88.18 \pm 21.21

mean value displayed (\pm 1 SD): normally distributed for both lichen species

† mean value displayed (\pm 1 SD): normally distributed for *Physcia* spp.

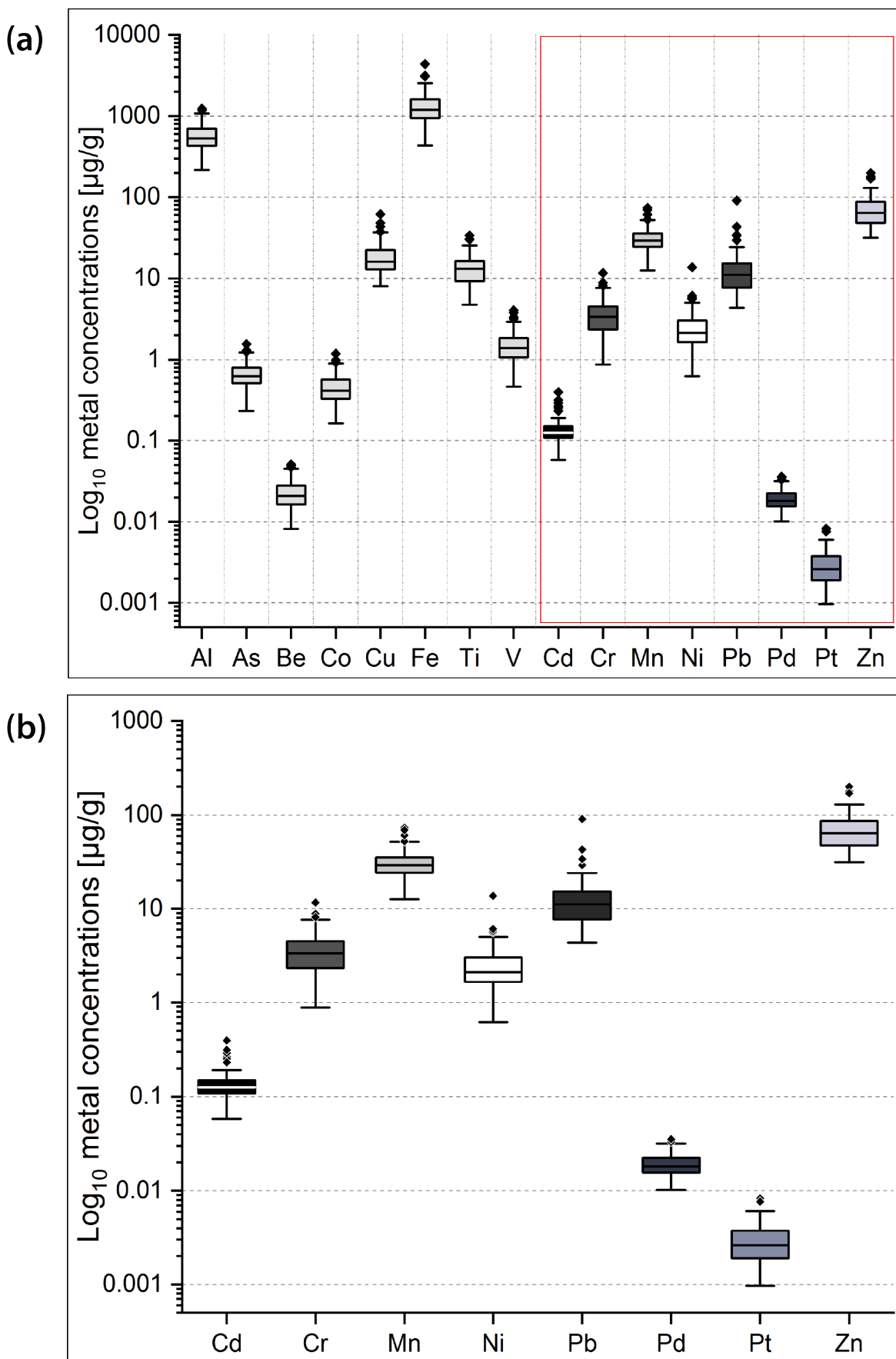


Figure 6-8: Box-Whisker plots (25th to 75th percentile, displayed with mean: red square, median line and extreme values: black diamond) of metal concentrations (y-axes presented as log₁₀-scale) recorded in urban samples of *X. parietina* (N=84), (a) for all analysed metals and (b) for target metals in this study

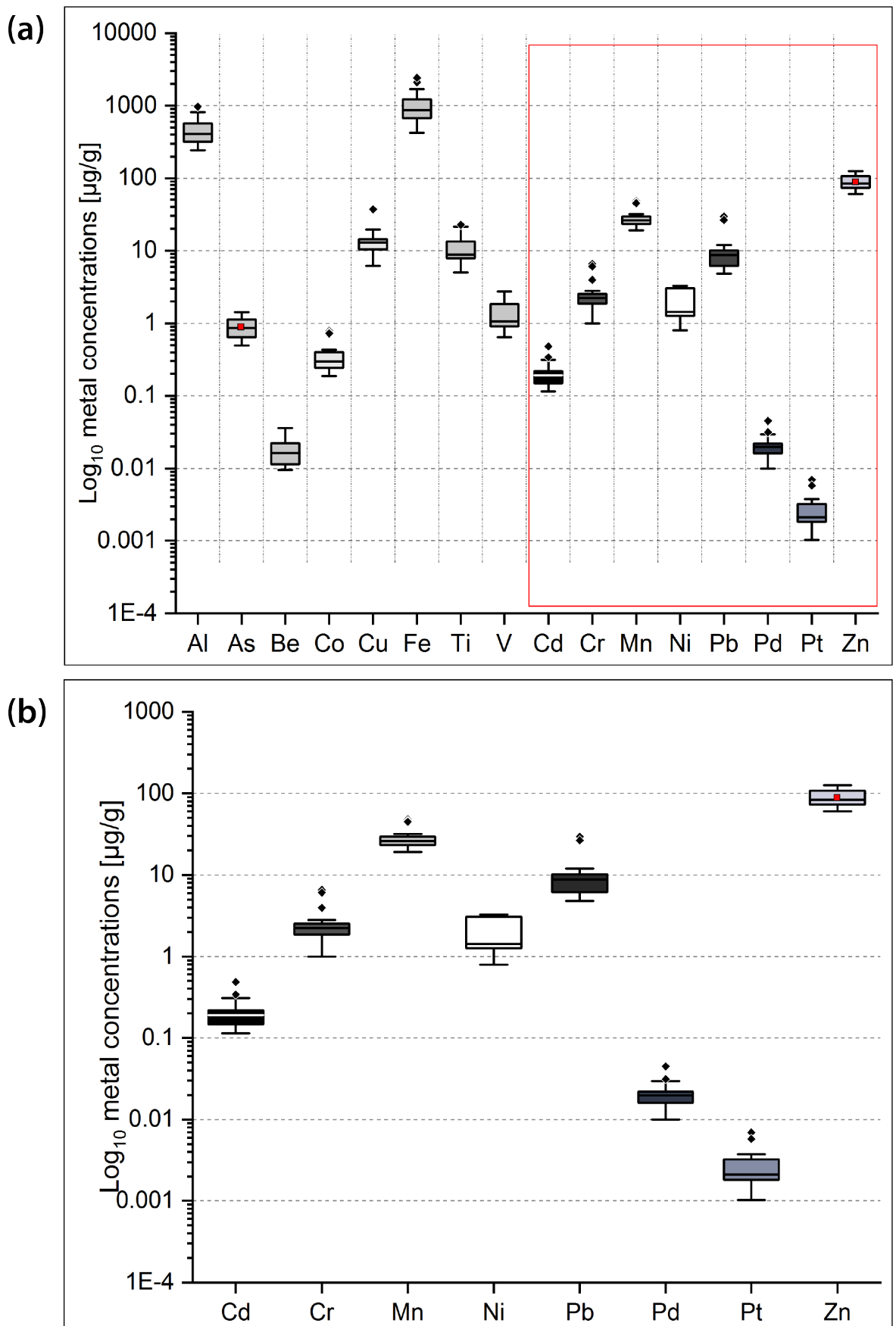


Figure 6-9: Box-Whisker plots (25th to 75th percentile, displayed with mean: red square, median line and extreme values: black diamond) of metal concentrations (y-axes presented as log₁₀-scale) recorded in urban samples of *Physica* spp. (N=17), (a) for all analysed metals and (b) for target metals in this study

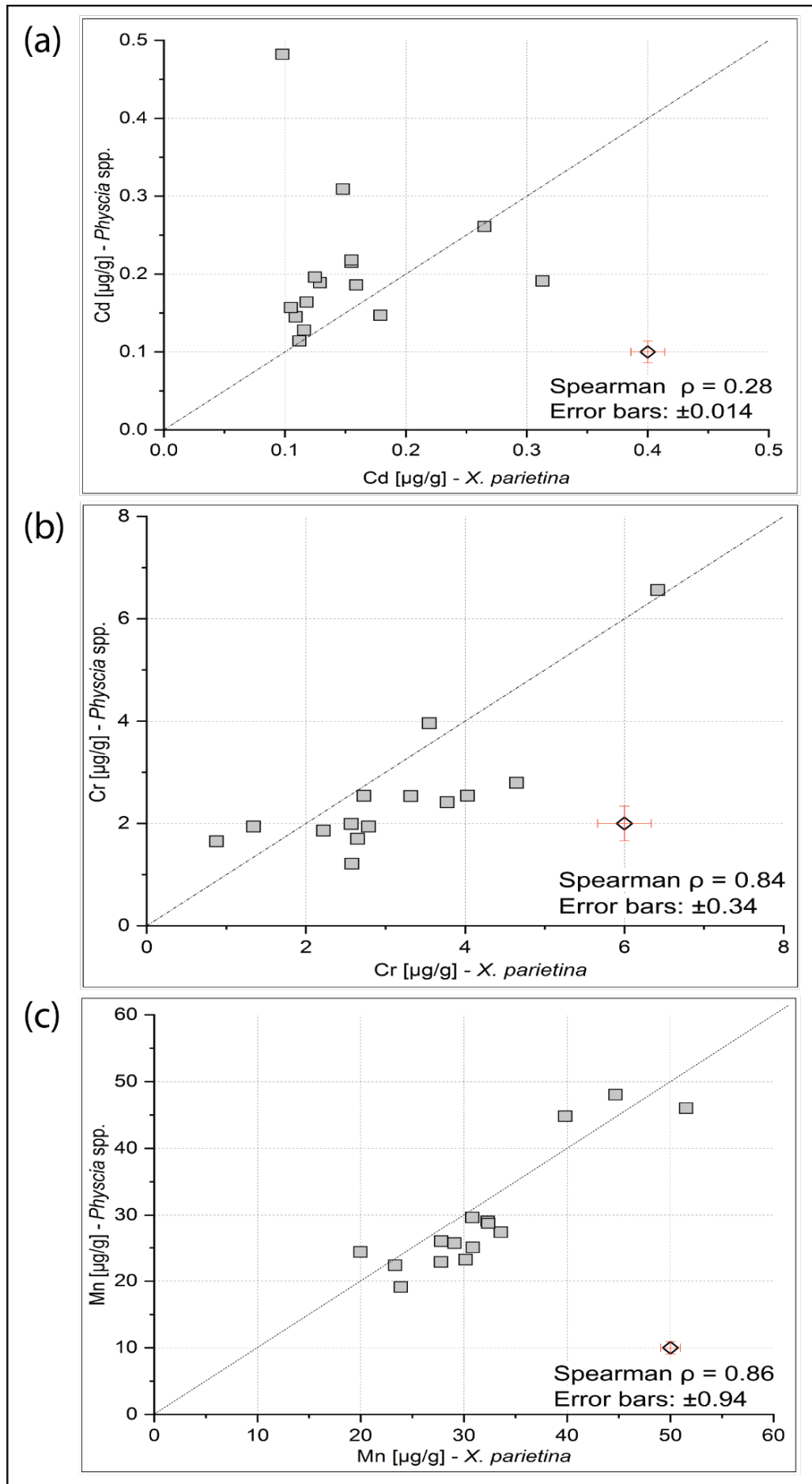
To compare both lichen species for their recorded metal concentrations and to investigate potential species-specific differences, a Wilcoxon test (non-parametric) was used (Table 6-13). Only sites that have been sampled and analysed for both lichens species (N=15) were used for comparison.

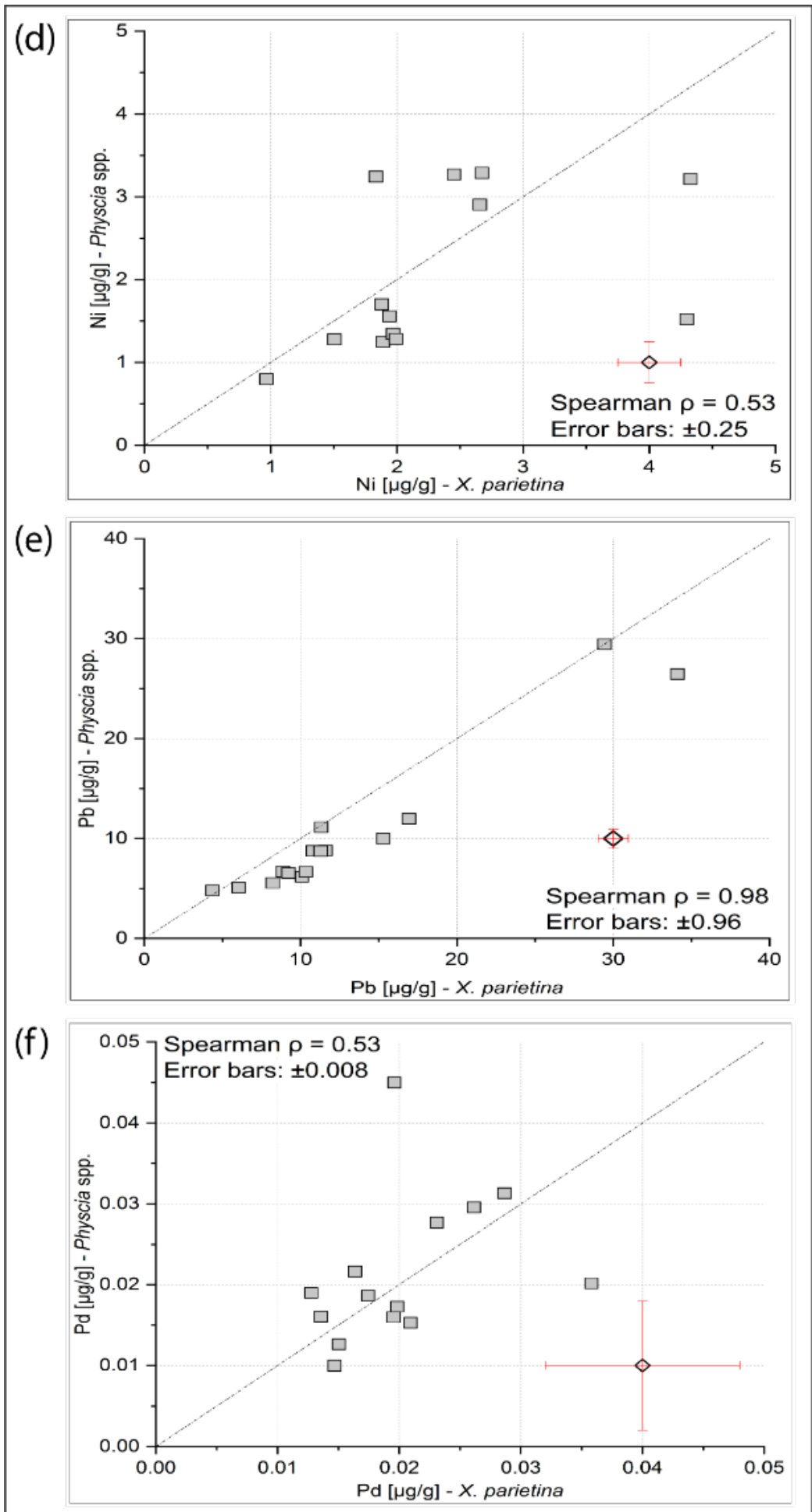
Significant differences ($p < 0.05$) for *X. parietina* and *Physcia* spp. were found for As and target metals Cd, Cr and Mn. In contrast highly significant differences ($p < 0.01$) were recorded for non-target metals: Al, Be, Co, Cu, Fe, Ti and V, and for target metals: Pb and Zn. No significant differences were recorded for Ni, Pd and Pt.

Table 6-13: Wilcoxon test (due to different outcomes of Shapiro-Wilk normality test) for comparison of metal concentrations in *X. parietina* and *Physcia* spp. sampled from the same sites (N=15), displayed with significance levels * $p < 0.05$, shaded in yellow and ** $p < 0.01$, shaded in green; key target metals presented in bold

Element	Wilcoxon (two-tailed)
Aluminium (Al)	0.0001**
Arsenic (As)	0.01*
Beryllium (Be)	0.0006**
Cadmium (Cd)	0.02*
Cobalt (Co)	0.0006**
Chromium (Cr)	0.02*
Copper (Cu)	0.005**
Iron (Fe)	0.0006**
Manganese (Mn)	0.04*
Nickel (Ni)	0.37
Lead (Pb)	0.0003**
Palladium (Pd)	0.72
Platinum (Pt)	0.12
Sulphur (S)	<0.0001**
Titanium (Ti)	0.0009**
Vanadium (V)	0.125
Zinc (Zn)	<0.0003**

Recorded concentrations for target metals in *X. parietina* compared to *Physcia* spp. are presented as scatter-plot in Figure 6-10a to h. Cadmium (Figure 6-10a) was recorded at higher concentrations in samples of *Physcia* spp. compared to *X. parietina*. Zinc was also found higher in *Physcia* spp. (Figure 6-10h) when compared to *X. parietina*. In contrast, concentrations of Cr, Mn, and Pb were recorded higher in *X. parietina* (at the same site; Figure 6-10b, c and e). No comparison was undertaken for Pd and Pt, due to non-significant differences and analytical errors (Figure 6-10f and g).





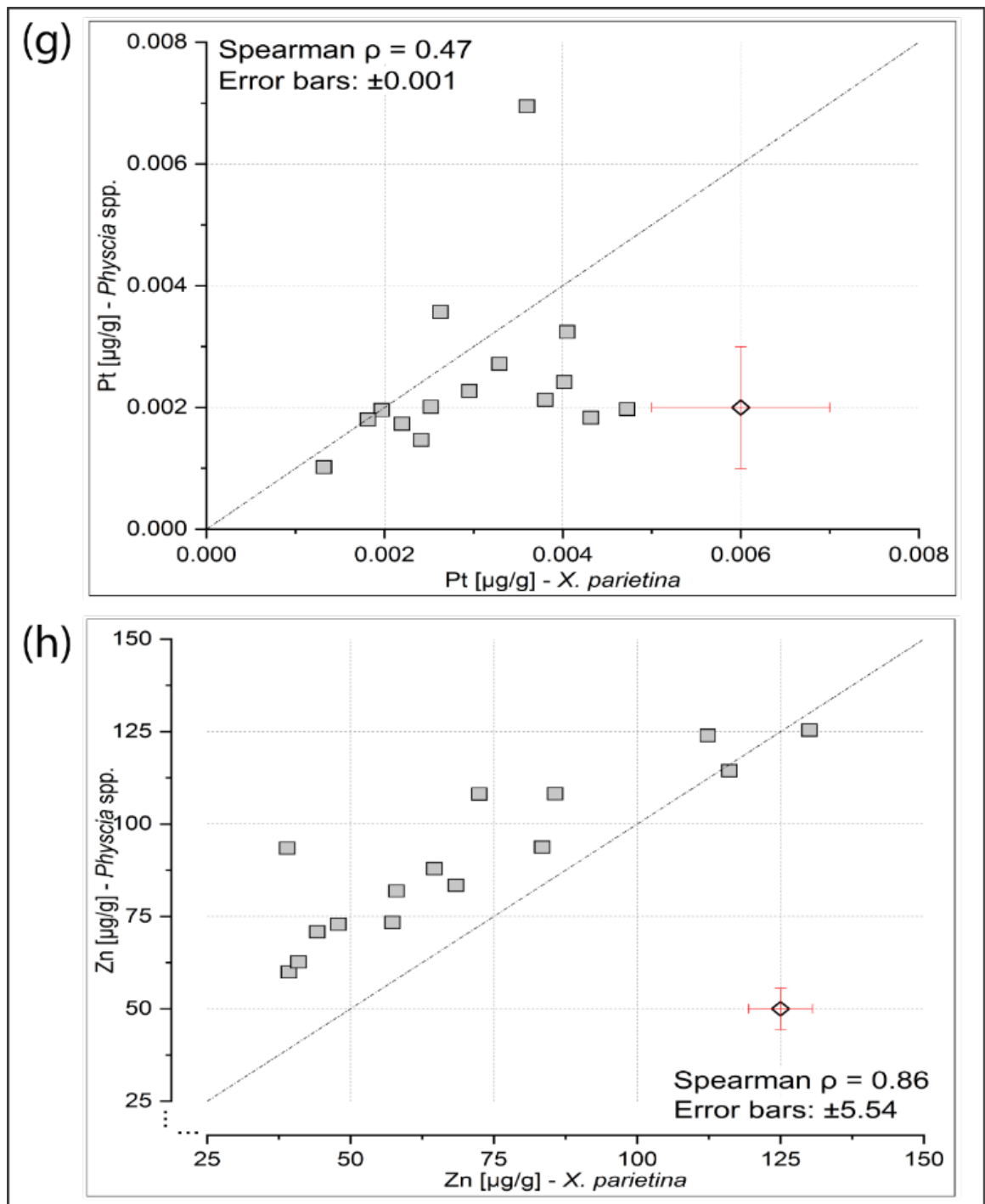


Figure 6-10: Comparison of (a) Cd, (b) Cr, (c) Mn, (d) Ni, (e) Pb, (f) Pd, (g) Pt and (h) Zn concentrations in *X. parietina* and *Physcia* spp. (X and Y error bars displayed on 'dummy value [white diamond]': lichen CRM derived, displayed as 1x SD; together with Spearman ρ for concentrations in lichen species)

6.3.5 Spatial variability of metal concentrations recorded in *X. parietina* and *Phyrcia* spp. samples across Manchester

Key target metal concentrations in both lichen species varied by sampling location and within lichen species. Figure 6-11 displays Cd concentrations recorded in *X. parietina* (a) and *Phyrcia* spp. (b). Elevated Cd concentrations (in *X. parietina*) were found across the research area, whereas highest Cd for *Phyrcia* spp. was found in the northeast of the research area.

Concentrations of Cr show a comparable pattern for both lichen species (Figure 6-12), with elevated Cr within the city centre and along the major road network. Moreover, elevated Cr was found at three sites for both, *X. parietina* (Figure 6-12a) and *Phyrcia* spp. (Figure 6-12b), suggesting site-specific Cr influences. However, for Cr temporal variability might be superimposed, as described in section 6.3.2, which needs to be taken into account.

Manganese (Mn) concentrations in both lichen species illustrate a similar spatial pattern (Figure 6-13), again with the three sites found high in Cr, having higher Mn concentrations. Manganese in lichens was more variable in *X. parietina* (Figure 6-13b) across Manchester, compared to *Phyrcia* spp. (Figure 6-13b). Highest concentrations were found within the city centre and along major roads.

Ni concentrations (in *X. parietina*; Figure 6-14) exhibited spatial variability across Manchester, with highest recorded concentrations along major roads north of 'Piccadilly Gardens' automated monitoring station. Elevated Ni was found within the city centre and along major roads within the research area. Nickel, recorded in *Phyrcia* spp. showed higher concentrations at sites also higher in Cr (Figure 6-12) and Mn (Figure 6-13), but lower compared to concentrations recorded in *X. parietina*.

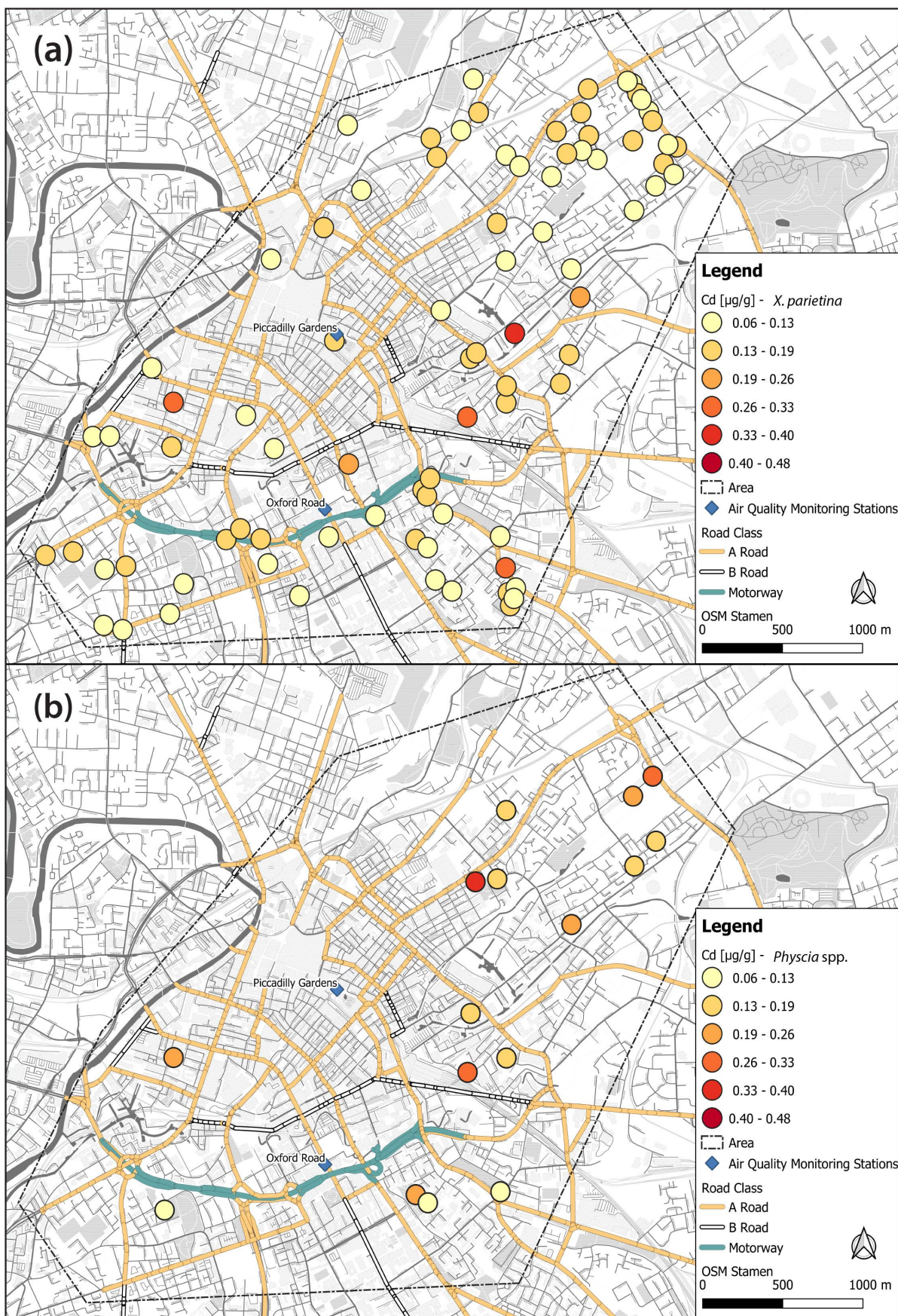


Figure 6-11: Cadmium (Cd) concentrations in (a) *X. parietina* (N = 84) and (b) *Physcia* spp. (N=17), displayed as colour-coded symbols and automated air quality monitoring stations are also shown; EU/UK limit value for Cd in air show in Table 2-1 (1-year average: 5 ng/m^3)



Figure 6-12: Chromium (Cr) concentrations in (a) *X. parietina* (N = 84) and (b) *Physcia* spp. (N=17), displayed as colour-coded symbols and automated air quality monitoring stations are also shown. A potential temporal influence, overlaid onto spatial variability needs to be considered for Cr concentrations in lichens; no EU/UK limit value available

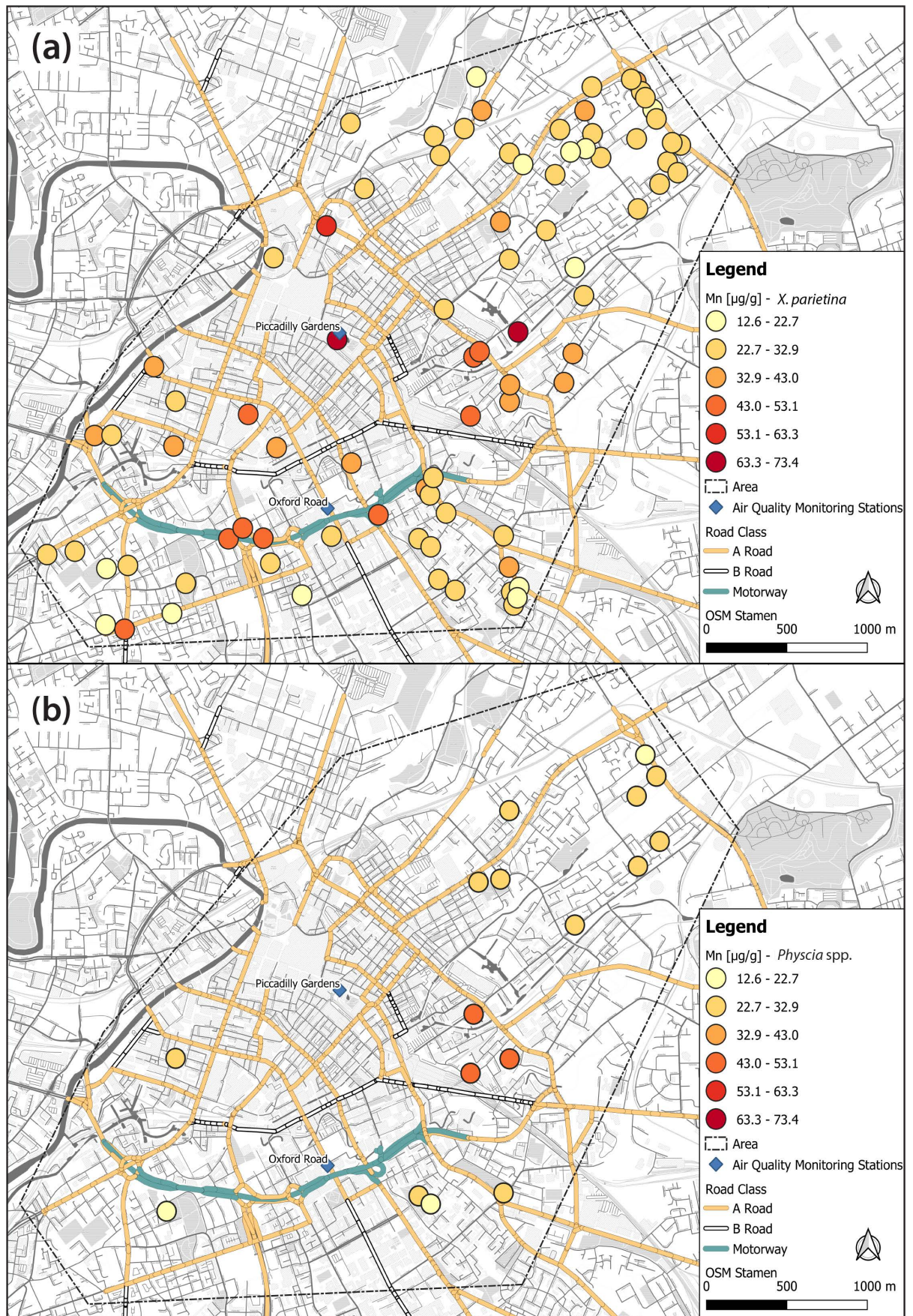


Figure 6-13: Manganese (Mn) concentrations in (a) *X. parietina* (N = 84) and (b) *Physcia* spp. (N=17), displayed as colour-coded symbols and automated air quality monitoring stations are also shown; no EU/UK limit value available

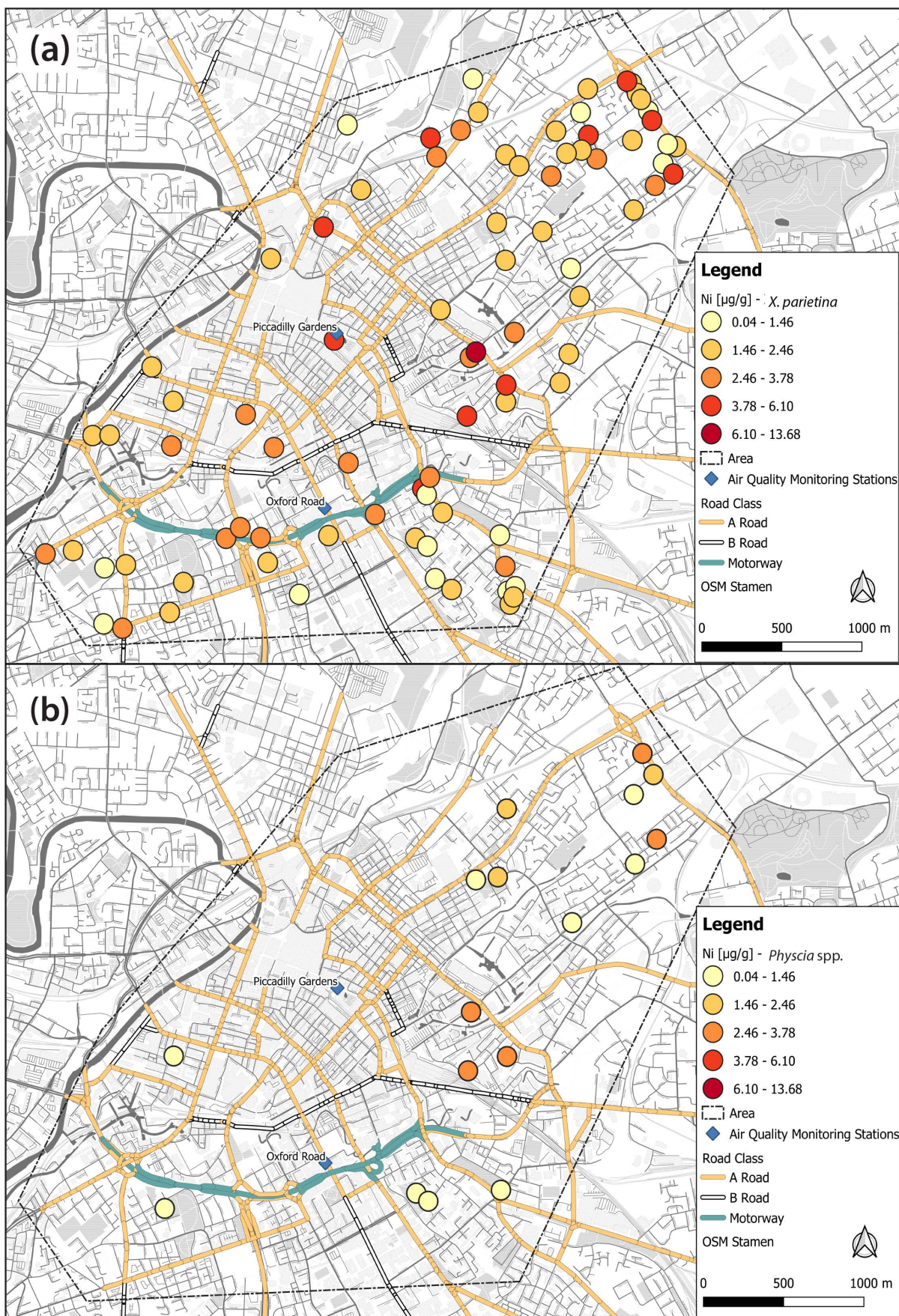


Figure 6-14: Nickel (Ni) concentrations in (a) *X. parietina* (N = 84) and (b) *Physcia* spp. (N=17), displayed as colour-coded symbols and automated air quality monitoring stations are also shown; EU/UK limit value shown in Table 2-1 (1-year average: 20 ng/m³)

Spatial variability of Pb concentrations in *X. parietina* and *Phyiscia* spp. is displayed in Figure 6-15a and b, respectively. Higher lead concentrations were found across the research area as a whole, with highest within the city centre and along the major road network. Comparable variability was found for *Phyiscia* spp. with highest Pb at sites already elevated in prior metals. Again, temporal variability of Pb concentrations need to be considered.

Platinum concentrations in *X. parietina* (Figure 6-16a) were found at higher concentrations along the major road network and around the city centre area, whereas highest Pt in *Phyiscia* spp. was recorded in the south of the research area (Figure 6-16b). Interestingly, the three sites that showed elevated metal concentrations (i.e. Cr, Mn, Ni and Pb) showed low Pt concentrations.

Figure 6-17a illustrates recorded Zn concentrations in *X. parietina*, with elevated concentrations within the city centre and 'hot-spots' located a major roads north of 'Piccadilly Gardens' and west of 'Oxford Road' automated monitoring stations. Zinc concentrations in *Phyiscia* spp. (Figure 6-17b) were found highest at three aforementioned sites. Elevated Zn was also recorded in the northeast of the research area.



Figure 6-15: Lead (Pb) concentrations in (a) *X. parietina* (N = 84) and (b) *Physcia* spp. (N=17), displayed as colour-coded symbols and automated air quality monitoring stations are also shown. A temporal influence, overlaid onto spatial variability for needs to be considered for Pb concentrations in lichens; EU/UK limit value shown in Table 2-1 (1-year average: $0.5 \mu\text{g/m}^3$)

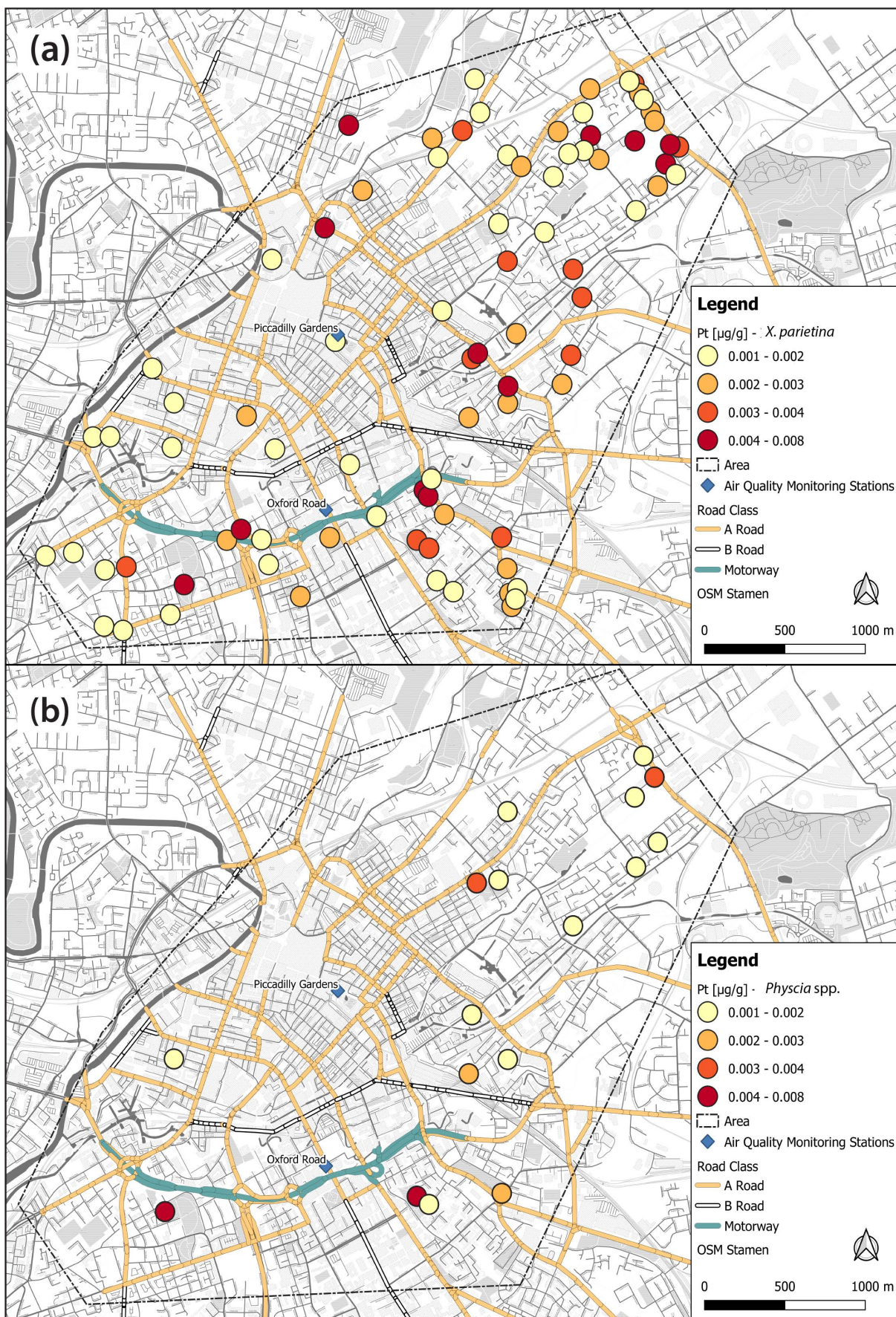


Figure 6-16: Platinum (Pt) concentrations in (a) *X. parietina* (N = 84) and (b) *Physcia* spp. (N=17), displayed as colour-coded symbols and automated air quality monitoring stations are also shown; no EU/UK limit value available

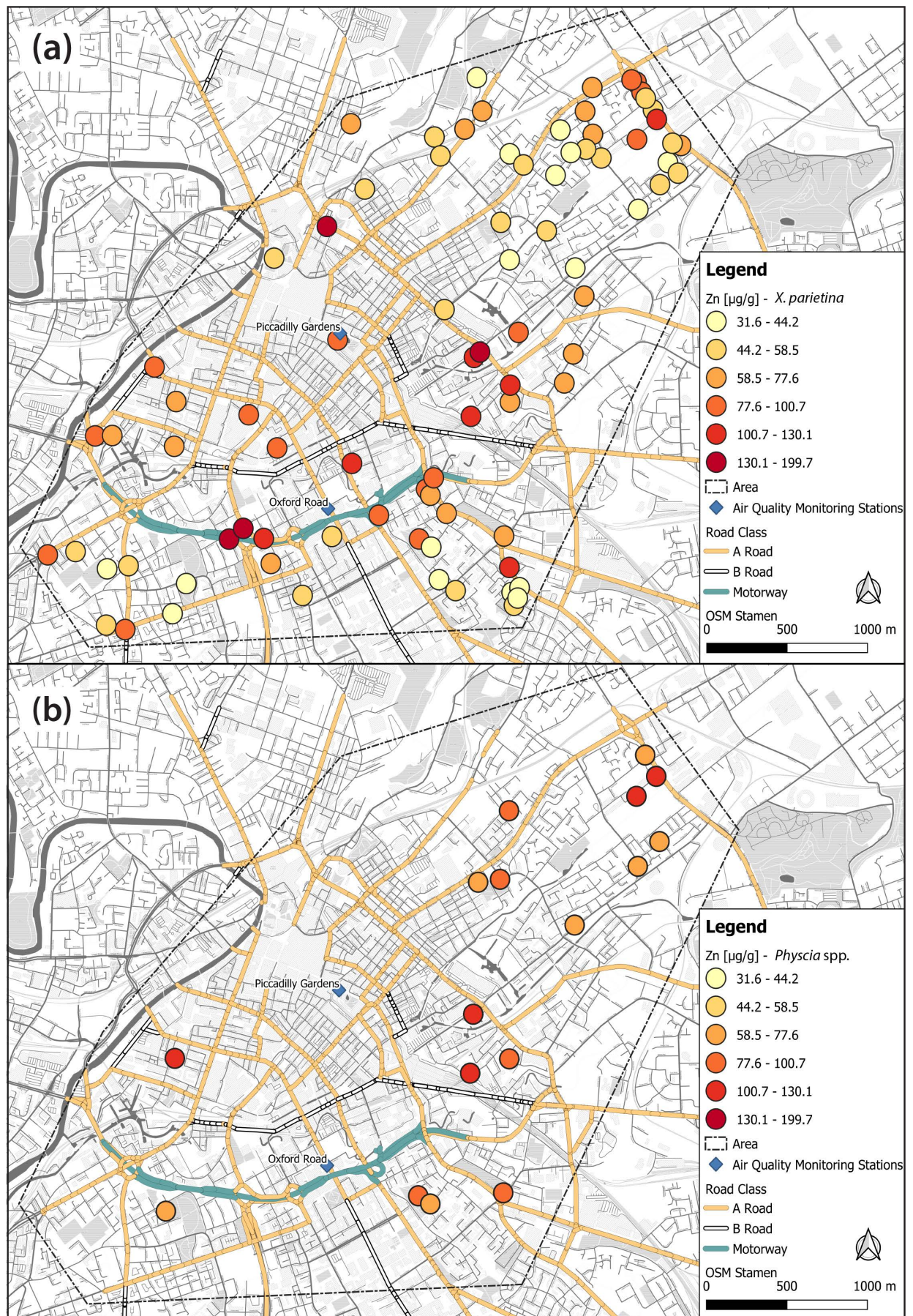


Figure 6-17: Zinc (Zn) concentrations in (a) *X. parietina* (N = 84) and (b) *Physcia* spp. (N=17), displayed as colour-coded symbols and automated air quality monitoring stations are also show; no EU/UK limit value available

Metal concentrations in both lichen species exhibit spatial variability across Manchester, suggesting potential sources, i.e. tyre and engine wear from cars (e.g. Ni and Cr), railway wear (Zn and Mn) and catalytic converters (Pt). Higher metal concentrations were generally recorded within the city centre and along the major road network (Figure 6-11 to Figure 6-17). Furthermore, species-specific differences for analysed metal concentrations were displayed, suggesting different uptake abilities and capabilities to respond to metal-induced stresses of *X. parietina*, compared to *Physcia* spp.

Urban influences, i.e. distribution and dispersion of pollutants, as well as species-specific differences in metal uptake abilities will be discussed later (section 6.4.4). Hereafter, urban *X. parietina* metal concentrations were compared to rural *X. parietina* samples, to evaluate differences in two contrasting environments.

6.3.6 Comparison of metal concentrations in rural and urban *X. parietina* lichens

Lichen metal concentrations, when compared for a rural and an urban environment, could potentially display varying pollution sources within these contrasting environments. Moreover, metal concentrations in an urban environment were considered to be higher and by testing elemental concentrations against a presumably 'cleaner' environment, could suggest the use of rural lichen samples as 'control' samples.

To compare urban and rural samples of *X. parietina* a Mann-Whitney test (non-parametric) was used, due to different sampling sizes (i.e. urban: N=84 [sampled during the initial sampling period in 2016/17] and rural: N=12) and different outcomes of Shapiro-Wilk tests for normal distribution of metal data.

Mann-Whitney test showed highly significant differences ($p < 0.001$; Table 6-14) for most metal concentrations, i.e. Cd, Cr, Ni, Pb and Zn, indicating additional metal influences on *X. parietina* across Manchester. No significant differences ($p > 0.05$) were found for Mn and Pt, respectively. Palladium is not considered, due to potential temporal bias in urban samples (Table 6-14). In general, concentrations in urban samples of *X. parietina* were usually higher and more variable (Table 6-12), compared to concentrations recorded in rural *X. parietina* samples (Table 6-10). Concentrations of metals sampled across the City of Manchester, were found to be significantly different from rural samples (Table 6-14). Figure 6-18 (a) to (g) illustrate concentrations of target metals in this study, recorded in urban and rural *X. parietina* samples.

Table 6-14: Mann-Whitney test output to assess whether there is a statistically significant difference between metal concentrations in urban (N=84) and rural (N=12) *X. parietina* samples; displayed as two-tailed p-value and significance levels (*p<0.05 and shaded in yellow; **p<0.01 and shaded in green); key target metals presented in bold (and shaded in grey)

Element	Mann-Whitney test (p-value, two-tailed)
Aluminium (Al)	<0.0001**
Arsenic (As)	0.0002**
Beryllium (Be)	<0.0001**
Cadmium (Cd)	<0.0001**
Cobalt (Co)	<0.0001**
Chromium (Cr)	<0.0001**
Copper (Cu)	<0.0001**
Iron (Fe)	<0.0001**
Manganese (Mn)	0.247
Nickel (Ni)	<0.0001**
Lead (Pb)	<0.0001**
Palladium (Pd)	0.03*
Platinum (Pt)	0.13
Sulphur (S)	0.009**
Titanium (Ti)	<0.0001**
Vanadium (V)	<0.0001**
Zinc (Zn)	<0.0001**

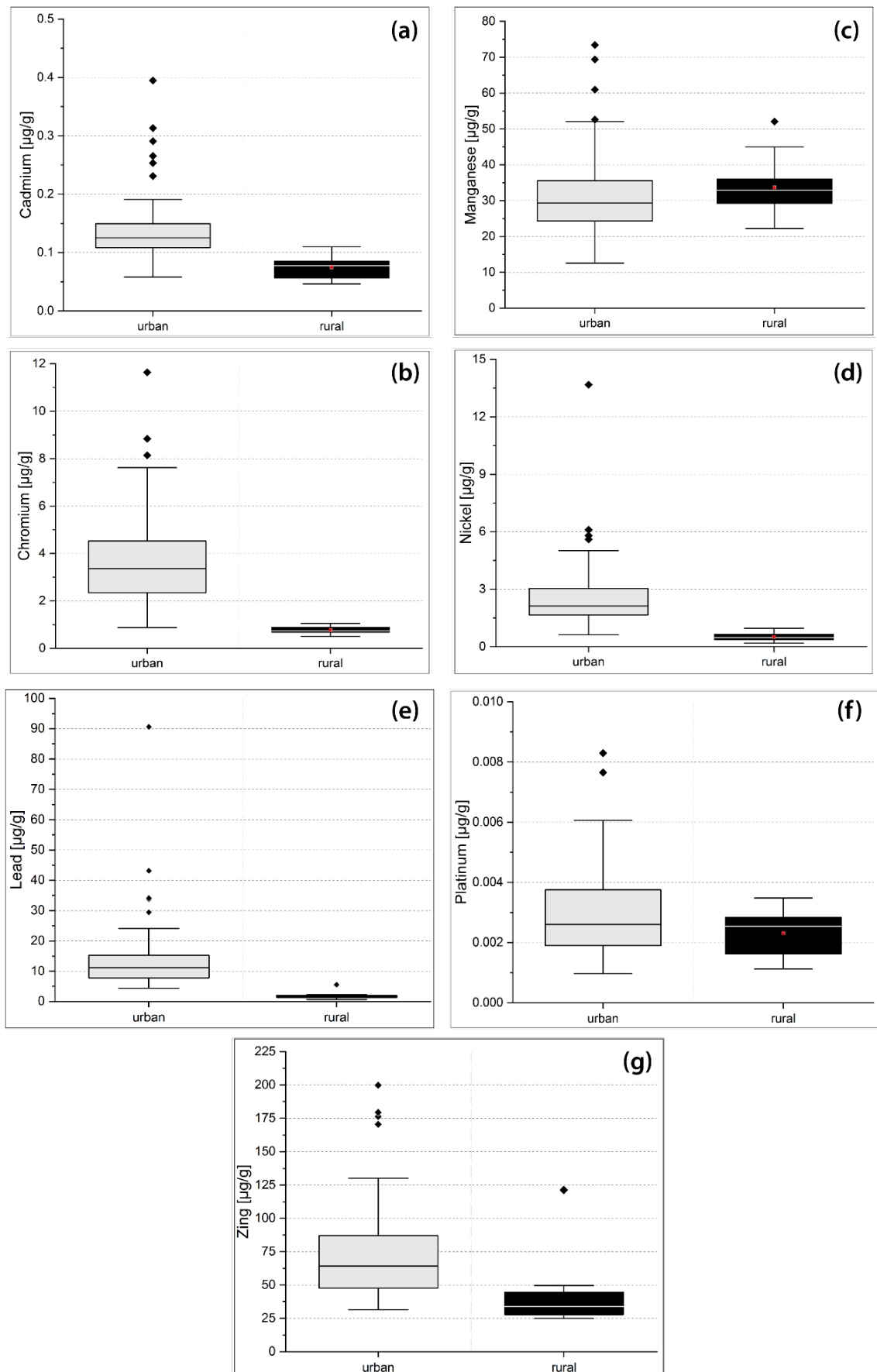


Figure 6-18: Box-whisker plots (25th to 75th percentile; with mean: red square for normally distributed metal concentrations; median line for non-normally distributed metal concentrations; extreme values: black diamonds) for (a) Cd, (b) Cr, (c) Mn, (d) Ni, (e) Pb, (f) Pt and (g) Zn in urban and rural samples of *X. parietina*

6.4 Interpretation and Discussion

6.4.1 Temporal variability of metal concentrations

High-spatial resolution sampling was undertaken during an initial sampling period in 2016/17. To evaluate potential temporal bias on lichen metal concentrations, a sub-set of sites were re-visited (same tree) in 2018 and analysed for metal concentrations. Temporal variability of metal concentrations (in *X. parietina*) was not recorded for most analysed target metals, i.e. Cd, Mn, Ni, Pt and Zn, whereas significant ($p < 0.05$) differences and highly significant differences were recorded for Cr and Pb and Pd, respectively. Palladium was discarded, whereas Pb and Cr were kept for spatial analysis, due to significant health risk of these elements (Morais et al., 2012; Jaishankar, Mathew, et al., 2014). Temporal variability of metal concentrations in *Phycia* spp. was not possible, due to re-sampling at one site only. Therefore, analysis of temporal variability in Manchester is related to *X. parietina* elemental concentrations.

Transplantation studies reported that most lichens respond to changing atmospheric metal concentrations within a few months (Bačkor and Loppi, 2009). Conti et al. (2004) reported changing metal concentrations in *E. prunastri*, deployed in urban, industrial and rural areas at Cassino (Italy) of Cd (62%), Cr (142%), Pb (168%) and Zn (654%) within a year. These authors also reported seasonal variability of metal concentrations in lichens, with regard to climatic factors and the ability of lichens to accumulate metals (Conti and Cecchetti, 2001; Conti et al., 2004). Deployment of *Flavoparmelia caperata* from a clean to polluted site and back (in Portugal) showed changing metal concentrations within two months (Godinho et al., 2011). Comparable findings were presented in lichen-biomonitoring studies, reporting changes in metal concentrations with regard to the specific site (i.e. rural, industrial, residential) between 6 to 15 months (Loppi et al., 2004; Kularatne and De Freitas, 2013; Paoli, Vannini, Fačkovcová, et al., 2018). Gerdol et al. (2014) used the moss *Tortula muralis* to assess spatio-temporal variation of metals in the urban environment of Ferrara (Italy) and suggested temporal trends reflecting the variation in proportional contributions of different emission sources (i.e. vehicular emissions). Metal concentrations in *X. parietina* were used in Cracow (Poland) to assess traffic-related influences within the urban area, reporting accumulation trends of Ni and Cr (and to a certain extent for Zn and Cd) in the lichen over time (Rola and Osyczka, 2019).

Weather conditions, i.e. rain can have an impact on lichen metal concentrations, either “washing-off” contaminated particles or contributing elements from rainfall (Knops et al., 1991; Bačkor and Loppi, 2009). Moreover, lichens are metabolically more active, when wet and temporal variations can be explained, i.e. higher mineral uptake in winter months (Nash and Gries, 1995; Bačkor and Loppi, 2009).

Therefore, (trace) elemental concentrations in lichens are greatly influenced by seasons (Corapi et al., 2014; Vannini et al., 2017). For instance, Kularatne and De Freitas (2013) reported higher on-thallus accumulation (dry deposition) during summer and lower during winter, with a direct impact on accumulation and release of metals from the lichen surface by rain. However, Bergamaschi et al. (2007) reported that concentrations in the lichen thalli varies according to the amount of pollutants, potentially producing biological stress, and in turn, altering uptake of elements. Rola and Osyczka (2019) reported different accumulation abilities in the vegetative parts (i.e. thallus and apothecia) in *X. parietina*. Certainly, metal accumulation within lichens is a complex and dynamic physiochemical process, influenced by many factors, including tree bark pH, climatic and topographic factors (Garty, 2001), which needs to be considered.

For Manchester, a general trend of increased metal concentrations between sampling periods was found. However, not statistically significant for most key target metals, i.e. Cd, Mn, Ni, Pt and Zn. Chromium and Pb were significantly different between sampling periods, with increased Cr and decreased Pb in *X. parietina*. Varying concentrations of metals could be related to biological stresses induced by high metal concentrations, and anatomical characteristics of the lichen (*X. parietina*). Higher Cr concentrations in *X. parietina* for the second sampling period could be related to sampling conditions, i.e. during the summer months, where dry deposition of metals are reportedly higher (Kularatne and De Freitas, 2013). Lichens were not washed before acid digestion, to include entrapped particulates on the lichen surface and obtain a ‘overall’ metal concentrations, rather than bioconcentrated portions (Forbes et al., 2015). However, 12 out of 17 sites showed increased Cr concentrations, suggesting additional influences, i.e. from vehicular emissions across Manchester (Taylor, 2006; Charron et al., 2019).

High Pb concentrations (up to 645 µg/g) were reported in 'road dusts' within the city centre of Manchester (Robertson et al., 2003; Taylor, 2006), suggesting entrapped particles on the lichen surface. Pb is preferentially stored at extracellular level (i.e. cell wall binding sites) in *X. parietina*, suggesting potential wash-off of particulates and 'binding site competition' with other metals (Paoli, Vannini, Monaci, et al., 2018). Therefore, decreased Pb in 2018 is potentially related to a wash-off effect from the lichen surface (Garty, 2001; Hauck and Huneck, 2007; Bačkor and Loppi, 2009).

Weather conditions during the sampling periods could explain slightly different concentrations, compared to the second sampling, for most metals (i.e. Cd, Mn, Ni, Pt and Zn). However, lichen samples were collected during dry conditions for both sampling periods, to minimise potential "wash-off" effects of metal containing particles (Bačkor and Loppi, 2009). Moreover, lichen age was reported to influence metal concentrations in lichens, with central parts (older) containing higher amounts of metals, compared to peripheral (younger) parts (Garty, 2001). Consequently, lichen age for sampled sites might play a role in recorded metal concentrations. In this study, lichens were sampled from twigs and small branches, to obtain younger lichen specimen and assess recent metal pollution. However, it is suggested that sampling should be undertaken during a shorter period, to minimise potential temporal and climatological effects.

The scope of this study was to elucidate high spatial resolution of metal concentrations. Temporal variability was considered, due to long sampling periods. However, for target metals (except Pb and Cr) no significant differences were found. Cr and Pb were further spatially analysed, due to their significant human health impacts. Therefore, spatial variability of metal concentration was considered valid for target metals (except Pd), which will be discussed in section 6.4.4. At first, urban and rural lichen samples will be discussed hereafter.

6.4.2 Can rural *X. parietina* lichens be used as 'control' samples for comparison with urban *X. parietina* for airborne metal concentrations?

Comparing lichens from different environments could be useful to assess the variation of pollution within different environments, and to potentially use samples from one environment as 'control' for the other. In this study, *X. parietina* samples from the City of Manchester were compared to *X. parietina*, sampled around a poultry farm (rural).

Metal concentrations in rural *X. parietina*, sampled around a poultry farm, were found to be variable, indicating site-specific sources. When compared with urban samples of *X. parietina*, majority of recorded metal concentrations were highly significant different at the level $p < 0.01$ (Table 6-14), suggesting additional influences on lichen metal concentrations in the urban environment of Manchester, i.e. from vehicular emissions (exhaust and non-exhaust; Taylor, 2006; Charron et al., 2019).

However, Mn and Pt did not show significant differences between urban and rural samples. Mn could therefore be related to bark Mn concentrations (Paul, 2005; Hauck et al., 2006), while Pt could potentially be emitted by surrounding vehicular traffic, as Pt is primarily emitted in metallic form (Schlögl et al., 1987; Stuben and Kupper, 2006; Zereini et al., 2007). Furthermore, fertilisers were found to contain 0.3 to 30 $\mu\text{g}/\text{kg}$ of Pt (Alt and Messerschmidt, 1993; WHO, 2000a) and could influence rural *X. parietina* samples. No significant differences for target metals (except Zn) with distance to poultry farm were found, suggesting to use samples >500 m away from the poultry farm, when analysing for Zn. For other metals, no 'minimum distance' can be stated. Additionally, temporal influences, between sampling in urban and rural locations could influence recorded metal concentrations. However, major differences in metal concentrations, with urban samples being significantly higher, indicate the beneficial use of sampled *X. parietina* samples around a poultry farm.

Therefore, additional influences on *X. parietina* in the urban environment of Manchester, from specific sources i.e. vehicular abrasion (e.g. Zn and Cd), engine wear, plating and alloys (e.g. Cd, Cr and Ni), tyre and brake wear, lubricating oils and paints (e.g. Cd, Mn and Zn) and catalytic converters (e.g. Pt; Taylor, 2006), are suggested.

6.4.3 Assessment of whether urban metal concentrations exhibit similar patterns and the potential for source apportionment

Cluster analysis was used to ascribe metals into groups (clusters), to maximise similarities between members of each group and to minimise similarities between groups (Legendre and Legendre, 1988; Trakhtenbrot and Kadmon, 2005). Key target metal concentrations in *X. parietina* were significantly ($p < 0.01$) positive correlated with each other (Table 6-15), indicating similar sources for particular metals. For instance, Zn, Cd and Mn were highly ($p < 0.01$) positive correlated with each other, suggesting vehicular emissions (especially tyre wear) as major source,

while Ni and Cr (Spearman $\rho = 0.61$; $p < 0.01$) are related to engine wear (Taylor, 2006). However, to further investigate similarities/dissimilarities between metals and assess potential sources, cluster analysis was undertaken for metal concentrations recorded in *X. parietina*.

Table 6-15: Spearman ρ correlation coefficients of ‘target’ metals recorded in urban *X. parietina* (N=84); displayed with significance levels (p-values; two-tailed; values presented in **bold**: significance level $p < 0.01$, shaded in green; underlined values: significance level $p < 0.05$; shaded in yellow)

Element		Cd	Cr	Ni	Mn	Pb	Pt	Zn
		Spearman ρ						
Cd	Significance level (p-value)		0.53	0.30	0.54	0.48	0.12	0.47
Cr		<0.01		0.61	0.76	0.78	<u>0.22</u>	0.74
Ni		<0.01	<0.01		0.53	0.51	-0.01	0.56
Mn		<0.01	<0.01	<0.01		0.81	0.13	0.79
Pb		<0.01	<0.01	<0.01	<0.01		<u>0.24</u>	0.83
Pt		0.29	<u><0.05</u>	0.93	0.25	<u><0.05</u>		0.15
Zn		<0.01	<0.01	<0.01	<0.01	<0.01	0.16	

Figure 6-19 illustrates the dendrogram of metal concentrations recorded in *X. parietina* and identified Ni and Pt being related (1) and so form the first main cluster (1). Nickel occurs naturally in soil, but is part of alloys, plating, colour and catalysts and emissions are related to industry and energy production (i.e. oil- and coal-burning power plants; ATDSR, 2005). Catalytic converters contain 1 to 3 g of Platinum and can be sources of platinum, due to Pt abrasion by mechanical and thermal impact, with reported Pt losses of 2 $\mu\text{g}/\text{km}$ travelled (for pellet-type catalyst, used in the US; WHO, 2000). However, Pt and Ni did not show a significant relationship and high dissimilarities (Figure 6-19), but concentrations were elevated for both elements along the major road network in Manchester (Figure 6-14 and Figure 6-16), suggesting vehicular emissions, i.e. from engine wear and catalytic converters (Taylor, 2006).

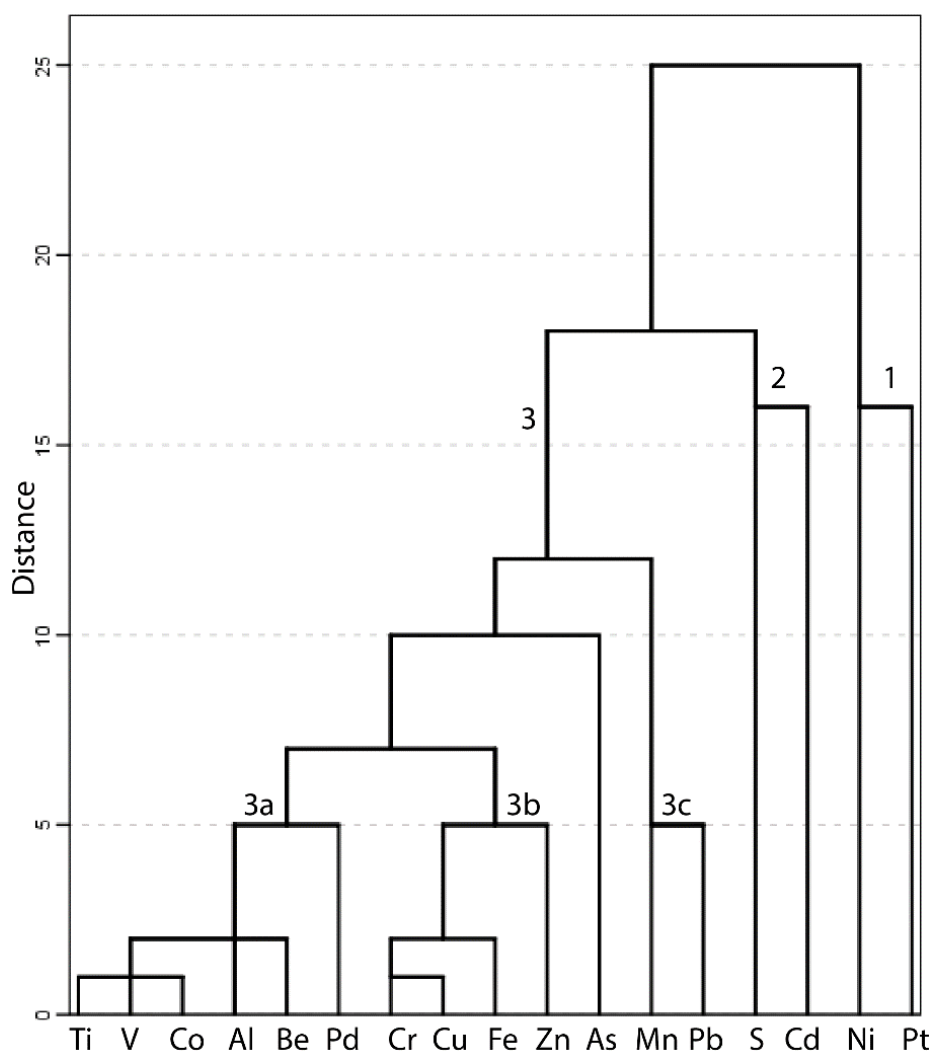


Figure 6-19: Dendrogram of elements in urban samples of *X. parietina* (using complete linkage and squared Euclidian Distance); shorter distances between elements show higher similarity, further distances illustrate dissimilarities.

The second cluster (2) in *X. parietina* was found for sulphur and Cd. Cadmium in urban environments originates from tyre wear and vehicular abrasion as well as from lubricating oils, alloys and pigments in paint and plastics (Taylor, 2006; ATSDR, 2008b; ICdA, 2019). The later could also indicate similar sources for Cd and S, due to the use of cadmium sulphide (CdS) as pigment ('cadmium yellow'; Smith, 2002), potentially used in automobile colours. Furthermore, energy production, i.e. fuel combustion like coal and oil and manufacturing processes (i.e. iron and steel) are primary sources of Cd and S in the environment (DEFRA, 2017a).

The third group has been further subdivided into 3a, 3b and 3c to investigate elemental relationships. Group 3a is not further discussed here, as Pd was disregarded form further analysis due to high temporal variability. Group 3b comprised of target elements Zn and Cr. Zinc and chromium, although being essential plant nutrient can induce toxicity at high levels and sources are related to

industrial (e.g. steel works, electroplating) and vehicular sources (Gough et al., 1979; Taylor, 2006; Uluozlu et al., 2007). Elevated concentrations for Cr and Zn were found close to major roads and within the city centre area (Figure 6-12 and Figure 6-17), Zinc and Cr were strongly positive correlated (Spearman $\rho = 0.74$; $p < 0.01$) with each other, suggesting vehicular origins (i.e. tyre and engine wear; Taylor, 2006) as primary sources.

In addition, Zn in road-dust sediments within the city centre of Manchester have been reported between 50 $\mu\text{g/g}$ to 796 $\mu\text{g/g}$ indicating additional local variability and thus potential site-specific influences on lichen metal concentrations (Robertson and Taylor, 2007). Urban soils have higher Zn concentrations, compared to natural soils (Lehmann and Stahr, 2007; Sandstead and Au, 2007) and elevated concentrations could be related to re-suspended soil particles. Nonetheless, tyre wear was reported a major source of Zn in urban areas (Wik and Dave, 2009).

Manganese (Mn) and lead (Pb) were located in cluster 3c, which are considered as traffic-related metals (Uluozlu et al., 2007). Lead was historically used as petrol additive and vehicular emissions were the primary sources of Pb, whereas nowadays, metal production and industrial lubricant combustion contain Pb (DEFRA, 2017a). Sources of Mn could be related to tyre wear and brake linings, additional to the geological background (Taylor, 2006). Manganese is used as a diesel fuel additive and could be further used as a tracer for railway wear (together with Cr and Fe) (Wang et al., 2003; Bukowiecki et al., 2007; Gehrig et al., 2007; Valotto et al., 2015). Manganese was highly significant ($p < 0.001$) positive correlated with Cr (Spearman $\rho = 0.76$; and Fe $\rho = 0.86$, $p < 0.001$) strongly suggesting sources from railway wear and vehicular sources. Lead (Pb) and Mn concentrations in road dust in Manchester have been found to range between 71 $\mu\text{g/g}$ to 594 $\mu\text{g/g}$ (Pb) and 70 $\mu\text{g/g}$ to 294 $\mu\text{g/g}$ (Zn), close to major traffic islands in the city centre of Manchester (Robertson and Taylor, 2007). Higher Pb concentrations were found at sampling sites close to major roads (Figure 6-13 and Figure 6-15), indicating roadside contaminated particles (Pb) and diesel exhausts (Mn) as potentially affecting lichen metal concentrations in Manchester.

6.4.4 Do *X. parietina* and *Physcia* spp. lichens record different airborne metal concentrations in the City of Manchester?

Two lichen species, *X. parietina* and *Physcia* spp. were used to analyse metal concentrations in the urban environment of Manchester. Interspecific analysis could inform the use of both lichen species for a combined (i.e. combining both to a single sample) or species-specific biomonitoring studies.

Significant differences between both lichen species was found for target metals, including Cd, Cr and Mn ($p < 0.05$) as well as Pb and Zn ($p < 0.01$), suggesting different uptake abilities between both lichen species and potential toxic effects. No significant difference was found for Ni and Pt.

Interestingly three sites, analysed for metal concentrations in *Physcia* spp. showed elevated metal concentrations for all target metal, except Pt (Figure 6-11 to Figure 6-17). This could be related to species-specific response to elevated airborne metal concentrations and/or the sampling locations specific surrounding, i.e. being located next to major tramlines and within a more industrial surrounding (e.g. parcel-delivery service and small businesses).

Lichens are able to cope with stresses induced by metal pollution through different adaptive mechanisms, i.e. sequestration, complexation and detoxification, including oxalates, extracellular phenols, chelation with lichen substances, cation binding by carboxyl, phosphate, amine and hydroxyl groups, exclusion (by the cell walls of both bionts) and intracellular accumulation within the plasmalemma (Bačkor and Loppi, 2009). Specific lichen substances, which include more than 800 aliphatic, cycloaliphatic, aromatic and terpenic known compounds, are involved in binding or chelation of heavy metals (Hauck and Huneck, 2007). For instance Kalinowska et al., (2015) reported that the pigment 'parietin' in the lichen *Xanthoria parietina* protects the photobiont cells from excessive cadmium, acting as cortex barrier for Cd^{2+} -ions. Similar protective effects were presented by Hauck and Huneck (2007) for 'physodalic acid' in *Hypogymnia physodes*. The mycobiont, in relation to the photobiont, making up 90% of total lichen biomass, is able to accumulate most metals, without being affected too seriously (Bačkor and Loppi, 2009). Other metals, including As, Cu, Zn, Ni and Cd showed to have toxic influences on photosynthetic pigments and the mycobiont of *X. parietina* (Pisani et al., 2009; Piovár et al., 2017).

Less availability and analysis of *Physcia* spp. (N=17) could indicate metal toxicity towards this particular lichen and potential detoxification methods of *X. parietina*, being able to cope with higher metal concentrations. Moreover, higher concentrations recorded in *X. parietina* could be related to the growth form of the lichen species in comparison to *Physcia* spp., i.e. entrapped metal-enriched particulates within the thallus of *X. parietina* and accumulation in apothecia, which are not present in *Physcia* spp. (Garty, 2001; Nash III, 2008; Rola and Osyczka, 2019). Metals contained by a lichen species is dependent (and refers to) its morphological and structural features, i.e. thin flat thalli provide high surface area to dry weight ratio (Nieboer et al., 1972; Chiarenzelli et al., 1997; Garty, 2001).

Therefore, different lichen species in the same location could contain different amounts of metals (Garty, 2001). However, accumulation of metals in lichens is a dynamic process and concentrations vary according to pollutants, inducing biological stress, and in turn, alter element uptake (Bergamaschi et al., 2007; Bačkor and Loppi, 2009). *X. parietina* and *Physcia* spp. are foliose lichens, and recorded metal concentrations illustrate species-specific uptake abilities of metals. Both lichen species provide beneficial information on airborne metal concentrations across the city centre of Manchester. However, lichen species should be used separately, when applied in biomonitoring studies.

6.4.5 Are lichen metal concentrations recorded for the City of Manchester comparable with other urban biomonitoring studies?

Lichen-derived metal concentrations were used to compare airborne metal concentrations for Manchester (UK) with other urban studies, to assess whether Manchester is a particularly polluted urban environment.

Table 6-16 displays the target metal concentrations for *X. parietina* and *Physcia* spp. in comparison to other European (including Turkey) lichen biomonitoring studies, primarily using *X. parietina* and *Physcia* spp. Another UK based study, actively deploying *Pseudevernia furfuracea* and *Parmelia sulcata* was included for further comparison. Concentrations of Pd and Pt are not further discussed due to temporal variability presented earlier (section 6.4.1) and unavailability of urban studies for comparison, respectively. Figure 6-20 and Figure 6-21 illustrate the comparison of target metal concentrations (as maximum concentrations) recorded in lichen biomonitoring studies.

It should be stated that comparison between Manchester and urban biomonitoring studies, include studies that have been undertaken between 2001 and 2015 and recorded values could show airborne metal concentrations before a reduction of emissions, i.e. by legislations and/or appropriate reduction controls. Therefore, more recent studies offer strongest like-for-like comparison of metal concentrations.

Table 6-16: Comparison of target metal concentrations (concentrations ranges) [in µg/g] recorded in this study and urban biomonitoring studies, using *X. parietina* and *Physcia* spp., displayed with lichen species and location the study was undertaken; additionally the study undertaken by Vingiani et al. (2015) using *Pseudevernia furfuracea* and *Parmelia sulcata* actively deployed in London (UK) was included; N/A represents that elements were not measured/reported in the particular study

	Lichen species	Location	Cd	Cr	Mn	Ni	Pb	Zn
This study	<i>X. parietina</i>	Manchester (UK)	0.06 to 0.40	0.88 to 11.64	12.57 to 73.41	0.62 to 13.68	4.37 to 90.60	31.56 to 199.73
This study	<i>Physcia</i> spp.	Manchester (UK)	0.11 to 0.48	1.0 to 6.56	19.10 to 48.04	0.80 to 3.29	4.79 to 29.43	59.95 to 125.36
Kurnaz and Cobanoglu (2017)	<i>Ph. adscendens</i>	Istanbul (Turkey)	0.28 to 3.79	2.45 to 11.79	5.76 to 68.39	7.16 to 18.50	13.11 to 37.47	11.27 to 129.57
Parzych et al. (2016)	<i>X. parietina</i>	Słupsk (Poland)	N/A	N/A	31.6 to 249.9	11.1 to 45.9	2.2 to 7.0	Up to 113.3
Vingiani et al. (2015)	<i>P. furfuracea</i> <i>P. sulcata</i>	London (UK)	0.2 to 0.9	0.1 to 1.5	N/A	0.1 to 2	10 to 40	100 to 700
Doğrul Demiray et al. (2012)	<i>X. parietina</i>	Kocaeli province (Turkey)	0.18 to 1.23	N/A	40 to 239	2.70 to 10.20	8 to 132	65 to 371
Owczarek et al. (2001)	<i>Ph. adscendens</i>	Rieti (Italy)	0.25 to 0.54	0.8 to 20.6	25.3 to 81.7	1.7 to 13.2	19.3 to 130.9	108.2 to 240.9

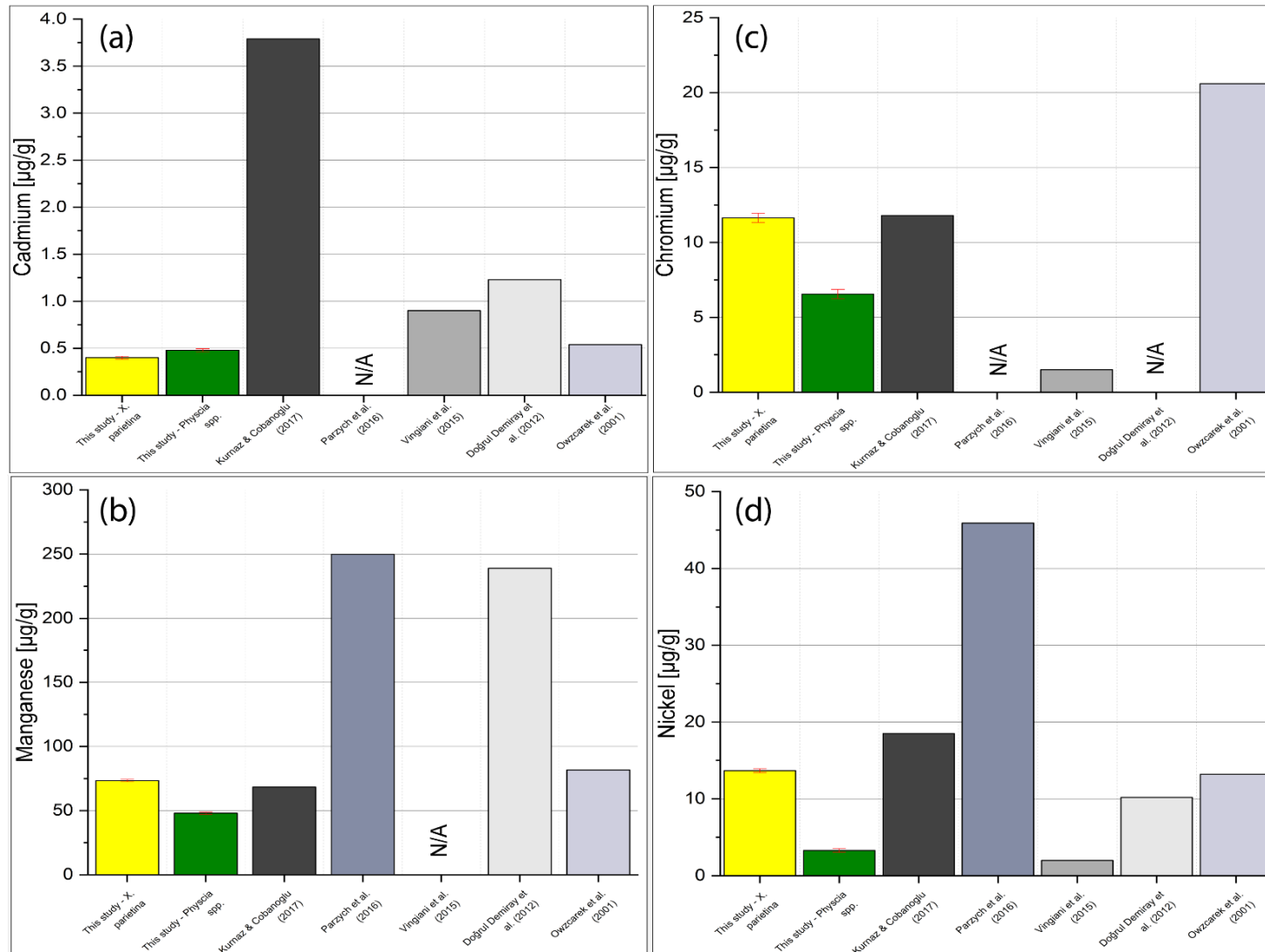


Figure 6-20: Maximum recorded concentrations of (a) Cd, (b) Mn, (c) Cr and (d) Ni recorded in this study, in comparison to urban lichen biomonitoring studies as presented in Table 6-16 (error bars as 1x Std.Dev. for *X. parietina* and *Physcia* spp.)

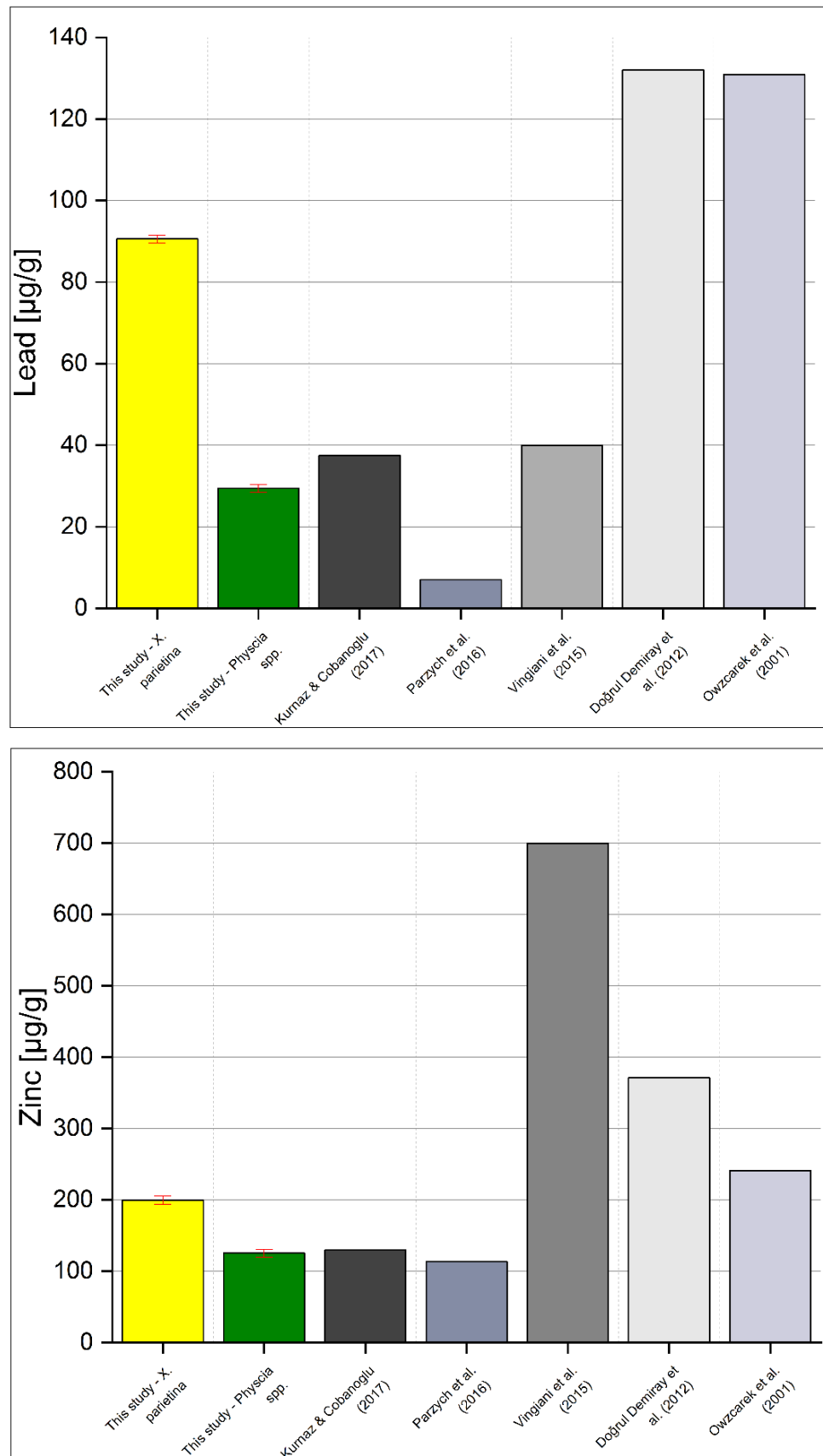


Figure 6-21: Maximum recorded concentrations of Lead (Pb) [above] and Zinc (Zn) [below] recorded in this study, in comparison to urban lichen biomonitoring studies as presented in Table 6-16 (error bars as 1x Std.Dev. for *X. parietina* and *Physcia* spp.)

Concentrations of Cd in *X. parietina* were comparable to concentrations recorded in Rieti (Italy) and lower compared to other studies, i.e. London and Istanbul (Figure 6-20a). Cd was related to vehicular emissions as major source in Istanbul (Doğrul Demiray et al., 2012). Similar results have been reported by Kurnaz and Cobanoglu (2017), with highest Cd close to major roads and in industrial areas of Kocaeli (Turkey). In general, concentrations of Cd in Manchester were also found at higher levels close to major roads, suggesting vehicular emissions as major Cd source. However, highest Cd in Manchester (0.40 µg/g) was found further away from a major road. Cd can be linked with fine particulates allowing long distance travel and therefore indicate potential influences (i.e. from traffic) further from a major road (Adamo et al., 2011; Vingiani et al., 2015). Therefore, Manchester was considered less polluted by Cd.

Manganese (Mn; Figure 6-20b) recorded in the urban areas of Słupsk and Istanbul were about threefold higher than recorded in Manchester (Doğrul Demiray et al., 2012; Parzych, Zdunczyk, et al., 2016). Concentrations of Mn in this study were found comparable to concentrations recorded by Kurnaz and Cobanoglu (2017) and Owczarek et al. (2001). Mn was reported to originate from exhaust fumes, tyre and brake wear and elevated concentrations were related to traffic density (Taylor, 2006; Kurnaz and Cobanoglu, 2017). However, Mn in lichen thalli is directly proportional to atmospheric concentrations, with about 50% of airborne Mn in urban areas being of natural (geological background) origin (Parzych, Zdunczyk, et al., 2016). Furthermore, bark pH can have an influence on lichen Mn concentrations (Paul, 2005; Hauck et al., 2006). Nonetheless, Mn concentrations recorded in Manchester were higher around the major road network and highest at 'Piccadilly Gardens', the main bus terminal within the city centre (3.700 daily; DfT, 2017), suggesting vehicular fuel emissions as major source of Mn, with more than 20% of busses in Manchester falling into the most polluting Euro 2-3 emission standard (Cox and Goggins, 2018). Furthermore, Mn is associated with railway abrasion (Gehrig et al., 2007) and higher Mn in lichens in close proximity to Piccadilly Gardens could be related to tram lines leading through the city centre.

Sources of Cr include vehicular wear, e.g. brake linings and lubricant oil (Taylor, 2006; Pulles et al., 2012; Charron et al., 2019). Concentrations (Figure 6-20c), recorded in *X. parietina* and *Physcia* spp. sampled across Manchester were found at comparable concentrations as reported by Kurnaz and Cobanoglu (2017), who found high Cr in highly trafficked areas, especially congested areas. Owczarek et al. (2001) reported vehicular sources as primary source of Cr in Rieti (Italy). Cr in Manchester, was found highest along the major road network, with highest Cr recorded at a sampling site close to a major junction, suggesting vehicular abrasions as major origin. In contrast, Vingiani et al. (2015) reported lower Cr in deployed lichens in London, next to a heavy to moderate traffic flow, when compared to concentrations found in Manchester. Manchester could therefore be more polluted with Cr, when compared to London. However, traffic flow and additional factors, such as meteorological conditions, traffic-fleet composition and particular urban surrounding could have influenced metal concentrations (Hertel and Goodsite, 2009; Charron et al., 2019).

Nickel (Ni) concentrations were found more variable in *X. parietina*, compared to *Physcia* spp. in Manchester. Comparable concentrations were found in Istanbul and Rieti, with regard to industrial activities and vehicular traffic, respectively (Owczarek et al., 2001; Doğrul Demiray et al., 2012). Higher Ni concentrations were found at roadside sampling sites (for *X. parietina*) across Manchester, which is in agreement with findings by Parzych et al. (2016) and Kurnaz and Cobanoglu (2017). Ni in *Physcia* spp. showed a slightly different pattern, with highest Ni at three sites, suggesting a 'local' influence. For instance, these sites are located within a more industrial/manufacturing surrounding and major railways, suggesting influences from combustion of fossil fuels (e.g. for power generation), steel manufacturing, electroplating and engine wear (Taylor, 2006; EEA, 2015). Nickel concentrations in *Physcia* spp. were highest (between 2.68 µg/g to 3.29 µg/g; Figure 6-14b) at sites, that also showed high concentrations for Cr (Figure 6-12) and Mn (Figure 6-13), indicating specific metal sources at these sites, potentially from engine wear (Ni), vehicular and railway abrasion (Cr and Mn; Taylor, 2006; Gehrig et al., 2007). In contrast, Ni is also found in soils (ATDSR, 2005) and elevated concentrations could be related to re-suspended particles. Vingiani et al. (2015) reported low Ni for London, which is comparable for concentrations in *Physcia* spp. However, Ni in Manchester was generally lower, when compared to other urban studies.

High Pb was reported by Owczarek et al. (2001) and Doğrul Demiray et al. (2012), with higher concentrations close to main roads and traffic counts. Robertson et al. (2003) reported Pb concentrations of 357 µg/g in road dust sediments in the inner city of Manchester, opposing to 185 µg/g outside the city centre. Due to its environmental persistence (primarily derived from petroleum fuels containing lead as antiknock) higher Pb could be related to re-suspended road dust (Barrett et al., 2010; Nagajyoti et al., 2010; Adamiec et al., 2016). Lead recorded in *X. parietina* in Manchester was high along the major road network, suggesting re-suspended dust (i.e. by traffic) as primary source of Pb (Figure 6-21). Kurnaz and Cobanoglu (2017) reported high Pb concentrations in *Ph. adscendens* in relation to traffic and location close to highways, which is in accordance with recorded concentrations in Manchester (for *Physcia* spp.). Lead concentrations recorded in Manchester (in *X. parietina*) are higher compared to London. This may be related to Manchester's industrial heritage and the environmental persistence of lead.

Highest Zn concentrations recorded in Manchester were about three and a half times lower compared to Zn in London (Vingiani et al., 2015). Highest Zn in Manchester was found at a site close to railway tracks, suggesting railway wear as potential source, as Zn is associated with abrasion of railway steel and overhead traction lines (Bukowiecki et al., 2007; Gehrig et al., 2007; Valotto et al., 2015). However, Zn was spatially variable across Manchester, with elevated levels recorded in the city centre and along the major road network, also suggesting tyre and vehicular abrasion (Taylor, 2006; Napier et al., 2008). Zn in road dust sediments in the city centre of Manchester was found to range between 402 µg/g to 1016 µg/g (Robertson et al., 2003), indicating potential re-suspended particles influencing lichen Zn. Furthermore, higher accumulation of Zn in younger parts of *P. sulcata*, and involvement of Zn in biochemical pathways was reported (Tyler et al., 1989; Cuny et al., 2004; Vingiani et al., 2015). Young specimen of *X. parietina* and *Physcia* spp. were sampled across Manchester and recorded Zn could be related to higher metabolic activity of younger lichen parts (Stefano Loppi et al., 1997; Godinho et al., 2009; Vingiani et al., 2015).

No comparison with other urban studies was possible for Platinum (Pt). However, Pt is a component of diesel after-treatment systems (diesel oxidation catalysts – DOC), especially in EURO 3 cars and higher and enters the environment as metal or oxide dusts (Gebel, 2000; ATSDR, 2008a; Matthaios et al., 2019). Therefore, elevated Pt in urban samples of *X. parietina* are suggested to be primarily related to vehicular emissions, i.e. from catalytic converters.

In general, airborne metal concentrations recorded in Manchester were lower, compared to other urban areas. Studies reported traffic as primary source of metals, i.e. Cd, Cr, Ni and Pb, whereas Mn and Zn could be related to railway wear, diesel fuels, as well as bark pH and/or lichen age. Elevated metal concentrations were recorded along the major road network and within the city centre, suggesting primarily vehicular origin. When comparing Manchester to London, airborne metal concentrations were found variable in both environments, with potential ‘urban’ specific influences, i.e. urban layout, traffic flow, fleet composition and speed, as well as meteorological data (Hertel and Goodsite, 2009; Janhäll, 2015; Charron et al., 2019).

Therefore, additional influences, with regard to the analysed geographic region, meteorological conditions, urban layouts and traffic conditions need to be taken into account when analysing airborne metal concentrations. Spatial variability of metal concentrations, with regard to Manchester’s urban structure will be discussed hereafter.

6.4.6 Exploring potential controls on urban metal concentrations in the City of Manchester Spatial variability of metal concentrations recorded in the City of Manchester

Spatial variability and site-specific influences on metal concentrations were presented earlier and findings suggested influences of the sampling locations’ specific surrounding. To further address spatial variability of target metals, metal concentrations were related to urban influencing factors, such as distance to major road, traffic counts, building density, distance to green space and distance to large point sources. These influencing factors could imply sources (i.e. vehicular and industrial emissions) and explain variability due to beneficial effect, i.e. by green spaces. Table 6-17 illustrates the Spearman ρ correlation coefficient of metal concentrations with urban influencing factors, as described in Table 6-5.

Table 6-17: Spearman ρ correlation coefficients and significance levels (* significant at the level: $p < 0.05$, shaded in yellow; ** significant at the level: $p < 0.01$, shaded in green) of lichen-derived metal concentrations and urban influencing factors to investigate potential controls on urban metal concentrations (MR = distance to major road, RdCl = Road class, TC = traffic counts, BH = mean surrounding building height; GS = distance to greenspace and PS = distance to large point source); key target metals in bold

Element	MR		RdCl		TC		BH		GS		PS	
	X. p.	Ph. spp.	X. p.	Ph. spp.	X. p.	Ph. spp.	X. p.	Ph. spp.	X. p.	Ph. spp.	X. p.	Ph. spp.
Al	-0.18	-0.20	-0.22*	-0.10	0.31*	0.49	0.20	0.01	0.35**	0.42	0.02	-0.15
Fe	-0.31**	-0.28	-0.31**	-0.10	0.26*	0.47	0.21	-0.17	0.32**	0.50	0.04	-0.13
Mn	-0.25*	-0.10	-0.24*	-0.20	0.17	0.36	0.22*	0.08	0.26*	0.67**	0.03	0.34
Ni	-0.09	-0.16	-0.11	0.42	0.20	0.59*	0.27*	-0.23	0.31**	0.61*	0.08	0.15
Pb	-0.21	-0.38	0.07	0.20	0.26*	0.60*	0.24*	0.08	0.26*	0.57*	0.05	0.07
Zn	-0.44**	-0.38	-0.38**	0	0.24*	0.21	0.32**	0.27	0.34**	0.22	-0.19	-0.14
Be	-0.21	-0.37	-0.19	0.05	0.36	0.28*	0.22*	-0.08	0.27*	0.41	-0.05	-0.24
Ti	-0.17	-0.35	-0.18	-0.15	0.28	0.62*	0.19	-0.04	0.36**	0.40	0.08	-0.21
V	-0.18	-0.45	-0.19	-0.05	0.30	0.57*	0.18	-0.14	0.37**	0.32	0.11	-0.32
Cr	-0.26*	-0.27	-0.25*	-0.10	0.25	0.56	0.31**	0.05	0.35**	0.47	0.08	0.03
Co	-0.17	-0.13	-0.16	0.15	0.29	0.41*	0.19	-0.04	0.36**	0.58*	0.05	-0.02
Cu	-0.25*	-0.25	-0.23*	-0.20	0.26	0.54	0.27*	0.04	0.39**	0.46	0.06	-0.03
As	-0.15	-0.25	-0.15	-0.10	0.22	0.61*	0.22	0.06	0.31**	0.21	0.01	-0.14
Pd	-0.15	-0.39	-0.13	0.08	0.03	0.57*	0.21	0.06	0.33**	0.45	0.02	0.11
Cd	-0.07	-0.33	0.01	0.41	0.09	0.38	0.20	0.16	0.21	0.32	0.06	0.2
Pt	-0.05	-0.41	-0.04	-0.19	0.14	-0.02	-0.03	0.23	0.14	-0.14	0.16	-0.15

Distance to road and road class

The major road network in Manchester comprises of A-, B-roads and motorways (UK Department of Transport, 2012). Sampling locations were analysed with respective distance to major road. Unclassified and minor roads, i.e. local roads for local traffic linking housing estates were not considered, as limited data (i.e. traffic counts on minor roads) was available. Therefore, major roads were considered as representative of potential high pollution source (with regard to traffic counts).

Significant negative correlation (in *X. parietina*) were found for distance to major road with Cr ($r = -0.26$; $p < 0.05$) and Mn ($r = -0.25$; $p < 0.05$), presented in Figure 6-22. Cr and Mn are linked to both, non-exhaust (Cr) and exhaust emissions (Mn), and decline with distance to road suggests vehicular emissions as potential source (Kurnaz and Cobanoglu, 2017; Charron et al., 2019).

Moreover, highly significant ($p < 0.01$) negative correlation of Zn concentrations and distance to major roads was found (Figure 6-22). Napier et al. (2008) reported a release of 89 μg Zn per kilometre and vehicle from non-exhaust vehicular parts, i.e. brake and tyre wear. Zn is a major constituent of brake pads (Hulskotte et al., 2014; Charron et al., 2019) and elevated concentrations close to a major road could be related to stop-and-go traffic, with regard to diurnal traffic patterns, i.e. slow traffic during peak times (see chapter 2; Figure 2-20).

In contrast, metals recorded in *Physcia* spp. did not show such a relation. Chromium is detrimental to plant growth and development and could indicate a toxic impact on *Physcia* spp., as less sites ($N=17$) were sampled for this lichen, compared to *X. parietina*, suggesting species-specific tolerance to high metal Cr concentrations (Sanità Di Toppi et al., 2004; Dzubaj et al., 2008; Kováčik et al., 2018). No significant relationship between distance to major road and Cd, Ni, Pb and Pt concentration was found for both lichen species, suggesting additional factors, i.e. traffic density, building structure and meteorological influences (e.g. 'wash-off' effects) on metal dispersion and distribution.

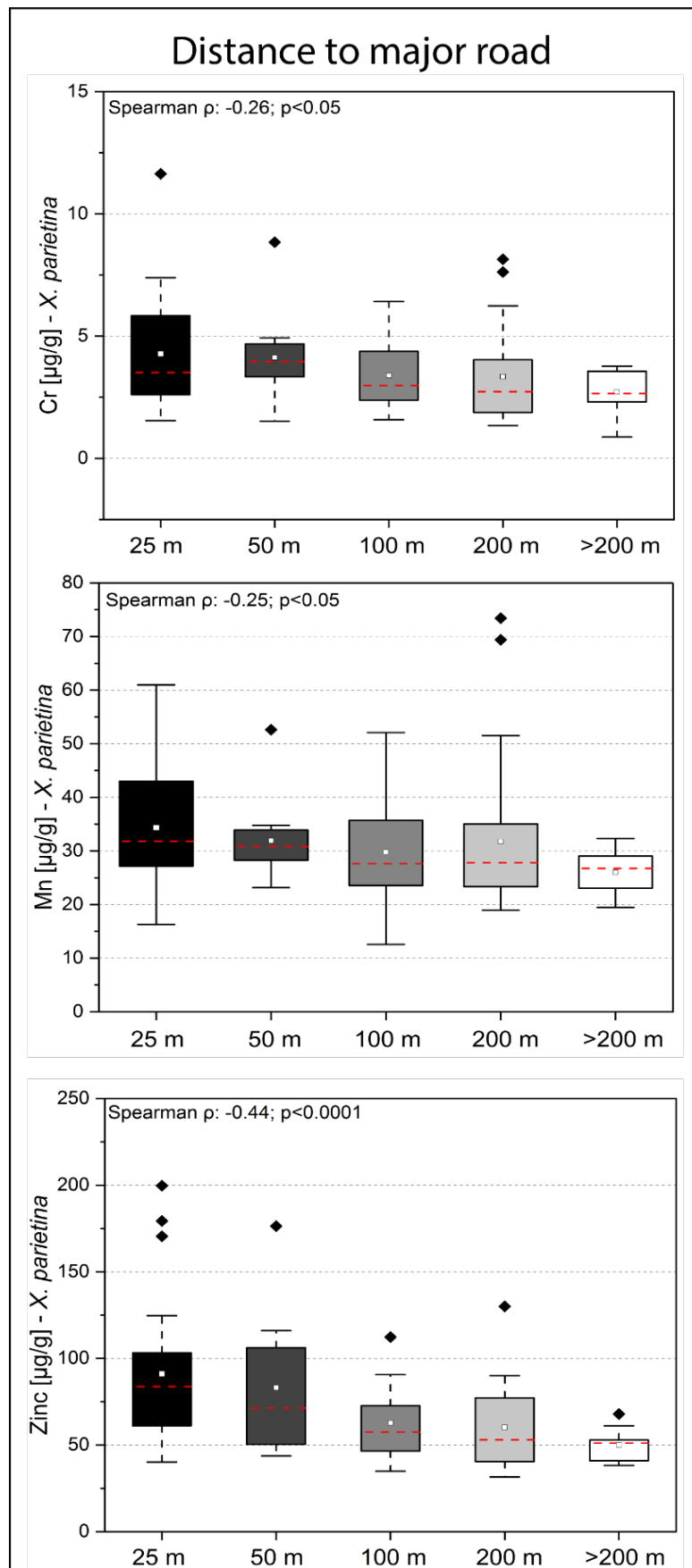


Figure 6-22: Box-whisker plots (25th to 75th percentile) of Cr, Mn and Zn concentration in *X. parietina* with distance to major road (major roads include A- and B- roads and motorways); displayed with mean values (white rectangle), median lines (red dashed line) and outliers (black diamonds)

Traffic counts

'Annual average daily traffic flow' represents the number of vehicles passing a point in the road network each day (DfT, 2017a). Sampling locations were compared to traffic counts (with respect to its location to major road).

Pb was positively correlated with traffic counts (*X. parietina*: $r = 0.26$; $p < 0.05$; *Ph. spp.*: $r = 0.60$; $p < 0.05$) and are presented in Figure 6-23b and d. Zn for *X. parietina* and Ni for *Physcia* spp. were significantly ($p < 0.05$) correlated to traffic counts (Figure 6-23a and c). High traffic counts could indicate re-suspension of soil particles and dust, which were reported to contain high concentrations of Pb and Zn in the city centre of Manchester (Robertson et al., 2003; Barrett et al., 2010). Additionally, abrasion of automobile tires contain about 1.5 to 2% Zn (Parzych, Zdunczyk, et al., 2016) and correlation with distance to road ($p < 0.001$) and traffic counts ($p < 0.05$) suggesting increases Zn in *X. parietina* due to vehicular emissions. Moreover, positive correlation of Pb with Zn ($r = 0.829$; $p < 0.01$), Mn ($r = 0.814$; $p < 0.01$); and Cd ($r = 0.482$; $p < 0.001$), sampled in *X. parietina* across Manchester suggest vehicular emissions as a major sources (Doğrul Demiray et al., 2012).

Nickel is an abundant natural element with anthropogenic emissions related to combustion of diesel and fuel oil combustion, metal processes and manufacturing (Nriagu, 1979; ATDSR, 2005; Xu et al., 2017; Defra, 2018a). Elevated Ni in *Physcia* spp. could be related to entrapped particulate-bound Ni, emitted from anthropogenic sources (i.e. combustion processes; Xu et al., 2017).

High concentrations of Cd, Cr, Ni, Pb and Zn have been reported in *Cladonia convoluta* sampled 1 m away from a road, with elevated Cd levels at 5-10 m and Pb up to 60 m away from the same road, with regard to prevailing wind (Tuba and Csintalan, 1993; Garty, 2001). Roadside samples across Manchester showed elevated levels for target metals, potentially originating from vehicular sources. About 1.65 billion vehicle miles were travelled in 2018 in Manchester (Defra, 2018b), indicating the potentially high impact of traffic on air quality across Manchester.

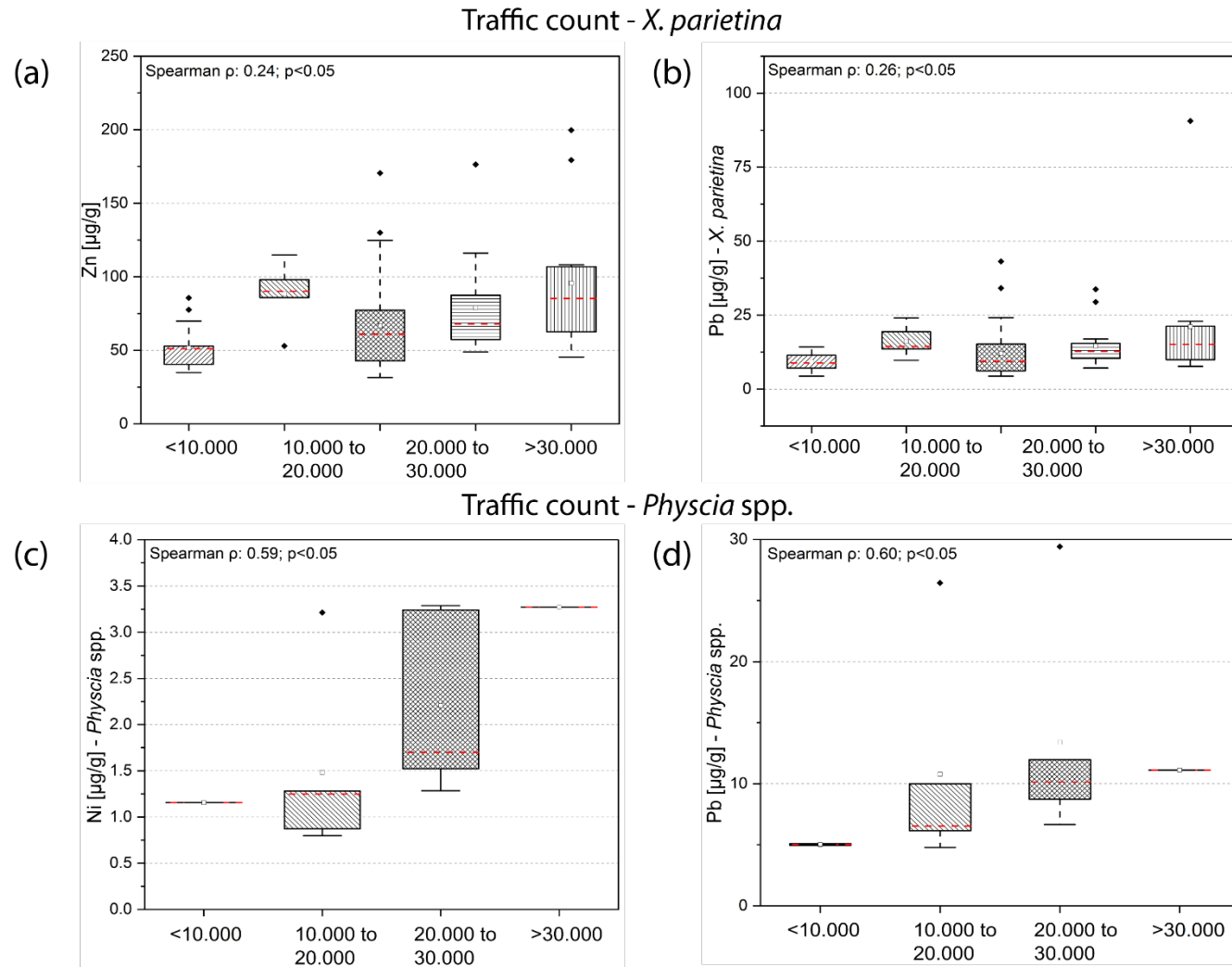


Figure 6-23: Box-whisker Plot (25th to 75th percentile, with mean value: white square, median line and extreme values: black diamond) of (significant) target metal concentrations in *X. parietina* (a) Zn and (b) Pb and *Physcia* spp. (c) Ni and (d) Pb and with traffic counts (AADF - annual average daily traffic flow, 2017)

Building heights

Compact urban forms (high-density) affect wind flow patterns, resulting in further pollutant accumulation and poor air quality (Buccolieri et al., 2009; Shen et al., 2017). Moreover, higher buildings lead to heavier pollution inside the street canyon, especially at pedestrian level (Fu et al., 2017). Surrounding building heights were significantly correlated with most target metals, except Pt (Figure 6-24). In contrast, for *Physcia* spp. no such relationship was found, again suggesting toxic effect of elevated metal concentrations on this lichen species (section 6.4.4), due to lower sampling density.

Findings for *X. parietina* suggest ‘canyoning’ effects across Manchester, with regard to site-specific surrounding building heights and could explain higher metal concentrations in the densely built-up area in the city centre of Manchester. Longley et al. (2004) reported the complex influence between urban topography, wind (within and above the canyon) and vertical turbulences by traffic on dispersion of pollutants. Therefore, impaired air ventilation and deteriorated air quality are primarily related to the city centre area of Manchester, suggesting potential health impacts by airborne metals in this area.

Distance to greenspaces and point sources

Urban greenspaces and vegetation (including trees) can improve air quality by filtering out various pollutants, i.e. NO_x, SO₂, PAHs and metals (Salmond et al., 2013; Janhäll, 2015; Nitsche et al., 2017). The city centre of Manchester contains about 14% green infrastructure and 5% tree cover (Gill et al., 2008; Manchester Green Infrastructure Strategy, 2015). Sampling sites were analysed with distance to greenspace under the assumption that sampling sites within greenspaces potentially show lower pollutant concentrations. Point sources include industrial and commercial sources that emit various pollutants, including metals such as Cd, Cr, Pb, Ni and Zn in Manchester (NAEI, 2015).

Metal concentrations recorded in *X. parietina* were significantly correlated (except Cd and Pt) with distance to greenspace. In contrast, Mn, Ni and Pb recorded in *Physcia* spp. were significantly positive correlated with distance to green space only. Significant relationships are not graphically displayed. No relationship was found with distance to point sources in both lichens. Findings suggest the positive influence of urban vegetation on metal concentrations in Manchester. However, potential surroundings, i.e. building heights and traffic counts at sampling locations might have a bigger influence, in comparison to urban vegetation and greenspaces. Analysed urban factors were 'measured' within a GIS and might not represent real world influencing factors. For instance, applied distances were measured disregarding the fact of surrounding buildings. Mean building heights, were included, but also might inaccurately represent the actual building heights. A multi-storey building on one side could thus influence the overall building height. However, highest buildings predominantly occur in the city centre (see chapter 2).

Additional factors, i.e. meteorological data, atmospheric stability and dispersion patterns of pollutants were not considered, but could be included in future work. However, analysed urban factors were considered to potentially assess sources, dispersion, and distribution of airborne metals that might result in higher pollutant loadings in lichens. Lichen-derived metal concentrations were further modelled, using regression analysis (section 6.4.7) incorporating the urban layout of Manchester.

Findings suggest vehicular emissions as sources of metal concentrations and potential beneficial effects of urban vegetation. Therefore, health risks by airborne metal concentrations are potentially highest within the city centre of Manchester and along the major road network.

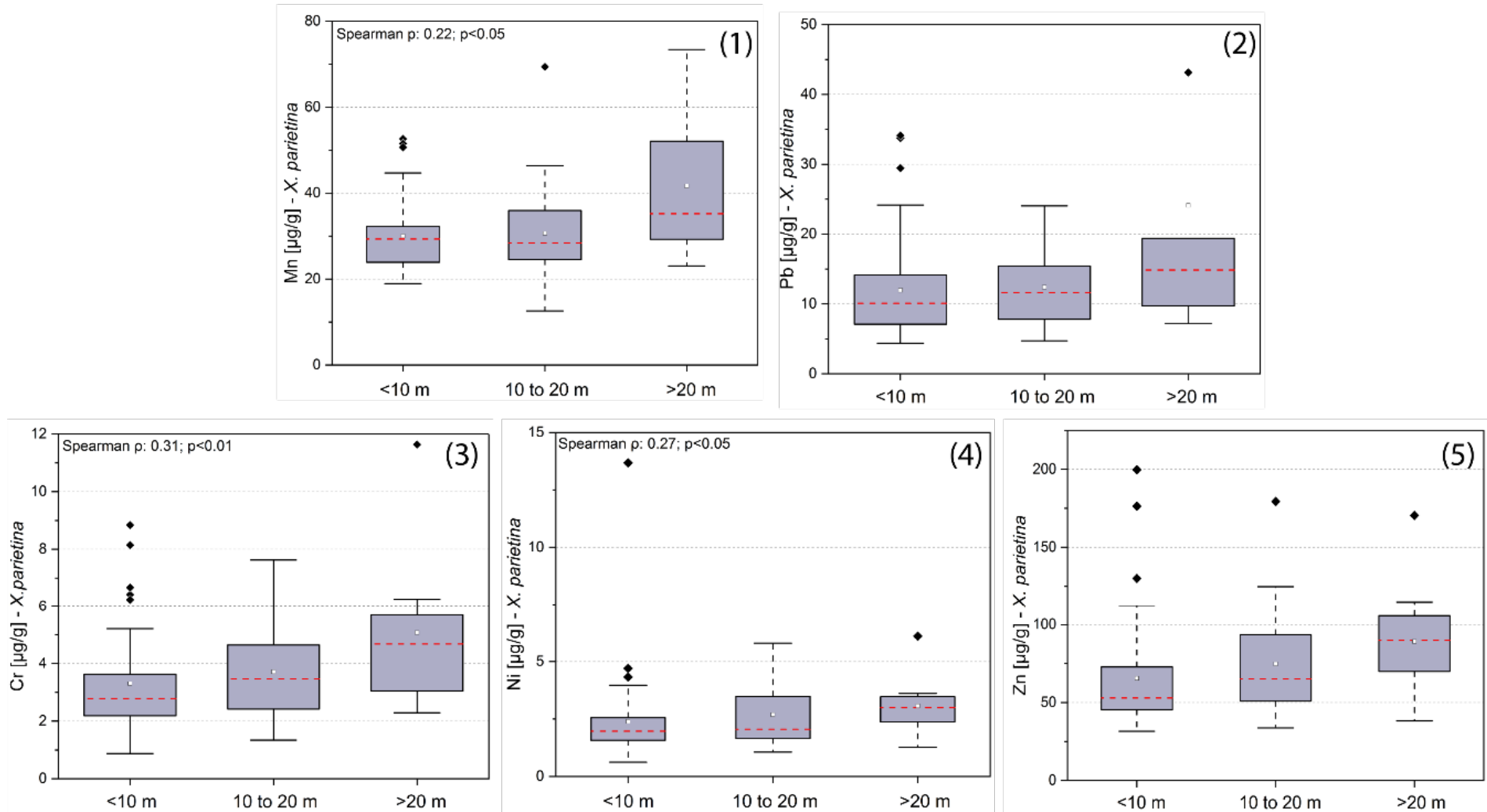
Building heights - *X. parietina*

Figure 6-24: Box-whisker plots (25th to 75th percentile; displayed with mean value: white square, median and extreme values: black diamonds) of building density/surrounding building heights and (significant) target metal concentrations for (1) Mn, (2) Pb, (3) Cr, (4) Ni and (5) Zn

6.4.7 Modelling approach of metal concentrations in urban *X. parietina* samples applying urban control factors

Significant relationships between metal concentrations and urban factors illustrate influences on distribution and dispersion of metals across the city centre of Manchester. To investigate spatial distribution and prediction of metals in the urban environment of Manchester (at un-sampled sites), metal concentrations were modelled using ‘Geographically Weighed Regression’ (GWR) together with urban influencing factors (section 6.3.5). GWR is able to capture spatial variations by allowing regression model parameters (i.e. urban variables previously described) to change over space (Yang and Wang, 2017) and was applied to lichen metal concentrations in association with urban factors. GWR was only applied for *X. parietina* samples, due to small sampling size and sampling distribution for *Physcia* spp.

Table 6-18 displays the ‘goodness of fit’ (R^2 -value) of GWR applied to metal concentrations. The R^2 -value may be interpreted as the proportion of dependent variable variance accounted for by the regression model (ESRI, 2019), i.e. explanation of the distribution of metal concentrations by the urban variables. Higher R^2 -values are preferable and indicates a better model (Ahn and Palmer, 2016; Yang et al., 2017).

Table 6-18: Goodness of Fit (R^2 -value) for GWR modelled metal concentrations, to investigate spatial distribution of metal concentrations by including urban factors.

Target metal	GWR: R^2
Cd	0.10
Cr	0.35
Mn	0.24
Ni	0.25
Pb	0.30
Pt	0.17
Zn	0.36

Distribution of metal concentrations at un-sampled sites, based on lichen-derived concentrations, in association with urban factors suggested that the applied modelling variables not fully explain spatial variability. Air quality studies incorporated meteorological data (i.e. precipitation, relative humidity and wind) as well as population data and total emission data of pollutants into GWR air quality models (Fang et al., 2015; Yang et al., 2017; Warsito et al., 2018).

Therefore, additional influences, such as meteorological data, sampling site specifics (i.e. twig bark pH) and population and emission data could improve modelling outcomes and should be further considered in further research. However, the scope of this study was to assess spatial variability of air quality, impaired by airborne metals across Manchester. Spatial variability of metals was presented and discussed (section 6.3.5 and section 6.4.5). Therefore, predicted metal concentrations are further discussed. Figure 6-25 to Figure 6-28 illustrate the predicted metal concentrations (by GWR).

In general, 'hotspot' areas of high metal concentrations were found across Manchester, around the motorway ('Mancunian Way') where the 'Oxford Road' monitoring station is located and along the major road north of 'Piccadilly Gardens' automated monitoring station. The 'Oxford Road' corridor is a key bus route into the city centre with about 2,400 busses daily (DfT, 2017a) and the main motorway ('Mancunian Way') is crossing through (with about 90,500 vehicles daily; DfT, 2017), suggesting higher emissions of metals due to higher traffic loads. Furthermore, higher metal concentrations along the A-road north of the city centre, also suggest vehicular emissions, with traffic counts between 15,700 to 35,600 vehicles daily (DfT, 2017a). In contrast, metal concentrations around 'Piccadilly Gardens' monitoring stations were lower, which could be related to its relatively open space, compared to the Oxford Road corridor, resulting in altered dispersion of metals. Interestingly, Pt concentrations were lower within the city centre, whereas higher in the north of the city centre Figure 6-27b. This could be related to restrictions of passenger cars within the city centre (and on Oxford Road) during daytimes (TfGM, 2019).

However, meteorological influences as well as traffic-related parameters (i.e. fleet composition, traffic-speed and flow) could influence dispersion of recorded metal concentrations across Manchester. As presented for Manchester (see chapter 2), traffic-flow and speed within the city centre are influenced by stop-and-go traffic and congestion during peak hours (i.e. <10 miles per hour during morning AM and PM peaks; chapter 2; Figure 2-20). Further investigating traffic-fleet composition and thus potential emission data could improve and re-define emissions across Manchester. Wind measurements at sampled locations could have further provided dispersion characteristics of pollutants. However, spatial variability of metal concentrations in lichens were found to be influenced by the specific urban layout.

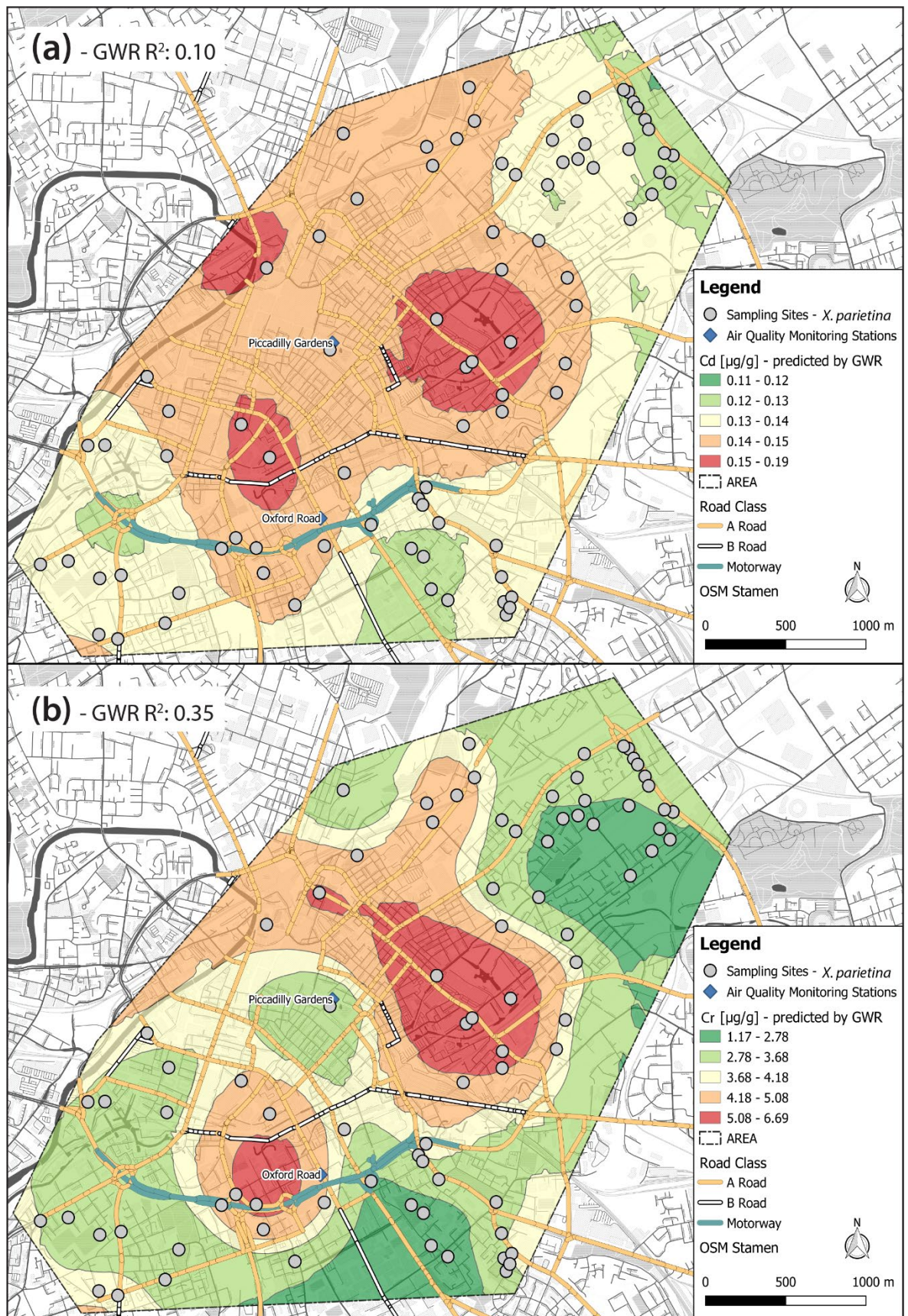


Figure 6-25: Predicted concentrations of (a) Cd and (b) Cr [$\mu\text{g/g}$] across the research area, with R^2 -value to display goodness of fit by GWR; air quality monitoring stations and sampling sites are also shown

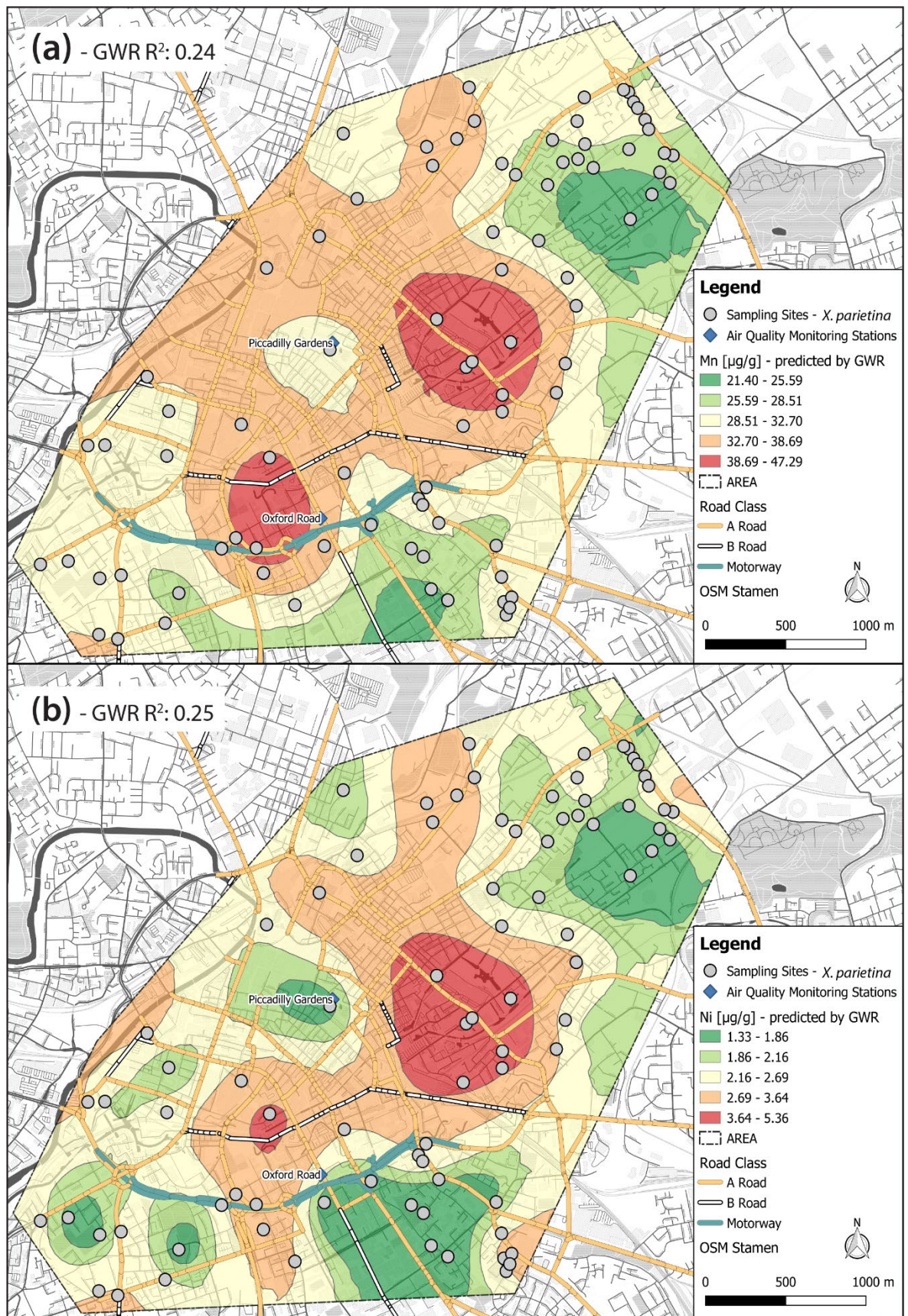


Figure 6-26: Predicted concentrations of (a) Mn and (b) Ni [$\mu\text{g/g}$] across the research area, with R^2 -value to display goodness of fit by GWR; air quality monitoring stations and sampling sites are also shown

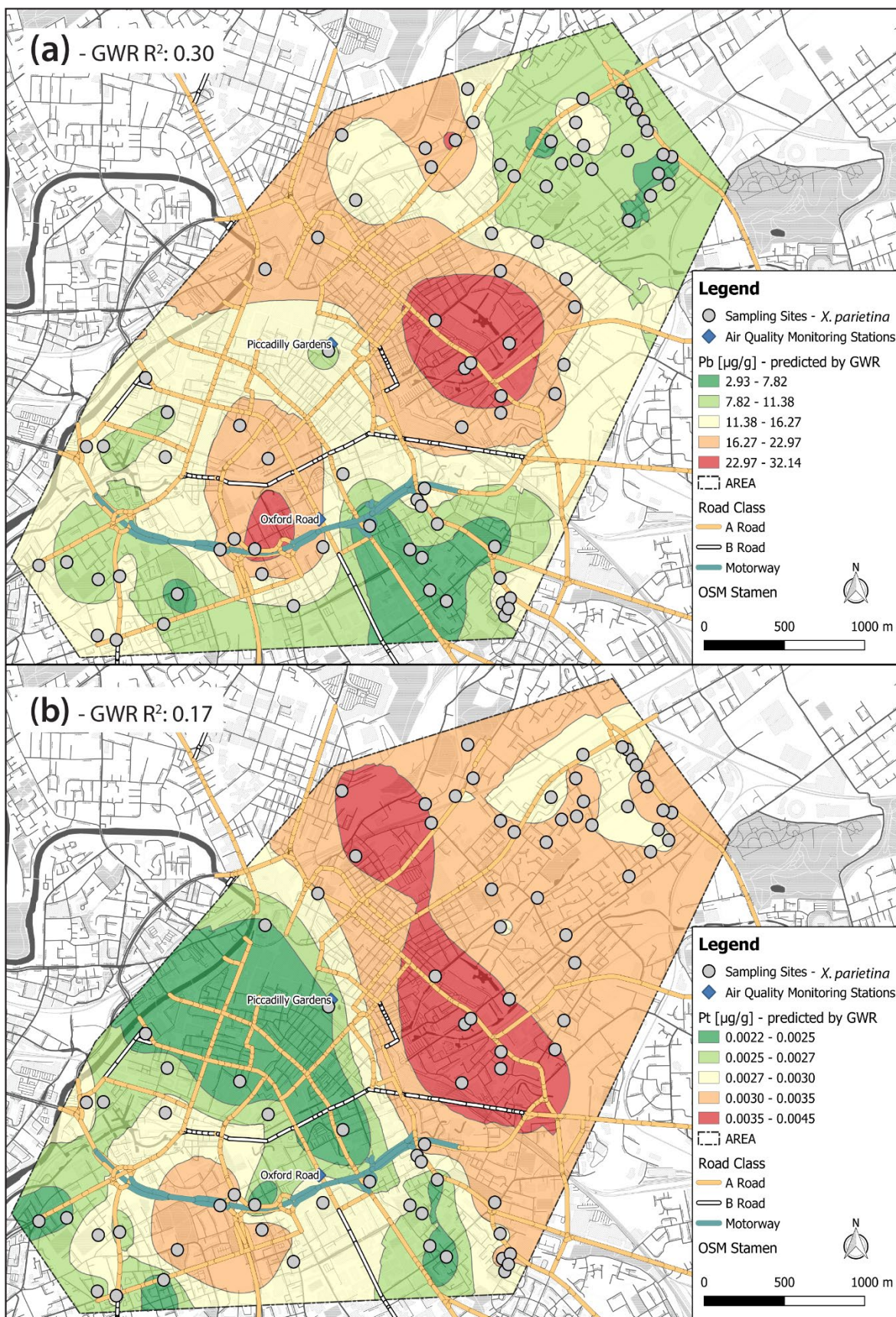


Figure 6-27: Predicted concentrations of (a) Pb and (b) Pt [$\mu\text{g/g}$] across the research area, with R^2 -value to display goodness of fit by GWR; air quality monitoring stations and sampling sites are also shown

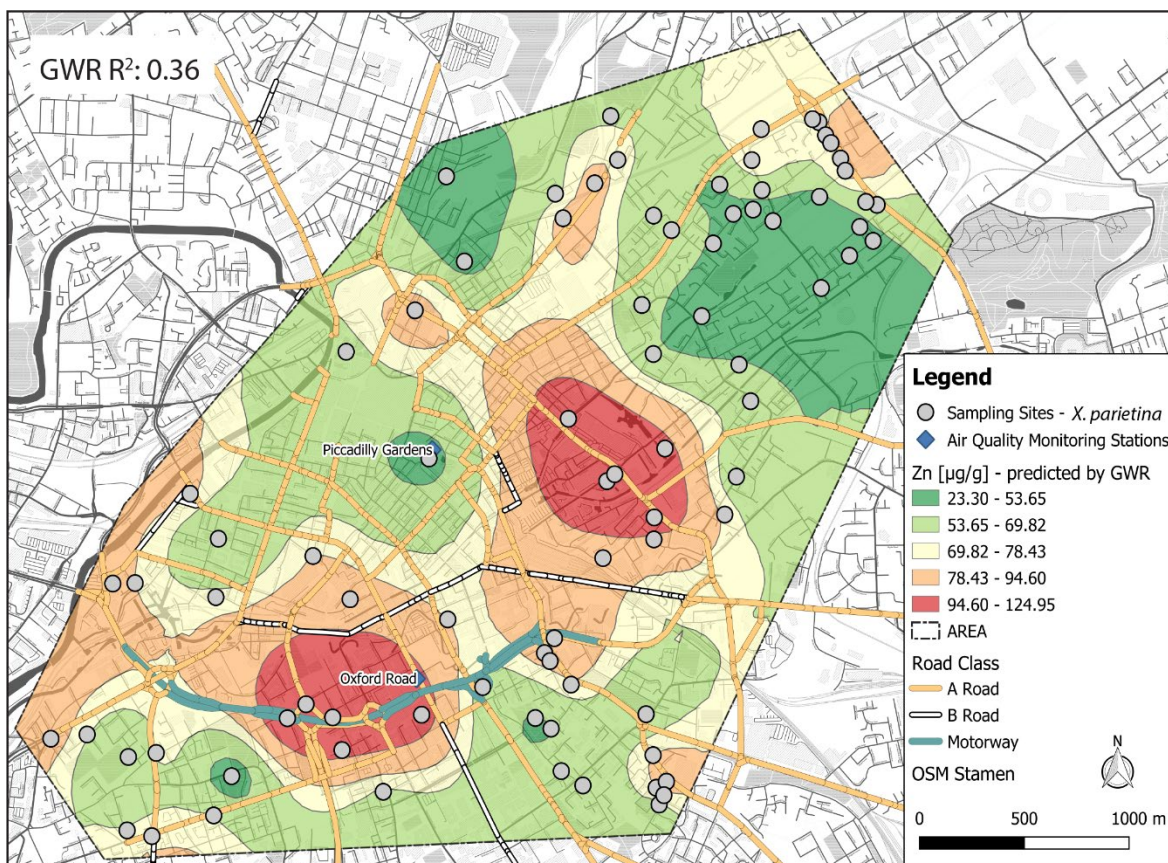


Figure 6-28: Predicted concentrations of (a) Zn [$\mu\text{g/g}$] across the research area, with R^2 -value to display goodness of fit by GWR; air quality monitoring stations and sampling sites are also shown

6.5 Conclusion

In this study target metals, known to be toxic to human health (i.e. Pb and Cd) and related to specific sources, i.e. vehicular, tyre and brake wear (i.e. Cr, Mn, Ni, Pd, Pt and Zn) were of particular interest.

Health relevant metals were recorded at higher concentrations along the major road network and within the city centre, indicating deteriorated air quality. Comparable distribution patterns were found for additional target metals. Therefore, metals recorded in lichens, primarily originate from traffic-related sources (i.e. tyres, brake lining and vehicular abrasion) with regard to traffic counts. Moreover, the urban layout of Manchester, i.e. building heights, resulting in canyoning effects seemed to affect dispersion and distribution of airborne metals.

Both automated air quality monitoring stations in Manchester do not record airborne metal concentrations and results presented indicate elevated airborne metals within the city centre that need to be further investigated. In particular, higher metal concentrations were recorded close to the 'Oxford Road' monitoring station, suggesting additional measurements of airborne metal concentrations.

Additional analysis of airborne metals, i.e. by passive sampling could provide information on breathable fractions (i.e. PM₁₀ and PM_{2.5}) of metals. PM₁₀ is measured at Oxford Road and further investigating metals (particle-bound) could be used to define potential health risks. However, elevated metal levels in lichens suggest increased health risks to Manchester's populations, in particular within the city centre and along the major road network. Traffic reduction and fleet improvements (i.e. bus and taxi fleet) could reduce emissions of metals (and particulates). However, even with electric vehicles non-exhaust emissions, i.e. vehicular abrasion, tyre and brake wear will be a major source of particulates and subsequently metals (Pant and Harrison, 2013; Timmers and Achten, 2016; Charron et al., 2019). Furthermore, rare-earth elements, such as neodymium (Nd) used in hybrid/electric cars was reported to cause lung embolism and liver damage (Rim et al., 2013). Therefore, emissions would potentially change from one relevant metal to another. Thus suggesting that traffic reduction, by improving public transport and improve cycling schemes would provide a viable option to reduce metal pollution within the city centre of Manchester. Nonetheless, high concentrations of metals are affecting the air quality and therefore the health of Manchester's urban population.

In conclusion, *X. parietina* and *Physcia* spp. provide a useful tool to assess spatial (and temporal) variability of airborne metals at a high spatial scale within an urban environment. In particular, at sites that are not continuously monitored by automated air quality monitoring stations, lichens provide fine spatial detail of deteriorated air quality and areas of health concern, which need further investigation and improvement.

Chapter 7-
Lichen
biomonitoring for
atmospheric PAH
source
apportionment and
toxicity assessment

7.1 Introduction

Atmospheric polycyclic aromatic hydrocarbons (PAHs) are of major concern for human health in urban areas (Vingiani et al., 2015). PAHs are known to be carcinogenic (especially lung, bladder and liver cancers) and are ubiquitous, persistent and highly lipo-soluble, i.e. able to accumulate in the food chain (International Programme on Chemical Safety (IPCS), 1996; Farmer, 1997; Kim et al., 2013; Garrido et al., 2014; International Agency for Research on Cancer (IARC), 2014; Augusto et al., 2016). These organic compounds are produced by incomplete combustion of coal, oil and wood, with anthropogenic emission sources including heating, industrial processes (i.e. chemical manufacturing, catalytic cracking and coking) and transportation, the latter primarily via road traffic exhaust emissions (Blasco et al., 2007; Kaya et al., 2012; Augusto, Máguas, et al., 2013; Augusto et al., 2015; Umweltbundesamt, 2016).

Continuous monitoring and recording of atmospheric PAH concentrations is undertaken at 31 sites across the UK (DEFRA, 2014c), although not at the two automated air quality monitoring stations within the city centre of Manchester, on Oxford Road and at Piccadilly Gardens. Consequently, additional information is needed to assess contemporary atmospheric PAH pollution within the City of Manchester, i.e. in this study by using lichen biomonitors to assess the spatial variability of PAH compounds and their concentrations, which can then be used to identify areas where negative human health impacts will be greatest.

Airborne PAHs can be accumulated by different plants, i.e. shrub/tree leaves/needles, mosses and lichens (Migaszewski et al., 2002; Piccardo et al., 2005; Blasco et al., 2007), the latter extensively used to biomonitor and evaluate air pollution/quality (Nimis et al., 1991; Giordani et al., 2002; Giordani, 2007; Pinho et al., 2012). Due to recent interest in persistent organic pollutants in the environment, several PAH-related lichen studies have been undertaken in urban areas, and to monitor traffic-sourced PAH pollution around the world (including in Europe and India), using either native or transplanted lichen species (Owczarek et al., 2001; Guidotti et al., 2003, 2009; Blasco et al., 2006; Domeño et al., 2006; Shukla and Upreti, 2009; Augusto et al., 2010; Shukla et al., 2012; Nascimbene et al., 2014; Kodnik et al., 2015). Only one such study focused on a UK urban area (i.e. London), using transplanted lichen *Pseudevernia furfuracea* (Vingiani et al., 2015). Furthermore, just a few studies previously used the lichen *Xanthoria parietina* and

only one used *Physcia adscendens* to assess PAH pollution in urban areas of Poland, Spain and Portugal (Owczarek et al., 2001; Domeño et al., 2006; Augusto et al., 2010). Therefore, lichens (*X. parietina* and *Physcia* spp.) can be used to assess spatial variability of PAHs across the City of Manchester.

In 1976 the U.S. Environmental Protection Agency (EPA) identified 16 PAHs of primary interest (from a much larger list of “129 Priority Pollutants”) for human health, which were implemented in environmental legislations throughout the world and which are routinely used in environmental studies (Andersson and Achten, 2015; Keith, 2015). These 16 PAHs are: naphthalene, acenaphthylene, acenaphthene, fluorene, phenanthrene, anthracene, fluoranthene, pyrene, benz[a]anthracene, chrysene, benzo[b]fluoranthene, benzo[k]fluoranthene, benzo[a]pyrene, indeno[1,2,3-cd]pyrene, dibenz[a,h]anthracene and benzo[ghi]perylene (EPA, 1999; Blasco et al., 2006, 2008; Lerda, 2011; Suvarapu and Baek, 2017). PAHs also have been classified into groups based on their carcinogenic potential (IARC, 2010; Lerda, 2011; Abdel-Shafy and Mansour, 2016; International Agency for Research on Cancer, 2018), as displayed in (Figure 7-1). Benzo[a]pyrene (group 1) has been extensively studied for its negative health effects and an association between benzo[a]pyrene exposure and cancer is supported (WHO, 2000b; U.S. EPA, 2017). Additionally, benz[a]anthracene and dibenz[a,h]anthracene are considered to be probably carcinogenic (group 2A), with chrysene, benzo[b]fluoranthene, benzo[k]fluoranthene and indeno[1,2,3-cd]pyrene possibly carcinogenic to humans (group 2B). These seven PAHs will be the main focus of analysis in this study, due to their (potential) severe deleterious impacts on human health (Figure 7-1).

Other 3- and 4-ring PAHs, i.e. fluoranthene, phenanthrene and pyrene, were further considered for analysis in this work due to their presence in air, lichens and their potential use to facilitate ‘fingerprinting’, or source apportionment, of PAH source(s) (Pozo et al., 2004; Blasco et al., 2006; Shukla and Upreti, 2009; Satya et al., 2012; Domínguez-Moruco et al., 2015; Loppi et al., 2015; Van der Wat and Forbes, 2015). Furthermore, total PAH profiles recorded in lichens will be presented, as interaction of PAHs with lichen’s surface is strongly dependent in which phase (i.e. gas-phase and/or particulate phase) they exist (Augusto et al., 2016). For instance, 2- and 3-ring PAHs primarily exist in the gas phase, whereas 5- and 6-ring PAHs are bound to particulates, and 4-ring can be present in both (Augusto et al., 2016).

Table 7-1: Classification of 16 EPA PAHs, based on their carcinogenic risk by the IARC (2010) that are adapted in legislations of the European Union (Lerda, 2011); ‘Not classified’ is used for PAHs which have not been assigned to a specific group by the IARC (2010), a classification different to ‘Group 3’ because the latter includes PAHs with inadequate evidence of carcinogenicity in humans (and inadequate or limited in experimental animals)

Carcinogenic group	PAH
Group 1: known to be carcinogenic to humans	Benzo[a]pyrene (BaP)
Group 2A: probably carcinogenic to humans	Benz[a]anthracene (BaA); Dibenz[a,h]anthracene (DahA)
Group 2B: possibly carcinogenic to humans	Chrysene (CHRY), Benzo[b]fluoranthene (BbF); Benzo[k]fluoranthene (BkF); Indeno[1,2,3-cd]pyrene
Group 3: not classifiable with regards to carcinogenicity to humans	Anthracene (ANC); Benzo[g,h,i]perylene (BghiP); Fluoranthene (FLT); Fluorene (FLU); Phenanthrene (PHE); Pyrene (PYR)
Not classified	Acenaphthylene (ACY); Acenaphthene (ACN); Naphthalene (NAP)

Polyurethane foam disks (PUF disks) are among the most commonly used passive air sampling devices, due to their ability to accumulate gaseous and particulate phase pollutants, as well as due to their cost effectiveness (Bohlin et al., 2014). PUF disks are capable of being deployed in many locations simultaneously (due to their relatively low cost), illustrating the possibility of undertaking air quality monitoring over large geographical scales to highlight spatial patterns, or temporal trends, of ‘persistent organic pollutants (POPs)’ (Harner et al., 2006; Klanova et al., 2006; Estellano et al., 2012). Specifically for PAHs (and other POPs), polyurethane foam disk passive samplers (PUF-PAS) have been applied previously in air quality monitoring studies, i.e. in Chile, Mexico, Sweden and the UK (Kohoutek et al., 2006; Bohlin et al., 2008; Harner et al., 2013; Klingberg et al., 2017).

Unfortunately, test deployment and solvent extraction of PUF disk samplers by ultrasonication did not achieve any acceptable results and is not described and discussed further here. PUF disk results would have provided additional information on spatial (and temporal) distribution on airborne PAHs and could have provided useful atmospheric PAH concentrations to ground-truth lichen PAH loadings.

This chapter presents the extraction, identification and quantification of PAHs from lichens sampled across the City of Manchester (UK). Results and discussion will primarily focus on PAHs derived from *X. parietina* lichens, due to small *Physcia* spp. sample size (N=3).

Interpretation and discussion focuses on lichen PAH compound concentrations, both in comparison to other urban studies and as an assessment of spatial variability of PAH concentrations within the study area. PAH source apportionment, or ‘fingerprinting’, and assessment of potential toxicity using ‘Toxic Equivalence Factors’ (TEFs), also are investigated. Finally, a conclusion about lichen-derived airborne PAH concentrations and their possible implications for poor quality air quality and deleterious human health implications within the city of Manchester will be drawn.

7.2 Research area – Manchester city centre

Atmospheric PAH concentrations have been reported to be extremely heterogeneous on a local urban scale, due to occurrence of several different PAH sources within urban environments (Lohmann et al., 2001). In the City of Manchester, PAH concentrations were measured previously between 1991 and 1995, using high-volume air samplers equipped with glass fibre filters and polyurethane foam plugs; total airborne PAH concentrations decreased from 115 ng/m³ in 1991 to 19 ng/m³ in 1995, following a decline in domestic fossil fuel combustion (Figure 7-1; Coleman et al., 1997; Howsam and Jones, 1998). Meijer et al. (2008) reported a change of UK PAH primary sources between the years 1991 and 2005, i.e. a transition from industrial processes (e.g. anode baking for the aluminium industry), which were the major sources of PAHs in 1991, to transportation/road traffic emissions that made up 65% of PAH emissions in 2005, with phenanthrene being a major contributor to atmospheric PAHs. Between 1991 and 2014, quarterly ambient airborne PAH concentrations were measured at ‘Manchester Law Court’ (Easting/Northing: 383375, 398260; UK-AIR ID: UKA00185; (DEFRA, 2014b), albeit with no data collection for 2012 (Figure 7-2). Since 2014, no airborne PAH concentration data have been collected for the City of Manchester, demonstrating the necessity for contemporary monitoring and assessment of PAH impacts on urban air quality.

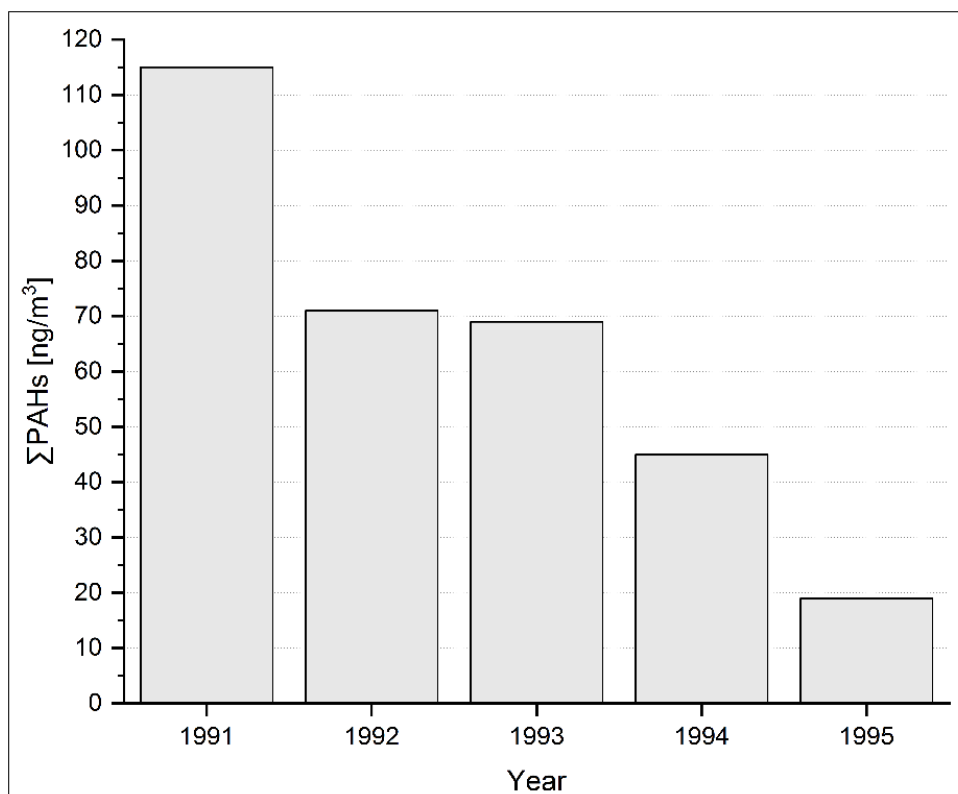


Figure 7-1: Total (Σ) PAHs measured at 'Manchester Law Courts' between 1991 and 1995 by high-volume air samplers (Coleman et al., 1997; Howsam and Jones, 1998)

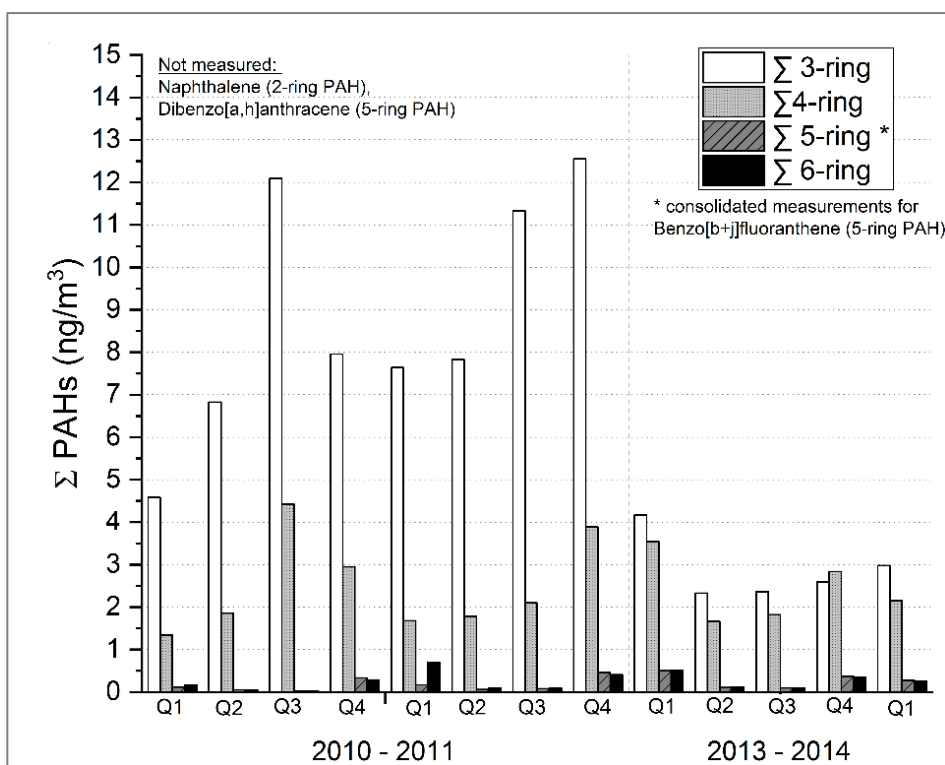


Figure 7-2: Quarterly PAH concentrations (particulate-phase and vapour-phase) measured at Manchester Law Court between 2010 and 2014; PAHs classified by number of rings; Naphthalene and dibenzo[a,h]anthracene were not measured, benzo[b]fluoranthene is included with benzo[j]fluoranthene (DEFRA, 2014b)

7.2.1 Lichen sampling for PAH extractions

In this study, *X. parietina* and *Physcia* spp. lichens were sampled from street trees that had previously been sampled for analysis of lichen CNS contents and stable-isotope ratios, as well as metal concentrations. Specifically, selection of sampling stations for this PAH investigation was informed by lichen N content (wt %; Chapter 3) and target metal concentrations (Chapter 6), i.e. vehicular-emitted metals Cd, Cr, Ni, Mn, Pb, Pd, Pt and Zn; Taylor, 2006; Robertson and Taylor, 2007). Different lichen nitrogen contents and metal concentrations, as recorded at selected sites, are interpreted to indicate different site-specific influences on lichen chemistry, i.e. higher and lower traffic-related emissions impacting localised air quality. For instance, higher nitrogen contents and elevated metal concentrations at sites close to major roads suggest vehicular emissions impacting negatively on airborne pollutant loading, which consequently could also be reflected by higher lichen PAH loadings (Table 7-2; MR labels, with daily traffic counts, where applicable). In contrast, sites located in, or proximal to, greenspaces (i.e. further away from major roads, labelled as GS in Table 7-2) were assumed to have been potentially less affected by airborne PAHs sourced from road traffic. Additionally, sites in a more residential surrounding also were re-sampled (labelled RES in Table 7-2), of which three sites are also located closer to a major road (labelled MR/RES, together with traffic counts).

No standardised approach has yet been formulated, when sampling biomonitors for organic analytes (Forbes et al., 2015). However, to minimise loss of more volatile compounds, lichen samples should be kept in paper bags and freezer stored until analysis (Forbes et al., 2015). Initial sampling was undertaken over a longer period of time in 2016 and 2017 and lichen samples were not stored in a freezer for analysis of CNS compounds, stable-isotope ratios and metal concentrations. It was therefore necessary to re-sample sites and process accordingly (i.e. immediate processing and freezer-stored) to assess PAH concentrations in lichens and minimise potential losses (see Chapter 2; Figure 2-24).

In total, 20 sites were re-visited (Table 7-2 and Figure 7-3) from May to September 2018 (specific lichen sampling dates in Appendix E-1). Lichens were collected from the same tree, as previously sampled for analysis of additional pollutants. Samples were obtained off twigs and small branches, at a height of 2 to 4 m, to acquire 'young' lichen specimen and assess recent atmospheric PAH pollution. The sampling period was undertaken during summer months, when PAH concentrations are reported to be lower (compared to winter months; Augusto, Máguas, et al., 2013). Lichens were sampled during dry days, to minimise variations due to rain wash-off (Forbes et al., 2015).

A potential temporal influence of PAHs recorded in lichens was considered. However, lichens absorb contaminants (and nutrients) more or less constantly throughout their lifecycle (Blasco et al., 2006). They are long-living organisms and thus integrate atmospheric pollutants over time, allowing to relate low levels of pollutants with long-term chronic effects on health (Augusto et al., 2007; Augusto, Pereira, et al., 2013). A potential temporal bias will be discussed later (section 7.4.3).

The collected lichens were stored in paper bags, immediately returned to the MMU laboratory and scraped-off the twigs and ground and homogenised into a powder using an agate pestle and mortar on the same day as collected. To avoid loss of volatile organic compounds, the prepared lichen material was stored in glass vials and freezer-stored, then subsequently freeze dried for 12h (-55°C; 0.03 mbar) using a 'Büchi L-200' freeze dryer, and stored in a freezer (-18°C) until solvent extraction of PAHs (González et al., 1996; Reis et al., 1999; Forbes et al., 2015).

Table 7-2: Sites re-sampled for lichens for PAH determinations across Manchester (Site ID; Figure 7-3) displayed with lichen N (wt%; Chapter 3) and target metals (Pb, Cd, Cr, Ni, Mn and Zn; Chapter 4) content, as well as rationale for sampling (MR = major road; GS = greenspace; RES = residential, with average annual daily traffic counts, where applicable; DfT, 2017); data values are displayed as three significant figures; * represents sites that have been sampled for both lichens, i.e. *X. parietina* and *Physcia* spp.

Site ID	N (wt%)	Pb [$\mu\text{g/g}$]	Cd [$\mu\text{g/g}$]	Cr [$\mu\text{g/g}$]	Ni [$\mu\text{g/g}$]	Mn [$\mu\text{g/g}$]	Zn [$\mu\text{g/g}$]	Site rationale
<i>Xanthoria parietina</i> (N=20)								
1	3.18	43.1	0.181	11.6	6.10	61.0	171	MR 15.600
2	2.18	13.7	0.0974	4.05	1.97	31.4	50.6	GS
3	3.04	13.8	0.139	3.41	1.82	31.7	77.5	MR 25.700
4	3.41	13.9	0.189	4.32	2.58	36.1	74.6	GS
5*	2.21	11.3	0.179	2.79	1.88	33.6	58.0	RES
6	2.86	10.8	0.118	3.78	2.66	32.3	47.9	GS
7	2.42	15.3	0.155	4.03	1.89	30.9	83.5	GS
8	3.60	14.4	0.147	3.89	1.84	35.8	60.4	RES
9	2.56	5.8	0.100	1.69	1.34	24.5	42.8	RES
10	3.35	22.9	0.147	6.67	2.83	50.6	199	MR 59.400
11	2.50	29.5	0.159	6.42	2.67	44.7	112	MR/RES 31.000
12	2.83	5.26	0.119	1.95	1.12	20.2	40.2	RES
13	2.82	20.2	0.136	7.39	5.60	41.8	108	MR 32.000
14	2.71	9.23	0.313	2.57	1.99	32.4	72.5	GS
15*	2.20	N/A	N/A	N/A	N/A	N/A	N/A	RES
16	2.68	9.99	0.0677	3.36	1.95	24.5	49.6	MR/RES 31.000
17	2.35	8.39	0.104	1.54	2.11	25.9	64.9	MR/RES 26.800
18	2.56	10.1	0.112	3.32	0.97	30.2	68.4	GS
19*	2.39	15.4	0.113	2.79	1.95	37.2	86.	MR 26.700
20	3.06	14.4	0.112	2.74	3.20	44.1	98.1	MR 10.200
<i>Physcia</i> spp. (N=3)								
5*	1.92	8.74	0.147	1.94	1.70	27.3	81.9	RES
15*	2.21	4.96	0.117	0.998	0.240	20.0	73.5	RES
19*	2.32	N/A	N/A	N/A	N/A	N/A	N/A	MR 26.700

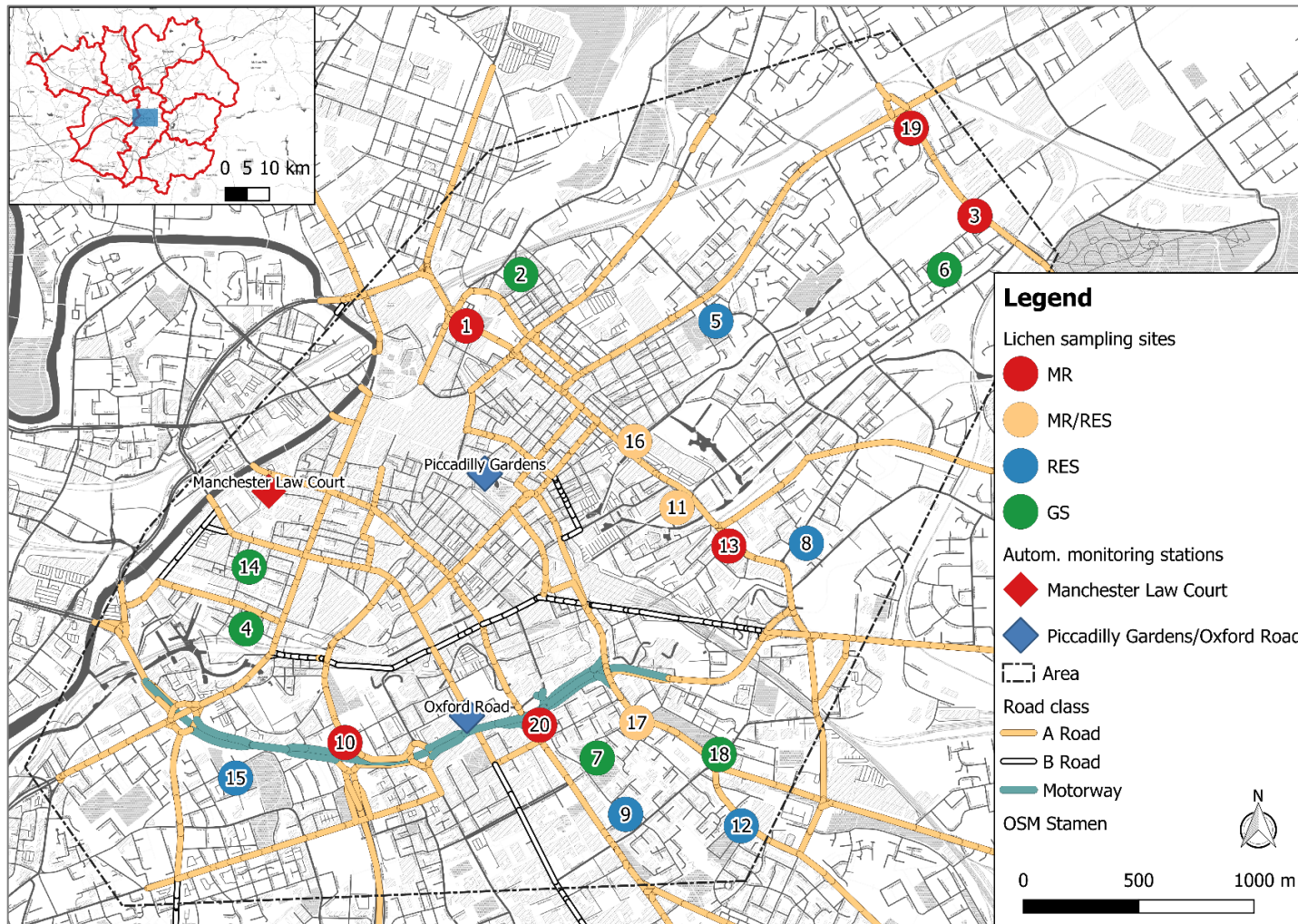


Figure 7-3: Lichen sampling sites (*X. parietina*, N=20; *Phyiscia* spp., N=3) for PAH extraction across the City of Manchester. Sampling sites are colour-coded by site rationale, as displayed in Table 7-2 (MR= major road, GS= greenspace and RES= residential). The two automated air quality monitoring stations and the PAH Andersen Sampler at 'Manchester Law Court' (PAH measurements undertaken until 2014) also are shown.

7.2.2 Solvent extraction of PAHs from lichen material

Different solvent extraction methods for determination of PAHs within lichens are described in the literature, i.e. Accelerated Solvent Extraction (ASE), Matrix Solid-Phase Dispersion (MSPD), Dynamic Sonication-Assisted Solvent Extraction (DSASE), ultrasonication, Soxhlet extraction and more recently QuEChERS (Quick, Easy, Cheap, Effective, Rugged and Safe) (Ockenden et al., 1998; Owczarek et al., 2001; Domeño et al., 2006; Blasco et al., 2007, 2011, Augusto et al., 2009, 2010; Guidotti et al., 2009; Vingiani et al., 2015; Concha-Graña et al., 2015; Kodnik et al., 2015; Wat and Forbes, 2019). Ultrasonication was used in this study, because ASE and DSASE equipment are not available at MMU and Soxhlet is a time and solvent consuming technique (Forbes et al., 2015). Moreover, ultrasonic-assisted extraction was reported to outperform Soxhlet to extract PAHs from pine needles (Ratola et al., 2006; Forbes et al., 2015) and ultrasonic extraction of PAHs has been successfully applied in environmental lichen studies (Table 7-3).

Table 7-3: Summary of studies that have solvent extracted PAHs from lichens using the ultrasonication technique, including geographical sampling area, extraction solvent (CYCLO = cyclohexane; DCM = dichloromethane) and volume, lichen mass and ultrasonication time

Author(s)	Geographical Area	Solvent used	Solvent volume	Lichen mass	Ultrasonication time
Protano et al. (2014)	Malagrotta area, Italy	CYCLO	30 ml	2.0 g	1 x 30 minutes
Fernández et al. (2011)	Caracas Valley, Venezuela	CYCLO-DCM (4:1, v:v)	30 ml	2.0 g	1 x 30 minutes
Käffer et al. (2012)	Porto Alegre, Brazil	DCM	15 ml	0.2 g	4 x 15 minutes
Guidotti et al. (2003, 2009)	Rieti, Italy	CYCLO	30 ml	2.0 g	1 x 30 minutes
Domeño et al. (2006)	Zaragoza city, Spain	DCM	15 ml	0.2 g	4 x 15 minutes
Owczarek et al. (2001)	Rieti, Italy	DCM	Not specified	1.0 g	2 x 20 minutes

Other lichen masses (up to 3.0 g), solvent volumes, sample clean-up procedures (i.e. filtering, solid-phase extraction (SPE), gel permeation chromatography) and analytical methods (i.e. HPLC and GC-MS) are likewise described within the scientific literature (Appendix E-2).

Based on the published solvent extraction techniques, including solvent type, subsequent clean-up steps and final analytical instrument, an ultrasonication solvent extraction method was set up for this study, to suit the equipment available at MMU and this methodology was initially tested for extraction/analysis on lichen material (*X. parietina*).

7.2.3 Testing SPE clean-up to determine best analytical practice

Solid-phase extraction (SPE) has become an alternative to conventional sample clean-up methods (i.e. column chromatography), which can be used to pre-concentrate components and clean-up matrices for sample analysis, by simultaneously reducing the solvent consumption (Blasco et al., 2007). SPE cartridges, consisting of 'polymerically bonded aminopropyl phase (-NH₂)' have been recommend to remove phenols, plant pigments and chlorophylls from the lichen matrix (Thurman and Mills, 1998; Blasco et al., 2007).

Once PAHs are extracted from a lichen sample, using one or more organic solvents, the solvents are passed through a solid-phase extraction (SPE) cartridge to: 1) concentrate the PAHs, by reducing solvent volume, and 2) remove other organic compounds that could result in a more complicated chromatograph that would impact on PAH identification and quantification. Therefore, before testing lichen PAH extraction, any possible influence of the solid-phase extraction (SPE) clean-up steps, and solvents used, was undertaken to determine the best analytical practice. Different solvents (repeated in triplicate; Table 7-4) were spiked with 1 ml biphenyl (C₁₂H₁₀) and a known concentration (2 µg/ml) of mixed PAH standard "Polynuclear Aromatic Hydrocarbon Mix" (TraceCERT®, 2000 µg/mL each component in methylene chloride: benzene (1:1) – Sigma-Aldrich) containing the 16 EPA PAHs targeted (Appendix E-4). These "spiked" solvents then were passed through SPE columns (Supelco LC-NH₂, 500 mg, 6 ml; CLWE method: **C**ondition, **L**oad, **W**ash and **E**lution; further described section 7.2.3), using a Supelco Visiprep™ Vacuum Manifold (12-port model, Sigma-Aldrich). The final solvent eluents were blown down to a smaller volume (~100µl) under nitrogen (N₂) and then made up to 1 ml with hexane and analysed using MMU's GC-MS (Agilent GC: 7980 and MS: 5977B; method specifications: Appendix E-5). Table 7-4 illustrates the recovery rates for each PAH and organic solvent/solvent mixture used for the SPE clean-up test.

Cyclohexane and hexane did not show recovery rates for some PAHs (especially high-molecular-weight PAHs), while some recovery rates were considered high (i.e. fluoranthene in hexane: 176%), due to potential contamination. In contrast, solvents/solvent mixtures containing dichloromethane, i.e. DCM:ACE, DCM and DCM:HEX were able to recover all PAHs. Recovery rates were poor for tested solvents, which could be related to PAHs retained on the SPE column (i.e. by not using enough solvent volume to elute the PAHs from the SPE column) and/or loss of analytes during the ultrasonication procedure (e.g. by evaporation).

Table 7-4: SPE clean-up test for solvents/solvent mixtures spiked with 2 ng/ml PAH Mix [triplicates for each solvent/solvent mixture] and obtained recovery rates (mean % \pm 1 standard deviation as %) by GC-MS analysis; #indicates that only one of three samples obtained PAHs

PAH [at 2 ng/ml]	DCM:ACE	CYCLO	DCM	DCM:HEX	HEX
Naphthalene	14 \pm 10%	18 \pm 16%	22 \pm 14%	20 \pm 16%	54 \pm 4%
Acenaphthylene	15 \pm 10%	40 \pm 12%	24 \pm 14%	21 \pm 15%	88 \pm 7%
Acenaphthene	15 \pm 10%	29 \pm 7%	27 \pm 16%	21 \pm 16%	68 \pm 10%
Fluorene	20 \pm 8%	49 \pm 2%	27 \pm 17%	21 \pm 15%	93 \pm 15%
Phenanthrene	16 \pm 7%	67 \pm 3%	26 \pm 14%	19 \pm 15%	126 \pm 18%
Anthracene	16 \pm 8%	77 \pm 2%	29 \pm 20%	28 \pm 16%	122 \pm 16%
Fluoranthene	20 \pm 11%	105 \pm 5%	29 \pm 17%	25 \pm 17%	176 \pm 21%
Pyrene	18 \pm 9%	100 \pm 4%	31 \pm 18%	28 \pm 18%	166 \pm 20%
Benzo[a]anthracene	10 \pm 8%	137 \pm 7%	21 \pm 15%	19 \pm 15%	N/A
Chrysene	24 \pm 13%	169 \pm 6%	21 \pm 15%	36 \pm 19%	N/A
Benzo[b]fluoranthene	21%#	195 \pm 9%	28 \pm 5%	28 \pm 18%	N/A
Benzo[k]fluoranthene	30 \pm 9%	N/A	41 \pm 19%	44 \pm 20%	N/A
Benzo[a]pyrene	19 \pm 9%	N/A	31 \pm 17%	28 \pm 18%	N/A
Indeno[1,2,3-cd]pyrene	17 \pm 7%	N/A	27 \pm 9%	22 \pm 13%	N/A
Dibenzo[a,h]anthracene	58%#	N/A	69 \pm 5%	48 \pm 21%	N/A
Benzo[ghi]perylene	23 \pm 13%	N/A	33 \pm 16%	33 \pm 12%	N/A

The SPE clean-up step favoured the use of DCM containing solvents for lichen extraction. DCM as solvent was previously applied in studies to extract PAHs from lichen material (Table 7-3) and was therefore further investigated with two different lichen masses (Table 7-5). Four sites that were resampled in 2018 (ID: 7; ID: 10; ID: 12 and ID: 15), for which sufficient lichen material was obtained (~2.5g), were extracted as described in Table 7-5 and were tested on MMU GC-MS and Waters equipment: GC-APCI-TQ-MS/MS (GC: Agilent 7890A, MS: Waters APGC Xevo TQ-XS) and GC-APCI-TOF-MS/MS (GC: Agilent 7890A; MS: Waters APGC Xevo G2-XS TOF).

Table 7-5: Solvent/solvent mixtures, lichen masses [g], solvent volumes and ultrasonication times used to test for optimal PAH extraction from lichen material

Test	Solvents	Solvent volumes [ml]	Ultrasonication times [min.]	Lichen masses [g]
(a)	Dichloromethane (DCM)	4x 15 (60)	4x 15 (60)	0.2
(b)	Dichloromethane (DCM)	4x 15 (60)	4x 15 (60)	1.0

GC-MS analysis at MMU was not able to detect extracted PAHs, potentially due to less sensitivity of the equipment, compared to Waters GC-systems. However, extraction of 1 g lichen material, analysed by GC-APCI-TQ-MS/MS reached the detection limit of the equipment, i.e. flattened peak shaped indicating detector overload, whereas 0.2 g of lichen material showed PAHs in the samples. Lichen material for further analysis was set to 0.2 g and subsequently, re-sampled sites (N=20) were extracted and analysed, as described in the following sections (7.2.4, extraction and 7.2.5, analysis).

7.2.4 PAH extraction applied to Manchester urban lichen samples

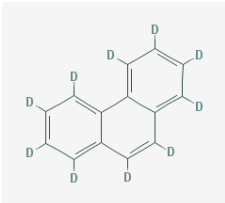
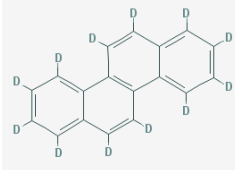
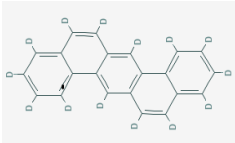
Figure 7-4 illustrates the solvent extraction procedure applied to the lichen sample for subsequent identification and quantification of PAHs. The procedure followed these steps:

1. About 0.2 g of each freeze-dried, ground and homogenised lichen sample (Domeño et al., 2006; Käffer et al., 2012) was weighed into pre-cleaned (fired at 400°C for 4h and DCM rinsed) glass vials. Prior to solvent extraction, all lichen samples were spiked with 10 µl of each of the three deuterated standards containing 0.5 ng/µl of deuterated PAHs (Table 7-6). Deuterated PAH standards are used to calculate the concentrations of

analytes of interest in the sample, and as a retention time reference for the identification of peaks in the GC-MS chromatogram (Bealey et al., 2008; Forbes et al., 2015; Moldoveanu and David, 2015). Deuterated PAHs (used as internal standards) elute in relative proximity to target analytes (i.e. 16 EPA PAHs) and chemically resemble the analytes (and are not naturally present in the lichen samples). Response factors of the individual PAHs relative to the deuterated PAHs are calculated using the ratio of the areas of individual PAHs and the internal standards (Poster et al., 1998).

Deuterated PAH standards were used for quantification of PAHs in lichens (Table 7-6), i.e. phenanthrene-d10 (for 2- and 3-ring PAHs), chrysene-d12 (for 4-ring PAHs) and dibenzo[a,h]anthracene-d14 (for 5- and 6-ring PAHs). For instance, phenanthrene-d10 was used for low-molecular weight PAHs (i.e. naphthalene, acenaphthylene, acenaphthene, fluorene, anthracene and phenanthrene (Table 7-6).

Table 7-6: Three deuterated PAH standards (no. of rings, molecular weight and structure) used for spiking of lichen samples before extraction, clean-up and GC analysis; deuterated standards were used for quantification of similar PAHs (i.e. phenanthrene-d10 for PAHs with 2- or 3-rings)

Deuterated standard	No. of rings	Molecular weight	structure	Used for quantification of
phenanthrene-d10 (C ₁₄ D ₁₀)	3	188.295		naphthalene acenaphthylene acenaphthene fluorene anthracene phenanthrene
chrysene-d12 (C ₁₈ D ₁₂)	4	240.367		fluoranthene pyrene benz[a]anthracene chrysene
dibenz[a,h]anthracene-d14 (C ₂₂ D ₁₄)	5	292.439		benzo[b]fluoranthene benzo[k]fluoranthene benzo[a]pyrene dibenzo[a,h]anthracene indeno[1,2,3-cd]pyrene dibenzo[g,h,i]perylene

2. 15 ml of dichloromethane (DCM) was added onto each lichen sample and the glass vials were ultrasonicated (covered with tin foil) for 15 minutes at room temperature, this extraction process was completed four times (total DCM volume $4 \times 15 \text{ ml} = 60 \text{ ml}$ (Domeño et al., 2006; Käffer et al., 2012). After each separate extraction, the sample glass vials were centrifuged at 4000 rpm for 10 min to separate lichen and DCM, with the DCM supernatant removed using glass Pasteur pipettes (fired at 400°C for 4h) and filtered through Whatman® 540 filter paper (Fernández et al., 2011) into new glass vials (pre-cleaned as described above).
3. The total 60 ml DCM extracts then were blown down under nitrogen (to ~3 ml) and subsequently cleaned using SPE. SPE cartridges (Supelco® LC-NH₂, 500 mg, 6 ml; new for each lichen sample) were topped up with 0.05 g anhydrous sodium sulphate (to remove traces of water) and 0.05 g of florisil (100-200 mesh, to remove secondary compounds, e.g. esters and glycerides), supplied from Sigma-Aldrich/Merck (Darmstadt, Germany; Domeño et al., 2006; Blasco et al., 2007, 2008, 2011; Nascimbene et al., 2014; Concha-Graña et al., 2015). CLWE (**C**ondition, **L**oad, **W**ash and **E**lution) then was used to prepare and extract PAHs from the ~3 ml DCM solutions. SPE conditioning (**C**) comprised 3 ml hexane and 6 ml DCM. DCM extraction solutions (~3 ml) then were added to the SPE cartridges (flow rate: 1-2 drops/sec; L) and, when the extraction solutions had passed through, the SPE cartridge bed was washed (W) with 0.5 ml hexane. 3 ml of hexane/DCM (v/v 3:1) then was used to elute (E) PAHs into new, pre-cleaned glass vials (Domeño et al., 2006; Käffer et al., 2012) ready for GC-MS analysis.
4. Toluene (20 µl) was added to each 3 ml hexane/DCM (v/v 3:1) eluent, to avoid evaporation to dryness and loss of more volatile compounds (i.e. naphthalene). These solutions were then blown down under nitrogen to ~100 µl, before transfer into GC-MS vials and PAH identification and quantification using GC-APCI-TQ MS/MS (Agilent GC 7890A, MS: Waters APGC Xevo TQ-XS) at Waters Corporation (Stamford Avenue, Wilmslow, SK9 4AX, UK) (Appendix E-3).

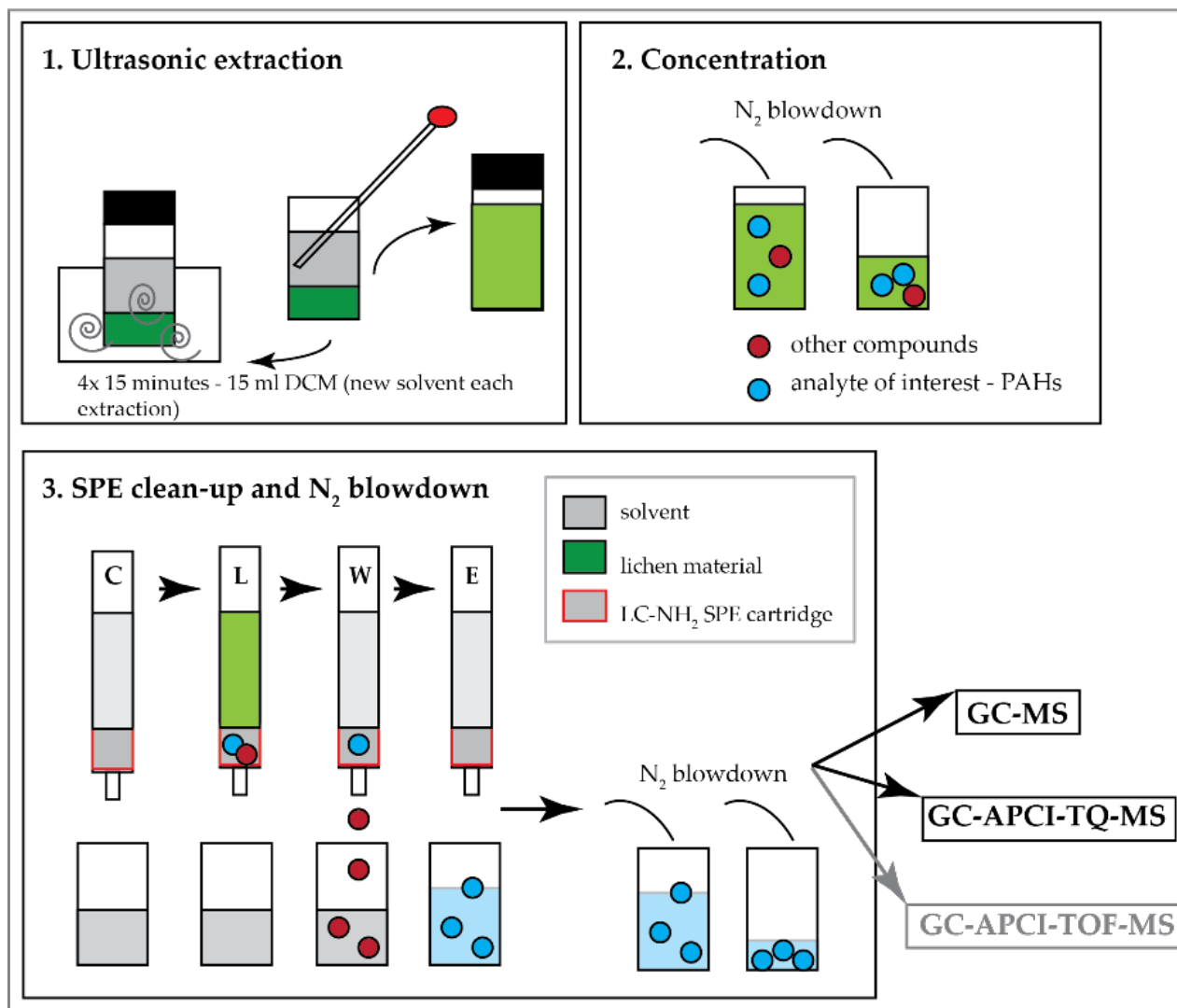


Figure 7-4: Schematic overview of solvent extraction process used for identification and quantification of lichen PAHs using ultrasonic-assisted extraction, sample concentration, SPE clean-up procedure and analysis by GC-MS and GC-APCI-TQ/TOF-MS/MS

7.2.5 PAH analysis using GC-MS, GC-APCI-TOF-MS/MS and GC-APCI-TQ-MS/MS

As described, MMU equipment was not able to detect PAHs in lichen extracts for undertaken tests using different masses. Changing of GC equipment, i.e. column, septa, inlet liner and ferrules and cleaning of the MS source improved instrument peak separation and shape. However, lichen-extracted PAHs could still not be determined. Subsequently, measurements were completed at Waters Corporation (in collaboration with Rhys G. Jones, Senior Research Scientist, Waters) using their GC-APCI-TQ-MS/MS (GC: Agilent 7890A, MS: Waters APGC Xevo TQ-XS): *Gas Chromatography Atmospheric Pressure Chemical Ionisation – Tandem Quadrupole – Mass Spectrometry*. TQ-MS/MS is able to achieve excellent sensitivity and quantification of compounds in difficult matrices, by using the MRM (Multiple Reaction Monitoring) feature, with low background noise to achieve low detection limits (Thurman and Ferrer, 2009). MRM is a mass spectrometry technique to monitor multiple product ions from one (or more) precursor ions, by collision, fragmentations and subsequently monitoring selected product ions (Thurman and Ferrer, 2009; Tollbäck, 2009; Murray et al., 2013). MRMs used for analysis of 16 EPA PAHs are displayed in the Appendix E-6.

GC-MS instrument programme specifications were based on EPA TO-13A: “Determination of Polycyclic Aromatic Hydrocarbons (PAHs) in Ambient Air Using Gas Chromatography/Mass Spectrometry (GC/MS)” (EPA, 1999). GC-MS conditions were adapted from this EPA method and adjusted (i.e. initial column temperature and hold time reduced, and temperature ramping expanded) to reduce analytical time, improve peak separation and recognition and were applied to the run on the Waters equipment (Table 7-7). Waters software ‘MassLynx V4.2 with TargetLynx XS’ was used to determine PAHs in lichen samples (with regard to prepared calibration standards; see Table 7-8).

Table 7-7: GC-APCI-TQ-MS/MS analytical conditions (adapted and changed from EPA TO-13A; EPA, 1999)

Conditions	
GC-APCI-TQ-MS/MS (Waters Corporation)	
Gas Chromatography	
Column	Rxi-5Sil-MS; -60°C to 350°C: 30m x 0.25 mm x 0.25 µm
Carrier Gas	Helium
Injection Volume	1 µl, split-less
Injector Temperature	310°C
Temperature Programme	
Initial Column Temp.	50°C
Initial Hold Time	2 minutes
Programme	20°C/min to 150°C (no hold) 10°C/min to 300°C (5 min. hold)
Final Temperature	300°C
Final Hold Time	5 Minutes
Mass Spectrometer	
Transfer Temperature	Line 280°C
Ionization Mode	Chemical ionisation (CI)
Mass Range	Multiple Reaction Monitoring (MRM)

PAH calibration standards were prepared from TCL PAH Mix (2000 µg/ml in benzene:dichloromethane – Sigma-Aldrich), which was diluted in hexane. Certified PAH concentrations are displayed in Appendix E-4. Each calibration standard (700 µl) was “spiked” with 100 µl of each of the three deuterated internal standard (containing 0.5 ng/µl) to a final volume of 1 ml. GC-APCI-TQ-MS/MS calibration was in the pg/µl range (Table 7-8), due to equipment sensitivity.

Table 7-8: PAH calibration standards (CS) prepared from 16 EPA PAH Mix for analysis by GC-APCI-TQ-MS/MS (in pg/μl and ng/μl)

CS0: Calibration "0"	GC-APCI-MS/MS [pg/μl]	
	pg/μl	ng/μl
CS1:	0.1 pg/μl	0.0001 ng/μl
CS2:	1 pg/μl	0.001 ng/ μl
CS3:	10 pg/μl	0.01 ng/μl
CS4:	100 pg/μl	0.1 ng/μl
CS5:	1000 pg/μl	1 ng/μl
CS6:	2000 pg/μl	2 ng/μl

7.2.6 Calculating of recovery rates and limits of detection and limits of quantification for PAHs recorded by GC-APCI-TQ-MS/MS

To calculate recovery percentages for PAHs, 0.2 g of unspiked lichen samples (N=4) were extracted following the same procedure as spiked samples (section 7.2.3). PAH concentrations obtained in unspiked samples were subtracted from spiked extracted lichens and used for calculation of spike recoveries (%) following Domeño et al., (2006).

$$\text{Spike recoveries (\%)} = \frac{\text{measured PAH (spiked)} - \text{PAH in unspiked}}{\text{PAH (known amount added to sample)}} \times 100$$

The extraction procedure blank was DCM (spiked with the same amount of deuterated standards as lichen material), passed through the same extraction cycle (4x ultrasonication), SPE clean-up step and subsequent analysis. The SPE clean-up blank consisted of DCM (spiked with deuterated standards) that was passed through the SPE clean-up step, to assess potential contamination and analyte retention during the SPE clean-up. The procedural blank was used for blank subtraction and analytical blanks (N=4, hexane) were used during the GC-APCI-TQ-MS/MS run to minimise cross-contamination and carry-over between sample analysis. Limits of detection and limits (LOD) of quantification (LOQ) were determined using standard solutions containing 0.1 pg/μl, 1 pg/μl, 10 pg/μl. The LOD is defined as the amount of analyte that generates a signal three times the noise, in the chromatogram close to the compound of interest, and LOQ being ten times the noise (Kodnik et al., 2015), following the calculations (1) for LOD and (2) for LOQ:

$$(1) \text{ LOD} = \frac{3.3 * \sigma}{S_{\text{calibration}}}$$

$$(2) \text{ LOQ} = \frac{10 * \sigma}{S_{\text{calibration}}}$$

where σ is the standard deviation of the response and $S_{\text{calibration}}$ is the slope of the calibration curve (European Medicines Agency, 1995; ICH, 1996; Shrivastava and Gupta, 2011). Method repeatability was assessed by analysing four spiked lichen samples with the 16 EPA PAHs mix (at 2 ng/ μ l). Average recovery rates (%), Limits of Detection (LOD) and Limits of Quantification (LOQ) and analytical precision derived from 10 pg/ μ l standards (as coefficient of variation - CV%) are presented in Table 7-9.

Table 7-9: Average recovery rates (%), LODs and LOQs (in pg – picogram) and coefficient of variation (CV%) for 16 EPA PAH compounds determined in spiked lichen samples (N=4, TCL PAH mix) and standard solutions (NAP= naphthalene; ACY= acenaphthylene; ACN= acenaphthene; FLU= fluorene; PHE= phenanthrene; ANT= anthracene; FLT= fluoranthene; PYR= pyrene; BaA= benz[a]anthracene; CHRY= chrysene; BbF= benzo[b]fluoranthene; BkF= benzo[k]Fluoranthene; BaP= benzo[a]pyrene; IcdP= indeno[1,2,3-cd]pyrene; DahA= dibenzo[a,h]anthracene; BghiP= benzo[g,h,i]perylene)

PAH	Recovery (%)	LOD / LOQ [in pg]		CV%	PAH	Recovery (%)	LOD / LOQ [in pg]		CV%
NAP	58	0.16	0.50	1.62	BaA	103	0.10	0.29	3.5
ACY	115	0.77	2.35	7.48	CHRY	74	0.62	1.86	0.3
ACN	118	0.30	0.92	2.58	BbF	135	0.94	2.85	13.8
FLU	76	0.23	0.70	8.57	BkF	74	0.91	2.76	11.8
PHE	66	0.43	1.31	6.64	BaP	154	0.92	2.78	13.4
ANT	62	0.63	1.90	5.72	IcdP	80	0.95	2.87	1.4
FLT	118	0.44	1.33	4.49	DahA	66	0.59	1.78	4.0
PYR	117	0.43	1.31	3.04	BghiP	67	0.39	1.19	5.3

7.2.7 Statistical analysis and data visualisation

Statistical analysis and data visualisation were undertaken using GraphPad Prism 7, SPSS Statistics 25 and Origin 2018. Geospatial mapping was undertaken in QGIS 3.42. – ‘Madeira’. Normality of lichen PAH concentrations was tested using a Shapiro-Wilk test, due to its higher statistical power regardless of sample size and distribution, when compared to other statistical tests (Mendes and Pala, 2003; Razali and Wah, 2011). Normality was tested for each analysed PAH for the whole set of 20 samples. Due to a non-normal distribution of concentrations for all measured PAH compounds (Shapiro-Wilk; $p < 0.05$), non-parametric statistical tests, e.g. correlation coefficient Spearman ρ , have been applied.

Grouping of data for statistical analysis of lichen PAHs with ‘urban factors’ was described in detail in chapter 2, i.e. classification of distance to major road based on NO_x decline within the first 200 m distance from major roads (i.e. motorways; Gilbert et al., 2003; Laffray et al., 2010; Bermejo-Orduna et al., 2014). Here distance to major road was sub-divided into two groups, i.e. <100 m and >100 m, as sampling sites were within 200 m of a major road and to assess potential traffic influences, close to highly trafficked roads.

Traffic counts count statistics (available for major roads; (DfT, 2017a) and the UKs ‘primary route network’ (including major roads: A-roads, B-roads and motorways; UK Department of Transport, 2012), respectively.

Surrounding building heights were calculated using the close (50 m buffer around the sampling location) surrounding the tree, using ‘OS building heights – alpha’ (Digimap - Ordnance Survey, 2017). Distances to greenspace (using ‘OS – Open Greenspace’ (Digimap - Ordnance Survey, 2018) classifications were based on human health studies, reporting decreased impacts of air pollution within 30 to 500 m of greenspaces (Dadvand, de Nazelle, et al., 2012; Dadvand, Sunyer, et al., 2012; Browning and Lee, 2017). Urban ‘variables’ that were used to assess potential controls on the spatial variability of PAH concentrations across the sampled area in Manchester are displayed in Table 7-10.

Table 7-10: Urban influencing factors and associated categories used to assess potential controls on the spatial variability of PAH concentrations

Urban influencing factor	Categories
Distance to major road (including A- and B-roads and motorways)	<100 m >100m
Traffic counts (annual average daily traffic flow)	<20.000 vehicles >20.000 vehicles
Distance to greenspace	1: <100 m 2: 100 to 200 m 3: 200 to 300m 4: 300 to 400 m 5: 400 to 500 m 6: >500 m
Building height (mean of surrounding buildings)	1: <10m 2: 10 to 20 m 3: >20 m

7.3 Results – lichen PAH concentrations

7.3.1 Type and concentrations of PAHs recorded in *X. parietina* and *Physcia* spp.

Analysed PAH concentrations in lichens were investigated by their overall PAH profile, i.e. PAH grouped by ring structure, to evaluate the uptake potential of lichens, with regard to physico-chemical properties of PAHs (being present in gas- and/or particulate-phase), and their indicative potential for particular sources. Following, target PAH concentrations based on toxicity groups (Table 7-1) are presented.

For 18 sites, all 16 EPA PAHs were recorded in analysed lichen samples. Anthracene was not recorded in two samples of *X. parietina* (ID: 2 and ID: 5), while dibenzo[a,h]anthracene was not recorded in one lichen sample of *Physcia* spp. (ID: 22). The total PAH profile recorded in both lichen species (summarised by ring numbers) are displayed in Table 7-11 and Figure 7-5. 4-ring PAHs (including fluoranthene, pyrene, benz[a]anthracene and chrysene) are most predominant PAHs across Manchester in both lichen species, with total concentrations of 189.82 ng/g and 20.76 ng/g, respectively.

Table 7-11: PAH concentrations (summarised by ring numbers) recorded in *X. parietina* and *Physcia* spp. to investigate species-specific uptake abilities of PAHs

	<i>X. parietina</i>	<i>Physcia</i> spp.
2-ring	7.23 ng/g	1.48 ng/g
3-ring	33.25 ng/g	9.61 ng/g
4-ring	189.82 ng/g	20.76 ng/g
5-ring	67.98 ng/g	5.96 ng/g
6-ring	46.13 ng/g	4.46 ng/g

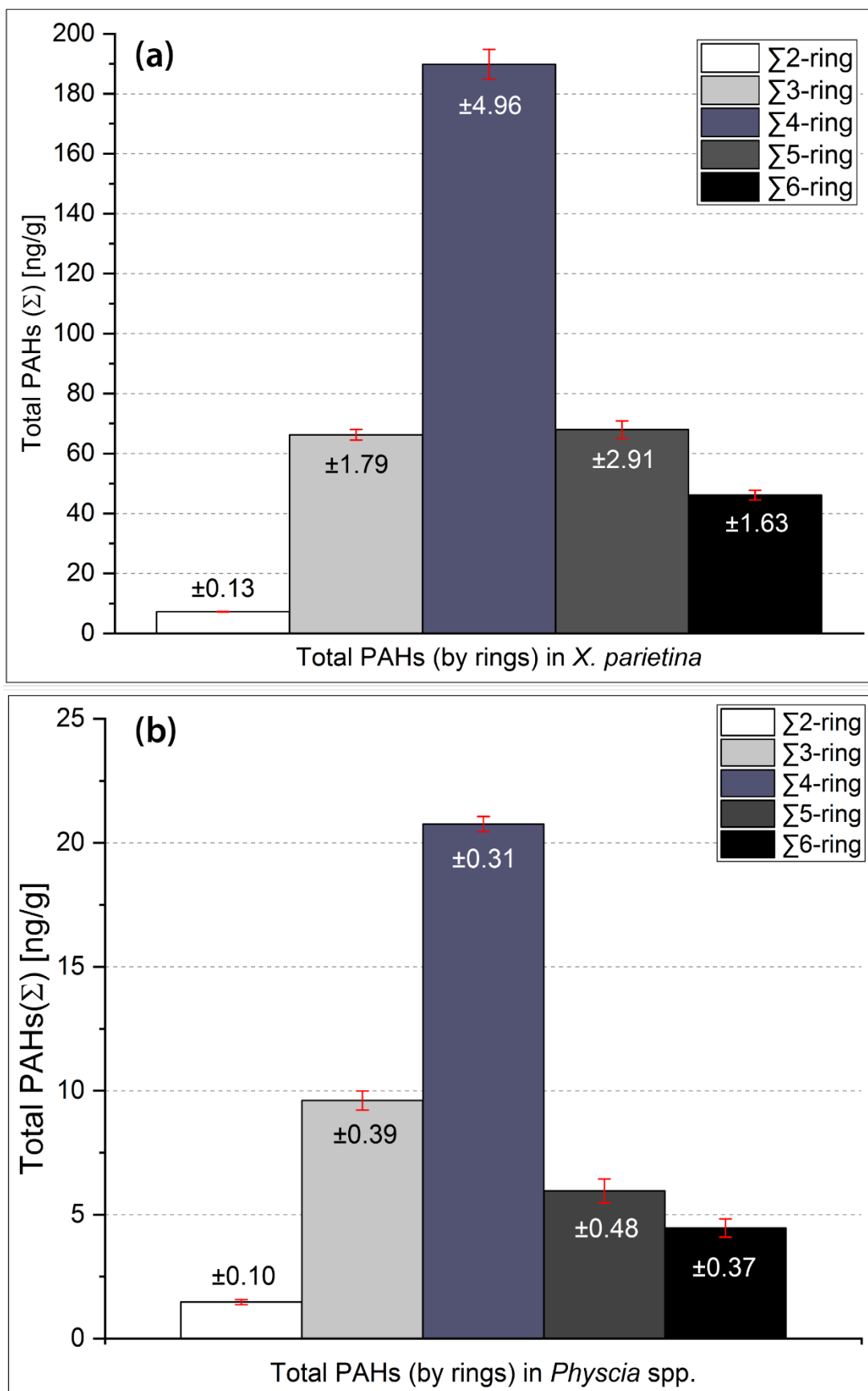


Figure 7-5: Total PAH concentrations (Σ by rings) recorded in: (a) *X. parietina* (N=20) and (b) *Physcia* spp. (N=3), with error bars and values within the bars (presented as 1x standard deviation of summarised ring-PAH concentrations, separately for *X. parietina* (a) and *Physcia* spp. (b))

Individual concentration ranges of recorded target PAHs are displayed in Table 7-12. Highest recorded concentrations in *X. parietina* were found for pyrene, fluoranthene and phenanthrene, which is comparable to highest concentrations found in *Physcia* spp. Benzo[a]pyrene (toxicity group 1) was recorded in both lichen species, with higher concentration ranges in *X. parietina*. Toxicity groups 2A and 2B PAHs were also found more variable in *X. parietina*, when compared to *Physcia* spp.

PAH concentrations by sites are displayed in Figure 7-6 and Figure 7-7 (colour coded by 'target' PAHs for this study, based on carcinogenicity, i.e. group 1: red, 2A: orange and 2B: yellow; traffic-related PAHs are displayed in green). PAHs (in %) summarised by ring-structure at sites for *X. parietina* (Figure 7-6) and *Physcia* spp. (Figure 7-7), are also included to indicate predominant PAHs in lichen profiles.

Table 7-12: PAH concentration ranges [in ng/g] of most toxic PAHs (group 1, 2A, 2B) and 'traffic-related' PAHs recorded in *X. parietina* (N=20) and *Physcia* spp. (N=3) across Manchester; colour-coded by toxicity potential (red-orange and yellow) and traffic-related emissions ((green)

Group	Target PAHs	<i>X. parietina</i>	<i>Physcia</i> spp.
‘traffic-related’	Phenanthrene (PHE)	1.32 to 7.55	2.07 to 2.77
	Fluoranthene (FLT)	1.32 to 9.90	1.87 to 2.50
	Pyrene (PYR)	1.84 to 9.63	3.10 to 3.44
2B	Chrysene (CHRY)	0.64 to 4.79	0.88 to 1.16
	Benzo[b]fluoranthene (BbF)	0.44 to 4.62	0.69 to 0.90
	Benzo[k]fluoranthene (BkF)	0.10 to 1.44	0.20 to 0.53
	Indeno[1,2,3-cd]pyrene (IcdP)	0.37 to 3.90	0.62 to 1.06
2A	Dibenzo[a,h]anthracene (DahA)	0.006 to 2.47	0.02 to 0.04
	Benz[a]anthracene (BaA)	0.31 to 2.95	0.31 to 0.57
1	Benzo[a]pyrene (BaP)	0.42 to 4.33	0.61 to 1.08

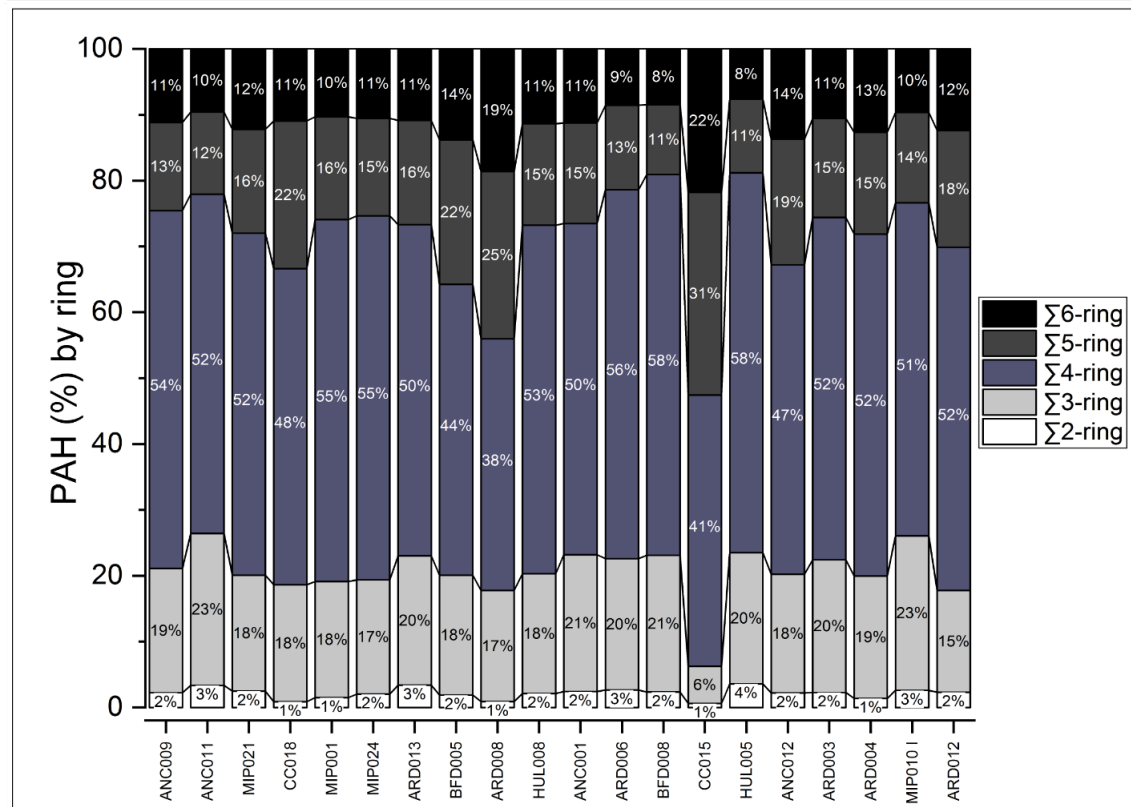
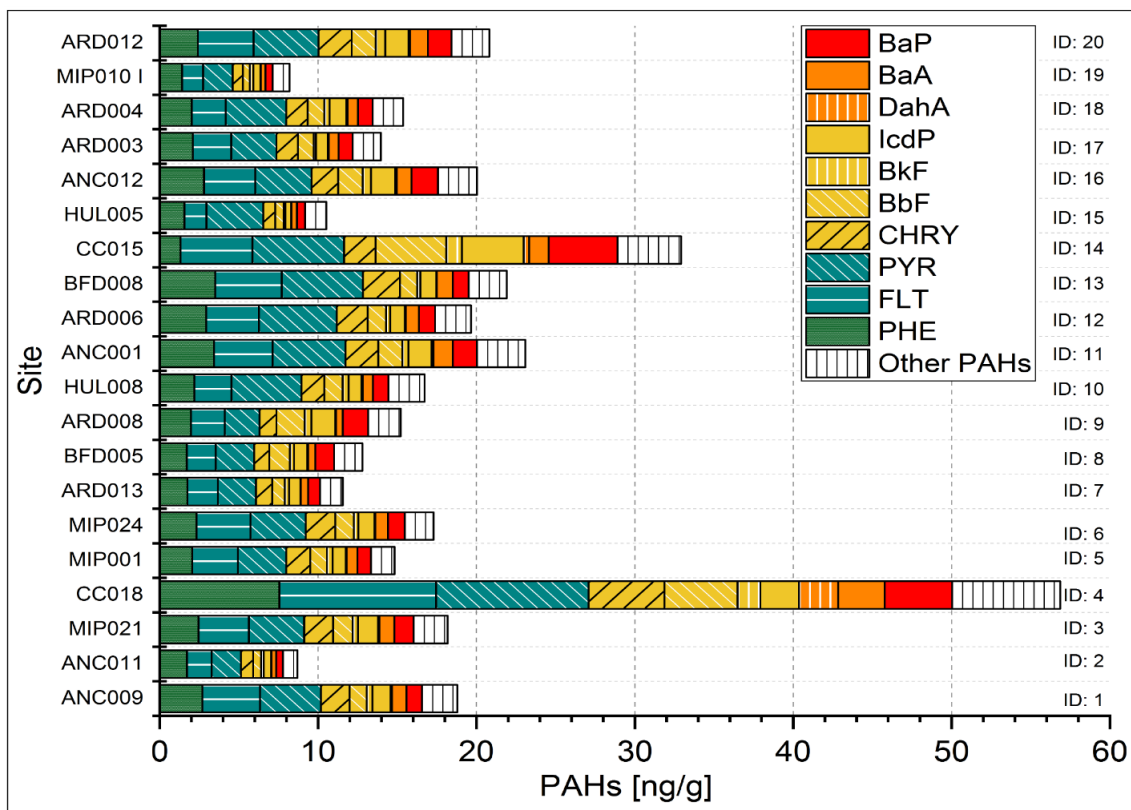


Figure 7-6: PAH concentrations (summarised by carcinogenic group 1: red, 2A: orange and 2B: yellow; traffic-related: green Σ PAHs: white) recorded at sampling sites for *X. parietina* (top panel) and PAHs (%) by ring-structure at sampling sites (bottom panel).

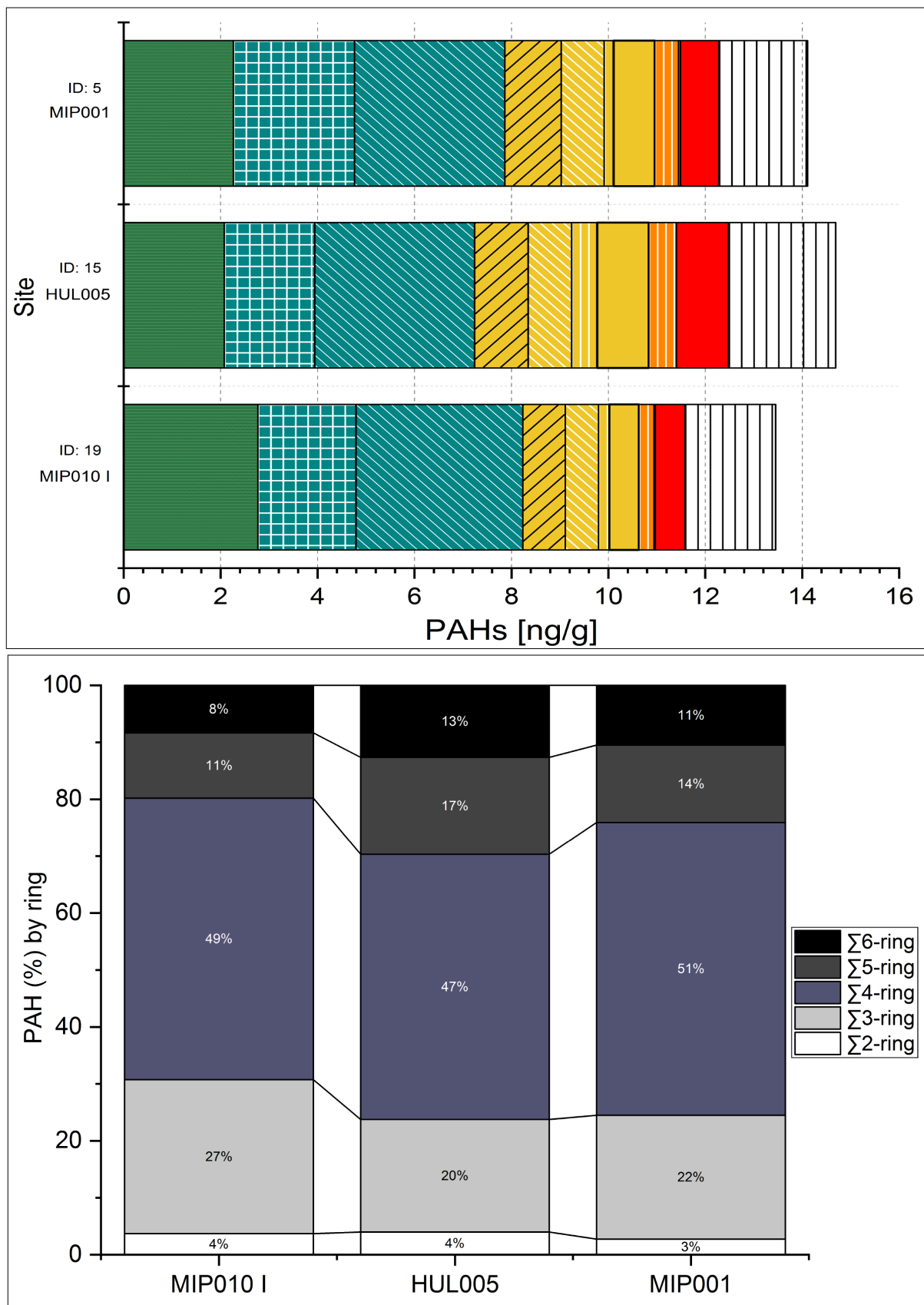


Figure 7-7: PAH concentrations (summarised by carcinogenic group 1: red, 2A: orange and 2B: yellow; traffic-related: green and other Σ PAHs: white) recorded at sampling sites for *Physcia* spp. (top panel) and PAHs (%) by ring-structure at sampling sites (bottom panel).

Mann-Whitney (non-parametric) tests were used to compare median values of target PAH concentrations for both lichen species, sampled from the same site (N=3; Table 7-13). No significant differences between median concentrations of PAHs in *X. parietina* and *Physcia* spp. was found. Comparison of target PAHs recorded in *X. parietina* and *Physcia* spp. are displayed in Figure 7-8 as box-whisker plots.

Results suggest site-specific influences of PAH on the lichen samples, with regard to its specific urban surrounding and potentially different PAH uptake abilities of lichen species (although not significantly different). Both will be discussed later in this chapter (section 7.6.1 and 7.6.3).

Table 7-13: Mann-Whitney test p-values presented for focus PAHs (target PAHs, including carcinogenicity groups 1, 2A and 2B) analysed in *X. parietina* and *Physcia* spp.

PAH	Mann-Whitney p-value
Traffic-related PAHs	
Phenanthrene	0.10
Fluoranthene	0.70
Pyrene	0.70
Group 2B PAHs	
Chrysene	0.70
Benzo[b]fluoranthene	0.70
Benzo[k]fluoranthene	>0.99
Indeno[1,2,3-cd]pyrene	0.20
Group 2A PAHs	
Benz[a]anthracene	>0.99
Dibenzo[a,h]anthracene	0.80
Group 1 PAH	
Benzo[a]pyrene	0.40

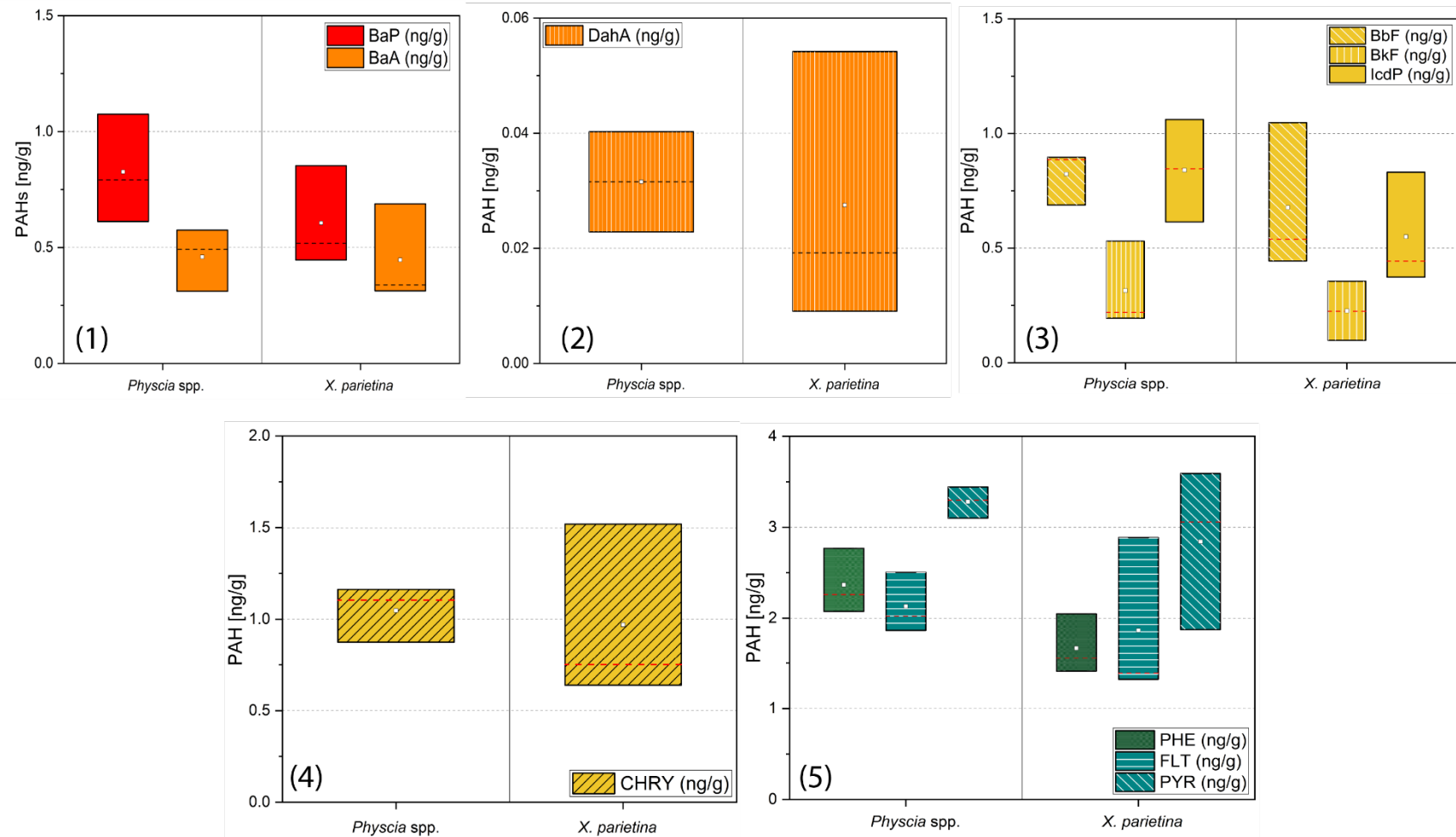


Figure 7-8: Box-Whisker plots (25th to 75th percentile) for PAH concentrations [in ng/g] recorded in *X. parietina* and *Physcia* spp. for (1) and (2) carcinogenicity group 1 and 2A: benzo[a]pyrene (BaP) and benz[a]anthracene (BaA); (2) carcinogenicity group 2B: dibenzo[a,h]anthracene (DaA), (3) benzo[b]fluoranthene (BbF), benzo[k]fluoranthene (BkF) and indeno[1,2,3-cd]pyrene (IcdP); (4) chrysene (CHRY) and (5) pyrene (PYR), fluoranthene (FLT) and phenanthrene (PHE)

7.3.2 Spatial variability of PAH concentrations

PAH concentrations recorded in *X. parietina* and *Physcia* spp. have been shown to be spatially variable across the city centre of Manchester, indicating site-specific sources with regard to the sample locations close surrounding (i.e. building density, distance to major road and traffic density). Due to small sample size for *Physcia* spp. (N=3), spatial variability is further analysed for *X. parietina* only.

Figure 7-9 displays the total concentrations of PAH recorded at each site, shown on the map with pie charts, illustrating the proportions of each PAH-ring group present within *X. parietina*. PAHs of the carcinogenic group 1 and 2A are displayed in Figure 7-10a, b and c, whereas Figure 7-11a, b, c and d illustrate the variability of group 2B PAHs. Figure 7-12a, b and c illustrates recorded concentrations of traffic-related PAHs in *X. parietina*.

Lichen PAH profiles at all sampling locations showed a predominance of 4-ring PAHs, including fluoranthene, pyrene, benz[a]anthracene and chrysene. Other PAH-ring profiles suggest site-specific influences (Figure 7-9), which will be further discussed later (section 7.5.3). Interestingly, two sites (ID: 4 and ID: 15) showed high concentrations for 'known' (group 1) and 'possibly' (2A) carcinogenic group PAHs and most group 2B PAHs (Figure 7-10 to Figure 7-12).

Results demonstrated spatial variability of PAHs across Manchester, with regard to ring-structure and specific health relevant PAHs.

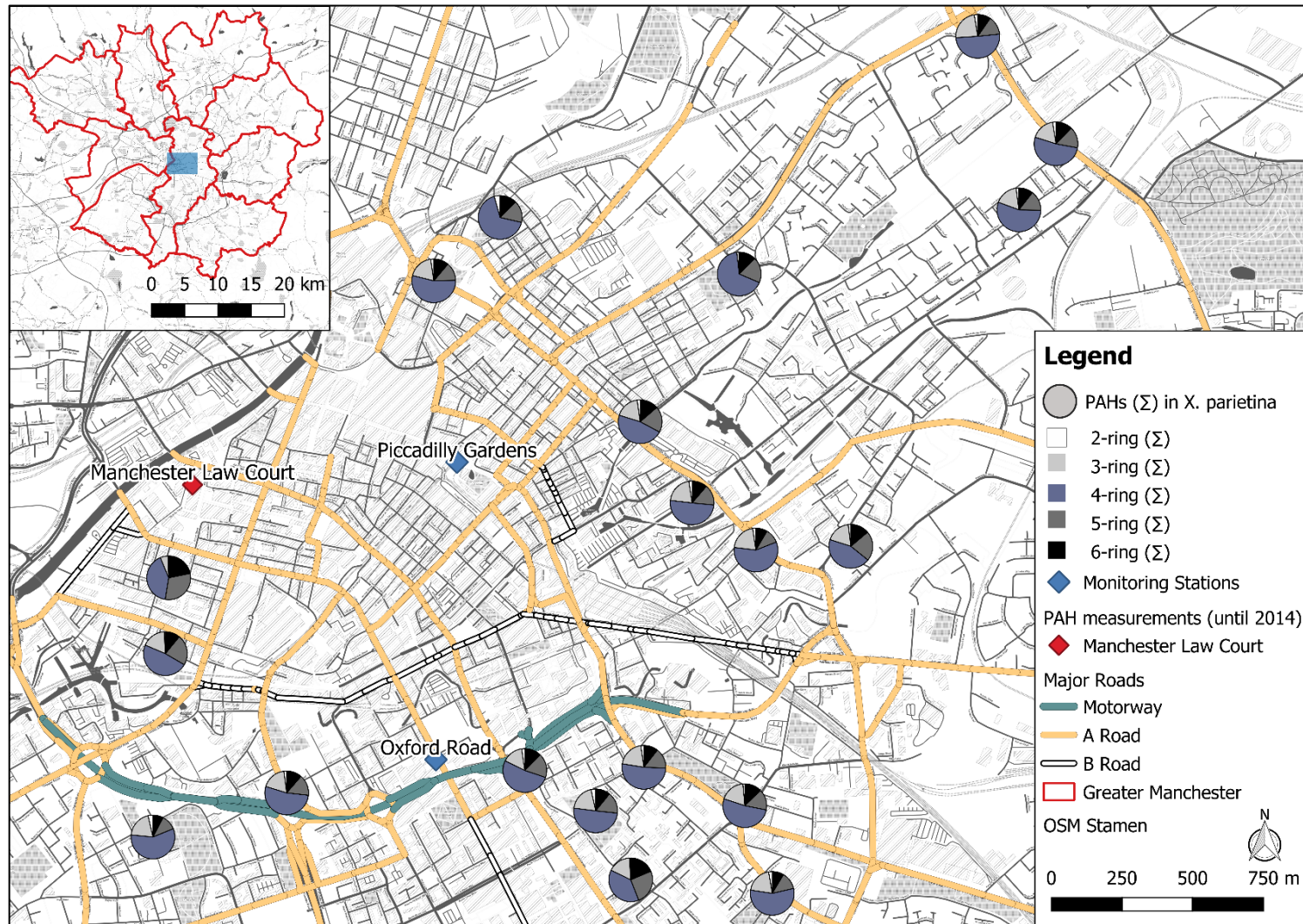


Figure 7-9: Summarized PAHs (Σ by rings) in *X. parietina* at analysed sites in Manchester, with major roads (A-, B-roads and motorway) and automated monitoring stations (blue) and PAH Andersen sampler (used for PAH measurements until 2014, red), illustrating lichen PAH profiles across Manchester.

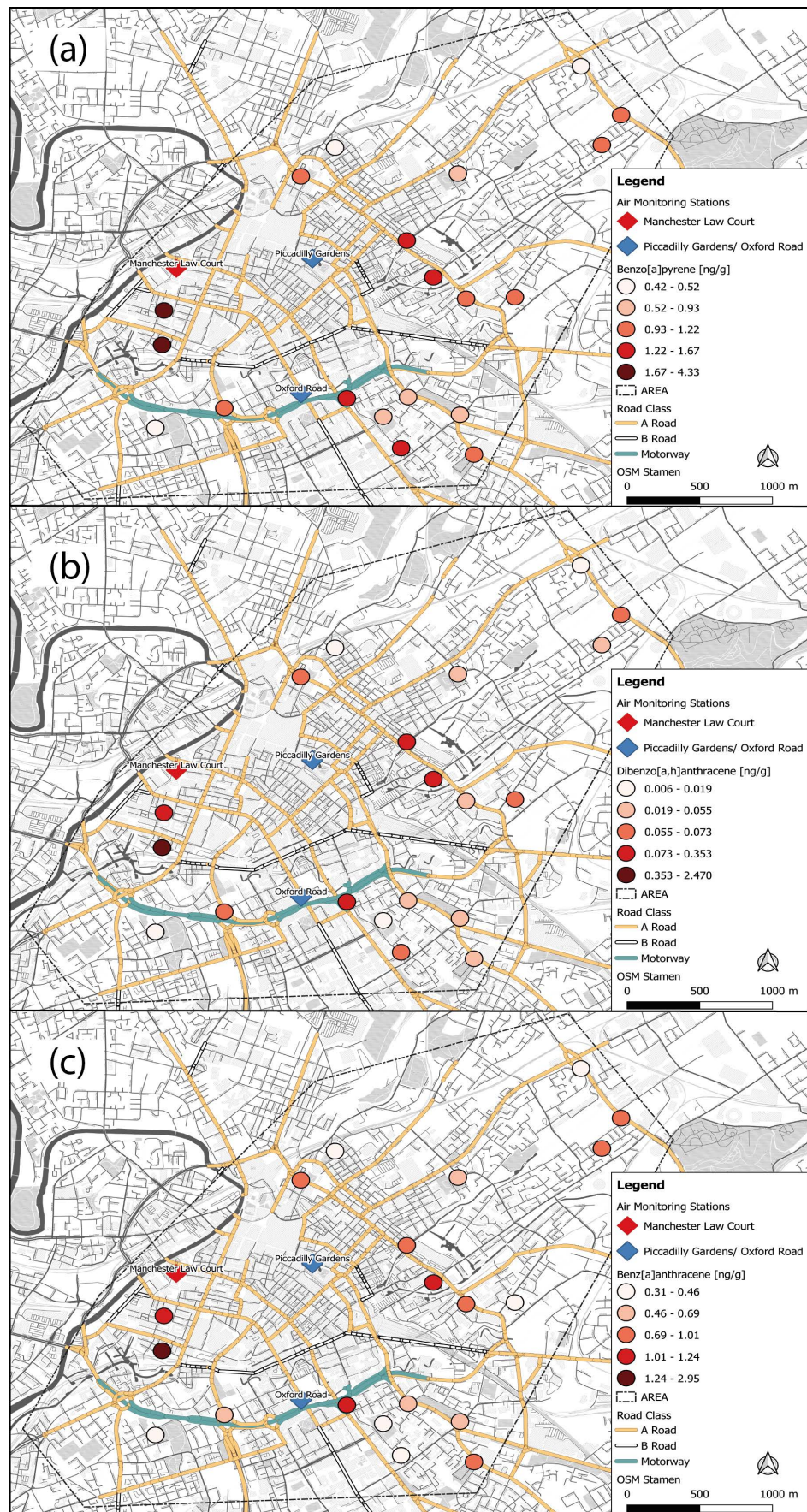
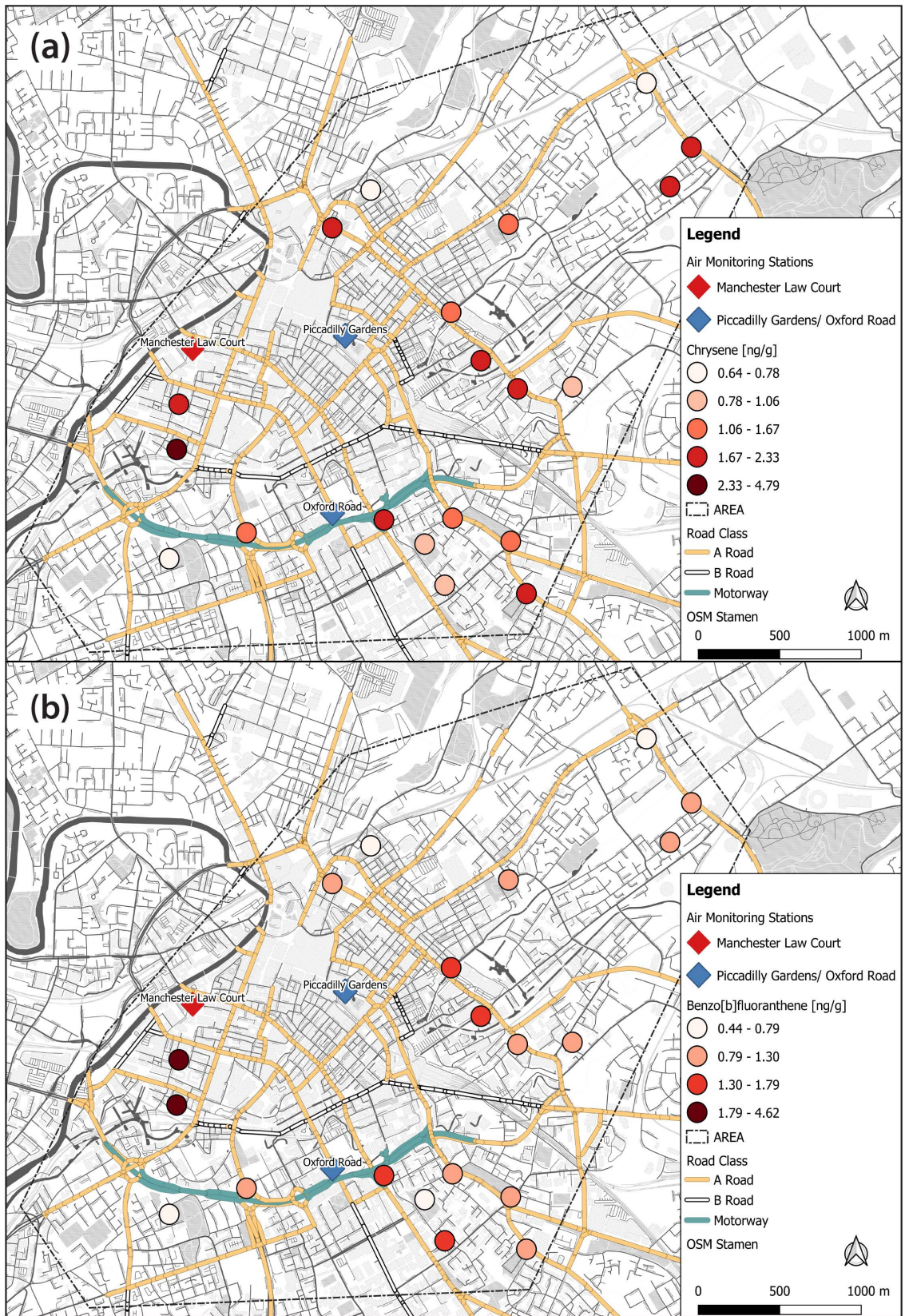


Figure 7-10: Concentrations of 'group 1 and group 2A' toxicity PAHs (a) benzo[a]pyrene, (b) dibenzo[a,h]anthracene and (c) benz[a]anthracene [in ng/g] recorded in *X. parietina* across the city centre of Manchester; displayed with automated monitoring stations (blue diamonds) and PAH monitoring station (in use until 2014; red diamond)



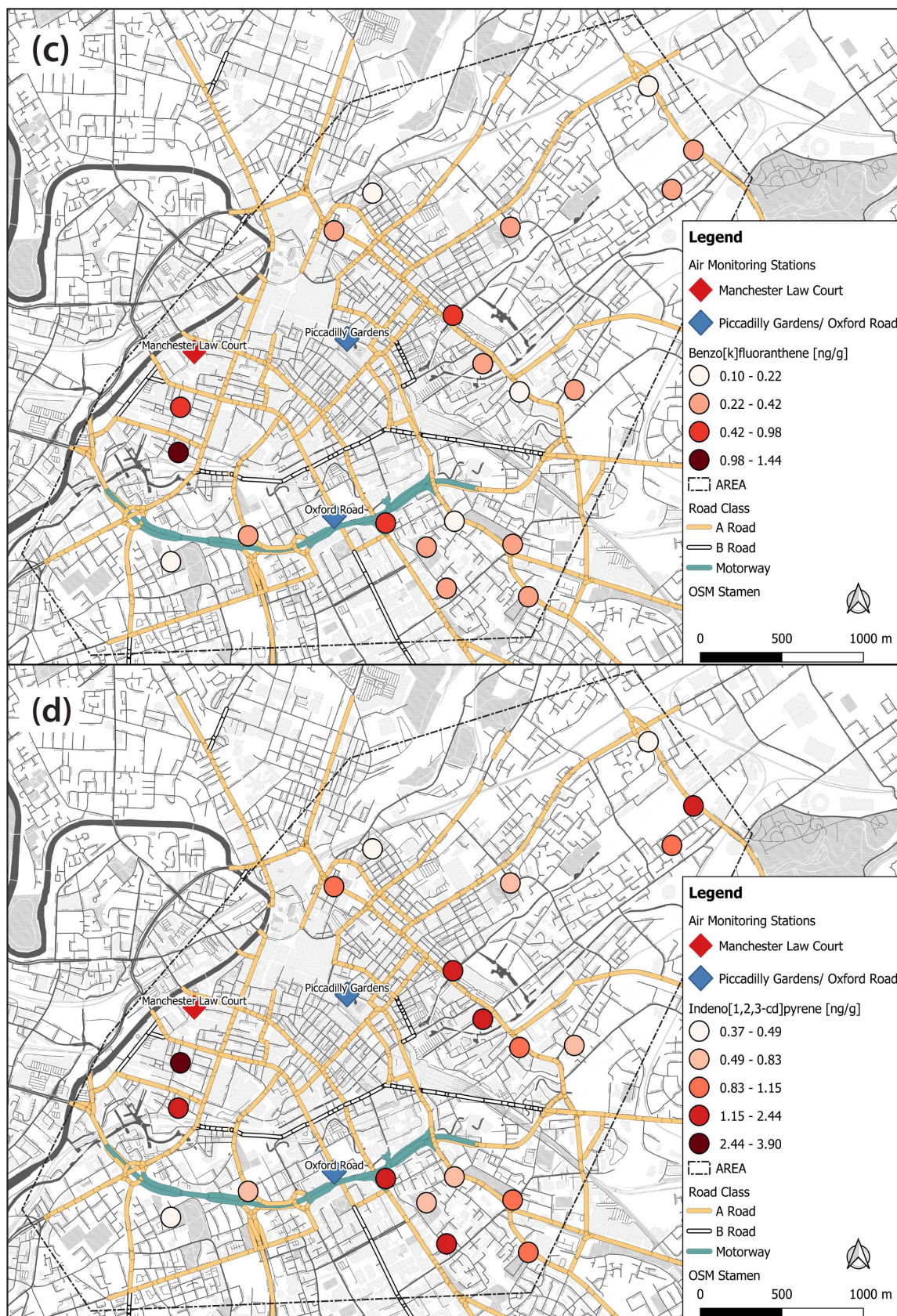


Figure 7-11: Concentrations of 'group 2B' toxicity PAHs (a) chrysene, (b) benzo[b]fluoranthene, (c) benzo[k]fluoranthene and (d) indeno[1,2,3-cd]pyrene [in ng/g] recorded in *X. parietina* across the city centre of Manchester; displayed with automated monitoring stations (blue diamonds) and PAH monitoring station (in use until 2014; red diamond)



Figure 7-12: Concentrations of ‘traffic-related PAHs’ (a) phenanthrene, (b) fluoranthene and (c) pyrene [in ng/g] recorded in *X. parietina* across the city centre of Manchester; displayed with automated monitoring stations (blue diamonds) and PAH monitoring station (in use until 2014; red diamond)

PAH concentrations were analysed in regard to potential urban influencing factors, i.e. distance to major road, traffic counts, distance to greenspaces and building heights to assess spatial variability across Manchester. PAH concentrations recorded in *X. parietina* were not drawn from a normal distribution (Shapiro-Wilk $p < 0.05$) and further analysis was performed using non-parametric statistical test. Table 7-14 displays correlation coefficient (Spearman ρ) for analysis of PAHs concentrations in lichens with urban influences, whereas Table 7-15 display statistical test outcomes (Mann-Whitney) between grouped data, i.e. distance to major road and traffic counts. Figure 7-13 to Figure 7-15 illustrate the statistical relationships and differences between groups (distance to major road and traffic counts) as box-whisker plots.

Table 7-14: Spearman ρ correlation coefficient of PAH concentrations (target' PAHs, Σ PAHs by ring structure) to investigate potential influences by the urban structure of Manchester (MR = distance to major road, TC = traffic counts, GS = distance to greenspace, PS = distance to point sources and BH = mean of surrounding building heights); *significant at the level $p < 0.05$ (underlined values; shaded in yellow), **significant at the level $p < 0.01$ (**bold values**; shaded in green)

PAH	MR	TC	GS	PS	BH
	Target PAHs				
PHE	<u>-0.66</u>**	-0.12	<u>0.63</u> *	0.18	0.12
FLT	-0.37	-0.41	0.33	0.15	0.17
PYR	<u>-0.46</u> *	-0.30	0.29	-0.08	0.34
CHRY	-0.43	-0.38	0.33	0.06	0.05
BbF	-0.11	-0.45	0.27	-0.10	-0.16
BkF	-0.14	<u>-0.47</u> *	0.08	-0.23	-0.11
IcdP	-0.25	<u>-0.49</u> *	0.17	-0.07	-0.10
BaA	-0.44	-0.36	0.32	0.05	0.10
DahA	-0.34	-0.38	0.43	-0.12	0.03
BaP	-0.16	-0.45	0.29	-0.08	-0.10
	PAHs summarised by ring structure				
2-ring	<u>-0.55</u> *	-0.12	<u>0.51</u> *	0.10	0.23
3-ring	<u>-0.66</u>**	-0.04	<u>0.61</u>**	0.34	0.02
4-ring	-0.41	-0.34	0.30	0.06	0.20
5-ring	-0.16	<u>-0.47</u> *	0.25	-0.20	-0.14
6-ring	-0.25	-0.45	0.22	-0.13	-0.08

Table 7-15: Mann-Whitney test for grouped data, to investigate differences between PAHs concentrations with distance to road and traffic count groups (distance to major road <100 m and >100; traffic counts <20,000 vehicles and >20,000 vehicles); significance differences presented in bold (* $p < 0.05$, shaded in yellow; ** $p < 0.01$ shaded in green)

Target PAHs	Mann-Whitney p-value (two-tailed)		PAHs by ring	Mann-Whitney p-value (two-tailed)	
	MR	TC		MR	TC
PHE	<0.01**	0.76	2-ring	<0.05*	0.97
FLT	0.12	0.17	3-ring	<0.01**	0.96
PYR	<0.05*	0.24	4-ring	0.08	0.20
CHRY	0.07	0.18	5-ring	0.52	0.08
BbF	0.68	0.12	6-ring	0.31	0.06
BkF	0.57	0.07			
IcdP	0.31	<0.05*			
BaA	0.06	0.18			
DahA	0.16	0.24			
BaP	0.52	0.12			

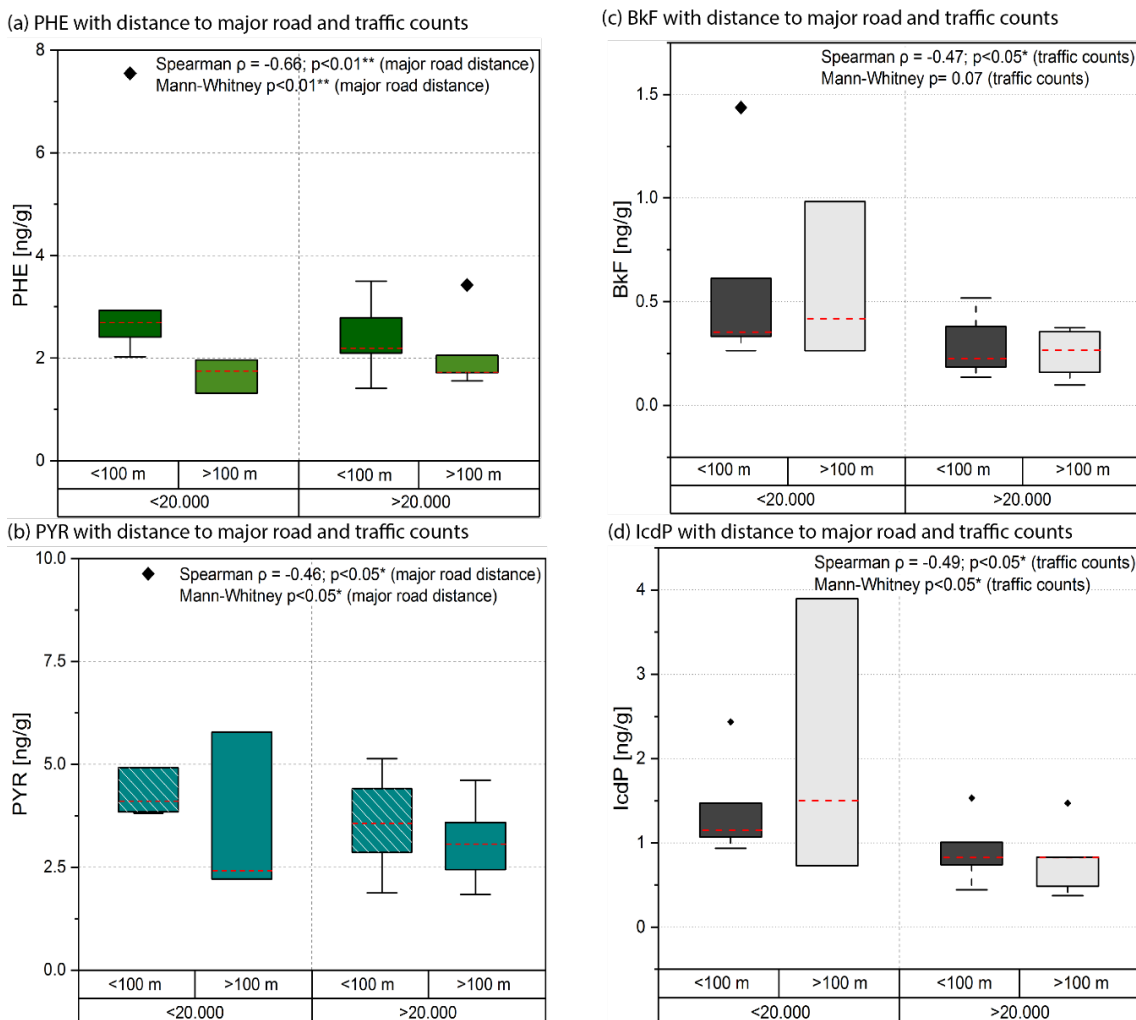


Figure 7-13: Box-Whisker plots (25th to 75th percentile) of (a) phenanthrene (PHE) and (b) pyrene (PYR) with distance to major road and traffic counts, (c) benzo[k]fluoranthene (BkF) and (d) indeno[1,2,3-cd]pyrene [IcdP] with distance to road and traffic counts; displayed median line (red dashed line) and Spearman ρ value and Mann-Whitney test, with significance level

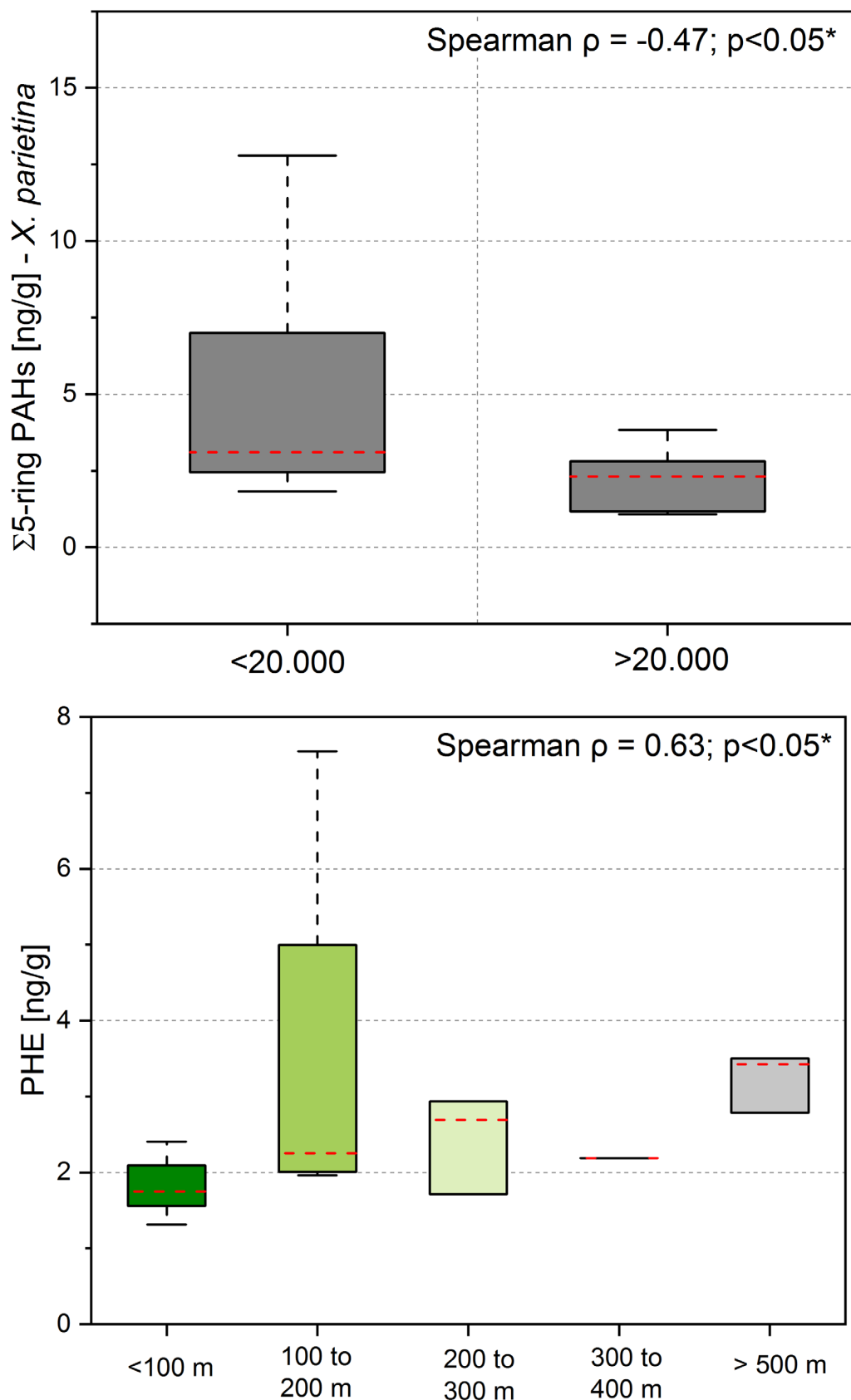


Figure 7-14: Box-Whisker plots (25th to 75th percentile) of $\Sigma 5$ -ring PAHs with traffic counts [upper panel] and phenanthrene concentrations with distance to green space [lower panel]; displayed with median line (red dashed line) and correlation statistics (Spearman ρ) and significance level

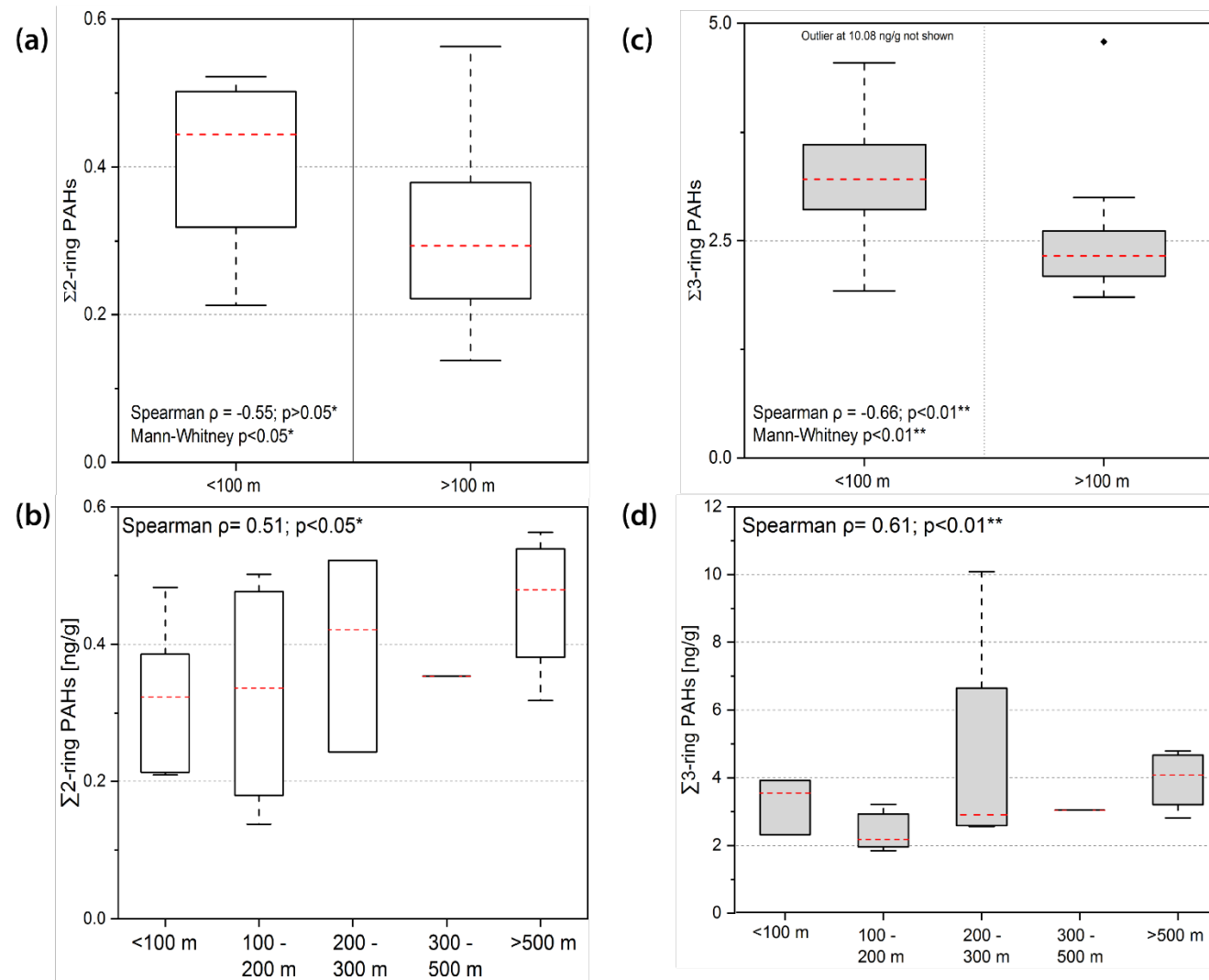


Figure 7-15: Box-Whisker plots (25th to 75th percentile) of $\Sigma 2$ -ring PAHs with (a) distance to road and (b) distance to greenspace and $\Sigma 3$ -ring PAHs with distance to road (c) and distance to greenspace (d); displayed with median line (red dashed line) and correlation and group statistics (with significance level; *significant at level $p < 0.05$; **significant at the level $p < 0.01$)

7.4 Interpretation and Discussion

7.4.1 Comparison of PAH concentrations recorded in *X. parietina* and *Phyiscia* spp.

Three sites were sampled for both lichen species, *X. parietina* and *Phyiscia* spp. and PAH concentrations recorded were compared for these sampling sites. Total PAHs were higher at two sampled sites for *Phyiscia* spp. (ID: 15 and ID: 19). High-molecular weighed PAHs that are associated to particles (e.g. indeno[1,2,3-cd]pyrene with PM_{2.5}; Wong et al., 2018) were found at higher concentrations for the two sites in *Phyiscia* spp., which could be related to entrapment of particulates by the lichen. The lichen's surface, structure and roughness allow the interception and retention of particles (Di Lella et al., 2003; Bergamaschi et al., 2007; Shukla et al., 2014). Species-specific differences for pollutant accumulation has been reported, i.e. *Usnea* species are more dependent on wet deposition, whereas *Parmelia* species accumulate more from dry deposition (Bosserman and Hagner, 1981; Bergamaschi et al., 2007). Differences between foliose lichens (i.e. *Flavoparmelia caperata* and *X. parietina*) have also been found (Nimis et al., 2001; Bergamaschi et al., 2007).

Low molecular weight PAHs (i.e. fluoranthene, phenanthrene and anthracene) were also found higher in *Phyiscia* spp., when compared to *X. parietina*. Blasco et al. (2011) reported different uptake abilities for *Parmelia sulcata*, *Ramalina farinacea*, *Evernia prunastri*, *Pseudevernia furfuracea*, *Usnea* spp. and *Lobaria pulmonaria*. However, they also reported higher accumulation of low-molecular weight PAHs (LMWs), i.e. 2-, 3- and 4-ring compounds, which is potentially related to their relative solubility in water and uptake by lichens via wet deposition, whereas high-molecular weight PAHs are associated with dry deposition (Blasco et al., 2011). The content of symbiotic algae is a key factor for gas-phase PAH accumulation in lichens (Kummerová et al., 2006; Augusto et al., 2015). Higher concentrations of LMW PAHs in *Phyiscia* spp. could be related to higher algae contents in the lichen. Moreover, higher concentrations of fluoranthene was found to affect photosynthesis in lichens (Kummerová et al., 2006, 2007). Fluoranthene was found more variable in *X. parietina* and less sites sampled for *Phyiscia* spp. could indicate toxic effects on *Phyiscia* spp.

Different uptake rates of PAHs might also be related to different molecular weights of compounds and resistances imposed by the thallus morphology (Collins and Farrar, 1978; Augusto et al., 2015). Both lichen species are foliose lichens ('leaf-like') and findings indicate specific capabilities of particle trapping. *X. parietina* consist of lobes, closely attached to the substrate, whereas *Physcia* spp. consist of small 'branches' that overhang from the substrate (see chapter 2 for lichen pictures).

Therefore, species-specific uptake abilities for PAHs are an important consideration, when analysing (urban) atmospheric pollution for PAHs. *X. parietina* and *Physcia* spp. used in this study did not show statistically significant differences in PAH concentrations. However, only three sites were sampled for both lichen species and compared. Hence, findings presented could be further investigated by extending the sampling for both lichen species. Environmental changes influence lichen morphology, physiology, chemistry and accumulation of pollutants (Nimis et al., 2002; Upreti et al., 2015). Findings suggest that, when using lichens to analyse atmospheric PAH concentrations, same species should be analysed to minimise potential species-specific uptake abilities. Specific PAHs might be more toxic to PAHs than others that needs to be further investigated.

7.4.2 Comparison of PAH concentrations recorded in Manchester with urban lichen-biomonitoring studies

Comparison of recorded concentrations in *X. parietina* and *Physcia* spp. showed lower concentrations of total PAHs in Manchester, compared to other urban lichen bio-monitoring studies (Table 7-16).

Table 7-16: Overview of PAH concentrations recorded in lichens in urban and traffic-related pollution studies to investigate differences between cities [shortened: excluding studies on landfill and mining sites; Augusto et al., 2016]

Lichen species	Topic and geographic area (and author)	Min/max concentrations [ng/g]
<i>Parmotrema hypoleucinum</i>	Urban, industrial, agricultural and forest – Sines (Portugal) Augusto et al., 2009	91-872 (overall)
<i>Remototrachyna awasthii</i>	Urban – Mahableshwar City (India) Bajpai et al., 2013	Max. 62340
<i>Parmelia sulcata</i>	Traffic – Somport tunnel (Spain and France) Blasco et al., 2006	910-1920
<i>Parmelia sulcata</i>	Traffic – Aragon Valley (Spain) Blasco et al., 2007	352-1652
<i>Evernia prunastri</i>	Traffic – Aragon Valley (Spain) Blasco et al., 2008	696-6240
<i>Parmelia sulcata, Lobaria pulmonaria, Evernia prunastri, Ramalina farinacea, Pseudevernia farinacea, Usnea sp.</i>	Traffic – Aspe and Aragon Valley (France and Spain) Blasco et al., 2011	238-6240 (overall)
<i>Xanthoria parietina</i>	Urban – Zaragoza City (Spain) Domeño et al., 2006	340
<i>Pyxine coralligera</i>	Urban – Caracas (Venezuela) Fernández et al., 2011	240-9080
<i>Pseudevernia furfuracea</i>	Traffic – Rieti, Latium (Italy) Guidotti et al., 2003	36-375
<i>Pseudevernia furfuracea</i>	Traffic – Viterbo, Latium (Italy) Guidotti et al., 2009	168-395
<i>Pseudevernia furfuracea</i>	Urban, industrial, agricultural and forest – Carnic pre-alps (Italy) Kodnik et al., 2015	48-1576
<i>Pseudevernia furfuracea</i>	Traffic – Dolomites, SE alps (Italy) Nascimbene et al., 2014	186-2130
<i>Xanthoparmelia mexicana</i>	Traffic – tunnels of Guanajuat City (Mexico) Puy-Alquiza et al., 2016	522-3571
<i>Rinodina sophodes</i>	Urban – Kanpur City (India) Satya et al., 2012	189-494
<i>Phaeophyscia hispidula</i>	Traffic – DehraDun City, Garhwal Himalayas (India) Shukla and Upreti, 2009	3380-25010
<i>Phaeophyscia hispidula, Phaeophyscia orbicularis, Heterodermia angustiloba, Dimelaena oreina</i>	Traffic, urban – Garhwal Himalayas, Uttaranchal (India) Shukla et al., 2010	683-33720
<i>Pyxine subcinerea</i>	Urban, industrial and forest – Haridwar (India) Shukla et al., 2012	1250-187300
<i>Dermatocarpon vellereum</i>	Urban – Rudraprayag, Central Garhwal Himalayas (India) Shukla et al., 2013	136-4961
<i>Pseudevernia furfuracea</i>	Urban – Naples (Italy) and London (UK) Vingiani et al., 2015	500 (85 in control samples)

The use of PAH rings are considered more indicative for pollutant sources, whereas concentrations provide information on the gradient of pollution (Augusto et al., 2009).

Within Manchester, 4-ring PAHs were predominantly contributing to the overall PAH profile in *X. parietina* and *Physcia* spp. (Table 7-17), which is comparable to findings presented by Augusto et al. (2010) for *X. parietina* in Sines (Portugal). In contrast, Blasco et al. (2006, 2008) reported predominance of 3-ring PAHs in *Evernia prunastri* and *Parmelia sulcata* along a national road in the Aragon Valley (Spain). Again, this could be related to species-specific uptake abilities of different lichens or varying sources in the different environments. However, Augusto et al. (2009) reported that PAH profiles recorded in lichens could be used to identify particular land-use types. For instance, 4-ring PAHs (i.e. fluoranthene, pyrene and chrysene) characterise the lichen profile in urban areas (i.e. emitted from vehicular emissions), whereas 5- and 6-ring PAHs (i.e. benzo[k]fluoranthene, benzo[g,h,i]perylene and indeno[1,2,3-cd]pyrene) characterise lichen PAH profiles from industrial areas (Guidotti et al., 2003; Augusto et al., 2009).

Table 7-17: PAH profile of *X. parietina* and *Physcia* spp. sampled across Manchester, for comparison with other urban studies

	<i>X. parietina</i>	<i>Physcia</i> spp.
2-ring	1% to 4%	3% to 4%
3-ring	6% to 23%	20% to 27%
4-ring	28% to 58%	47% to 51%
5-ring	11% to 31%	11% to 17%
6-ring	8% to 22%	8% to 13%

5- and 6-ring PAHs were found to contribute to a higher extent to the overall PAH profile in Manchester, when compared to other urban areas. For instance, Augusto et al. (2010) reported contributions of 5% (5-ring) and 2% (6-ring) to the total PAH profile in *X. parietina*. Higher concentrations of 5- and 6-ring PAHs recorded in Manchester could be related to vehicular fleets (i.e. cars, busses, taxis and trucks). Diesel vehicles have higher particulate emissions than gasoline-fuel cars (Ravindra, Sokhi, et al., 2008). Additionally, elevated concentrations of 5- and 6-ring PAHs recorded could be related to their lower volatility and particulates deposited (i.e. from diesel and gasoline cars) on the lichen surface (Khalili et al., 1995; Howsam et al., 2000, 2001; Shukla et al., 2013; Wong et al., 2018).

A study undertaken in London (UK) also reported increased accumulation of 4-, 5- and 6-ring PAHs in deployed *Pseudevernia furfuracea*, which is comparable with PAH profiles recorded in Manchester. Hence, findings suggest the contribution of particle-bound PAHs to the overall lichen profile within both urban environments.

Target PAH concentrations, i.e. by toxicity groups and traffic-related, are displayed in Figure 7-16. Recorded concentrations are much lower, when compared to other European urban studies. However, phenanthrene, fluoranthene and pyrene were highest in *X. parietina* and *Physcia* spp., which is comparable to other studies. Findings suggest vehicular emissions, in particular for fluoranthene and pyrene, as primary source of PAHs in Manchester. Furthermore, phenanthrene is derived from motorised traffic, especially diesel trucks (Blasco et al., 2006; Shukla and Upreti, 2009; Satya et al., 2012).

The most toxic PAH benzo[a]pyrene was found at lower concentrations in Manchester. Within the UK, benzo[a]pyrene is primarily emitted by domestic coal and wood burning and industrial processes (PHE CRCE, 2018). However, elevated benzo[a]pyrene in particulates was related to heavy traffic (trucks and lorries), suggesting a potential source (Mastral et al., 2003). Moreover, benzo[a]pyrene is primarily adsorbed to particles and less prone to long-range transport, suggesting local sources (e.g. industry and vehicular) in Manchester.

About 12.4 million diesel cars (40% of licensed cars) are registered within the UK (DfT, 2017b). Within Manchester, about 80% of NO_x emissions are associated to diesel vehicles (Regan, 2018). Charron et al. (2019) reported relationships between NO_x and fluoranthene and pyrene (but not for phenanthrene) in the urban area of Grenoble (France), further suggesting vehicular emissions in Manchester. Elevated NO₂ concentrations were recorded in Manchester (see chapter 3) and therefore suggesting potential emissions of PAHs primarily related to diesel vehicles.

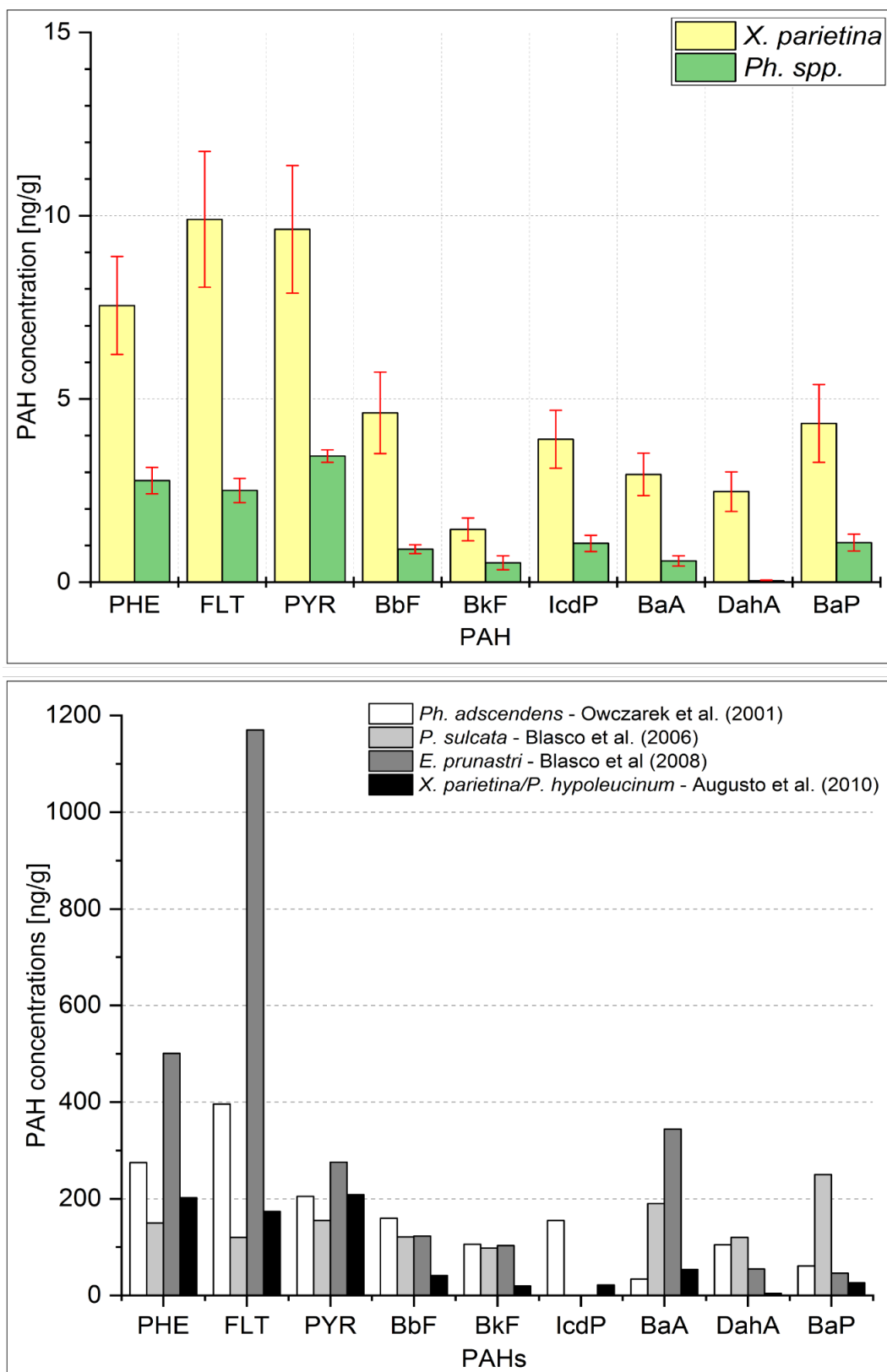


Figure 7-16: Maximum PAH concentrations recorded in *X. parietina* and *Physcia* spp. for 'target PAHs' (upper panel); displayed with 1x specific PAH-derived standard deviation in the lichen species (*X. p.*: 0.31 ng/g to 1.85 ng/g; *Ph. spp.*: 0.02 ng/g to 0.36 ng/g) and maximum PAH concentrations (same PAHs) from European (urban/traffic) biomonitoring studies (lower panel); PHE= phenanthrene, FLT= fluoranthene, PYR= pyrene, BbF= benzo[b]fluoranthene, BkF= benzo[k]fluoranthene, IcdP= indeno[1,2,3-cd]pyrene, BaA= benz[a]anthracene, DahA= dibenzo[a,h]anthracene, BaP= benzo[a]pyrene

Findings presented showed lower recorded PAHs in lichens in the City of Manchester, compared to other European studies. Therefore, air quality in Manchester is potentially less as affected by PAHs. However, it should be noted that some studies have been undertaken more than ten years ago and PAH concentrations might have decreased and cities might be less polluted today.

Lower PAH concentrations across Manchester suggest minor PAH emissions, which is in accordance with emission reduction reported by Meijer et al. (2008). However, transport was reported to be responsible for 65% of total PAH emissions within the UK (in 2005; Meijer et al., 2008). 4-ring PAHs were highest in *X. parietina* and *Phyiscia* spp., with fluoranthene, pyrene and phenanthrene (a 3-ring PAH) found at highest concentrations. Therefore, vehicular emissions are potentially the primary source of these PAHs across Manchester.

In contrast, 5- and 6-ring PAH were also found at higher concentrations in Manchester. A comparable study reported elevated 5- and 6-ring PAHs in lichens from London (UK), suggesting comparable PAH profiles across the UK. However, 5- and 6-ring PAHs are primarily particle-bound and suggest local sources (i.e. vehicular and industrial emissions) in Manchester. Therefore, it could be important to further analyse particulates across Manchester (i.e. PM₁₀ and/or PM_{2.5}) to investigate potential PAH sources. From a human health perspective, high molecular weight PAHs are more carcinogenic than low-molecular weight PAHs (Shukla et al., 2014) and their association with particulates could provide additional information on human health impacts.

However, spatial variability of PAH recorded in both lichen species was presented (section 7.4.2), with regard to urban influencing factors, i.e. distance to road and traffic counts, which is discussed hereafter.

7.4.3 Spatial variability of PAH concentrations in the urban environment of Manchester

Lichens were sampled over a period of five months (May to September 2018), indicating potential temporal variability, super-imposed on spatial variability. Atmospheric PAH concentrations have been reported to be influenced by wind, precipitation and photochemistry, with higher concentrations in winter months and lower during warmer months (Mastral et al., 2003; Augusto, Máguas, et al., 2013; Garrido et al., 2014).

Seasonal variation is an important factor, that needs to be taken into account for lichen PAH biomonitoring studies (Augusto et al., 2016). For instance, Kodnik et al. (2015) reported higher PAH concentrations in transplanted *Pseudevernia furfuracea* during winter months, compared to summer months in NE Italy. Augusto, Pereira, et al. (2013) highlighted the drawback of lichen derived PAH concentrations and their “translation” into atmospheric concentrations and used a combined approach, using *Parmotrema hypoleucinum* and particulate-phase samplers (active air sampling) in Portugal. They reported that lichen were able to reflect a retroactive period (between 45 and 60 days) and seasonal variation in lichen and active sampler follow a similar trend. Similar results were reported in studies, using *Ramalina fastigiata* and *Evernia prunastri* transplants and passive air samplers, containing polyurethane foam discs, and highlight the translation of lichen PAH values into atmospheric concentrations (Domínguez-Morueco et al., 2015; Loppi et al., 2015).

Moreover, meteorological variables (i.e. temperature, atmospheric pressure, relative humidity and wind speed) influence PAH concentrations, in both, lichens and air (Augusto, Pereira, et al., 2013; Garrido et al., 2014). Monitoring of atmospheric PAHs, i.e. by high-volume and passive monitoring devices reported similar seasonality (higher in winter and lower in summer) of PAH concentrations (Augusto, Pereira, et al., 2013; Garrido et al., 2014; Hsu et al., 2015; Pozo et al., 2015; Evci et al., 2016). Therefore, additional analysis of meteorological data and temporal variability of atmospheric concentrations, i.e. by passive sampling approaches is suggested.

Lichen sampling was undertaken during dry days (in summer months) to minimise variations due to rain wash-off (Forbes et al., 2015). Lichens absorb contaminants (and nutrients) more or less constantly throughout their lifecycle (Blasco et al., 2006). They are long-living organisms and thus integrate atmospheric pollutants over time, allowing to relate low levels of pollutants with long-term chronic effects on health (Augusto et al., 2007; Augusto, Pereira, et al., 2013).

Spatial variability of PAHs in lichens was presented in section 7.3.2. PAHs of the carcinogenetic group 1 (Figure 7-10a, b and c) and 2A (Figure 7-10a, b and c) were found highest at two sites (ID: 4 and ID: 14), with concentrations >3 ng/g of benzo[a]pyrene. Benzo[a]pyrene (BaP) is emitted by vehicles with and without catalytic converters and higher concentrations in *X. parietina* suggest vehicular emissions (Rogge et al., 1993; Blasco et al., 2006).

However, highest benzo[a]pyrene in Manchester was recorded at sites located within greenspaces, and in close proximity (<500 m) to railway lines. Malawska and Wiołkomirski (2001) reported elevated PAH concentrations in dandelion (*Taraxacum officinale*) and soils sampled along a railway junction in Poland. PAHs originating from rail transportation is related to diesel and diesel-electric locomotives, of which older engines produce large amounts of 'black smoke' and may be a significant source of PAHs (European Commission, 2001; Ravindra, Sokhi, et al., 2008). Both sites also showed elevated levels in phenanthrene (Figure 7-12a) and pyrene (Figure 7-12c), which were also reported to be related to diesel engines (Sawant et al., 2007).

The EU target value for ambient PAHs is 1 ng/m³, considering benzo[a]pyrene as the marker of carcinogenic risk and is estimated as annual average of total content in PM₁₀ (EU, 2004; Slezakova et al., 2010). Elevated levels of benzo[a]pyrene were also recorded at sites close to major roads across Manchester, suggesting benzo[a]pyrene bound to particulates (PM_{2.5} and PM₁₀) entrapped on the lichen surface (Slezakova et al., 2010; Augusto et al., 2016).

Therefore, elevated benzo[a]pyrene recorded in lichens at analysed sites suggest traffic (i.e. diesel-fueled vehicles) and railway emissions as sources of PAHs, posing a potential human health risk, as it is bound to breathable fractions of particulates (Slezakova et al., 2010).

Furthermore, these two sites showed elevated levels for high-molecular weight PAHs, including dibenzo[a,h]anthracene, benz[a]anthracene, benzo[b]- and benzo[k]fluoranthene and indeno[1,2,3-cd]pyrene (Figure 7-10 and Figure 7-11), further suggesting particulate-bound PAHs entrapped within the lichen surface. Indeno[1,2,3-cd]pyrene is emitted by diesel and gasoline engines and is associated with PM_{2.5} (Khalili et al., 1995; Wong et al., 2018). However, indeno[1,2,3-cd]pyrene was significantly ($p < 0.05$) negative correlated with traffic counts, with higher concentrations further away from major roads and less traffic (section 7.4.2; Figure 7-13d). This could be related to transport of particulates further away from mobile sources (i.e. highly-trafficked roads) and/or industrial emissions, which are a major contributor to of 5- and 6-ring PAHs (Augusto et al., 2009; Shukla et al., 2012, 2014).

Interestingly 5-ring PAHs were found to be significantly negative correlated with traffic counts (Figure 7-14), with higher loadings recorded in lichens, with less traffic. This could be related to site-specific surroundings, i.e. building heights (and

accompanied 'canyoning effects') and/or meteorological condition (during the sampling period) and dispersion of pollutants. Slezakova et al. (2010) reported higher concentrations of 5- and 6-ring PAHs in particulate matter (PM) at traffic influenced sites. For instance, Napier et al. (2008) reported PAH emissions from cars in the UK, being primarily related to oil losses, followed by exhaust emissions, tyre erosion and brake wear, with regard to traffic flow. Traffic flows, especially travelling speed in Manchester have been found at ranges from 0 to 20 miles per hour (mph) during AM and PM peaks, suggesting additional vehicle related (diesel and gasoline) emissions (Napier et al., 2008; Satya et al., 2012; Highway Forecasting and Analytical Services, 2015). Contribution of 5- and 6-ring PAHs in both lichen species sampled across Manchester, indicate largely particulate influences on lichen PAH profiles (Figure 7-16).

High-molecular PAHs (i.e. indeno[1,2,3-cd]pyrene, dibenzo[a,h]anthracene and benzo[a]pyrene) were highly significant ($p < 0.001$) correlated with each other (Spearman $\rho > 0.8$ for all three PAHs), suggesting similar sources. Possanzini et al. (2004) reported percentages of PAHs found in particulate phase, with 89% for benzo[a]pyrene and 100% for indeno[1,2,3-cd]pyrene, respectively. Thus, concentrations recorded in both lichen species are regarded to be associated to the particulate phase. Other group 2B PAHs were also found at higher concentrations along the major road network, i.e. benzo[k]fluoranthene and chrysene, which were also found to be related to traffic-related particulates (Slezakova et al., 2010). However, chrysene and benzo[k]fluoranthene were reported as markers for coal combustion (Khalili et al., 1995; Smith and Harrison, 1998; Ravindra et al., 2007; Ravindra, Sokhi, et al., 2008; Ravindra, Wauters, et al., 2008). The use of coal within the UK and Greater Manchester has significantly decreased since 1990 (Douglas et al., 2002; DEFRA, 2017e), suggesting minor importance of coal as contributor to ambient PAH concentrations.

In conclusion, high-molecular weight PAHs are considered to be toxic to human health and elevated levels found across Manchester are potentially related to distribution of particulates (PM_{10} and $PM_{2.5}$), due to vehicular emissions (Slezakova et al., 2010). Therefore, these PAHs pose a significant threat to human health and need to be further investigated, i.e. by passive sampling and analysis of particle-bound PAHs.

Concentrations of traffic PAHs were highest for phenanthrene, fluoranthene and pyrene (Figure 7-12) in both lichen species, which is comparable to other urban and traffic-related studies (Figure 7-16). Phenanthrene, pyrene and benzo[b]fluoranthene are associated to combustion processes (especially fossil fuels), with phenanthrene indicating motorized traffic, in particular diesel trucks (Kavouras et al., 2001; Blasco et al., 2006). Phenanthrene was found to be a major constituent in UK air measurements in 2005 and is also emitted by vehicles, i.e. lubricant oil and exhausts (Meijer et al., 2008; Napier et al., 2008). However, predominance of 4-ring PAHs suggest primarily traffic-related emissions as major sources of PAH in Manchester.

Phenanthrene ($p < 0.01$) and pyrene were significantly ($p < 0.05$) negative correlated with distance to major road and distance groups (<100m and >100m) were significantly different (Figure 7-13a and Table 7-15). Additionally, 2-ring PAHs (Spearman $\rho = -0.55$, $p < 0.05$) and 3-ring PAHs (Spearman $\rho = -0.66$, $p < 0.01$) were significantly correlated with distance to major road (Figure 7-15a and c). 2-ring-PAHs are associated with light vehicular traffic and lower concentrations with increasing distance to road suggest vehicular emissions, in proximity to major roads as primary PAH source (Guidotti et al., 2003; Blasco et al., 2006; Shukla and Upreti, 2009; Satya et al., 2012).

Highly significant correlation ($p < 0.001$) was found for fluorene (FLU), phenanthrene (PHE) and anthracene (ANT; correlation matrix of PAHs displayed in Appendix E-7) with Spearman ρ coefficients of 0.93 (FLU and PHE), 0.84 (FLU and ANT) and 0.90 (PHE and ANT). These PAHs, together with pyrene are present partially or totally in vapour phase in the atmosphere and therefore can be more easily accumulated by lichens (i.e. *X. parietina* and *Physcia* spp.; Guidotti et al., 2003).

Studies reported the uptake and deposition of PAHs by and on tree leaves and needles, suggesting interception of urban green with atmospheric PAHs (Howsam et al., 2000, 2001; De Nicola et al., 2017; Zha et al., 2017). Moreover, meteorological and climate conditions also play a crucial role in dispersion of low-molecular PAHs (Pankow et al., 1993; Zielinska et al., 2004; Hussain et al., 2018). 2- and 3-ring PAHs were correlated with distance to greenspace, suggesting interception of urban vegetation close to urban green, potentially by uptake of gaseous and deposited particulate-bound PAHs. PAHs consisting of 2- and 3-rings primarily exist in the gaseous phase and are more volatile compared to PAHs with

>5-rings (Howsam et al., 2001; Augusto et al., 2016). However, more volatile PAHs (present in the gaseous phase) can be transported and dispersed in more remote areas, whereas high-molecular PAHs are closely linked to the emission source (Thomas, 1986; Vingiani et al., 2015).

Potential positive influences of greenspace in Manchester were suggested, although distance measurements (i.e. within a GIS) might not fully represent the sampling site, i.e. dispersion and canyoning effects of surrounding buildings. However, 2- and 3-ring PAHs contributed to a lesser extent to the lichen PAH profile, suggesting beneficial interception by urban vegetation (i.e. for sampling sites within greenspaces). Furthermore, lower concentrations at particular sampling sites might be related to dispersion and meteorological and climatic conditions affecting PAHs, due to higher volatility of 2- and 3-ring PAHs.

Therefore, analysis of additional tree compartments, e.g. tree leaves and bark could improve the understanding of potential interception of urban green in Manchester. Moreover, lichen sampling during colder month, when no leaves are present, could further indicate 'seasonal' contribution of PAHs to the overall lichen profile.

Spatial variability of PAHs in Manchester appeared to be primarily related to vehicular and railway emissions, with regard to the specific sampling site. To further investigate PAH profiles and 'fingerprint' particular sources, analysed PAHs were compared using PAH ratios, presented hereafter.

7.4.4 Using PAH ratios to 'fingerprint' major sources of PAHs in the urban environment of Manchester

Atmospheric PAHs in urban areas originate from numerous sources, from both petrogenic (i.e. crude oil and gasoline, heating oil, asphalt and coal) and pyrogenic (i.e. combustion engines, fires and furnaces; EPRI, 2008). Pyrogenic PAHs are formed during 'pyrolysis', i.e. burning organic substances at high temperatures, with low or no oxygen present and sources include incomplete combustion of motor fuels and fuel oils for heating (Hussain et al., 2018). In contrast, PAHs that are generated at lower temperatures and are released by crude oil and crude oil products (and fuel spills), i.e. gasoline and motor oil are termed 'petrogenic' (Tolosa et al., 1996; WHO, 2003; Masih and Taneja, 2006; Seo et al., 2007; Hussain et al., 2018).

Differentiation between PAH sources (i.e. coal-, wood- or oil-based) can be performed by chemical fingerprinting, through studying the behaviour of different chemical indicators (Hussain et al., 2018). For instance, temperature impart information in identifying PAH sources, i.e. higher temperatures tend to generate PAHs with fewer alkylated chains compared to that under low temperatures (Abdel-Shafy and Mansour, 2016; Hussain et al., 2018). In general 'pyrogenic' PAHs consist of larger rings, compared to 'petrogenic' PAHs (Pampanin and Sydnnes, 2013; Hussain et al., 2018).

Dispersion of PAHs is controlled by thermodynamic properties and kinetic characteristics, during low-temperature and high-temperature processes, respectively (Alberty and Reif, 1988; Hussain et al., 2018). Phenanthrene, for example, is thermochemically more stable than anthracene, with higher molar fraction of phenanthrene compared to anthracene at lower temperatures. In contrast, combustion of organic matter at high temperatures is characterised by low phenanthrene/anthracene ratio (Baumard et al., 1998; Hussain et al., 2018). The use of diagnostic ratios between PAHs to assess the origin of PAHs, was proposed by Yunker et al. (2002). PAH ratios are based on measurements from suspended particulates and river sediments, however, several studies have applied the indicator ratios in lichen-biomonitoring studies (Blasco et al., 2006, 2008; Shukla and Upreti, 2009; Fernández et al., 2011; Shukla et al., 2012; Augusto et al., 2016). Therefore, using specific ratios between PAHs can be used to distinguish between sources. For instance, phenanthrene/anthracene to distinguish petroleum from combustion, fluoranthene/fluoranthene + pyrene to distinguish petroleum combustion from other types (e.g. grass, wood and coal and diesel). Nonetheless, environmental samples contain PAHs from multiple sources, which needs to be taken into account, when analysing diagnostic ratios for PAHs. Diagnostic ratios that incorporate PAH of main interest were considered for ratio-analysis of lichen-derived PAHs in Manchester (Table 7-18). Additionally, combustion PAHs (PAH_{comb}) against total PAHs (PAH_{total}) was used as an indicator for combustion sources that can be used together with other ratios to confirm the origin (Hwang et al., 2003; Augusto et al., 2016). PAHs considered as PAH_{comb} were summarised as $\sum PAH_{comb}$ including fluoranthene, pyrene, benzo[a]anthracene, chrysene, benzo[b]fluoranthene, benzo[k]fluoranthene, benzo[a]pyrene, indeno[1,2,3-cd]pyrene and benzo[ghi]perylene (Prahl and Carpenter, 1983; Hwang et al., 2003). Table 7-19 displays the analysed PAH ratios and their primary origin.

Table 7-18: PAH ratios applied in lichen biomonitoring studies to address major pollution sources (ANT= anthracene; PHE= phenanthrene; FLT= fluoranthene; PYR= pyrene; BaA= benzo[a]anthracene and CHRY= chrysene)

PAH ratios	Source
PHE/ANT	<10 – vehicular emissions >10 – petrogenic sources (Petroleum)
ANT/(ANT+PHE)	<0.10 – Petroleum >0.10 – Combustion
FLT/(FLT+PYR)	>0.5 – grass, wood, coal combustion 0.4-0.5 fuel combustion (gasoline, diesel, crude oil) <0.4 – Petroleum
FLT/PYR	<1.0 – vehicular emissions >1 – combustion
BaA/(BaA/CHRY)	<0.2 - petrogenic >0.35 – fuel combustion
PAH _{comb} /PAH _{total}	≥0.7 - combustion

References: Augusto et al., 2016; Blasco et al., 2011, 2008, 2006; Fernández et al., 2011; Satya et al., 2012; Shukla et al., 2012; Shukla and Upreti, 2009; Yunker et al., 2002; Hwang et al., 2003

Table 7-19: Site-IDs displayed with analysed diagnostic PAH ratios to evaluate PAH sources/origin; N/A – not calculated due to no data for anthracene (ANT) at both sites

ID	ANT/(ANT+PHE)	BaA/(BaA+CHRY)	FLT/PYR	PHE/ANT	FLT/(FLT+PYR)	PAH _{comb} /PAH _{total}
1	petroleum	petrogenic	vehicular emissions	vehicular emissions	fuel combustion	combustion
2	N/A	petrogenic	vehicular emissions	N/A	fuel combustion	combustion
3	petroleum	petrogenic	vehicular emissions	vehicular emissions	fuel combustion	combustion
4	combustion	pyrogenic	combustion	vehicular emissions	grass, wood and coal combustion	combustion
5	N/A	petrogenic	vehicular emissions	N/A	fuel combustion	combustion
6	petroleum	petrogenic	vehicular emissions	vehicular emissions	fuel combustion	combustion
7	petroleum	petrogenic	vehicular emissions	petrogenic	fuel combustion	combustion
8	petroleum	petrogenic	vehicular emissions	vehicular emissions	fuel combustion	combustion
9	petroleum	petrogenic	vehicular emissions	petrogenic	fuel combustion	combustion
10	combustion	petrogenic	vehicular emissions	vehicular emissions	petroleum	combustion
11	combustion	pyrogenic	vehicular emissions	vehicular emissions	fuel combustion	combustion
12	combustion	petrogenic	vehicular emissions	vehicular emissions	fuel combustion	combustion
13	combustion	petrogenic	vehicular emissions	vehicular emissions	fuel combustion	combustion
14	combustion	pyrogenic	vehicular emissions	vehicular emissions	fuel combustion	combustion
15	petroleum	petrogenic	vehicular emissions	petrogenic	fuel combustion	combustion
16	combustion	pyrogenic	vehicular emissions	vehicular emissions	fuel combustion	combustion
17	petroleum	petrogenic	vehicular emissions	vehicular emissions	fuel combustion	combustion
18	combustion	petrogenic	vehicular emissions	vehicular emissions	petroleum	combustion
19	combustion	petrogenic	vehicular emissions	vehicular emissions	fuel combustion	combustion
20	combustion	petrogenic	vehicular emissions	vehicular emissions	fuel combustion	combustion

ANT = Anthracene, PHE = Phenanthrene, FLT = Fluoranthene, PYR = Pyrene, BaA = Benzo[a]anthracene, CHRY = Chrysene, PAH_{comb} = Σ combustion PAHs and PAH_{total} = all Σ 16 PAHs

Diagnostic ratios of ANT/(ANT+PHE) were almost evenly distributed with 44% of sites showing ratios <0.10 and 56% of sites showing ratios >0.10 , illustrating 'petrogenic' and 'pyrogenic' PAH sources across Manchester (Table 7-19; Figure 7-17). In contrast, other urban studies reported a clearer distinction between sources using ANT/(ANT+PHE) ratios (Blasco et al., 2006; Shukla and Upreti, 2009; Satya et al., 2012). Findings for this study suggest that this ratio might not be a good indicator to 'fingerprint' specific sources in Manchester, due to site-specific compound influences. However, when using PHE/ANT ratios (N=18, *X. parietina*) primarily showed vehicular emissions as main PAH source at most sites (83%), whereas only three sites indicated 'petrogenic' sources (Figure 7-18). Ratios <10 (PHE/ANT) suggest traffic as primary source, due to phenanthrene being emitted from diesel trucks (Shukla and Upreti, 2009). Higher phenanthrene concentrations compared to anthracene could also be related to higher thermodynamic stability of phenanthrene (Zhou et al., 2005; Shukla and Upreti, 2009).

Ratios of BaA/(BaA+CHRY) <0.2 showed petrogenic sources for 85% of analysed sites. Pyrogenic sites were found at four sites across Manchester (Figure 7-19). Interestingly, these four sites also showed 'pyrogenic/combustion' sources for ANT/(ANT+PHE) ratios. In contrast, Blasco et al. (2006) reported a clear distinction using BaA/(BaA+CHRY) ratios in highly trafficked areas. Comparable to ANT/(ANT+PHE) results for BaA/(BaA+CHRY) might not be a useful ratio to investigate particular sources in Manchester, but rather suggest a mixture of PAH sources.

A ratio of about 0.6 for FLT/PYR was reported a clear indicator of vehicle emissions (Neilson, 1998; Blasco et al., 2006). All sites, except one (ID: 4) showed ratios <1 for FLT/PYR (Figure 7-20), suggesting vehicular emissions as primary source. However, FLT/PYR ratios ranged between 0.39 to 1.02, again indicating a mixture of compounds at analysed sites. In contrast, ratios of FLT/(FLT+PYR) between 0.4-0.5 illustrate fuel combustion (gasoline, diesel and crude oil) as source of PAHs, which was found for the majority of sites (85%). Two sites showed petroleum (<0.4 ; ID: 10 and 18) and one site grass, wood and coal combustion (FLT/FLT+PYR >0.5 ; ID: 4) as PAH origin (Figure 7-21). Interestingly, all analysed samples in *X. parietina* showed PAH_{comb}/PAH_{total} ratios >0.7 , thus suggesting combustion processes as major PAH source (Figure not shown).

Findings presented suggest a complex mixture of PAHs in the urban environment of Manchester that to a certain extent could be explained by using PAH ratios. The use of ratios, to 'fingerprint' pollution sources is a more recent method and is still insufficient to generalise conclusions (Augusto et al., 2016). Moreover, PAHs react differently in the atmosphere (e.g. benzo[a]pyrene] and anthracene), resulting in atmospheric PAH ratios deviating from those in source emissions (Schauer et al., 1996; Fraser et al., 1998; Yunker et al., 2002)

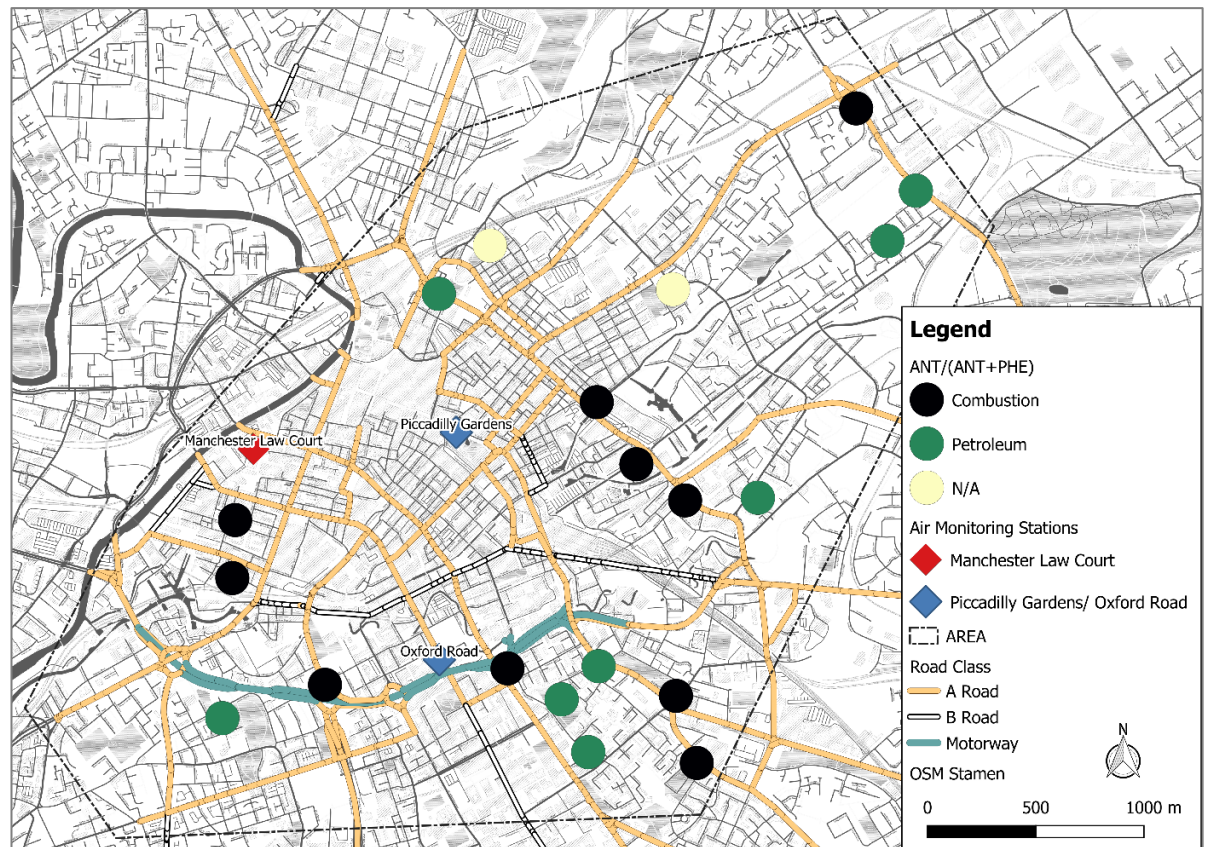


Figure 7-17: Ratios of ANT/(ANT+PHE) at analysed sites (recorded in *X. parietina*); displayed with monitoring stations and PAH measurement station (in use until 2014), N/A – ANT has not been found in samples

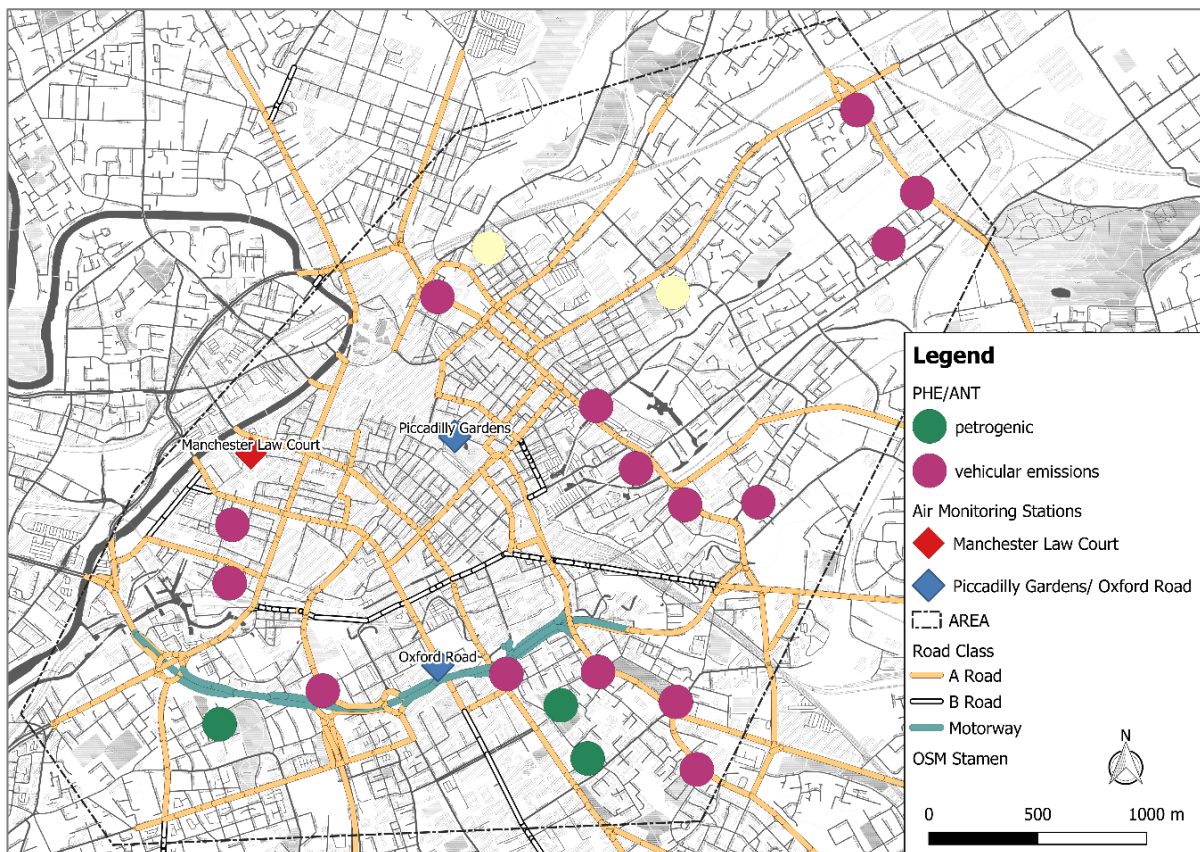


Figure 7-18: Ratios of PHE/ANT at analysed sites (recorded in *X. parietina*); displayed with monitoring stations (blue diamond) and PAH measurement station (in use until 2014)

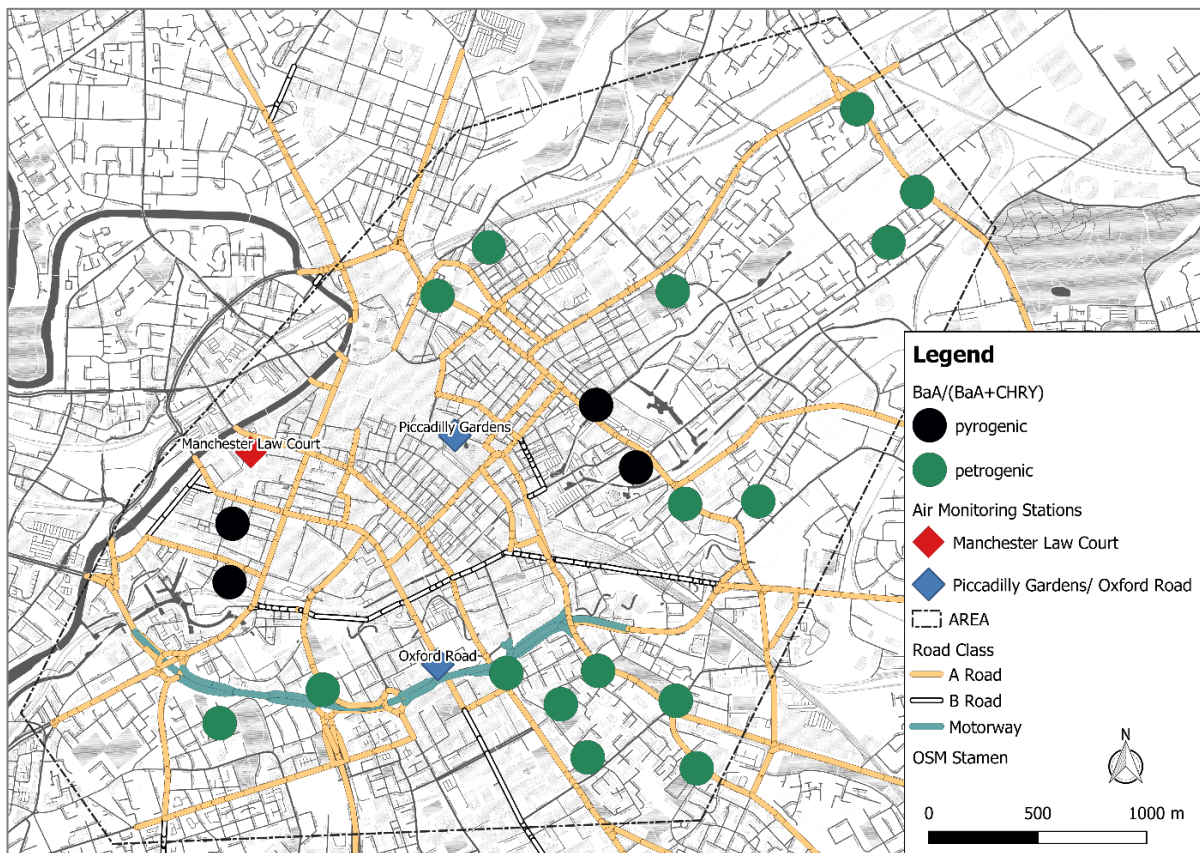


Figure 7-19: Ratios of BaA/(BaA+CHRY) at analysed sites (recorded in *X. parietina*); displayed with monitoring stations and PAH measurement station (in use until 2014)

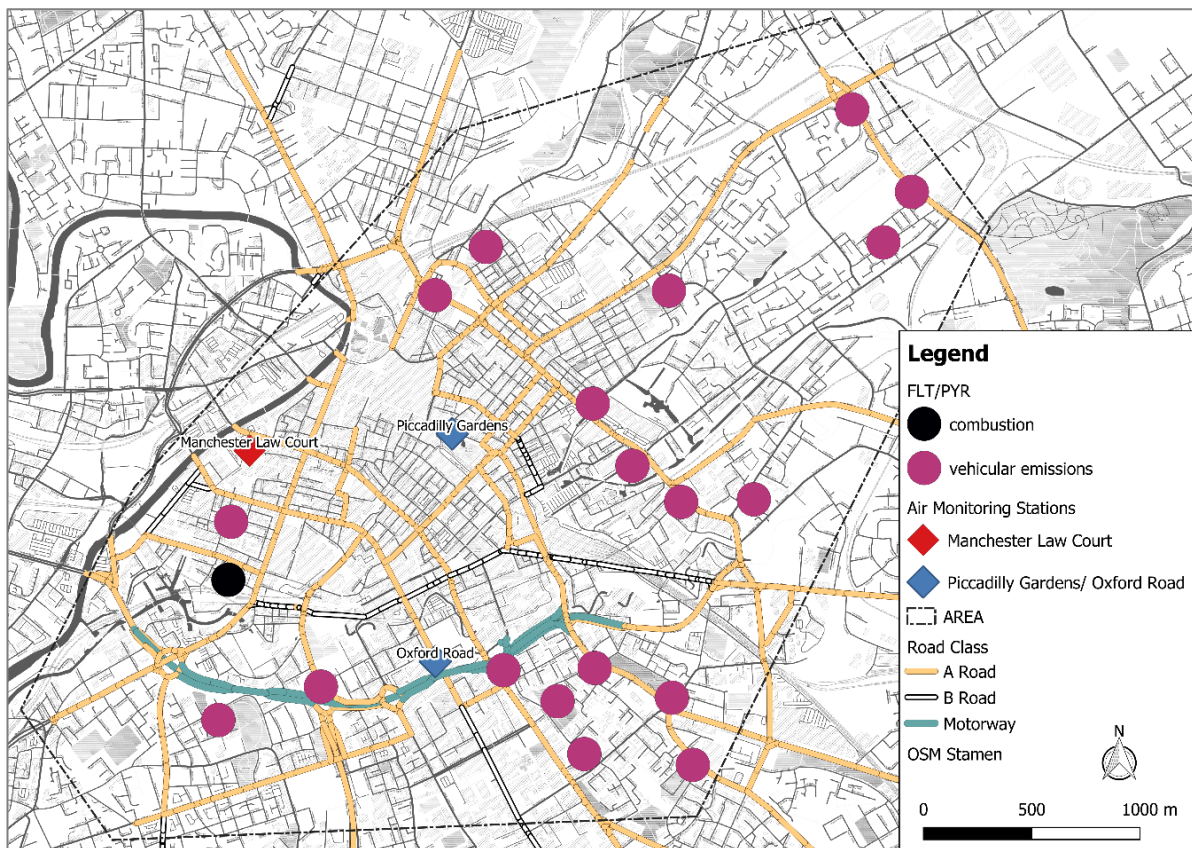


Figure 7-20: Ratios of FLT/PYR at analysed sites (recorded in *X. parietina*); displayed with monitoring stations (blue diamond) and PAH measurement station (in use until 2014)

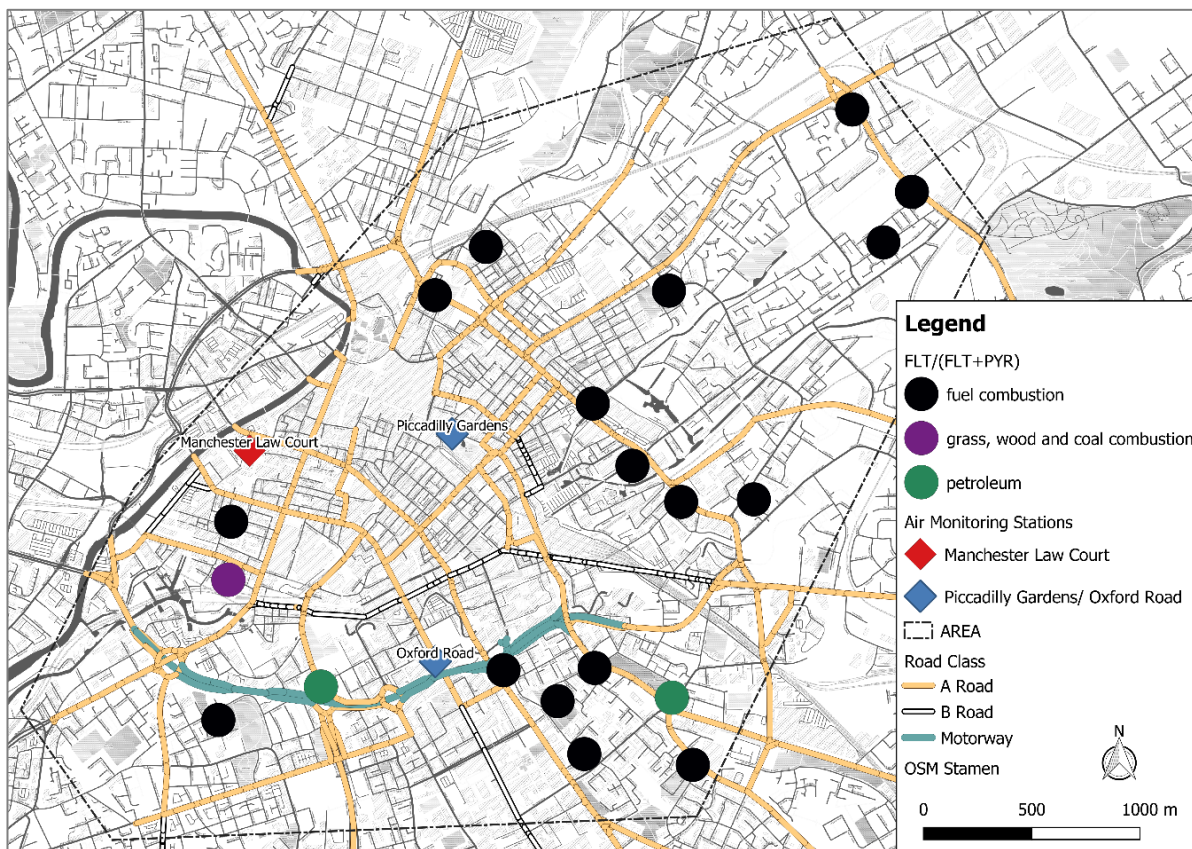


Figure 7-21: Ratios of FLT/(FLT+PYR) at analysed sites (recorded in *X. parietina*); displayed with monitoring stations (blue diamond) and PAH measurement station (in use until 2014)

Using a single ratio to conclude sources could lead to misleading results and the use of cross-plots of ratios could provide safer interpretation (Yunker et al., 2002). PAH sources, derived in this study were 'cross-plotted' to further investigate potential sources.

Figure 7-22 displays the ratios of $ANT/(ANT+PHE)$ plotted against $BaA/(BaA+CHRY)$. Both ratios showed differences in potential sources across Manchester, i.e. combustion or petrogenic. Results show three patterns for combustion, mixture and petrogenic PAHs. Increased PAHs of petrogenic origin could be related to higher asphalt abrasion and additional dripping of fuels and lubricant oils from cars (EPRI, 2008). Interestingly, two sites (ID: 4 and ID: 14), both located in a green surrounding, showed 'combustion' as major source of PAHs. Both sites are located in proximity (<500 m) to major railway lines in Manchester. Potential emissions of PAHs from railway could be related to diesel and diesel-electric locomotives, influencing PAH ratios (for $BaA/BaA+CHRY$) at these particular site (European Commission, 2001).

In contrast, three sites (ID: 7, ID: 9 and ID: 15) showed 'petrogenic' origin of PAHs. All sites are located in a greenspace/residential surrounding. Petroleum-derived PAHs could explain 'local sources', as tyre particles, asphalt and lubricant oils are associated with local sources of PAHs (European Commission, 2001; Blasco et al., 2011). For all other analysed sites, a mixture of 'petrogenic' and 'combustion' sources aggravates source apportionment in lichen samples across Manchester, using these ratios.

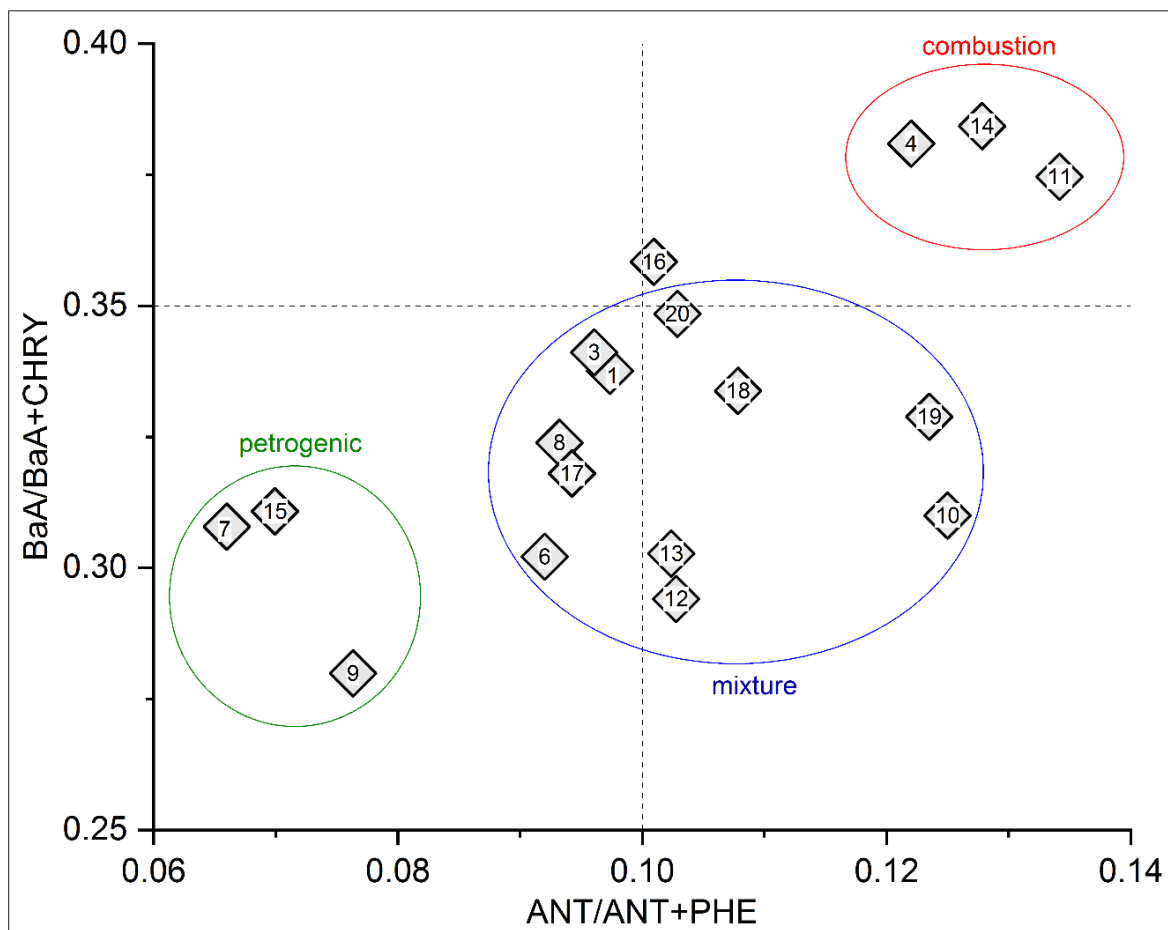


Figure 7-22: Scatter-plot of ANT/ANT+PHE and BaA/BaA+CHRY ratios recorded at sampling sites (*X. parietina*); displayed with cluster of primary sources, i.e. petrogenic, petrogenic/combustion (mixture) and fuel combustion; dotted lines represent ratio thresholds

Ratios of FLT/PYR (>1) and PHE/ANT (<10) can be used to identify combustion sources, whereas ratios <1 (FLT/PYR) and >10 (PHE/ANT) indicate petroleum sources (Baumard et al., 1998; Satya et al., 2012). In this study, ratios of FLT/PYR <1 and PHE/ANT <10 suggest different sources of PAH (Augusto et al., 2016). Again three sites (ID: 7, 9 and 15) suggest petrogenic sources, which is comparable to other ratios presented. However, a clear differentiation cannot be stated for these ratios and a rather complex mixture of PAH compounds is suggested (Table 7-19; Figure 7-23). Furthermore, Blasco et al. (2011) reported PHE/ANT >10 and FLT/PYR >1 for sites close to major roads, suggesting a mixture of PAH compounds. They also reported that PHE/ANT is dependent on the lichen species, indicating use of the same species when evaluating potential sources. Findings once again could not specifically identify sources of PAHs using FLT/PYR and PHE/ANT, but suggest a complex mixture of PAH sources across Manchester.

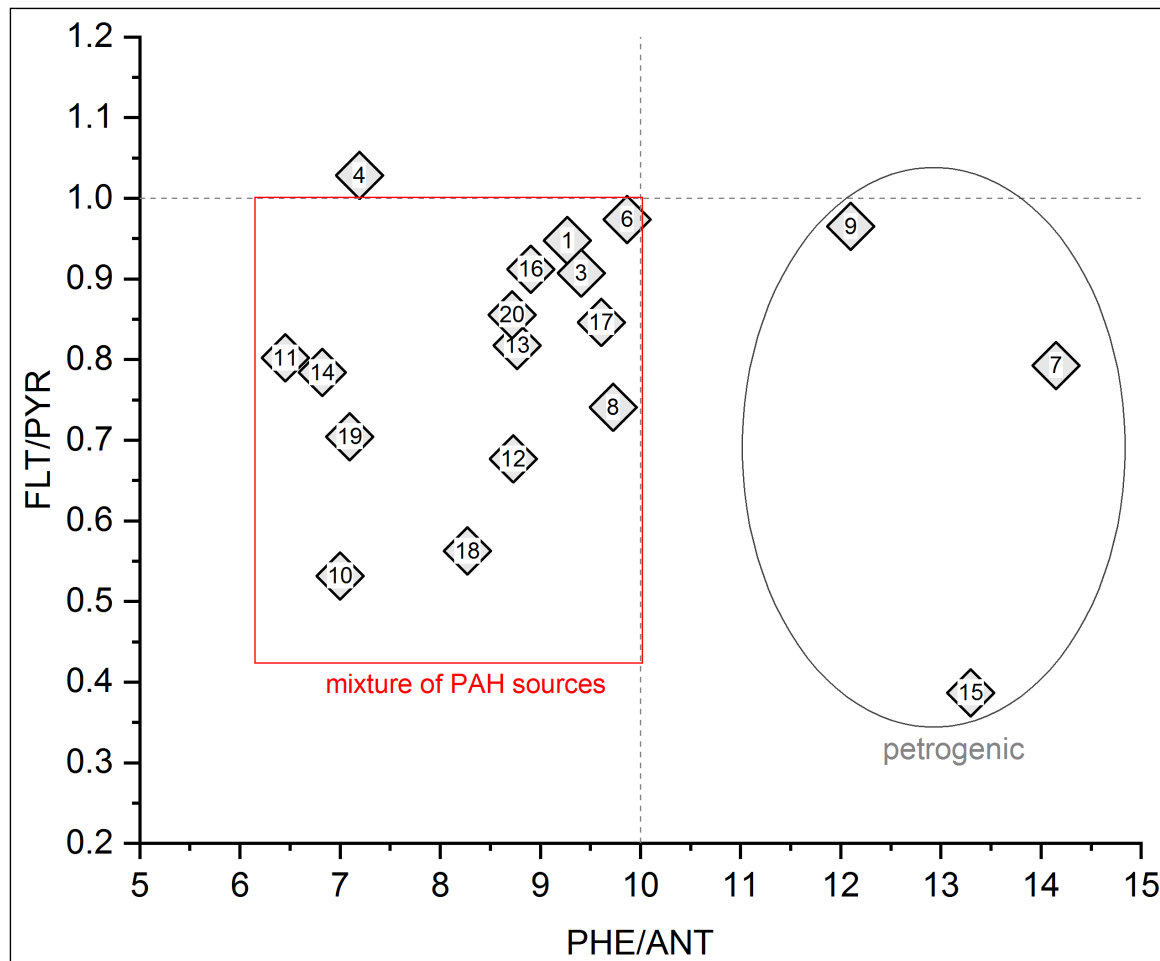


Figure 7-23: Scatter-plot of PHE+ANT and FLT+PYR ratios recorded at sampling sites (*X. parietina*); displayed with cluster of primary sources, i.e. vehicular emissions; lines represent ratio thresholds

Using $FLT/(FLT+PYR)$ could provide a finer classification of potential PAH sources, as a ratio between 0.4 and 0.5 suggests gasoline and diesel combustion by cars and trucks (Blasco et al., 2006; Shukla and Upreti, 2009; Satya et al., 2012; Shukla et al., 2012; Augusto et al., 2016). Here, a finer differentiation is possible, as the majority of sites (12 out of 20) suggest vehicular emissions as primary PAH source. Once more, three sites (ID: 7, 9 and 15) suggest additional sources (i.e. petrogenic; $PHE/ANT > 10$) of PAHs. A similar statement can be made for sites ID: 10 and ID: 18, which suggest vehicular emissions ($PHE/ANT < 10$) and in contrast petrogenic sources ($FLT/(FLT+PYR) < 0.4$). Both sites are located in close distance to highly trafficked roads, with about 17.000 and 58.000 vehicles daily (DfT, 2017a), suggesting contribution of petrogenic sources (for $FLT/FLT+PYR$), i.e. from tyre and asphalt particles in *X. parietina*. Moreover, ID: 4 suggested the influence of 'grass, wood and coal combustion' as major PAH source. Therefore, different sources seemed to influence lichen PAH loadings and thus analysed PAH ratios at particular sites, complicating source apportionment.

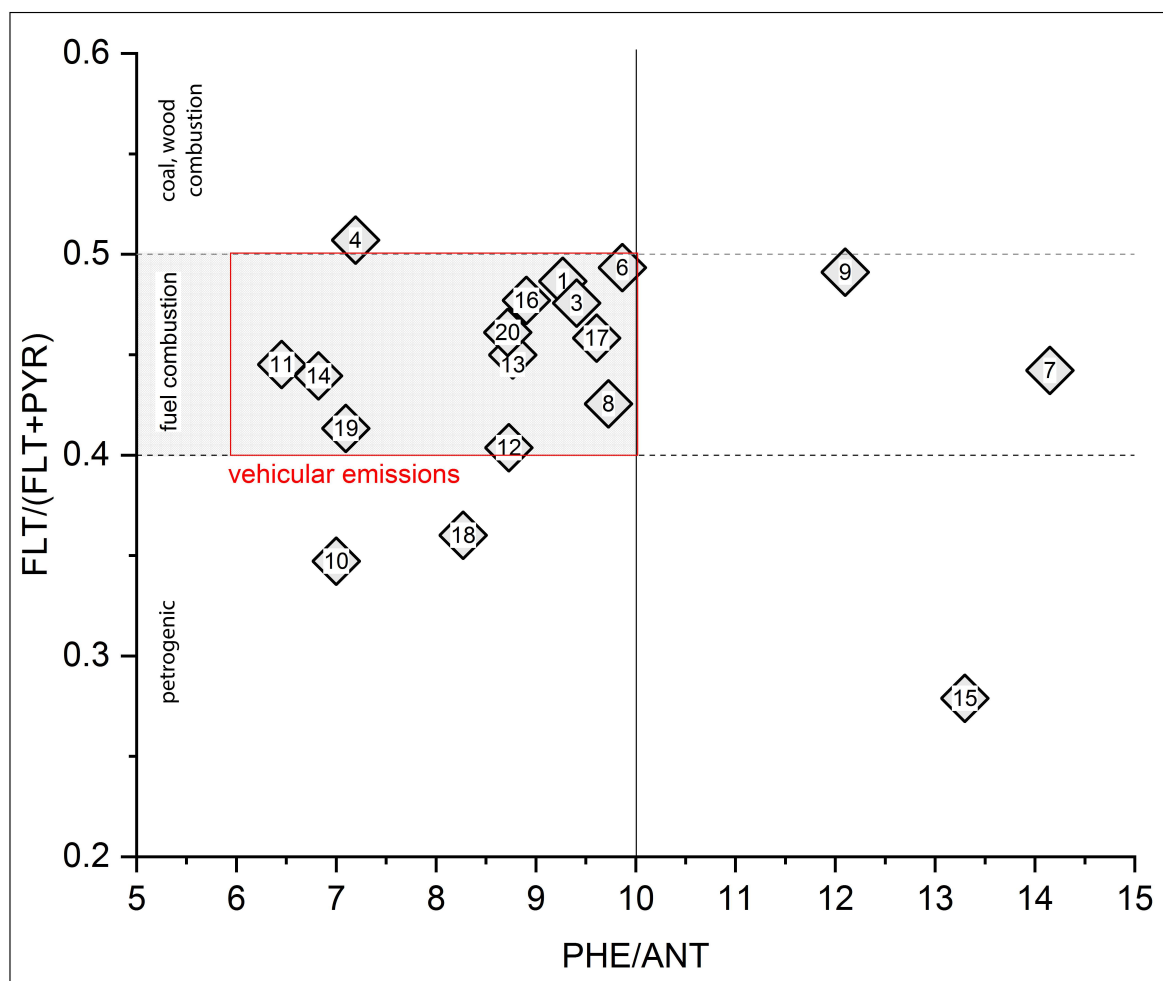


Figure 7-24: Scatter-plot of PHE+ANT and FLT/FLT+PYR ratios recorded at sampling sites (*X. parietina*); displayed with cluster of primary sources, i.e. vehicular emissions; lines represent ratio thresholds

In contrast, combustion PAHs (PAH_{comb}) including ≥ 4 -rings PAHs (i.e. fluoranthene, pyrene, benz[a]anthracene, chrysene, benzo[b]- and benzo[k]fluoranthene, benzo[a]pyrene, indeno[1,2,3-cd]pyrene and benzo[g,h,i]perylene) contributed to more than 70% of the total PAH concentrations at analysed sites (Figure 7-25). Combustion is the typical source for high-molecular weight PAHs, while an enrichment in low-molecular PAHs is more common for fresh fuels, i.e. petrogenic origin (Masclat et al., 1987; Budzinski et al., 1997; Hwang et al., 2003). Total combustion PAHs (PAH_{comb}) with total PAHs (PAH_{total}) is considered as an additional indicator of combustion sources, together with other ratios (Hwang et al., 2003; Augusto et al., 2016). All sites showed PAH_{comb}/PAH_{total} ratios > 0.7 , suggesting combustion sources as primary PAH source, which is in accordance with findings by Hwang et al. (2003) for ratios > 0.7 in city centres (in Korea, Mexico and the US) using pine needles as biomonitors.

However, results presented showed increased 4-, 5- and 6-ring PAHs across Manchester, with a higher contribution of 5- and 6-ring PAHs to the overall profile, which is comparable to findings presented in London (UK; Vingiani et al. 2015). Moreover, the lower stability of low-molecular weight PAHs could be related to lower concentrations recorded. Therefore, combustion PAHs might not be sufficient to provide information on source apportionment for the city of Manchester and could be used to compare with other urban areas and/or rural sites.

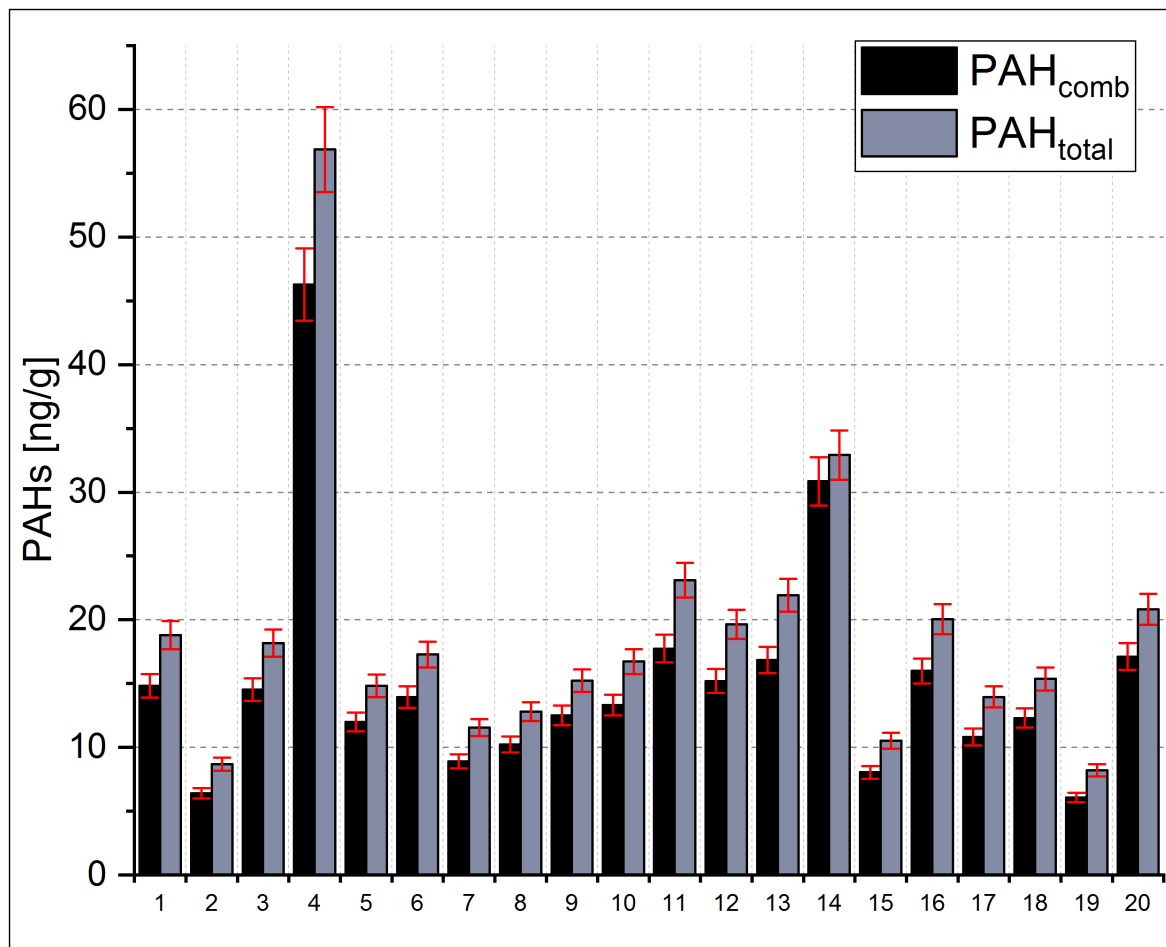


Figure 7-25: Total PAHs (PAH_{total}) and combustion PAHs (PAH_{comb}) at each sampling site (error bars presented as 10 µg/µl standard CV% of total PAHs and combustion PAHs [4,5 and 6-ring] with 5.86% PAH_{total} and 6.12% PAH_{comb})

To further investigate potential influences of vehicular emissions, ratios were compared to distance to road and traffic counts and are displayed in Figure 7-26. Due to small sample size (N=20) and to assess fine spatial detail, major road distances were only grouped into 1: <100 m and 2: >100 m and traffic counts were grouped into <20,000 Vehicles and >20,000 vehicles (based on daily average traffic, DfT, 2017; Table 7-10). For analysed ratios, no clear differentiation, with regard to road distance and traffic was found.

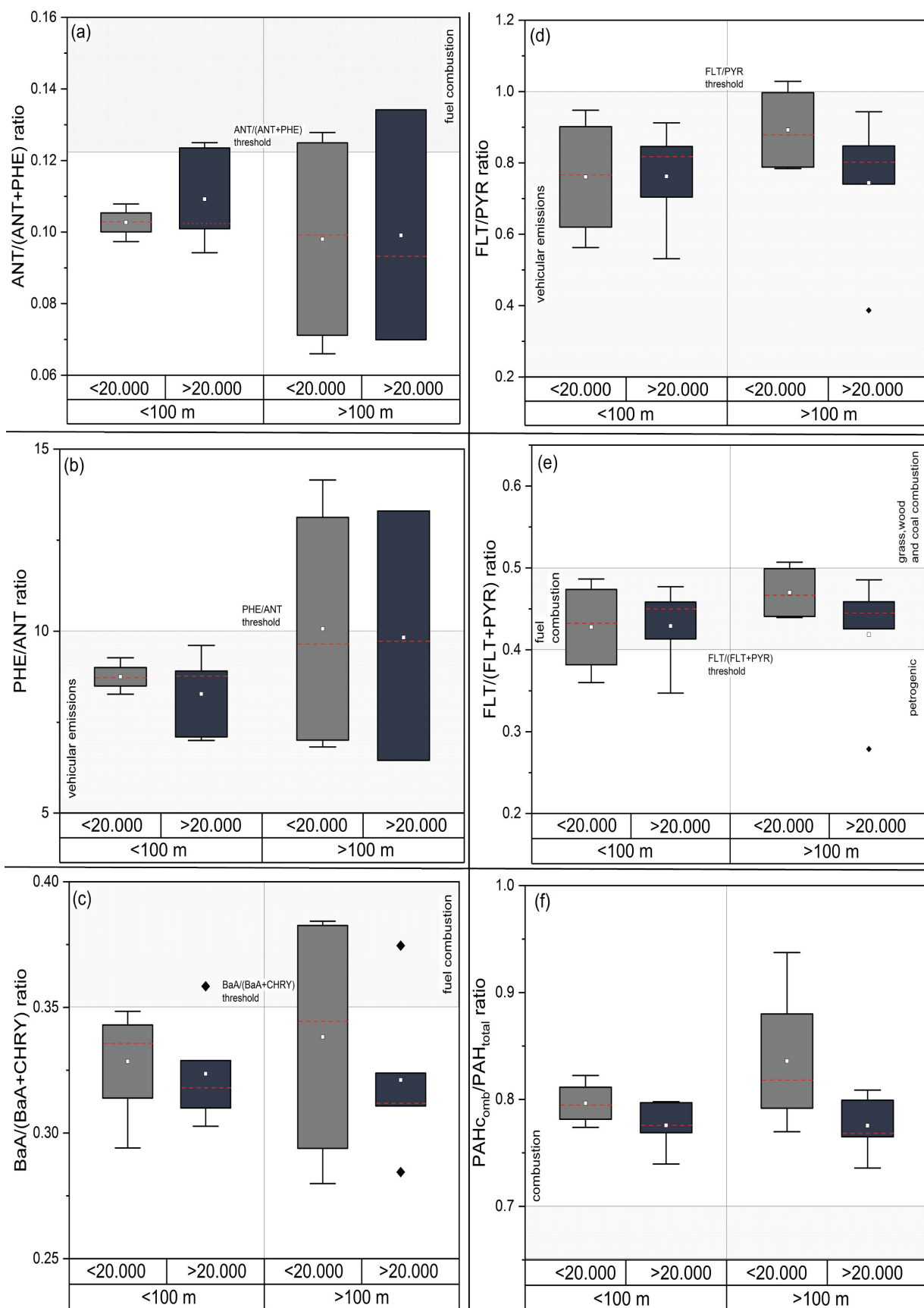


Figure 7-26: PAH ratios and distances to major road of (a) ANT/ANT+PHE, (b) PHE/ANT (c) BaA/BaA+CHRY, (d) FLT/PYR and (e) FLT/PFLT+PYR and (f) PAH_{comb}/PAH_{total}; displayed with thresholds and potential PAH origins

Marr et al. (2006) reported diurnal traffic patterns of gasoline and diesel vehicles on PAH emissions. Within the UK, 37.7 million vehicles are licensed, of which 83% were cars, 10% light-good vehicles (LGVs) and 1% heavy-goods vehicles (HGVs) (DfT, 2017b). 59% of cars are petrol cars, whereas 40% are diesel-powered cars (DfT, 2017b). Therefore, potential variability of vehicular fleets (i.e. diesel and gasoline cars, LGVs and HGVs) could influence the particular lichen PAH profile. Traffic count data is primarily available for major roads (counted or estimated; DfT, 2017a) and site-specific traffic data was not available.

Moreover, it should be stated, that these ratios should be taken with care, due to a data obtained from 20 sampling sites (for *X. parietina*) only. However, these ratios are a useful tool to evaluate potential origins of PAHs and help to interpret PAH results in lichens. However, photochemical reactions and chemical transformations after emissions (from any sources) can alter the pollutant composition of what was really emitted and different accumulation abilities by different lichen species are considered as main issues, when using PAH ratios (Augusto et al., 2016). Additional ratios (i.e. BaP/BaP+CHRY and Bbk/BbF among others) have been suggested that could be applied to (re-)define fingerprinting of PAH sources (Pandey et al., 1999; Park et al., 2002; Ravindra, Sokhi, et al., 2008).

In conclusion, analysed PAH ratios suggest different sources and a mixture of compounds within the city of Manchester. Site-specific differences were found, i.e. for three sites primarily suggesting 'petrogenic' sources. Spatial variability of PAHs and PAH ratios showed that PAHs occur in complex mixtures rather than individual compounds (PHE CRCE, 2018), potentially explaining particular site differences in PAH profiles. However, PAH ratios need to be further investigated. For instance, extending the sampling towards more rural areas could aid further 'fingerprint' sources of PAHs. Moreover, plant leaves have been reported to be a main sink of airborne PAHs and might intercept PAH accumulation in lichens within green spaces (Satya et al., 2012). This suggests that additional environmental compartments (i.e. tree leaves and needles) could be used to investigate PAH profiles across Manchester and identify potential interferences. Therefore, PAH ratios applied in this study need further investigation, to specifically identify PAH sources in the city of Manchester.

7.4.5 The carcinogenic potential of PAHs recorded across Manchester

Analysed PAH concentrations recorded in *X. parietina*, sampled across the City of Manchester could provide information on human exposure assessment. The methodology to evaluate the toxicity and assess the risks of a mixture of structurally related chemicals with a common mechanism of action, was developed by the U.S. Environmental Protection Agency (EPA; U.S. EPA, 1993). It is an estimate of the relative toxicity of a chemical compared to a reference chemical (U.S. EPA, 1993). The carcinogenic risk of PAH mixtures is expressed as equivalent concentrations of benzo[a]pyrene ($BaP_{eq.}$), based on individual PAH carcinogenic potency relative to that of benzo[a]pyrene (Augusto, Pereira, et al., 2013). So-called Toxic Equivalence Factors (TEFs) have been developed and are used to assess PAH mixture toxicity (Nisbet and LaGoy, 1992; U.S. EPA, 1993; Augusto, Pereira, et al., 2013). TEFs are calculated according (Eq. 1) and TEFs developed by Nisbet and LaGoy (1992) are most commonly (Table 7-20) used to assess PAH mixture carcinogenicity and can be used to evaluate human health risk associated with exposure to PAHs (Tsai et al., 2001; Fang et al., 2002; Augusto, Pereira, et al., 2013).

$$(Eq. 1) \quad BaP_{eq.} = \sum_{i=1}^{16} (C_i \times TEF_i)$$

With C_i being the concentration of the PAH and TEF_i is the TEF for the specific PAH. For each sampling site (of *X. parietina*; $N=20$) the total carcinogenic potency was calculated for each of the 16 EPA PAHs. Total carcinogenic potency (sum of $BaP_{eq.}$ for 16 EPA PAHs) was calculated using median PAH concentrations (Sarigiannis et al., 2015), as lichen PAH concentrations followed a asymmetric distribution. Figure 7-27 displays the TEFs of PAHs contributing to the toxicity profile of the 16 EPA PAHs recorded in *X. parietina*.

Table 7-20: Toxic Equivalent Factors for 16 EPA PAHs (Nisbet and LaGoy, 1992) and $\Sigma\text{BaP}_{\text{eq}}$ for each PAH

PAH	Toxic Equivalence Factor (TEQ)	$\Sigma\text{BaP}_{\text{eq}}$ PAH
Naphthalene	0.001	0.0004
Acenaphthylene	0.001	0.0002
Acenaphthene	0.001	0.0001
Fluorene	0.001	0.0002
Phenanthrene	0.001	0.002
Anthracene	0.01	0.002
Fluoranthene	0.001	0.003
Pyrene	0.001	0.004
Banz[a]anthracene	0.1	0.08
Chrysene	0.01	0.02
Benzo[b]fluoranthene	0.1	0.12
Benzo[k]fluoranthene	0.1	0.03
Benzo[a]pyrene	1	1.02
Dibenzo[a,h]anthracene	5*	0.29
Indeno[1,2,3-cd]pyrene	0.1	0.10
Benzo[g,h,i]perylene	0.01	0.009

*a TEF of 1 appears to be appropriate for high doses of DahA but the TEF of 5 is considered more likely to be applicable to environmental exposure (Nisbet and LaGoy, 1992)

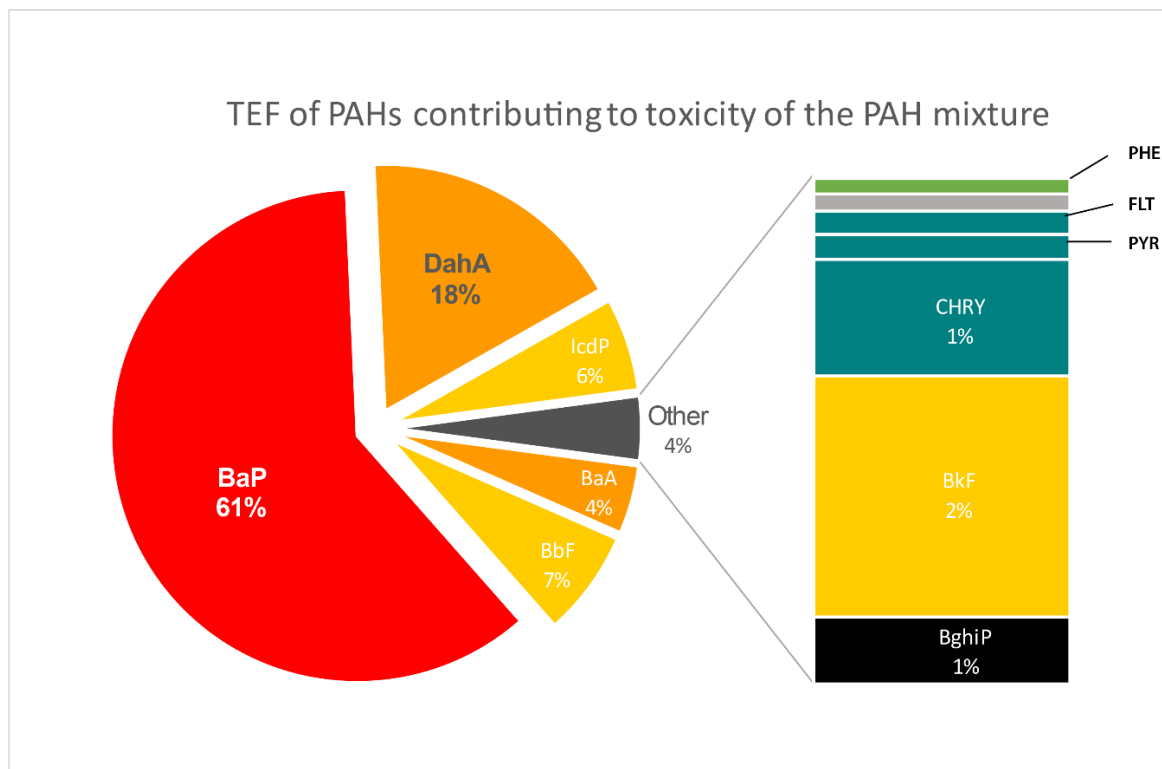


Figure 7-27: TEF of PAHs contribution to toxicity/carcinogenicity of the PAH mixture recorded in *X. parietina*, presented as pie-chart and exploded bar-chart; colour-coded by carcinogenicity of target PAHs, group 1: red, group 2A: orange, group 2B: yellow and traffic-related PAHs: green

The complex mixture of PAH derived from extracted lichens is dominated by benzo[a]pyrene and dibenz[a,h]anthracene, making up about 79% of the toxicological potential of analysed PAHs across Manchester (Figure 7-27). indeno[1,2,3-cd]pyrene, benzo[b]- and benzo[k]fluoranthene and benzo[a]anthracene are contributing to a total of 19% to the total carcinogenic potential of the PAH mixture (Figure 7-27). All other PAHs showed minor contribution to the total toxicity potential.

Benzo[a]pyrene and dibenz[a,h]anthracene are both considered toxic pollutants, dominating the carcinogenicity of PAH mixtures with 61% related to dibenzo[a,h]anthracene and 18% for benzo[a]pyrene (Figure 7-27). Likewise, Kumar et al.(2014) reported benzo[a]pyrene and dibenzo[a,h]anthracene as the two most toxic and carcinogenic PAHs found in roadside soils. Fang et al.(2002) reported benzo[a]pyrene making up 49% of the carcinogenic potency in Taichun City (Taiwan). Petry et al. (1996) reported the carcinogenic potency of benzo[a]pyrene alone in the range of 27% to 67%. Carcinogenic PAHs (group 2B), such as indeno[1,2,3-cd]pyrene (IcdP) and benz[a]anthracene (BaA) comprise a smaller amount of TEF, but contribute to 4% (for BaA) and 6% (IcdP) to the carcinogenic potency of the PAH mixture (Figure 7-27).

Benzo[b]fluoranthene and benzo[k]fluoranthene contribute to about 9% to the toxic potential in lichen-derived PAHs (Figure 7-27). Other PAHs, such as naphthalene, acenaphthylene and acenaphthene only play a minor role in the carcinogenic potential, due to their higher volatility compared to high-molecular PAHs (Mackay and Callcott, 1998).

In contrast, Achten and Andersson (2015) mentioned that the use of 16 EPA priority PAHs is strongly underestimating the toxic potential, by missing highly toxic PAHs on the list, by missing alkylated derivatives and by missing heterocyclic aromatic compounds of known toxicity, frequently occurring. For instance, Yagishita et al. (2015) included benzo[c]fluorine, cyclopenta[c,d]pyrene and benzo[j]fluoranthene additional to the 16 EPA PAH, due to their known carcinogenic potential. Lammel (2015) reported that nitro- and oxy-PAHs, posing a high health risk, should be included in ambient monitoring studies. Samburova et al. (2017) analysed 88 gas and particle phase PAHs and reported that 16 EPA PAHs only contributed to 14.4% of the toxic equivalency (TEF), resulting in a high underestimation of potential health impacts.

Accordingly, TEFs analysed in *X. parietina*, showed the potential impact of high-molecular PAHs on human health across Manchester. In particular, benzo[a]pyrene contributed 61% to the PAH toxicity profile. As previously stated, high-molecular weight PAHs are primarily bound to particulates, in particular in the breathable fraction (PM₁₀ and PM_{2.5}) could pose a significant health risk, especially at sites with high traffic counts (Slezakova et al., 2010). Therefore, additional analysis of lichen samples could improve fine spatial detail of PAH concentrations and further including additional 'health-relevant' PAHs could benefit a more detailed human health assessment.

7.5 Conclusion

This study aimed to assess the spatial distribution of PAHs across Manchester, including potential source apportionment and health risk assessment. Concentrations found in lichens were found at lower concentrations compared to other urban areas, which are in accordance with reported reduction in PAH emissions across the UK (Meijer et al., 2008). However, lichen-derived PAHs across Manchester showed spatial variability, with predominance of 4-ring PAHs that suggested vehicular emission as primary source. Moreover, 5- and 6-ring PAHs were found at higher concentrations, suggesting particulate-bound PAHs (from local sources) affecting air quality in Manchester. Sampling design, i.e. during which season sampling will be undertaken, should be considered, when analysing lichens for PAHs. Additional sampling, especially during the winter months, could further provide beneficial information on temporal PAH concentrations across Manchester. However, in order to ensure temporal (and spatial) representation, long-term measurements and continuous sampling at a large number of sites (on a broad scale), is required (Shukla et al., 2014). Although not measured continuously, PAHs are still present in the urban air of Manchester, resulting in impaired air quality. Applying a lichen biomonitoring approach was able to detect spatially variable PAH concentrations. Findings presented suggest potential health risk across Manchester primarily related to particulate-bound PAHs. Additional sampling and increasing the spatial density of samples could improve the high-spatial resolution approach.

Chapter 8-

Conclusions and

recommendations

The aim of this study was to document and assess spatial variability of air quality, using lichens as biomonitors. A high-spatial resolution biomonitoring approach was used to assess fine spatial detail of air quality in the City of Manchester, with focus on carbon, nitrogen and sulphur contents, stable-isotope-ratio signatures, and metal and polycyclic aromatic hydrocarbon (PAH) concentrations. Passive monitoring devices, i.e. NO_x diffusion tubes were used to ground-truth the lichen dataset and to assess spatio-temporal variability of NO₂ concentrations.

In conclusion, a high spatial lichen-biomonitoring approach provides a useful tool to assess air quality in the urban environment of Manchester. Furthermore, a wide range of pollutants can be addressed. However, they will not replace continuous measurements, but can as an aid to investigate and identify areas of concern regarding human health risks.

This summary chapter aims to provide an overall conclusion for this undertaken research project and to provide recommendations for potential further research. For each chapter the main findings are presented, including potential future work and recommendations.

Chapter 3 – Epiphytic lichen diversity and air quality in Manchester

Lichen diversity can provide a rapid and low-cost approach to assess environmental quality, allowing evaluation of long-term effects of air quality. This chapter aimed to use lichen diversity, combined with passively-derived NO₂ concentrations, to assess a 'general' overview of air quality across Manchester.

Predominance of eutrophication species indicate influences on nitrogen compounds across Manchester, suggesting the under representation of automated monitoring stations and measurements of NO_x and NH_x compounds. This is of particular interest for potential health implications across Manchester, with lichens providing an 'early warning system' that can be used easily to investigate potential areas of concern. However, potential toxic effects of pollutants on nitrogen-sensitive lichens and colonisation abilities of particular species should be considered. Lichen diversity was investigated with regard to NO₂ concentrations, whereas importance of other pollutants (i.e. O₃ and organic compounds) might be underestimated and need further consideration. Additional, site-specific influences, including bark pH, bark surface roughness, urban microclimates as well as urban structures influencing the dispersion and distribution of pollutants need further investigation.

Findings suggested deteriorated air quality, primarily by NO₂ across the City of Manchester. Exceedances of the WHO limit value (40 µg/m³) suggest potential health impacts at locations that are not continuously measured by automated monitoring locations that should be further investigated by applying additional monitoring methods, i.e. as described here: lichen diversity and passive monitoring devices. Both methods provide additional cost-effective and easy-to-use tools to assess potential 'hot-spot' locations over a large geographical area (i.e. urban environment) and over a long period of time (here: 12-months). This could be of particular interest for local authorities and stakeholders trying to address air quality problems. For Manchester in particular, 80% of NO₂ emissions are related to traffic and improvements are necessary to reduce NO₂ within the city centre, i.e. by improving the fleet composition (e.g. buses and taxis), reducing public access and public transport improvements and thus reducing negative health effects. However, lichen diversity and diffusion tubes can be considered as 'indicative' methods and further analysis of pollutant loadings in lichens was undertaken to investigate air quality in more detail and relate pollutants to specific sources.

Chapter 4 - Lichen CNS compounds and stable-isotope ratios ($\delta^{13}\text{C}$, $\delta^{15}\text{N}$ and $\delta^{34}\text{S}$)

Indicative measurements of air quality across Manchester showed deteriorated air quality with regard to eutrophication compounds, i.e. nitrogen dioxide (NO₂). Carbon, nitrogen and sulphur contents and stable-isotope-ratio signatures in lichens were further used to potentially identify major pollutant sources in the urban environment of Manchester.

In particular, lichen N wt% and S wt% combined with their stable-isotope ratio signatures ($\delta^{15}\text{N}$ and $\delta^{34}\text{S}$) suggested anthropogenic influences, i.e. vehicular emissions and industrial/residential combustion. Elevated nitrogen contents in lichens could be used to identify areas of higher NO₂, which could then be further investigated, i.e. by passive monitoring approaches. Therefore, providing a cost-effective for local authorities and stakeholders (i.e. NGOs) to investigate air quality in more detail and investigate areas of concern without the use of installing new measurement stations and/or using additional labour-intensive methods.

However, 'fingerprinting' specific sources using stable-isotope signatures of lichens was not possible and therefore suggesting a complex mixture of sources, in particular for N and S compounds. This indicates a vast research potential by investigating stable-isotopic compositions of potential sources that affected lichens in the urban environment of Manchester, i.e. precipitation, vehicular emissions and particulate matter.

In contrast, C wt% and $\delta^{13}\text{C}$ signatures of lichens did not provide a useful tool to address pollution sources across Manchester. However, both seemed to be influenced by meteorological and micro-climatic conditions and therefore suggest the use of C wt% and $\delta^{13}\text{C}$ values to investigate climate change in (urban) environments with lichens, which again could be aided by the lichen diversity. Combining indicative measurements (i.e. NO_x diffusion tubes) and chemical data (i.e. CNS contents and stable-isotope ratios) provide additional tools to assess spatial variability of air quality, which could not only be used in urban environments (i.e. in rural areas, as applied in this study).

Chapter 5 – Development of a new method to quantify nitrate and ammonium in lichens

Nitrogen contents in combination with $\delta^{15}\text{N}$ values and NO_2 measurements indicated the suitability of lichens (and passive sampling devices) to assess nitrogen pollution in an urban environment. However, not only NO_x compounds but also NH_x compounds are affecting air quality and human health. Nitrate (NO_3^-) and ammonium (NH_4^+) were considered to affect lichen bulk N contents and isotope ratio signatures and potentially improve source apportionment studies.

Methodological development was undertaken (using KCl) to extract NO_3^- and NH_4^+ from lichen material, providing an entirely new method to extract and separate nitrogen compounds for biomonitoring and human health purposes. Both compounds are precursors of particulate matter and are related to adverse human health impacts. This method could be applied to different environments and investigate the influence of NO_3^- and NH_4^+ , and thus aiding to identify the extent of these compounds within an environment. Additionally, the entirely new method could be applied to other (bio-)monitors, i.e. mosses and tree leaves.

Findings suggest the use of a single lichen species (highly N-tolerant to evaluate and compare the influences of nitrogen compounds on air quality in different (urban) environments. This is in accordance with findings in chapter 3 (lichen diversity and NO₂ measurements) and chapter 4 (CNS wt% and stable-isotope ratio signatures). Therefore, the first three chapters of this study showed the particular advantageous use of lichens (cost-effective and easy-to-use) to assess air quality, in particular regarding nitrogen compounds. However, additional research potential, by investigating particulate matter (i.e. via passive sampling and extraction) could further provide information on contribution of NO₃⁻ and NH₄⁺ to lichen nitrogen loadings and human health impact studies, especially at fine spatial detail.

Chapter 6 - Lichen biomonitoring of spatial variability of airborne metal pollution

Determination of metal concentrations in lichens has been used in numerous studies to assess environmental pollution in (urban) environments. However, this study aimed to assess airborne metal pollution within the City of Manchester at fine spatial detail, with focus on human health relevant studies (i.e. Pb and Cd) and metals from different vehicular compounds (i.e. Cr, Mn, Ni, Pd, Pt and Zn) that also can pose a significant threat to human health.

Elevated nitrogen contents, less negative $\delta^{15}\text{N}$ values, as well as NO₃⁻ and NH₄⁺ concentrations in lichens indicated traffic-related sources (as well as a complex mixture of sources) across Manchester. Investigating lichen metal concentrations further provided information on potential (vehicular) sources, i.e. exhaust and non-exhaust emissions. Metal concentrations are not continuously measured across Manchester, illustrating the beneficial use of lichens to monitor airborne metals. However, additional variables, such as bark pH, climatic and topographic factors should be included to investigate metal concentrations in lichens. Health impacts of elevated metal concentrations could be of particular interest for people living close to major roads and within the city centre. Especially, the environmentally persistent element lead (Pb) was found at high concentrations in Manchester, indicating health risks decades after phasing out lead in petrol. Combining a biomonitoring approach, together with soil and/or road dust analysis could further provide insights into distribution and potential sources of health relevant metals (i.e. Pb and Cd) within an urban environment.

Particulate matter (PM) is measured at 'Piccadilly Gardens' monitoring station, but does not provide information on metal concentrations. Lichens could be used to assess 'hot-spots' of airborne metals and to identify areas that need improvement, i.e. by adding pollutant barriers, such as trees and or green barriers between roads. This is particularly important for residential areas in proximity to highly-trafficked roads and lichens could be used to assess pre- and post installation of such barriers or road improvement works. However, installation of green barriers or planting of new trees might not be possible with an densely built-up urban centre, whereas facade greening could improve air quality by interception metal-containing particles (and other pollutants). Again, this could be investigated with a lichen biomonitoring, prior and subsequent improvements. Moreover, lichen metal concentrations that indicate particular sources (i.e. vehicular) could also provide information on further investigations, especially for organic pollutants, such as aromatic hydrocarbons (e.g. PAHs).

Chapter 7 - Lichen biomonitoring for atmospheric PAH source apportionment and toxicity assessment

Polycyclic aromatic hydrocarbons (PAHs) are a major concern for human health and lichen analysis provided an insight into atmospheric PAH concentrations in Manchester, which are not continuously measured at automated monitoring stations. Closed measurements of PAHs in Manchester in 2014, by high-volume sampler at 'Manchester Law Courts' indicated that PAH concentrations were below the EU limit value (1 ng/m³, expressed as concentration of benzo[a]pyrene; European Commission, 2018). However, lichen PAH concentrations, although being low compared to other urban lichen biomonitoring studies, provided beneficial results and illustrated spatial variability of PAHs across Manchester. Therefore, lichens are considered a useful tool to assess airborne PAHs, which could aid local authorities to reconsider PAH measurements. Moreover, extending the lichen analysis for additional PAHs, i.e. extending the 16 EPA priority PAHs and include nitro-, oxy-, alkylated-, amino- and higher molecular weight PAHs (Andersson and Achten, 2015), could provide additional research potential when using lichens as biomonitors.

Furthermore, other persistent organic compounds (e.g. PCBs, PCDFs and PCDDs) that pose a potential health impact could be implemented in the analysis, and provide finer spatial detail of organic pollutants across Manchester and other urban environments. Lichen PAH profiles suggest a complex mixture of PAH sources within the urban environment of Manchester, complication source apportionment. In this study, only 20 sites were analysed, not achieving a high spatial resolution of PAHs in Manchester. Further sampling and analysis is suggested to assess fine spatial detail. Moreover, method adjustments, as suggested by Wat and Forbes (2019) using 'QuEChERS' (Quick, Easy, Cheap, Effective, Rugged and Safe) could improve spatial coverage and reducing time and labour, by analysing more samples in shorter amount of time.

Toxicity assessment, using lichen PAHs concentrations showed major contributions by benzo[a]pyrene and dibenzo[a,h]anthracene, which are considered 'carcinogenic' and probably 'carcinogenic' to human health. Recent research suggest to include additional PAHs to further investigate potential toxicity of PAHs, i.e. including secondary PAH reaction products (Andersson and Achten, 2015; Samburova et al., 2017). Lichens could therefore be used to assess spatial 'hot-spots' of PAH pollution, which could be further investigated by passive monitoring approaches, i.e. using PUF disk samplers. Passive monitoring could provide a seasonal overview of PAH concentrations for Manchester and identify areas of concern. Moreover methodological development for PUF disk extraction using an ultrasonic-assisted extraction method could be further investigated (as initiated by this research project) as an alternative to conventional extraction procedures (i.e. time- and solvent-consuming Soxhlet).

There is apparently growing interest in the public according health impacts of deteriorated air quality, suggesting the need for additional monitoring methods, which can be easily (and cost-effectively) be applied by different stakeholders, such as local authorities and NGOs to address air pollution and investigate public health, particularly at not continuously monitored locations. Moreover, a lichen biomonitoring approach could be used to assess a comparison before and after improvements were implemented (i.e. road, fleet improvements and urban greening).

In this study, lichen diversity and chemically analysed pollutant loadings, combined with passive monitoring devices (NO_x diffusion tubes), did provide a beneficial tool to assess spatial variability of air quality in the urban environment of Manchester. Therefore, this cost-effective approach could be applied to other (urban) environments, providing the possibility for comparison of air quality across the UK. Additionally, a lichen biomonitoring and/or passive sampling study could be used in a citizen science context. For instance, the 'Clean Air Campaign' by Friends of the Earth (UK) used NO_x diffusion tube kits to assess NO₂ concentrations (on a local scale, including Manchester; Friends of the Earth (UK), 2017). For Greater Manchester in particular, 'Clean Air Greater Manchester provides a NO_x diffusion tube network (N=272) to support automated measurements (GMCA and TfGM, 2019), which could be additionally supported by lichen (chemical) analysis. Moreover, air quality improvements (i.e. by improving bus and car fleets) and introducing a 'Clean Air Zone' (by 2021) in Manchester (GMCA and TfGM, 2019) can be investigated using the outlined approach, allowing to compare air quality throughout the years and to assess the efficiency of (implemented) improvement plans.

Another potential research project could include the use of lichens as 'travelers' in commuting cars and/or to assess differences between indoor and outdoor air pollution, as described by Paoli et al. (2019). For instance, assessing air quality along Europe's and Manchester's busiest bus route (Oxford Road) could provide valuable insights for Manchester's local authorities on where and how to improve traffic-flow, fleet composition, installing of green-barriers and potential human health risks during a daily commute.

However, there is vast research potential, especially with emerging pollutants of concern (i.e. secondary reaction products), further methodological development (including lichen extraction and passive sampling devices), as well as health risk assessments by 'translating' lichen pollutant loadings into atmospheric concentrations (in particular for health risk assessment via inhalation) that can be addressed in future research.

References

- Abd Razak, A., Hagishima, A., Ikegaya, N. and Tanimoto, J. (2013) 'Analysis of airflow over building arrays for assessment of urban wind environment.' *Building and Environment*. Elsevier Ltd, 59, January, pp. 56–65.
- Abdel-Shafy, H. I. and Mansour, M. S. M. (2016) 'A review on polycyclic aromatic hydrocarbons: Source, environmental impact, effect on human health and remediation.' *Egyptian Journal of Petroleum*. Egyptian Petroleum Research Institute, 25(1) pp. 107–123.
- Abdul-Razzaq, W. and Gautam, M. (2001) 'Discovery of magnetite in the exhausted material from a diesel engine.' *Applied Physics Letters*, 78(14) pp. 2018–2019.
- Achakulwisut, P., Brauer, M., Hystad, P. and Anenberg, S. C. (2019) 'Global, national, and urban burdens of paediatric asthma incidence attributable to ambient NO₂ pollution: estimates from global datasets.' *The Lancet Planetary Health*. The Author(s). Published by Elsevier Ltd. This is an Open Access article under the CC BY NC ND 4.0 license, 5196(19).
- Achten, C. and Andersson, J. T. (2015) 'Overview of Polycyclic Aromatic Compounds (PAC).' *Polycyclic Aromatic Compounds*, 35(2–4) pp. 177–186.
- Adamiec, E., Jarosz-Krzemińska, E. and Wieszała, R. (2016) 'Heavy metals from non-exhaust vehicle emissions in urban and motorway road dusts.' *Environmental Monitoring and Assessment*, 188(6) p. 369.
- Adamo, P., Giordano, S., Sforza, A. and Bargagli, R. (2011) 'Implementation of airborne trace element monitoring with devitalised transplants of *Hypnum cupressiforme* Hedw.: Assessment of temporal trends and element contribution by vehicular traffic in Naples city.' *Environmental Pollution*.
- Addison, P. A. and Puckett, K. J. (1980) 'Deposition of atmospheric pollutants as measured by lichen element content in the Athabasca oil sands area.' *Canadian Journal of Botany*, 58(22) pp. 2323–2334.
- AEA Energy and Environment (2008) *Diffusion Tubes for Ambient NO₂ Monitoring: Practical Guidance for Laboratories and Users*. ED48673043. Didcot.
- Agilent Technologies (2006) 'ICP-MS: Inductively Coupled Plasma Mass Spectrometry' p. 84.
- Agilent Technologies (2019) *Multi-Element Calibration standards*. [Online] [Accessed on 21st February 2019] [https://www.agilent.com/en/products/icp-ms/icp-ms-supplies/standards/icp-ms-calibration-standards-\(multi-element\)](https://www.agilent.com/en/products/icp-ms/icp-ms-supplies/standards/icp-ms-calibration-standards-(multi-element)).
- Aguilera, I., Sunyer, J., Fernández-Patier, R., Hoek, G., Aguirre-Alfaro, A., Meliefste, K., Bombol-Mingarro, M. T., Nieuwenhuijsen, M. J., Herce-Garraleta, D. and Brunekreef, B. (2008) 'Estimation of outdoor NO_x, NO₂, and BTEX exposure in a cohort of pregnant women using land use regression modeling.' *Environmental Science and Technology*.
- Aguinis, H., Gottfredson, R. K. and Joo, H. (2013) 'Best-Practice Recommendations for Defining, Identifying, and Handling Outliers.' *Organizational Research Methods*, 16(2) pp. 270–301.
- Ahn, K. H. and Palmer, R. (2016) 'Regional flood frequency analysis using spatial proximity and basin characteristics: Quantile regression vs. parameter regression technique.' *Journal of Hydrology*.
- Air Quality England (2018a) *Air Pollution Report - Manchester Piccadilly (MAN7)*. Manchester.
- Air Quality England (2018b) *Manchester Oxford Road (MAN1) - Exceedence Summary*. [Online] [Accessed on 25th June 2018] http://www.airqualityengland.co.uk/site/exceedence?site_id=MAN1.
- Air Quality Expert Group (2004) *Nitrogen Dioxide in the United Kingdom*. London.

- Air Quality Expert Group (2007) *Trends in Primary Nitrogen Dioxide in the United Kingdom*. London.
- Aksu, A. (2015) 'Sources of metal pollution in the urban atmosphere (A case study: Tuzla, Istanbul).' *Journal of Environmental Health Science and Engineering*. Journal of Environmental Health Science and Engineering, 13(1) p. 79.
- Alam, A. and Hatzopoulou, M. (2014) 'Reducing transit bus emissions: Alternative fuels or traffic operations?' *Atmospheric Environment*. Elsevier Ltd, 89 pp. 129–139.
- Alberty, R. A. and Reif, A. K. (1988) 'Standard Chemical Thermodynamic Properties of Polycyclic Aromatic Hydrocarbons and Their Isomer Groups I. Benzene Series.' *Journal of Physical and Chemical Reference Data*, 17(1) pp. 241–253.
- Alt, F. and Messerschmidt, J. (1993) *Edelmetallemission durch Katalysatoren-Beitrag der Analytischen Chemie zur Abschätzung des Gefahrenpotentials. Akute und chronische Toxizität von Spurenelementen V*. Kiel: Wissenschaftliche Verlagsgesellschaft mbH Stuttgart.
- Alvi, M. U., Chishtie, F., Shahid, I., Mahmud, T. and Hussain, R. (2018) 'Traffic -and Industry-Related Air Pollution Exposure Assessment in an Asian Megacity.' *Clean - Soil, Air, Water*, 46(1) pp. 1–20.
- Andersen, H. V. and Hovmand, M. F. (1999) 'Review of dry deposition measurements of ammonia and nitric acid to forest.' *Forest Ecology and Management*, 114(1) pp. 5–18.
- Andersson, J. T. and Achten, C. (2015) 'Time to Say Goodbye to the 16 EPA PAHs? Toward an Up-to-Date Use of PACs for Environmental Purposes.' *Polycyclic Aromatic Compounds*, 35(2–4) pp. 330–354.
- Andersson, J. T. and Achten, C. (2015) 'Time to Say Goodbye to the 16 EPA PAHs? Toward an Up-to-Date Use of PACs for Environmental Purposes.' *Polycyclic Aromatic Compounds*, 35(2–4) pp. 330–354.
- Andrews, A. (2014) *The Clean Air Handbook*. London.
- AQEG (2012) *Fine Particulate Matter in the United Kingdom*.
- AQEG (2018) *Air Pollution from Agriculture*.
- Asman, W. A. H., Sutton, M. A. and Schjørring, J. K. (1998) 'Ammonia: Emission, atmospheric transport and deposition.' *New Phytologist*.
- Asta, J., Erhardt, W., Ferrette, M., Fornasier, F., Kirschbaum, U., Nimis, P. L., Purvis, O. W., Pirintzos, S., Scheidegger, C., Van Haluwyn, C. and Wirth, V. (2002) 'Mapping Lichen Diversity As An Indicator Of Environmental Quality.' In Nimis, P., Scheidegger, C., and Wolseley, P. A. (eds) *Monitoring with Lichens - Monitoring Lichens*. 1st ed., Dordrecht: Springer Science + Business Media B.V., pp. 273–278.
- Asta, J., Ferretti, M. and Fornasier, M. F. (2002) 'European guideline for mapping lichen diversity as an indicator of environmental stress.'
- Astel, A. M., Chepanova, L. and Simeonov, V. (2011) 'Soil contamination interpretation by the use of monitoring data analysis.' *Water, Air, and Soil Pollution*.
- ATSDR (2005) *Nickel - ToxFAQs™*. Atlanta, GA.
- Atkins, C. H. F., Sandalls, J., Law, D. V., Hough, A. M. and Stevenson, K. J. (1986) *The Measurement of Nitrogen Dioxide in the Outdoor Environment Using Passive Diffusion Tube Samplers*.
- Atkinson, R. W., Fuller, G. W., Anderson, H. R., Harrison, R. M. and Armstrong, B. (2010) 'Urban ambient particle metrics and health: A time-series analysis.' *Epidemiology*, 21(4) pp. 501–511.
- ATSDR (2004a) 'Ammonia - ToxFAQs™,' (September).
- ATSDR (2004b) *Cobalt - ToxFAQs™*. Atlanta, Ga.
- ATSDR (2004c) *Copper - ToxFAQs™*. Atlanta, GA.
- ATSDR (2005) *Zinc - ToxFAQs™*. Atlanta.
- ATSDR (2008a) *Aluminum- ToxFAQs™*. Atlanta.

- ATSDR (2008b) *Toxicological Profile for Cadmium*. Atlanta, GA.
- ATSDR (2012a) *Manganese - ToxFAQs™*. Atlanta, GA.
- ATSDR (2012b) *Vanadium - ToxFAQs™*. Atlanta, GA.
- ATSDR (2015) 'Toxicological Profile: Nitrate and Nitrite.' *U.S. Department of Health and Human Services*, (July).
- ATSDR (2018) *ATSDR Toxic Substances Portal*. Toxicological Profiles. [Online] [Accessed on 10th December 2018] <https://www.atsdr.cdc.gov/substances/index.asp>.
- Augusto, S., Máguas, C. and Branquinho, C. (2013) 'Guidelines for biomonitoring persistent organic pollutants (POPs), using lichens and aquatic mosses – A review.' *Environmental Pollution*, 180, September, pp. 330–338.
- Augusto, S., Máguas, C., Matos, J., Pereira, M. J. and Branquinho, C. (2010) 'Lichens as an integrating tool for monitoring PAH atmospheric deposition: A comparison with soil, air and pine needles.' *Environmental Pollution*, 158(2) pp. 483–489.
- Augusto, S., Máguas, C., Matos, J., Pereira, M. J., Soares, A. and Branquinho, C. (2009) 'Spatial Modeling of PAHs in Lichens for Fingerprinting of Multisource Atmospheric Pollution.' *Environmental Science & Technology*, 43(20) pp. 7762–7769.
- Augusto, S., Pereira, M. J., Máguas, C. and Branquinho, C. (2013) 'A step towards the use of biomonitors as estimators of atmospheric PAHs for regulatory purposes.' *Chemosphere*. Elsevier Ltd, 92(5) pp. 626–632.
- Augusto, S., Pereira, M. J., Máguas, C., Soares, A. and Branquinho, C. (2012) 'Assessing human exposure to polycyclic aromatic hydrocarbons (PAH) in a petrochemical region utilizing data from environmental biomonitors.' *Journal of Toxicology and Environmental Health - Part A: Current Issues*, 75(13–15) pp. 819–830.
- Augusto, S., Pereira, M. J., Soares, A. and Branquinho, C. (2007) 'The contribution of environmental biomonitoring with lichens to assess human exposure to dioxins.' *International Journal of Hygiene and Environmental Health*.
- Augusto, S., Shukla, V., Upreti, D. K., Paoli, L., Vannini, A., Loppi, S., Nerín, C., Domeño, C. and Schumacher, M. (2016) 'Biomonitoring of Airborne Persistent Organic Pollutants Using Lichens.' In Tom, M., Vuković, G., and Aničić Uroević, M. (eds) *Biomonitoring of Air Pollution Using Mosses and Lichens: A Passive and Active Approach - State of the Art Research and Perspectives*. Nova Science Publishers, Incorporated, pp. 2–41.
- Augusto, S., Sierra, J., Nadal, M. and Schumacher, M. (2015) 'Tracking polycyclic aromatic hydrocarbons in lichens: It's all about the algae.' *Environmental Pollution*. Elsevier Sci Ltd, Oxford, England, 207, December, pp. 441–445.
- Avalos, A. and Vicente, C. (1985) 'Phytochrome enhances nitrate reductase activity in the lichen *Evernia prunastri*.' *Canadian Journal of Botany*, 63(8) pp. 1350–1354.
- Bačkor, M. and Loppi, S. (2009) 'Interactions of lichens with heavy metals.' *Biologia Plantarum*, 53(2) pp. 214–222.
- Baffi, C., Bettinelli, M., Beone, G. M. and Spezia, S. (2002) 'Comparison of different analytical procedures in the determination of trace elements in lichens.' *Chemosphere*, 48(3) pp. 299–306.
- Baird, C. and Cann, M. C. (2008) *Environmental Chemistry*. 4th ed., New York: W.H. Freeman.
- Bajpai, R., Karakoti, N. and Upreti, D. K. (2013) 'Performance of a naturally growing Parmelioid lichen *Remototrachyna awasthii* against organic and inorganic pollutants.' *Environmental Science and Pollution Research*.
- Balmes, J. R., Fine, J. M. and Sheppard, D. (1987) 'Symptomatic Bronchoconstriction after Short Term Inhalation of Sulfur Dioxide.' *American Review of Respiratory Disease*, 136(5) pp. 1117–1121.
- Barabasz, W., Albińska, D., Jaśkowska, M. and Lipiec, J. (2002) 'Ecotoxicology of Aluminium.' *Polish Journal of Environmental Studies*.

- Bargagli, R. (1998) *Trace elements in terrestrial plants: An ecophysiological approach to biomonitoring and biorecovery*. 6th ed., Berlin: Springer.
- Bari, A., Ferraro, V., Wilson, L. R., Luttinger, D. and Husain, L. (2003) 'Measurements of gaseous HONO, HNO₃, SO₂, HCl, NH₃, particulate sulfate and PM_{2.5} in New York, NY.' *Atmospheric Environment*.
- Barkman, J. J. (1963) 'De epifythen-flora en vegetatie van Midden-Limburg (België).' *Verhandeling der Koninklijke Nederlandse Akademie van Wetenschappen, Afdeling Natuurkunde.*, 54 pp. 1–46.
- Barrett, J. E. S., Taylor, K. G., Hudson-Edwards, K. A. and Charnock, J. M. (2010) 'Solid-phase speciation of Pb in urban road dust sediment: A XANES and EXAFS study.' *Environmental Science and Technology*, 44(8) pp. 2940–2946.
- Barrett, J. E. S., Taylor, K. G., Hudson-Edwards, K. a, Charnock, J. M., Arrett, J. E. S. B., Aylor, K. G. T. and Dwards, K. a H. U. (2011) 'Solid-phase speciation of Zn in road dust sediment.' *Mineralogical Magazine*, 75(October) pp. 2611–2629.
- Barrett, S. R. H., Speth, R. L., Eastham, S. D., Von Schneidemesser, E., Kuik, F., Mar, K. A. and Butler, T. (2017) 'Environmental Research Letters Potential reductions in ambient NO₂ concentrations from meeting diesel vehicle emissions standards Potential reductions in ambient NO₂ concentrations from meeting diesel vehicle emissions standards.' *Environ. Res. Lett.*, 12(2).
- Barth, A., Brucker, N., Moro, A. M., Nascimento, S., Goethel, G., Souto, C., Fracasso, R., Sauer, E., Altknecht, L., da Costa, B., Duarte, M., Menezes, C. B., Tasca, T., Arbo, M. D. and Garcia, S. C. (2017) 'Association between inflammation processes, DNA damage, and exposure to environmental pollutants.' *Environmental Science and Pollution Research*. *Environmental Science and Pollution Research*, 24(1) pp. 353–362.
- Bartholomeß, H. (n.d.) *Flechten als Bioindikatoren für Umweltbelastungen*. Stuttgart.
- Bartholomeß, H. and John, E. (1997) *Luftqualität - Selbst bestimmt*. 1st ed., Stuttgart: Verlag Stephanie Nagelschmid.
- Batts, J. E., Batts, B. D. and Krouse, H. R. (1996) 'd¹³C of lichens as environmental monitors.' In van Arsen, B. G. K. (ed.) *Australian Organic Geochemistry Conference Abstracts*. Fremantle, Washington, p. 52.
- Batts, J. E., Calder, L. J. and Batts, B. D. (2004) 'Utilizing stable isotope abundances of lichens to monitor environmental change.' *Chemical Geology*, 204(3–4) pp. 345–368.
- Batty, K., Bates, J. W. and Bell, J. N. (2003) ' A transplant experiment on the factors preventing lichen colonization of oak bark in southeast England under declining SO₂ pollution .' *Canadian Journal of Botany*.
- Baumard, P., Budzinski, H., Michon, Q., Garrigues, P., Burgeot, T. and Bellocq, J. (1998) 'Origin and Bioavailability of PAHs in the Mediterranean Sea from Mussel and Sediment Records.' *Estuarine, Coastal and Shelf Science*, 47(1) pp. 77–90.
- Bealey, W., Long, S., Spurgeon, D., Leith, I. and Cape, J. (2008) *Review and implementation study of biomonitoring for assessment of air quality outcomes*. Bristol.
- Beauchamp, M., Malherbe, L., Letinois, L. and Fouquet, C. De (2012) 'Spatial representativeness of an air quality monitoring station. Delimitation of exceedances areas.' *Proceedings Geostats 2012* pp. 1–5.
- Beck, A. and Mayr, C. (2012) 'Nitrogen and carbon isotope variability in the green-algal lichen *Xanthoria parietina* and their implications on mycobiont-photobiont interactions.' *Ecology and Evolution*, 2(12) pp. 3132–3144.
- Bellinger, D. C. (2005) 'Teratogen update: Lead and pregnancy.' *Birth Defects Research Part A - Clinical and Molecular Teratology*.
- Bener, A., Kamal, M. and Shanks, N. J. (2007) 'Impact of asthma and air pollution on school attendance of primary school children: Are they at increased risk of school

- absenteeism?' *Journal of Asthma*, 44(4) pp. 249–252.
- Bergamaschi, L., Rizzio, E., Giaveri, G., Loppi, S. and Gallorini, M. (2007) 'Comparison between the accumulation capacity of four lichen species transplanted to a urban site.' *Environmental Pollution*, 148(2) pp. 468–476.
- Berglen, T. F., Myhre, G., Isaksen, I. S. A., Vestreng, V. and Smith, S. J. (2007) 'Sulphate trends in Europe: Are we able to model the recent observed decrease?' *Tellus, Series B: Chemical and Physical Meteorology*, 59(4) pp. 773–786.
- Berkowicz, R. (2000) 'A simple model for urban background pollution.' *Environmental Monitoring and Assessment*, 65(1) pp. 259–267.
- Bermejo-Orduna, R., McBride, J. R., Shiraishi, K., Elustondo, D., Lasheras, E. and Santamaría, J. M. (2014) 'Biomonitoring of traffic-related nitrogen pollution using *Letharia vulpina* (L.) Hue in the Sierra Nevada, California.' *Science of the Total Environment*. Elsevier B.V., 490 pp. 205–212.
- Bettinelli, M., Perotti, M., Spezia, S., Baffi, C., Beone, G. M., Alberici, F., Bergonzi, S., Bettinelli, C., Cantarini, P. and Mascetti, L. (2002) 'The role of analytical methods for the determination of trace elements in environmental biomonitors.' *Microchemical Journal*, 73(1–2) pp. 131–152.
- Biazrov, L. G. (2010) 'Die Dynamik der Artendiversität epiphytischer Flechten im Nordbezirk von Moskau (Russland)'. *Archive der Lichenology*, 6 pp. 1–8.
- Biazrov, L. G. (2012) 'Values of stable carbon isotopes ($\delta^{13}\text{C}$) in the thalli of the arid vagrant lichen *Xanthoparmelia camtschadalis* along an altitudinal gradient in the Khangai Plateau as a reflection of the spatial and ecological heterogeneity of the semiarid region of Mongol.' *Arid Ecosystems*, 2(1) pp. 54–60.
- Bigi, A. and Harrison, R. M. (2012) 'Analysis of the air pollution climate at a background site in the Po valley †' pp. 552–563.
- Bishop, G. A., Peddle, A. M., Stedman, D. H. and Zhan, T. (2010) 'On-road emission measurements of reactive nitrogen compounds from three California Cities.' *Environmental Science and Technology*.
- Bishop, G. A. and Stedman, D. H. (2015) 'Reactive Nitrogen Species Emission Trends in Three Light-/Medium-Duty United States Fleets.' *Environmental Science and Technology*, 49(18) pp. 11234–11240.
- Blasco, M., Domeño, C., Bentayeb, K. and Nerín, C. (2007) 'Solid-phase extraction clean-up procedure for the analysis of PAHs in lichens.' *International Journal of Environmental Analytical Chemistry*, 87(12) pp. 833–846.
- Blasco, M., Domeño, C., López, P. and Nerín, C. (2011) 'Behaviour of different lichen species as biomonitors of air pollution by PAHs in natural ecosystems.' *Journal of Environmental Monitoring*, 13(9) p. 2588.
- Blasco, M., Domeño, C. and Nerín, C. (2006) 'Use of Lichens as Pollution Biomonitors in Remote Areas: Comparison of PAHs Extracted from Lichens and Atmospheric Particles Sampled in and Around the Somport Tunnel (Pyrenees).' *Environmental Science & Technology*, 40(20) pp. 6384–6391.
- Blasco, M., Domeño, C. and Nerín, C. (2008) 'Lichens biomonitoring as feasible methodology to assess air pollution in natural ecosystems: Combined study of quantitative PAHs analyses and lichen biodiversity in the Pyrenees Mountains.' *Analytical and Bioanalytical Chemistry*, 391(3) pp. 759–771.
- Boamponsem, L. K. and de Freitas, C. R. (2017) 'Validation of *Parmotrema reticulatum* as a biomonitor of elemental air pollutants in Auckland, New Zealand.' *Journal of the Royal Society of New Zealand*. Taylor & Francis, 0(0) pp. 1–19.
- Boersma, K. F., Jacob, D. J., Trainic, M., Rudich, Y., DeSmedt, I., Dirksen, R. and Eskes, H. J. (2009) 'Validation of urban NO_2 concentrations and their diurnal and seasonal variations observed from the SCIAMACHY and OMI sensors using in situ surface measurements in Israeli cities.' *Atmospheric Chemistry and Physics*, 9(12) pp. 3867–3879.

- Bohlin, P., Audy, O., Škrdlíková, L., Kukučka, P., Příbylová, P., Prokeš, R., Vojta, Š. and Klánová, J. (2014) 'Outdoor passive air monitoring of semi volatile organic compounds (SVOCs): a critical evaluation of performance and limitations of polyurethane foam (PUF) disks.' *Environ. Sci.: Processes Impacts*, 16(3) pp. 433–444.
- Bohlin, P., Jones, K. C., Tovalin, H. and Strandberg, B. (2008) 'Observations on persistent organic pollutants in indoor and outdoor air using passive polyurethane foam samplers.' *Atmospheric Environment*, 42(31) pp. 7234–7241.
- Boleij, J. S. M., Lebre, E., Hoek, F., Noy, D. and Brunekreef, B. (1986) 'The use of palmes diffusion tubes for measuring NO₂ in homes.' *Atmospheric Environment* (1967).
- Boltersdorf, S. H., Pesch, R. and Werner, W. (2014) 'Comparative use of lichens, mosses and tree bark to evaluate nitrogen deposition in Germany.' *Environmental Pollution*. Elsevier Ltd, 189, June, pp. 43–53.
- Boltersdorf, S. H. and Werner, W. (2014) 'Lichens as a useful mapping tool?—an approach to assess atmospheric N loads in Germany by total N content and stable isotope signature.' *Environmental Monitoring and Assessment*, 186(8) pp. 4767–4778.
- Boltersdorf, S. and Werner, W. (2013) 'Source attribution of agriculture-related deposition by using total nitrogen and $\delta^{15}\text{N}$ in epiphytic lichen tissue, bark and deposition water samples in Germany.' *Isotopes in Environmental and Health Studies*, 49(2) pp. 197–218.
- Bosserman, R. W. and Hagner, J. E. (1981) 'Elemental Composition of Epiphytic Lichens from Okefenokee Swamp.' *The Bryologist*, 84(1) p. 48.
- Boudsocq, S., Niboyet, A., Lata, J. C., Raynaud, X., Loeuille, N., Mathieu, J., Blouin, M., Abbadie, L. and Barot, S. (2012) 'Plant Preference for Ammonium versus Nitrate: A Neglected Determinant of Ecosystem Functioning?' *The American Naturalist*, 180(1) pp. 60–69.
- Bourguignon, D. (2018) *Air quality. Pollution sources and impacts, EU legislation and international agreements*. Brussels: European Parliament Research Service (EPRS).
- Bowatte, G., Lodge, C. J., Knibbs, L. D., Erbas, B., Perret, J. L., Jalaludin, B., Morgan, G. G., Bui, D. S., Giles, G. G., Hamilton, G. S., Wood-Baker, R., Thomas, P., Thompson, B. R., Matheson, M. C., Abramson, M. J., Walters, E. H. and Dharmage, S. C. (2018) 'Traffic related air pollution and development and persistence of asthma and low lung function.' *Environment International*, 113(January) pp. 170–176.
- Bower, J. S., Lampert, J. E., Stevenson, K. J., Atkins, D. H. F. and Law, D. V. (1991) 'A diffusion tube survey of NO₂ levels in urban areas of the U.K.' *Atmospheric Environment. Part B, Urban Atmosphere*, 25(2) pp. 255–265.
- Boyd, H. B., Pedersen, F., Cohr, K. H., Damborg, A., Jakobsen, B. M., Kristensen, P. and Samsøe-Petersen, L. (1999) 'Exposure scenarios and guidance values for urban soil pollutants.' *Regulatory Toxicology and Pharmacology*, 30(3) pp. 197–208.
- Braga, R. S., Barone, P. M. V. B. and Galvão, D. S. (1999) 'Identifying carcinogenic activity of methylated polycyclic aromatic hydrocarbons (PAHs).' *Journal of Molecular Structure: THEOCHEM*, 464(1–3) pp. 257–266.
- Branquinho, C., Brown, D. H. and Catarino, F. (1997) 'The cellular location of Cu in lichens and its effects on membrane integrity and chlorophyll fluorescence.' *Environmental and Experimental Botany*, 38(2) pp. 165–179.
- Branquinho, C., Brown, D. H., Máguas, C. and Catarino, F. (1997) 'Lead (Pb) uptake and its effects on membrane integrity and chlorophyll fluorescence in different lichen species.' *Environmental and Experimental Botany*, 37(2–3) pp. 95–105.
- Brauer, M. (2016) *Poor air quality kills 5.5 million worldwide annually*. UBC News. Vancouver. [Online] <http://news.ubc.ca/2016/02/12/poor-air-quality-kills-5-5-million-worldwide-annually/>.
- Bremner, J. M. and Keeney, D. R. (1966) 'Determination and Isotope-Ratio Analysis of

- Different Forms of Nitrogen in Soils: 3. Exchangeable Ammonium, Nitrate, and Nitrite by Extraction-Distillation Methods¹.' *Soil Science Society of America Journal*, 30(5) p. 577.
- Britter, R. E. and Hanna, S. R. (2003) 'Flow and Dispersion in Urban Areas.' *Annual Review of Fluid Mechanics*, 35(1) pp. 469–496.
- Brown, D. H. (1996) 'Urban, industrial and agricultural effects on lichens' pp. 257–281.
- Brown, D. H. and Beckett, R. P. (1983) 'Differential Sensitivity of Lichens to Heavy Metals.' *Annals of botany*, 52 pp. 51–57.
- Browning, M. and Lee, K. (2017) 'Within what distance does “greenness” best predict physical health? A systematic review of articles with gis buffer analyses across the lifespan.' *International Journal of Environmental Research and Public Health*, 14(7) pp. 1–21.
- de Bruin, M. (1990) 'Applying biological monitors and neutron activation analysis in studies of heavy-metal air pollution.' *International Atomic Energy Agency bulletin*, 32(4) pp. 22–27.
- Brunekreef, B. and Holgate, S. T. (2002) 'Air pollution and health.' *The Lancet*, 360(9341) pp. 1233–1242.
- Buccolieri, R., Gromke, C., Di Sabatino, S. and Ruck, B. (2009) 'Aerodynamic effects of trees on pollutant concentration in street canyons.' *Science of the Total Environment*.
- Buccolieri, R., Sandberg, M. and Di Sabatino, S. (2010) 'City breathability and its link to pollutant concentration distribution within urban-like geometries.' *Atmospheric Environment*.
- Budzinski, H., Jones, I., Bellocq, J., Piérard, C. and Garrigues, P. (1997) 'Evaluation of sediment contamination by polycyclic aromatic hydrocarbons in the Gironde estuary.' *In Marine Chemistry*.
- Bukowiecki, N., Gehrig, R., Hill, M., Lienemann, P., Zwicky, C. N., Buchmann, B., Weingartner, E. and Baltensperger, U. (2007) 'Iron, manganese and copper emitted by cargo and passenger trains in Zürich (Switzerland): Size-segregated mass concentrations in ambient air.' *Atmospheric Environment*, 41(4) pp. 878–889.
- Bush, T., Smith, S., Stevenson, K. and Moorcroft, S. (2001) 'Validation of nitrogen dioxide diffusion tube methodology in the UK.' *Atmospheric Environment*, 35(2) pp. 289–296.
- Buzica, D. and Gerboles, M. (2008) *Monitor Determination of NO₂ and SO₂ by ion chromatography in ambient air by use of membrane – closed Palmes tube*.
- Buzica, D., Gerboles, M. and Amantini, L. (2003) *Laboratory and Field Inter-comparisons of NO₂ Diffusive Samplers*. Ispra, Italy.
- Caballero, S., Esclapez, R., Galindo, N., Mantilla, E. and Crespo, J. (2012) 'Use of a passive sampling network for the determination of urban NO₂ spatiotemporal variations.' *Atmospheric Environment*. Elsevier Ltd, 63(2) pp. 148–155.
- Camargo, J. A. and Alonso, Á. (2006) 'Ecological and toxicological effects of inorganic nitrogen pollution in aquatic ecosystems: A global assessment.' *Environment International*, 32(6) pp. 831–849.
- Campbell, G. W., Stedman, J. R. and Stevenson, K. (1994) 'A survey of nitrogen dioxide concentrations in the United Kingdom using diffusion tubes, July-December 1991.' *Atmospheric Environment*.
- Cape, J. N. (2005) 'The Use of Passive Diffusion Tubes for Measuring Concentrations of Nitrogen Dioxide in Air.' *Critical Reviews in Analytical Chemistry*, 39(4) pp. 289–310.
- Cape, J. N., Tang, Y. S., Van Dijk, N., Love, L., Sutton, M. A. and Palmer, S. C. F. (2004) 'Concentrations of ammonia and nitrogen dioxide at roadside verges, and their contribution to nitrogen deposition.' *Environmental Pollution*, 132(3) pp. 469–478.
- Cariolet, J. M., Colombert, M., Vuillet, M. and Diab, Y. (2018) 'Assessing the resilience of urban areas to traffic-related air pollution: Application in Greater Paris.' *Science of*

- the Total Environment*. Elsevier B.V., 615 pp. 588–596.
- Carré, J., Gatimel, N., Moreau, J., Parinaud, J. and Léandri, R. (2017) 'Does air pollution play a role in infertility?: A systematic review.' *Environmental Health: A Global Access Science Source*. Environmental Health, 16(1) pp. 1–16.
- Carreras, H. A. and Pignata, M. L. (2002) 'Biomonitoring of heavy metals and air quality in Cordoba City, Argentina, using transplanted lichens.' *Environmental Pollution*, 117(1) pp. 77–87.
- Carreras, H. A., Rodriguez, J. H., González, C. M., Wannaz, E. D., Garcia Ferreyra, F., Perez, C. A. and Pignata, M. L. (2009) 'Assessment of the relationship between total suspended particles and the response of two biological indicators transplanted to an urban area in central Argentina.' *Atmospheric Environment*.
- Casas, L., Cox, B., Bauwelinck, M., Nemery, B., Deboosere, P. and Nawrot, T. S. (2017) 'Does air pollution trigger suicide? A case-crossover analysis of suicide deaths over the life span.' *European Journal of Epidemiology*. Springer Netherlands, 32(11) pp. 973–981.
- Case, J. W. and Krouse, H. R. (1980) 'Variations in sulphur content and stable sulphur isotope composition of vegetation near a SO₂ source at Fox Creek, Alberta, Canada.' *Oecologia*, 44(2) pp. 247–257.
- Casquero-Vera, J. A., Lyamani, H., Titos, G., Borrás, E., Olmo, F. J. and Alados-Arboledas, L. (2019) 'Impact of primary NO₂ emissions at different urban sites exceeding the European NO₂ standard limit.' *Science of the Total Environment*. Elsevier B.V., 646(2) pp. 1117–1125.
- Castello, M. and Skert, N. (2005) 'Evaluation of lichen diversity as an indicator of environmental quality in the North Adriatic submediterranean region.' *Science of the Total Environment*, 336(1–3) pp. 201–214.
- Cattle, J. A., McBratney, A. B. and Minasny, B. (2002) 'Kriging Method Evaluation for Assessing the Spatial Distribution of Urban Soil Lead Contamination.' *Journal of Environment Quality*, 31(5) p. 1576.
- Chapin, F. S., Bloom, A. J., Field, C. B. and Waring, R. H. (1987) 'Plant responses to multiple environmental factors.' *BioScience*, 37(1) pp. 49–57.
- Charron, A., Polo-Rehn, L., Besombes, J.-L., Golly, B., Buisson, C., Chanut, H., Marchand, N., Guillaud, G. and Jaffrezo, J.-L. (2019) 'Identification and quantification of particulate tracers of exhaust and non-exhaust vehicle emissions.' *Atmospheric Chemistry and Physics Discussions*, October, pp. 1–32.
- Chen, H., Kwong, J. C., Copes, R., Tu, K., Villeneuve, P. J., van Donkelaar, A., Hystad, P., Martin, R. V., Murray, B. J., Jessiman, B., Wilton, A. S., Kopp, A. and Burnett, R. T. (2017) 'Living near major roads and the incidence of dementia, Parkinson's disease, and multiple sclerosis: a population-based cohort study.' *The Lancet*, 389(10070) pp. 718–726.
- Chiarenzelli, J. R., Aspler, L. B., Ozarko, D. L., Hall, G. E. M., Powis, K. B. and Donaldson, J. A. (1997) 'Heavy metals in lichens, southern district of Keewatin, Northwest Territories, Canada.' *Chemosphere*.
- Cipollini, M. L., Drake, B. G. and Whigham, D. (1993) 'International Association for Ecology Effects of Elevated CO₂ on Growth and Carbon / Nutrient Balance in the Deciduous Woody.' *Oecologia*, 96(3) pp. 339–346.
- Cislaghi, C. and Nimis, P. L. (1997) 'Lichens, air pollution and lung cancer.' *Nature*, 387(6632) pp. 463–464.
- City of Trees (2018) *City of Trees - About City of Trees*. [Online] [Accessed on 27th May 2018] <http://www.cityoftrees.org.uk/about-city-trees>.
- Clapp, L. J. and Jenkin, M. E. (2001) 'Analysis of the relationship between ambient levels of O₃, NO₂ and NO as a function of NO_x in the UK.' *Atmospheric Environment*, 35(36) pp. 6391–6405.
- Clark, I. (ed.) (1979) *Practical Geostatistics*. London: Applied Science Publishers Ltd.

- Clark, I. and Harper, W. V. (eds) (2007a) *Practical Geostatistics 2000: Answers to the Exercises*. Scotland: Geostokos (Ecosse) Ltd.,
- Clark, I. and Harper, W. V. (eds) (2007b) *Practical Geostatistics 2000*. Scotland: Geostokos (Ecosse) Ltd.
- Clark, I. and Harper, W. V. (eds) (2008) *Practical Geostatistics 2000: Case Studies*. Scotland: Geostokos (Ecosse) Ltd.
- Coccaro, D. M. B., Saiki, M., Vasconcellos, M. B. A. and Marecelli, M. P. (2000) 'Analysis of *Canoparmelia texana* lichens collected in Brazil by neutron activation analysis.' *In Biomonitoring of Atmospheric Pollution (with Emphasis on Trace Elements) — BioMap. Proc. of an Int. Workshop Organized by the International Atomic Energy Agency in Cooperation with the Instituto Tecnológico Nuclear*. Lisbon, Portugal, pp. 143–148.
- Cole, T. C. H. (2015) *Wörterbuch der Biologie*. 4. Auflage, Berlin, Heidelberg: Springer Verlag.
- Coleman, P. J., Lee, R. G. M., Alcock, R. E. and Jones, K. C. (1997) 'Observations on PAH, PCB, and PCDD/F trends in U.K. Urban air, 1991- 1995.' *Environmental Science and Technology*, 31(7) pp. 2120–2124.
- Collins, C. R. and Farrar, J. F. (1978) 'Structural resistances to mass transfer in the lichen *Xanthoria parietina*.' *New Phytologist*, 81(1) pp. 71–83.
- COMEAP (2018) *Associations of long-term average concentrations of nitrogen dioxide with mortality*.
- Concha-Graña, E., Muniategui-Lorenzo, S., De Nicola, F., Aboal, J. R., Rey-Asensio, A. I., Giordano, S., Reski, R., López-Mahía, P. and Prada-Rodríguez, D. (2015) 'Matrix solid phase dispersion method for determination of polycyclic aromatic hydrocarbons in moss.' *Journal of Chromatography A*, 1406, August, pp. 19–26.
- Conti, M. E. and Cecchetti, G. (2001) 'Biological monitoring: lichens as bioindicators of air pollution assessment - A review.' *Environmental Pollution*, 114(3) pp. 471–492.
- Conti, M. E. and Tudino, M. B. (2016) 'Lichens as Biomonitors of Heavy-Metal Pollution.' *Comprehensive Analytical Chemistry*, 73 pp. 117–145.
- Conti, M. E., Tudino, M., Stripeikis, J. and Cecchetti, G. (2004) 'Heavy metal accumulation in the Lichen *Evernia prunastri* transplanted at urban, rural and industrial sites in Central Italy.' *Journal of Atmospheric Chemistry*, 49(1–3) pp. 83–94.
- Cooper, E., Arioli, M., Carrigan, A. and Lindau, L. A. (2014) 'Exhaust emissions of transit buses: Brazil and India case studies.' *Research in Transportation Economics*. Elsevier Ltd, 48 pp. 323–329.
- Corapi, A., Gallo, L., Nicolardi, V., Lucadamo, L. and Loppi, S. (2014) 'Temporal trends of element concentrations and ecophysiological parameters in the lichen *Pseudevernia furfuracea* transplanted in and around an industrial area of S Italy.' *Environmental Monitoring and Assessment*.
- Cortecci, G. and Longinelli, A. (1970) 'Isotopic composition of sulfate in rain water, Pisa, Italy.' *Earth and Planetary Science Letters*.
- Coskun, M., Steinnes, E., Coskun, M. and Cayir, A. (2009) 'Comparison of epigeic moss (*Hypnum cupressiforme*) and lichen (*Cladonia rangiformis*) as biomonitor species of atmospheric metal deposition.' *Bulletin of Environmental Contamination and Toxicology*.
- Costa, M. (1997) 'Toxicity and carcinogenicity of Cr(VI) in animal models and humans.' *Critical Reviews in Toxicology*.
- Costa, M., Yan, Y. and Salnikow, K. (2003) 'Molecular mechanisms of nickel carcinogenesis: gene silencing by nickel delivery to the nucleus and gene activation/inactivation by nickel-induced cell signaling.' *Journal of Environmental Monitoring*, 5(2) pp. 222–223.
- Cox, E. and Goggins, D. (2018) *Atmosphere: Towards a proper Strategy for Tackling Greater Manchester's Air Pollution Crisis*. Greater Manchester.

- Crittenden, P. D. (1994) 'Does nitrogen supply limit the growth of lichens?' *Cryptogamic Botany*, 4 pp. 143–155.
- Crittenden, P. D. (1996) 'The Effect of Oxygen Deprivation on Inorganic Nitrogen Uptake in an Antarctic Macrolichen.' *The Lichenologist*, 28(4) p. 347.
- Crittenden, P. D. (1998) 'Nutrient exchange in an Antarctic macrolichen during summer snowfall-snow melt events.' *New Phytologist*, 139(4) pp. 697–707.
- Cuny, D., Van Haluwyn, C., Shirali, P., Zerimech, F., Jérôme, L. and Haguenoer, J. M. (2004) 'Cellular impact of metal trace elements in terricolous lichen *Diploschistes muscorum* (Scop.) R. Sant. - Identification of oxidative stress biomarkers.' *Water, Air, and Soil Pollution*.
- Dadvand, P., de Nazelle, A., Figueras, F., Basagaña, X., Su, J., Amoly, E., Jerrett, M., Vrijheid, M., Sunyer, J. and Nieuwenhuijsen, M. J. (2012) 'Green space, health inequality and pregnancy.' *Environment International*. Elsevier Ltd, 40(1) pp. 110–115.
- Dadvand, P., Sunyer, J., Basagaña, X., Ballester, F., Lertxundi, A., Fernández-Somoano, A., Estarlich, M., García-Esteban, R., Mendez, M. A. and Nieuwenhuijsen, M. J. (2012) 'Surrounding Greenness and Pregnancy Outcomes in Four Spanish Birth Cohorts.' *Environmental Health Perspectives*, 120(10) pp. 1481–1487.
- Dahlman, L., Palmqvist, K. and Näsholm, T. (2002) 'Growth, nitrogen uptake, and resource allocation in the two tripartite lichens *Nephroma arcticum* and *Peltigera aphthosa* during nitrogen stress.' *New Phytologist*, 153(2) pp. 307–315.
- Dahlman, L., Persson, J., Näsholm, T. and Palmqvist, K. (2003) 'Carbon and nitrogen distribution in the green algal lichens *Hypogymnia physodes* and *Platismatia glauca* in relation to nutrient supply.' *Planta*.
- Dahlman, L., Persson, J., Palmqvist, K. and Näsholm, T. (2004) 'Organic and inorganic nitrogen uptake in lichens.' *Planta*, 219(3) pp. 459–67.
- Dämmgen, U., Walker, K., Grünhage, L. and Jäger, H.-J. (2011) 'The Atmospheric Sulphur Cycle.' *In*.
- Davies, L., Bates, J. W., Bell, J. N. B., James, P. W. and Purvis, O. W. (2007) 'Diversity and sensitivity of epiphytes to oxides of nitrogen in London.' *Environmental Pollution*, 146(2) pp. 299–310.
- Defra (2018a) *Air Pollution in the UK 2017*.
- Defra (2018b) *Road traffic statistics - Local authority: Manchester*. [Online] [Accessed on 31st May 2019] <https://roadtraffic.dft.gov.uk/local-authorities/85>.
- DEFRA (2003) 'Part IV of Environment Act 1995: Local Air Quality Management Technical Guidance. LAQM.TG(03).' Department for Environment, Food & Rural Affairs.
- DEFRA (2007) *The Air Quality Strategy for England, Scotland, Wales and Northern Ireland: Volume 1*.
- DEFRA (2009) 'Local Air Quality Management.' *Environment*, (February).
- DEFRA (2010) *The Air Quality Standards Regulation 2010*. United Kingdom.
- DEFRA (2011) 'What are the causes of air Pollution' pp. 1–5.
- DEFRA (2014a) *Air Pollution Background Concentration Maps: A User Guide for Local Authorities*. (v1.0).
- DEFRA (2014b) *PAH Andersen - Manchester Law Courts*. [Online] [Accessed on 7th January 2018] https://uk-air.defra.gov.uk/data/non-auto-data?uka_id=UKA00185&network=pah&s=View+Site.
- DEFRA (2014c) *Polycyclic Aromatic Hydrocarbons (PAH) - network information*. [Online] [Accessed on 7th January 2018] <https://uk-air.defra.gov.uk/networks/network-info?view=pah>.
- DEFRA (2017a) 'Air Pollution in the UK 2016.' *Annual Report 2016 Issue 2*, (September) p. 131.
- DEFRA (2017b) 'Air Quality A Briefing for Directors of Public Health.' *Department for*

- Environment Food & Rural Affairs*, (March) p. 11.
- DEFRA (2017c) *Background Mapping Data for Local Authorities*. [Online] [Accessed on 1st October 2019] <https://uk-air.defra.gov.uk/data/laqm-background-home>.
- DEFRA (2017d) *Background Mapping data for local authorities - 2017*. [Online] [Accessed on 12th December 2018] <https://uk-air.defra.gov.uk/data/laqm-background-home>.
- DEFRA (2017e) *Defra National Statistics Release: Air quality statistics in the UK 1987 to 2016*. London (National Statistics).
- DEFRA (2018a) *Air Quality England - webpage: Manchester Piccadilly*. [Online] [Accessed on 25th September 2018] http://www.airqualityengland.co.uk/site/latest?site_id=MAN3.
- DEFRA (2018b) *Air Quality England - webpage: Oxford Road*. [Online] [Accessed on 25th September 2018] http://www.airqualityengland.co.uk/site/data?site_id=MAN1.
- DEFRA (2018c) *Clean Air Strategy 2018*. London.
- DEFRA (2018d) *UK Air - Polycyclic Aromatic Hydrocarbons (PAH)*. [Online] [Accessed on 13th December 2018] <https://uk-air.defra.gov.uk/networks/network-info?view=pah>.
- DEFRA (2019a) *Clean Air Strategy*.
- DEFRA (2019b) *UK Air - Monitoring Networks*. [Online] [Accessed on 17th April 2019] <https://uk-air.defra.gov.uk/networks/>.
- DEFRA and DfT (2017) *UK plan for tackling roadside nitrogen dioxide concentrations: Detailed plan*.
- Degraeuwe, B., Thunis, P., Clappier, A., Weiss, M., Lefebvre, W., Janssen, S. and Vranckx, S. (2017) 'Impact of passenger car NO_x emissions on urban NO₂ pollution – Scenario analysis for 8 European cities.' *Atmospheric Environment*. Elsevier, 171(2) pp. 330–337.
- Demetriades, A. (2011) 'Understanding the Quality of Chemical Data from the Urban Environment – Part 2: Measurement Uncertainty in the Decision-Making.' In Locutura, J., Demetriades, A., and Ottesen, R. T. (eds) *Mapping the chemical environment in urban areas*. 1st ed., Oxford - UK: John Wiley & Sons Ltd, pp. 77–98.
- Desnoues, N., Lin, M., Guo, X., Ma, L., Carreño-Lopez, R. and Elmerich, C. (2003) 'Nitrogen fixation genetics and regulation in a *Pseudomonas stutzeri* strain associated with rice.' *Microbiology*.
- Desyana, R. D., Sulistyantara, B., Nasrullah, N. and Fatimah, I. S. (2017) 'Study of the effectiveness of several tree canopy types on roadside green belt in influencing the distribution of NO₂ gas emitted from transportation.' *IOP Conference Series: Earth and Environmental Science*, 58.
- DfT (2017a) *Road traffic statistics*. [Online] <https://www.gov.uk/government/publications/road-traffic-estimates-great-britain-jan-to-mar-q1-2014%5Cnhttps://www.gov.uk/government/collections/road-traffic-statistics>.
- DfT (2017b) *Vehicle Licensing Statistics: 2017 (Revised)*.
- Digimap - Ordnance Survey (2016) *OS Open Roads*. [Online] [Accessed on 17th June 2017] <https://www.ordnancesurvey.co.uk/business-and-government/products/os-open-roads.html>.
- Digimap - Ordnance Survey (2017) *OS Building Heights (Alpha)*. [Online] [Accessed on 11th December 2018] https://digimap.edina.ac.uk/webhelp/os/data_information/os_products/os_building_heights.htm.
- Digimap - Ordnance Survey (2018) *OS Open Greenspace*. [Online] [Accessed on 12th December 2018] https://digimap.edina.ac.uk/webhelp/os/data_information/os_products/os_open_grreenspace.htm.

- Dijkema, M. B. A., van Strien, R. T., van der Zee, S. C., Mallant, S. F., Fischer, P., Hoek, G., Brunekreef, B. and Gehring, U. (2016) 'Spatial variation in nitrogen dioxide concentrations and cardiopulmonary hospital admissions.' *Environmental Research*. Elsevier, 151 pp. 721–727.
- Van Dobben, H. F. and Braak, C. J. F. te. (1999) 'Ranking of epiphytic lichen sensitivity to air pollution using survey data: A comparison of indicator scales.' *Lichenologist*.
- Van Dobben, H. F. and Ter Braak, C. J. F. (1998) 'Effects of atmospheric NH₃ on epiphytic lichens in the Netherlands: The pitfalls of biological monitoring.' *Atmospheric Environment*, 32(3) pp. 551–557.
- Van Dobben, H. F., Wolterbeek, H. T., Wamelink, G. W. W. and Ter Braak, C. J. F. (2001) 'Relationship between epiphytic lichens, trace elements and gaseous atmospheric pollutants.' *Environmental Pollution*, 112(2) pp. 163–169.
- Dobre, A., Arnold, S. J., Smalley, R. J., Boddy, J. W. D., Barlow, J. F., Tomlin, A. S. and Belcher, S. E. (2005) 'Flow field measurements in the proximity of an urban intersection in London, UK.' *Atmospheric Environment*, 39(26) pp. 4647–4657.
- Dobson, F. S. (2011) *Lichens - An Illustrated Guide to the British and Irish Species*. 6th ed., Slough: The Richmond Publishing Co. Ltd.
- Doğrul Demiray, A., Yolcubal, I., Akyol, N. H. and Çobanoğlu, G. (2012) 'Biomonitoring of airborne metals using the Lichen *Xanthoria parietina* in Kocaeli Province, Turkey.' *Ecological Indicators*, 18 pp. 632–643.
- Domeño, C., Blasco, M., Sánchez, C. and Nerín, C. (2006) 'A fast extraction technique for extracting polycyclic aromatic hydrocarbons (PAHs) from lichens samples used as biomonitors of air pollution: Dynamic sonication versus other methods.' *Analytica Chimica Acta*, 569(1–2) pp. 103–112.
- Domínguez-Morueco, N., Augusto, S., Trabalón, L., Pocurull, E., Borrull, F., Schuhmacher, M., Domingo, J. L. and Nadal, M. (2015) 'Monitoring PAHs in the petrochemical area of Tarragona County, Spain: comparing passive air samplers with lichen transplants.' *Environmental Science and Pollution Research*. Environmental Science and Pollution Research pp. 11890–11900.
- Dongarrà, G. and Varrica, D. (1998) 'The presence of heavy metals in air particulate at Vulcano island (Italy).' *Science of the Total Environment*, 212(1) pp. 1–9.
- Dore, C., Murrells, T., Passant, N., Hobson, M., Thistlethwaite, G., Wagner, a, Li, Y., Bush, T., King, K., Norris, J., Coleman, P., Walker, C., Stewart, R., Tsagatakis, I., Conolly, C., Brophy, N. and Hann, M. (2008) 'UK emissions of air pollutants 1970 to 2006.' *AEA Energy &*
- Douglas, I., Hodgson, R. and Lawson, N. (2002) 'Industry, environment and health through 200 years in Manchester.' *Ecological Economics*, 41(2) pp. 235–255.
- Dzubaj, A., Bačkor, M., Tomko, J., Peli, E. and Tuba, Z. (2008) 'Tolerance of the lichen *Xanthoria parietina* (L.) Th. Fr. to metal stress.' *Ecotoxicology and Environmental Safety*, 70(2) pp. 319–326.
- Eberlein-König, B., Przybilla, B., Kühnl, P., Pechak, J., Gebefügi, I., Kleinschmidt, J. and Ring, J. (1998) 'Influence of airborne nitrogen dioxide or formaldehyde on parameters of skin function and cellular activation in patients with atopic eczema and control subjects.' *Journal of Allergy and Clinical Immunology*, 101(1) pp. 141–143.
- EEA (2015) *Air quality in Europe — 2015 report*. EEA Report No 5/2015.
- EEA (2016) *Air pollutant emissions data viewer (Gothenburg Protocol, LRTAP Convention) 1990 - 2016*.
- Eliasson, I., Offerle, B., Grimmond, C. S. B. and Lindqvist, S. (2006) 'Wind fields and turbulence statistics in an urban street canyon.' *Atmospheric Environment*, 40(1) pp. 1–16.
- Elliott, E. M., Kendall, C., Wankel, S. D., Burns, D. A., Boyer, E. W., Harlin, K., Bain, D. J. and Butler, T. J. (2007) 'Nitrogen isotopes as indicators of NO_x source contributions

- to atmospheric nitrate deposition across the midwestern and northeastern United States.' *Environmental Science and Technology*, 41(22) pp. 7661–7667.
- Endlicher, W. (2012) *Einführung in die Stadtökologie - Grundzüge des urbanen Mensch-Umwelt-Systems*. Stuttgart: Verlag Eugen Ulmer, UTB.
- Environment Agency (2018) *The state of the environment: air quality*. Rotherham.
- EPA (1999) *Method TO-13A: Compendium of Methods for the Determination of Toxic Organic Compounds in Ambient Air Second Edition Compendium Method TO-13A Determination of Polycyclic Aromatic Hydrocarbons (PAHs) in Ambient Air Using Gas Chromatography / Mass Spectrom*. Epa. Cincinnati, OH.
- EPA (2007) *Method 9210A - Potentiometric Determination of Nitrate*.
- EPA (2008) 'Idling Vehicle Emissions for Passenger Cars, Light-Duty Trucks, and Heavy-Duty Trucks.' U.S. Environmental Protection Agency (EPA) p. 6.
- EPA (2014) 'Priority Pollutant List.' U.S. Environmental Protection Agency.
- EPRI (2008) *Examination of the Sources of Polycyclic Aromatic Hydrocarbon (PAH) in Urban Background Soil*. Paolo Alto, CA.
- ESRI (2016) 'ArcGIS Desktop: ArcMap 10.5.' Redlands, CA: Environmental Research Institute.
- ESRI (2019) *ArcGIS Pro tool reference*. [Online] [Accessed on 14th February 2019] <http://pro.arcgis.com/en/pro-app/tool-reference/main/arcgis-pro-tool-reference.htm>.
- Esslab (2017) *Inorganic Ventures - Interactive Periodic Table*. [Online] [Accessed on 4th December 2017] <http://www.esslab.com/iv-periodic.html>.
- Estellano, V. H., Pozo, K., Harner, T., Corsolini, S. and Focardi, S. (2012) 'Using PUF disk passive samplers to simultaneously measure air concentrations of persistent organic pollutants (POPs) across the Tuscany region, Italy.' *Atmospheric Pollution Research*. Elsevier, 3(1) pp. 88–94.
- EU (2004) 'Directive 2004/107/EC of the European Parliament and of the Council relating to arsenic, cadmium, mercury, nickel and polycyclic aromatic hydrocarbons in ambient air.' *Official Journal of the European Union*, L23/3 pp. 3–16.
- EU (2008) 'Directive 2008/50/EC of the European Parliament and of the Council of 21 May 2008 on ambient air quality and cleaner air for Europe.' *Official Journal of the European Union*, 152(51) pp. 1–44.
- European Commission (2001) *Ambient air pollution by Polycyclic Aromatic Hydrocarbons (PAH) - Position Paper*.
- European Commission (2018) *Air Quality Standards*. [Online] [Accessed on 11th October 2018] <http://ec.europa.eu/environment/air/quality/standards.htm>.
- European Environment Agency (2018) 'Exhaust emissions from road transport – Update Jul. 2018.' *EMEP/EEA* p. 143.
- European Medicines Agency (1995) *Note for Guidance on Validation of Analytical Procedures: Text and Methodology (CPMP/ICH/381/95)*. London.
- Evans, A. N. G. (1996) *Characterizing atmospheric sulphur using lichen and rain in eastern Newfoundland*. Memorial University of Newfoundland, Canada.
- Evci, Y. M., Esen, F. and Taşdemir, Y. (2016) 'Monitoring of Long-Term Outdoor Concentrations of PAHs with Passive Air Samplers and Comparison with Meteorological Data.' *Archives of Environmental Contamination and Toxicology*, 71(2) pp. 246–256.
- Falla, J., Laval-Gilly, P., Henryon, M., Morlot, D. and Ferard, J. F. (2000) 'Biological air quality monitoring: A review.' *Environmental Monitoring and Assessment*.
- Fang, C., Liu, H., Li, G., Sun, D. and Miao, Z. (2015) 'Estimating the impact of urbanization on air quality in China using spatial regression models.' *Sustainability (Switzerland)*, 7(11) pp. 15570–15592.
- Fang, G. C., Chang, K. F., Lu, C. and Bai, H. (2002) 'Toxic equivalency factors study of polycyclic aromatic hydrocarbons (PAHs) in Taichung City, Taiwan.' *Toxicology and*

Industrial Health, 18(6) pp. 279–288.

- Fantozzi, F., Monaci, F., Blanusa, T. and Bargagli, R. (2015) 'Spatio-temporal variations of ozone and nitrogen dioxide concentrations under urban trees and in a nearby open area.' *Urban Climate*. Elsevier B.V., 12(2) pp. 119–127.
- Farmer, P. B. (1997) 'Diesel fuel and exhaust emissions: Is there a human carcinogenic risk?' *The Lancet*, 350(9085) p. 1118.
- Faustini, A., Rapp, R. and Forastiere, F. (2014) 'Nitrogen dioxide and mortality: Review and meta-analysis of long-term studies.' *European Respiratory Journal*.
- Felix, J. D. and Elliott, E. M. (2014) 'Isotopic composition of passively collected nitrogen dioxide emissions: Vehicle, soil and livestock source signatures.' *Atmospheric Environment*. Elsevier Ltd, 92 pp. 359–366.
- Felix, J. D., Elliott, E. M., Gish, T. J., McConnell, L. L. and Shaw, S. L. (2013) 'Characterizing the isotopic composition of atmospheric ammonia emission sources using passive samplers and a combined oxidation-bacterial denitrifier approach.' *Rapid Communications in Mass Spectrometry*, 27(20) pp. 2239–2246.
- Felix, J. D., Elliott, E. M. and Shaw, S. L. (2012) 'Nitrogen isotopic composition of coal-fired power plant NO_x: Influence of emission controls and implications for global emission inventories.' *Environmental Science and Technology*, 46(6) pp. 3528–3535.
- Fenger, J. (1999) 'Urban air quality.' *Atmospheric Environment*, 33(29) pp. 4877–4900.
- Fenger, J. (2009) 'Air pollution in the last 50 years – From local to global.' *Atmospheric Environment*. Elsevier Ltd, 43(1) pp. 13–22.
- Fernández, R., Galarraga, F., Benzo, Z., Márquez, G., Fernández, A. J., Requiza, M. G. and Hernández, J. (2011) 'Lichens as biomonitors for the determination of polycyclic aromatic hydrocarbons (PAHs) in Caracas Valley, Venezuela.' *International Journal of Environmental Analytical Chemistry*, 91(3) pp. 230–240.
- Finlayson-Pitts, B. J. and Pitts, J. N. (1999) *Chemistry of the Upper and Lower Atmosphere - Theory, Experiments, and Applications*. 1st ed., New York: Academic Press.
- Fogel, M. L., Wooller, M. J., Cheeseman, J., Smallwood, B. J., Roberts, Q., Romero, I. and Meyers, M. J. (2008) 'Unusually negative nitrogen isotopic compositions ($\delta^{15}\text{N}$) of mangroves and lichens in an oligotrophic, microbially-influenced ecosystem.' *Biogeosciences*, 5(6) pp. 1693–1704.
- Fontaras, G., Franco, V., Dilara, P., Martini, G. and Manfredi, U. (2014) 'Development and review of Euro 5 passenger car emission factors based on experimental results over various driving cycles.' *Science of the Total Environment*.
- Forbes, P. B. C. (2015) 'Monitoring of Air Pollutants: Sampling, Sample Preparation and Analytical Techniques.' In Forbes, P. B. C. (ed.) *Comprehensive Analytical Chemistry*. Amsterdam, Boston, London, New York, Oxford, Paris, San Diego, San Francisco, Singapore, Sydney, Tokyo: Elsevier B.V., pp. 239–267.
- Forbes, P. B. C., van der Wat, L. and Kroukamp, E. M. (2015) 'Monitoring of Air Pollutants Sampling, Sample Preparation and Analytical Techniques - Biomonitors.' In Forbes, P. (ed.) *Comprehensive Analytical Chemistry*. Elsevier B.V., pp. 53–108.
- Forman, R. T. T. (2014) 'Urban Air.' In Forman, R. T. T. (ed.) *Urban Ecology - Science of Cities*. Cambridge: Cambridge University Press, pp. 125–148.
- Fotheringham, A. S., Brunson, C. and Charlton, M. (eds) (2002) *Geographically weighted regression: the analysis of spatially varying relationships*. Chichester (UK).
- Franzen-Reuter, I. (2004) *Untersuchungen zu den Auswirkungen atmosphärischer Stickstoffeinträge auf epiphytische Flechten und Moose im Hinblick auf die Bioindikation*. Rheinischen Friedrich-Wilhelms-Universität Bonn.
- Fraser, M. P., Cass, G. R., Simoneit, B. R. T. and Rasmussen, R. A. (1998) 'Air quality model evaluation data for organics. 5. C₆-C₂₂ nonpolar and semipolar aromatic compounds.' *Environmental Science and Technology*.
- Frati, L. and Brunialti, G. (2006) 'Long-Term Biomonitoring with Lichens: Comparing Data from Different Sampling Procedures.' *Environmental Monitoring and Assessment*,

119(1–3) pp. 391–404.

- Frati, L., Caprasecca, E., Santoni, S., Gaggi, C., Guttova, A., Gaudino, S., Pati, A., Rosamilia, S., Pirintsos, S. A. and Loppi, S. (2006) 'Effects of NO₂ and NH₃ from road traffic on epiphytic lichens.' *Environmental Pollution*, 142(1) pp. 58–64.
- Frati, L., Santoni, S., Nicolardi, V., Gaggi, C., Brunialti, G., Guttova, A., Gaudino, S., Pati, A., Pirintsos, S. A. and Loppi, S. (2007) 'Lichen biomonitoring of ammonia emission and nitrogen deposition around a pig stockfarm.' *Environmental Pollution*, 146(2) pp. 311–316.
- Freer-Smith, P. H., Holloway, S. and Goodman, A. (1997) 'The uptake of particulates by an urban woodland: Site description and particulate composition.' *Environmental Pollution*.
- Freyer, H. D. (1978) 'Seasonal trends of NH + 4 and NO – 3 nitrogen isotope composition in rain collected at Jülich, Germany.' *Tellus*, 30(3) pp. 83–92.
- Friends of the Earth (UK) (2017) *Clean Air Campaign*. [Online] [Accessed on 29th May 2019] <https://friendsoftheearth.uk/clean-air/results>.
- Fry, B. (2006) *Stable Isotope Ecology*. 3rd ed., New York: Springer Science + Business Media, LLC.
- Fu, X., Liu, J., Ban-Weiss, G. A., Zhang, J., Huang, X., Ouyang, B., Popoola, O. and Tao, S. (2017) 'Effects of canyon geometry on the distribution of traffic-related air pollution in a large urban area: Implications of a multi-canyon air pollution dispersion model.' *Atmospheric Environment*. Elsevier Ltd, 165 pp. 111–121.
- Gadsdon, S. R., Dagley, J. R., Wolseley, P. A. and Power, S. A. (2010) 'Relationships between lichen community composition and concentrations of NO₂ and NH₃.' *Environmental Pollution*. Elsevier Ltd, 158(8) pp. 2553–2560.
- Gadsdon, S. R. and Power, S. A. (2009) 'Quantifying local traffic contributions to NO₂ and NH₃ concentrations in natural habitats.' *Environmental Pollution*. Elsevier Ltd, 157(10) pp. 2845–2852.
- Gaio-Oliveira, G., Branquinho, C., Maguas, C. and Martins-Loucao, M. A. (2001) 'The concentration of nitrogen in nitrophilous and non-nitrophilous lichen species.' *Symbiosis*, 31(1–3) pp. 187–199.
- Gaio-Oliveira, G., Dahlman, L., Palmqvist, K. and Máguas, C. (2004) 'Ammonium uptake in the nitrophytic lichen *Xanthoria parietina* and its effects on vitality and balance between symbionts.' *The Lichenologist*, 36(1) pp. 75–86.
- Gaio-Oliveira, G., Dahlman, L., Palmqvist, K. and Máguas, C. (2005) 'Responses of the lichen *Xanthoria parietina* (L.) Th. Fr. to varying thallus nitrogen concentrations.' *Lichenologist*, 37(2) pp. 171–179.
- Gaio-Oliveira, G., Dahlman, L., Palmqvist, K., Martins-Loução, M. A. and Máguas, C. (2005) 'Nitrogen uptake in relation to excess supply and its effects on the lichens *Evernia prunastri* (L.) Ach and *Xanthoria parietina* (L.) Th. Fr.' *Planta*, 220(5) pp. 794–803.
- Gair, A. J. and Penkett, S. A. (1995) 'The effects of wind speed and turbulence on the performance of diffusion tube samplers.' *Atmospheric Environment*.
- Galimov, E. M. (2000) 'Carbon isotope composition of Antarctic plants.' *Geochimica et Cosmochimica Acta*, 64(10) pp. 1737–1739.
- Galloway, J. N., Townsend, A. R., Erisman, J. W., Bekunda, M., Cai, Z., Freney, J. R., Martinelli, L. A., Seitzinger, S. P. and Sutton, M. A. (2008) 'Transformation of the Nitrogen Cycle: Recent Trends, Questions, and Potential Solutions.' *Science*, 320(May) pp. 889–892.
- Garrido, A., Jiménez-Guerrero, P. and Ratola, N. (2014) 'Levels, trends and health concerns of atmospheric PAHs in Europe.' *Atmospheric Environment*, 99, December, pp. 474–484.
- Garty, J. (2001) 'Biomonitoring Atmospheric Heavy Metals with Lichens: Theory and Application.' *Critical Reviews in Plant Sciences*, 20(4) pp. 309–372.
- Garty, J., Galun, M. and Kessel, M. (1979) 'Localization of heavy metals and other elements

in the lichen thallus.' *New Phytologist*.

- Garza, A., Vega, R. and Soto, E. (2006) 'Cellular mechanisms of lead neurotoxicity.' *Medical science monitor : international medical journal of experimental and clinical research*.
- Gaston, K. (2010) 'Urban environments and ecosystem functions.' *Urban ecology*. ... pp. 35–52.
- Gauslaa, Y. (2014) 'Rain, dew, and humid air as drivers of morphology, function and spatial distribution in epiphytic lichens.' *The Lichenologist*, 46(01) pp. 1–16.
- Gauslaa, Y., Yemets, O. A., Asplund, J. and Solhaug, K. A. (2016) 'Carbon based secondary compounds do not provide protection against heavy metal road pollutants in epiphytic macrolichens.' *Science of the Total Environment*. Elsevier B.V., 541 pp. 795–801.
- Gebel, T. (2000) 'Toxicology of platinum, palladium, rhodium, and their compounds.' In Zereini, F. and Alt, F. (eds) *Anthropogenic Platinum-Group Element Emissions*. Berlin, Heidelberg: Springer Akademischer Verlag, pp. 245–255.
- Gehrig, R., Hill, M., Lienemann, P., Zwicky, C. N., Bukowiecki, N., Weingartner, E., Baltensperger, U. and Buchmann, B. (2007) 'Contribution of railway traffic to local PM10 concentrations in Switzerland.' *Atmospheric Environment*, 41(5) pp. 923–933.
- Gerboles, M., Buzica, D. and Amantini, L. (2005) 'Modification of the Palmes diffusion tube and semi-empirical modelling of the uptake rate for monitoring nitrogen dioxide.' *Atmospheric Environment*.
- Gerdol, R., Bragazza, L., Marchesini, R., Medici, A., Pedrini, P., Benedetti, S., Bovolenta, A. and Coppi, S. (2002) 'Use of moss (*Tortula muralis* Hedw.) for monitoring organic and inorganic air pollution in urban and rural sites in Northern Italy.' *Atmospheric Environment*.
- Gerdol, R., Marchesini, R., Iacumin, P. and Brancaleoni, L. (2014) 'Monitoring temporal trends of air pollution in an urban area using mosses and lichens as biomonitors.' *Chemosphere*. Elsevier Ltd, 108 pp. 388–395.
- Geyer, A., Alicke, B., Ackermann, R., Martinez, M., Harder, M., Brune, W., di Carlo, P., Williams, E., Jobson, T., Hall, S., Shetter, R. and Stutz, J. (2003) 'Direct observations of daytime NO₃: Implications for urban boundary layer chemistry.' *Journal of Geophysical Research*, 108(D12) p. 4368.
- Gilbert, N. L., Woodhouse, S., Stieb, D. M. and Brook, J. R. (2003) 'Ambient nitrogen dioxide and distance from a major highway.' *Science of the Total Environment*, 312(1–3) pp. 43–46.
- Gill, S. E., Handley, J. F., Ennos, A. R., Pauleit, S., Theuray, N. and Lindley, S. J. (2008) 'Characterising the urban environment of UK cities and towns: A template for landscape planning.' *Landscape and Urban Planning*, 87(3) pp. 210–222.
- Giordani, P. (2007) 'Is the diversity of epiphytic lichens a reliable indicator of air pollution? A case study from Italy.' *Environmental Pollution*, 146(2) pp. 317–323.
- Giordani, P. and Brunialti, G. (2015) 'Sampling and Interpreting Lichen Diversity Data for Biomonitoring Purposes.' In Upreti, D. K., Divakar, P. K., Shukla, V., and Bajpai, R. (eds) *Recent Advances in Lichenology: Modern Methods and Approaches in Biomonitoring and Bioprospection, Volume 1*. New Delhi: Springer India, pp. 19–45.
- Giordani, P., Brunialti, G. and Alleleo, D. (2002) 'Effects of atmospheric pollution on lichen biodiversity (LB) in a Mediterranean region (Liguria, northwest Italy).' *Environmental Pollution*, 118(1) pp. 53–64.
- Giordani, P., Brunialti, G., Calderisi, M., Malaspina, P. and Frati, L. (2018) 'Beta diversity and similarity of lichen communities as a sign of the times.' *The Lichenologist*, 50(03) pp. 371–383.
- GMCA and TfGM (2019) *Clean Air Greater Manchester*. [Online] [Accessed on 19th April 2019] <https://cleanairgm.com/>.
- GMUE (2017) *Distribution of Fungi and Lichen in Greater Manchester*. [Online] [Accessed on 28th May 2019] <https://www.gbif.org/dataset/0415af37-8cdd-4bb0-b16c->

e06783d19d71.

- Godinho, R. M., Verburg, T. G., Freitas, M. C. and Wolterbeek, H. T. (2009) 'Accumulation of trace elements in the peripheral and central parts of two species of epiphytic lichens transplanted to a polluted site in Portugal.' *Environmental Pollution*.
- Godinho, R. M., Verburg, T. G., Freitas, M. do C. and Wolterbeek, H. T. (2011) 'Dynamics of element accumulation and release of *Flavoparmelia caperata* during a long-term field transplant experiment.' *International Journal of Environment and Health*, 5(1/2) p. 49.
- Godinho, R. M., Wolterbeek, H. T., Verburg, T. and Freitas, M. C. (2008) 'Bioaccumulation behaviour of transplants of the lichen *Flavoparmelia caperata* in relation to total deposition at a polluted location in Portugal.' *Environmental Pollution*, 151(2) pp. 318–325.
- Gombert, S., Asta, J. and Seaward, M. R. . (2003) 'Correlation between the nitrogen concentration of two epiphytic lichens and the traffic density in an urban area.' *Environmental Pollution*, 123(2) pp. 281–290.
- Gombert, S., Asta, J. and Seaward, M. R. D. (2004) 'Assessment of lichen diversity by index of atmospheric purity (IAP), index of human impact (IHI) and other environmental factors in an urban area (Grenoble, southeast France).' *Science of the Total Environment*, 324(1–3) pp. 183–199.
- Gómez-Baggethun, E. and Barton, D. N. (2013) 'Classifying and valuing ecosystem services for urban planning.' *Ecological Economics*. Elsevier B.V., 86 pp. 235–245.
- Gómez, B., Gómez, M., Sanchez, J. ., Fernández, R. and Palacios, M. . (2001) 'Platinum and rhodium distribution in airborne particulate matter and road dust.' *Science of The Total Environment*, 269(1–3) pp. 131–144.
- González, C. M., Casanovas, S. S. and Pignata, M. L. (1996) 'Biomonitoring of air pollutants from traffic and industries employing *Ramalina ecklonii* (Spreng.) Mey. and Flot. in Córdoba, Argentina.' *Environmental Pollution*, 91(3) pp. 269–277.
- Google (2018) *Google Earth V 7.1.1.1888; Manchester (UK)*.
- Gough, L. P., Shacklette, H. T. and Case, A. A. (1979) 'Element Concentrations Toxic to Plants, Animals , and Man.' *Geological Survey Bulletin*, 1466 p. i-iii; 1-80.
- Greater Manchester Combined Authority (GMCA) (2018) *Who we are*. [Online] [Accessed on 10th April 2018] <https://www.greatermanchester-ca.gov.uk/about>.
- Grimmond, C. S. B. and Oke, T. R. (1999) 'Aerodynamic Properties of Urban Areas Derived from Analysis of Surface Form.' *Journal of Applied Meteorology*, 38(9) pp. 1262–1292.
- Grindon, L. H. (1859) *The Manchester flora*. 1st., London: William White.
- Grubbs, F. E. (1969) 'Procedures for Detecting Outlying Observations in Samples.' *Technometrics*.
- Guerreiro, C., Gonzalez Ortiz, A., de Leeuw, F., Viana, M. and Horalek, J. (2016) *Air quality in Europe — 2016 report*. Copenhagen.
- Guidotti, M., Stella, D., Dominici, C., Blasi, G., Owczarek, M., Vitali, M. and Protano, C. (2009) 'Monitoring of Traffic-Related Pollution in a Province of Central Italy with Transplanted Lichen *Pseudovernia furfuracea*.' *Bulletin of Environmental Contamination and Toxicology*, 83(6) pp. 852–858.
- Guidotti, M., Stella, D., Owczarek, M., De Marco, A. and De Simone, C. (2003) 'Lichens as polycyclic aromatic hydrocarbon bioaccumulators used in atmospheric pollution studies.' *Journal of Chromatography A*, 985(1–2) pp. 185–190.
- Gulia, S., Nagendra, S. M. S., Khare, M. and Khanna, I. (2015) 'Urban air quality management-A review.' *Atmospheric Pollution Research*. Elsevier, 6(2) pp. 286–304.
- Gulliver, J., de Hoogh, K., Fecht, D., Vienneau, D. and Briggs, D. (2011) 'Comparative assessment of GIS-based methods and metrics for estimating long-term exposures to air pollution.' *Atmospheric Environment*.

- Gurbanov, R. and Unal, D. (2019) 'The biomolecular alterations in *cladonia convoluta* in response to lead exposure.' *Spectroscopy Letters*. Taylor & Francis, 0(0) pp. 1–8.
- Haberzettl, P. (2018) 'Circadian toxicity of environmental pollution. Inhalation of polluted air to give a precedent.' *Current Opinion in Physiology*. Current Opinion in Psychology, 5 pp. 16–24.
- Hagman, R., Weber, C. and Amundsen, A. H. (2015) 'Emissions from new vehicles - trustworthy?,' (x) pp. 0–3.
- Hall, J., Bealey, B. and Wadsworth, R. (2006) 'Assessing the risks of air pollution impacts to the condition of Areas/Sites of Special Scientific Interest in the UK,' (387).
- Halsall, C., Burnett, V., Davis, B., Jones, P., Pettit, C. and Jones, K. C. (1993) 'PCBs and PAHs in U.K. urban air.' *Chemosphere*. Pergamon-Elsevier Sci Ltd, Oxford, England, 26(12) pp. 2185–2197.
- Van Haluwyn, C. and Van Herk, C. M. (2002) 'Bioindication: The Community Approach.' In Nimis, P. L., Scheidegger, C., and Wolseley, P. A. (eds) *Monitoring with Lichens - Monitoring Lichens*. 1., Dordrecht: Springer Science + Business Media B.V., pp. 39–65.
- Hangartner, M. (2001) *Influence of meteorological factors on the performance of diffusive samplers*. Brown, R. H., Hafkenscheid, T. L., Saunders, K. J., Borowiak, A., and De Saeger, E. (eds) *Measuring Air Pollutants by Diffusive Sampling*. Montpellier, France.
- Hansen, T. S., Kruse, M., Nissen, H., Glasius, M. and Lohse, C. (2001) 'Hansen, T.S., Kruse, M., Nissen, H., Glasius, M. and Lohse, C., 2001. Measurements of nitrogen dioxide in Greenland using Palmes diffusion tubes. *Journal of Environmental Monitoring*, 3(1): 13.' *Journal of Environmental Monitoring*, 3(1) pp. 139–145.
- Hargreaves, K. J. (1989) *The development and application of diffusion tubes for air pollution measurements*. University of Nottingham.
- Harner, T., Bartkow, M., Holoubek, I., Klanova, J., Wania, F., Gioia, R., Moeckel, C., Sweetman, A. J. and Jones, K. C. (2006) 'Passive air sampling for persistent organic pollutants: Introductory remarks to the special issue.' *Environmental Pollution*, 144(2) pp. 361–364.
- Harner, T., Su, K., Genualdi, S., Karpowicz, J., Ahrens, L., Mihele, C., Schuster, J., Charland, J. P. and Narayan, J. (2013) 'Calibration and application of PUF disk passive air samplers for tracking polycyclic aromatic compounds (PACs).' *Atmospheric Environment*, 75 pp. 123–128.
- Harvey, R. G. (1998) 'ENvironmental Chemistry of PAHs.' In Neilson, A. H. (ed.) *The Handbook of Environmental Chemistry - PAHs and Related Compounds*. Berlin, Heidelberg: Springer Verlag.
- Hauck, M. (2010) 'Ammonium and nitrate tolerance in lichens.' *Environmental Pollution*. Elsevier Ltd, 158(5) pp. 1127–1133.
- Hauck, M. (2011) 'Eutrophication threatens the biochemical diversity in lichens.' *The Lichenologist*, 43(02) pp. 147–154.
- Hauck, M., Böning, J., Jacob, M., Dittrich, S., Feussner, I. and Leuschner, C. (2013) 'Lichen substance concentrations in the lichen *Hypogymnia physodes* are correlated with heavy metal concentrations in the substratum.' *Environmental and Experimental Botany*. Elsevier B.V., 85 pp. 58–63.
- Hauck, M. and Huneck, S. (2007) 'Lichen substances affect metal adsorption in *Hypogymnia physodes*.' *Journal of chemical ecology*, 33(1) pp. 219–223.
- Hauck, M., Mulack, C. and Paul, A. (2002) 'Manganese uptake in the epiphytic lichens *Hypogymnia physodes* and *Lecanora conizaeoides*.' *Environmental and Experimental Botany*. Elsevier, 48(2) pp. 107–117.
- Hauck, M., Paul, A. and Spribille, T. (2006) 'Uptake and toxicity of manganese in epiphytic cyanolichens.' *Environmental and Experimental Botany*, 56(2) pp. 216–224.
- Hawksworth, D. L. (1970) 'Lichens as litmus for air pollution: a historical review.'

- International Journal of Environmental Studies*, 1(1–4) pp. 281–296.
- Hawksworth, D. L. and Rose, F. (1970) 'Qualitative Scale for estimating Sulphur Dioxide Air Pollution in England and Wales using Epiphytic Lichens.' *Nature*, 227(5254) pp. 145–148.
- Heal, M. R. and Cape, J. N. (1997) 'A numerical evaluation of chemical interferences in the measurement of ambient nitrogen dioxide by passive diffusion samplers.' *Atmospheric Environment*.
- Heal, M. R., Kirby, C. and Cape, J. N. (2000) 'Systematic biases in measurement of urban nitrogen dioxide using passive diffusion samplers.' *Environmental Monitoring and Assessment*.
- Heaton, T. H. E. (1986) 'Isotopic studies of nitrogen pollution in the hydrosphere and atmosphere: A review.' *Chemical Geology: Isotope Geoscience Section*, 59(C) pp. 87–102.
- Heaton, T. H. E., Spiro, B. and Robertson, S. M. C. (1997) 'Potential canopy influences on the isotopic composition of nitrogen and sulphur in atmospheric deposition.' *Oecologia*, 109(4) pp. 600–607.
- Heidorn, K. C. and Yap, D. (1986) 'A synoptic climatology for surface ozone concentrations in Southern Ontario, 1976-1981.' *Atmospheric Environment* (1967).
- Hengl, T. (2009) *A Practical guide to Geostatistical Mapping. Scientific and Technical Research series*.
- Henschel, S., Le Tertre, A., Atkinson, R. W., Querol, X., Pandolfi, M., Zeka, A., Haluza, D., Analitis, A., Katsouyanni, K., Bouland, C., Pascal, M., Medina, S. and Goodman, P. G. (2016) 'Trends of nitrogen oxides in ambient air in nine European cities between 1999 and 2010.' *Atmospheric Environment*, 117 pp. 234–241.
- Van Herk, C. M. (1999) 'Mapping of ammonia pollution with epiphytic lichens in the Netherlands.' *Lichenologist*, 31(1) pp. 9–20.
- Van Herk, C. M. (2001) 'Bark pH and susceptibility to toxic air pollutants as independent causes of changes in epiphytic lichen composition in space and time.' *Lichenologist*, 33(5) pp. 419–441.
- Van Herk, C. M. (2003) 'A changing lichen flora The effects of short and long distance nitrogen deposition on epiphytic lichens.' In Lambley, P. and Wolseley, P. A. (eds) *Lichens in a changing pollution environment: English Nature Research Reports*. Peterborough: English Nature, pp. 13–20.
- Van Herk, C. M., Mathijssen-Spiekman, E. A. M. and De Zwart, D. (2003) 'Long distance nitrogen air pollution effects on lichens in Europe.' *Lichenologist*, 35(4) pp. 347–359.
- Hertel, O. and Goodsite, M. E. (2009) 'Urban Air Pollution Climates throughout the World.' *Air Quality in Urban Environments* pp. 1–22.
- Hewitt, C. N. (1991) 'Spatial variations in nitrogen dioxide concentrations in an urban area.' *Atmospheric Environment. Part B. Urban Atmosphere*, 25(3) pp. 429–434.
- Highway Forecasting and Analytical Services (2015) *HFAS Report 1843 - Transport Statistics Manchester 2014, Appendix 3: Traffic flow, road accidents and congestion plots*. Manchester.
- Hirner, A. V., Rehage, H. and Sulkowski, M. (2000) *Umweltgeochemie - Herkunft, Mobilität und Analyse von Schadstoffen in der Pedosphäre*. 1. edition, Darmstadt: Steinkopff Verlag.
- Hoefs, J. (2009) *Stable Isotope Geochemistry*. Springer. 6th ed., Berlin, Heidelberg: Springer Verlag.
- Howsam, M. and Jones, K. C. (1998) 'Sources of PAHs in the Environment.' In Neilson, A. H. (ed.) *The Handbook of Environmental Chemistry - PAHs and Related Compounds*. Berlin, Heidelberg: Springer Verlag, pp. 137–175.
- Howsam, M., Jones, K. C. and Ineson, P. (2000) 'PAHs associated with the leaves of three deciduous tree species. I--Concentrations and profiles.' *Environmental pollution (Barking, Essex : 1987)*, 108(3) pp. 413–24.

- Howsam, M., Jones, K. C. and Ineson, P. (2001) 'PAHs associated with the leaves of three deciduous tree species. II: Uptake during a growing season.' *Chemosphere*, 44(2) pp. 155–164.
- Hsu, Y.-M., Harner, T., Li, H. and Fellin, P. (2015) 'PAH Measurements in Air in the Athabasca Oil Sands Region.' *Environmental Science & Technology* p. 150416093308006.
- Hu, S., Herner, J. D., Shafer, M., Robertson, W., Schauer, J. J., Dwyer, H., Collins, J., Huai, T. and Ayala, A. (2009) 'Metals emitted from heavy-duty diesel vehicles equipped with advanced PM and NOx emission controls.' *Atmospheric Environment*. Elsevier Ltd, 43(18) pp. 2950–2959.
- Hüls, A., Vierkötter, A., Gao, W., Krämer, U., Yang, Y., Ding, A., Stolz, S., Matsui, M., Kan, H., Wang, S., Jin, L., Krutmann, J. and Schikowski, T. (2016) 'Traffic-Related Air Pollution Contributes to Development of Facial Lentigines: Further Epidemiological Evidence from Caucasians and Asians.' *Journal of Investigative Dermatology*. Elsevier Ltd, 136(5) pp. 1053–1056.
- Hulskotte, J. H. J., Roskam, G. D. and Denier van der Gon, H. A. C. (2014) 'Elemental composition of current automotive braking materials and derived air emission factors.' *Atmospheric Environment*.
- Hussain, K., Hoque, R. R., Balachandran, S., Medhi, S., Idris, M. G., Rahman, M. and Hussain, F. L. (2018) *Monitoring and Risk Analysis of PAHs in the Environment. Handbook of Environmental Materials Management*.
- Hwang, H. M., Wade, T. L. and Sericano, J. L. (2003) 'Concentrations and source characterization of polycyclic aromatic hydrocarbons in pine needles from Korea, Mexico, and United States.' *Atmospheric Environment*.
- IARC (2010) 'IARC monographs on the evaluation of carcinogenic risks to humans.' *IARC Monographs on the Evaluation of Carcinogenic Risks to Humans*. Lyon: International Agency for Research on Cancer (IARC).
- ICdA (2019) *Cadmium emissions*. International Cadmium Association. [Online] [Accessed on 4th March 2019] <https://www.cadmium.org/environment/cadmium-emissions>.
- ICH (1996) *International Conference on Harmonization (ICH) of Technical Requirements for the Registration of Pharmaceuticals for Human Use, Validation of analytical procedures: Text and Methodology. Ich-Q2B*.
- International Agency for Research on Cancer (2018) *IARC Monographs on the Evaluation of Carcinogenic Risks to Humans*. [Online] [Accessed on 17th July 2018] <https://monographs.iarc.fr/agents-classified-by-the-iarc/>.
- International Agency for Research on Cancer (IARC) (2014) 'Diesel and Gasoline Engine Exhausts and Some Nitroarenes.' Cedex, Geneva: International Agency for Research on Cancer, WHO Press p. 714.
- International Programme on Chemical Safety (IPCS) (1996) 'Diesel engines - The use of diesel engines is increasing steadily. What are the pros and cons?' *The Newsletter of the International Programme on Chemical Safety*. December, p. 8.
- Isaaks, E. H. and Srivastava, R. M. (eds) (1989) *An Introduction to Applied Geostatistics*. Oxford: Oxford University Press.
- Jaishankar, M., Mathew, B. B., Shah, M. S., T.P., K. M. and K.R., S. G. (2014) 'Biosorption of Few Heavy Metal Ions Using Agricultural Wastes.' *Journal of Environment Pollution and Human Health*, 2(1) pp. 1–6.
- Jaishankar, M., Tseten, T., Anbalagan, N., Mathew, B. B. and Beeregowda, K. N. (2014) 'Toxicity, mechanism and health effects of some heavy metals.' *Interdisciplinary Toxicology*, 7(2) pp. 60–72.
- James, P. and Bound, D. (2009) 'Urban morphology types and open space distribution in urban core areas.' *Urban Ecosystems*, 12(4) pp. 417–424.
- Janhäll, S. (2015) 'Review on urban vegetation and particle air pollution – Deposition and dispersion.' *Atmospheric Environment*, 105, March, pp. 130–137.

- Järup, L. (2003) 'Hazards of heavy metal contamination.' *British Medical Bulletin*, 68 pp. 167–182.
- Jeran, Z., Jaimovi, R., Batič, F. and Mavsar, R. (2002) 'Lichens as integrating air pollution monitors.' *Environmental Pollution*, 120 pp. 107–113.
- Johansson, O., Nordin, A., Olofsson, J. and Palmqvist, K. (2010) 'Responses of epiphytic lichens to an experimental whole-tree nitrogen-deposition gradient.' *The New Phytologist*, 188(4) pp. 781–795.
- Jones, D. L., Shannon, D., Murphy, D. V. and Farrar, J. (2004) 'Role of dissolved organic nitrogen (DON) in soil N cycling in grassland soils.' *Soil Biology and Biochemistry*, 36(5) pp. 749–756.
- Jones, D. L. and Willett, V. B. (2006) 'Experimental evaluation of methods to quantify dissolved organic nitrogen (DON) and dissolved organic carbon (DOC) in soil.' *Soil Biology and Biochemistry*, 38(5) pp. 991–999.
- Jordanova, N., Jordanova, D., Henry, B., Le Goff, M., Dimov, D. and Tsacheva, T. (2006) 'Magnetism of cigarette ashes.' *Journal of Magnetism and Magnetic Materials*, 301(1) pp. 50–66.
- Journel, A. G. and Huijbregts, C. J. (eds) (1978) *Mining Geostatistics*. London: Academic Press.
- Jovan, S., Riddell, J., Padgett, P. E. and Nash, T. H. (2012) 'Eutrophic lichens respond to multiple forms of N: Implications for critical levels and critical loads research.' *Ecological Applications*, 22(7) pp. 1910–1922.
- Kadowaki, S. (1986) 'On the Nature of Atmospheric Oxidation Processes of SO₂ to Sulfate and of NO₂ to Nitrate on the Basis of Diurnal Variations of Sulfate, Nitrate, and Other Pollutants in an Urban Area,' 20(12) pp. 1249–1253.
- Käffer, M. I., Lemos, A. T., Apel, M. A., Rocha, J. V., Martins, S. M. D. A. and Vargas, V. M. F. (2012) 'Use of bioindicators to evaluate air quality and genotoxic compounds in an urban environment in Southern Brazil.' *Environmental pollution (Barking, Essex : 1987)*. Elsevier Ltd, 163 pp. 24–31.
- Käffer, M. I., Martins, S. M. D. A., Alves, C., Pereira, V. C., Fachel, J. and Vargas, V. M. F. (2011) 'Corticolous lichens as environmental indicators in urban areas in southern Brazil.' *Ecological Indicators*.
- Kalinowska, R., Bačkor, M. and Pawlik-Skowrońska, B. (2015) 'Parietin in the tolerant lichen *Xanthoria parietina* (L.) Th. Fr. increases protection of *Trebouxia* photobionts from cadmium excess.' *Ecological Indicators*, 58 pp. 132–138.
- Kampa, M. and Castanas, E. (2008) 'Human health effects of air pollution.' *Environmental Pollution*, 151(2) pp. 362–367.
- Kasper-Giebl, A. and Puxbaum, H. (1999) 'Deposition of particulate matter in diffusion tube samplers for the determination of NO₂ and SO₂.' *Atmospheric Environment*, 33(8) pp. 1323–1326.
- Kavouras, I. G., Koutrakis, P., Tsapakis, M., Lagoudaki, E., Stephanou, E. G., Von Baer, D. and Oyola, P. (2001) 'Source apportionment of urban particulate aliphatic and polynuclear aromatic hydrocarbons (PAHs) using multivariate methods.' *Environmental Science and Technology*.
- Kaya, E., Dumanoglu, Y., Kara, M., Altıok, H., Bayram, A., Elbir, T. and Odabasi, M. (2012) 'Spatial and temporal variation and air-soil exchange of atmospheric PAHs and PCBs in an industrial region.' *Atmospheric Pollution Research*. Elsevier, 3(4) pp. 435–449.
- Keeney, D. R. and Nelson, D. W. (1982) 'Nitrogen - inorganic forms.' *Methods of soil analysis. Part 2. Chemical and microbiological properties*.
- Keith, L. H. (2015) 'The Source of U.S. EPA's Sixteen PAH Priority Pollutants.' *Polycyclic Aromatic Compounds*, 35(2–4) pp. 147–160.
- Khalili, N. R., Scheff, P. A. and Holsen, T. M. (1995) 'PAH source fingerprints for coke ovens, diesel and, gasoline engines, highway tunnels, and wood combustion

- emissions.' *Atmospheric Environment*, 29(4) pp. 533–542.
- Khan, M. A. H., Morris, W. C., Watson, L. A., Galloway, M., Hamer, P. D., Shallcross, B. M. A., Percival, C. J. and Shallcross, D. E. (2015) 'Estimation of Daytime NO₃ Radical Levels in the UK Urban Atmosphere Using the Steady State Approximation Method.' *Advances in Meteorology*, 2015(2) pp. 1–9.
- Kielhorn, J., Melber, C., Keller, D. and Mangelsdorf, I. (2002) 'Palladium – A review of exposure and effects to human health.' *International Journal of Hygiene and Environmental Health*, 205(6) pp. 417–432.
- Kienzl, K., Riss, A., Vogel, W., Hackl, J. and Götz, B. (2003) 'Bioindicators and biomonitors for policy, legislation and administration.' In Markert, B. A., Breure, A. M., and Zechmeister, H. G. (eds) *Bioindicators & Biomonitors: Principles, Concepts and Applications*. Oxford - UK: Elsevier, pp. 85–123.
- Kim, K.-H., Jahan, S. A., Kabir, E. and Brown, R. J. C. (2013) 'A review of airborne polycyclic aromatic hydrocarbons (PAHs) and their human health effects.' *Environment International*. Elsevier Ltd, 60 pp. 71–80.
- Kim, S. Y., Peel, J. L., Hannigan, M. P., Dutton, S. J., Sheppard, L., Clark, M. L. and Vedal, S. (2012) 'The temporal lag structure of short-term associations of fine particulate matter chemical constituents and cardiovascular and respiratory hospitalizations.' *Environmental Health Perspectives*, 120(8) pp. 1094–1099.
- King, K., Hall, T., Twigg, R., Hulse, L., Street, S., Ol, R., Brown, S., Scott, J., Jones, R., Place, K. and Street, D. (2016) *2015 Air Quality Updating and Screening Assessment for Greater Manchester In fulfillment of Part IV of the Environment Act 1995 Local Air Quality Management Date February 2016*. Greater Manchester.
- Kirby, C., Fox, M. and Waterhouse, J. (2000) 'Reliability of nitrogen dioxide passive diffusion tubes for ambient measurement: In situ properties of the triethanolamine absorbent.' *Journal of Environmental Monitoring*.
- Kirby, C., Fox, M., Waterhouse, J. and Drye, T. (2001) 'Influence of environmental parameters on the accuracy of nitrogen dioxide passive diffusion tubes for ambient measurement.' In *Journal of Environmental Monitoring*.
- Kirchner, M., Jakobi, G., Feicht, E., Bernhardt, M. and Fischer, A. (2005) 'Elevated NH₃ and NO₂ air concentrations and nitrogen deposition rates in the vicinity of a highway in Southern Bavaria.' *Atmospheric Environment*, 39(25) pp. 4531–4542.
- Kirschbaum, U. and Wirth, V. (2010) *Flechten erkennen - Umwelt bewerten*. 3. edition, Wiesbaden: Hessisches Landesamt für Umwelt und Geologie.
- Klanova, J., Kohoutek, J., Hamplova, L., Urbanova, P. and Holoubek, I. (2006) 'Passive air sampler as a tool for long-term air pollution monitoring: Part 1. Performance assessment for seasonal and spatial variations.' *Environmental Pollution*, 144 pp. 393–405.
- Klimek, B., Tarasek, A. and Hajduk, J. (2015) 'Trace element concentrations in lichens collected in the beskidy mountains, the outer western carpathians.' *Bulletin of Environmental Contamination and Toxicology*, 94(4) pp. 532–536.
- Klingberg, J., Broberg, M., Strandberg, B., Thorsson, P. and Pleijel, H. (2017) 'Influence of urban vegetation on air pollution and noise exposure – A case study in Gothenburg, Sweden.' *Science of The Total Environment*. Elsevier B.V., 599–600 pp. 1728–1739.
- Knops, J. M. H., Nash III, T. H., Boucher, V. L. and Schlesinger, W. H. (1991) 'Mineral Cycling and Epiphytic Lichens: Implications at the Ecosystem Level.' *The Lichenologist*, 23(03) pp. 309–321.
- Kobza, J. and Geremek, M. (2017) 'Do the pollution related to high-traffic roads in urbanised areas pose a significant threat to the local population?' *Environmental Monitoring and Assessment*. Environmental Monitoring and Assessment, 189(1) p. 33.
- Koch, N. M., Lucheta, F., Käffer, M. I., Martins, S. M. de A. and Vargas, V. M. F. (2018) 'Air quality assessment in different urban areas from Rio Grande do Sul State, Brazil,

- using lichen transplants.' *Anais da Academia Brasileira de Ciencias*, 90(2) pp. 2233–2248.
- Kodnik, D., Candotto Carniel, F., Lichen, S., Tolloj, A., Barbieri, P. and Tretiach, M. (2015) 'Seasonal variations of PAHs content and distribution patterns in a mixed land use area: A case study in NE Italy with the transplanted lichen *Pseudevernia furfuracea*.' *Atmospheric Environment*. Elsevier Ltd, 113 pp. 255–263.
- Kohoutek, J., Holoubek, I. and Klanova, J. (2006) 'Methodology of passive sampling.' *OCOEN, sro Brno/RECETOX MU Brno. TOCOEN REPORT*, 300(300) pp. 1–14.
- Koohgoli, R., Hudson, L., Naidoo, K., Wilkinson, S., Chavan, B. and Birch-Machin, M. A. (2017) 'Bad air gets under your skin.' *Experimental Dermatology*, (November) pp. 1–4.
- Kostruykova, A. M., Krupnova, T. G., Mashkova, I. V. and Shelkanova, E. E. (2017) 'Monitoring Air Quality Using Lichens In Chelyabinsk, Russian Federation.' *International Journal of GEOMATE*, 12(34) pp. 101–106.
- Kot-Wasik, A., Zabiegała, B., Urbanowicz, M., Dominiak, E., Wasik, A. and Namieśnik, J. (2007) 'Advances in passive sampling in environmental studies.' *Analytica Chimica Acta*, 602(2) pp. 141–163.
- Kováčik, J., Dresler, S., Peterková, V. and Babula, P. (2018) 'Metal-induced oxidative stress in terrestrial macrolichens.' *Chemosphere*, 203 pp. 402–409.
- Král, R., Krýžová, L. and Liška, J. (1989) 'Background concentrations of lead and cadmium in the lichen *Hypogymnia physodes* at different altitudes.' *Science of the Total Environment, The*.
- Kricke, R. and Loppi, S. (2002) 'Bioindication: The I.A.P. Approach.' In Nimis, P. L., Scheidegger, C., and Wolseley, P. A. (eds) *Monitoring with Lichens - Monitoring Lichens*. 1., Dordrecht: Springer Science + Business Media B.V., pp. 21–39.
- Krige, D. G. (1984) 'Geostatistics and the definition of uncertainty.' *Transactions of the Institution of Mining and Metallurgy (Section A: Mining Industry)*, 94(A41-47).
- Krouse, H. R. and Herbert, H. K. (1996) 'd13C‰ systematics of the lichens *Ramalina celastri* and *Ramalina subfraxinea* var. *confirmata*, coastal Eastern Australia and adjacent hinterland. In: van Aarsen, B.G.K. (Ed.), *Australian Organic Geochemistry Conf.* In van Arsen, B. G. . (ed.) *Australian Organic Geochemistry Conference Abstracts*. Fremantle, Washington, pp. 69–70.
- Krupa, S. V. (2003) 'Effects of atmospheric ammonia (NH₃) on terrestrial vegetation: A review.' *Environmental Pollution*, 124(2) pp. 179–221.
- Krupa, S. V. and Legge, A. H. (2000) 'Passive sampling of ambient, gaseous air pollutants: An assessment from an ecological perspective.' *Environmental Pollution*, 107(1) pp. 31–45.
- Kubota, T., Miura, M., Tominaga, Y. and Mochida, A. (2008) 'Wind tunnel tests on the relationship between building density and pedestrian-level wind velocity: Development of guidelines for realizing acceptable wind environment in residential neighborhoods.' *Building and Environment*, 43(10) pp. 1699–1708.
- Kukutschová, J., Moravec, P., Tomášek, V., Matějka, V., Smolík, J., Schwarz, J., Seidlerová, J., Šafářová, K. and Filip, P. (2011) 'On airborne nano/micro-sized wear particles released from low-metallic automotive brakes.' *Environmental Pollution*, 159(4) pp. 998–1006.
- Kularatne, K. I. A. and De Freitas, C. R. (2013) 'Epiphytic lichens as biomonitors of airborne heavy metal pollution.' *Environmental and Experimental Botany*. Elsevier B.V., 88 pp. 24–32.
- Kumar, K. S., Han, Y.-S., Choo, K.-S., Kong, J.-A. and Han, T. (2009) 'Chlorophyll fluorescence based copper toxicity assessment of two algal species.' *Toxicology and Environmental Health Sciences*, 1(1) pp. 17–23.
- Kumar, V., Kothiyal, N. C., Saruchi, Mehra, R., Parkash, A., Sinha, R. R., Tayagi, S. K. and Gaba, R. (2014) 'Determination of some carcinogenic PAHs with toxic equivalency

- factor along roadside soil within a fast developing northern city of India.' *Journal of Earth System Science*, 123(3) pp. 479–489.
- Kummerová, M., Barták, M., Dubová, J., Tříska, J., Zubrová, E. and Zezulka, Š. (2006) 'Inhibitory effect of fluoranthene on photosynthetic processes in lichens detected by chlorophyll fluorescence.' *Ecotoxicology*, 15(2) pp. 121–131.
- Kummerová, M., Zezulka, Š., Krulová, J. and Tříska, J. (2007) 'Photoinduced toxicity of fluoranthene on primary processes of photosynthesis in lichens.' *Lichenologist*, 39(1) pp. 91–100.
- Kurnaz, K. and Cobanoglu, G. (2017) 'Biomonitoring of air quality in istanbul metropolitan territory with epiphytic lichen *Physcia adscendens* (FR.) H. Olivier.' *Fresenius Environmental Bulletin*, 26(12) pp. 7296–7308.
- Kurppa, M., Hellsten, A., Auvinen, M., Raasch, S., Vesala, T. and Järvi, L. (2018) 'Ventilation and air quality in city blocks using large-eddy simulation-urban planning perspective.' *Atmosphere*, 9(2) pp. 1–27.
- Kuttler, W. (2013) *Klimatologie. 2.*, Paderborn: Verlag Ferdinand Schöningh.
- Kwak, H. Y., Ko, J., Lee, S. and Joh, C. H. (2017) 'Identifying the correlation between rainfall, traffic flow performance and air pollution concentration in Seoul using a path analysis.' *Transportation Research Procedia*. Elsevier B.V., 25 pp. 3556–3567.
- De La Cruz, A. R. H., De La Cruz, J. K. H., Tolentino, D. A. and Gioda, A. (2018) 'Trace element biomonitoring in the Peruvian andes metropolitan region using *Flavoparmelia caperata* lichen.' *Chemosphere*. Elsevier Ltd, 210 pp. 849–858.
- Laffray, X., Rose, C. and Garrec, J. P. (2010) 'Biomonitoring of traffic-related nitrogen oxides in the Maurienne valley (Savoie, France), using purple moor grass growth parameters and leaf 15N/14N ratio.' *Environmental Pollution*. Elsevier Ltd, 158(5) pp. 1652–1660.
- Lam, M. M., Engwall, M., Denison, M. S. and Larsson, M. (2018) 'Methylated polycyclic aromatic hydrocarbons and/or their metabolites are important contributors to the overall estrogenic activity of polycyclic aromatic hydrocarbon-contaminated soils.' *Environmental Toxicology and Chemistry*, 37(2) pp. 385–397.
- Lambley, P. and Wolseley, P. (2003) *Lichens in a changing pollution environment: English Nature Research Reports. English Nature Research Report*. Peterborough.
- Lammel, G. (2015) 'Polycyclic Aromatic Compounds in the Atmosphere – A Review Identifying Research Needs.' *Polycyclic Aromatic Compounds*, 35(2–4) pp. 316–329.
- Lang, G. E., Reiners, W. A. and Heier, R. K. (1976) 'Potential alteration of precipitation chemistry by epiphytic lichens.' *Oecologia*, 25(3) pp. 229–241.
- Lanzafame, R., Monforte, P. and Scandura, F. P. (2016) 'Comparative Analyses of Urban Air Quality Monitoring Systems: Passive Sampling and Continuous Monitoring Stations.' *Energy Procedia*. Elsevier B.V., 101(2) pp. 321–328.
- Lapworth, A. and McGregor, J. (2008) 'Seasonal variation of the prevailing wind direction in Britain.' *Weather*, 63(12) pp. 361–364.
- Largueche, F.-Z. B. (2006) 'Estimating Soil Contamination with Kriging Interpolation Method.' *American Journal of Applied Sciences*, 3(6) pp. 1894–1898.
- Larsen, R. S., Bell, J. N. B., James, P. W., Chimonides, P. J., Rumsey, F. J., Tremper, A. and Purvis, O. W. (2007) 'Lichen and bryophyte distribution on oak in London in relation to air pollution and bark acidity.' *Environmental Pollution*, 146(2) pp. 332–340.
- Larsen Vilsholm, R., Wolseley, P. A., Söchting, U. and Chimonides, P. J. (2009) 'Biomonitoring with lichens on twigs.' *Lichenologist*. Manchester Metropolitan University, 41(2) pp. 189–202.
- Laumbach, R. J. and Kipen, H. M. (2012) 'Respiratory health effects of air pollution: Update on biomass smoke and traffic pollution.' *Journal of Allergy and Clinical Immunology*. Elsevier Ltd, 129(1) pp. 3–11.

- Lawrey, J. D. and Diedrich, P. (2018) *Lichenicolous fungi - worldwide checklist, including isolated cultures and sequences available*. [Online] [Accessed on 23rd January 2019] www.lichenicolous.net.
- Laxen, D. and Wilson, P. (2002) *Compilation of Diffusion Tube Collocation Studies Carried Out by Local Authorities*.
- Leavy, A. L. (2009) *Insights into the Variables Controlling Human Exposure to Ultrafine Particle Concentrations in Urban Affinity Zones*. University of Manchester, UK.
- Lee, B. E., Ha, E. H., Park, H. S., Kim, Y. J., Hong, Y. C., Kim, H. and Lee, J. T. (2003) 'Exposure to air pollution during different gestational phases contributes to risks of low birth weight.' *Human reproduction (Oxford, England)*, 18(3) pp. 638–43.
- Lee, H. S., Kang, C. M., Kang, B. W. and Kim, H. K. (1999) 'Seasonal variations of acidic air pollutants in Seoul, South Korea.' *Atmospheric Environment*.
- Lee, J. H., Kim, J. S., Min, B. H., Kim, S. T. and Kim, J. H. (1998) 'Determination of anions in certified reference materials by ion chromatography.' *Journal of Chromatography A*, 813(1) pp. 85–90.
- Lee, Y. I., Lim, H. S. and Yoon, H. I. (2009) 'Carbon and nitrogen isotope composition of vegetation on King George Island, maritime Antarctic.' *Polar Biology*, 32(11) pp. 1607–1615.
- Legendre, P. C. and Legendre, L. (1988) 'Numerical Ecology, Volume 24.' (*Developments in Environmental Modelling*).
- Lehmann, A. and Stahr, K. (2007) 'Nature and significance of anthropogenic urban soils.' *Journal of Soils and Sediments*, 7(4) pp. 247–260.
- Lei, H. and Wuebbles, D. J. (2013) 'Chemical competition in nitrate and sulfate formations and its effect on air quality.' *Atmospheric Environment*. Elsevier Ltd, 80 pp. 472–477.
- Leiser, C. L., Hanson, H. A., Sawyer, K., Steenblik, J., Al-Dulaimi, R., Madsen, T., Gibbins, K., Hotaling, J. M., Ibrahim, Y. O., VanDerslice, J. A. and Fuller, M. (2018) 'Acute effects of air pollutants on spontaneous pregnancy loss: a case-crossover study.' *Fertility and Sterility*. Elsevier Inc. pp. 1–6.
- Leith, I. D., Van Dijk, N., Pitcairn, C. E. R., Wolseley, P. A., Whitfield, C. P. and Sutton, M. A. (2005) 'Biomonitoring methods for assessing the impacts of nitrogen pollution: refinement and testing.' *JNCC Report No. 386*, (386) p. 282.
- Di Lella, L. A., Frati, L., Loppi, S., Protano, G. and Riccobono, F. (2003) 'Lichens as biomonitors of uranium and other trace elements in an area of Kosovo heavily shelled with depleted uranium rounds.' *Atmospheric Environment*.
- Lerda, D. (2011) 'Polycyclic Aromatic Hydrocarbons (PAHs) Factsheet.' *Environmental Protection*. Geel, Belgium: European Commission p. 34.
- Levia, D. F. (2002) 'Nitrate sequestration by corticolous macrolichens during winter precipitation events.' *International Journal of Biometeorology*, 46(2) pp. 60–65.
- Li, J. and Heap, A. D. (2008) 'A review of spatial interpolation methods for environmental scientists.' *Canberra: Geoscience Australia*.
- Limbeck, A. and Puls, C. (2011) 'Particulate emissions from on-road vehicles.' In Zereini, F. and Wiseman, C. L. S. (eds) *Urban Airborne Particulate Matter: Origin, Chemistry, Fate and Health Impacts*, pp. 63–80.
- Lin, Y. P., Chang, T. K., Shih, C. W. and Tseng, C. H. (2002) 'Factorial and indicator kriging methods using a geographic information system to delineate spatial variation and pollution sources of soil heavy metals.' *Environmental Geology*.
- Liu, J., Zhang, Y., Liu, X., Tang, A., Qiu, H. and Zhang, F. (2016) 'Concentrations and isotopic characteristics of atmospheric reactive nitrogen around typical sources in Beijing, China.' *Journal of Arid Land*, 8(6) pp. 910–920.
- Liu, T.-L., Juang, K.-W. and Lee, D.-Y. (2006) 'Interpolating Soil Properties Using Kriging Combined with Categorical Information of Soil Maps.' *Soil Science Society of America Journal*, 70(4) p. 1200.

- Liu, T., Wang, X., Deng, W., Zhang, Y., Chu, B., Ding, X., Hu, Q., He, H. and Hao, J. (2015) 'Role of ammonia in forming secondary aerosols from gasoline vehicle exhaust.' *Science China Chemistry*.
- Lo, K. W. and Ngan, K. (2015) 'Characterising the pollutant ventilation characteristics of street canyons using the tracer age and age spectrum.' *Atmospheric Environment*, 122 pp. 611–621.
- Loader, A. (2006) *NO₂ Diffusion Tubes for LAQM: Guidance Note for Local Authorities*. Harwell.
- Lohmann, R., Corrigan, B. P., Howsam, M., Jones, K. C. and Ockenden, W. A. (2001) 'Further developments in the use of semipermeable membrane devices (SPMDs) as passive air samplers for persistent organic pollutants: Field application in a spatial survey of PCDD/Fs and PAHs.' *Environmental Science and Technology*, 35(12) pp. 2576–2582.
- Longley, I. D., Gallagher, M. W., Dorsey, J. R., Flynn, M. and Barlow, J. F. (2004) 'Short-term measurements of airflow and turbulence in two street canyons in Manchester.' *Atmospheric Environment*, 38(1) pp. 69–79.
- López-Veneroni, D. (2009) 'The stable carbon isotope composition of PM_{2.5} and PM₁₀ in Mexico City Metropolitan Area air.' *Atmospheric Environment*, 43(29) pp. 4491–4502.
- Loppi, S. (2019) 'May the Diversity of Epiphytic Lichens Be Used in Environmental Forensics?' *Diversity*, 11(3) p. 36.
- Loppi, S. and De Dominicis, V. (1996) 'Lichens as long-term biomonitors of air quality in central Italy.' *Acta Botanica Neerlandica*, 45(4) pp. 563–570.
- Loppi, S., Frati, L., Paoli, L., Bigagli, V., Rossetti, C., Bruscoli, C. and Corsini, A. (2004) 'Biodiversity of epiphytic lichens and heavy metal contents of *Flavoparmelia caperata* thalli as indicators of temporal variations of air pollution in the town of Montecatini Terme (central Italy).' *Science of the Total Environment*, 326(1–3) pp. 113–122.
- Loppi, S., Giovannelli, L., Pirintsos, S. A., Putorti, E. and Corsini, A. (1997) 'Lichens as bioindicators of recent changes in air quality (Montecatini Terme, Italy).' *Ecologia Mediterranea*, 23 pp. 53–56.
- Loppi, S., Nelli, L., Ancora, S. and Bargagli, R. (1997) 'Accumulation of Trace Elements in the Peripheral and Central Parts of a Foliose Lichen Thallus.' *The Bryologist*, 100(2) p. 251.
- Loppi, S., Pirintsos, S. A. and De Dominicis, V. (1999) 'Soil contribution to the elemental composition of epiphytic lichens (Tuscany, central Italy).' *Environmental Monitoring and Assessment*, 58(2) pp. 121–131.
- Loppi, S., Pozo, K., Estellano, V. H., Corsolini, S., Sardella, G. and Paoli, L. (2015) 'Accumulation of polycyclic aromatic hydrocarbons by lichen transplants: Comparison with gas-phase passive air samplers.' *Chemosphere*. PERGAMON-ELSEVIER SCIENCE LTD, THE BOULEVARD, LANGFORD LANE, KIDLINGTON, OXFORD OX5 1GB, ENGLAND, 134, September, pp. 39–43.
- Loubet, B., Asman, W. A. H., Theobald, M. R., Hertel, O., Tang, Y. S., Robin, P., Hassouna, M., Dammgén, U., Genermont, S., Cellier, P. and Sutton, M. A. (2009) 'Ammonia Deposition Near Hot Spots: Processes, Models and Monitoring Methods.' *In Atmospheric Ammonia*, pp. 205–263.
- Mackay, D. and Callcott, D. (1998) 'Partitioning and Physical Chemical Properties of PAHs.' *In Neilson, A. H. (ed.) The Handbook of Environmental Chemistry - PAHs and Related Compounds*. Berlin, Heidelberg: Springer Verlag, pp. 325–346.
- Máguas, C., Pinho, P., Branquinho, C., Hartard, B. and Lakatos, M. (2013) 'Carbon-Water-Nitrogen relationships between lichens and the atmosphere: Tools to understand metabolism and ecosystem change.' *MycKeys*, 6 pp. 95–106.
- Maher, B. A., Ahmed, I. A. M., Karloukovski, V., Maclaren, D. A. and Foulds, P. G. (2016)

- 'Magnetite pollution nanoparticles in the human brain.' *Proceedings of the National Academy of Sciences of the United States of America* pp. 3–7.
- Majumder, S., Mishra, D., Ram, S. S., Jana, N. K., Santra, S., Sudarshan, M. and Chakraborty, A. (2013) 'Physiological and chemical response of the lichen, *Flavoparmelia caperata* (L.) Hale, to the urban environment of Kolkata, India.' *Environmental Science and Pollution Research*, 20(5) pp. 3077–3085.
- Malaspina, P., Tixi, S., Brunialti, G., Frati, L., Paoli, L., Giordani, P., Modenesi, P. and Loppi, S. (2014) 'Biomonitoring urban air pollution using transplanted lichens: element concentrations across seasons.' *Environmental science and pollution research international*, 21(22) pp. 12836–42.
- Malawska, M. and Wiołkomirski, B. (2001) 'An Analysis of Soil and Plant (*Taraxcum Officinale*) Contamination with Heavy Metals and Polycyclic Aromatic Hydrocarbons (PAHs) in the Area of the Railway Junction Ława Główna, Poland.' *Water, Air, and Soil Pollution*, 127(1/4) pp. 339–349.
- Mamane, Y. and Dzubay, T. G. (1988) 'Fly ash concentrations in Philadelphia aerosol determined by electron microscopy.' *Water, Air, and Soil Pollution*.
- Manchester City Council (2016a) *Manchester's State of the City Report 2016 - Transport*. *Manchester State of the City Report 2016*. Manchester.
- Manchester City Council (2016b) *Manchester - Factsheet [Updated January 2016]*. *Factsheet*. Manchester.
- Manchester City Council (2017) *State of the City Report 2017*. Manchester.
- Manchester City Council (2018) *Air quality information and campaigns - nature and sources of air pollutants*. [Online] [Accessed on 12th December 2018] https://secure.manchester.gov.uk/info/100006/environmental_problems/2942/air_quality_information_and_campaigns/5.
- Manchester Green Infrastructure Strategy* (2015). Manchester.
- Markert, B. A., Breure, A. M. and Zechmeister, H. G. (2003) 'Bioindicators & Biomonitors Principles, Concepts and Applications.' In Markert, B. A., Breure, A. M., and Zechmeister, H. G. (eds) *Trace Metals and other Contaminants in the Environment* 6. Amsterdam, Boston, London, New York, Oxford, Paris, San Diego, San Francisco, Singapore, Sydney, Tokyo: Elsevier Sci Ltd, Oxford, England, p. 1017.
- Marr, L. C., Dzepina, K., Jimenez, J. L., Reisen, F., Bethel, H. L., Arey, J., Gaffney, J. S., Marley, N. A., Molina, L. T. and Molina, M. J. (2006) 'Sources and transformations of particle-bound polycyclic aromatic hydrocarbons in Mexico City.' *Atmospheric Chemistry and Physics*, 6(6) pp. 1733–1745.
- Martin, C. L., Allan, J. D., Crosier, J., Choularton, T. W., Coe, H. and Gallagher, M. W. (2011) 'Seasonal variation of fine particulate composition in the centre of a UK city.' *Atmospheric Environment*. PERGAMON-ELSEVIER SCIENCE LTD, THE BOULEVARD, LANGFORD LANE, KIDLINGTON, OXFORD OX5 1GB, ENGLAND, 45(26) pp. 4379–4389.
- Martin, S. and Griswold, W. (2009) 'Human Health Effects of Heavy Metals.' *Environmental Science and Technology Briefs*, 15 pp. 1–6.
- Martinez-Argudo, I., Little, R., Shearer, N., Johnson, P. and Dixon, R. (2005) 'Nitrogen fixation: key genetic regulatory mechanisms.' *Biochemical Society Transactions*.
- Masclat, P., Bresson, M. A. and Mouvier, G. (1987) 'Polycyclic aromatic hydrocarbons emitted by power stations, and influence of combustion conditions.' *Fuel*.
- Masih, A. and Taneja, A. (2006) 'Polycyclic aromatic hydrocarbons (PAHs) concentrations and related carcinogenic potencies in soil at a semi-arid region of India.' *Chemosphere*.
- Maslaňáková, I., Biřová, I., Goga, M., Kuchár, M. and Bačkor, M. (2015) 'Differences Between Sensitivity of Mycobiont and Photobiont of *Cladonia* sp. Lichens to Different Types of Nitrogen Exposure.' *Water, Air, & Soil Pollution*, 226(8) p. 243.
- Mastral, A. M., López, J. M., Callén, M. S., García, T., Murillo, R. and Navarro, M. V. (2003)

- 'Spatial and temporal PAH concentrations in Zaragoza, Spain.' *Science of the Total Environment*, 307(1–3) pp. 111–124.
- Matsumoto, S. T., Mantovani, M. S., Malagutti, M. I. A., Dias, A. L., Fonseca, I. C. and Marin-Morales, M. A. (2006) 'Genotoxicity and mutagenicity of water contaminated with tannery effluents as evaluated by the micronucleus test and comet assay using the fish *Oreochromis niloticus* and chromosome aberrations in onion root-tips.' *Genetics and Molecular Biology*, 29(1) pp. 148–158.
- Matthaios, V. N., Kramer, L. J., Sommariva, R., Pope, F. D. and Bloss, W. J. (2019) 'Investigation of vehicle cold start primary NO₂ emissions from ambient monitoring data in the UK and their implications for urban air quality.' *Atmospheric Environment*. Elsevier, 199(2) pp. 402–414.
- May, T. W., Wiedmeyer, R. H., Chaudhary-webb, M., Paschal, D. C., Elliott, W. C., Hopkins, H. P., Ghazi, a M., Ting, B. C., Romieu, I., Vicente, O., Pelfort, E., Martinez, L., Olsina, R., Marchevsky, E., Chen, H. P., Miller, D. T. and Morrow, J. C. (1998) 'A table of polyatomic interferences in ICP-MS.' *Atomic Spectroscopy*, 19(5) pp. 150–155.
- Mayer, H. (1999) 'Air pollution in cities.' *Atmospheric Environment*, 33(24–25) pp. 4029–4037.
- Maynard, D. G. and Kalra, Y. P. (1993) 'Nitrate and Exchangeable Ammonium Nitrogen.' In Carter, M. R. (ed.) *Soil sampling and Methods of Analysis*. 1st editio, Boca Raton: Lewis Publishers, pp. 25–38.
- McFadyen, G. G. and Cape, J. N. (2005) 'Peroxyacetyl nitrate in eastern Scotland.' *Science of the Total Environment*.
- McLean, A. and Drabble, J. (2015) *2014 Detailed Air Quality Assessment for Greater Manchester*. Manchester.
- Meijer, S. N., Sweetman, A. J., Halsall, C. J. and Jones, K. C. (2008) 'Temporal trends of polycyclic aromatic hydrocarbons in the U.K. atmosphere: 1991-2005.' *Environmental Science and Technology*, 42(9) pp. 3213–3218.
- Mekhtiyeva, V. L., Gavrilov, E. Y. and Pankina, R. G. (1976) 'Sulphur isotopic composition in land plants.' *Geochemistry International*, 13 pp. 85–88.
- Mendes, M. and Pala, A. (2003) 'Type I Error Rate and Power of Three Normality Tests.' *Information Technology Journal*, 2(2) pp. 135–139.
- Meng, Z., Xu, X., Wang, T., Zhang, X., Yu, X., Wang, S., Lin, W., Chen, Y., Jiang, Y. and An, X. (2010) 'Ambient sulfur dioxide, nitrogen dioxide, and ammonia at ten background and rural sites in China during 2007 e 2008.' *Atmospheric Environment*. Elsevier Ltd, 44(21–22) pp. 2625–2631.
- Met Office (2015) *UK-climate: regional climates*. [Online] [Accessed on 3rd March 2016] <http://www.metoffice.gov.uk/climate/uk/regional-climates/nw>.
- Met Office (2018) *When does spring start?* [Online] [Accessed on 29th November 2018] <https://www.metoffice.gov.uk/learning/seasons/spring/when-does-spring-start>.
- Michalski, R. and Kurzyca, I. (2014) 'Determination of nitrogen species (Nitrate, Nitrite and Ammonia Ions) in Environmental Samples by Ion Chromatography.' *Polish Journal of Environmental Studies*, 15(July) pp. 5–18.
- Michalski, R., Lyko, A. and Kurzyca, I. (2012) 'Matrix Influences on the Determination of Common Ions by using Ion Chromatography Part 1--Determination of Inorganic Anions.' *Journal of Chromatographic Science*, 50(6) pp. 482–493.
- Mielke, H. W. (1997) 'Urbane Geochemie: Prozesse, Muster und Auswirkungen auf die menschliche Gesundheit.' In *Geochemie und Umwelt: Relevante Prozesse in Atmo-, Pedo- und Hydrosphäre*. Berlin; Heidelberg; New York; Barcelona; Budapest; Hong Kong; London; Mailand; Paris; Santa Clara; Singapur; Tokio: Springer Verlag, pp. 169–180.
- Mielke, H. W., Gonzales, C. R., Smith, M. K. and Mielke, P. W. (1999) 'The urban environment and children's health: Soils as an integrator of lead, zinc, and cadmium

- in New Orleans, Louisiana, U.S.A.' *Environmental Research*.
- Mielke, H. W. and Reagan, P. L. (1998) 'Soil is an important pathway of human lead exposure.' *Environmental Health Perspectives*.
- Migaszewski, Z. M., Gałuszka, A. and Paślawski, P. (2002) 'Polynuclear aromatic hydrocarbons, phenols, and trace metals in selected soil profiles and plant bioindicators in the Holy Cross Mountains, South-Central Poland.' *Environment International*, 28(4) pp. 303–313.
- Mikhailova, I. N. (2017) 'Initial stages of recovery of epiphytic lichen communities after reduction of emissions from a copper smelter.' *Russian Journal of Ecology*, 48(4) pp. 335–339.
- Miller, J. E. and Brown, D. H. (1999) 'Studies of Ammonia Uptake and Loss by Lichens.' *The Lichenologist*, 31(01) p. 85.
- Mills, I. C., Atkinson, R. W., Kang, S., Walton, H. and Anderson, H. R. (2015) 'Quantitative systematic review of the associations between short-term exposure to nitrogen dioxide and mortality and hospital admissions.' *BMJ Open*.
- Miranda, A. I., Silveira, C., Ferreira, J., Monteiro, A., Lopes, D., Relvas, H., Roebeling, P., Borrego, C., Turrini, E. and Volta, M. (2014) 'Urban air quality plans in Europe: a review on applied methodologies.' In *WIT Transactions on Ecology and the Environment*, pp. 315–326.
- Moldanová, J., Grennfelt, P. and Jonsson, A. (2011) 'Nitrogen as threat to European air quality.' In Sutton, M. A. and et al. (eds) *The European Nitrogen Assessment*. Cambridge University Press, pp. 405–433.
- Moldoveanu, S. and David, V. (2015) 'Solvent Extraction.' In Moldoveanu, S. and David, V. (eds) *Modern Sample Preparation for Chromatography*. 1st Editio, pp. 131–189.
- Morais, S., e Costa, F. G. and Lourdes Pereir, M. de (2012) 'Heavy Metals and Human Health.' In Oosthuizen, J. (ed.) *Environmental Health - Emerging Issues and Practice*. InTech, p. 64.
- Moschandreas, D. J., Relwani, S. M., Taylor, K. C. and Mulik, J. D. (1990) 'A laboratory evaluation of a nitrogen dioxide personal sampling device.' *Atmospheric Environment Part A, General Topics*.
- Motulsky, H. J. and Brown, R. E. (2006) 'Detecting outliers when fitting data with nonlinear regression - A new method based on robust nonlinear regression and the false discovery rate.' *BMC Bioinformatics*, 7 pp. 1–20.
- Mumtaz, M. and George, J. (1999) *Toxicological Profile for Polycyclic Aromatic Hydrocarbons, U.S. Department of Health & Human Services, Public Health Service, Agency for Toxic Substances and Disease Registry, Washington, D.C., August, 1985*.
- Munzi, S., Correia, O., Silva, P., Lopes, N., Freitas, C., Branquinho, C. and Pinho, P. (2014) 'Lichens as ecological indicators in urban areas: Beyond the effects of pollutants.' *Journal of Applied Ecology* pp. 1750–1757.
- Murray, K. K., Boyd, R. K., Eberlin, M. N., Langley, G. J., Li, L. and Naito, Y. (2013) 'Definitions of terms relating to mass spectrometry (IUPAC Recommendations 2013).' *Pure and Applied Chemistry*.
- NAEI (2013) *Emissions from large NAEI point sources*. [Online] [Accessed on 12th August 2016] <http://naei.beis.gov.uk/data/map-large-source>.
- NAEI (2015) *Emissions from NAEI large point sources*. [Online] [Accessed on 12th December 2018] <http://naei.beis.gov.uk/data/map-large-source>.
- NAEI (2016) *UK emissions data selector - Ammonia*. [Online] [Accessed on 1st October 2019] <http://naei.beis.gov.uk/data/data-selector-results?q=114381>.
- NAEI (2018a) *Data Selector - Carbon monoxide (CO) and Sulphur dioxide (SO2)*. [Online] [Accessed on 25th October 2018] <http://naei.beis.gov.uk/data/data-selector?view=air-pollutants>.
- NAEI (2018b) *Data Selector - Nitrogen dioxides (NOx)*. [Online]

- <http://naei.beis.gov.uk/data/data-selector?view=air-pollutants>.
- NAEI (2018c) *Overview of air pollutants*. [Online] <http://naei.beis.gov.uk/overview/overview>.
- NAEI (2018d) *Pollutant Information: Ammonia*. [Online] [Accessed on 1st May 2018] http://naei.beis.gov.uk/overview/pollutants?pollutant_id=21.
- NAEI (2018e) *Pollutant Information: Carbon Monoxide*. [Online] [Accessed on 13th July 2018] http://naei.beis.gov.uk/overview/pollutants?pollutant_id=4.
- NAEI (2018f) *Pollutant Information: Nitrogen Oxides*. [Online] [Accessed on 1st May 2018] http://naei.beis.gov.uk/overview/pollutants?pollutant_id=6.
- NAEI (2018g) *Pollutant Information: Sulphur Dioxide*. [Online] [Accessed on 13th July 2018] http://naei.beis.gov.uk/overview/pollutants?pollutant_id=8.
- Naeth, M. A. and Wilkinson, S. R. (2008) 'Lichens as Biomonitors of Air Quality around a Diamond Mine, Northwest Territories, Canada.' *Journal of Environment Quality*, 37(5) p. 1675.
- Nagajyoti, P. C., Lee, K. D. and Sreekanth, T. V. M. (2010) 'Heavy metals, occurrence and toxicity for plants: A review.' *Environmental Chemistry Letters*, 8(3) pp. 199–216.
- Nahm, K. H. (2005) 'Evaluation of the nitrogen content in poultry manure.' *World's Poultry Science Journal*, 59(01) pp. 77–88.
- Napier, F., D'Arcy, B. and Jefferies, C. (2008) 'A review of vehicle related metals and polycyclic aromatic hydrocarbons in the UK environment.' *Desalination*, 226(1–3) pp. 143–150.
- Nascimbene, J., Tretiach, M., Corana, F., Lo Schiavo, F., Kodnik, D., Dainese, M. and Mannucci, B. (2014) 'Patterns of traffic polycyclic aromatic hydrocarbon pollution in mountain areas can be revealed by lichen biomonitoring: A case study in the Dolomites (Eastern Italian Alps).' *Science of The Total Environment*. Elsevier B.V., 475, March, pp. 90–96.
- Nash III, T. H. (1973) 'Sensitivity of Lichens to Sulfur Dioxide.' *The Bryologist*, 76(3) pp. 333–339.
- Nash III, T. H. (2008) *Lichen Biology*. 2nd ed., Cambridge, New York, Melbourne, Madrid, Cape Town, Singapore, Sao Paulo, Delhi: Cambridge University Press.
- Nash, T. H. and Gries, C. (1995) 'The use of lichens in atmospheric deposition studies with an emphasis on the Arctic.' *Science of the Total Environment*.
- National Center for Biotechnology Information (2018) *Pubchem Open Chemistry Database*. [Online] [Accessed on 23rd October 2018] <https://pubchem.ncbi.nlm.nih.gov/>.
- NBN (2019) *NBN Atlas*. [Online] [Accessed on 28th May 2019] [https://regions.nbnatlas.org/Local Authorities GB/Manchester%2520District%2520\(B\)#group=Fungi&subgroup=&from=2010&to=2019&tab=speciesTab](https://regions.nbnatlas.org/LocalAuthorities/GB/Manchester%2520District%2520(B)#group=Fungi&subgroup=&from=2010&to=2019&tab=speciesTab).
- Neilson, A. H. (ed.) (1998) *The Handbook of Environmental Chemistry - PAHs and Related Compounds*. 3rd ed., Berlin, Heidelberg: Springer Verlag.
- Neuhauser, B., Dynowski, M., Mayer, M. and Ludewig, U. (2007) 'Regulation of NH₄⁺ Transport by Essential Cross Talk between AMT Monomers through the Carboxyl Tails.' *PLANT PHYSIOLOGY*.
- De Nicola, F., Concha Graña, E., López Mahía, P., Muniategui Lorenzo, S., Prada Rodríguez, D., Retuerto, R., Carballeira, A., Aboal, J. R. and Fernández, J. Á. (2017) 'Evergreen or deciduous trees for capturing PAHs from ambient air? A case study.' *Environmental Pollution*, 221 pp. 276–284.
- Nieboer, E., Ahmed, H. M., Puckett, K. J. and Richardson, D. H. S. (1972) 'Heavy metal content of lichens in relation to distance from a nickel smelter in sudbury, ONTARIO.' *The Lichenologist*.
- Nieboer, E., Puckett, K. J. and Grace, B. (1976) 'The uptake of nickel by *Umbilicaria muhlenbergii*: a physicochemical process.' *Canadian Journal of Botany*, 54(8) pp.

724–733.

- Nimis, P. L., Andreussi, S. and Pittao, E. (2001) 'The performance of two lichen species as bioaccumulators of trace metals.' *Science of the Total Environment*.
- Nimis, P. L. and Bargagli, R. (1999) 'LINEE-GUIDA PER L' UTILIZZO DI LICHENI EPIFITI COME BIOACCUMULATORI DI METALLI IN TRACCIA.' *Proc. Workshop Biomonitoraggio della qualità dell'aria sul territorio nazionale*. Roma: ANPA-Serie pp. 279–287.
- Nimis, P. L., Castello, M. and Perotti, M. (1990) 'Lichens as Biomonitors of Sulphur Dioxide Pollution in La Spezia (Northern Italy).' *The Lichenologist*, 22(03) pp. 333–344.
- Nimis, P. L., Ciccarelli, A., Lazzarin, G., Bargagli, R., Benedet, A., Castello, M., Gasparo, D., Lausi, D., Olivieri, S. and Tretiach, M. (1989) 'I licheni come bioindicatori inquinamento atmosferico nell'area di Schio-Thiene-Breganze (VI).' *Bollettino del Museo civico di Storia Naturale di Verona*, 16 pp. 1–154.
- Nimis, P. L., Lazzarin, A., Lazzarin, G. and Gasparo, D. (1991) 'Lichens as bioindicators of air pollution by SO₂ in the Veneto region (NE Italy).' *Studia Geobotanica*, 11 pp. 3–76.
- Nimis, P. L. and Purvis, O. W. (2002) 'Monitoring Lichens as Indicators of Pollution.' In Nimis, P. L., Scheidegger, C., and Wolseley, P. A. (eds) *Monitoring with Lichens - Monitoring Lichens*. 1st ed., Dordrecht: Springer Science + Business Media B.V., pp. 7–10.
- Nimis, P. L., Scheidegger, C. and Wolseley, P. A. (2002) *Monitoring with Lichens - Monitoring Lichens*. Nimis, P. L., Scheidegger, C., and Wolseley, P. A. (eds). 1st ed., Dordrecht: Springer Science + Business Media B.V.
- Nimis, P. L., Scheidegger, C. and Wolseley, P. A. (2002) 'Monitoring with Lichens — Monitoring Lichens.' In Nimis, P. L., Scheidegger, C., and Wolseley, P. A. (eds) *Monitoring with Lichens — Monitoring Lichens*. 1st ed., Dordrecht: Springer Science + Business Media B.V., pp. 1–4.
- Nimis, P. L., Wolseley, P. and Martellos, S. (2009) 'A key to common lichens on trees in England.' *Key to nature*.
- Nisbet, I. C. T. and LaGoy, P. K. (1992) 'Toxic equivalency factors (TEFs) for polycyclic aromatic hydrocarbons (PAHs).' *Regulatory Toxicology and Pharmacology*, 16(3) pp. 290–300.
- Nitsche, M., Nurmatov, N., Hensgen, F. and Wachendorf, M. (2017) 'Heavy metals and polycyclic aromatic hydrocarbons in urban leaf litter designated for combustion.' *Energies*, 10(3).
- Norman, A.-L. (2004) 'Insights into the biogenic contribution to total sulphate in aerosol and precipitation in the Fraser Valley afforded by isotopes of sulphur and oxygen.' *Journal of Geophysical Research*, 109(D5) p. D05311.
- Nriagu, J. O. (1979) 'Global inventory of natural and anthropogenic emissions of trace metals to the atmosphere.' *Nature*.
- Núñez-Alonso, D., Pérez-Arribas, L. V., Manzoor, S. and Cáceres, J. O. (2019) 'Statistical Tools for Air Pollution Assessment: Multivariate and Spatial Analysis Studies in the Madrid Region.' *Journal of Analytical Methods in Chemistry*, 2019 pp. 1–9.
- Nybakken, L., Johansson, O. and Palmqvist, K. (2009) 'Defensive compound concentration in boreal lichens in response to simulated nitrogen deposition.' *Global Change Biology*, 15(9) pp. 2247–2260.
- O'Brien, T., Xu, J. and Patierno, S. R. (2001) 'Effects of glutathione on chromium-induced DNA crosslinking and DNA polymerase arrest.' *Molecular and Cellular Biochemistry*, 222(1–2) pp. 173–182.
- Ockenden, W. A., Steinnes, E., Parker, C. and Jones, K. C. (1998) 'Observations on Persistent Organic Pollutants in Plants: Implications for Their Use as Passive Air Samplers and for POP Cycling.' *Environmental Science & Technology*, 32(18) pp. 2721–2726.

- OECD (2019) *Functional Urban Areas - United Kingdom*.
- Office for National Statistics (2013) *2011 Census: Characteristics of Built-Up Areas*. London.
- Oiamo, T. H., Johnson, M., Tang, K. and Luginaah, I. N. (2015) 'Assessing traffic and industrial contributions to ambient nitrogen dioxide and volatile organic compounds in a low pollution urban environment.' *Science of the Total Environment*. Elsevier B.V., 529 pp. 149–157.
- Oke, T. R. (1988) 'Street design and urban canopy layer climate.' *Energy and Buildings*, 11(1–3) pp. 103–113.
- Olivier, J. G. J., Bouwman, A. F., Van Der Hock, K. W. and Berdowski, J. J. M. (1998) 'Global air emission inventories for anthropogenic sources of NO, NH, and N₂O in 1990.' *Environmental Pollution* 102 pp. 135–148.
- Olsen, H. B., Berthelsen, K., Andersen, H. V. and Sørensen, U. (2010) 'Xanthoria parietina as a monitor of ground-level ambient ammonia concentrations.' *Environmental Pollution*. Elsevier Ltd, 158(2) pp. 455–461.
- OPAL (2015a) *Air Survey results - lichens on trees*. [Online] [Accessed on 28th May 2019] <https://www.opalexplornature.org/lichen-results-map>.
- OPAL (2015b) 'Lichen Identification Guide.' FSC Publications.
- Owczarek, M., Guidotti, M., Blasi, G., De Simone, C., De Marco, A. and Spadoni, M. (2001) 'Traffic pollution monitoring using lichens as bioaccumulators of heavy metals and polycyclic aromatic hydrocarbons.' *Fresenius Environmental Bulletin*, 10(1) pp. 42–45.
- Palacios, M. A., Gómez, M. M., Moldovan, M., Morrison, G., Rauch, S., McLeod, C., Ma, R., Laserna, J., Lucena, P., Caroli, S., Alimonti, A., Petrucci, F., Bocca, B., Schramel, P., Lustig, S., Zischka, M., Wass, U., Stenbom, B., Luna, M., Saenz, J. C., Santamaría, J. and Torrens, J. M. (2000) 'Platinum-group elements: Quantification in collected exhaust fumes and studies of catalyst surfaces.' *Science of the Total Environment*.
- Palmes, E. D., Gunnison, A. F., DiMattio, J. and Tomczyk, C. (1976) 'Personal sampler for nitrogen dioxide.' *American Industrial Hygiene Association Journal*, 37(10) pp. 570–577.
- Palmqvist, K., Campbell, D., Ekblad, A. and Johansson, H. (1998) 'Photosynthetic capacity in relation to nitrogen content and its partitioning in lichens with different photobionts.' *Plant, Cell and Environment*, 21(4) pp. 361–372.
- Palmqvist, K. and Dahlman, L. (2006) 'Responses of the green algal foliose lichen *Platismatia glauca* to increased nitrogen supply.' *The New phytologist*, 171(2) pp. 343–56.
- Pampanin, D. M. and Sydnes, M. O. (2013) 'Chapter 5: Polycyclic aromatic hydrocarbons a constituent of Petroleum: Presence and influence in the aquatic environment.' *In Hydrocarbon*.
- Pandey, P. K., Patel, K. S. and Lenicek, J. A. N. (1999) 'Polycyclic Aromatic Hydrocarbons: Need for assessment of Health Risks in India? Study of An Urban-Industrial Location in India.' *Environ Monit Assess*.
- Pankow, J. F., Storey, J. M. E. and Yamasaki, H. (1993) 'Effects of relative humidity on gas/particle partitioning of semivolatile organic compounds to urban particulate matter.' *Environmental Science & Technology*, 27(10) pp. 2220–2226.
- Pannullo, F., Lee, D., Waclawski, E. and Leyland, A. H. (2015) 'Improving spatial nitrogen dioxide prediction using diffusion tubes: A case study in West Central Scotland.' *Atmospheric Environment*. Elsevier Ltd, 118 pp. 227–235.
- Pant, P. and Harrison, R. M. (2013) 'Estimation of the contribution of road traffic emissions to particulate matter concentrations from field measurements: A review.' *Atmospheric Environment*.
- Paoli, L., Corsini, A., Bigagli, V., Vannini, J., Bruscoli, C. and Loppi, S. (2012) 'Long-term

- biological monitoring of environmental quality around a solid waste landfill assessed with lichens.' *Environmental Pollution*. Elsevier Ltd, 161, February, pp. 70–75.
- Paoli, L., Maccelli, C., Guarnieri, M., Vannini, A. and Loppi, S. (2019) 'Lichens "travelling" in smokers' cars are suitable biomonitors of indoor air quality.' *Ecological Indicators*.
- Paoli, L., Maslaňáková, I., Grassi, A., Bačkor, M. and Loppi, S. (2015) 'Effects of acute NH₃ air pollution on N-sensitive and N-tolerant lichen species.' *Ecotoxicology and Environmental Safety*, 122 pp. 377–383.
- Paoli, L., Vannini, A., Fačkovcová, Z., Guarnieri, M., Bačkor, M. and Loppi, S. (2018) 'One year of transplant: Is it enough for lichens to reflect the new atmospheric conditions?' *Ecological Indicators*, 88(January) pp. 495–502.
- Paoli, L., Vannini, A., Monaci, F. and Loppi, S. (2018) 'Competition between heavy metal ions for binding sites in lichens: Implications for biomonitoring studies.' *Chemosphere*. Elsevier Ltd, 199 pp. 655–660.
- Park, S. S., Kim, Y. J. and Kang, C. H. (2002) 'Atmospheric polycyclic aromatic hydrocarbons in Seoul, Korea.' *Atmospheric Environment*.
- Parra, M. A., Elustondo, D., Bermejo, R. and Santamaría, J. M. (2008) 'Ambient air levels of volatile organic compounds (VOC) and nitrogen dioxide (NO₂) in a medium size city in Northern Spain.' *Science of the Total Environment*, The. Elsevier B.V., 407(3) pp. 999–1009.
- Parzych, A., Astel, A., Zdunczyk, A. and Surowiec, T. (2016) 'Evaluation of urban environment pollution based on the accumulation of macro- and trace elements in epiphytic lichens.' *Journal of Environmental Science and Health Part A-Toxic/Hazardous Substances & Environmental Engineering*. Taylor & Francis, 51(4) pp. 297–308.
- Parzych, A., Zdunczyk, A. and Astel, A. (2016) 'Epiphytic lichens as bioindicators of air pollution by heavy metals in an urban area (northern Poland),' 21(3) pp. 781–795.
- Paul, A. (2005) *Manganese as a site factor for epiphytic lichens*. Georg-August-Universität zu Göttingen.
- Paustenbach, D. J. (2000) 'The practice of exposure assessment: A state-of-the-art review.' *Journal of Toxicology and Environmental Health - Part B: Critical Reviews*, 3(3) pp. 179–291.
- Pavlova, E. A. and Maslov, A. I. (2008) 'Nitrate uptake by isolated bionts of the lichen *Parmelia sulcata*.' *Russian Journal of Plant Physiology*, 55(4) pp. 475–479.
- Pearson, J., Wells, D. M., Seller, K. J., Bennett, A., Soares, A., Woodall, J. and Ingrouille, M. J. (2000) 'Traffic exposure increases natural ¹⁵N and heavy metal concentrations in mosses.' *New Phytologist*, 147(2000) pp. 317–326.
- Pearson, L. and Skye, E. (1965) 'Air Pollution Affects Pattern of Photosynthesis in *Parmelia sulcata*, a Corticolous Lichen.' *Science*, 148(3677) pp. 1600–1602.
- Pedersen, M., Giorgis-Allemand, L., Bernard, C., Aguilera, I., Andersen, A.-M. N., Ballester, F., Beelen, R. M. J., Chatzi, L., Cirach, M., Danileviciute, A., Dedele, A., Eijdsen, M. van, Estarlich, M., Fernández-Somoano, A., Fernández, M. F., Forastiere, F., Gehring, U., Grazuleviciene, R., Gruziova, O., Heude, B., Hoek, G., Hoogh, K. de, van den Hooven, E. H., Håberg, S. E., Jaddoe, V. W. V., Klümper, C., Korek, M., Krämer, U., Lerchundi, A., Lepeule, J., Nafstad, P., Nystad, W., Patelarou, E., Porta, D., Postma, D., Raaschou-Nielsen, O., Rudnai, P., Sunyer, J., Stephanou, E., Sørensen, M., Thiering, E., Tuffnell, D., Varró, M. J., Vrijkotte, T. G. M., Wijga, A., Wilhelm, M., Wright, J., Nieuwenhuijsen, M. J., Pershagen, G., Brunekreef, B., Kogevinas, M. and Slama, R. (2013) 'Ambient air pollution and low birthweight: a European cohort study (ESCAPE).' *The Lancet Respiratory Medicine*, 1(9) pp. 695–704.
- Peled, R. (2011) 'Air pollution exposure: Who is at high risk?' *Atmospheric Environment*. Elsevier Ltd, 45(10) pp. 1781–1785.
- Perrino, C., Catrambone, M., Menno Di Bucchianico, D. and Allegrini, I. (2002) 'Gaseous

- ammonia in the urban area of Rome, Italy and its relationship with traffic emissions.' *Atmospheric Environment*.
- Peterson, B. S., Rauh, V. A., Bansal, R., Hao, X., Toth, Z., Nati, G., Walsh, K., Miller, R. L., Arias, F., Semanek, D. and Perera, F. (2015) 'Effects of prenatal exposure to air pollutants (polycyclic aromatic hydrocarbons) on the development of brain white matter, cognition, and behavior in later childhood.' *JAMA Psychiatry*, 72(6) pp. 531–540.
- Petry, T., Schmid, P. and Schlatter, C. (1996) 'The use of toxic equivalency factors in assessing occupational and environmental health risk associated with exposure to airborne mixtures of polycyclic aromatic hydrocarbons (PAHs).' *Chemosphere*, 32(4) pp. 639–648.
- PHE CRCE (2018) *Polycyclic aromatic hydrocarbons (Benzo[a]pyrene) - Toxicological Overview*.
- Piccardo, M. T., Pala, M., Bonaccorso, B., Stella, A., Redaelli, A., Paola, G. and Valerio, F. (2005) 'Pinus nigra and Pinus pinaster needles as passive samplers of polycyclic aromatic hydrocarbons.' *Environmental Pollution*, 133(2) pp. 293–301.
- Pienaar, J. J., Beukes, J. P., Van Zyl, P. G., Aherne, J. and Lehmann, C. M. B. (2015) 'Passive Diffusion Sampling Devices for Monitoring Ambient Air Concentrations.' In Forbes, P. B. C. (ed.) *Comprehensive Analytical Chemistry*. Elsevier B.V., pp. 13–52.
- Pinho, P., Augusto, S., Branquinho, C., Bio, A., Pereira, M. J., Soares, A. and Catarino, F. (2004) 'Mapping lichen diversity as a first step for air quality assessment.' *Journal of Atmospheric Chemistry*.
- Pinho, P., Augusto, S., Martins-Loução, M. A., Pereira, M. J., Soares, A., Máguas, C. and Branquinho, C. (2008) 'Causes of change in nitrophytic and oligotrophic lichen species in a Mediterranean climate: Impact of land cover and atmospheric pollutants.' *Environmental Pollution*, 154(3) pp. 380–389.
- Pinho, P., Barros, C., Augusto, S., Pereira, M. J., Máguas, C. and Branquinho, C. (2017) 'Using nitrogen concentration and isotopic composition in lichens to spatially assess the relative contribution of atmospheric nitrogen sources in complex landscapes.' *Environmental Pollution*, 230(November) pp. 632–638.
- Pinho, P., Bergamini, A., Carvalho, P., Branquinho, C., Stofer, S., Scheidegger, C. and Máguas, C. (2012) 'Lichen functional groups as ecological indicators of the effects of land-use in Mediterranean ecosystems.' *Ecological Indicators*. Elsevier Ltd, 15(1) pp. 36–42.
- Pinho, P., Branquinho, C., Cruz, C., Tang, Y. S., Dias, T., Rosa, A. P., Máguas, C., Martins-Loução, and M. A. S., Parto, M.-A. and Sutton, M. A. (2009) 'Assessment of Critical Levels of Atmospheric Ammonia for Lichen Diversity in Cork-Oak Woodland, Portugal.' In Sutton, M. A., Reis, S., and Baker, S. (eds) *Atmospheric Ammonia: Detecting Emission Changes and Environmental Impacts*. Dordrecht: Springer Netherlands, pp. 109–123.
- Piovár, J., Weidinger, M., Bačkor, M., Bačkorová, M. and Lichtscheidl, I. (2017) 'Short-term influence of Cu, Zn, Ni and Cd excess on metabolism, ultrastructure and distribution of elements in lichen *Xanthoria parietina* (L.) Th. Fr.' *Ecotoxicology and Environmental Safety*, 145(May) pp. 408–419.
- Pisani, T., Munzi, S., Paoli, L., Bačkor, M. and Loppi, S. (2009) 'Physiological effects of arsenic in the lichen *Xanthoria parietina* (L.) Th. Fr.' *Chemosphere*, 76(7) pp. 921–926.
- Plaisance, H., Sagnier, I., Saison, J. Y., Galloo, J. C. and Guillermo, R. (2002) 'Performances and application of a passive sampling method for the simultaneous determination of nitrogen dioxide and sulfur dioxide in ambient air.' *Environmental Monitoring and Assessment*, 79(3) pp. 301–315.
- Pohl, C. and Saini, C. (2014) *Determination of Common Anions and Oxyhalides in Environmental Samples: Selecting the Proper Mobile Phase and Column*.

Sunnycale.

- Possanzini, M., Di Palo, V., Gigliucci, P., Tomasi Scianò, M. C. and Cecinato, A. (2004) 'Determination of phase-distributed PAH in Rome ambient air by denuder/ GC-MS method.' *Atmospheric Environment*, 38(12) pp. 1727–1734.
- Poster, D. L., Sander, L. C. and Wise, S. A. (1998) 'Chromatographic Methods of Analysis for the Determination of PAHs in Environmental Samples.' In Neilson, A. H. (ed.) *The Handbook of Environmental Chemistry - PAHs and Related Compounds*. 3rd ed., Berlin, Heidelberg: Springer-Verlag, pp. 77–135.
- Pozo, K., Estellano, V. H., Harner, T., Diaz-Robles, L., Cereceda-Balic, F., Etcharren, P., Pozo, K., Vidal, V., Guerrero, F. and Vergara-Fernández, A. (2015) 'Assessing Polycyclic Aromatic Hydrocarbons (PAHs) using passive air sampling in the atmosphere of one of the most wood-smoke-polluted cities in Chile: The case study of Temuco.' *Chemosphere*. Elsevier Ltd, 134 pp. 475–481.
- Pozo, K., Harner, T., Shoeib, M., Urrutia, R., Barra, R., Parra, O. and Focardi, S. (2004) 'Passive-sampler derived air concentrations of persistent organic pollutants on a north-south transect in Chile.' *Environmental Science and Technology*, 38(24) pp. 6529–6537.
- Prahl, F. G. and Carpenter, R. (1983) 'Polycyclic aromatic hydrocarbon (PAH)-phase associations in Washington coastal sediment.' *Geochimica et Cosmochimica Acta*, 47(6) pp. 1013–1023.
- Protano, C., Guidotti, M., Owczarek, M., Fantozzi, L., Blasi, G. and Vitali, M. (2014) 'Polycyclic aromatic hydrocarbons and metals in transplanted lichen (*Pseudovernia furfuracea*) at sites adjacent to a solidwaste landfill in central Italy.' *Archives of Environmental Contamination and Toxicology*, 66(4) pp. 471–481.
- Pulles, T., Denier van der Gon, H., Appelman, W. and Verheul, M. (2012) 'Emission factors for heavy metals from diesel and petrol used in European vehicles.' *Atmospheric Environment*.
- Purvis, O. W., Chimonides, J., Din, V., Erotokritou, L., Jeffries, T., Jones, G. C., Louwhoff, S., Read, H. and Spiro, B. (2003) 'Which factors are responsible for the changing lichen floras of London?' *Science of the Total Environment*, 310(1–3) pp. 179–189.
- Puy-Alquiza, M. J., Reyes, V., Wrobel, K., Wrobel, K., Torres Elguera, J. C. and Miranda-Aviles, R. (2016) 'Polycyclic aromatic hydrocarbons in urban tunnels of Guanajuato city (Mexico) measured in deposited dust particles and in transplanted lichen *Xanthoparmelia mexicana* (Gyeln.) Hale.' *Environmental Science and Pollution Research*.
- Quevauviller, P., Herzig, R. and Muntau, H. (1996) *The certification of the contents (mass fractions) of Al, As, Cd, Cr, Cu, Hg, Ni, Pb and Zn in lichen CRM 482*.
- Ratola, N., Lacorte, S., Alves, A. and Barceló, D. (2006) 'Analysis of polycyclic aromatic hydrocarbons in pine needles by gas chromatography-mass spectrometry. Comparison of different extraction and clean-up procedures.' *Journal of Chromatography A*, 1114(2) pp. 198–204.
- Ravindra, K., Sokhi, R. and Van Grieken, R. (2008) 'Atmospheric polycyclic aromatic hydrocarbons: Source attribution, emission factors and regulation.' *Atmospheric Environment*, 42(13) pp. 2895–2921.
- Ravindra, K., Wauters, E. and Van Grieken, R. (2007) 'Spatial and temporal variations in particulate Polycyclic Aromatic Hydrocarbon (PAH) levels over Menen (Belgium) and their relation with air mass trajectories.' In *Developments in Environmental Science*, pp. 838–841.
- Ravindra, K., Wauters, E. and Van Grieken, R. (2008) 'Variation in particulate PAHs levels and their relation with the transboundary movement of the air masses.' *Science of The Total Environment*, 396(2–3) pp. 100–110.
- Razali, N. M. and Wah, Y. B. (2011) 'Power comparisons of Shapiro-Wilk, Kolmogorov-Smirnov, Lilliefors and Anderson-Darling tests.' *Journal of Statistical Modeling and Analytics*, 2(1) pp. 21–33.

- Red Rose Forest (2008) *Manchester Tree Audit Phase 2: The Location and Function of Trees in the City - Executive Summary*. Manchester.
- Regan, D. (2018) *Manchester Public Health Annual Report 2018*. Manchester.
- Reis, M. A., Alves, L. C., Freitas, M. C., Van Os, B. and Wolterbeek, H. T. (1999) 'Lichens (*Parmelia sulcata*) time response model to environmental elemental availability.' *Science of the Total Environment*, 232(1–2) pp. 105–115.
- Rendu, J.-M. (1978) *An Introduction to Geostatistical Methods of Mineral Evaluation*. Johannesburg: South African Institute of Mining and Metallurgy.
- Ribeiro, M. C., Pinho, P., Llop, E., Branquinho, C. and Pereira, M. J. (2016) 'Geostatistical uncertainty of assessing air quality using high-spatial-resolution lichen data: A health study in the urban area of Sines, Portugal.' *Science of the Total Environment*. Elsevier B.V., 562 pp. 740–750.
- Ribeiro, M. C., Pinho, P., Llop, E., Branquinho, C., Sousa, A. J. and Pereira, M. J. (2013) 'Multivariate geostatistical methods for analysis of relationships between ecological indicators and environmental factors at multiple spatial scales.' *Ecological Indicators*. Elsevier Ltd, 29 pp. 339–347.
- Richardson, D. H. S. (1993) *Pollution monitoring with lichens*. Slough: The Richmond Publishing Co. Ltd.
- Rim, K. T., Koo, K. H. and Park, J. S. (2013) 'Toxicological Evaluations of Rare Earths and Their Health Impacts to Workers: A Literature Review.' *Safety and Health at Work*.
- Robertson, D. J. and Taylor, K. G. (2007) 'Temporal variability of metal contamination in urban road-deposited sediment in Manchester, UK: Implications for urban pollution monitoring.' *Water, Air, and Soil Pollution*, 186(1–4) pp. 209–220.
- Robertson, D. J., Taylor, K. G. and Hoon, S. R. (2003) 'Geochemical and mineral magnetic characterisation of urban sediment particulates, Manchester, UK.' *Applied Geochemistry*, 18(2) pp. 269–282.
- Rogge, W. F., Hildemann, L. M., Mazurek, M. a., Cass, G. R. and Simoneit, B. R. T. (1993) 'Sources of fine organic aerosol. 2. Noncatalyst and catalyst-equipped automobiles and heavy-duty diesel trucks.' *Environmental Science & Technology*, 27(4) pp. 636–651.
- Rola, K. and Osyczka, P. (2019) 'Temporal changes in accumulation of trace metals in vegetative and generative parts of *Xanthoria parietina* lichen thalli and their implications for biomonitoring studies.' *Ecological Indicators*. Elsevier, 96(August 2018) pp. 293–302.
- Romary, T., de Fouquet, C. and Malherbe, L. (2011) 'Sampling design for air quality measurement surveys: An optimization approach.' *Atmospheric Environment*. Elsevier Ltd, 45(21) pp. 3613–3620.
- Rose, C. I. and Hawksworth, D. L. (1981) 'Lichen recolonization in London's cleaner air.' *Nature*, 289 pp. 289–292.
- Royal Society of Chemistry (2018) *Chemspider*. [Online] [Accessed on 23rd October 2018] <http://www.chemspider.com/>.
- Ruoss, E. (1999) 'How agriculture affects lichen vegetation in Central Switzerland.' *Lichenologist*, 31(1) pp. 63–73.
- Russell, K. M., Galloway, J. N., Macko, S. A., Moody, J. L. and Scudlark, J. R. (1998) 'Sources of nitrogen in wet deposition to the Chesapeake Bay region.' *Atmospheric Environment*, 32(14–15) pp. 2453–2465.
- Russow, R., Veste, M. and Littmann, T. (2004) 'Using the natural ¹⁵N abundance to assess the main nitrogen inputs into the sand dune area of the north-western Negev Desert (Israel).' *Isotopes in Environmental and Health Studies*, 40(1) pp. 57–67.
- Salem, A. A., Soliman, A. A. and El-Haty, I. A. (2009) 'Determination of nitrogen dioxide, sulfur dioxide, ozone, and ammonia in ambient air using the passive sampling method associated with ion chromatographic and potentiometric analyses.' *Air Quality, Atmosphere and Health*, 2(3) pp. 133–145.

- Salit, M. L. and Turk, G. C. (1998) 'A Drift Correction Procedure.' *Analytical Chemistry*, 70(15) pp. 3184–3190.
- Salmond, J. A. and McKendry, I. G. (2009) 'Influences of Meteorology on Air Pollution Concentrations and Processes in Urban Areas.' In Harrison, R. M. and Hester, R. E. (eds) *Air Quality in Urban Environments*. Cambridge: Royal Society of Chemistry (Issues in Environmental Science and Technology), pp. 23–42.
- Salmond, J. A., Williams, D. E., Laing, G., Kingham, S., Dirks, K., Longley, I. and Henshaw, G. S. (2013) 'The influence of vegetation on the horizontal and vertical distribution of pollutants in a street canyon.' *Science of The Total Environment*. Elsevier B.V., 443, January, pp. 287–298.
- Salsac, L., Chaillou, S., Morot-Gaudry, J.-F., Lesaint, C. and Jolivoie, E. (1987) 'Nitrate and ammonium nutrition in plants.' *Plant Physiology and Biochemistry*, 25 pp. 805–812.
- Samburova, V., Zielinska, B. and Khlystov, A. (2017) 'Do 16 Polycyclic Aromatic Hydrocarbons Represent PAH Air Toxicity?' *Toxics*, 5(3) p. 17.
- Sanchez, B., Santiago, J. L., Martilli, A., Martin, F., Borge, R., Quaassdorff, C. and de la Paz, D. (2017) 'Modelling NOX concentrations through CFD-RANS in an urban hot-spot using high resolution traffic emissions and meteorology from a mesoscale model.' *Atmospheric Environment*. Elsevier Ltd, 163(X) pp. 155–165.
- Sandstead, H. H. and Au, W. (2007) 'Zinc.' In Nordberg, G. F., Fowler, B. A., Nordberg, M., and Friberg, L. T. (eds) *Handbook on the Toxicology of Metals*. 3rd ed., Elsevier B.V., pp. 925–947.
- Sanità Di Toppi, L., Musetti, R., Marabottini, R., Corradi, M. G., Vattuone, Z., Favali, M. A. and Badiani, M. (2004) 'Responses of *Xanthoria parietina* thalli to environmentally relevant concentrations of hexavalent chromium.' *Functional Plant Biology*.
- Sarigiannis, D. A., Karakitsios, S. P., Zikopoulos, D., Nikolaki, S. and Kermenidou, M. (2015) 'Lung cancer risk from PAHs emitted from biomass combustion.' *Environmental Research*. Elsevier, 137 pp. 147–156.
- Satya, Upreti, D. K. and Patel, D. K. (2012) 'Rinodina sophodes (Ach.) Massal.: a bioaccumulator of polycyclic aromatic hydrocarbons (PAHs) in Kanpur City, India.' *Environmental Monitoring and Assessment*, 184(1) pp. 229–238.
- Sawant, A. A., Nigam, A., Miller, J. W., Johnson, K. C. and Cocker, D. R. (2007) 'Regulated and Non-Regulated Emissions from In-Use Diesel-Electric Switching Locomotives.' *Environmental Science & Technology*, 41(17) pp. 6074–6083.
- SAWG (2002) *Appendix E - SAWG Enclosure A - Measurement Error*.
- Schaefer, M. (2012) *Wörterbuch der Ökologie*. 5., Heidelberg: Spektrum Akademischer Verlag.
- Schauer, J., Rogge, W., Hildemann, L., Mazurek, M., Cass, G. and Simoneit, B. (1996) 'Source apportionment of airborne particulate matter using organic compounds as tracers.' *Atmospheric Environment*, 41 pp. 241–259.
- Schlögl, R., Indlekofer, G. and Oelhafen, P. (1987) 'Mikropartikelemissionen von Verbrennungsmotoren mit Abgasreinigung – Röntgen-Photoelektronenspektroskopie in der Umweltanalytik.' *Angewandte Chemie*, 99(4) pp. 312–322.
- Schnelle-Kreis, J., Sklorz, M., Herrmann, H. and Zimmermann, R. (2007) 'Quellen, Vorkommen, Zusammensetzung Atmosphärische Aerosole.' *Chemie in Unserer Zeit*, 41(3) pp. 220–230.
- Schraufnagel, D. E., Balmes, J. R., Cowl, C. T., De Matteis, S., Jung, S.-H., Mortimer, K., Perez-Padilla, R., Rice, M. B., Riojas-Rodriguez, H., Sood, A., Thurston, G. D., To, T., Vanker, A. and Wuebbles, D. J. (2019) 'Air Pollution and Noncommunicable Diseases.' *Chest*. Elsevier Inc, 155(2) pp. 409–416.
- Seaward, M. R. D. (2003) *Lichens and hypertrophication*. Lambley, P. and Wolseley, P. (eds) *Lichens in a changing pollution environment: English Nature Research Reports*. Peterborough.

- Seed, L., Wolseley, P., Gosling, L., Davies, L. and Power, S. A. (2013) 'Modelling relationships between lichen bioindicators, air quality and climate on a national scale: Results from the UK OPAL air survey.' *Environmental Pollution*. Elsevier Ltd, 182, November, pp. 437–447.
- Seinfeld, J. H. and Pandis, S. N. (1997) *Atmospheric Chemistry and Physics: from Air Pollution to Climate Change*. John Wiley & Sons.
- Seo, J.-S., Keum, Y.-S., Harada, R. M. and Li, Q. X. (2007) 'Isolation and Characterization of Bacteria Capable of Degrading Polycyclic Aromatic Hydrocarbons (PAHs) and Organophosphorus Pesticides from PAH-Contaminated Soil in Hilo, Hawaii.' *Journal of Agricultural and Food Chemistry*, 55(14) pp. 5383–5389.
- Sernander, R. (1926) *Stockholms Natur*. Stockholm: Almqvist and Wiksel.
- Shapiro, I. A. (1983) 'Activities of nitrate reductase and glutamine synthetase in lichens.' *Soviet Plant Physiology*, 30 pp. 539–542.
- Shapiro, I. A. (1984) 'Activities of nitrate reductase and glutamine synthetase in lichens.' *Soviet Plant Physiology*, 30 pp. 539–542.
- Shapiro, I. A. (1985) 'Nitrate reductase activity in the lichen *Lobaria pulmonaria*.' *Soviet Plant Physiology*, 32 pp. 397–401.
- Shapiro, I. A. (1987) 'Effects of lichen substances on nitrate reductase activity in the lichen *Lobaria pulmonaria*.' *Soviet Plant Physiology*, 34 pp. 255–258.
- Shapiro, I. A. and Nifontova, M. G. (1991) 'Effects of sulfur dioxide and gamma-radiation on the nitrate reductase activity in the lichen *Lobaria pulmonaria* (L.) Hoffm.' *Soviet Journal of Ecology*, 22 pp. 47–51.
- Sharp, Z. (2017) *Principles of Stable Isotope Geochemistry*. 2nd editio, Pearson.
- Shen, J., Gao, Z., Ding, W. and Yu, Y. (2017) 'An investigation on the effect of street morphology to ambient air quality using six real-world cases.' *Atmospheric Environment*. Elsevier Ltd, 164 pp. 85–101.
- Shrivastava, A. and Gupta, V. B. (2011) 'Methods for the determination of limit of detection and limit of quantitation of the analytical methods.' *Chronicles of Young Scientists*, 2(1) pp. 21–25.
- Shukla, V., D.K., U. and Bajpai, R. (2014) *Lichens to Biomonitor the Environment. Lichens to Biomonitor the Environment*. New Delhi: Springer India.
- Shukla, V., Patel, D. K., Upreti, D. K. and Yunus, M. (2012) 'Lichens to distinguish urban from industrial PAHs.' *Environmental Chemistry Letters*, 10(2) pp. 159–164.
- Shukla, V. and Upreti, D. K. (2009) 'Polycyclic aromatic hydrocarbon (PAH) accumulation in lichen, *Phaeophyscia hispidula* of DehraDun City, Garhwal Himalayas.' *Environmental Monitoring and Assessment*, 149(1–4) pp. 1–7.
- Shukla, V., Upreti, D. K., Patel, D. K. and Tripathi, R. (2010) 'Accumulation of Polycyclic Aromatic Hydrocarbons in some lichens of Garhwal Himalayas, India.' *International Journal of Environment and Waste Management*, 5(1/2) p. 104.
- Shukla, V., Upreti, D. K., Patel, D. K. and Yunus, M. (2013) 'Lichens reveal air PAH fractionation in the Himalaya.' *Environmental Chemistry Letters*, 11(1) pp. 19–23.
- Sigma-Aldrich (2017) *Certificate of Analysis Nutrients - WP (Whole-volume)*.
- Silberstein, L., Siegel, B. Z., Siegel, S. M., Mukhtar, A. and Galun, M. (1996a) 'Comparative Studies on *Xanthoria Parietina*, a Pollution Resistant Lichen, and *Ramalina Duriaei*, a Sensitive Species. I. Effects of Air Pollution on Physiological Processes.' *The Lichenologist*, 28(04) pp. 355–365.
- Silberstein, L., Siegel, B. Z., Siegel, S. M., Mukhtar, A. and Galun, M. (1996b) 'Comparative Studies on *Xanthoria Parietina*, a Pollution Resistant Lichen, and *Ramalina Duriaei*, a Sensitive Species. I. Effects of Air Pollution on Physiological Processes.' *The Lichenologist*, 28(04) p. 355.
- Silveira, C., Roebeling, P., Lopes, M., Ferreira, J., Costa, S., Teixeira, J. P., Borrego, C. and Miranda, A. I. (2016) 'Assessment of health benefits related to air quality

- improvement strategies in urban areas: An Impact Pathway Approach.' *Journal of Environmental Management*, 183 pp. 694–702.
- Sims, D., Hudson, A., Park, J., Hodge, V., Porter, H. and Spaulding, W. (2017) 'Buellia dispersa (Lichens) Used as Bio-Indicators for Air Pollution Transport: A Case Study within the Las Vegas Valley, Nevada (USA).' *Environments*, 4(4) p. 94.
- Slezakova, K., Castro, D., Pereira, M. C., Morais, S., Delerue-Matos, C. and Alvim-Ferraz, M. C. (2010) 'Influence of traffic emissions on the carcinogenic polycyclic aromatic hydrocarbons in outdoor breathable particles.' *Journal of the Air and Waste Management Association*, 60(4) pp. 393–401.
- Sloof, J. E. and Wolterbeek, B. T. (1993) 'Substrate influence on epiphytic lichens.' *Environmental Monitoring and Assessment*, 25(3) pp. 225–234.
- De Sloover, J. and LeBlanc, F. (1968) 'Mapping of atmospheric pollution on the basis of lichen sensitivity.' In Misra, R. and Gopal, B. (eds) *Proceedings of the Symposium in Recent Advances in Tropical Ecology, International Society for Tropical Ecology*. Banaras Hindu University, Varanasi: International Society for Tropical Ecology, pp. 42–56.
- Smith, C. W., Aptroot, A., Coppins, B. J., Fletcher, A., Gilbert, O. L., James, P. W. and Wolseley, P. A. (eds) (2009) *The Lichens of Great Britain and Ireland*. 2nd ed., British Lichen Society.
- Smith, D. C. (1960) 'Studies in the Physiology of Lichens I. The Effects of Starvation and of Ammonia Absorption upon the Nitrogen Content of *Peltigera polydactyla*.' *Ann Bot N.S.*, 24(93) pp. 52–62.
- Smith, D. J. T. and Harrison, R. M. (1998) 'Polycyclic Aromatic Hydrocarbons in Atmospheric Particles.' In Harrison, R. M. and Van Grieken, R. (eds) *Atmospheric Particles*. Wiley.
- Smith, H. M. (ed.) (2002) *High Performance Pigments*. Wiley VCH.
- Smith, S. and Read, D. (1997) *Mycorrhizal Symbiosis*. *Mycorrhizal Symbiosis*. 2nd ed., San Diego, CA, USA: Academic Press, Harcourt Brace Co.
- Søchting, U. (1995) 'Lichens as monitors of nitrogen deposition.' *Cryptogamic Botany*, 5 pp. 264–269.
- Son, J. Y., Lee, J. T., Kim, K. H., Jung, K. and Bell, M. L. (2012) 'Characterization of fine particulate matter and associations between particulate chemical constituents and mortality in Seoul, Korea.' *Environmental Health Perspectives*, 120(6) pp. 872–878.
- Sparrius, L. B. (2007) 'Response of epiphytic lichen communities to decreasing ammonia air concentrations in a moderately polluted area of The Netherlands.' *Environmental Pollution*, 146(2) pp. 375–379.
- Spier, L., Van Dobben, H. and Van Dort, K. (2010) 'Is bark pH more important than tree species in determining the composition of nitrophytic or acidophytic lichen floras?' *Environmental Pollution*. Elsevier Ltd, 158(12) pp. 3607–3611.
- Spiro, B., Morrison, J. and Purvis, O. W. (2002) 'Sulphur Isotopes in Lichens as Indicators of Sources.' In Nimis, P. L., Scheidegger, C., and Wolseley, P. A. (eds) *Monitoring with Lichens - Monitoring Lichens*. 1st ed., Dordrecht: Springer Science + Business Media B.V., pp. 311–315.
- Spribile, T., Tuovinen, V., Resl, P., Vanderpool, D., Wolinski, H., Aime, M. C., Schneider, K., Stabentheiner, E., Toome-heller, M., Thor, G., Mayrhofer, H. and Mccutcheon, J. P. (2016) 'Basidiomycete yeasts in the cortex of ascomycete macrolichens,' 8287.
- State, G., Popescu, I. V., Radulescu, C., Macris, C., Stihi, C., Gheboianu, A., Dulama, I. and Nițescu, O. (2012) 'Comparative studies of metal air pollution by atomic spectrometry techniques and biomonitoring with moss and lichens.' *Bulletin of Environmental Contamination and Toxicology*.
- Sterry, P. (2007) *Collins Complete Guide to British Trees*. London: HarperCollins Publisher Ltd.
- Stritzke, F., Diemel, O. and Wagner, S. (2015) 'TDLAS-based NH₃ mole fraction

- measurement for exhaust diagnostics during selective catalytic reduction using a fiber-coupled 2.2- μm DFB diode laser.' *Applied Physics B: Lasers and Optics*.
- Stuben, D. and Kupper, T. (2006) 'Anthropogenic emission of Pd and traffic-related PGEs-Results based on monitoring with sewage sludge.' In Zereini, F. and Alt, F. (eds) *Palladium Emissions in the Environment: Analytical Methods, Environmental Assessment and Health Effects*. New York: Springer-Verlag, pp. 325–341.
- Sujetovienė, G. (2017) 'Epiphytic Lichen Diversity as Indicator of Environmental Quality in an Industrial Area (Central Lithuania).' *Polish Journal of Ecology*, 65(1) pp. 38–45.
- Sujetovienė, G. and Galinytė, V. (2016) 'Effects of the urban environmental conditions on the physiology of lichen and moss.' *Atmospheric Pollution Research*, 7 pp. 1–8.
- Sun, K., Tao, L., Miller, D. J., Khan, M. A. and Zondlo, M. A. (2014) 'On-road ammonia emissions characterized by mobile, open-path measurements.' *Environmental Science and Technology*.
- Sun, K., Tao, L., Miller, D. J., Pan, D., Golston, L. M., Zondlo, M. A., Griffin, R. J., Wallace, H. W., Leong, Y. J., Yang, M. M., Zhang, Y., Mauzerall, D. L. and Zhu, T. (2017) 'Vehicle Emissions as an Important Urban Ammonia Source in the United States and China.' *Environmental Science and Technology*, 51(4) pp. 2472–2481.
- Sutcliffe, M. (2009) *British Lichens - Species Gallery*. [Online] [Accessed on 10th October 2017] <http://www.uklichens.co.uk/speciesgallery.html#L>.
- Sutton, M. ., Dragosits, U., Tang, Y. . and Fowler, D. (2000) 'Ammonia emissions from non-agricultural sources in the UK.' *Atmospheric Environment*, 34(6) pp. 855–869.
- Sutton, M. A., Milford, C., Dragosits, U., Place, C. J., Singles, R. J., Smith, R. I., Pitcairn, C. E. R., Fowler, D., Hill, J., ApSimon, H. M., Ross, C., Hill, R., Jarvis, S. C., Pain, B. F., Phillips, V. C., Harrison, R., Moss, D., Webb, J., Espenhahn, S. E., Lee, D. S., Hornung, M., Ulyett, J., Bull, K. R., Emmett, B. A., Lowe, J. and Wyers, G. P. (1998) 'Dispersion, deposition and impacts of atmospheric ammonia: Quantifying local budgets and spatial variability.' In *Environmental Pollution*.
- Sutton, M. A., Pitcairn, C. E. R. and Whitfield, C. P. (2004) *Bioindicator and biomonitoring methods for assessing the effects of atmospheric nitrogen on statutory nature conservation sites. JNCC Report No. 356*.
- Suvarapu, L. N. and Baek, S.-O. (2017) 'Biomonitoring of Atmospheric Polycyclic Aromatic Hydrocarbons: A Mini Review.' *Mini-Reviews in Organic Chemistry*, 14(6) pp. 496–500.
- Taylor, K. G. (2006) 'Urban Environments.' In Perry, C. T. and Taylor, K. G. (eds) *Environmental Sedimentology*. Oxford (UK): Blackwell Publishing, pp. 190–222.
- Teeri, J. A. (1981) 'Stable Carbon Isotope Analysis of Mosses and Lichens Growing in Xeric and Moist Habitats.' *The Bryologist*, 84(1) pp. 82–84.
- TfGM (2016) *Greater Manchester Air Quality Action Plan 2016-2021*. Greater Manchester.
- TfGM (2019) *Oxford Road has changed*.
- TfGM and GMCA (2016) *Greater Manchester Low-Emission Strategy*. Greater Manchester.
- The Royal College of Physicians (2016) *Every breathe we take: the lifelong impact of air pollution - Report of a working party*. London.
- The World Bank and Institute for Health Metrics and Evaluation (2014) *The Cost of Air Pollution*. Seattle: OECD.
- Thermo Fisher Scientific (2018a) 'Dionex™ Seven Anion Standard II.'
- Thermo Fisher Scientific (2018b) 'Dionex™ Six Cation Standard I.'
- Thomas, W. (1986) 'Representativity of mosses as biomonitor organisms for the accumulation of environmental chemicals in plants and soils.' *Ecotoxicology and Environmental Safety*.
- Thurman, E. M. and Ferrer, I. (2009) 'Comparison of Quadrupole Time-of-Flight, Triple Quadrupole, and Ion-Trap Mass Spectrometry/Mass Spectrometry for the Analysis of Emerging Contaminants' pp. 14–31.

- Thurman, E. M. and Mills, M. S. (1998) *Solid-Phase Extraction: Principles and Practice*. New York: Wiley-Interscience.
- Timmers, V. R. J. H. and Achten, P. A. J. (2016) 'Non-exhaust PM emissions from electric vehicles.'
- Tiwari, A. K. and Singh, A. K. (2014) 'Hydrogeochemical investigation and groundwater quality assessment of Pratapgarh district, Uttar Pradesh.' *Journal of the Geological Society of India*.
- Tollbäck, J. (2009) *New methods for determination of airborne pollutants*. Stockholm University.
- Tolosa, I., Bayona, J. M. and Albaigés, J. (1996) 'Aliphatic and polycyclic aromatic hydrocarbons and sulfur/oxygen derivatives in Northwestern Mediterranean sediments: Spatial and temporal variability, fluxes, and budgets.' *Environmental Science and Technology*, 30(8) pp. 2495–2503.
- Tóth, G., Hermann, T., Szatmári, G. and Pásztor, L. (2016) 'Maps of heavy metals in the soils of the European Union and proposed priority areas for detailed assessment.' *Science of the Total Environment*. The Authors, 565 pp. 1054–1062.
- Tozer, W. C., Hackell, D., Miers, D. B. and Silvester, W. B. (2005) 'Extreme isotopic depletion of nitrogen in New Zealand lithophytes and epiphytes; the result of diffusive uptake of atmospheric ammonia?' *Oecologia*, 144(4) pp. 628–635.
- Trakhtenbrot, A. and Kadmon, R. (2005) 'Environmental cluster analysis as tool for selecting complementary networks of conservation sites.' *Ecological Applications*, 15(1) pp. 335–345.
- Trees & Design Action Group (2012) 'Trees in the Townscape: A Guide for Decision Makers.'
- Trust, B. A. and Fry, B. (1992) 'Stable sulphur isotopes in plants: a review.' *Plant, Cell and Environment*, 15(9) pp. 1105–1110.
- Tsai, P. J., Shieh, H. Y., Lee, W. J. and Lai, S. O. (2001) 'Health-risk assessment for workers exposed to polycyclic aromatic hydrocarbons (PAHs) in a carbon black manufacturing industry.' *Science of the Total Environment*.
- Tuba, Z. and Csintalan, Z. (1993) 'Bioindication of road motor traffic caused heavy metal pollution by lichen transplants.' In Markert, B. A. (ed.) *Plants as Biomonitors, Indicators for Heavy metals in the Terrestrial Environment*. Weinheim and New York: VCH, pp. 329–341.
- Tuckey, J. W. (1977) 'Exploratory data analysis.' Reading: Addison-Wesley.
- Tuduri, L., Millet, M., Briand, O. and Montury, M. (2012) 'Passive air sampling of semi-volatile organic compounds.' *TrAC - Trends in Analytical Chemistry*. Elsevier Ltd, 31(2) pp. 38–49.
- Tuovinen, V., Ekman, S., Thor, G., Vanderpool, D., Spribille, T. and Johannesson, H. (2018) 'Two Basidiomycete Fungi in the Cortex of Wolf Lichens' pp. 1–8.
- Twigg, M. M., Di Marco, C. F., Leeson, S., van Dijk, N., Jones, M. R., Leith, I. D., Morrison, E., Coyle, M., Proost, R., Peeters, A. N. M., Lemon, E., Frelink, T., Braban, C. F., Nemitz, E. and Cape, J. N. (2015) 'Water soluble aerosols and gases at a UK background site – Part 1: Controls of PM_{2.5} and PM₁₀; aerosol composition.' *Atmospheric Chemistry and Physics*, 15(14) pp. 8131–8145.
- Tyler, G., Pålsson, A. M. B., Bengtsson, G., Bååth, E. and Tranvik, L. (1989) 'Heavy-metal ecology of terrestrial plants, microorganisms and invertebrates - A review.' *Water, Air, and Soil Pollution*.
- Tynnyrinen, S., Palomäki, V., Holopainen, T. and Karenlampi, L. (1992) 'Comparison of Several Bioindicator Methods in Monitoring the Effects on Forest of a Fertilizer Plant and a Strip Mine.' *Annales Botanici Fennici*, 29(1) pp. 11–24.
- Tzamkiozis, T., Ntziachristos, L. and Samaras, Z. (2010) 'Diesel passenger car PM emissions: From Euro 1 to Euro 4 with particle filter.' *Atmospheric Environment*.

- Elsevier Ltd, 44(7) pp. 909–916.
- U.S. EPA (1993) *Provisional Guidance for Qualitative Risk Assessment of Polycyclic Aromatic Hydrocarbons (EPA/600/R-93/089)*. Washington D.C.
- U.S. EPA (2017) *Toxicological Review of Benzo[a]pyrene [CASRN 50-32-8]*.
- UK Department of Transport (2012) 'Guidance on Road Classification and the Primary Route Network,' (January).
- Uluozlu, O. D., Kinalioglu, K., Tuzen, M. and Soylak, M. (2007) 'Trace metal levels in lichen samples from roadsides in East Black Sea region, Turkey.' *Biomedical and environmental sciences: BES*, 20(3) pp. 203–7.
- Umweltbundesamt (2016) *Polyzyklische Aromatische Kohlenwasserstoffe Umweltschädlich! Giftig! Unvermeidbar?* Dessau-Roßlau.
- Upreti, D. K., Divakar, P. K., Shukla, V. and Bajpai, R. (2015) *Recent advances in lichenology: Modern methods and approaches in Lichen systematics and culture techniques. Recent Advances in Lichenology: Modern Methods and Approaches in Lichen Systematics and Culture Techniques, Volume 2*. New York, Dodrecht, London: Springer India.
- Valotto, G., Rampazzo, G., Visin, F., Gonella, F., Cattaruzza, E., Glisenti, A., Formenton, G. and Tieppo, P. (2015) 'Environmental and traffic-related parameters affecting road dust composition: A multi-technique approach applied to Venice area (Italy).' *Atmospheric Environment*. Elsevier Ltd, 122, December, pp. 596–608.
- Vannini, A., Paoli, L., Nicolardi, V., Di Lella, L. A. and Loppi, S. (2017) 'Seasonal variations in intracellular trace element content and physiological parameters in the lichen *Evernia prunastri* transplanted to an urban environment.' *Acta Botanica Croatica*, 76(2) pp. 171–176.
- Vardoulakis, S., Solazzo, E. and Lumbreras, J. (2011) 'Intra-urban and street scale variability of BTEX, NO₂ and O₃ in Birmingham, UK: Implications for exposure assessment.' *Atmospheric Environment*, 45(29) pp. 5069–5078.
- VDI (1995) 'Richtlinie 3799. Blatt I: Ermittlung und Beurteilung phytotoxischer Wirkungen von Immissionen mit Flechten: Flechtenkartierung.' Duesseldorf: Verein Deutscher Ingenieure (VDI).
- Vingiani, S., Adamo, P. and Giordano, S. (2004) 'Sulphur, nitrogen and carbon content of *Sphagnum capillifolium* and *Pseudevernia furfuracea* exposed in bags in the Naples urban area.' *Environmental Pollution*, 129(1) pp. 145–158.
- Vingiani, S., De Nicola, F., Purvis, W. O., Concha-Graña, E., Muniategui-Lorenzo, S., López-Mahía, P., Giordano, S. and Adamo, P. (2015) 'Active Biomonitoring of Heavy Metals and PAHs with Mosses and Lichens: a Case Study in the Cities of Naples and London.' *Water, Air, & Soil Pollution*. Springer, Dordrecht, Netherlands, 226(8 (Article 240)) pp. 1–12.
- Wada, E., Ando, T. and Kumazawa, K. (1995) 'Biodiversity of stable isotope ratios.' In Wada, E., Yoneyama, T., Minagawa, M., Ando, T., and Fry, B. . (eds) *Stable Isotopes in the Biosphere*. Kyoto: Kyoto University Press, Japan, pp. 7–14.
- Wada, E. and Hattori, E. (1990) *Nitrogen in the Sea: Forms, Abundance and Rate Processes*. CRC, Boca, Raton, FL. Boca Raton, FL: CRC Press.
- Wade, A. E. (1953) 'the British Anaptychia and Physciae' pp. 126–144.
- Wadleigh, M. A. (2003) 'Lichens and atmospheric sulphur: What stable isotopes reveal.' *Environmental Pollution*, 126(3) pp. 345–351.
- Wadleigh, M. A. and Blake, D. M. (1999) 'Tracing sources of atmospheric sulphur using epiphytic lichens.' *Environmental Pollution*, 106(3) pp. 265–271.
- Walton, R. T., Mudway, I. S., Dundas, I., Marlin, N., Koh, L. C., Aitlhadj, L., Vulliamy, T., Jamaludin, J. B., Wood, H. E., Barratt, B. M., Beevers, S., Dajnak, D., Sheikh, A., Kelly, F. J., Griffiths, C. J. and Grigg, J. (2016) 'Air pollution, ethnicity and telomere length in east London schoolchildren: An observational study.' *Environment International*, 96 pp. 41–47.

- Wang, Y. F., Huang, K. L., Li, C. T., Mi, H. H., Luo, J. H. and Tsai, P. J. (2003) 'Emissions of fuel metals content from a diesel vehicle engine.' *Atmospheric Environment*, 37(33) pp. 4637–4643.
- Warsito, B., Yasin, H., Ispriyanti, D. and Hoyyi, A. (2018) 'Robust geographically weighted regression of modeling the Air Polluter Standard Index (APSI).' *Journal of Physics: Conference Series*, 1025(1) p. 012096.
- Van der Wat, L. and Forbes, P. B. C. (2015) 'Lichens as biomonitors for organic air pollutants.' *Trends in Analytical Chemistry*. Elsevier B.V., 64 pp. 165–172.
- Wat, L. Van Der and Forbes, P. B. C. (2019) 'Comparison of extraction techniques for polycyclic aromatic hydrocarbons from lichen biomonitors.' *Environmental Science and Pollution Research*, (2006).
- Watmough, S. a., McDonough, A. M. and Raney, S. M. (2014) 'Characterizing the influence of highways on springtime NO₂ and NH₃ concentrations in regional forest monitoring plots.' *Environmental Pollution*. Elsevier Ltd, 190(2) pp. 150–158.
- Watson, J. G. (2002) 'Visibility: Science and Regulation.' *Journal of the Air & Waste Management Association*. Taylor & Francis Group, 52(6) pp. 628–713.
- Webb, J., Menzi, H., Pain, B. F., Misselbrook, T. H., Dämmgen, U., Hendriks, H. and Döhler, H. (2005) 'Managing ammonia emissions from livestock production in Europe.' *Environmental Pollution*, 135(3 SPEC. ISS.) pp. 399–406.
- Webster, R. and Oliver, M. A. (2007) *Geostatistics for Environmental Scientists. Geostatistics for Environmental Scientists: Second Edition*. Chichester, UK: John Wiley & Sons, Ltd (Statistics in Practice).
- Wheeler, A. J., Smith-doiron, M., Xu, X., Gilbert, N. L. and Brook, J. R. (2008) 'Intra-urban variability of air pollution in Windsor, Ontario — Measurement and modeling for human exposure assessment \$,' 106 pp. 7–16.
- Whitehead, J. D., Longley, I. D. and Gallagher, M. W. (2007) 'Seasonal and diurnal variation in atmospheric ammonia in an urban environment measured using a quantum cascade laser absorption spectrometer.' *Water, Air, and Soil Pollution*, 183(1–4) pp. 317–329.
- Whitworth Meteorological Observatory - Data Archive (2018). [Online] [Accessed on 16th October 2018] <http://whitworth.cas.manchester.ac.uk/2018/>.
- WHO (1999) *Monitoring ambient air quality for health impact assessment. WHO regional publications European series*. Copenhagen.
- WHO (2000a) 'Platinum.' *In Air Quality Guidelines for Europe, Copenhagen: World Health Organization, Regional Office for Europe*. 2nd ed., Copenhagen: World Health Organisation, pp. 1–273.
- WHO (2000b) 'Polycyclic aromatic hydrocarbons (PAHs).' *In*. Copenhagen: World Health Organization Regional Office for Europe, pp. 1–24.
- WHO (2003) *Polynuclear aromatic hydrocarbons in drinking-water. Background document for development of WHO guidelines for drinking-water quality (WHO/SDE/WSH/03.04/59)*. Geneva.
- WHO (2006) 'WHO Air quality guidelines for particulate matter, ozone, nitrogen dioxide and sulfur dioxide: global update 2005: summary of risk assessment.' *Geneva: World Health Organization* pp. 1–22.
- WHO (2013a) *Health risks of air pollution in Europe – HRAPIE project*. Copenhagen.
- WHO (2013b) *Review of evidence on health aspects of air pollution – REVIHAAP Project*. Copenhagen.
- WHO (2015) 'United Kingdom: WHO statistical profile.' *WHO statistical profile*. Geneva: World Health Organization p. 3.
- WHO (2018) *Air Pollution*. [Online] [Accessed on 11th June 2018] <http://www.who.int/airpollution/en/>.
- Widory, D. (2006) 'Combustibles, fuels and their combustion products: A view through

- carbon isotopes.' *Combustion Theory and Modelling*, 10(5) pp. 831–841.
- Widory, D. (2007) 'Nitrogen isotopes: Tracers of origin and processes affecting PM10 in the atmosphere of Paris.' *Atmospheric Environment*, 41(11) pp. 2382–2390.
- Wik, A. and Dave, G. (2009) 'Occurrence and effects of tire wear particles in the environment - A critical review and an initial risk assessment.' *Environmental Pollution*.
- Williams, G. (1996) 'Manchester.' *Cities*, 13(3) pp. 203–212.
- Winckelmans, E., Cox, B., Martens, E., Fierens, F., Nemery, B. and Nawrot, T. S. (2015) 'Fetal growth and maternal exposure to particulate air pollution - More marked effects at lower exposure and modification by gestational duration.' *Environmental Research*. Elsevier, 140, July, pp. 611–618.
- Wirth, V. (1995) *Flechtenflora*. 2. edition, Stuttgart: Eugen Ulmer GmbH & Co.
- Wiseman, R. D. and Wadleigh, M. A. (2002) 'Lichen response to changes in atmospheric sulphur: Isotopic evidence.' *Environmental Pollution*, 116(2) pp. 235–241.
- Wolseley, P. A., Leith, I. D., van Dijk, N. and Sutton, M. A. (2009) 'Macrolichens on Twigs and Trunks as Indicators of Ammonia Concentrations Across the UK – a Practical Method.' In Sutton, M. A., Reis, S., and Baker, S. M. H. (eds) *Atmospheric Ammonia: Detecting Emission Changes and Environmental Impacts*. Dordrecht: Springer Netherlands, pp. 101–108.
- Wolseley, P. A. and Pryor, K. V. (1999) 'The potential of epiphytic twig communities on *Quercus petraea* in a Welsh woodland site (tycanol) for evaluating environmental changes.' *Lichenologist*, 31(1) pp. 41–61.
- Wolseley, P. A., Theobald, M. R., James, P. W. and Sutton, M. A. (2006) 'Detecting changes in epiphytic lichen communities at sites affected by atmospheric ammonia from agricultural sources.' *Lichenologist*, 38(2) pp. 161–176.
- Wolterbeek, H. T., Garty, J., Reis, M. A. and Freitas, M. . (2003) 'Biomonitoring in use: lichens and metal air pollution.' In Markert, B. A., Breure, A. M., and Zechmeister, H. G. (eds) *Trace Metals and other Contaminants in the Environment 6*. Amsterdam, Boston, London, New York, Oxford, Paris, San Diego, San Francisco, Singapore, Sydney, Tokyo: Elsevier Science, pp. 377–419.
- Wong, C. S. C., Li, X. and Thornton, I. (2006) 'Urban environmental geochemistry of trace metals.' *Environmental Pollution*, 142(1) pp. 1–16.
- Wong, S. C. (1990) 'Elevated atmospheric partial pressure of CO₂ and plant growth - II. Non-structural carbohydrate content in cotton plants and its effect on growth parameters.' *Photosynthesis Research*.
- Wong, T. H., Lee, C. L., Su, H. H., Lee, C. L., Wu, C. C., Wang, C. C., Sheu, C. C., Lai, R. S., Leung, S. Y., Lin, C. C., Wei, Y. F., Wang, C. J., Lin, Y. C., Chen, H. L., Huang, M. S., Yen, J. H., Huang, S. K. and Suen, J. L. (2018) 'A prominent air pollutant, Indeno[1,2,3-cd]pyrene, enhances allergic lung inflammation via aryl hydrocarbon receptor.' *Scientific Reports*. Springer US, 8(1) pp. 1–11.
- Xu, H., Ho, S. S. H., Cao, J., Guinot, B., Kan, H., Shen, Z., Ho, K. F., Liu, S., Zhao, Z., Li, J., Zhang, N., Zhu, C., Zhang, Q. and Huang, R. (2017) 'A 10-year observation of PM_{2.5}-bound nickel in Xi'an, China: Effects of source control on its trend and associated health risks.' *Scientific Reports*. Nature Publishing Group, 7(1) p. 41132.
- Yagishita, M., Kageyama, S., Ohshima, S., Matsumoto, M., Aoki, Y., Goto, S. and Nakajima, D. (2015) 'Atmospheric concentration and carcinogenic risk of polycyclic aromatic hydrocarbons including benzo[c]fluorene, cyclopenta[c,d]pyrene, and benzo[j]fluoranthene in Japan.' *Atmospheric Environment*. Elsevier Ltd, 115 pp. 263–268.
- Yamamoto, N., Kabeya, N., Onodera, M., Takahashi, S., Komori, Y., Nakazuka, E. and Shirai, T. (1988) 'Seasonal variation of atmospheric ammonia and particulate ammonium concentrations in the urban atmosphere of Yokohama over a 5-year period.' *Atmospheric Environment (1967)*.

- Yamamoto, N., Nishiura, H., Honjo, T., Ishikawa, Y. and Suzuki, K. (1995) 'A long-term study of atmospheric ammonia and particulate ammonium concentrations in Yokohama, Japan.' *Atmospheric Environment*, 29(1) pp. 97–103.
- Yang, X., Wang, S., Zhang, W., Zhan, D. and Li, J. (2017) 'The impact of anthropogenic emissions and meteorological conditions on the spatial variation of ambient SO₂ concentrations: A panel study of 113 Chinese cities.' *Science of the Total Environment*. Elsevier B.V., 584–585 pp. 318–328.
- Yang, Z. and Wang, J. (2017) 'A new air quality monitoring and early warning system: Air quality assessment and air pollutant concentration prediction.' *Environmental Research*. Elsevier Inc., 158(June) pp. 105–117.
- Yeatman, S. G., Spokes, L. J., Dennis, P. F. and Jickells, T. D. (2001) 'Comparisons of aerosol nitrogen isotopic composition at two polluted coastal sites.' *Atmospheric Environment*.
- Yoo, J. and Ready, R. (2016) 'The impact of agricultural conservation easement on nearby house prices: Incorporating spatial autocorrelation and spatial heterogeneity.' *Journal of Forest Economics*.
- Yunker, M. B., Macdonald, R. W., Vingarzan, R., Mitchell, R. H., Goyette, D. and Sylvestre, S. (2002) 'PAHs in the Fraser River basin: A critical appraisal of PAH ratios as indicators of PAH source and composition.' *Organic Geochemistry*.
- Zabiegała, B., Kot-Wasik, A., Urbanowicz, M. and Namieśnik, J. (2010) 'Passive sampling as a tool for obtaining reliable analytical information in environmental quality monitoring.' *Analytical and bioanalytical chemistry*, 396 pp. 273–296.
- Zereini, F., Contact Information, F. A., Rankenburg, K., Beyer, J.-M. and Artelt, S. (1997) 'Verteilung von Platingruppenelementen (PGE) in den Umweltkompartimenten Boden, Schlamm, Straßenstaub, Straßenkehrgut und Wasser.' *Springer*.
- Zereini, F., Wiseman, C. and Püttmann, W. (2007) 'Changes in palladium, platinum, and rhodium concentrations, and their spatial distribution in soils along a major highway in Germany from 1994 to 2004.' *Environmental Science and Technology*, 41(2) pp. 451–456.
- Zha, Y., Liu, X., Sun, K., Tang, J. and Zhang, Y. L. (2017) 'Polycyclic aromatic hydrocarbons (PAHs) concentration levels, pattern, source identification, and human risk assessment in foliar dust from urban to rural areas in Nanjing, China.' *Human and Ecological Risk Assessment*, 7039(October) pp. 1–18.
- Zhou, J., Wang, T., Huang, Y., Mao, T. and Zhong, N. (2005) 'Size distribution of polycyclic aromatic hydrocarbons in urban and suburban sites of Beijing, China.' *Chemosphere*.
- Zhu, G., Guo, Q., Xiao, H., Chen, T. and Yang, J. (2017) 'Multivariate statistical and lead isotopic analyses approach to identify heavy metal sources in topsoil from the industrial zone of Beijing Capital Iron and Steel Factory.' *Environmental Science and Pollution Research*.
- Zielinska, B., Sagebiel, J., Arnott, W. P., Rogers, C. F., Kelly, K. E., Wagner, D. A., Lighty, J. S., Sarofim, A. F. and Palmer, G. (2004) 'Phase and Size Distribution of Polycyclic Aromatic Hydrocarbons in Diesel and Gasoline Vehicle Emissions.' *Environmental Science and Technology*.
- Zierdt, M. (1997) *Umweltmonitoring mit natuerlichen Indikatoren: Pflanzen, Boden, Wasser und Luft*. Berlin: Springer Verlag.
- Zivin, J. G. and Neidell, M. (2012) 'The Impact of Pollution on Worker Productivity.' *American Economic Review*, 102(7) pp. 3652–3673.

Appendices

Appendix A – Lichen diversity and air quality (Chapter 3)

Appendix A-1: NO_x diffusion tube data – site ID with name and XY-coordinates (OSGB 1936 – British National Grid), nitrogen and sulphur contents (wt%) of *X. parietina* and *Physcia* spp. with NO_x tube deployment site NO₂ (mean) and SO₂ (median) concentrations (N/A – not applicable, values not analysed)

ID	Site-ID	X	Y	NO ₂ [$\mu\text{g}/\text{m}^3$] \pm 1x Std.Dev.	N wt% (Xp)	N wt% (Ph)
1	ANC001 I	385143	398190	43.95 \pm 10.73	2.50	2.48
2	ANC003	384734	398978	33.09 \pm 8.95	3.59	3.73
3	ANC009	384231	398977	39.54 \pm 10.8	3.18	N/A
4	ANC011	384467	399200	28.91 \pm 8.24	2.18	3.01
5	ANC012	384960	398477	37.37 \pm 10.74	2.68	3.31
6	ARD001	384890	397470	43.81 \pm 9.03	2.61	2.84
7	ARD004	385326	397120	35.67 \pm 8.32	2.56	2.51
8	ARD005	385024	396794	27.94 \pm 8.45	2.48	2.71
9	ARD012	384548	397247	41.43 \pm 10.29	3.06	2.77
10	ARD013	384798	397104	29.35 \pm 7.76	2.42	2.31
11	BFD002	385829	398555	29.58 \pm 8.60	1.01	1.79
12	BFD005	385704	398035	28.16 \pm 10.67	3.60	3.88
13	CC001	385123	397837	40.18 \pm 9.38	3.04	3.00
14	CC003	383836	397553	32.08 \pm 6.42	3.77	3.99
15	CC006	383517	398334	37.61 \pm 9.33	2.42	2.28
16	CC007	383902	398788	33.45 \pm 8.10	3.07	3.31
17	CC008	384382	397558	41.55 \pm 9.49	3.18	3.47
18	CC009	384295	398297	39.51 \pm 7.67	2.95	2.81
19	CC011	384003	398020	41.79 \pm 8.21	3.03	N/A
20	CC012	382892	397730	30.41 \pm 9.09	2.02	2.07
21	CC015	383290	397932	28.04 \pm 6.72	2.71	2.18
22	CC017	383273	397492	33.76 \pm 10.04	2.81	2.97
23	CC018	383277	397664	32.64 \pm 6.81	3.41	3.19
24	CC021	384516	398751	36.30 \pm 7.77	1.96	2.64
25	CC025	384409	397812	41.70 \pm 9.76	3.55	N/A
26	CHE001	385166	399865	23.28 \pm 8.96	2.45	2.45
27	HUL001	383876	396960	35.24 \pm 10.21	3.02	2.70
28	HUL002	384072	396768	29.68 \pm 8.30	1.84	1.97
29	HUL005	383231	397017	26.66 \pm 8.00	2.20	2.21
30	HUL008	383705	397171	50.00 \pm 9.90	3.35	3.20
31	HUL016	383263	396662	30.25 \pm 11.61	2.05	1.94
32	HUL021 I	382970	396570	45.70 \pm 11.65	3.28	N/A
33	HUL024	382661	397036	25.23 \pm 8.66	3.07	3.36
34	HUL027	384271	397097	33.21 \pm 8.75	3.05	3.83
35	MIP001	385312	398998	31.33 \pm 12.90	2.21	1.92
36	MIP002	385653	399279	27.25 \pm 8.95	2.44	2.48
37	MIP007	386160	399492	26.68 \pm 8.50	2.88	2.86
38	MIP010 II	386128	399848	31.26 \pm 10.38	2.70	1.11
39	MIP014	385684	399549	28.01 \pm 9.09	2.55	2.31
40	MIP016	384938	399397	33.42 \pm 8.95	3.03	3.90
41	MIP017	385369	399408	25.40 \pm 9.75	2.78	2.51

42	MIP018	385199	399664	32.41 ± 8.79	3.02	2.82
43	MIP021	386434	399454	30.75 ± 13.31	3.04	3.03
44	MIP024	386302	399221	27.01 ± 10.71	2.86	2.68
45	MIP025	385597	398946	27.56 ± 9.46	2.48	2.75

Appendix A-2: Lichen diversity data, including site-ID, XY-coordinates (OSGB1936), tree species, and lichens found; diversity values for reference and eutrophication species (by cardinal direction) and number of reference and eutrophication species found by tree

ID	Lichen surveying and mapping		Diversity values - reference and eutrophication species								tree ref. species	tree eutro. species
	ID/name and tree species	lichens found	Reference species				Eutrophication species					
			N	E	S	W	N	E	S	W		
1	BFD002 (X: 385845, Y: 398563): <i>Acer</i>	<i>Xanthoria parietina</i>					0	0	5	3	3	37
		<i>Physcia tenella</i>					4	3	5	5		
		<i>Xanthoria ucrainica</i>					1	5	4	2		
		<i>Candelariella reflexa</i>	2	0	0	0						
		<i>Parmelia sulcata</i>	0	0	0	1						
		Sum (frequency)	2	0	0	1	5	8	14	10		
2	BFD008 (X: 385361, Y: 398038): <i>Fraxinus</i>	<i>Xanthoria ucrainica</i>					0	1	5	0	10	23
		<i>Physcia tenella</i>					4	4	4	4		
		<i>Buellia punctata</i>	0	1	1	1						
		<i>Candelariella reflexa</i>	3	1	0	3						
		Sum (frequency)	3	2	1	4	4	5	9	4		
3	BFD007 (X: 385366, Y: 397922): <i>Acer</i>	<i>Lecanora expallens</i>	1	1	0	0					10	20
		<i>Buellia punctata</i>	1	1	0	0						
		<i>Physcia tenella</i>					1	2	5	4		
		<i>Candelariella reflexa</i>	1	1	2	2						
		<i>Xanthoria ucrainica</i>					0	1	2	1		
		<i>Phaeophyscia orbicularis</i>					0	0	4	0		
		Sum (frequency)	3	3	2	2	1	3	11	5		
4	BFD006 (X: 385662, Y: 397913): <i>Quercus</i>	<i>Lecanora chlorotera</i>	2	0	1	3					15	0
		<i>Buellia punctata</i>	1	0	1	1						
		<i>Lecanora expallens</i>	2	3	1	1						
		Sum (frequency)	4	3	3	5						
5	BFD005 (X: 385681, Y: 398061): <i>Tilia</i>	<i>Buellia punctata</i>	2	2	1	3					19	20
		<i>Lecanora chlorotera</i>	2	2	0	4						
		<i>Physcia tenella</i>					5	2	5	4		
		<i>Candelariella reflexa</i>	0	0	0	3						
		<i>Xanthoria parietina</i>					0	1	3	0		
		<i>Xanthoria ucrainica</i>					1	0	0	0		
		Sum (frequency)	4	4	1	10	5	3	8	4		
6	HUL001 (X:383876, Y: 396960): <i>Fraxinus</i>	<i>Buellia punctata</i>	1	0	1	0					9	1
		<i>Lecanora chlorotera</i>	2	0	0	0						
		<i>Lecanora expallens</i>	2	0	1	2						
		<i>Physcia tenella</i>					0	0	1	0		
		Sum (frequency)	5	0	2	2	0	0	1	0		
7	HUL008 (X: 383705, Y: 397171): <i>Acer</i>	<i>Xanthoria parietina</i>					1	0	0	2	2	36
		<i>Physcia tenella</i>					4	4	2	3		
		<i>Xanthoria ucrainica</i>					5	5	5	5		
		<i>Candelariella reflexa</i>	2	0	0	0						
		Sum (frequency)	2	0	0	0	10	9	7	10		
8	MIP012 (X: 385838, Y: 399661): <i>Acer</i>	<i>Xanthoria parietina</i>					4	2	2	0	12	23
		<i>Physcia tenella</i>					4	4	2	3		
		<i>Candelariella reflexa</i>	0	5	5	2						
		<i>Xanthoria ucrainica</i>					0	0	0	2		
		Sum (frequency)	0	5	5	2	8	6	4	5		
9	MIP013 (X: 385886, Y: 399523): <i>Fraxinus</i>	<i>Physcia tenella</i>					5	5	5	5	17	41
		<i>Xanthoria parietina</i>					2	2	1	2		
		<i>Buellia punctata</i>	2	2	3	3						
		<i>Lecanora chlorotera</i>	2	1	2	2						
		<i>Xanthoria ucrainica</i>					0	5	5	4		
Sum (frequency)	4	3	5	5	7	12	11	11				
10	MIP006 (X: 385938, Y: 399381): <i>Fraxinus</i>	<i>Xanthoria ucrainica</i>					2	4	1	4	12	21
		<i>Lecanora chlorotera</i>	2	1	0	3						
		<i>Physcia tenella</i>					2	3	3	2		
		<i>Lecidella elaeochroma</i>	2	1	1	0						
		<i>Lecanora expallens</i>	1	0	0	0						
		<i>Lepraria incana</i>	0	1	0	0						
Sum (frequency)	5	3	1	3	4	7	4	6				

11	MIP008 I (X: 386283, Y: 399611): <i>Tilia</i>	<i>Lecanora chlorotera</i>	1	1	0	2					18	16
		<i>Candelariella reflexa</i>	3	4	1	2						
		<i>Physcia tenella</i>					0	5	1	5		
		<i>Xanthoria ucrainica</i>					0	2	0	0		
		<i>Melanohalea exasperata</i>	0	1	1	0						
		<i>Buellia punctata</i>	0	0	1	1						
		<i>Xanthoria parietina</i>					0	0	2	1		
Sum (frequency)	4	6	3	5	0	7	3	6				
12	MIP009 II (X: 386190, Y: 399774): <i>Fraxinus</i>	<i>Xanthoria parietina</i>					3	2	2	3	11	38
		<i>Physcia tenella</i>					5	4	5	5		
		<i>Candelariella reflexa</i>	5	4	0	2						
		<i>Xanthoria ucrainica</i>					0	4	4	0		
		<i>Physcia adscendens</i>					0	0	0	1		
Sum (frequency)	5	4	0	2	8	10	11	9				
13	MIP010 I (X: 386158, Y: 399834): <i>Quercus</i>	<i>Xanthoria parietina</i>					2	3	5	5	13	49
		<i>Physcia tenella</i>					5	5	5	5		
		<i>Physcia adscendens</i>					2	1	2	0		
		<i>Buellia punctata</i>	2	0	0	0						
		<i>Xanthoria ucrainica</i>					3	1	2	3		
		<i>Candelariella reflexa</i>	5	5	0	0						
		<i>Melanohalea exasperata</i>	1	0	0	0						
Sum (frequency)	8	5	0	0	12	10	14	13				
14	MIP011 (X: 385833, Y: 399803): <i>Acer</i>	<i>Physcia tenella</i>					2	3	3	4	5	13
		<i>Xanthoria ucrainica</i>					1	0	0	0		
		<i>Lepraria incana</i>	1	0	0	0						
		<i>Phaeophyscia orbicularis</i>	0	0	1	1						
		<i>Buellia punctata</i>	0	0	0	2						
Sum (frequency)	1	0	1	3	3	3	3	4				
15	MIP014 (X: 385681, Y: 399559): <i>Acer</i>	<i>Phaeophyscia orbicularis</i>					2	1	1	0	14	30
		<i>Physcia tenella</i>					5	5	5	5		
		<i>Xanthoria parietina</i>					1	1	3	5		
		<i>Candelariella reflexa</i>	2	5	2	0						
		<i>Buellia punctata</i>	0	0	0	1						
Sum (frequency)	4	6	3	1	6	6	8	10				
16	MIP022 (X: 386381, Y: 399468): <i>Fraxinus</i>	<i>Physcia tenella</i>					5	5	4	5	3	43
		<i>Xanthoria parietina</i>					4	4	3	5		
		<i>Xanthoria ucrainica</i>					3	0	0	1		
		<i>Candelariella reflexa</i>	2	1	0	0						
		<i>Physcia adscendens</i>					0	0	3	1		
		Sum (frequency)	2	1	0	0	12	9	10	12		
17	MIP020 (X: 386352, Y: 399353): <i>Fraxinus</i>	<i>Physcia tenella</i>					5	3	4	4	23	26
		<i>Xanthoria ucrainica</i>					3	3	4	0		
		<i>Lecanora chlorotera</i>	1	0	0	2						
		<i>Buellia punctata</i>	1	0	0	2						
		<i>Candelariella reflexa</i>	3	3	5	4						
		<i>Lecanora expallens</i>	0	2	0	0						
		Sum (frequency)	5	5	5	8	8	6	8	4		
18	MIP024 (X: 386302, Y: 399221): <i>Acer</i>	<i>Physcia tenella</i>					5	5	4	5	10	31
		<i>Xanthoria parietina</i>					2	0	4	2		
		<i>Candelariella reflexa</i>	2	4	0	0						
		<i>Xanthoria ucrainica</i>					1	0	0	0		
		<i>Punctelia subrudecta</i>	0	4	0	0						
		<i>Physcia adscendens</i>					0	0	1	2		
		Sum (frequency)	2	8	0	0	8	5	9	9		
19	MIP038 (X: 386167, Y: 399073): <i>Acer</i>	<i>Physcia tenella</i>					5	5	5	5	14	31
		<i>Xanthoria parietina</i>					1	3	3	1		
		<i>Candelariella reflexa</i>	5	5	2	1						
		<i>Buellia punctata</i>	0	1	0	0						
		<i>Physcia adscendens</i>					0	0	1	0		
		<i>Xanthoria ucrainica</i>					0	0	1	1		
Sum (frequency)	5	6	2	1	6	8	10	7				
20	MIP039 (X: 385774, Y: 399073): <i>Acer</i>	<i>Physcia tenella</i>					5	4	2	5	8	23
		<i>Xanthoria parietina</i>					2	0	0	2		
		<i>Lepraria incana</i>	1	0	0	0						
		<i>Phaeophyscia orbicularis</i>					1	0	0	2		
		<i>Candelariella reflexa</i>	1	2	4	0						
Sum (frequency)	2	2	4	0	8	4	2	9				

21	MIP025 (X: 385597, Y: 398946): <i>Acer</i>	<i>Physcia tenella</i>					5	5	4	4	21	24	
		<i>Candelariella reflexa</i>	5	5	5	5							
		<i>Xanthoria ucrainica</i>					0	1	2	0			
		<i>Parmelia sulcata</i>	0	1	0	0							
		<i>Phaeophyscia orbicularis</i>					0	0	3	0			
		Sum (frequency)	5	6	5	5	5	6	9	4			
22	ANC007 (X: 385176, Y: 398981): <i>Acer</i>	<i>Candelariella reflexa</i>	0	3	5	1						10	2
		<i>Lepraria incana</i>	0	1	0	0							
		<i>Xanthoria ucrainica</i>					0	0	1	0			
		<i>Physcia tenella</i>					0	0	1	0			
		Sum (frequency)	0	4	5	1	0	0	2	0			
23	MIP001 (X: 385312, Y: 398998): <i>Acer</i>	<i>Physcia tenella</i>					5	5	5	5	15	25	
		<i>Xanthoria ucrainica</i>					1	0	0	0			
		<i>Xanthoria parietina</i>					1	0	0	1			
		<i>Candelariella reflexa</i>	4	5	1	5							
		<i>Phaeophyscia orbicularis</i>					1	0	1	0			
		Sum (frequency)	4	5	1	5	8	5	6	6			
24	MIP002 (X: 385653, Y: 399279): <i>Acer</i>	<i>Physcia tenella</i>					1	0	0	2	18	17	
		<i>Lecanora expallens</i>	3	0	0	1							
		<i>Candelariella reflexa</i>	4	4	0	3							
		<i>Parmelia sulcata</i>	0	1	1	0							
		<i>Xanthoria parietina</i>					0	4	3	1			
		<i>Xanthoria ucrainica</i>					0	0	1	5			
		<i>Lecanora chlorotera</i>	0	0	0	1							
		Sum (frequency)	7	5	1	5	1	4	4	8			
25	MIP005 (X: 385843, Y: 399434): <i>Acer</i>	<i>Physcia tenella</i>					1	0	0	2	13	4	
		<i>Lecanora chlorotera</i>	0	2	3	0							
		<i>Buellia punctata</i>	0	2	3	1							
		<i>Lecanora expallens</i>	0	0	1	0							
		<i>Candelariella reflexa</i>	0	0	0	1							
		<i>Xanthoria parietina</i>					0	0	0	1			
		Sum (frequency)	0	4	7	2	1	0	0	3			
26	MIP015 (X: 385454, Y: 399341): <i>Acer</i>	<i>Candelariella reflexa</i>	0	5	0	0					7	3	
		<i>Physcia tenella</i>					0	0	2	1			
		<i>Buellia punctata</i>	0	0	0	2							
		Sum (frequency)	0	5	0	2	0	0	2	1			
27	MIP017 (X: 385369, Y: 399408): <i>Acer</i>	<i>Physcia tenella</i>					3	5	5	5	16	40	
		<i>Physcia adscendens</i>					0	1	4	1			
		<i>Xanthoria parietina</i>					3	3	3	4			
		<i>Physcia aipolia</i>	0	2	2	0							
		<i>Parmelia sulcata</i>	0	0	1	0							
		<i>Candelariella reflexa</i>	5	3	0	3							
		<i>Xanthoria ucrainica</i>					0	0	0	3			
		Sum (frequency)	5	5	3	3	6	9	12	13			
28	MIP016 (X: 384938, Y: 399397): <i>Fraxinus</i>	<i>Candelariella reflexa</i>	5	4	2	4					15	19	
		<i>Physcia tenella</i>					5	3	4	5			
		<i>Xanthoria ucrainica</i>					0	0	1	0			
		<i>Xanthoria parietina</i>					0	0	0	1			
		Sum (frequency)	5	4	2	4	5	3	5	6			
29	CHE001 (X: 385166, Y: 399865): <i>Fraxinus</i>	<i>Physcia tenella</i>					5	5	5	5	29	27	
		<i>Xanthoria parietina</i>					2	1	1	2			
		<i>Candelariella reflexa</i>	5	5	4	5							
		<i>Parmelia sulcata</i>	1	3	1	2							
		<i>Xanthoria ucrainica</i>					0	0	1	0			
		<i>Buellia punctata</i>	0	0	0	1							
		<i>Evernia prunastri</i>	0	0	0	2							
		Sum (frequency)	6	8	5	10	7	6	7	7			
30	CHE002 (X: 384901, Y: 399510): <i>Fraxinus</i>	<i>Buellia punctata</i>	2	0	0	1					15	3	
		<i>Lecanora hagenii</i>					1	0	0	0			
		<i>Physcia tenella</i>					2	0	0	0			
		<i>Candelariella reflexa</i>	3	2	5	2							
		Sum (frequency)	5	2	5	3	3	0	0	0			

31	ARD001 (X: 384890, Y: 397470): <i>Fraxinus</i>	<i>Xanthoria ucrainica</i>					3	1	5	5	5	17
		<i>Physcia tenella</i>					2	0	0	1		
		<i>Lepraria lobifigans</i>	0	0	5	0						
		Sum (frequency)	0	0	5	0	5	1	5	6		
32	ARD002 I (X: 384869, Y: 397365): <i>Fraxinus</i>	<i>Candelariella reflexa</i>	5	5	4	1					16	45
		<i>Xanthoria parietina</i>					5	2	4	4		
		<i>Physcia tenella</i>					3	3	5	5		
		<i>Physcia adscendens</i>					1	0	1	0		
		<i>Phaeophyscia orbicularis</i>					2	1	0	0		
		<i>Xanthoria ucrainica</i>					1	0	3	5		
		<i>Flavoparmelia soledians</i>	0	0	1	0						
Sum (frequency)	5	5	5	1	12	6	13	14				
33	ARD003 (X: 384969, Y: 397257): <i>Acer</i>	<i>Physcia tenella</i>					3	4	4	4	18	34
		<i>Parmelia sulcata</i>	1	0	0	2						
		<i>Xanthoria ucrainica</i>					1	0	0	0		
		<i>Xanthoria parietina</i>					0	4	5	3		
		<i>Candelariella reflexa</i>	0	5	5	5						
		<i>Phaeophyscia orbicularis</i>					0	0	2	2		
		<i>Physcia adscendens</i>					0	0	1	1		
Sum (frequency)	1	5	5	7	4	8	12	10				
34	ARD006 I (X: 385359, Y: 396932): <i>Acer</i>	<i>Parmelia sulcata</i>	3	1	1	0					17	49
		<i>Physcia tenella</i>					5	5	5	5		
		<i>Xanthoria parietina</i>					4	5	4	3		
		<i>Melanohalea exasperata</i>	1	0	0	2						
		<i>Xanthoria ucrainica</i>					3	0	1	1		
		<i>Candelariella reflexa</i>	0	5	4	0						
		<i>Phaeophyscia orbicularis</i>					0	1	0	1		
<i>Physcia adscendens</i>					0	2	2	2				
Sum (frequency)	4	6	5	2	12	13	12	12				
35	ARD006 II (X: 385410, Y: 396748): <i>Fraxinus</i>	<i>Physcia tenella</i>					5	5	5	5	9	43
		<i>Physcia adscendens</i>					3	0	3	2		
		<i>Xanthoria parietina</i>					3	0	3	2		
		<i>Parmelia sulcata</i>	0	1	2	0						
		<i>Xanthoria ucrainica</i>					0	1	5	1		
		<i>Candelariella reflexa</i>	0	1	3	0						
		<i>Lepraria lobifigans</i>	0	1	0	0						
<i>Evernia prunastri</i>	0	0	1	0								
Sum (frequency)	0	3	6	0	11	6	16	10				
36	ARD006 III (X: 385387, Y: 396705): <i>Fraxinus</i>	<i>Physcia tenella</i>					5	5	5	5	12	50
		<i>Xanthoria parietina</i>					2	1	1	4		
		<i>Xanthoria ucrainica</i>					4	1	3	5		
		<i>Candelariella reflexa</i>	2	5	0	3						
		<i>Physcia adscendens</i>					0	2	1	1		
		<i>Phaeophyscia orbicularis</i>					0	2	2	1		
		<i>Physcia aipolia</i>	0	0	1	0						
<i>Evernia prunastri</i>	0	0	0	1								
Sum (frequency)	2	5	1	4	11	11	12	16				
37	ARD012 (X: 384548, Y: 397247): <i>Acer</i>	<i>Physcia tenella</i>					1	5	5	5	11	20
		<i>Candelariella reflexa</i>	0	5	5	0						
		<i>Phaeophyscia orbicularis</i>					0	0	2	1		
		<i>Parmelia sulcata</i>	0	0	0	1						
		<i>Xanthoria parietina</i>					0	0	0	1		
Sum (frequency)	0	5	5	1	1	5	7	7				
38	ARD013 (X: 384798, Y: 397104): <i>Acer</i>	<i>Physcia tenella</i>					5	3	5	5	25	24
		<i>Xanthoria ucrainica</i>					2	0	0	2		
		<i>Candelariella reflexa</i>	5	4	5	0						
		<i>Xanthoria parietina</i>					1	0	0	1		
		<i>Lecanora chlorotera</i>	2	0	0	0						
		<i>Lepraria incana</i>	1	4	0	0						
		<i>Buellia punctata</i>	0	2	0	0						
		<i>Parmelia sulcata</i>	0	0	1	0						
<i>Melanohalea exasperata</i>	0	0	0	1								
Sum (frequency)	8	10	6	1	8	3	5	8				
39	ARD013 I (X: 384873, Y: 397055): <i>Acer</i>	<i>Physcia tenella</i>					5	5	5	3	14	25
		<i>Candelariella reflexa</i>	5	4	1	2						
		<i>Lecidella elaeochroma</i>	2	0	0	0						
		<i>Phaeophyscia orbicularis</i>					5	0	0	0		
		<i>Xanthoria ucrainica</i>					0	1	0	0		
		<i>Xanthoria parietina</i>					0	0	0	1		
Sum (frequency)	7	4	1	2	10	6	5	4				
40	ARD005 (X: 385024, Y: 396794): <i>Acer</i>	<i>Physcia tenella</i>					5	5	3	4	15	26
		<i>Candelariella reflexa</i>	5	5	4	1						
		<i>Xanthoria ucrainica</i>					1	0	0	3		
		<i>Xanthoria parietina</i>					0	2	0	0		
		<i>Phaeophyscia orbicularis</i>					0	2	0	1		
Sum (frequency)	5	5	4	1	6	9	3	8				

41	ARD008 (X: 384921, Y: 396860): <i>Acer</i>	<i>Physcia tenella</i>					5	5	3	3	8	18	
		<i>Candelariella reflexa</i>	0	5	1	0							
		<i>Xanthoria ucrainica</i>					0	1	0	0			
		<i>Lepraria incana</i>	0	1	0	0							
		<i>Xanthoria parietina</i>					0	0	1	0			
		<i>Evernia prunastri</i>	0	0	0	1							
		Sum (frequency)	0	6	1	1	5	6	4	3			
42	HUL021 (X: 382850, Y: 396595): <i>Fraxinus</i>	<i>Xanthoria ucrainica</i>					5	5	5	5	2	29	
		<i>Buellia punctata</i>	2	0	0	0							
		<i>Physcia tenella</i>					3	1	1	3			
		<i>Phaeophyscia orbicularis</i>					0	0	0	1			
		Sum (frequency)	2	0	0	0	8	6	6	9			
43	CC010 (X: 382786, Y: 397728): <i>Prunus</i>	<i>Physcia tenella</i>					1	1	2	1	5	6	
		<i>Lecanora hagenii</i>	1	0	0	0							
		<i>Candelariella reflexa</i>	0	2	0	0							
		<i>Buellia punctata</i>	0	0	1	0							
		<i>Lepraria incana</i>	0	0	0	1							
		<i>Xanthoria parietina</i>					0	0	0	1			
		Sum (frequency)	1	2	1	1	1	1	2	2			
44	CC012 (X: 382892, Y: 397730): <i>Tilia</i>	<i>Lecidella elaeochroma</i>	1	0	0	1					23	8	
		<i>Buellia punctata</i>	2	0	0	1							
		<i>Lepraria incana</i>	1	1	0	0							
		<i>Lecanora chlorotera</i>	1	0	1	0							
		<i>Physcia tenella</i>					0	3	0	0			
		<i>Candelariella reflexa</i>	0	5	5	3							
		<i>Lecania spp.</i>	0	1	0	0							
		<i>Phaeophyscia orbicularis</i>					0	0	2	3			
		Sum (frequency)	5	7	6	5	0	3	2	3			
45	CC015 (X: 383290, Y: 397932): <i>Tilia</i>	<i>Arthonia radiata</i>	1	0	0	1					9	3	
		<i>Buellia punctata</i>	0	2	0	0							
		<i>Physcia tenella</i>					0	1	0	0			
		<i>Xanthoria ucrainica</i>					0	0	0	2			
		Sum (frequency)	1	2	4	2	0	1	0	2			
46	CC014 (X: 383156, Y: 398139): <i>Acer</i>	<i>Physcia tenella</i>					4	0	0	0	0	10	
		<i>Phaeophyscia orbicularis</i>					2	2	1	1			
		Sum (frequency)	0	0	0	0	6	2	1	1			
47	HUL026 (X: 382856, Y: 396932): <i>Acer</i>	<i>Xanthoria ucrainica</i>					2	1	1	0	15	19	
		<i>Physcia tenella</i>					4	5	5	1			
		<i>Arthonia radiata</i>	1	0	0	1							
		<i>Candelariella reflexa</i>	0	4	2	0							
		<i>Lepraria incana</i>	0	1	0	0							
		<i>Buellia punctata</i>	0	0	3	1							
		<i>Lecanora chlorotera</i>	0	0	1	0							
		<i>Lecania spp.</i>	0	0	0	1							
		Sum (frequency)	1	5	6	3	6	6	6	1			
		<i>Physcia tenella</i>					4	3	2	0			
48	HUL024 (X: 382664, Y: 397041): <i>Acer</i>	<i>Phaeophyscia orbicularis</i>					3	1	0	2	18	15	
		<i>Lepraria incana</i>	3	0	0	1							
		<i>Candelariella reflexa</i>	2	0	2	0							
		<i>Buellia punctata</i>	0	3	4	1							
		<i>Arthonia radiata</i>	0	0	2	0							
		Sum (frequency)	5	3	8	2	7	4	2	2			
		<i>Physcia tenella</i>					5	4	5	4			
49	ANC003 (X: 384734, Y: 398978): <i>Tilia</i>	<i>Buellia punctata</i>	2	0	0	0					28	23	
		<i>Candelariella reflexa</i>	4	5	5	5							
		<i>Xanthoria parietina</i>					1	0	1	2			
		<i>Xanthoria ucrainica</i>					1	0	0	0			
		<i>Lepraria incana</i>	0	1	0	0							
		<i>Lecanora expallens</i>	0	3	0	0							
		<i>Parmelina tiliacea</i>	0	0	1	2							
		Sum (frequency)	6	9	6	7	7	4	6	6			
		<i>Physcia tenella</i>					5	5	5	5			
50	HUL025 (X: 383832, Y: 397110): <i>Acer</i>	<i>Phaeophyscia orbicularis</i>					4	4	0	4	14	53	
		<i>Xanthoria parietina</i>					2	2	1	0			
		<i>Candelariella reflexa</i>	4	0	4	5							
		<i>Arthonia punctiformis</i>	1	0	0	0							
		<i>Physcia adscendens</i>					0	1	1	0			
		<i>Xanthoria ucrainica</i>					0	5	5	4			
		Sum (frequency)	5	0	4	5	11	17	12	13			

51	CC008 (X: 384382, Y: 397558): <i>Acer</i>	<i>Physcia tenella</i>					4	0	4	4	6	21	
		<i>Arthonia punctiformis</i>	2	0	0	0							
		<i>Phaeophyscia orbicularis</i>					0	0	2	1			
		<i>Candelariella reflexa</i>	0	0	1	2							
		<i>Xanthoria ucrainica</i>					0	0	3	3			
		<i>Parmelia sulcata</i>	0	0	0	1							
		Sum (frequency)	2	0	1	3	4	0	9	8			
52	CC025 (X: 384409, Y: 397812): <i>Acer</i>	<i>Xanthoria parietina</i>					2	4	0	1	20	30	
		<i>Physcia tenella</i>					5	5	3	3			
		<i>Candelariella reflexa</i>	5	5	0	1							
		<i>Phaeophyscia orbicularis</i>					4	1	0	2			
		<i>Buellia grisovirens</i>	0	0	4	5							
		Sum (frequency)	5	5	4	6	11	10	3	6			
53	HUL027 (X: 384256, Y: 397121): <i>Tilia</i>	<i>Physcia tenella</i>						5	5	5	5	16	35
		<i>Buellia grisovirens</i>	1	0	1	0							
		<i>Lepraria incana</i>	2	0	0	0							
		<i>Buellia punctata</i>	0	1	1	1							
		<i>Xanthoria parietina</i>					0	4	0	0			
		<i>Candelariella reflexa</i>	0	1	5	2							
		<i>Xanthoria ucrainica</i>					0	2	5	2			
		<i>Physcia adscendens</i>					0	0	1	0			
		<i>Lecanora chlorotera</i>	0	0	1	0							
		<i>Phaeophyscia orbicularis</i>					0	0	0	1			
				Sum (frequency)	3	2	8	3	5	11	11		
54	HUL020 (X: 382990, Y: 396950): <i>Acer</i>	<i>Physcia tenella</i>						5	4	4	3	18	19
		<i>Buellia punctata</i>	2	1	1	2							
		<i>Lepraria incana</i>	3	0	0	2							
		<i>Lecanora chlorotera</i>	2	0	0	2							
		<i>Arthonia punctiformis</i>	1	1	0	0							
		<i>Xanthoria ucrainica</i>					0	0	3	0			
		<i>Candelariella reflexa</i>	0	0	1	0							
		Sum (frequency)	8	2	2	6	5	4	7	3			
55	HUL023 (X: 382488, Y: 397017): <i>Tilia</i>	<i>Lecanora conizaeoides</i>	5	3	3	2						41	24
		<i>Physcia tenella</i>					4	4	5	5			
		<i>Buellia punctata</i>	1	0	1	0							
		<i>Parmelia sulcata</i>	1	0	0	0							
		<i>Xanthoria parietina</i>					3	0	1	2			
		<i>Candelariella reflexa</i>	2	4	5	3							
		<i>Arthonia punctiformis</i>	0	2	2	0							
		<i>Lecidella elaeochroma</i>	0	4	3	0							
		Sum (frequency)	9	13	14	5	7	4	6	7			
56	HUL014 (X: 383349, Y: 396842): <i>Acer</i>	<i>Physcia tenella</i>					4	5	5	5	10	44	
		<i>Physcia adscendens</i>					2	1	0	2			
		<i>Xanthoria ucrainica</i>					5	5	5	5			
		<i>Buellia punctata</i>	3	1	0	1							
		<i>Arthonia punctiformis</i>	0	1	3	0							
		<i>Lecanora chlorotera</i>	0	1	0	0							
		Sum (frequency)	3	3	3	1	11	11	10	12			
57	ANC002 (X: 385366, Y: 398773): <i>Fraxinus</i>	<i>Xanthoria parietina</i>					1	2	0	1	10	8	
		<i>Physcia tenella</i>					1	1	1	1			
		<i>Candelariella reflexa</i>	2	0	3	0							
		<i>Arthonia punctiformis</i>	0	1	0	0							
		<i>Buellia punctata</i>	0	1	1	1							
		<i>Lecanora conizaeoides</i>	0	0	0	1							
		Sum (frequency)	2	2	4	2	2	3	1	2			
58	CC021 (X: 384516, Y: 398751): <i>Tilia</i>	<i>Buellia punctata</i>	2	0	1	0					16	9	
		<i>Candelariella reflexa</i>	4	1	4	4							
		<i>Physcia tenella</i>					0	5	0	3			
		<i>Xanthoria ucrainica</i>					0	0	1	0			
		Sum (frequency)	6	1	5	4	0	5	1	3			

Appendix A-3: NO_x diffusion tube locations (ID, site-ID and XY-coordinates, OSGB1936) and calculated NO₂ concentrations [in µg/m³] for each bi-weekly deployment period (1) to (24); concentrations <20 µg/m³ shaded in blue, concentrations between 40 to 50 µg/m³ shaded in light yellow, concentrations >50 µg/m³ shaded in dark yellow; missing equipment/values shaded in red

ID	ID/site	X	Y	NO ₂ (1)	NO ₂ (2)	NO ₂ (3)	NO ₂ (4)	NO ₂ (5)	NO ₂ (6)	NO ₂ (7)	NO ₂ (8)	NO ₂ (9)	NO ₂ (10)
1	ANC001 I	385143	398190	36.91	34.77	39.24	36.87	38.35	41.71	33.60	47.18	51.10	60.86
2	ANC003	384734	398978	26.39	26.67	29.23	33.19	34.02	38.00	29.36	36.02	46.88	42.42
3	ANC009	384231	398977	31.36	35.25	35.99	39.07	35.02	40.60	46.33	48.17	57.80	52.43
4	ANC011	384467	399200	20.50	22.19	22.72	27.31	29.85	30.20	30.95	35.15	41.63	40.65
5	ANC012	384960	398477	30.37	27.18	32.48	32.83	36.50	39.60	40.09	42.30	50.67	59.09
6	ARD001	384890	397470	39.99	31.05	37.56	43.11	46.10	43.57	46.33	54.10	52.12	62.63
7	ARD004	385326	397120	28.35	24.73	30.79	31.72	33.28	40.97	41.56	43.12	47.81	44.18
8	ARD005	385024	396794	20.09	14.69	20.00	25.48	24.76	26.86	29.36	34.57	42.21	43.60
9	ARD012	384548	397247	35.86	29.56	21.01	39.44	41.30	36.51	56.94	38.23	56.42	59.09
10	ARD013	384798	397104	23.84	16.55	23.27	26.58	26.61	27.23	28.30	34.57	41.35	40.65
11	BFD002	385829	398555	23.80	18.78	21.72	26.21	27.64	31.32	28.83	38.64	42.08	39.59
12	BFD005	385704	398035	21.02	16.18	23.72	22.54	27.64		32.54	32.54	37.79	44.91
13	CC001	385123	397837	30.58	30.77	33.73	39.81	37.24	43.94	51.64	43.12	62.30	48.22
14	CC003	383836	397553	26.39	21.45	24.47	29.89	36.50	35.30	35.09	38.46	36.82	39.35
15	CC006	383517	398334	25.94	25.92	30.04	34.66	37.35	41.71	38.38	44.74	48.95	51.25
16	CC007	383902	398788	23.30		23.97	27.68	26.90	36.14	29.89	34.98	38.11	42.67
17	CC008	384382	397558	30.66	30.03	33.73	37.60	34.02		47.93	48.55	61.59	55.05
18	CC009	384295	398297	32.76	30.68	33.80	36.13	37.72	43.20	45.27	43.83	43.53	51.56
19	CC011	384003	398020	32.84	32.26	33.23	40.91	42.16	45.05	46.33	45.28	52.39	44.77
20	CC012	382892	397730	26.02	18.84	25.52	28.05	29.20	33.54	29.89	38.76	40.37	39.47
21	CC015	383290	397932	21.90	19.21	22.47	24.74	23.58	30.57	26.17	31.73	38.11	34.86
22	CC017	383273	397492	25.27	26.30	29.73	33.56	36.24	40.97	36.78	42.02	47.95	43.60
23	CC018	383277	397664		23.69	24.27	31.72	29.85	39.11	27.23	43.25	39.08	38.18
24	CC021	384516	398751	28.29	25.92	32.30	33.19	32.54	41.71	37.31	43.40	48.63	38.52
25	CC025	384409	397812	29.18	36.74	36.99	41.65	39.57	40.60	41.03	48.55	47.52	50.08

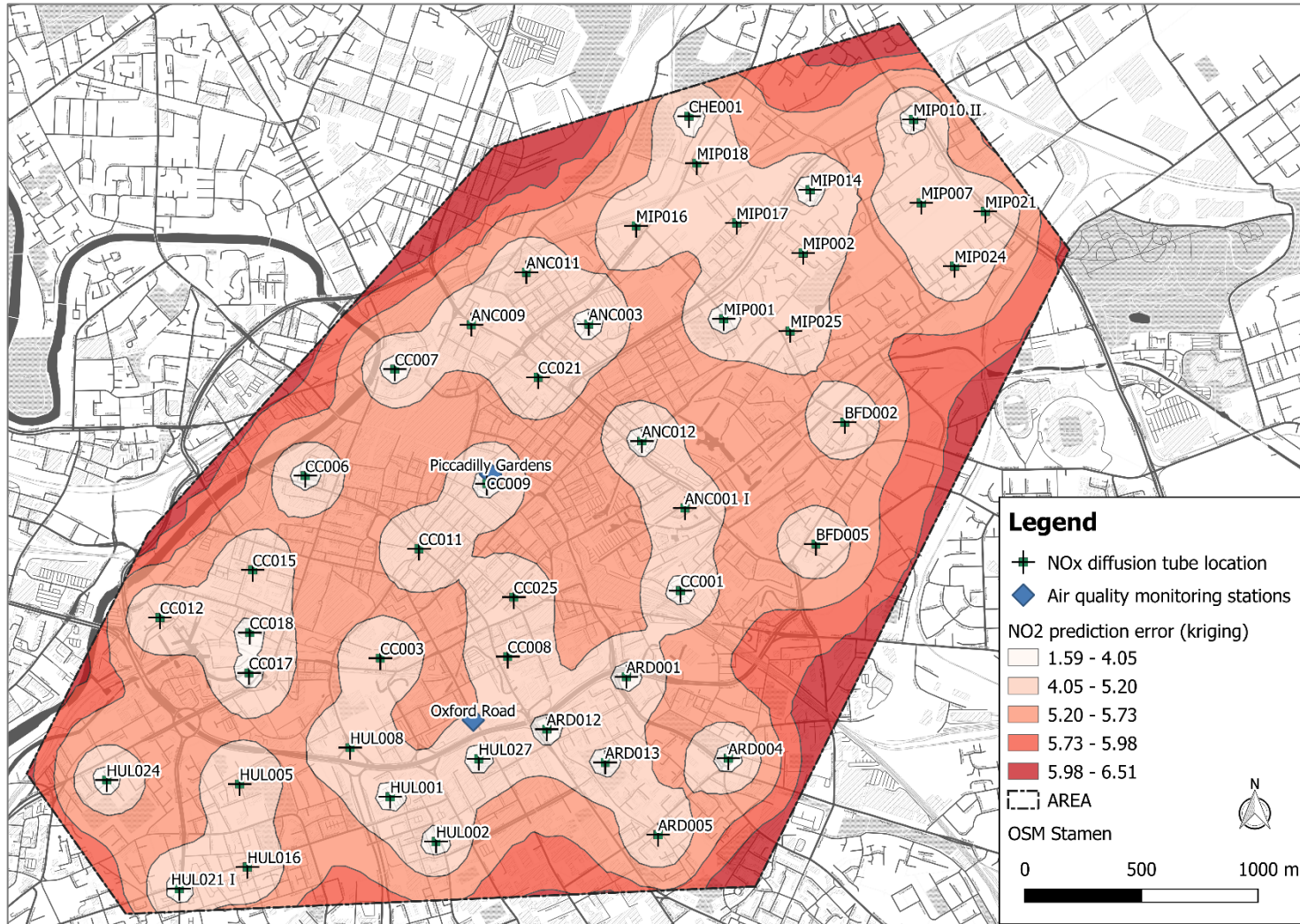
26	CHE001	385166	399865	17.03	13.61	16.99	18.86	19.20	25.00	23.52	25.63	37.36	37.82	
27	HUL001	383876	396960	28.36	22.50	25.22	31.36	32.44	33.54	34.13	41.90	50.39	46.54	
28	HUL002	384072	396768	20.46	16.92	21.47	21.43	25.79	27.60	30.42	36.20	38.76	35.35	
29	HUL005	383231	397017	18.16	18.04	17.96	24.30	26.61	31.69	24.58	34.07	33.16	31.81	
30	HUL008	383705	397171	45.66	40.35	40.82	47.38	44.25	65.48	51.64	55.15	59.87	61.86	
31	HUL016	383263	396662	20.09	16.55	18.50	19.23	27.27	29.83	29.36	37.83	42.21	44.18	
32	HUL021 I	382970	396570					42.01	40.31	45.80	58.01	49.07	58.58	54.20
33	HUL024	382661	397036	19.71	13.95	18.25	22.47		27.23	20.34	31.63	30.15	39.47	
34	HUL027	384271	397097	22.16	20.27	21.76	26.50	29.20	30.57	26.70	33.35	38.33	34.86	
35	MIP001	385312	398998	23.14		23.27	27.97	27.64	29.09	25.11	35.79	42.51	40.06	
36	MIP002	385653	399279	21.32	18.41	21.76	24.67	27.64	25.37	30.42	33.35	36.93	36.53	
37	MIP007	386160	399492		14.69	18.21	24.37	22.84	29.17	30.51	29.29	38.65	37.23	
38	MIP010 II	386128	399848	23.72	18.41	17.96	35.03	28.38	25.82	33.17	30.51	39.08	37.70	
39	MIP014	385684	399549	33.20	16.92	23.52	30.25	25.79	24.33	31.04	31.73	39.08	35.94	
40	MIP016	384938	399397	28.18	24.73	33.48	30.25	32.81	34.29	34.66	38.23	42.51	49.04	
41	MIP017	385369	399408	19.91	15.48	22.51	28.70		23.52		30.91	12.88	41.36	
42	MIP018	385199	399664	28.27	22.94	25.97	29.06	31.70	30.57	41.56	35.39	37.36	47.27	
43	MIP021	386434	399454	21.49	17.29	19.46	25.48	26.16	29.55	23.59	42.30	8.16	49.63	
44	MIP024	386302	399221		20.64	18.21	22.17	20.25	23.52	29.36	33.76	36.93	45.50	
45	MIP025	385597	398946	23.87	18.14	27.42	24.08	23.95	26.94	30.51	36.20	35.21	40.65	

ID	NO ₂ (11)	NO ₂ (12)	NO ₂ (13)	NO ₂ (14)	NO ₂ (15)	NO ₂ (16)	NO ₂ (17)	NO ₂ (18)	NO ₂ (19)	NO ₂ (20)	NO ₂ (21)	NO ₂ (22)	NO ₂ (23)	NO ₂ (24)
1	61.76	49.99	56.85	49.64	68.54	28.45	49.79	41.58	53.55	35.72	35.62	33.77	33.63	35.37
2	41.44	36.95	52.50	34.19	50.80	23.22	29.44	28.94	34.25	26.36	30.22	18.82	18.79	26.00
3	42.38	48.12	50.09	41.72	60.07	21.99	36.73	29.35	47.81	32.92	30.97	24.22	32.88	27.70
4	48.94	22.06	39.58	32.21	34.27	33.05	28.23	24.76	30.08	20.96	22.10	19.65	17.08	19.60
5	57.26	38.47	48.22	42.91	50.39	20.09	31.64	38.65	44.68	26.82	34.77	24.64	21.29	26.00
6		45.17	46.10	57.79	57.82	31.90	39.57	45.63	44.38	41.47		31.70	32.02	33.67

7	54.92	40.24	43.46	43.57	36.39	25.87	29.04	35.61	39.54	27.00	36.15	27.13	23.91	26.85
8	41.86	40.42	30.66	33.70	36.80	22.40	27.01	26.43	29.37	19.15	23.02	20.49	19.21	18.32
9	65.27	43.89	39.70	50.28	47.31	26.42	37.14	35.61	40.99	38.16	42.93	36.68	37.15	38.35
10	40.85	37.87	35.18	41.59	40.72	26.25	28.23	24.35	29.37	20.39	25.56	24.22	19.64	21.31
11	45.24	35.00	42.96	31.03	42.86	19.65	25.59	29.86	33.21	19.86	24.71	21.73	20.92	18.75
12	48.24	35.55	41.46	33.80	44.75	13.05	22.18	29.02	29.55	19.47	27.68	14.26	11.96	17.90
13	53.75	41.95	48.97	43.70	49.74	24.05	38.82	39.91	42.59	32.62	39.96	27.96	26.90	31.96
14	47.67	37.94	37.70	34.88	21.37	30.18	32.78	31.44	35.81	28.37	27.59	30.04	26.05	24.29
15	58.93	44.44	52.35	41.59	37.90	36.74	42.81	36.03	34.25	25.97	30.55	28.79	27.75	25.57
16	52.91	42.62	45.59	38.55	31.04	26.50	37.54	35.61	38.42	26.74	28.02	25.05	23.48	
17	57.70	46.75	40.71	49.24	42.11	23.96	42.53	42.67	47.81	29.06	37.42	39.59	42.27	34.62
18	53.75	47.07	46.85	42.12	47.98	29.36	39.16	33.11	50.42	31.37	33.18	30.87	34.59	29.83
19	61.63	44.38	40.71	38.83	53.38	41.25	47.67	38.95	53.55	33.78	34.77	38.34	33.73	26.85
20	55.58	14.48	37.70	33.80	41.93	24.86	34.30	26.43	34.77	21.34	28.44	22.98	21.78	21.73
21	46.01		35.07	29.04	30.24	28.95	30.25	29.77	33.73	22.12	25.90	20.07	21.35	19.18
22	54.74	7.35	39.20	35.67	38.70	35.92	35.62	33.53	42.07	26.74	27.59	25.47	28.18	17.05
23	47.02	31.61	39.20	34.88	38.30	28.13	36.73	30.19	38.42	25.97	25.48	27.54	28.18	22.59
24	56.26	41.40	49.11	41.72	29.83	26.50	38.35	35.20	36.33	31.76	32.24	30.87	33.73	26.00
25	64.15	44.27	44.09	42.38	60.30	27.63	49.29	46.46	51.98	31.76	32.34	24.22	35.87	34.09
26	39.73	30.61	31.32	28.96	37.49	14.81	19.92	22.74	29.46	15.99	15.39	13.43	13.20	10.65
27	63.46	43.53	39.32	43.96	44.08	25.27	38.76	33.11	40.03	26.59	27.25	27.13	24.34	22.59
28	48.39	42.80	29.53	31.72	39.11	32.64	35.11	28.52	38.09	21.22	23.86	23.81	25.19	17.90
29	44.87	37.69	28.78	36.07	34.27	23.22	29.44	23.93	32.28	17.91	20.90	13.43	20.07	16.62
30	68.98	50.47	50.24	60.94	58.46	33.87	44.84	43.96	61.81	49.32	49.70	30.87	40.56	43.47
31	54.92	45.17	36.31	40.81	41.24	28.13	33.09	31.53	35.18	22.04	25.56	2.26	24.77	20.03
32	84.05	47.55	49.11	47.12	47.31	32.23	37.54	44.51	43.90	35.27	39.96	35.43	33.30	34.52
33	49.89	32.94	26.14	29.75	13.71	24.93	28.63	24.76		19.98	18.78	18.82	18.36	
34	56.26	43.16	41.20	39.23	40.03	37.33	39.97	37.17	38.69	31.13	30.64	21.73		23.44
35	79.79	35.55	40.83	30.63	40.03	21.04	26.34	29.02	36.33	19.86	25.06	17.16	23.91	20.46

36	51.25	34.82	36.95	34.49	37.20	16.18	24.07	25.26	27.47	17.92	21.68	17.58	17.51	15.34
37	44.24	39.94	35.07	25.48	32.35	19.21	25.59	24.42	31.64	15.60	21.75	15.92	16.60	20.94
38	66.27	38.47	36.20	28.56	40.44	26.33	28.61	33.21	38.82	18.70		25.05	28.52	20.09
39	53.25	36.83	37.33	26.59	35.18	16.13	25.21	28.19	30.08	16.38	22.10	19.65	16.18	17.47
40	56.26	43.23	39.70	29.75	35.88	15.69	31.64	32.37	34.66	22.18	30.55		23.91	24.72
41	47.74	33.90	40.83	28.25	35.07	16.13	26.34	21.91	28.51	14.44	21.26	16.33	17.51	15.34
42	53.75	41.03	41.08	38.04	40.72	20.97	29.07	32.37	32.06	26.05	27.17	18.82	25.19	21.31
43	68.78	41.40	39.96		44.08	31.53	32.39	30.70	43.11	24.50	23.02	22.15	27.25	15.34
44	56.76	28.60	39.20	26.27	37.90	19.21	22.94	20.65	32.16	15.99	22.17	21.32	16.18	11.51
45	51.75	33.54	40.83	26.98	37.20	17.45	23.32	26.51	31.12	18.70	22.53	13.84	14.52	16.19

Appendix A-4: NO₂ (mean) concentrations kriging error maps, displayed as prediction errors



Appendix B – Lichen carbon, nitrogen and sulphur contents (wt%) and stable-isotope ratio signatures ($\delta^{13}\text{C}$, $\delta^{15}\text{N}$ and $\delta^{34}\text{S}$) (Chapter 4)

Appendix B-1: Sampling sites for lichens (*X. parietina* and *Physcia* spp.), including XY-coordinates (OSGB1935 –British National Grid), tree species lichens were sampled from, sampling direction and sampling date and description of surrounding

ID	ID/Name	X	Y	Tree species	Sampling Direction	Sampling Date	Surrounding
1	CC001	385123	397837	<i>Acer pseudoplatanus</i>	East	21.06.2016	industry/ manufacturing
2	ANC001 I	385143	398190	<i>Tilia cordata</i>	Southeast	21.06.2016	manufacturing/ road
3	ANC001 II	385180	398222	<i>Tilia cordata</i>	East/Northeast	21.06.2016	manufacturing/ road
4	BFD001	385420	398339	<i>Salix species</i>	North to East	21.06.2016	residential
5	BFD002	385829	398555	<i>Sorbus species</i>	East to South	21.06.2016	industry/ manufacturing
6	BFD008	385368	398023	<i>Fraxinus excelsior</i>	East to South	22.06.2016	industry/ manufacturing/ road
7	BFD007	385366	397922	<i>Acer pseudoplatanus</i>	North to East	22.06.2016	industry/ manufacturing
8	BFD006	385662	397913	<i>Quercus robur</i>	South to West	22.06.2016	green/ road
9	BFD005	385704	398035	<i>Tilia cordata</i>	West/Southwest	22.06.2016	green/ road/ residential
10	BFD004	385760	398209	<i>Platanus x hispanica</i>	South	22.06.2016	road/ residential
11	HUL002	384072	396768	<i>Tilia species</i>	East to South	30.06.2016	road/ residential
12	HUL001	383876	396960	<i>Fraxinus excelsior</i>	East to South	30.06.2016	residential / road
13	HUL004	383616	397107	<i>Crataegus species</i>	West	30.06.2106	road/ residential
14	HUL005	383231	397017	<i>Acer species</i>	South to West	30.06.2016	residential / road / green
15	HUL008	383705	397171	<i>Acer species</i>	West to North	30.06.2016	road/green
16	MIP012	385838	399661	<i>Acer species</i>	South to West	05.07.2016	road/ residential
17	MIP013	385886	399523	<i>Fraxinus excelsior</i>	North/Northeast	05.07.2016	road/green
18	MIP006	385938	399381	<i>Fraxinus excelsior</i>	North/Northeast	05.07.2016	road/industry
19	MIP007	386160	399492	<i>Sorbus species</i>	East to South	05.07.2016	industry/green
20	MIP008 I	386283	399611	<i>Tilia species</i>	East to South	05.07.2016	road/industry
21	MIP008 II	386261	399667	<i>Fraxinus excelsior</i>	West to North	05.07.2016	road/green
22	MIP009 I	386215	399738	<i>Fraxinus excelsior</i>	North to East	06.07.2016	road/green
23	MIP009 II	386190	399774	<i>Fraxinus excelsior</i>	East	06.07.2016	road/green

24	MIP010 I	386158	399834	<i>Quercus species</i>	East to South	06.07.2016	road/green
25	MIP010 II	386128	399848	<i>Fraxinus excelsior</i>	North/Northeast	06.07.2016	road/green
26	MIP011	385883	399803	<i>Acer species</i>	East to South	06.07.2016	road
27	MIP014	385684	399549	<i>Acer species</i>	North	06.07.2016	residential/road
28	MIP022	386381	399468	<i>Fraxinus excelsior</i>	North	12.07.2016	road/green
29	MIP021	386434	399454	<i>Fraxinus excelsior</i>	North to East	12.07.2016	road/green
30	MIP020	386352	399353	<i>Fraxinus excelsior</i>	East to South	12.07.2016	residential/green
31	MIP023	386415	399289	<i>Prunus species</i>	East to South	12.07.2016	residential
32	MIP024	386302	399221	<i>Acer species</i>	East to South	12.07.2016	green/residential
33	MIP038	386167	399073	<i>Acer species</i>	South to West	14.07.2016	green/residential
34	MIP039	385774	398723	<i>Acer species</i>	South	14.07.2016	green/road
35	MIP025	385597	398946	<i>Acer species</i>	South to West	14.07.2016	green/residential
36	ANC007	385176	398981	<i>Acer species</i>	East to South	14.07.2016	green
37	MIP001	385312	398998	<i>Acer species</i>	Northwest to Northeast	14.07.2016	green/road
38	MIP002	385653	399279	<i>Acer species</i>	South to West	19.07.2016	residential
39	MIP003	385749	399415	<i>Corylus colurna</i>	East	19.07.2016	residential/green
40	MIP005	385843	399434	<i>Acer species</i>	West	19.07.2016	green
41	MIP015	385454	399341	<i>Acer species</i>	North to South	19.07.2016	residential/road
42	MIP017	385369	399408	<i>Acer species</i>	South	03.08.2016	residential
43	MIP018	385199	399664	<i>Acer species</i>	West/Northwest	03.08.2016	green/road
44	MIP016	384938	399397	<i>Fraxinus excelsior</i>	South to West	09.08.2016	green/road
45	MIP016 I	385089	399557	<i>Fraxinus excelsior</i>	Northwest	09.08.2016	green/road
46	CHE001	385166	399865	<i>Fraxinus excelsior</i>	North/Northeast	09.08.2016	green/residential
47	CHE002	384901	399510	<i>Fraxinus excelsior</i>	North/Northeast	09.08.2016	residential
48	CHE004	384382	399591	<i>Sorbus aucuparia</i>	East to South	16.08.2016	road/industry
49	ANC011	384467	399200	<i>Quercus pubescens</i>	North to East	16.08.2016	green
50	ANC009	384231	398977	<i>Crataegus species</i>	West to East	16.08.2016	road
51	ARD001	384890	397470	<i>Fraxinus excelsior</i>	South to West	17.08.2016	road
52	ARD002	384843	397402	<i>Ulmus species</i>	East	17.08.2016	green/road/residential
53	ARD002 I	384869	397365	<i>Fraxinus excelsior</i>	East - South - West	17.08.2016	green/road
54	ARD003	384969	397257	<i>Acer species</i>	North/Northwest	17.08.2016	green/manufacturing

55	ARD004	385326	397120	<i>Acer cappadocicum</i>	East to South	17.08.2016	green/road
56	ARD007	385359	396932	<i>Carpinus betulus</i>	East	30.08.2016	road/industry
57	ARD006	385422	396810	<i>Carpinus betulus</i>	West - North - East	30.08.2016	green/residential
58	ARD006 I	385373	396782	<i>Acer species</i>	South to West	30.08.2016	green/residential
59	ARD006 II	385410	396748	<i>Fraxinus excelsior</i>	West to North	30.08.2016	green/residential
60	ARD006 III	385387	396705	<i>Fraxinus excelsior</i>	North	30.08.2016	green/residential
61	ARD012	384548	397247	<i>Acer species</i>	West/Southwest	01.09.2016	road
62	ARD013	384798	397104	<i>Acer species</i>	North to East	01.09.2016	green/residential
63	ARD013 I	384873	397055	<i>Acer species</i>	Northwest to East	01.09.2016	green/residential
64	ARD005	385024	396794	<i>Acer species</i>	North to South	01.09.2016	residential
65	ARD008	384921	396860	<i>Acer species</i>	East	01.09.2016	residential
66	HUL016	383263	396662	<i>Tilia platyphyllos</i>	North	09.05.2017	residential/road
67	HUL021	382850	396595	<i>Fraxinus excelsior</i>	West to North	10.05.2017	residential
68	HUL026	382857	396932	<i>Acer pseudoplatanus</i>	East to South	26.05.2017	green/residential
69	HUL024	382661	397036	<i>Acer pseudoplatanus</i>	South to Northeast	26.05.2017	residential
70	HUL023	382488	397017	<i>Tilia platyphyllos</i>	North to East	27.09.2017	road
71	CC017	383273	397492	<i>Fraxinus excelsior</i>	North	11.05.2017	canal
72	CC012 I	382786	397728	<i>Prunus avium</i>	Northwest to Northeast	11.05.2017	road
73	CC012	382892	397730	<i>Tilia cordata</i>	West to North	11.05.2017	construction site/residential
74	CC018	383277	397664	<i>Sorbus species</i>	Northeast to East	24.05.2017	green/ residential
75	CC015	383290	397932	<i>Tilia platyphyllos</i>	West to Northwest	23.05.2017	green
76	CC014	383156	398139	<i>Acer platanoides</i>	North to Northeast	24.05.2017	road
77	ANC012	384960	398477	<i>Robinia pseudoacacia</i>	Northwest to East	31.05.2017	residential/ canal
78	ANC002	385366	398773	<i>Fraxinus excelsior</i>	South to Northeast	09.10.2017	residential green
79	ANC003	384734	398978	<i>Tilia cordata</i>	South to West	31.05.2017	road
80	CC003	383836	397553	<i>Prunus species</i>	West	05.07.2017	canal/residential
81	CC004	383917	397652	<i>Sorbus aucuparia</i>	South to West	25.10.2017	road
82	CC006	383517	398334	<i>Tilia cordata</i>	West to East	26.10.2017	road
83	CC007	383902	398788	<i>Quercus petraea</i>	West to East	04.07.2017	green
84	CC021	384516	398751	<i>Tilia platyphyllos</i>	West to East	09.10.2017	residential
85	CC009	384295	398297	<i>Quercus robur</i>	South to West	05.07.2017	built-up

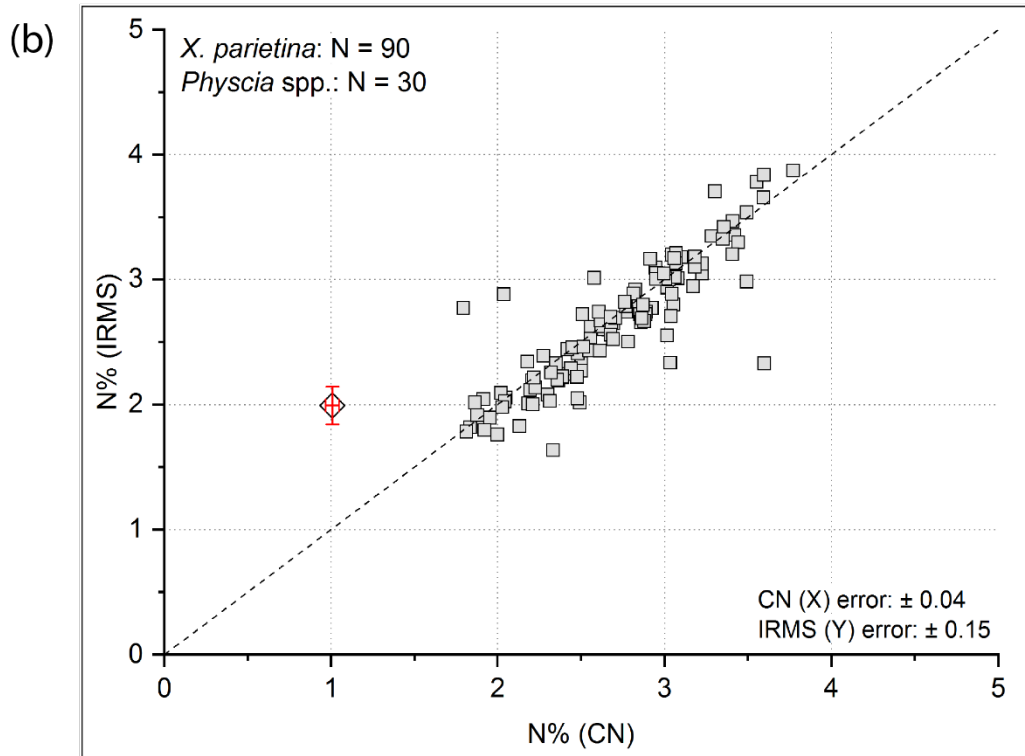
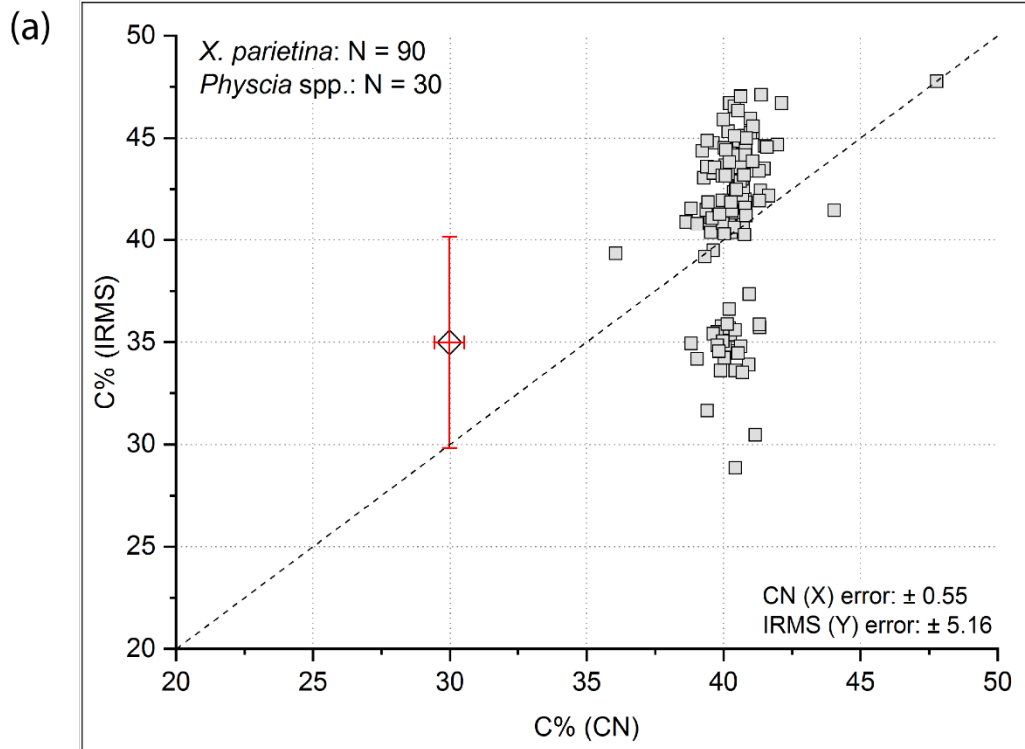
86	HUL025	383832	397110	<i>Acer platanoides</i>	East to West	14.06.2017	road/construction
87	CC025	384409	397812	<i>Acer platanoides</i>	South to West	13.07.2017	car park/rail
88	CC008	384382	397558	<i>Acer platanoides</i>	West to North	13.07.2017	green/road
89	CC011	384003	398020	<i>Catalpa species</i>	North to West	05.07.207	built-up
90	HUL021 I	382968	396568	<i>Acer platanoides</i>	West to East	28.09.2017	road
91	HUL027	384256	397121	<i>Fraxinus excelsior</i>	East	26.09.2017	green
92	HUL014	383349	396842	<i>Acer pseudoplatanus</i>	West to North	28.09.2017	green/residential/school
93	HUL020	382990	396950	<i>Acer pseudoplatanus</i>	South to West	27.09.2017	residential/road
94	CC016	383741	397851	<i>Carpinus betulus</i>	West to East	26.10.2017	road/residential

Appendix B-2: NO_x diffusion tube locations, with XY-coordinates (OSGB1936- British National Grid) and CNS contents (wt%) and stable-isotope ratio signatures ($\delta^{13}\text{C}$, $\delta^{15}\text{N}$ and $\delta^{34}\text{S}$) for *Xanthoria parietina* (Xp) and *Physcia* spp. (Ph)

ID	Site-ID	X	Y	N wt% (Xp)	$\delta^{15}\text{N}$ (Xp)	C wt% (Xp)	$\delta^{13}\text{C}$ (Xp)	S wt% (Xp)	$\delta^{34}\text{S}$ (Xp)	N wt% (Ph)	$\delta^{15}\text{N}$ (Ph)	C wt% (Ph)	$\delta^{13}\text{C}$ (Ph)	S wt% (Ph)	$\delta^{34}\text{S}$ (Ph)
1	ANC001 I	385143	398190	2.50	-6.83	40.70	-26.09	0.38	8.45	2.48	-7.39	40.93	-26.49	0.25	7.72
2	ANC003	384734	398978	3.59	-4.74	40.21	-26.00	0.55	7.17	3.73	-5.57	46.12	-25.14	0.44	7.26
3	ANC009	384231	398977	3.18	-3.38	40.52	-25.15	0.52	10.10	N/A	N/A	N/A	N/A	N/A	N/A
4	ANC011	384467	399200	2.18	-9.46	40.62	-24.93	0.35	9.40	3.01	-9.42	42.58	-25.96	0.30	8.25
5	ANC012	384960	398477	2.68	-6.34	40.04	-25.39	0.48	6.82	3.31	-6.51	47.56	-24.78	0.40	6.46
6	ARD001	384890	397470	2.61	-6.44	39.93	-25.41	0.45	8.57	2.84	-8.20	47.23	-25.53	0.35	7.70
7	ARD004	385326	397120	2.56	-7.37	40.81	-24.35	0.41	6.75	2.51	-8.02	41.06	-25.42	0.28	7.76
8	ARD005	385024	396794	2.48	-8.94	40.70	-24.11	0.45	8.09	2.71	-9.86	46.85	-24.89	0.32	8.32
9	ARD012	384548	397247	3.06	-6.99	38.82	-25.92	0.48	8.21	2.77	-9.12	43.02	-25.09	0.30	8.02
10	ARD013	384798	397104	2.42	-9.86	39.96	-23.83	0.46	7.54	2.31	-11.83	40.77	-23.96	0.23	8.31
11	BFD002	385829	398555	1.01	-4.57	41.15	-24.92	0.53	8.65	1.79	-7.32	44.04	-24.91	0.29	8.23
12	BFD005	385704	398035	3.60	-5.03	40.43	-25.70	0.50	8.98	3.88	-7.27	43.36	-25.88	0.41	8.85
13	CC001	385123	397837	3.04	-10.43	39.90	-25.22	0.49	7.29	3.00	-7.75	40.83	-25.35	0.38	7.57
14	CC003	383836	397553	3.77	-4.60	39.95	-24.07	0.73	6.35	3.99	-5.27	42.33	-24.19	0.42	6.30
15	CC006	383517	398334	2.42	-7.75	39.68	-25.94	0.41	7.04	2.28	-9.36	40.40	-27.58	0.30	7.43
16	CC007	383902	398788	3.07	-7.37	40.09	-25.20	0.55	6.53	3.31	-8.24	43.28	-26.74	0.36	6.96

17	CC008	384382	397558	3.18	-7.26	39.78	-25.79	0.54	7.22	3.47	-8.98	47.20	-25.76	0.42	7.07
18	CC009	384295	398297	2.95	-4.68	39.03	-26.67	0.47	6.98	2.81	-7.94	42.68	-26.46	0.34	6.70
19	CC011	384003	398020	3.03	-5.23	40.26	-25.38	0.39	6.55	N/A	N/A	N/A	N/A	N/A	N/A
20	CC012	382892	397730	2.02	-10.58	39.97	-24.88	0.44	6.58	2.07	-11.87	42.01	-25.33	0.25	6.13
21	CC015	383290	397932	2.71	-8.61	39.83	-24.38	0.52	7.74	2.18	-9.81	40.52	-24.65	0.28	7.65
22	CC017	383273	397492	2.81	-10.01	40.99	-24.74	0.65	1.34	2.97	-10.26	46.03	-24.86	0.41	1.48
23	CC018	383277	397664	3.41	-5.52	40.69	-25.21	0.63	4.61	3.19	-7.71	43.80	-25.66	0.42	5.30
24	CC021	384516	398751	1.96	-9.28	38.63	-25.36	0.30	7.90	2.64	-9.12	46.09	-26.02	0.28	7.95
25	CC025	384409	397812	3.55	-4.44	40.23	-24.39	0.65	7.26	N/A	N/A	N/A	N/A	N/A	N/A
26	CHE001	385166	399865	2.45	-11.52	40.20	-25.44	0.46	8.38	2.45	-12.89	42.17	-24.95	0.27	7.86
27	HUL001	383876	396960	3.02	-6.33	40.28	-23.93	0.49	7.31	2.70	-8.49	38.43	-24.42	0.30	7.30
28	HUL002	384072	396768	1.84	-6.43	40.65	-24.73	0.30	9.65	1.97	-6.59	44.21	-25.58	0.20	9.00
29	HUL005	383231	397017	2.20	-9.11	40.78	-24.37	0.35	8.76	2.21	-9.27	40.40	-24.67	0.23	9.18
30	HUL008	383705	397171	3.35	-1.59	39.76	-26.19	0.58	6.62	3.20	-3.71	43.23	-25.87	0.39	7.78
31	HUL016	383263	396662	2.05	-8.35	40.42	-25.18	0.38	9.07	1.94	-8.84	40.42	-24.48	0.23	8.70
32	HUL021 I	382968	396568	3.28	-3.84	40.09	-26.38	0.55	7.38	N/A	N/A	N/A	N/A	N/A	N/A
33	HUL024	382661	397036	3.07	-5.94	40.16	-25.38	0.55	8.17	3.36	-6.05	48.60	-25.10	0.42	7.42
34	HUL027	384255	397121	3.05	N/A	39.71	N/A	N/A	N/A	3.83	-7.71	45.02	-25.11	0.40	6.57
35	MIP001	385312	398998	2.21	-8.96	40.39	-23.55	0.37	7.64	1.92	-10.36	40.03	-24.38	0.19	7.85
36	MIP002	385653	399279	2.44	-9.17	41.34	-24.35	0.37	8.61	2.48	-8.24	48.72	-25.30	0.26	8.71
37	MIP007	386160	399492	2.88	-6.37	40.06	-24.73	0.44	8.62	2.86	-7.31	41.96	-24.88	0.31	8.36
38	MIP010 II	386128	399848	2.70	-7.59	40.56	-24.17	0.46	7.18	1.11	-8.15	18.37	-23.84	0.11	8.59
39	MIP014	385684	399549	2.55	-8.05	40.26	-25.47	0.43	10.05	2.31	-7.97	44.62	-25.22	0.23	9.44
40	MIP016	384938	399397	3.03	-5.84	39.63	-23.49	0.56	8.97	3.90	-6.26	48.40	-24.59	0.44	7.84
41	MIP017	385369	399408	2.78	-8.80	40.30	-22.44	0.40	9.90	2.51	-8.86	41.37	-23.97	0.32	8.77
42	MIP018	385199	399664	3.02	-5.45	39.61	-25.24	0.54	7.86	2.82	-7.75	46.65	-25.46	0.31	8.36
43	MIP021	386434	399454	3.04	-7.27	40.92	-24.00	0.57	9.16	3.03	-7.87	41.29	-24.63	0.39	8.67
44	MIP024	386302	399221	2.86	-9.46	40.69	-23.86	0.45	8.51	2.68	-10.44	41.65	-24.93	0.29	8.74
45	MIP025	385597	398946	2.48	-10.15	39.40	-24.88	0.37	8.86	2.75	-9.32	46.45	-25.24	0.32	8.67

Appendix B-3: Comparison of carbon (wt%) and nitrogen (wt%) contents for lichen samples analysed by CN analyser and IRMS; error bars are presented as 1x Std. Dev. of analysed lichen CRM (N=32, CN analyser; N= 43, IRMS) carbon and nitrogen contents, by analytical instrument



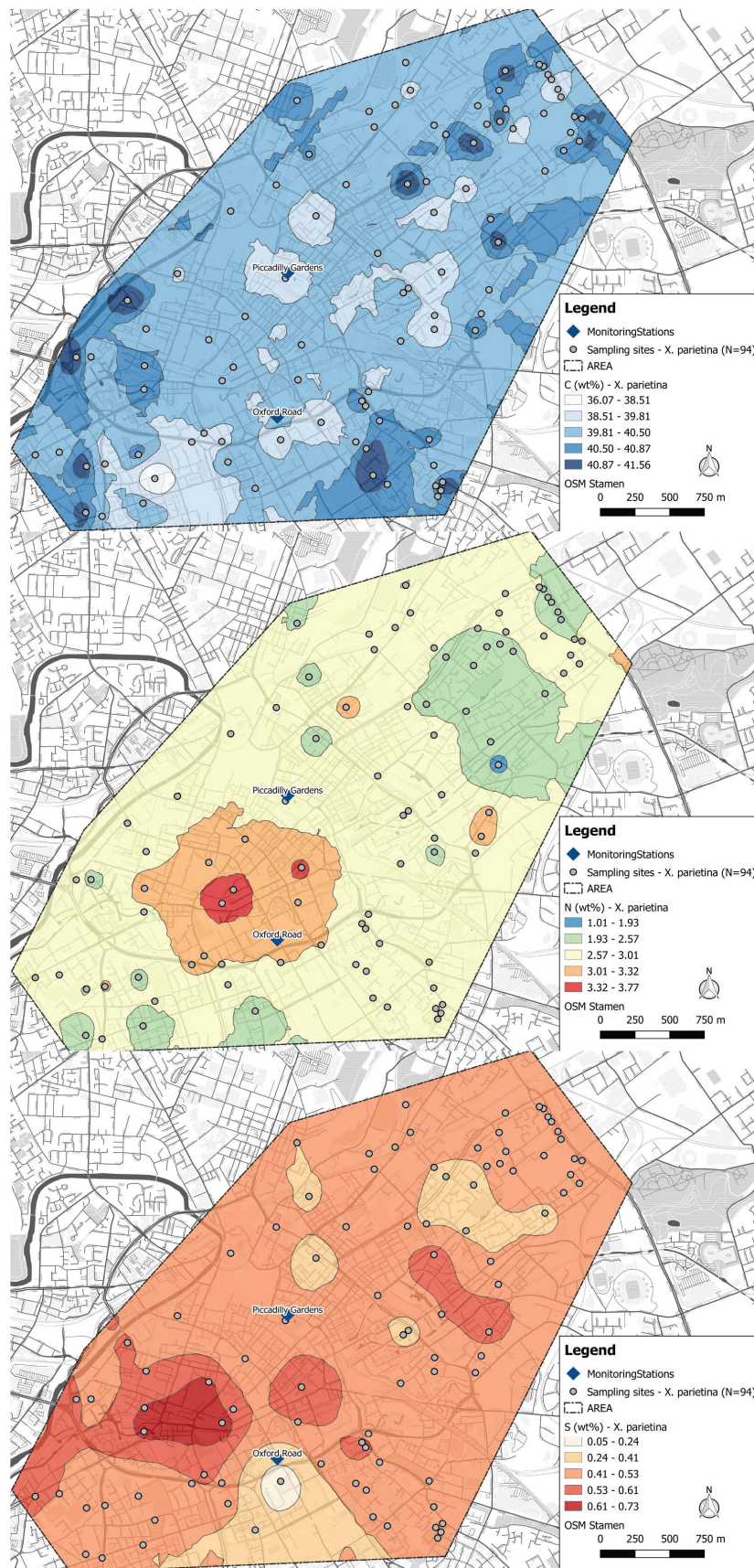
ID	ID/name	X	Y	N wt% (Xp)	C wt% (Xp)	S wt% (Xp)	$\delta^{15}\text{N}$ (Xp)	$\delta^{13}\text{C}$ (Xp)	$\delta^{34}\text{S}$ (Xp)	N wt% (Ph)	C wt% (Ph)	S wt% (Ph)	$\delta^{15}\text{N}$ (Ph)	$\delta^{13}\text{C}$ (Ph)	$\delta^{34}\text{S}$ (Ph)
1	ANC001 I	385143	398190	2.502	40.700	0.382	-6.83	-26.09	8.45	2.479	40.93	0.249	-7.39	-26.49	7.72
2	ANC001II	385180	398222	3.051	39.760	0.320	-6.99	-26.07	6.48	3.036	39.04	0.334	-7.19	-27.37	7.80
3	BFD001	385420	398339	2.926	39.370	0.548	-6.88	-24.89	8.00						
4	CC001	385123	397837	3.044	39.900	0.489	-10.43	-25.22	7.29	2.996	40.83	0.379	-7.75	-25.35	7.57
5	BFD002	385829	398555	1.010	41.150	0.526	-4.57	-24.92	8.65	1.794	44.04	0.289	-7.32	-24.91	8.23
6	BFD004	385760	398209	3.421	40.370	0.562	-5.59	-24.19	7.65	3.588	41.538	0.397	-6.72	-25.01	7.09
7	BFD007	385366	397922	2.038	38.820	0.530	-5.65	-23.36	8.85	2.579	40.82	0.346	-7.27	-24.41	8.11
8	BFD005	385704	398035	3.598	40.430	0.504	-5.03	-25.70	8.98	3.878	43.362	0.408	-7.27	-25.88	8.85
9	BFD006	385662	397913	2.636	40.750	0.481	-7.30	-25.20	8.87	2.494	40.14	0.236	-8.40	-24.83	9.05
10	BFD008	385368	398023	2.824	39.280	0.462	-7.53	-24.03	7.99	2.944	41.277	0.341	-6.02	-24.33	8.52
11	HUL001	383876	396960	3.015	40.280	0.489	-6.33	-23.93	7.31	2.703	38.430	0.302	-8.49	-24.42	7.30
12	HUL002	384072	396768	1.837	40.650	0.304	-6.43	-24.73	9.65	1.966	44.206	0.205	-6.59	-25.58	9.00
13	HUL004	383616	397107	3.226	39.540	0.501	-1.58	-24.58	7.85	3.470	42.295	0.389	-2.03	-25.34	7.37
14	HUL005	383231	397017	2.197	40.780	0.349	-9.11	-24.37	8.76	2.21	40.4	0.227	-9.27	-24.67	9.18
15	HUL008	383705	397171	3.349	39.760	0.584	-1.59	-26.19	6.62	3.203	43.226	0.388	-3.71	-25.87	7.78
16	MIP012	385838	399661	3.081	40.720	0.462	-3.54	-25.10	7.54	2.873	40.27	0.297	-4.24	-25.44	8.05
17	MIP013	385886	399523	2.890	40.580	0.451	-7.30	-23.58	9.50	2.780	44.154	0.338	-8.73	-23.55	9.22
18	MIP007	386160	399492	2.878	40.060	0.438	-6.37	-24.73	8.62	2.863	41.96	0.308	-7.31	-24.88	8.36
19	MIP008 II	386261	399667	1.999	39.320	0.350	-11.35	-24.49	7.02	1.813	40.22	0.228	-11.40	-25.58	7.01
20	MIP006	385938	399381	2.503	39.520	0.538	-8.41	-25.12	8.09	2.764	40.79	0.346	-7.55	-24.45	8.11
21	MIP008 I	386283	399611	2.131	39.620	0.291	-7.95	-24.06	7.20	2.614	39.43	0.231	-4.96	-25.52	7.77
22	CHE001	385166	399865	2.449	40.200	0.457	-11.52	-25.44	8.38	2.450	42.165	0.269	-12.89	-24.95	7.86
23	MIP016 I	385089	399557	2.665	40.060	0.446	-6.70	-23.99	9.42	2.909	43.784	0.338	-7.56	-24.53	8.90
24	ANC011	384467	399200	2.184	40.620	0.349	-9.46	-24.93	9.40	3.012	42.575	0.302	-9.42	-25.96	8.25
25	MIP021	386434	399454	3.040	40.920	0.572	-7.27	-24.00	9.16	3.030	41.290	0.392	-7.87	-24.63	8.67
26	CHE002	384901	399510	2.888	40.420	0.492	-8.53	-25.70	8.45	0.804	11.728	0.051	-10.75	-24.50	6.25
27	ANC009	384231	398977	3.183	40.520	0.515	-3.38	-25.15	10.10						

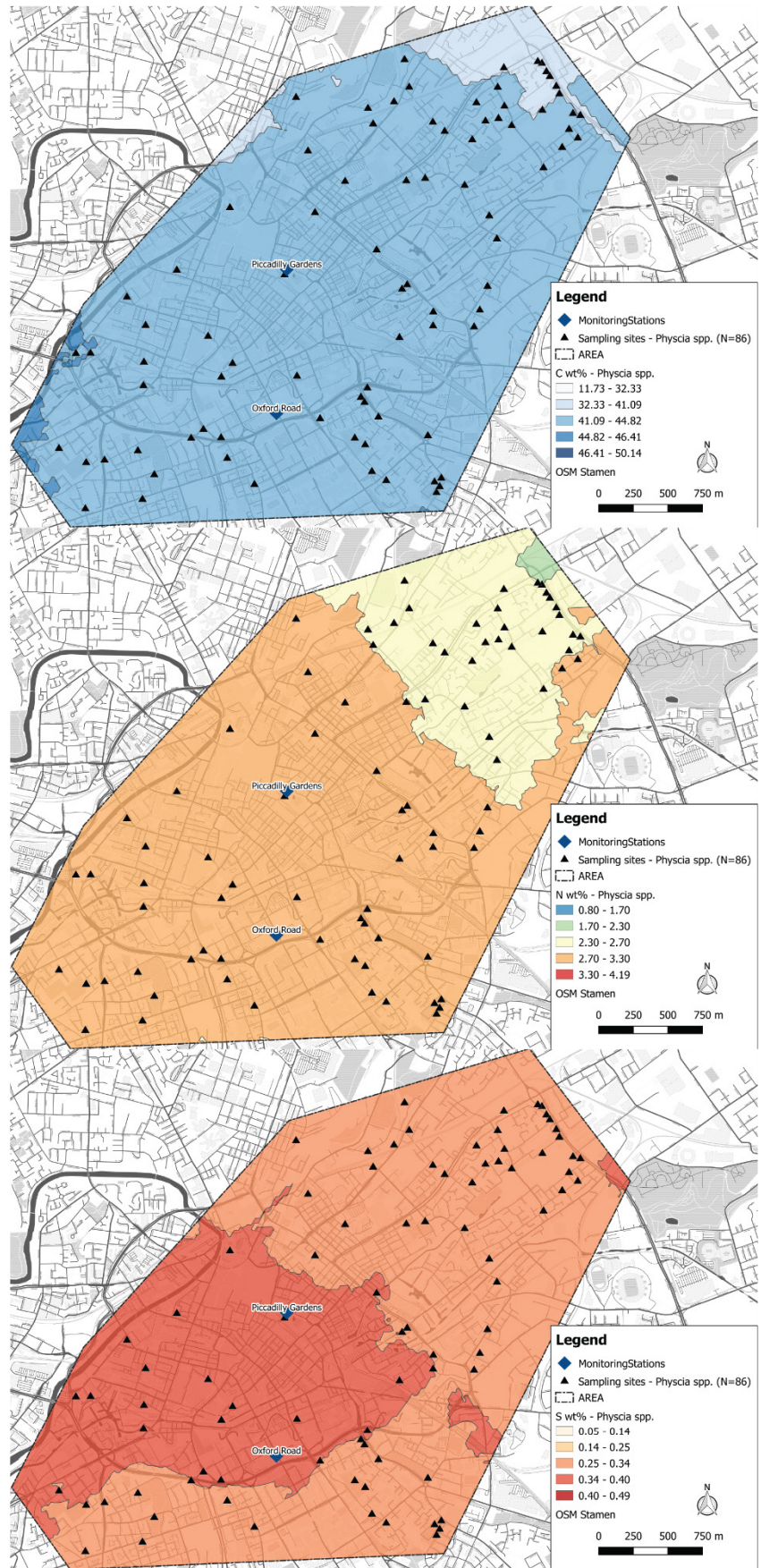
28	ARD007	385359	396932	3.172	39.580	0.549	-6.00	-24.13	9.08						
29	ARD004	385326	397120	2.559	40.810	0.411	-7.37	-24.35	6.75	2.514	41.06	0.277	-8.02	-25.42	7.76
30	MIP039	385774	398723	2.358	40.610	0.398	-9.62	-24.65	8.06	2.028	40.74	0.237	-11.31	-24.88	8.72
31	CHE004	384382	399591	2.389	40.730	0.398	-8.52	-23.34	8.52	2.692	41.31	0.300	-6.95	-24.34	7.46
32	ARD002	384843	397402	2.996	40.920	0.548	-6.88	-25.77	8.34	2.795	40.350	0.291	-8.47	-25.13	8.90
33	MIP010 I	386158	399834	2.388	40.680	0.392	-9.49	-24.49	7.74	2.321	41.59	0.262	-9.57	-25.45	8.33
34	ARD002 I	384869	397365	3.493	40.430	0.621	-5.84	-24.25	7.29	3.817	42.415	0.432	-5.33	-24.89	7.11
35	ANC007	385176	398981	2.621	41.560	0.451	-9.14	-24.95	6.78	2.735	46.117	0.326	-9.00	-25.66	7.34
36	MIP011	385883	399803	2.772	40.990	0.481	-5.77	-24.53	8.23	2.678	42.11	0.301	-6.13	-25.28	8.35
37	ARD013	384798	397104	2.421	39.960	0.462	-9.86	-23.83	7.54	2.313	40.77	0.225	-11.83	-23.96	8.31
38	MIP020	386352	399353	3.044	40.040	0.535	-5.96	-24.39	8.07	3.710	41.357	0.404	-5.56	-24.89	7.55
39	ARD013 I	384873	397055	2.953	40.990	0.461	-4.98	-24.51	6.69	2.769	41.3	0.297	-6.94	-24.86	7.64
40	MIP009 II	386190	399774	2.618	40.250	0.491	-7.80	-23.85	7.32	3.058	41.08	0.386	-7.06	-24.55	7.34
41	MIP022	386381	399468	2.365	40.640	0.456	-9.46	-24.55	8.43	2.711	41.828	0.321	-8.28	-24.12	7.23
42	MIP010 II	386128	399848	2.695	40.560	0.456	-7.59	-24.17	7.18	1.112	18.368	0.114	-8.15	-23.84	8.59
43	MIP014	385684	399549	2.549	40.260	0.432	-8.05	-25.47	10.05	2.307	44.616	0.230	-7.97	-25.22	9.44
44	MIP024	386302	399221	2.859	40.690	0.452	-9.46	-23.86	8.51	2.677	41.65	0.288	-10.44	-24.93	8.74
45	MIP018	385199	399664	3.023	39.610	0.537	-5.45	-25.24	7.86	2.816	46.649	0.306	-7.75	-25.46	8.36
46	ARD012	384548	397247	3.062	38.820	0.483	-6.99	-25.92	8.21	2.774	43.020	0.303	-9.12	-25.09	8.02
47	MIP017	385369	399408	2.783	40.300	0.399	-8.80	-22.44	9.90	2.508	41.37	0.316	-8.86	-23.97	8.77
48	MIP016	384938	399397	3.026	39.630	0.564	-5.84	-23.49	8.97	3.904	48.400	0.442	-6.26	-24.59	7.84
49	MIP023	386415	399289	3.055	40.780	0.481	-8.04	-24.32	7.78	3.068	48.483	0.319	-7.99	-24.67	7.92
50	ARD006 I	385373	396782	2.854	40.570	0.442	-9.09	-24.69	7.51	2.606	48.213	0.309	-10.82	-25.77	8.26
51	MIP009 I	386215	399738	2.217	39.410	0.421	-9.83	-23.63	8.06	1.88	40.08	0.278	-10.74	-24.65	6.92
52	MIP001	385312	398998	2.206	40.390	0.366	-8.96	-23.55	7.64	1.921	40.03	0.188	-10.36	-24.38	7.85
53	MIP038	386167	399073	2.301	39.850	0.368	-9.37	-24.09	8.25	2.044	40.61	0.222	-10.62	-25.26	8.98
54	MIP015	385454	399341	2.227	40.570	0.376	-8.66	-24.25	9.70	2.398	47.032	0.294	-9.03	-25.11	8.14
55	MIP002	385653	399279	2.439	41.340	0.368	-9.17	-24.35	8.61	2.477	48.722	0.263	-8.24	-25.30	8.71
56	MIP025	385597	398946	2.477	39.400	0.374	-10.15	-24.88	8.86	2.754	46.453	0.318	-9.32	-25.24	8.67

57	ARD001	384890	397470	2.608	39.930	0.455	-6.44	-25.41	8.57	2.843	47.232	0.345	-8.20	-25.53	7.70
58	MIP005	385843	399434	1.865	41.320	0.408	-9.01	-24.96	10.56	2.118	43.443	0.246	-9.60	-24.20	9.55
59	ARD003	384969	397257	2.351	40.800	0.439	-8.59	-24.51	8.95	2.485	46.070	0.316	-8.66	-24.88	8.35
60	MIP003	385749	399415	2.411	39.970	0.422	-10.60	-24.05	7.24	2.215	50.136	0.301	-11.79	-26.04	8.00
61	ARD006	385422	396810	2.825	41.030	0.465	-7.92	-24.44	7.96	2.766	45.667	0.333	-9.61	-25.36	8.68
62	ARD005	385024	396794	2.480	40.700	0.446	-8.94	-24.11	8.09	2.708	46.854	0.317	-9.86	-24.89	8.32
63	ARD008	384921	396860	2.558	41.500	0.419	-9.20	-24.39	7.61	2.822	48.239	0.305	-9.99	-25.46	7.70
64	ARD006 III	385387	396705	3.017	40.440	0.547	-8.34	-24.25	7.53	2.993	42.552	0.348	-8.94	-24.97	8.12
65	ARD006 II	385410	396748	2.625	41.040	0.434	-9.72	-23.71	9.25	2.974	44.461	0.355	-9.38	-24.36	8.31
66	CC014	383156	398139	3.226	41.480	0.545	-6.30	-24.38	7.17	3.446	47.395	0.406	-7.89	-25.47	7.09
67	CC015	383290	397932	2.705	39.830	0.516	-8.61	-24.38	7.74	2.178	40.52	0.282	-9.81	-24.65	7.65
68	CC003	383836	397553	3.771	39.950	0.727	-4.60	-24.07	6.35	3.991	42.333	0.421	-5.27	-24.19	6.30
69	ANC003	384734	398978	3.594	40.210	0.553	-4.74	-26.00	7.17	3.729	46.122	0.438	-5.57	-25.14	7.26
70	CC017	383273	397492	2.814	40.990	0.654	-10.01	-24.74	1.34	2.970	46.027	0.408	-10.26	-24.86	1.48
71	HUL021	382850	396595	1.915	41.080	0.386	-13.62	-24.08	7.87	1.989	42.847	0.234	-14.16	-24.71	7.80
72	CC007	383902	398788	3.070	40.090	0.555	-7.37	-25.20	6.53	3.306	43.280	0.358	-8.24	-26.74	6.96
73	HUL025	383832	397110	2.952	39.630	0.493	-7.45	-25.06	8.05	2.916	40.41	0.404	-7.37	-25.40	6.72
74	HUL016	383263	396662	2.050	40.420	0.382	-8.35	-25.18	9.07	1.942	40.423	0.229	-8.84	-24.48	8.70
75	HUL026	382857	396932	2.333	41.150	0.272	-8.48	-23.40	9.34	3.026	49.290	0.369	-8.34	-24.83	7.75
76	CC009	384295	398297	2.950	39.030	0.469	-4.68	-26.67	6.98	2.809	42.681	0.345	-7.94	-26.46	6.70
77	CC018	383277	397664	3.408	40.690	0.630	-5.52	-25.21	4.61	3.186	43.800	0.418	-7.71	-25.66	5.30
78	CC012 I	382786	397728	3.005	41.310	0.574	-5.00	-26.02	8.28	3.907	48.394	0.492	-4.62	-25.85	7.21
79	CC012	382892	397730	2.021	39.970	0.443	-10.58	-24.88	6.58	2.065	42.007	0.249	-11.87	-25.33	6.13
80	HUL024	382661	397036	3.069	40.160	0.552	-5.94	-25.38	8.17	3.363	48.603	0.417	-6.05	-25.10	7.42
81	ANC012	384960	398477	2.681	40.040	0.478	-6.34	-25.39	6.82	3.308	47.560	0.399	-6.51	-24.78	6.46
82	CC025	384409	397812	3.554	40.230	0.647	-4.44	-24.39	7.26						
83	CC008	384382	397558	3.183	39.780	0.536	-7.26	-25.79	7.22	3.465	47.196	0.418	-8.98	-25.76	7.07
84	HUL021 I	382968	396568	3.284	40.090	0.551	-3.84	-26.38	7.38						
85	CC006	383517	398334	2.418	39.680	0.408	-7.75	-25.94	7.04	2.275	40.4	0.301	-9.36	-27.58	7.43

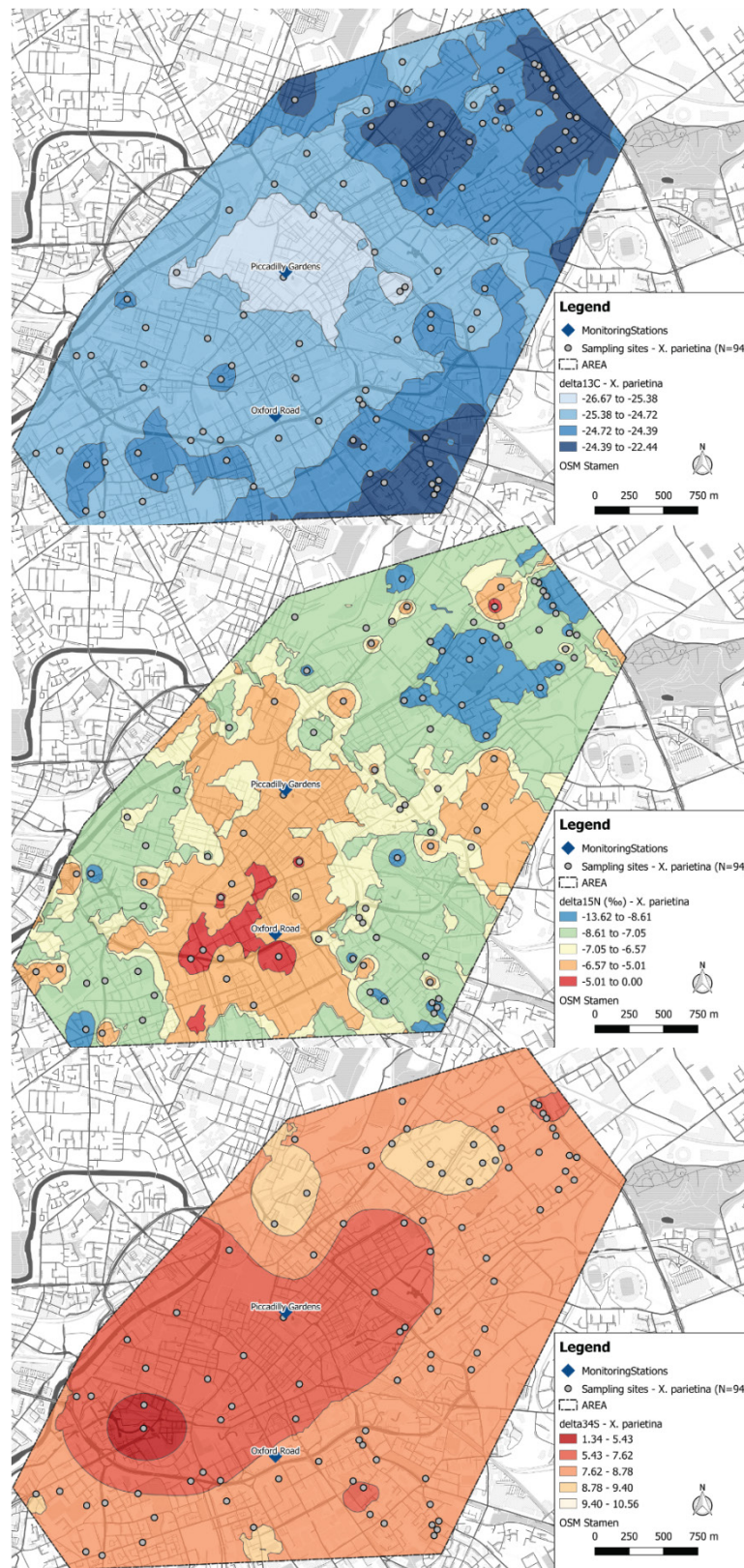
86	HUL027	384256	397121	3.049	39.710					3.826	45.022	0.396	-7.71	-25.11	6.57
87	CC016	383741	397851	3.357	40.430	0.655	-7.34	-25.39	7.59	3.596	47.78	0.450	-8.53	-25.81	8.14
88	CC021	384516	398751	1.955	38.630	0.296	-9.28	-25.36	7.90	2.639	46.088	0.276	-9.12	-26.02	7.95
89	CC011	384003	398020	3.03	40.26	0.388	-5.23	-25.38	6.55						
90	HUL023	382488	397017	2.947	40.000	0.571	-4.85	-24.98	9.40						
91	HUL020	382990	396950	3.410	39.390	0.602	-6.87	-25.05	7.39	4.191	47.178	0.443	-7.08	-25.73	7.59
92	CC004	383917	397652	3.441	40.470	0.532	-5.92	-24.57	7.97	3.673	46.051	0.437	-5.99	-25.77	6.91
93	HUL014	383349	396842	2.618	36.070	0.457	-7.49	-24.29	7.58	3.302	40.62		-7.68	-25.45	7.54
94	ANC002	385366	398773	3.101	39.230	0.630	-7.49	-24.31	7.38						

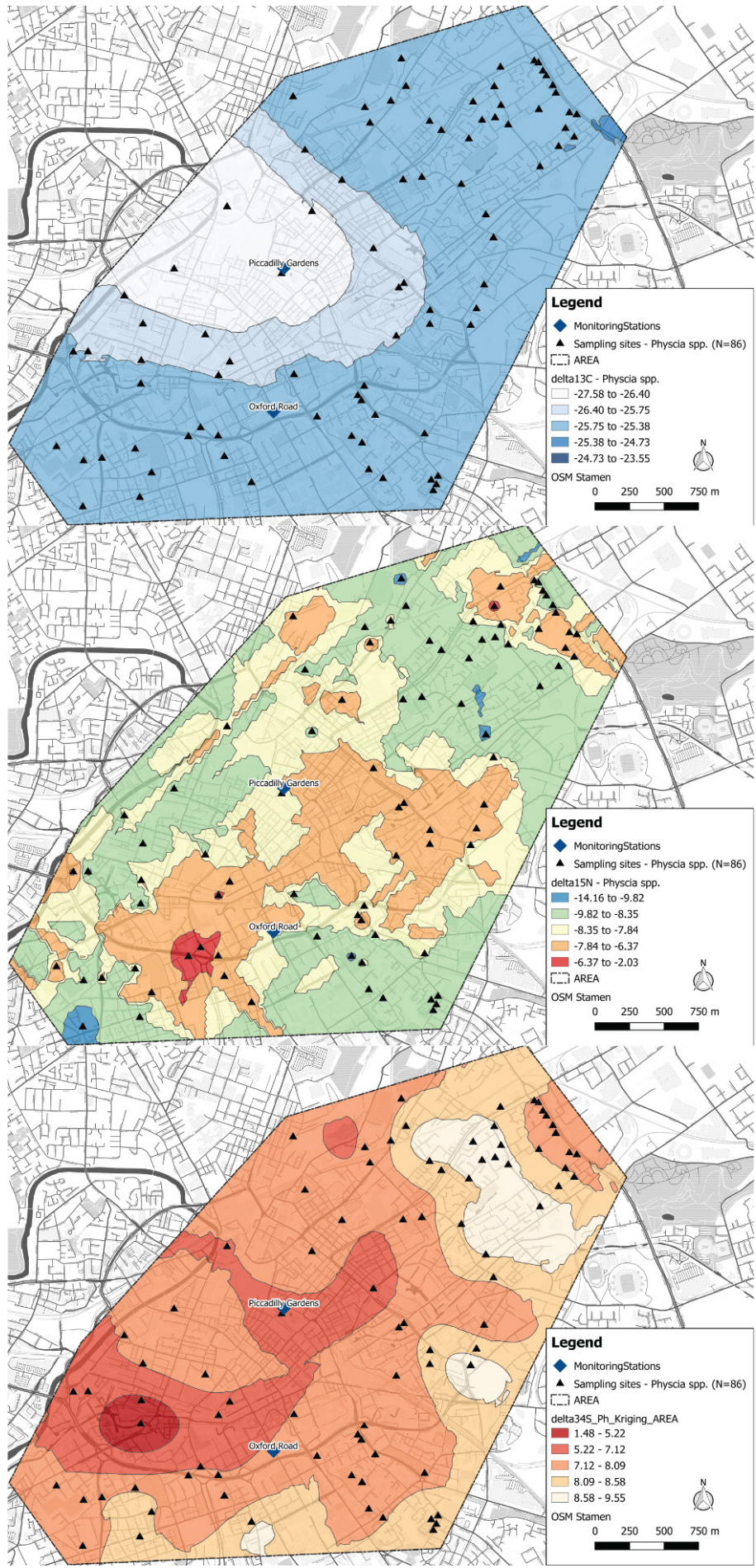
Appendix B-4: CNS contents (wt%) – *X. parietina* (N=94) and *Physcia* spp. (N=86), interpolated by ordinary kriging (upper panel: carbon wt%, middle panel: nitrogen wt% and lower panel: sulphur wt%)



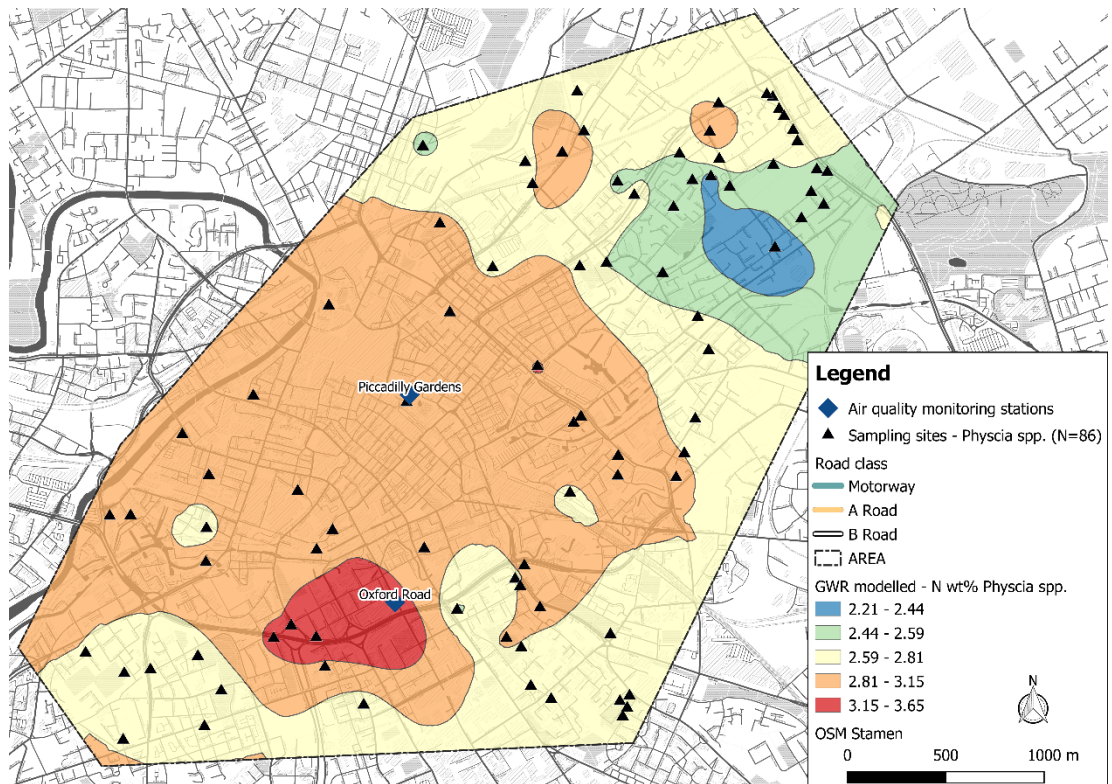


Appendix B-5: Stable-isotope ratio signatures - *X. parietina* (N=94) and *Physcia* spp. (N=86), interpolated by ordinary kriging (upper panel: $\delta^{13}\text{C}$ ‰, middle panel: $\delta^{15}\text{N}$ ‰ and lower panel: $\delta^{34}\text{S}$ ‰)





Appendix B-6: GWR modelled (predicted values) of N wt% in *Physcia* spp. (N=86)



Appendix C – Lichen nitrate (NO₃⁻) and ammonium (NH₄⁺) concentrations (Chapter 5)

Appendix C-1: Revisited sampling sites (N=17, *X. parietina*) for analysis of nitrate and ammonium concentrations, displayed with XY-coordinates, NO₃⁻ and NH₄⁺ concentrations, as well as nitrogen contents (wt%) for sampling undertaken and 2016/17 (1) and same site in 2018 (2)

ID	Site	X	Y	lichen spec	Nitrate (1)	Nitrate (2)	Ammonium (1)	Ammonium (2)	N wt% (1)	N wt% (2)
1	ARD008	384921	396860	Xp	100.039	106.882	8.043	2.409	2.527	2.646
2	MIP001	385312	398998	Xp	35.572	5.944	5.111	2.723	2.19	2.418
3	ARD003	384969	397257	Xp	64.432	111.984	7.481	2.901	2.327	2.851
4	BFD005	385704	398035	Xp	49.684	3.357	11.280	2.695	3.598	3.185
5	ARD012	384548	397247	Xp	88.520	17.591	11.030	2.729	3.062	3.152
6	MIP010 I	386158	399834	Xp	109.513	4.431	5.058	1.961	2.388	2.229
7	ANC012	384960	398477	Xp	5.319	29.065	11.110	3.719	2.649	3.188
8	CC018	383277	397664	Xp	75.799	26.932	10.587	4.261	3.202	3.761
9	MIP021	386434	399454	Xp	91.287	18.515	8.998	3.687	3.040	2.956
10	ARD004	385326	397120	Xp	46.710	12.444	12.923	2.570	2.168	2.781
11	BFD008	385368	398023	Xp	37.575	125.622	5.772	3.796	2.824	3.513
12	ANC011	384467	399200	Xp	36.748	N/A	5.610	1.899	2.184	2.153
13	MIP024	386302	399221	Xp	45.178	16.479	7.987	3.337	2.656	3.024
14	ARD006	385422	396810	Xp	71.807	71.807	2.428	2.428	2.918	N/A
15	HUL008	383705	397171	Xp	27.397	29.259	9.352	3.359	3.324	3.212
16	ARD013	384798	397104	Xp	50.419	9.852	5.941	1.719	2.421	2.26
17	ANC009	384231	398977	Xp	94.341	16.240	11.861	3.893	3.183	3.45

Appendix C-2: Nitrate and ammonium concentrations (per site) recorded in *X. parietina* (N=87), using 3% KCl and 6h extraction time; red shaded field indicate no recorded nitrate and/or ammonium

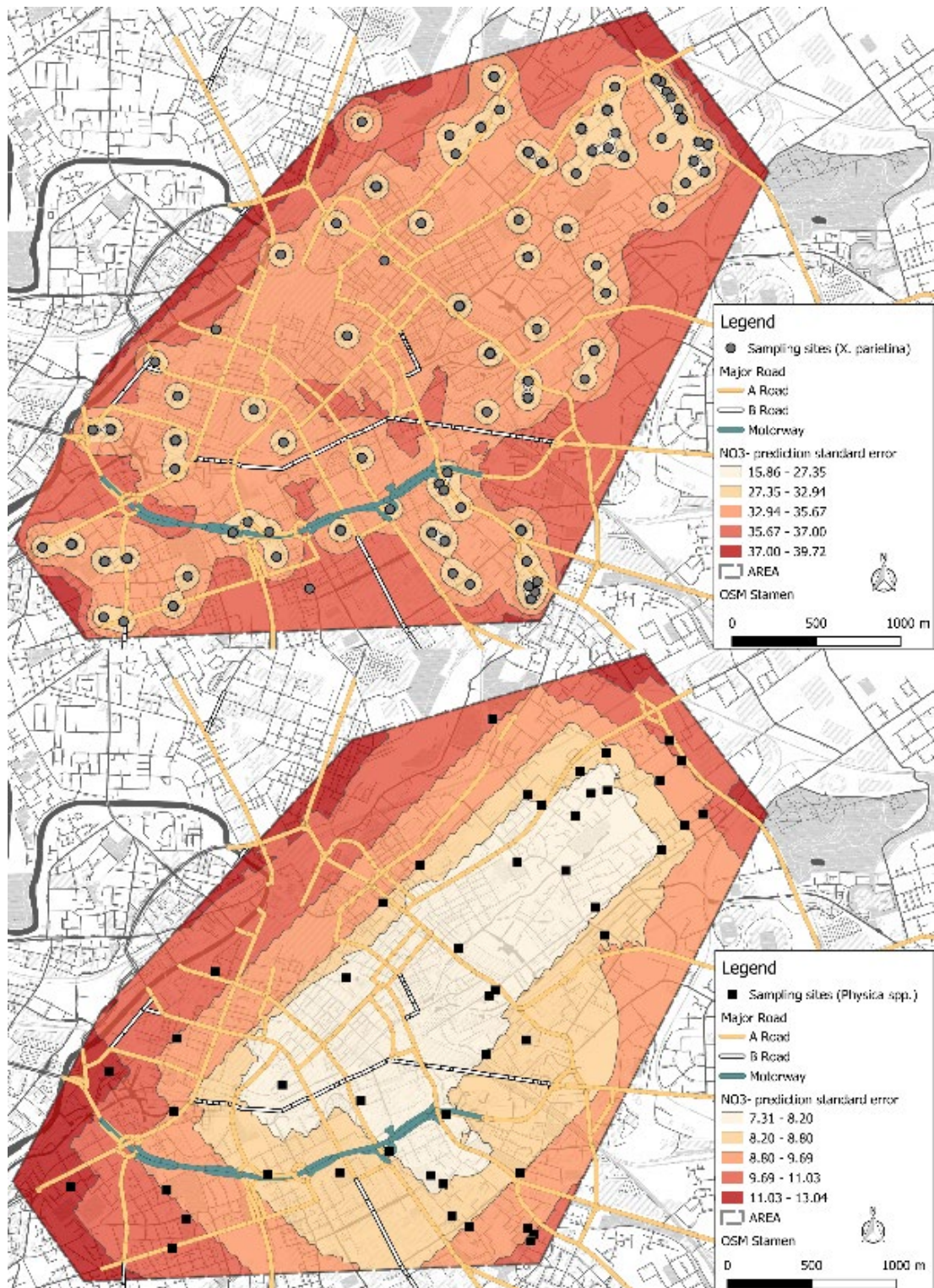
ID	NAME	X	Y	lichen species	Nitrate (mg/kg)	Ammonium (mg/kg)
1	MIP011	385883	399803	Xp	87.15	5.53
2	BFD008	385368	398023	Xp	37.57	5.77
3	MIP007	386160	399492	Xp	40.62	6.18
4	ARD013	384798	397104	Xp	50.42	5.94
5	BFD001	385420	398339	Xp	12.56	7.44
6	CHE004	384382	399591	Xp	43.36	5.19
7	MIP009 II	386190	399774	Xp	142.73	5.68
8	HUL001	383876	396960	Xp	45.73	7.10
9	ANC011	384467	399200	Xp	36.75	5.61
10	ARD007	385359	396932	Xp	76.08	10.41
11	MIP013	385886	399523	Xp	37.66	6.96
12	HUL002	384072	396768	Xp		3.18
13	CC001	385123	397837	Xp	9.96	7.44
14	MIP021	386434	399454	Xp	91.29	9.00
15	ANC009	384231	398977	Xp	94.34	11.86
16	ARD012	384548	397247	Xp	88.52	11.03
17	CHE001	385166	399865	Xp	54.01	7.39
18	BFD005	385704	398035	Xp	49.68	11.28
19	MIP010 I	386158	399834	Xp	109.51	5.06
20	CHE002	384901	399510	Xp	54.00	8.59
21	MIP008 II	386261	399667	Xp	18.88	4.28
22	MIP008 I	386283	399611	Xp	35.436	4.172
23	MIP001	385312	398998	Xp	35.572	5.111
24	ARD001	384890	397470	Xp	90.591	8.800
25	BFD004	385760	398209	Xp	31.301	11.907
26	ANC012	384960	398477	Xp	5.319	11.110
27	MIP014	385684	399549	Xp	136.434	5.958
28	HUL025	383832	397110	Xp	26.220	10.888
29	ARD005	385024	396794	Xp	59.611	7.139
30	CC008	384382	397558	Xp	93.590	14.842
31	CC009	384295	398297	Xp	21.886	12.646
32	MIP016 I	385089	399557	Xp	56.818	8.127
33	HUL027	384256	397121	Xp	20.295	10.832
34	CC012	382892	397730	Xp	38.648	5.581
35	MIP002	385653	399279	Xp	62.314	5.323
36	CC018	383277	397664	Xp	75.799	10.587
37	MIP015	385454	399341	Xp	53.510	5.331
38	MIP003	385749	399415	Xp	62.478	6.641
39	ARD002	384843	397402	Xp	78.993	9.584
40	MIP006	385938	399381	Xp	24.651	4.971
41	CC016	383741	397851	Xp	21.258	13.288
42	MIP025	385597	398946	Xp	38.006	6.167
43	ARD003	384969	397257	Xp	64.432	7.481
44	MIP020	386352	399353	Xp	115.851	9.645
45	HUL016	383263	396662	Xp	30.388	7.687
46	HUL021 I	382968	396568	Xp	33.875	12.889
47	MIP010 II	386128	399848	Xp	73.401	6.104
48	MIP017	385369	399408	Xp	62.030	6.997
49	HUL021	382850	396595	Xp	28.113	5.258
50	HUL014	383349	396842	Xp	1.015	11.840

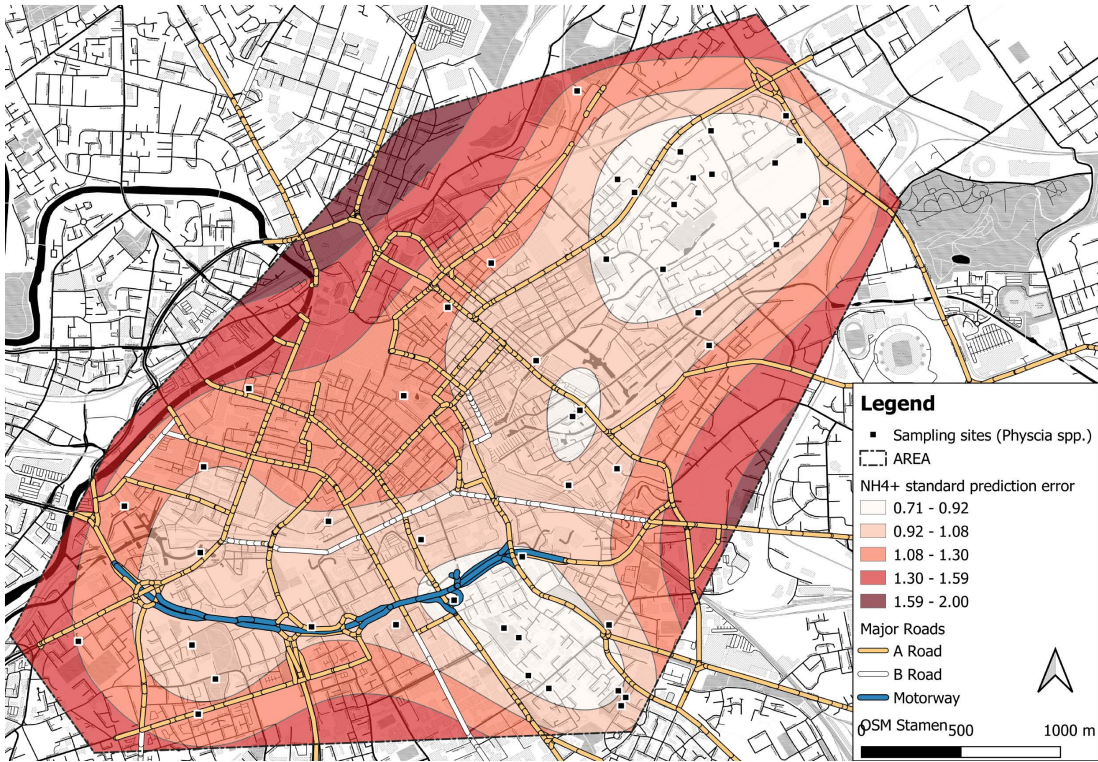
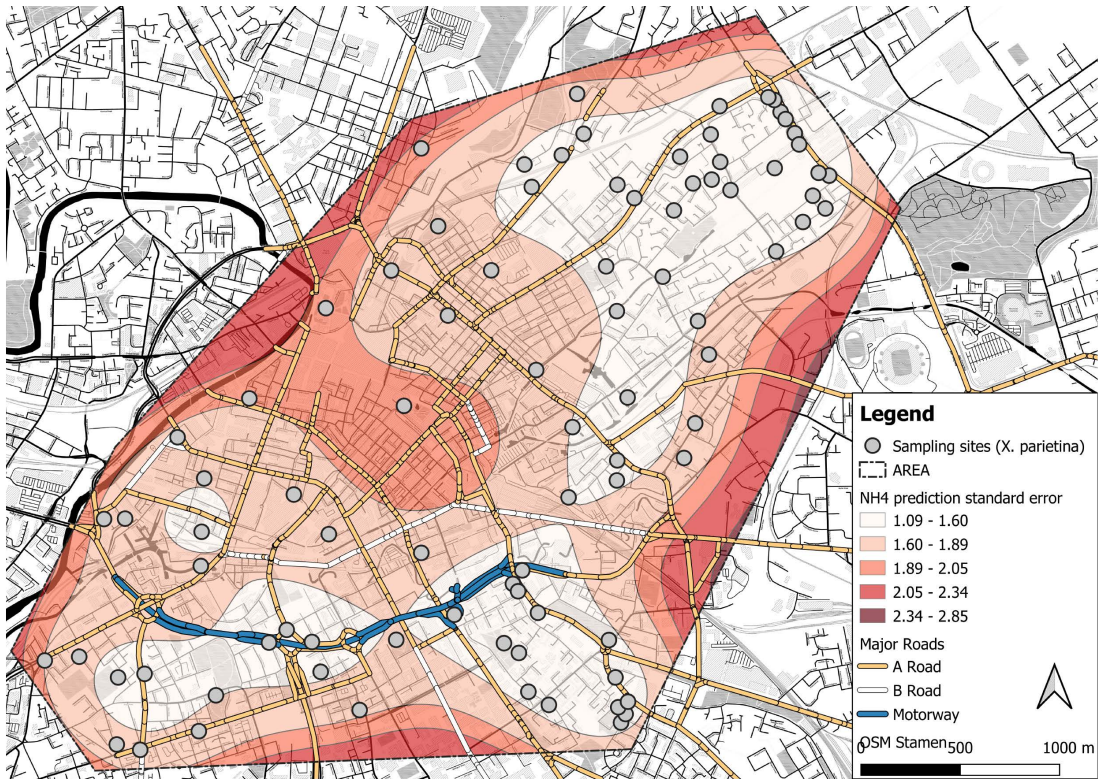
51	MIP038	386167	399073	Xp	45.847	3.986
52	CC007	383902	398788	Xp	12.874	11.685
53	BFD002	385829	398555	Xp	46.767	12.857
54	BFD007	385366	397922	Xp	24.857	7.691
55	HUL020	382990	396950	Xp	64.356	15.690
56	ARD006 III	385387	396705	Xp	96.652	10.488
57	MIP016	384938	399397	Xp	66.301	10.185
58	ARD008	384921	396860	Xp	100.039	8.043
59	HUL008	383705	397171	Xp	27.397	9.352
60	MIP024	386302	399221	Xp	45.178	7.987
61	HUL026	382857	396932	Xp	25.590	6.587
62	ANC002	385366	398773	Xp	33.061	12.374
63	HUL024	382661	397036	Xp	43.517	9.350
64	MIP005	385843	399434	Xp	37.943	4.433
65	MIP022	386381	399468	Xp	57.846	5.773
66	ARD006 II	385410	396748	Xp	97.718	17.565
67	ARD004	385326	397120	Xp	46.710	12.923
68	ARD006 I	385373	396782	Xp	47.442	18.980
69	MIP023	386415	399289	Xp	50.668	18.216
70	CC012 I	382786	397728	Xp	77.033	24.031
71	ARD002 I	384869	397365	Xp	88.586	23.349
72	MIP009 I	386215	399738	Xp	137.966	10.189
73	ARD013 I	384873	397055	Xp	34.494	16.559
74	MIP012	385838	399661	Xp	44.817	16.578
75	CC004	383917	397652	Xp	25.028	27.742
76	HUL004	383616	397107	Xp	50.505	17.652
77	ANC001 I	385143	398190	Xp	10.604	11.824
78	CC015	383290	397932	Xp	19.525	18.756
79	HUL023	382488	397017	Xp	19.519	22.979
80	MIP039	385774	398723	Xp	49.570	13.789
81	MIP018	385199	399664	Xp	59.540	18.499
82	ARD006	385422	396810	Xp	85.033	20.486
83	CC014	383156	398139	Xp	58.928	24.705
84	ANC003	384734	398978	Xp	62.946	14.866
85	CC017	383273	397492	Xp	52.091	9.311
86	CC006	383517	398334	Xp		9.873
87	CC021	384516	398751	Xp		7.265

Appendix C-3: Nitrate and ammonium concentrations (per site) recorded in *Physcia* spp. (N=48), using 3% KCl and 6h extraction time; red shaded field indicate no recorded nitrate and/or ammonium

ID	NAME	X	Y	lichen species	Nitrate (ppm)	Ammonium (ppm)
1	MIP038	386167	399073	Ph	43.562	2.911
2	MIP009 I	386215	399738	Ph	104.375	2.703
3	MIP024	386302	399221	Ph	33.646	3.081
4	MIP001	385312	398998	Ph	29.501	2.690
5	CC015	383290	397932	Ph	9.978	5.278
6	HUL005	383231	397017	Ph	19.464	4.881
7	ARD004	385326	397120	Ph	38.479	3.940
8	BFD007	385366	397922	Ph	4.428	15.486
9	MIP039	385774	398723	Ph	24.957	8.613
10	ANC001 I	385143	398190	Ph	5.599	9.002
11	ARD013 I	384873	397055	Ph	25.997	10.521
12	CC001	385123	397837	Ph	13.458	10.992
13	MIP007	386160	399492	Ph	33.231	7.746
14	MIP008 I	386283	399611	Ph	43.688	11.224
15	ARD013	384798	397104	Ph	22.387	7.456
16	MIP017	385369	399408	Ph	31.692	9.507
17	CC008	384382	397558	Ph	4.652	8.167
18	HUL016	383263	396662	Ph	29.127	5.590
19	CC017	383273	397492	Ph	66.233	5.160
20	MIP025	385597	398946	Ph	40.966	6.100
21	HUL024	382661	397036	Ph	14.381	6.925
22	CC004	383917	397652	Ph	4.994	7.116
23	MIP002	385653	399279	Ph	70.272	4.457
24	HUL027	384256	397121	Ph	3.407	9.273
25	MIP005	385843	399434	Ph	52.624	4.498
26	ARD001	384890	397470	Ph	97.875	5.300
27	CC012	382892	397730	Ph	42.630	5.448
28	ARD006 I	385373	396782	Ph	33.810	4.311
29	CC021	384516	398751	Ph	6.220	8.176
30	ARD012	384548	397247	Ph	56.675	5.991
31	CC009	384295	398297	Ph	0.796	10.679
32	ANC003	384734	398978	Ph	6.920	7.922
33	ARD008	384921	396860	Ph	95.476	5.043
34	MIP015	385454	399341	Ph	48.590	4.113
35	ARD005	385024	396794	Ph	22.913	4.066
36	MIP023	386415	399289	Ph	48.693	5.480
37	ARD006 II	385410	396748	Ph	67.442	5.615
38	ANC012	384960	398477	Ph	12.558	7.206
39	MIP014	385684	399549	Ph	169.790	6.175
40	ANC001 II	385180	398222	Ph	5.170	5.065
41	MIP012	385838	399661	Ph	27.609	6.602
42	BFD002	385829	398555	Ph	6.863	8.424
43	HUL014	383349	396842	Ph		7.298
44	CHE001	385166	399865	Ph	16.839	6.394
45	MIP003	385749	399415	Ph	19.304	5.420
46	CC006	383517	398334	Ph		6.710
47	HUL025	383832	397110	Ph	5.458	7.210
48	ARD006 III	385387	396705	Ph	17.036	8.205

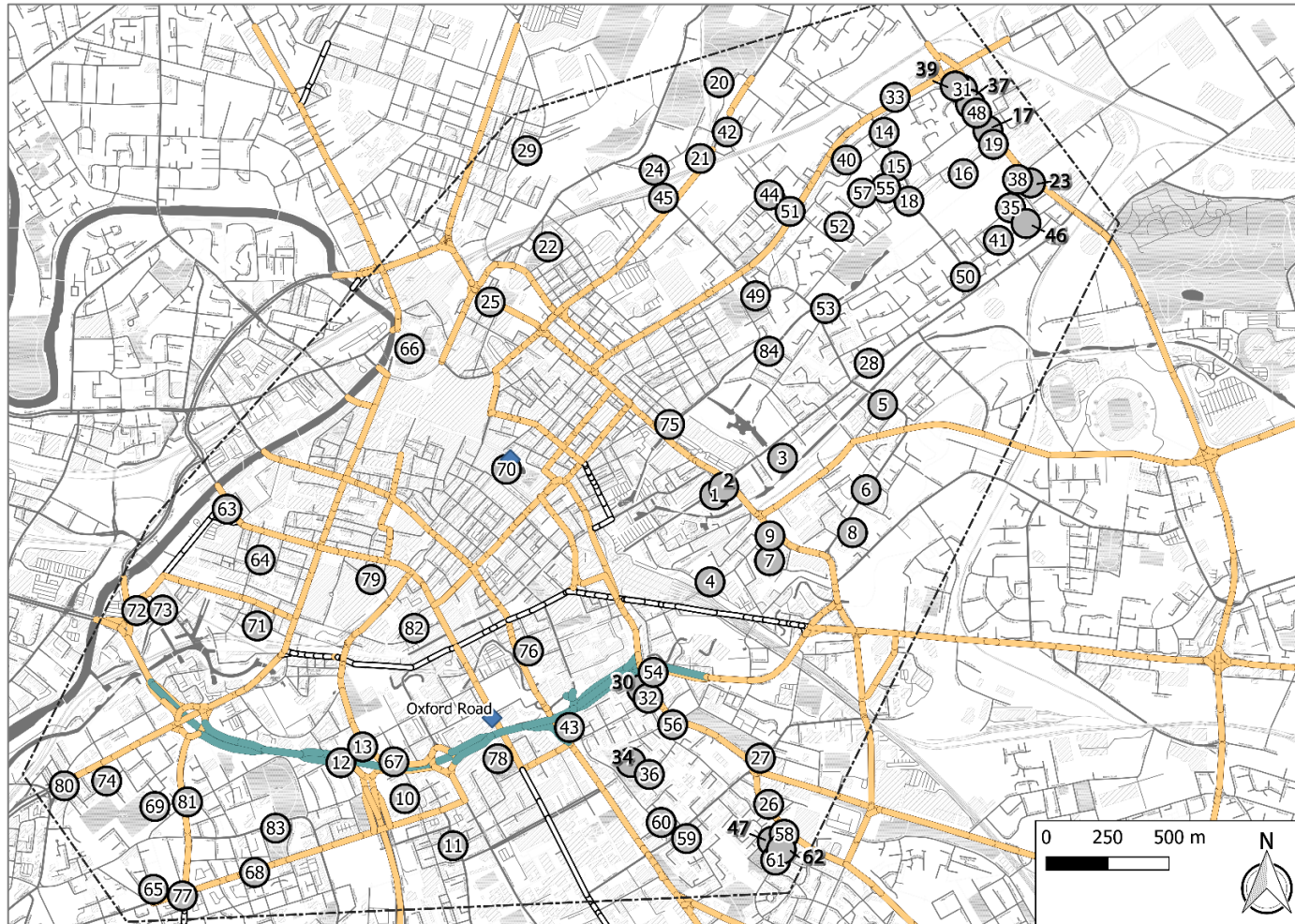
Appendix C-4: Ordinary kriging error maps, for *X. parietina* (upper panel) and *Physcia* spp. (lower panel) and nitrate and ammonium concentrations





Appendix D – Lichen metal concentrations (Chapter 6)

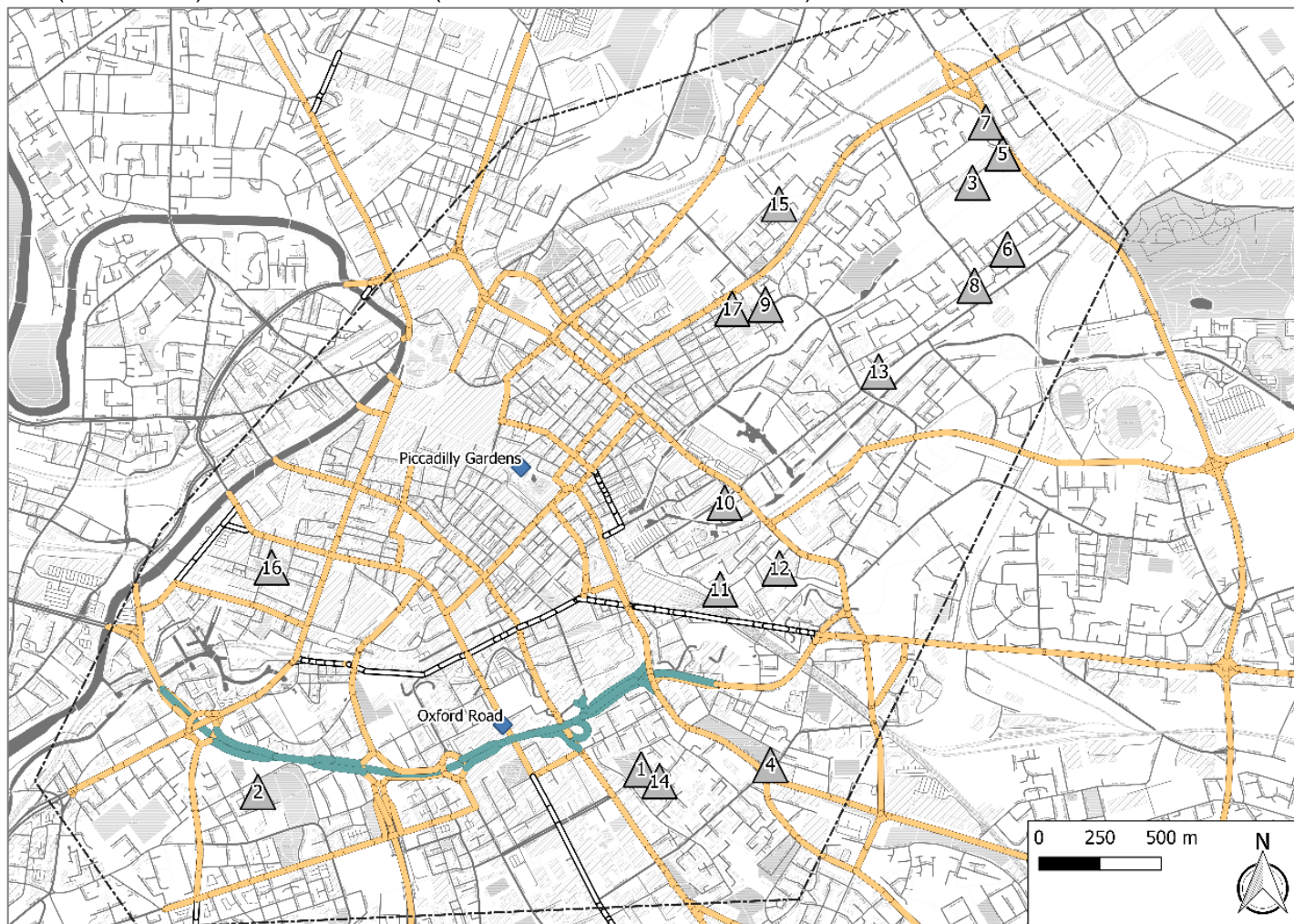
Appendix D-1: Sampling sites for *X. parietina* (grey circle, N=84) with site ID and automated air quality monitoring stations; and recorded metal concentrations [in $\mu\text{g/g}$] for sampled sites (Table below) with XY-coordinates (OSGB1936 – British national Grid)



ID	ID/name	X	Y	Al [µg/g]	Fe [µg/g]	Mn [µg/g]	Ni [µg/g]	Pb [µg/g]	S [µg/g]	Zn [µg/g]	Be [µg/g]	Ti [µg/g]	V [µg/g]	Cr [µg/g]	Co [µg/g]	Cu [µg/g]	As [µg/g]	Pd [µg/g]	Cd [µg/g]	Pt [µg/g]
1	ANC001 I	385143	398190	1075.289	2219.428	44.679	2.674	29.445	4025.545	112.330	0.038	21.718	2.548	6.420	0.816	36.887	0.779	0.026	0.159	0.004
2	ANC001 II	385180	398222	1176.697	3068.778	52.607	13.676	33.742	3333.063	176.346	0.051	30.507	3.348	8.838	1.181	47.932	1.063	0.033	0.141	0.008
3	BFD001	385420	398339	1229.776	2450.289	73.414	3.448	90.603	5266.034	90.056	0.047	29.956	3.795	5.699	0.988	25.828	1.277	0.030	0.395	0.003
4	CC001	385123	397837	957.554	3129.549	51.529	4.326	34.115	4640.417	130.052	0.036	24.346	3.177	8.142	0.898	43.086	1.007	0.029	0.265	0.003
5	BFD002	385829	398555	617.147	1155.403	26.688	1.568	17.729	5167.279	77.249	0.023	13.030	1.448	3.148	0.374	17.443	0.864	0.017	0.253	0.004
6	BFD004	385760	398209	1011.074	2362.708	36.610	2.423	24.161	5841.991	71.235	0.037	24.891	2.916	6.242	0.848	26.567	0.995	0.026	0.137	0.004
7	BFD007	385366	397922	852.287	1588.321	39.825	2.453	11.331	5176.176	64.603	0.029	23.092	2.381	3.550	0.693	18.645	0.719	0.020	0.129	0.003
8	BFD005	385704	398035	721.590	1584.137	35.774	1.836	14.136	5191.655	60.493	0.023	15.441	1.772	3.875	0.580	23.801	0.739	0.023	0.147	0.003
9	BFD008	385368	398023	980.021	2484.723	41.812	5.601	20.243	4496.115	108.101	0.034	25.439	2.660	7.388	0.758	33.400	0.812	0.029	0.136	0.006
10	HUL001	383876	396960	507.191	1021.483	24.124	2.343	7.647	4877.192	68.689	0.017	11.434	1.142	3.487	0.396	17.617	0.562	0.016	0.125	0.002
11	HUL002	384072	396768	580.521	1094.707	22.393	1.318	9.761	2953.593	53.007	0.019	14.000	1.358	2.724	0.418	16.184	0.478	0.022	0.075	0.003
12	HUL004	383616	397107	1059.927	2528.789	46.387	3.515	21.609	5290.958	179.342	0.042	25.350	2.834	6.840	0.926	36.720	0.962	0.032	0.133	0.003
13	HUL008	383705	397171	1055.026	2470.321	50.632	2.832	22.903	5304.323	199.734	0.045	20.166	2.754	6.670	0.849	37.635	1.249	0.036	0.147	0.005
14	MIP012	385838	399661	488.043	1024.020	35.362	1.265	9.649	4603.495	70.650	0.017	10.126	1.173	2.291	0.390	15.030	0.625	0.014	0.134	0.002
15	MIP013	385886	399523	543.475	1212.996	26.752	4.378	11.042	4376.093	61.138	0.024	13.778	1.476	3.717	0.464	26.237	0.713	0.022	0.159	0.008
16	MIP007	386160	399492	520.861	1024.710	27.788	1.505	11.601	4401.046	85.679	0.020	10.586	1.308	2.219	0.406	12.885	1.048	0.020	0.155	0.005
17	MIP008 II	386261	399667	466.427	946.319	19.632	0.620	7.108	3737.317	50.958	0.017	10.988	0.970	2.158	0.272	11.631	0.433	0.016	0.082	0.003
18	MIP006	385938	399381	545.026	1177.754	24.603	2.796	11.862	4411.717	51.531	0.020	13.929	1.437	3.562	0.433	16.220	0.761	0.021	0.108	0.003
19	MIP008 I	386283	399611	740.482	1676.328	30.811	4.298	16.944	3108.198	116.085	0.029	17.523	1.970	4.647	0.562	17.627	0.763	0.036	0.148	0.003
20	CHE001	385166	399865	360.849	843.166	19.221	1.061	6.138	4332.244	33.743	0.012	9.004	0.856	1.757	0.272	10.811	0.419	0.016	0.114	0.002
21	MIP016 I	385089	399557	436.638	1442.561	26.388	2.976	9.696	4126.409	69.904	0.021	10.557	1.525	4.666	0.414	14.872	0.612	0.017	0.115	0.004
22	ANC011	384467	399200	625.896	1428.445	31.415	1.968	13.652	3561.388	50.629	0.027	15.457	1.663	4.054	0.561	15.709	0.556	0.018	0.097	0.003
23	MIP021	386434	399454	711.279	1608.279	31.672	1.824	13.805	5231.950	77.568	0.028	15.033	1.856	3.407	0.574	22.390	0.839	0.021	0.139	0.004
24	CHE002	384901	399510	522.846	1179.066	26.339	5.799	9.900	4707.559	58.479	0.019	10.458	1.334	3.467	0.397	13.605	0.560	0.016	0.130	0.003
25	ANC009	384231	398977	1231.083	4349.374	60.959	6.103	43.138	5441.819	170.464	0.051	33.612	4.051	11.638	1.190	61.545	1.306	0.035	0.181	0.005
26	ARD007	385359	396932	1048.977	2073.049	42.508	3.465	19.004	5878.737	124.717	0.041	23.697	2.761	5.413	0.777	25.268	0.948	0.024	0.291	0.003
27	ARD004	385326	397120	593.682	1324.334	30.174	0.966	10.085	4087.529	68.411	0.019	11.675	1.327	3.318	0.342	17.333	0.524	0.017	0.112	0.004
28	MIP039	385774	398723	218.243	438.066	19.987	0.040	4.370	4115.462	40.953	< LLD	4.766	0.458	0.878	0.168	8.297	0.232	<LLD	0.125	0.004
29	CHE004	384382	399591	703.020	1498.206	29.047	1.462	16.776	4003.073	67.899	0.023	16.230	1.888	3.362	0.567	19.163	0.658	0.022	0.101	0.005
30	ARD002	384843	397402	763.788	1657.678	34.545	5.017	13.548	5037.582	97.518	0.030	17.382	1.857	4.930	0.565	22.583	0.746	0.027	0.131	0.005
31	MIP010 I	386158	399834	491.187	1292.143	37.233	1.954	15.427	3855.142	86.536	0.017	10.872	1.199	2.794	0.436	15.989	0.548	0.021	0.113	0.004
32	ARD002 I	384869	397365	675.991	1360.919	31.711	1.392	11.779	5847.840	72.806	0.028	13.806	1.590	3.440	0.472	21.177	0.645	0.022	0.147	0.005
33	MIP011	385883	399803	650.430	1695.435	31.919	1.542	19.628	4601.603	65.098	0.024	16.388	1.833	4.337	0.507	21.850	0.727	0.015	0.154	0.003
34	ARD013	384798	397104	1038.547	1704.231	30.857	1.891	15.293	4713.506	83.452	0.042	22.249	2.135	4.030	0.618	15.831	0.966	0.023	0.155	0.004
35	MIP020	386352	399353	547.188	1053.889	28.825	0.625	11.451	4870.745	40.493	0.029	7.242	1.189	1.555	0.398	12.816	0.977	0.016	0.130	0.006
36	ARD013 I	384873	397055	431.735	675.585	23.343	0.285	6.039	4474.628	44.222	< LLD	7.996	0.871	1.341	0.286	10.759	0.493	0.013	0.116	0.004
37	MIP009 II	386190	399774	566.216	1509.668	29.367	2.309	14.694	4514.156	80.963	0.026	13.240	1.501	4.609	0.522	22.242	0.663	0.019	0.154	0.003
38	MIP022	386381	399468	480.044	1046.482	23.151	0.864	8.784	4354.014	51.168	0.016	9.332	1.073	2.187	0.330	14.112	0.536	0.018	0.110	0.006
39	MIP010 II	386128	399848	457.931	1464.952	29.288	3.967	15.229	4253.958	95.334	0.014	9.120	0.966	1.964	0.266	9.304	0.419	0.014	0.099	0.002
40	MIP014	385684	399549	363.112	1010.805	29.653	1.659	7.012	3687.883	43.006	0.036	23.311	2.296	5.214	0.602	24.794	0.789	0.026	0.164	0.003

41	MIP024	386302	399221	579.872	1379.971	32.302	2.659	10.802	4255.048	47.906	0.026	14.044	1.453	3.775	0.433	22.058	0.592	0.020	0.118	0.003
42	MIP018	385199	399664	525.435	1375.541	36.571	1.910	9.372	4648.801	66.015	0.021	12.066	1.429	3.556	0.404	18.414	0.599	0.016	0.129	0.002
43	ARD012	384548	397247	856.661	2035.981	44.131	3.201	14.434	4799.271	98.051	0.027	14.245	1.544	2.736	0.458	13.281	0.828	0.018	0.112	0.002
44	MIP017	385369	399408	417.243	1154.248	29.091	1.941	8.876	3773.200	38.973	0.015	10.517	1.225	2.729	0.365	16.062	0.522	0.014	0.105	0.002
45	MIP016	384938	399397	506.990	1408.146	30.224	3.035	10.030	4762.762	48.888	0.020	13.647	1.543	3.548	0.438	18.499	0.535	0.017	0.137	0.002
46	MIP023	386415	399289	372.438	931.625	25.423	4.704	7.046	4492.622	52.855	0.015	8.801	1.130	1.770	0.273	10.547	0.592	0.014	0.104	0.002
47	ARD006 I	385373	396782	323.438	641.472	30.811	1.442	5.750	4015.628	43.704	0.013	6.511	0.774	1.522	0.251	10.160	0.382	0.014	0.131	0.003
48	MIP009 I	386215	399738	379.819	1099.443	23.896	1.834	10.346	3619.157	57.339	0.017	8.824	1.063	2.578	0.324	15.044	0.504	0.016	0.098	0.002
49	MIP001	385312	398998	536.163	1074.075	33.572	1.880	11.280	3289.630	58.037	0.021	13.285	2.058	2.787	0.436	13.055	1.557	0.021	0.179	0.002
50	MIP038	386167	399073	457.019	930.847	27.776	1.970	8.217	3680.824	39.265	0.013	12.732	1.193	2.649	0.337	13.454	0.449	0.015	0.109	0.002
51	MIP015	385454	399341	433.713	1017.438	22.396	1.918	7.214	3444.388	46.287	0.018	13.331	1.203	2.635	0.350	13.604	0.471	0.017	0.109	0.003
52	MIP002	385653	399279	260.872	602.949	23.138	3.784	4.368	3544.676	34.940	0.011	6.225	0.685	1.357	0.197	8.755	0.333	0.011	0.079	0.002
53	MIP025	385597	398946	649.155	1468.338	31.189	2.289	14.269	3560.742	51.058	0.014	11.413	1.071	2.307	0.318	12.128	0.478	0.013	0.125	0.002
54	ARD001	384890	397470	577.775	1455.593	30.134	2.692	11.205	4368.790	80.531	0.030	14.726	1.674	3.114	0.524	16.228	0.997	0.019	0.134	0.002
55	MIP005	385843	399434	347.714	765.125	19.474	1.577	6.634	3058.195	52.901	0.014	9.008	0.888	1.810	0.280	10.929	0.488	0.014	0.092	0.002
56	ARD003	384969	397257	407.986	991.592	25.931	2.113	8.394	4107.574	64.854	0.011	5.674	0.707	1.540	0.200	10.051	0.317	0.012	0.104	0.003
57	MIP003	385749	399415	302.812	654.765	18.928	2.457	5.439	4155.975	37.289	0.011	6.584	0.756	1.930	0.225	10.484	0.470	0.010	0.132	0.002
58	ARD006	385422	396810	272.218	635.830	20.235	1.119	5.263	4220.133	40.215	0.013	6.389	0.793	1.945	0.241	11.778	0.698	0.016	0.119	0.002
59	ARD005	385024	396794	479.067	916.828	24.622	2.179	6.513	4094.925	46.808	0.028	11.620	1.249	2.439	0.406	12.357	0.567	0.017	0.117	0.002
60	ARD008	384921	396860	306.226	654.644	24.540	1.337	5.746	3803.826	42.802	0.014	6.461	0.752	1.693	0.227	10.140	0.391	0.015	0.100	0.002
61	ARD006 III	385387	396705	471.866	969.979	25.134	2.130	8.394	4829.923	51.403	0.019	11.776	1.421	3.630	0.507	20.747	0.758	0.027	0.191	0.003
62	ARD006 II	385410	396748	341.205	666.164	21.274	1.657	7.787	4290.199	34.847	0.018	6.633	0.846	1.580	0.291	10.784	0.430	0.013	0.122	0.002
63	CC014	383156	398139	520.447	1244.457	35.939	2.191	10.453	4816.054	97.970	0.020	13.420	1.285	3.856	0.374	18.954	0.547	0.017	0.124	0.001
64	CC015	383290	397932	370.340	857.170	32.354	1.993	9.223	4444.113	72.486	0.015	8.854	0.920	2.570	0.261	13.344	0.400	0.015	0.313	0.001
65	HUL021	382850	396595	226.091	451.640	12.568	1.192	4.731	3081.222	47.621	0.010	5.645	0.547	1.722	0.164	8.002	0.305	0.011	0.083	0.001
66	CC007	383902	398788	499.555	1072.103	29.219	1.761	13.476	4732.079	51.238	0.018	13.828	1.216	3.043	0.350	14.594	0.514	0.017	0.120	0.001
67	HUL025	383832	397110	985.992	2018.807	45.942	3.467	16.129	4679.974	105.744	0.050	18.648	2.446	6.257	0.604	24.916	1.162	0.024	0.157	0.001
68	HUL016	383263	396662	336.881	747.682	16.293	1.540	5.298	3239.805	42.214	0.012	7.884	0.848	2.420	0.238	10.967	0.313	0.015	0.058	0.002
69	HUL026	382857	396932	275.813	528.146	19.471	1.039	4.985	3494.372	31.562	0.011	6.577	0.637	1.878	0.194	9.176	0.342	0.012	0.119	0.002
70	CC009	384295	398297	562.546	2454.001	69.386	4.249	24.033	4288.827	85.887	0.024	13.450	1.567	7.623	0.540	24.695	0.826	0.022	0.157	0.002
71	CC018	383277	397664	674.294	1414.039	36.058	2.577	13.916	5252.039	74.631	0.031	16.492	1.792	4.316	0.464	19.282	0.771	0.022	0.189	0.001
72	CC012 I	382786	397728	642.079	1562.071	33.272	2.392	12.757	5212.277	87.482	0.024	16.133	1.667	4.370	0.414	24.243	0.733	0.018	0.094	0.002
73	CC012	382892	397730	587.566	1187.301	26.007	1.807	12.399	3477.683	63.632	0.028	15.318	1.332	2.918	0.366	14.690	0.633	0.017	0.117	0.002
74	HUL024	382661	397036	400.013	822.818	23.300	2.128	8.700	4841.249	45.419	0.017	8.624	1.020	2.468	0.347	14.126	0.505	0.022	0.143	0.002
75	ANC012	384960	398477	508.378	1155.019	24.483	1.949	9.992	4386.346	49.644	0.021	12.936	1.283	3.359	0.339	14.787	0.598	0.017	0.068	0.002
76	CC008	384382	397558	688.082	1510.994	34.782	2.697	13.582	4934.119	114.842	0.028	15.637	1.685	4.698	0.479	17.863	1.230	0.023	0.231	0.001
77	HUL021 I	382968	396568	747.822	2114.585	43.526	3.234	13.911	4679.283	100.700	0.025	17.296	2.098	6.532	0.606	32.790	0.787	0.028	0.124	0.002
78	HUL027	384256	397121	480.614	907.110	23.812	1.655	7.816	4641.733	50.940	0.020	10.010	1.078	2.760	0.337	14.041	0.534	0.016	0.100	0.003
79	CC016	383741	397851	700.964	1692.044	52.064	3.020	18.211	5674.236	90.610	0.028	19.607	1.931	4.439	0.813	25.237	0.894	0.025	0.084	0.003
80	HUL023	382488	397017	560.740	1563.610	29.189	3.222	20.896	4702.426	93.370	0.022	11.923	1.541	4.701	0.464	36.220	0.706	0.022	0.151	0.002
81	HUL020	382990	396950	484.346	1149.317	28.396	1.859	7.168	5115.195	52.387	0.019	11.282	1.136	3.463	0.394	17.577	0.556	0.020	0.156	0.004
82	CC004	383917	397652	741.504	2015.524	35.027	3.614	19.382	4956.982	90.040	0.025	18.346	2.219	5.653	0.621	28.363	0.720	0.022	0.122	0.002
83	HUL014	383349	396842	394.997	736.976	22.925	1.798	6.320	3975.203	38.882	0.016	8.309	0.868	2.377	0.305	11.487	0.566	0.018	0.107	0.005
84	ANC002	385366	398773	470.044	846.219	23.045	2.375	7.179	5339.568	38.260	0.019	10.803	1.116	2.397	0.334	15.084	0.551	0.020	0.095	0.004

Appendix D-2: Sampling sites for *Physcia* spp. (grey triangle, N=17) with site ID and automated air quality monitoring stations; and recorded metal concentrations [in $\mu\text{g/g}$] for sampled sites (Table below) with XY-coordinates (OSGB1936 – British national Grid)



ID	ID/name	X	Y	Al [µg/g]	Fe [µg/g]	Mn [µg/g]	Ni [µg/g]	Pb [µg/g]	S [µg/g]	Zn [µg/g]	Be [µg/g]	Ti [µg/g]	V [µg/g]	Cr [µg/g]	Co [µg/g]	Cu [µg/g]	As [µg/g]	Pd [µg/g]	Cd [µg/g]	Pt [µg/g]
1	ARD013	384798	397104	693.868	1116.986	25.053	1.248	10.002	2628.580	93.760	0.026	13.778	1.837	2.542	0.403	14.338	1.416	0.028	0.215	0.007
2	HUL005	383231	397017	243.213	422.206	19.995	0.240	4.963	2573.366	73.503	0.010	5.021	0.647	0.998	0.205	8.452	0.494	0.020	0.117	0.006
3	MIP007	386160	399492	427.442	869.664	25.984	1.279	8.787	3234.582	108.176	0.016	8.849	1.187	1.860	0.378	13.020	1.343	0.017	0.218	0.002
4	ARD004	385326	397120	442.320	998.730	23.210	0.798	6.158	2872.988	83.409	0.014	9.878	1.096	2.534	0.262	14.420	0.891	0.019	0.114	0.003
5	MIP008 I	386283	399611	572.419	1229.521	29.634	1.521	11.971	2676.345	114.412	0.022	13.357	1.605	2.795	0.435	14.973	1.098	0.020	0.309	0.004
6	MIP024	386302	399221	469.298	1225.323	29.060	2.904	8.753	2750.755	72.885	0.017	9.049	1.063	2.415	0.315	14.053	0.506	0.016	0.164	0.002
7	MIP009 I	386215	399738	264.426	820.246	19.102	3.242	6.655	2097.063	73.363	0.018	8.293	2.667	1.213	0.225	6.207	0.701	0.022	0.482	0.002
8	MIP038	386167	399073	316.633	675.814	22.858	1.344	5.541	2082.493	59.948	0.011	7.445	0.871	1.700	0.270	9.435	0.729	0.013	0.145	0.001
9	MIP001	385312	398998	410.208	824.029	27.328	1.700	8.739	2008.259	81.863	0.017	7.830	1.002	1.937	0.305	10.745	0.857	0.015	0.147	0.002
10	ANC001 I	385143	398190	967.442	2092.540	48.040	3.287	29.426	2830.062	123.911	0.036	21.369	2.619	6.559	0.787	38.082	1.129	0.030	0.186	0.002
11	CC001	385123	397837	748.636	2410.563	46.009	3.214	26.448	3429.384	125.362	0.028	18.672	2.749	6.083	0.747	37.006	1.206	0.031	0.261	0.003
12	BFD007	385366	397922	812.440	1691.596	44.818	3.270	11.122	3432.949	87.912	0.027	22.684	2.530	3.957	0.728	19.432	1.195	0.045	0.189	0.002
13	MIP039	385774	398723	249.839	521.687	24.371	0.873	4.792	2325.144	62.664	0.010	5.663	0.662	1.650	0.187	9.337	0.611	0.020	0.196	0.002
14	ARD013 I	384873	397055	356.086	618.182	22.372	1.155	5.082	2821.005	70.818	0.013	8.091	0.988	1.937	0.242	10.393	0.883	0.019	0.128	0.002
15	MIP017	385369	399408	328.952	881.466	25.696	1.557	6.695	2676.064	93.447	0.012	8.859	1.035	2.542	0.293	13.541	0.866	0.016	0.157	0.002
16	CC015	383290	397932	277.370	585.635	28.712	1.282	6.535	2361.268	108.108	0.011	7.420	0.905	1.990	0.201	11.093	0.638	0.010	0.191	0.001
17	ANC007	385176	398981	325.596	683.024	31.825	1.283	10.141	2848.753	65.585	0.011	8.015	0.785	2.234	0.263	11.661	0.642	0.022	0.340	0.004

Appendix D-3: Rural lichen samples (N=12, *X. parietina*) and analysed CNS contents (in wt%), stable-isotope ratio signatures ($\delta^{13}\text{C}$, $\delta^{15}\text{N}$ and $\delta^{34}\text{S}$, in ‰), nitrate and ammonium concentrations (in mg/kg) and analysed metal concentrations (in µg/g)

ID	Sample ID	lichen species	Dist_to_Farm	C (wt%)	N (wt%)	S (wt%)	d15N	d13C	d34S	Nitrate	Ammonium	Al [µg/g]	Fe [µg/g]	Mn [µg/g]	Ni [µg/g]	Pb [µg/g]	S [µg/g]	Zn [µg/g]	Be [µg/g]	Ti [µg/g]	V [µg/g]	Cr [µg/g]	Co [µg/g]	Cu [µg/g]	As [µg/g]	Pd [µg/g]	Cd [µg/g]	Pt [µg/g]
1	PF001	Xp	150	43.3	3.439	0.353	-6.36	-23.42	9.44	15.599	9.181	175.352	212.156	44.959	0.371	0.666	2856.240	32.073	0.007	3.941	0.430	<LLD	0.083	3.881	0.233	0.017	0.050	0.003
2	PF002	Xp	310	42.8	3.342	0.332	-8.09	-23.04	10.88	5.807	9.457	267.457	265.349	28.680	0.875	1.187	2800.353	35.544	0.010	5.537	0.586	0.646	0.100	4.483	0.302	0.011	0.056	0.001
3	PF003	Xp	15	42.04	4.22	0.420	4.44	-23.09	8.42	34.836	12.175	263.877	368.565	35.110	0.750	1.588	3942.135	121.341	0.012	2.892	0.799	0.771	0.164	6.793	0.388	0.020	0.077	0.003
4	PF004	Xp	135	41.45	3.808	0.521	0.03	-22.75	9.96	45.958	13.060	334.963	424.749	34.091	0.899	2.184	4730.076	44.542	0.011	7.478	0.923	0.864	0.174	7.597	0.486	0.019	0.086	0.003
5	PF005	Xp	175	41.39	3.949	0.515	-2.69	-22.00	12.75	11.616	13.365	341.419	375.426	34.463	0.781	1.737	4555.892	49.587	0.011	6.103	0.806	0.707	0.150	6.350	0.434	0.015	0.070	0.003
6	PF006	Xp	70	42.22	3.872	0.453	-1.05	-22.32	10.99	38.459	11.377	370.223	439.227	30.849	0.673	2.110	4363.493	44.842	0.013	6.602	0.957	0.916	0.178	6.728	0.441	0.019	0.085	0.002
7	PF007	Xp	555	42.76	3.51	0.427	-6.59	-22.81	13.40	24.928	10.241	343.047	376.048	36.910	0.548	1.620	4034.837	24.943	0.011	6.052	0.673	0.700	0.142	4.943	0.503	0.019	0.078	0.003
8	PF008	Xp	1690	42.68	3.206	0.403	-7.61	-22.26	14.19	3.851	9.824	280.859	348.768	22.232	0.617	5.496	3900.652	29.421	0.010	9.424	0.785	1.051	0.142	8.931	1.757	0.014	0.101	0.003
9	PF009	Xp	2775	41.97	3.392	0.235	-2.67	-22.43	11.01	9.992	11.546	535.111	595.794	23.060	1.142	1.508	2152.103	36.571	0.017	11.203	1.020	0.887	0.245	5.050	0.411	0.017	0.058	0.002
10	PF010	Xp	3005	42.23	3.416	0.400	-5.95	-22.09	14.13	1.068	8.538	272.523	330.677	52.064	0.523	1.364	3980.835	26.192	0.010	5.381	0.586	0.501	0.134	4.722	0.357	0.016	0.110	0.002
11	PF011	Xp	1040	43.04	3.086	0.342	-10.09	-22.46	12.73		8.989	315.381	325.262	29.802	0.477	1.286	3518.414	24.935	0.009	7.654	0.718	0.678	0.130	4.751	0.285	0.012	0.082	0.001
12	PF012	Xp	390	42.67	3.396	0.462	-6.67	-22.56	13.50	11.382	9.406	353.951	377.033	31.818	0.605	1.458	4357.843	31.230	0.011	8.044	0.851	0.739	0.147	5.316	0.390	0.011	0.046	0.001

Appendix D-4: Decision matrix used for analysed metals in lichen samples, with potential interferences and decision which analytical instrument ICP-OES or ICP-MS concentrations were reported

Element	Interferences	Decision
Al	<u>ICP-OES:</u> U, Ce (394.4nm) <u>ICP-MS:</u> $^{12}\text{C}^{15}\text{N}^+$, $^{13}\text{C}^{14}\text{N}^+$, $^{1}\text{H}^{12}\text{C}^{14}\text{N}^+$, $^{11}\text{B}^{16}\text{O}^+$, $^{54}\text{Cr}^{2+}$, $^{54}\text{Fe}^{2+}$	ICP-OES (167.0nm)
As	<u>ICP-OES:</u> Cr (189.0nm); V, Ge (193.7nm) <u>ICP-MS:</u> $^{40}\text{Ar}^{35}\text{Cl}^+$, $^{59}\text{Co}^{16}\text{O}^+$, $^{36}\text{Ar}^{38}\text{Ar}^1\text{H}^+$, $^{38}\text{Ar}^{37}\text{Cl}^+$, $^{36}\text{Ar}^{39}\text{K}^+$, $^{150}\text{Nd}^{2+}$, $^{150}\text{Sm}^{2+}$, $^{43}\text{Ca}^{16}\text{O}_2$, $^{23}\text{Na}^{12}\text{C}^{40}\text{Ar}$, $^{12}\text{C}^{31}\text{PO}_2^+$	ICP-MS (with He)
Be		ICP-MS (without He)
Cd	<u>ICP-OES:</u> Pt, Ir (214.4nm); Co, Ir, As, Pt (228.8nm) <u>ICP-MS:</u> $^{95}\text{Mo}^{16}\text{O}^+$, $^{39}\text{K}^{216}\text{O}^+$	ICP-MS (with He)
Co	<u>ICP-OES:</u> W, Re, Al, Ta (237.8nm) <u>ICP-MS:</u> $^{42}\text{Ca}^{16}\text{O}^1\text{H}^+$, $^{40}\text{Ar}^{18}\text{O}^1\text{H}^+$, $^{36}\text{Ar}^{23}\text{Na}^+$, $^{43}\text{Ca}^{16}\text{O}^+$, $^{24}\text{Mg}^{35}\text{Cl}^+$, $^{40}\text{Ar}^{19}\text{F}^+$	ICP-MS (with He)
Cr	<u>ICP-MS:</u> $^{35}\text{Cl}^{16}\text{O}^1\text{H}^+$, $^{40}\text{Ar}^{12}\text{C}^+$, $^{36}\text{Ar}^{16}\text{O}^+$, $^{37}\text{Cl}^{15}\text{N}^+$, $^{34}\text{S}^{18}\text{O}^+$, $^{36}\text{S}^{16}\text{O}^+$, $^{38}\text{Ar}^{14}\text{N}^+$, $^{36}\text{Ar}^{15}\text{N}^1\text{H}^+$, $^{35}\text{Cl}^{17}\text{O}^+$	ICP-MS (with He)
Cu	<u>ICP-OES:</u> Pb, Ir, Ni, W (224.7nm); Nb, U, Th, Mo, Hf (324.7nm) <u>ICP-MS:</u> $^{40}\text{Ar}^{23}\text{Na}^+$, $^{47}\text{Ti}^{16}\text{O}^+$, $^{14}\text{N}^{12}\text{C}^{37}\text{Cl}^+$, $^{16}\text{O}^{12}\text{C}^{35}\text{Cl}^+$, $^{44}\text{Ca}^{18}\text{O}^1\text{H}^+$, $^{23}\text{Na}^{40}\text{Ca}^+$, $^{31}\text{P}^{16}\text{O}_2^+$, $^{46}\text{Ca}^{16}\text{O}^1\text{H}^+$, $^{36}\text{Ar}^{12}\text{C}^{14}\text{N}^1\text{H}^+$, $^{16}\text{O}^{12}\text{C}^{35}\text{Cl}^+$	ICP-MS (with He)
Fe	<u>ICP-OES:</u> Hf, Nb (259.9nm) <u>ICP-MS:</u> $^{40}\text{Ar}^{16}\text{O}^1\text{H}^+$, $^{40}\text{Ca}^{16}\text{O}^1\text{H}^+$, $^{40}\text{Ar}^{17}\text{O}^+$, $^{38}\text{Ar}^{18}\text{O}^1\text{H}^+$, $^{38}\text{Ar}^{19}\text{F}^+$	ICP-OES (259.9nm)
Mn	<u>ICP-MS:</u> $^{40}\text{Ar}^{14}\text{N}^1\text{H}^+$, $^{39}\text{K}^{16}\text{O}^+$, $^{37}\text{Cl}^{18}\text{O}^+$, $^{40}\text{Ar}^{15}\text{N}^+$, $^{38}\text{Ar}^{17}\text{O}^+$, $^{36}\text{Ar}^{18}\text{O}^1\text{H}^+$, $^{38}\text{Ar}^{16}\text{O}^1\text{H}^+$, $^{37}\text{Cl}^{17}\text{O}^1\text{H}^+$, $^{23}\text{Na}^{32}\text{S}^+$, $^{36}\text{Ar}^{19}\text{F}^+$	ICP-OES (257.0nm)
Ni	<u>ICP-OES:</u> Sb, Ta, Co (231.6nm) <u>ICP-MS:</u> $^{43}\text{Ca}^{16}\text{O}^1\text{H}^+$, $^{44}\text{Ca}^{16}\text{O}^+$, $^{23}\text{Na}^{37}\text{Cl}^+$	ICP-OES (231.6nm)
Pb	<u>ICP-OES:</u> Bi, Nb (220.3nm) <u>ICP-MS:</u> $^{192}\text{Pt}^{16}\text{O}^+$, $^{192}\text{Os}^{16}\text{O}^+$	ICP-OES (220.3nm)
Pd	<u>ICP-MS:</u> $^{40}\text{Ar}^{65}\text{Cu}$, $^{89}\text{Y}^{16}\text{O}$	ICP-MS (without He)
Pt	<u>ICP-MS:</u> $^{179}\text{Hf}^{16}\text{O}$	ICP-MS (without He)
S	<u>ICP-MS:</u> $^{32}\text{S} - ^{16}\text{O}_2^+$, $^{14}\text{N}^{18}\text{O}^+$, $^{15}\text{N}^{17}\text{O}^+$, $^{14}\text{N}^{17}\text{O}^1\text{H}^+$, $^{15}\text{N}^{16}\text{O}^1\text{H}^+$, $^{34}\text{S} - ^{15}\text{N}^{18}\text{O}^+$, $^{14}\text{N}^{18}\text{O}^1\text{H}^+$, $^{15}\text{N}^{17}\text{O}^1\text{H}^+$, $^{16}\text{O}^{17}\text{O}^+$, $^{16}\text{O}^{21}\text{H}^+$, $^{33}\text{S}^+$, $^{32}\text{S}^1\text{H}^+$	ICP-OES (182.0nm)
Ti	<u>ICP-MS:</u> $^{32}\text{S}^{14}\text{N}^1\text{H}^+$, $^{30}\text{Si}^{16}\text{O}^1\text{H}^+$, $^{32}\text{S}^{15}\text{N}^+$, $^{33}\text{N}^{14}\text{N}^+$, $^{33}\text{S}^{14}\text{N}^+$, $^{15}\text{N}^{16}\text{O}_2^+$, $^{14}\text{N}^{16}\text{O}_2^1\text{H}^+$, $^{12}\text{C}^{35}\text{Cl}^+$, $^{31}\text{P}^{16}\text{O}^+$	ICP-MS (with He)
V	<u>ICP-MS:</u> $^{34}\text{S}^{16}\text{O}^1\text{H}^+$, $^{35}\text{Cl}^{16}\text{O}^+$, $^{38}\text{Ar}^{-13}\text{C}^+$, $^{36}\text{Ar}^{15}\text{N}^+$, $^{36}\text{Ar}^{14}\text{N}^1\text{H}^+$, $^{37}\text{Cl}^{14}\text{N}^+$, $^{36}\text{S}^{15}\text{N}^+$, $^{33}\text{S}^{18}\text{O}^+$, $^{34}\text{S}^{17}\text{O}^+$, $^{102}\text{Ru}^{+2}$, $^{102}\text{Pd}^{+2}$	ICP-MS (with He)

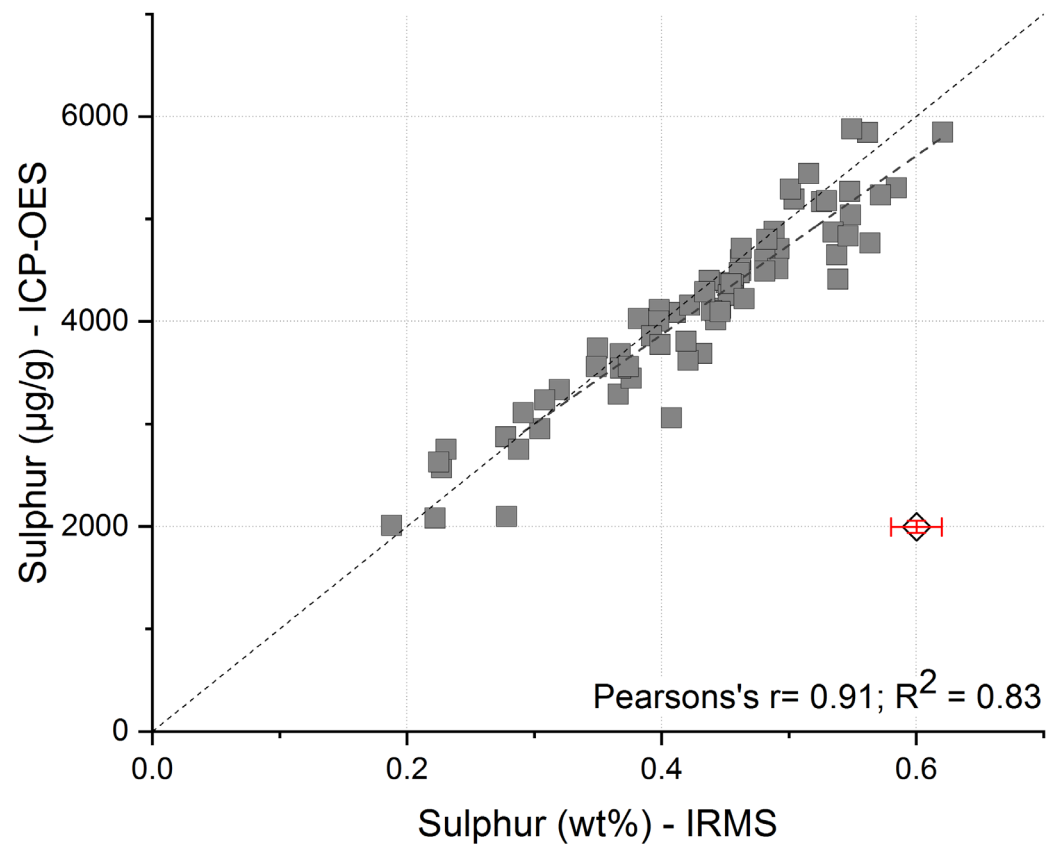
Appendix D-5: Descriptive statistics (min – max range, $\bar{x} \pm 1x$ SD and \tilde{x}) for comparison of metal concentrations [$\mu\text{g/g}$] recorded in *X. parietina* (N=17) for sampling periods (2016/17 and 2018). Metal concentrations for both years are shown for the sampled sites in 2016/17 that have been re-sampled in 2018

Element	2016-2017			2018		
	Min - Max	$\bar{x} \pm 1x$ SD	\tilde{x}	Min - Max	$\bar{x} \pm 1x$ SD	\tilde{x}
Aluminium (Al)	272.22 – 1231.08	682.96 \pm 273.69	625.90	430.24 – 2620.44	954.92 \pm 554.33	789.03
Arsenic (As)	0.32 – 1.56	0.75 \pm 0.31	0.74	0.36 – 1.26	0.76 \pm 0.26	0.67
Beryllium (Be)	0.01 – 0.05	0.03 \pm 0.01	0.03	0.02 – 0.09	0.04 \pm 0.02	0.03
Cadmium (Cd)	0.07 – 0.19	0.13 \pm 0.03	0.12	0.09 – 0.24	0.14 \pm 0.05	0.13
Cobalt (Co)	0.20 – 1.19	0.51 \pm 0.25	0.46	0.34 – 1.14	0.59 \pm 0.24	0.47
Chromium (Cr)	1.54 – 11.64	4.06 \pm 2.46	3.41	2.37 – 10.88	5.11 \pm 2.45	3.99
Copper (Cu)	10.05 – 61.55	21.02 \pm 12.85	15.99	11.31 – 46.68	21.26 \pm 9.60	17.52
Iron (Fe)	635.83 – 4349.37	1608.01 \pm 861.57	1414.04	858.95 – 3628.14	1840 \pm 836.80	1445.30
Manganese (Mn)	20.04 – 60.96	34.46 \pm 9.66	32.30	24.61 – 65.62	40.13 \pm 13.13	34.13
Nickel (Ni)	0.97 – 6.10	2.45 \pm 1.40	1.95	1.25 – 6.71	2.77 \pm 1.41	2.25
Lead (Pb)	5.26 – 43.14	15.00 \pm 9.15	13.80	5.54 – 27.19	12.23 \pm 7.26	9.09
Palladium (Pd)	0.01 – 0.04	0.02 \pm 0.006	0.02	0.02 – 0.05	0.03 \pm 0.007	0.03
Platinum (Pt)	0.001 – 0.006	0.003 \pm 0.001	0.003	0.002 – 0.007	0.004 \pm 0.001	0.003
Sulphur (S)	3289.63 – 5441.82	4395.21 \pm 630.58	4255.05	3134.94 – 5528.69	4275.99 \pm 706.14	4471.01
Titanium (Ti)	5.67 – 33.61	15.35 \pm 7.18	14.25	12.00 – 55.32	23.77 \pm 11.38	20.23
Vanadium (V)	0.71 – 4.05	1.74 \pm 0.82	1.66	1.12 – 4.30	2.25 \pm 0.97	1.75

Appendix D-6: Site-specific metal concentrations recorded in *X. parietina* (N=15) during for sampling undertaken in 2016/17 [upper table] and same sites re-visited in 2018 [lower table]

Sample ID	Al	Fe	Mn	Ni	Pb	S	Zn	Be	Ti	V	Cr	Co	Cu	As	Pd	Cd	Pt
ANC001 I	1075.289	2219.428	44.67866	2.67369	29.44523	4025.545	112.33	0.03844	21.71761	2.54767	6.41964	0.81603	36.8872	0.77932	0.02615	0.15862	0.0038
ANC009	1231.083	4349.374	60.95866	6.1028	43.13843	5441.819	170.4636	0.05088	33.61185	4.05095	11.63783	1.1903	61.54524	1.30593	0.03526	0.18082	0.00536
ANC011	625.8957	1428.445	31.41521	1.96793	13.65188	3561.388	50.62911	0.02657	15.45726	1.66306	4.05401	0.56071	15.70896	0.55597	0.01812	0.0974	0.00348
ANC012	508.3778	1155.019	24.48279	1.94919	9.9917	4386.346	49.64423	0.02148	12.9356	1.28309	3.35861	0.3393	14.78725	0.59841	0.01653	0.06767	0.00191
ARD003	407.9862	991.5922	25.93071	2.11325	8.39396	4107.574	64.85385	0.0112	5.67436	0.7071	1.54029	0.19954	10.05069	0.31673	0.0121	0.10428	0.00252
ARD004	593.6821	1324.334	30.17368	0.96572	10.08493	4087.529	68.41148	0.01887	11.6747	1.32735	3.3177	0.34153	17.3332	0.52405	0.01745	0.11225	0.00405
ARD006	272.2184	635.8295	20.23528	1.1186	5.26288	4220.133	40.21494	0.01333	6.38924	0.79348	1.94466	0.24056	11.77797	0.69805	0.016	0.11872	0.00207
ARD008	306.2257	654.6444	24.54014	1.3367	5.74567	3803.826	42.80234	0.01359	6.46079	0.75179	1.69251	0.22727	10.14007	0.3908	0.01548	0.10044	0.00178
ARD012	856.6613	2035.981	44.13115	3.20072	14.4337	4799.271	98.05061	0.02658	14.24464	1.54421	2.73603	0.45774	13.28144	0.82786	0.01824	0.11205	0.00195
ARD013	1038.547	1704.231	30.85673	1.89122	15.29287	4713.506	83.45175	0.04197	22.24943	2.13502	4.03036	0.61764	15.83059	0.96557	0.02309	0.15497	0.0036
BFD005	721.5895	1584.137	35.77418	1.8364	14.13628	5191.655	60.49273	0.02349	15.44142	1.77223	3.87514	0.57974	23.80071	0.73911	0.02258	0.14678	0.00312
BFD008	980.0208	2484.723	41.81167	5.6007	20.24282	4496.115	108.1007	0.03406	25.43868	2.66041	7.38849	0.75819	33.39959	0.8116	0.02941	0.13579	0.00568
CC018	674.294	1414.039	36.05759	2.57729	13.9163	5252.039	74.63057	0.03132	16.49153	1.79173	4.31644	0.46448	19.28173	0.77122	0.02163	0.18878	0.00126
MIP001	536.1629	1074.075	33.5718	1.88009	11.27997	3289.63	58.03709	0.02062	13.28519	2.05781	2.78738	0.43626	13.05531	1.55693	0.02093	0.17935	0.00197
MIP010 I	491.1869	1292.143	37.23264	1.95404	15.42706	3855.142	86.5362	0.017	10.87161	1.19861	2.79442	0.43609	15.9891	0.54813	0.02119	0.11271	0.00397
MIP021	711.2789	1608.279	31.67239	1.82394	13.80472	5231.95	77.56813	0.02818	15.03264	1.85582	3.4075	0.57401	22.38956	0.83911	0.02053	0.13888	0.00362
MIP024	579.872	1379.971	32.30216	2.65864	10.80248	4255.048	47.90618	0.02555	14.04367	1.45291	3.77453	0.43328	22.05798	0.59174	0.01954	0.11757	0.00295
Sample ID	Al	Fe	Mn	Ni	Pb	S	Zn	Be	Ti	V	Cr	Co	Cu	As	Pd	Cd	Pt
ANC001 I	1792.46	3255.808	65.62184	4.48036	27.18949	3647.132	130.3163	0.08864	55.31455	4.29498	10.88202	1.13744	35.22186	1.25978	0.04042	0.18065	0.00497
ANC009	1234.695	3628.14	56.76095	4.46695	26.60497	5021.384	123.5255	0.04986	34.88547	3.9111	9.57516	1.05863	46.6842	1.2468	0.04539	0.20682	0.00477
ANC011	430.2436	1042.971	24.61283	1.40995	6.91387	3134.935	40.04341	0.02254	14.47681	1.49486	3.37324	0.42615	15.45265	0.60313	0.01922	0.08776	0.00219
ANC012	919.333	2075.055	40.24713	2.88262	14.55323	4609.281	85.91027	0.04029	30.73565	2.45085	5.92125	0.6236	24.98299	0.87553	0.03035	0.09378	0.00267
ARD003	747.1325	1421.954	37.17304	2.01007	8.59499	4643.357	60.32175	0.02644	19.14231	1.74016	3.94606	0.46362	15.64447	0.57222	0.0216	0.13205	0.00264
ARD004	661.335	1445.298	31.23017	2.2173	7.75242	4144.648	73.06158	0.02553	15.71659	1.59161	3.85217	0.40409	17.51746	0.60934	0.02353	0.14538	0.00214
ARD006	624.4792	1264.928	31.10311	1.94723	9.09338	3879.334	57.78385	0.02262	15.26686	1.64941	3.36867	0.41879	14.90455	0.56067	0.03244	0.12251	0.00291
ARD008	496.7994	858.9486	29.66835	1.25155	5.54171	3774.346	47.41719	0.02142	12.54375	1.20551	2.36474	0.33651	11.3119	0.48835	0.0221	0.10094	0.00179
ARD012	1280.282	2484.662	52.92603	3.16917	12.28275	4601.568	83.41412	0.04706	34.94217	3.08732	6.81425	0.7373	23.68071	0.83808	0.03234	0.15547	0.00672
ARD013	789.0277	1356.446	30.31528	2.0724	8.97433	3623.194	51.34924	0.03027	20.23304	1.75315	3.48753	0.49664	13.66608	0.61021	0.02617	0.10562	0.00242
BFD005	823.6318	1573.862	34.1256	3.08357	9.36418	4617.259	67.79457	0.02686	22.65254	1.89532	4.66168	0.47187	18.10479	0.67379	0.02099	0.21013	0.00304
BFD008	2620.44	2599.642	56.49619	3.54352	13.47732	5450.339	91.75318	0.0393	30.48982	3.25902	7.18103	0.72903	31.9207	0.92695	0.03951	0.19919	0.00456
CC018	1152.302	2881.701	62.3483	6.7124	25.88036	5528.691	102.9365	0.05418	32.22479	3.19635	7.04386	0.86479	28.08516	1.13242	0.03745	0.2408	0.00502
MIP001	510.8547	1005.068	29.98033	1.43897	7.26501	3756.653	61.31045	0.02078	11.99796	1.11895	2.61345	0.34393	12.29542	0.35561	0.02704	0.08995	0.00397
MIP010 I	619.4799	1420.692	32.40669	2.25336	10.71467	3239.869	85.72185	0.02399	15.75797	1.48233	3.99015	0.44927	16.91616	0.5819	0.02783	0.12899	0.00306
MIP021	948.514	1782.984	35.34019	2.63909	7.47527	4548.815	65.68547	0.03308	22.59872	2.45035	4.71065	0.60775	21.95355	0.81911	0.02577	0.10835	0.00352
MIP024	582.6888	1185.132	31.81162	1.5958	6.20874	4471.007	48.7714	0.02061	15.13112	1.58007	3.06613	0.39327	13.12027	0.67494	0.02134	0.08954	0.00251

Appendix D-7: Comparison of analytical instruments (ICP-OES and IRMS) for sulphur concentrations in lichen (error bars represented by 1x Std. Dev. of CRM on dummy value – IRMS: ± 0.02 and ICP-OES: ± 59.11 ; displayed with Pearson's r)



Appendix E – Lichen PAH concentrations (Chapter 7)

Appendix D-1: Lichen sampling sites for PAH analysis, displayed with Site-ID, XY-coordinates (OSGB1936 – British National Grid), sampled lichen species and sampling date (lichen samples were processed and frozen on the same day)

ID	ID/Name	X	Y	lichen species	sampling date
1	ARD004	385326	397120	X. parietina	09/05/2018
2	ARD012	384548	397247	X. parietina	09/05/2018
3	ARD013	384798	397104	X. parietina	09/05/2018
4	HUL008	383705	397171	X. parietina	10/07/2018
5	MIP021	386434	399454	X. parietina	04/09/2018
6	BFD005	385704	398035	X. parietina	24/07/2018
7	HUL005	383231	397017	X. parietina	10/07/2018
				Ph. spp	10/07/2018
8	BFD008	385368	398023	X. parietina	24/07/2018
9	ARD006	385422	396810	X. parietina	11/07/2018
10	ARD008	384921	396860	X. parietina	11/07/2018
11	ARD003	384969	397257	X. parietina	10/07/2018
12	MIP010 I	386158	399834	X. parietina	04/09/2018
				Ph. spp	04/09/2018
13	MIP001	385312	398998	X. parietina	04/09/2018
14				Ph. spp	04/09/2018
15	MIP024	386302	399221	X. parietina	04/09/2018
16	CC018	383277	397664	X. parietina	12/09/2018
17	CC015	383290	397932	X. parietina	12/09/2018
				Ph. spp	12/09/2018
18	ANC001 I	385143	398190	X. parietina	10/10/2018
19	ANC009	384231	398977	X. parietina	10/10/2018
20	ANC011	384467	399200	X. parietina	10/10/2018
21	ANC012	384960	398477	X. parietina	10/10/2018

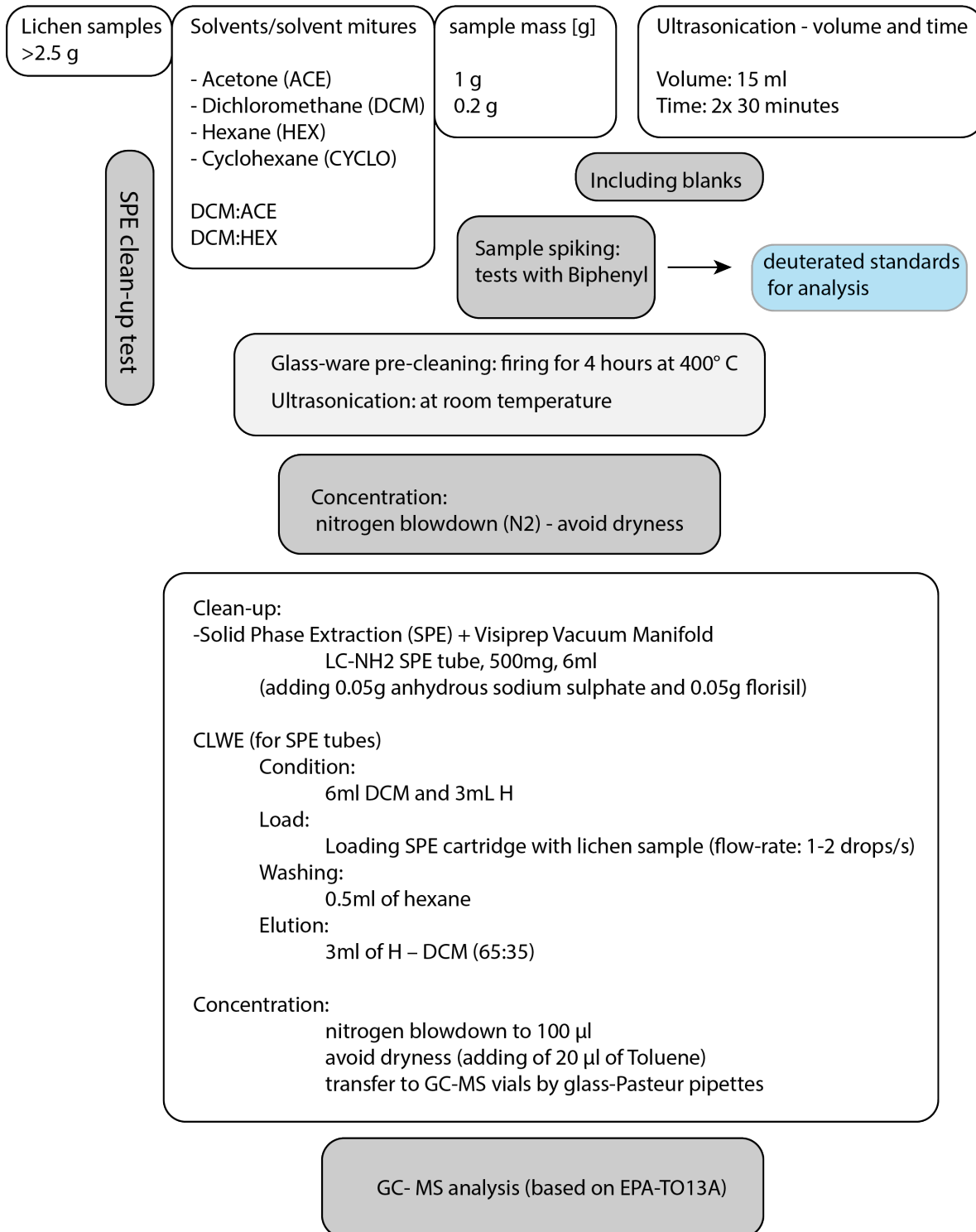
Appendix D-2: Method overview applied to extract PAHs from lichen material, including sample mass, sample additions, spiking standards and extraction solvents, volume of solvent used, extraction method, time and concentrations technique. Clean-up step, column additions (if column clean-up used), final solvent and pre-analysis preparations as well as analysis method used are described. References (see reference list) are also displayed

#	samples mass	additional to samples	spiking	extraction solvent(s)	volume of solvent [ml]	extraction method	extraction time	evaporation/concentration	post clean-up/purification	column additions	final solvent (measurement)	before analysis	instrument	source/paper
1	0.6g	Na2SO4 (0.6g) and florisil (0.6g)	surrogate standard: Wellington L429-IS (100µL, 1.2 µg/ml)	dichloromethane/acetone (1:1)		Accelerated Solvent Extractor (ASE X-100)	30min (3x10min)	rotary evaporated	column chromatography: alumina, eluting with dichloromethane		cyclohexane	evaporation to dryness by nitrogen stream, residue	GC-MS	Kodnik et al. 2015
2	2g		phenanthrene-d10	hexane	300ml	Soxhlet	24h	rotavapor	column with silica gel (2g) and Na2SO4 (0.5g)		isooctane		GC-MS	Loppi et al. 2015
3	0.25g	dispersant material C18 (0.5g)	anthracene-d10	hexane; dichloromethane/hexane mix (v:v, 20:80)	10 ml [both]	Matrix Solid-Phase Dispersion (MSPD)			Syncore SPE				PTV-GC-EI-MS-MS	Vingiani et al. 2015; Concha-Graña et al. 2015
4	0.6-0.8g			acetone/hexane (v/v, 1:1)	150ml	Automated Soxhlet Extraction	120min (2x60min)	concentrated to 2 to 5mL (before purification)	SPE clean-up (LC-NH2 SPE tubes, added with 0.05g anhydrous sodium sulphate and 0.05g florisil), elution with hexane-dichloromethane (65:35)	0.05g anhydrous sodium sulfate, 0.05g florisil	hexane-dichloromethane (65:35)	to 0.5mL under a nitrogen stream	GC-MS	Nascimbene et al. 2014
5	2g		perylene-d12	cyclohexane	30ml	ultrasonic bath	60min (2x30min)	concentrated to 2ml (before purification), rotavapor	filtering and repeat of extraction		isooctane		GC-MS	Protano et al. 2014
6	2g			dichloromethane		Soxhlet	16h		silica gel column	anhydrous sodium sulfate	acetonitrile		HPLC	Shukla et al. 2013
7	2g		surrogate mixture (Naphthalene-d8, acenaphthene-d10, phenanthrene-d10, chrysene-d12, perylene-d12)	hexane/dichloromethane (1:1, v:v)		Accelerated Solvent Extractor (ASE350)	24min (3x7min)	rotary evaporator	alumina/silica gel, gel permeation chromatography (GPC)	anhydrous sodium sulfate	hexane-dichloromethane (1:1)	rotary evaporation and nitrogen stream	GC-MS	Yang et al. 2013
8	0.2g (triplicates)			dichloromethane	100ml	Soxhlet	16h		silica gel column	anhydrous sodium sulfate	acetonitrile		HPCL	Shukla et al. 2012




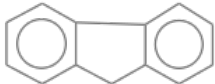
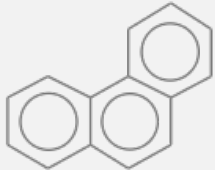

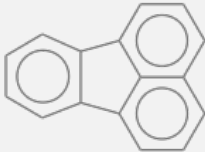

9	0.2g (triplicates)		PAH mixture (Sigma-Aldrich, USA)	dichloromethane	15ml	ultrasonic bath	60min (4x15min)		florisil (0.1g) and anhydrous sodium sulfate (0.1g) to lichen samples; elution with hexane-dichloromethane (3:1)		hexane-dichloromethane (3:1)	concentration under nitrogen stream	GC-MS	Käffer et al. 2012
10	0.2g (triplicates)			hexane	20ml	dynamic sonication-assisted solvent extraction (DSASE)	10min		SPE clean up - normal phase -NH2 column	anhydrous sodium sulfate, florisil	hexane:dichloromethane (65:35)	concentration under nitrogen stream	GC-MS	Blasco et al. 2007, 2008, 2011
11	2g			acetonitrile	200ml	Soxhlet	24h	rotary vacuum evaporation (purified N2)	florisil column		acetonitrile	stream of purified N2	HPCL	Augusto et al. 2010, 2009
12	2g		perylene-d12 and isoctane	cyclohexane	30ml	ultrasonic bath	60min (2x30min)	concentrated at 2ml before purification	filtering (and repeated extraction); silica gel in dichloromethane (glass column); elution of dichloromethane, pre-elution with pentane	anhydrous sodium sulfate	dichloromethane-pentane (2:3, v/v)	rotavapor concentrated to 1ml	GC-MS	Guidotti et al. 2009
13	0.2g		PAH mixture	hexane	20ml	dynamic sonication-assisted solvent extraction (DSASE)	10min	rotary evaporator	florisil (0.1g) and anhydrous sodium sulfate (0.1g) to spiked sample, alumina glass column	anhydrous sodium sulfate	hexane-dichloromethane (3:1)	concentrated to 500µl	GC-MS	Domeño et al. 2006
	0.2		PAH mixture	dichloromethane	15ml	ultrasonic bath	60min (4x15min)							
	0.2	anhydrous sodium sulfate	PAH mixture	dichloromethane	250ml	Soxhlet	6h							
14	2g		EPA working standard solution (100 µg/ml) in hexane	cyclohexane	30ml	ultrasonic bath (Branson)	60min (2x30min)		filtering (No.40 Whatman), glass chromatography column (activated silica gel in dichloromethane)	anhydrous sodium sulfate	25ml methylene chloride-pentane (2:3, v:v)		GC-MS	Guidotti et al. 2003
15	1g			dichloromethane		ultrasonic bath	40min (2x20min)	rotavapor (dried under nitrogen)			soctane		GC-MS	Owczarek et al. 2001
16	3g		13C12 PCB recovery standard (2.5ng)	dichloromethane		Soxhlet	4h		blowdown under nitrogen, alumina/silica gel chromatography, gel permeation chromatography and silica gel fractionation	15g anhydrous sodium sulfate	dodecane (GC internal standards - PCB congeners); isoctane (GC internal standard (TCMX))		GC-MSD	Ockenden et al. 1998

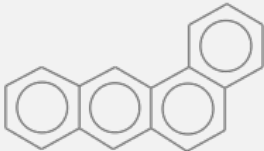
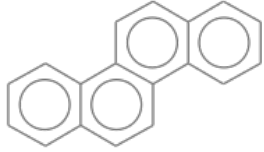
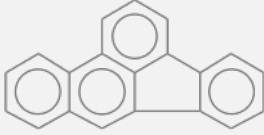
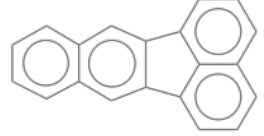
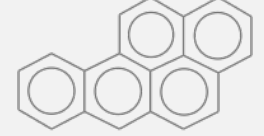
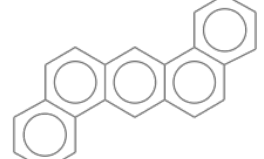

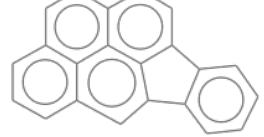
Appendix D 3: Experimental protocol - lichen material extraction for PAHs; initial

Experimental protocol - lichen extraction for PAHs



Appendix D-4: PAHs in certified reference material (CRM) with CAS number, concentrations (from the certificate of analysis values, reported for 'Supelco TCL PAH Mix' by Sigma-Aldrich) and ring structure (EPA, 1999; NIST, 2018)

Analyte – PAH with chemical formula	CAS#	Certified Conc. (±Uncertainty) [µg/ml]	PAH ring structure
Napthalene C ₁₀ H ₈	91-20-3	1994.0 ± 8.2	
Acenaphthylene C ₁₂ H ₈	208-96-8	1988.2 ± 6.5	
Acenaphthene C ₁₂ H ₁₀	83-32-9	19886.4 ± 44	
Fluorene C ₁₃ H ₁₀	86-73-7	1974.4 ± 7.3	
Phenanthrene C ₁₄ H ₁₀	85-01-8	1960.4 ± 7.4	
Anthracene C ₁₄ H ₁₀	120-12-7	1980.4 ± 16	
Fluoranthene C ₁₆ H ₁₀	206-44-0	1990.0 ± 12	
Pyrene C ₁₆ H ₁₀	129-00-0	1984.2 ± 7.3	

Benz[a]anthracene C₁₈H₁₂	56-55-3	1970.4 ± 8.3	
Chrysene C₁₈H₁₂	218-01-9	2000.0 ± 8.7	
Benzo[b]fluoranthene C₂₀H₁₈	205-99-2	1999.9 ± 14	
Benzo[k]fluoranthene C₂₀H₁₂	207-08-9	1990.2 ± 10	
Benzo[a]pyrene C₂₀H₁₂	50-32-8	1999.9 ± 11	
Dibenz[a,h]anthracene C₂₂H₁₄	53-70-3	1966.4 ± 12	
Benzo[ghi]perylene C₂₂H₁₂	191-24-2	1988.2 ± 7.2	
Indeno[1,2,3-cd]pyrene C₂₂H₁₂	193-39-5	1980.4 ± 13	

Appendix D-5: GC-MS conditions for analysis of lichen PAH concentrations at Manchester Metropolitan University

Conditions	
GC-MS (Manchester Metropolitan University)	
Gas Chromatography	
Column	HP-5ms Ultra Inert; -60°C to 325°C (350°C): 30m x 20µm x 0.25µm
Carrier Gas	Helium
Injection Volume	1 µl, split-less
Injector Temperature	280°C
Temperature Programme	
Initial Column Temp.	50°C
Initial Hold Time	2 minutes
Programme	20°C/min to 150°C (no hold) 10°C/min to 300°C (5 min. hold)
Final Temperature	300°C
Final Hold Time	5 Minutes
Mass Spectrometer	
Transfer Line Temperature	300°C
Ionization Mode	EI
Mass Range	m/z: 50.00 to 305.00; Full Scan Mode & Selected Ion Monitoring (SIM)
Scan Time	Scan Speed (u/s): 391 (N=4); Frequency: 1.5 (scans/sec)

Appendix D-6: Identification of 16 EPA PAHs by Multiple Reaction Monitoring (MRM), with retention times (RT) and MRMs (m/z-values) and applied collision energies

Compound	RT	MRMs (m/z)	Collision energy (V)
Naphthalene	6.38	128.06 > 128.06	30
		128.06 > 102.10	20
		128.06 > 77.10	30
Acenaphthylene	8.43	152.08 > 150.08	30
		152.08 > 126.08	27
		152.08 > 102.08	30
Acenaphthene	8.70	154.08 > 152.08	27
		154.08 > 126.07	45
		154.08 > 102.09	45
Fluorene	9.57	166.08 > 164.08	32
		166.08 > 139.05	35
		166.08 > 115.07	35
Phenanthrene Anthracene	11.38	178.08 > 176.08	32
	11.48	178.08 > 151.09	35
		178.08 > 126.07	40
Fluoranthene Pyrene	13.92	202.08 > 200.08	36
	14.39	202.08 > 150.07	45
		202.08 > 126.05	45
Benz[a]anthracene Chrysene	17.17	228.09 > 226.09	50
	17.23	228.09 > 200.10	50
		228.09 > 176.08	50
Benzo[b]fluoranthene Benzo[k]fluoranthene Benzo[a]pyrene	19.49	252.09 > 250.09	45
	19.55	252.09 > 224.08	55
	20.11	252.09 > 200.08	55
Dibenzo[a,h]anthracene	22.22	278.11 > 276.11	40
		278.11 > 250.10	55
		278.11 > 226.10	50
Indeno[1,2,3-cd]pyrene Benzo[ghi]perylene	22.15	276.09 > 274.09	50
	22.59	276.09 > 248.10	55
		276.09 > 224.10	70
Deuterated PAH standards			
Phenanthrene-d10	11.33	188.29 > 184.11	32
		188.29 > 158.10	35
		188.14 > 132.09	40
Chrysene-d12	17.18	240.17 > 236.14	50
		240.17 > 208.11	50
		240.17 > 184.14	50
Dibenzo[a,h]anthracene-d14	22.17	292.20 > 288.17	40
		292.20 > 260.14	55
		292.20 > 236.14	50

Appendix D-7: Correlation matrix of PAHs, displayed as Pearson's r colour-coded by significance level: p<0.05 shaded in yellow and p<0.01 shaded in green

Naphthalene	Naphthalene															
Acenaphthylene	0.523	Acenaphthylene														
Acenaphthene	0.459	0.430	Acenaphthene													
Fluorene	0.729	0.701	0.829	Fluorene												
Phenanthrene	0.820	0.645	0.744	0.928	Phenanthrene											
Anthracene	0.738	0.686	0.674	0.839	0.901	Anthracene										
Fluoranthene	0.528	0.433	0.696	0.675	0.702	0.699	Fluoranthene									
Pyrene	0.550	0.642	0.475	0.576	0.576	0.701	0.805	Pyrene								
Benz[a]anthracene	0.567	0.459	0.671	0.662	0.677	0.703	0.949	0.820	Benz[a]anthracene							
Chrysene	0.624	0.511	0.677	0.729	0.765	0.761	0.965	0.808	0.947	Chrysene						
Benzo[b]fluoranthene	0.212	0.146	0.577	0.457	0.406	0.340	0.650	0.513	0.693	0.651	Benzo[b]fluoranthene					
Benzo[k]fluoranthene	0.024	0.162	0.460	0.319	0.274	0.333	0.556	0.442	0.629	0.528	0.800	Benzo[k]fluoranthene				
Benzo[a]pyrene	0.239	0.114	0.591	0.469	0.421	0.346	0.690	0.529	0.738	0.680	0.988	0.768	Benzo[a]pyrene			
Dibenzo[a,h]anthracene	0.269	0.259	0.654	0.537	0.438	0.472	0.680	0.573	0.759	0.638	0.859	0.824	0.866	Dibenzo[a,h]anthracene		
Indeno[1,2,3-cd]pyrene	0.183	0.159	0.638	0.507	0.468	0.408	0.756	0.549	0.794	0.720	0.890	0.853	0.913	0.851	I[cd]pyrene	
Benzo[g,h,i]perylene	0.170	0.232	0.532	0.465	0.409	0.399	0.651	0.567	0.692	0.612	0.929	0.872	0.919	0.919	0.911	B[g,h,i]P

Appendix F – Modelling data groups

Appendix F- 1: Grouping of 'Manchester's urban factors' used for modelling of lichen-derived pollutant loadings including traffic data, building characteristics and others, i.e. point source and greenspace distance

Traffic data	Building characteristics	Other
<p>Road class</p> <ul style="list-style-type: none">1: M - motorway2: A - A-road3: B- B-road4: U - unclassified	<p>Mean building height</p> <ul style="list-style-type: none">1: <10 m2: 10 to 20 m3: >20 m	<p>Point source</p> <ul style="list-style-type: none">1: <500 m2: 500 to 1000 m3: 1000 to 2000 m4: >2000 m
<p>Distance major road</p> <ul style="list-style-type: none">1: <25 m2: 25 to 50 m3: 50 to 100 m4: 100 to 200 m5: >200 m	<p>Height-to-Width ratio</p> <ul style="list-style-type: none">1: <0.52: 0.5 to 13: 1 to 1.54: 1.5 to 25: >2	<p>Distance greenspace</p> <ul style="list-style-type: none">1: <100 m2: 100 to 200 m3: 200 to 300 m4: 300 to 400 m5: 400 to 500 m6: >500 m
<p>Traffic counts</p> <ul style="list-style-type: none">0: N/A1: <10,0002: 10,000 to 20,0003: 20,000 to 30,0004: >30,000	<p>Street canyon</p> <ul style="list-style-type: none">0: No1: Yes - buildings on two cardinal directions2: Yes - sampling location surrounded by buildings ('dead'end)	

Appendix F-2: Lichen sampling sites (N=94), displayed with XY-coordinates (OSGB – British National Grid) and grouping according to procedure described in chapter 2; classification numbers according to Appendix F-1; RdCl = Road class, MR = Distance to major road (class), BH = mean building height [in m] and BH_gr = grouped data, SC = Street canyon, H/W = height-to-width ratio TC = Traffic counts with TC_all = all vehicles (annual average daily traffic flow, 2017; empty field – no data available), PS = Distance to point source, GS = distance to greenspace

ID	ID/name	X	Y	RdCl	MR	BH	BH_gr	SC	H/W	TC	TC_all	PS	GS
1	ANCO01 I	385143	398190	2	3	8.39	1	2	3	3	29416	3	6
2	ANCO01 II	385180	398222	4	2	9.45	1	0	1	3	29416	3	6
3	BFD001	385420	398339	4	4	34.05	3	0	1	4	30935	3	6
4	CC001	385123	397837	4	4	7.33	1	1	3	2	18195	3	6
5	BFD002	385829	398555	4	4	9.3	1	1	2	2	12349	3	3
6	BFD004	385760	398209	4	4	7.73	1	1	2	2	12349	3	2
7	BFD007	385366	397922	4	4	8.2	1	2	2	4	30935	3	5
8	BFD005	385704	398035	4	4	7.15	1	0	1	4	30935	3	3
9	BFD006	385662	397913	2	2	7.40	1	0	1	3	21122	3	4
10	BFD008	385368	398023	4	1	12.04	2	1	2	4	30935	3	6
11	HUL001	383876	396960	4	3	9.43	1	2	2	4	44514	1	4
12	HUL002	384072	396768	4	4	9.6	1	2	3	1	8119	1	4
13	HUL004	383616	397107	1	1	10.61	2	2	1	4	74010	2	3
14	HUL005	383231	397017	4	4	11.08	2	0	1	4	74010	2	1
15	HUL008	383705	397171	2	1	10.9	2	1	1	4	58142	1	4
16	MIP012	385838	399661	4	3	22.48	3	0	1	2	16561	2	3
17	MIP013	385886	399523	4	5	15.1	2	1	3	2	16561	2	2
18	MIP007	386160	399492	4	4	10.63	2	0	1	0		2	1
19	MIP008 II	386261	399667	2	1	0.00	1	0	1	3	26732	2	2
20	MIP006	385938	399381	4	5	13.6	2	1	2	0		3	2
21	MIP008 I	386283	399611	4	2	10.18	2	1	2	3	26732	2	3
22	CHE001	385166	399865	4	4	12.01	2	0	1	2	14972	3	3
23	MIP016 I	385089	399557	2	2	39.9	3	0	1	0		3	3
24	ANCO11	384467	399200	4	4	0.00	1	0	1	3	21426	4	1
25	MIP021	386434	399454	2	1	0.00	1	0	1	0		2	2
26	CHE002	384901	399510	4	4	10.8	2	1	2	0		3	4
27	ANCO09	384231	398977	2	1	27.18	3	1	5	2	15885	3	3
28	ARD007	385359	396932	2	1	10.78	2	1	2	2	16953	2	2
29	ARD004	385326	397120	2	2	0.00	1	0	1	2	16953	2	1
30	MIP039	385774	398723	4	5	7.86	1	1	4	2	12349	3	3
31	CHE004	384382	399591	4	5	7.81	1	2	2	3	20337	4	2
32	ARD002	384843	397402	2	2	12.76	2	0	1	3	26034	2	3
33	MIP010 I	386158	399834	2	1	11.1	2	0	1	3	26732	2	1
34	ARD002 I	384869	397365	4	2	8.9	1	0	1	3	26034	2	2
35	ANCO07	385176	398981	4	3	8.95	1	1	1	3	20592	3	2
36	MIP011	385883	399803	2	2	12.6	2	0	1	2	16561	2	2
37	ARD013	384798	397104	4	4	12.97	2	0	1	2	19766	1	1
38	MIP020	386352	399353	4	4	9.27	1	0	1	0		3	1
39	ARD013 I	384873	397055	4	4	12.95	2	1	2	2	19766	1	1
40	MIP009 II	386190	399774	4	1	7.72	1	0	1	3	26732	2	1

41	MIP022	386381	399468	4	2	0.00	1	0	1	0		2	2
42	MIP010 II	386128	399848	2	1	8.03	1	0	1	2	16561	2	1
43	MIP014	385684	399549	4	3	8.21	1	2	2	0		3	1
44	MIP024	386302	399221	4	5	8.28	1	0	1	0		3	1
45	MIP018	385199	399664	2	1	9.75	1	0	1	2	14972	3	2
46	ARD012	384548	397247	1	1	0.00	1	0	1	1	9883	1	1
47	MIP017	385369	399408	4	4	7.93	1	0	1	0		3	2
48	MIP016	384938	399397	4	2	6.1	1	0	1	3	20592	3	3
49	MIP023	386415	399289	4	4	9.09	1	2	2	0		3	1
50	ARD006 I	385373	396782	4	3	8.14	1	0	1	2	12739	2	4
51	MIP009 I	386215	399738	4	1	5.23	1	0	1	3	26732	2	1
52	MIP001	385312	398998	4	4	0.00	1	0	1	3	20592	3	2
53	MIP038	386167	399073	4	5	0.00	1	0	1	0		3	2
54	MIP015	385454	399341	2	1	8.3	1	2	1	0		3	2
55	MIP002	385653	399279	4	4	6.77	1	2	2	0		3	2
56	MIP025	385597	398946	4	5	8.31	1	0	1	0		3	2
57	ARD001	384890	397470	2	1	7.87	1	0	1	4	32699	2	3
58	MIP005	385843	399434	4	5	0.00	1	1	3	0		3	2
59	ARD003	384969	397257	4	1	12.3	2	1	3	3	26034	2	1
60	MIP003	385749	399415	4	4	7.06	1	0	1	0		3	2
61	ARD006	385422	396810	2	1	10.75	2	2	2	2	12739	2	3
62	ARD005	385024	396794	4	4	6.67	1	2	3	2	19766	1	1
63	ARD008	384921	396860	4	4	6.77	1	2	3	2	19766	1	2
64	ARD006 III	385387	396705	4	4	9.53	1	0	1	2	12739	2	3
65	ARD006 II	385410	396748	4	3	10.17	2	0	1	2	12739	2	3
66	CC014	383156	398139	2	1	18.53	2	1	4	2	12838	2	3
67	CC015	383290	397932	4	4	15.9	2	2	3	2	11095	2	1
68	CC003	383836	397553	4	3	18.10	2	2	3	2	17088	2	6
69	ANC003	384734	398978	4	3	9.30	1	0	1	2	12732	3	3
70	CC017	383273	397492	2	2	10.60	2	0	1	2	17836	2	3
71	HUL021	382850	396595	4	3	13.73	2	2	3	2	11814	3	2
72	CC007	383902	398788	4	3	28.63	3	1	3	2	15007	3	1
73	HUL025	383832	397110	2	1	41.33	3	0	1	4	58142	1	4
74	HUL016	383263	396662	2	1	10.62	2	2	2	2	10979	3	1
75	HUL026	382857	396932	4	4	6.87	1	1	2	2	11856	3	1
76	CC009	384295	398297	4	4	16.83	2	0	1	1	3963	3	1
77	CC018	383277	397664	4	3	10.37	2	1	4	2	17836	2	2
78	CC012 I	382786	397728	2	2	8.6	1	1	1	3	29603	1	3
79	CC012	382892	397730	4	3	10.2	2	2	2	3	29603	2	2
80	HUL024	382661	397036	4	3	8.38	1	2	2	4	30213	2	1
81	ANC012	384960	398477	4	2	19.28	2	0	1	3	29416	3	6
82	CC025	384409	397812	4	3	27.30	3	2	5	1	3056	2	1
83	CC008	384382	397558	4	2	23.33	3	2	4	1	8159	1	3
84	HUL021 I	382968	396568	3	1	10.77	2	2	2	2	11814	3	2
85	CC006	383517	398334	4	2	18.09	2	1	3	1	6989	3	2
86	HUL027	384256	397121	2	3	19.45	2	0	1	4	93593	1	1
87	CC016	383741	397851	4	3	28.62	3	2	4	2	10048	2	3
88	CC021	384516	398751	4	2	12.79	2	1	2	2	16723	3	3
89	CC011	384003	398020	2	1	22.40	3	1	5	1	8224	2	4
90	HUL023	382488	397017	2	1	12	2	2	1	4	30213	2	2
91	HUL020	382990	396950	2	1	11.1	2	2	1	2	11856	3	2
92	CC004	383917	397652	4	4	29.78	3	2	5	1	8805	2	5
93	HUL014	383349	396842	4	4	0.00	1	0	1	2	10979	2	1
94	ANC002	385366	398773	4	5	29.76	3	0	1	2	11856	3	2